NASA/CR-2006-214511



Improved Airport Noise Modeling for High Altitudes and Flexible Flight Operations

David W. Forsyth and Jesse I. Follet
Boeing Commercial Airplane Company, Seattle, Washington

October 2006

The NASA STI Program Office . . . in Profile

Since its founding, NASA has been dedicated to the advancement of aeronautics and space science. The NASA Scientific and Technical Information (STI) Program Office plays a key part in helping NASA maintain this important role.

The NASA STI Program Office is operated by Langley Research Center, the lead center for NASA's scientific and technical information. The NASA STI Program Office provides access to the NASA STI Database, the largest collection of aeronautical and space science STI in the world. The Program Office is also NASA's institutional mechanism for disseminating the results of its research and development activities. These results are published by NASA in the NASA STI Report Series, which includes the following report types:

- TECHNICAL PUBLICATION. Reports of completed research or a major significant phase of research that present the results of NASA programs and include extensive data or theoretical analysis. Includes compilations of significant scientific and technical data and information deemed to be of continuing reference value. NASA counterpart of peer-reviewed formal professional papers, but having less stringent limitations on manuscript length and extent of graphic presentations.

- TECHNICAL MEMORANDUM. Scientific and technical findings that are preliminary or of specialized interest, e.g., quick release reports, working papers, and bibliographies that contain minimal annotation. Does not contain extensive analysis.

- CONTRACTOR REPORT. Scientific and technical findings by NASA-sponsored contractors and grantees.

- CONFERENCE PUBLICATION. Collected papers from scientific and technical conferences, symposia, seminars, or other meetings sponsored or co-sponsored by NASA.

- SPECIAL PUBLICATION. Scientific, technical, or historical information from NASA programs, projects, and missions, often concerned with subjects having substantial public interest.

- TECHNICAL TRANSLATION. English-language translations of foreign scientific and technical material pertinent to NASA's mission.

Specialized services that complement the STI Program Office's diverse offerings include creating custom thesauri, building customized databases, organizing and publishing research results ... even providing videos.

For more information about the NASA STI Program Office, see the following:

- Access the NASA STI Program Home Page at ***http://www.sti.nasa.gov***

- E-mail your question via the Internet to help@sti.nasa.gov

- Fax your question to the NASA STI Help Desk at (301) 621-0134

- Phone the NASA STI Help Desk at (301) 621-0390

- Write to:
 NASA STI Help Desk
 NASA Center for AeroSpace Information
 7121 Standard Drive
 Hanover, MD 21076-1320

NASA/CR-2006-214511



Improved Airport Noise Modeling for High Altitudes and Flexible Flight Operations

David W. Forsyth and Jesse I. Follet
Boeing Commercial Airplane Company, Seattle, Washington

National Aeronautics and
Space Administration

Langley Research Center
Hampton, Virginia 23681-2199

Prepared for Langley Research Center
under Contract NAS1-00086

October 2006

Available from:

NASA Center for AeroSpace Information (CASI)
7121 Standard Drive
Hanover, MD 21076-1320
(301) 621-0390

National Technical Information Service (NTIS)
5285 Port Royal Road
Springfield, VA 22161-2171
(703) 605-6000

Table of Contents

1 Summary 5

2 Introduction 6

3 Study Tasks 7

3.1 Standardized Modeling Assumptions 7

3.1.1 Standardizing Takeoff Weight vs. INM Stage Length 7

3.1.2 Modification of NPD Data to Different Atmospheric Absorption Standard 10

3.1.3 Adjustment of NPD Data to Account for Different Weather Conditions 11

3.2 Approach and Landing Noise Modeling 25

3.2.1 Effect of Aircraft Configuration on Approach Noise 25

3.3 Comparison of INM Predictions with Certification Measurements 29

3.3.1 Certification Flight Profiles 29

3.3.2 Boeing Noise Power Distance Curves (NPD) 30

3.3.3 Comparison of Noise Calculation Methods 30

3.3.4 Comparison of FAR 36 Takeoff Noise Results 30

3.4 Modeling Derated Thrust Takeoffs 36

3.4.1 Effect of Derate on Noise Contours 36

4 Conclusions and Recommendations 40

Bibliography 41

Appendix A Comparison of INM 5.0a through 6.2 Beta Using Noise Monitoring and Radar Data Collected at Denver International Airport

Appendix B Reduced Thrust Departures from a High Altitude Airport Using Procedure Steps with the Integrated Noise Model

THIS PAGE INTENTIONALLY LEFT BLANK

List of Figures

Figure 1: Takeoff Weights vs. Trip Length for 737-300s 8
Figure 2: Takeoff Weights vs. Trip Length for 757-200s 9
Figure 3: Takeoff Weights vs. Trip Length for 777-200s 9
Figure 4: dBA Contours Adjusted (Black) and Unadjusted (Grey) to SAE AIR-1845 for the 737-700 10
Figure 5: dBA Contours Adjusted (Black) and Unadjusted (Grey) to SAE AIR-1845 for the 757-200 11
Figure 6: dBA Contours Adjusted (Black) and Unadjusted (Grey) to CAN7 SAE AIR-1845 for the 747-400 11
Figure 7: Atmospheric Absorptions Used in NPD Adjustment Comparisons 12
Figure 8: Difference in SEL Calculated between Baseline and Dry Day (757-200RR) 13
Figure 9: Difference in LAmax Calculated between Baseline and Dry Day (757-200RR) 14
Figure 10: Difference in SEL Calculated between Baseline and Cool Day (757-200RR) 14
Figure 11: Difference in LAmax Calculated between Baseline and Cool Day (757-200RR) 15
Figure 12: Difference in SEL Calculated between Baseline and Dry Day (757-200PW) 15
Figure 13: Difference in LAmax Calculated between Baseline and Dry Day (757-200PW) 16
Figure 14: Difference in SEL Calculated between Baseline and Cool Day (757-200PW) 16
Figure 15: Difference in LAmax Calculated between Baseline and Dry Day (757-200PW) 17
Figure 16: Difference in SEL Calculated between Baseline and Dry Day (737-400) 17
Figure 17: Difference in LAmax Calculated between Baseline and Dry Day (737-400) 18
Figure 18: Difference in SEL Calculated between Baseline and Cool Day (737-400) 18
Figure 19: Difference in LAmax Calculated between Baseline and Cool Day (737-400) 19
Figure 20: Difference in SEL Calculated between Baseline and Dry Day (737-700) 19
Figure 21: Difference in LAmax Calculated between Baseline and Dry Day (737-700) 20
Figure 22: Difference in SEL Calculated between Baseline and Cool Day (737-700) 20
Figure 23: Difference in LAmax Calculated between Baseline and Cool Day (737-700) 21
Figure 24: Difference in SEL Calculated between Baseline and Dry Day (747-400) 21
Figure 25: Difference in LAmax Calculated between Baseline and Dry Day (747-400) 22
Figure 26: Difference in SEL Calculated between Baseline and Cool Day (747-400) 22
Figure 27: Difference in LAmax Calculated between Baseline and Cool Day (747-400) 23
Figure 28: Difference in SEL Calculated between Baseline and Dry Day (777-200) 23
Figure 29: Difference in LAmax Calculated between Baseline and Dry Day (777-200) 24
Figure 30: Difference in SEL Calculated between Baseline and Cool Day (777-200) 24
Figure 31: Difference in LAmax Calculated between Baseline and Cool Day (777-200) 25
Figure 32: Effect of Configuration on dBA Contour of the 737-800 Using the Standard Approach 27
Figure 33: Effect of Configuration on dBA Contour of the 737-800 Using a CDA Type Approach 27
Figure 34: Effect of Configuration on dBA Contour of the 777-200 Using a Standard Approach 28
Figure 35: Effect of Configuration on dBA Contour of the 757-300 Using a Standard Approach 28
Figure 36: Effect of Configuration on dBA Contour of the 757-300 Using a CDA Approach 29
Figure 37: 737-700 Cutback Flight Profile for 154,500 lbs 33
Figure 38: Comparison between Certification EPNL to the INM Predictions and INM Predictions with INM Built Procedure Profile for 737-700 at 154,500 lbs TOGW 33
Figure 39: Comparison between Certification EPNL to the INM Predictions for 717-200 34
Figure 40: Comparison between Certification EPNL to the INM Predictions for 737-700 34
Figure 41: Comparison between Certification EPNL to the INM Predictions for 747-400 35
Figure 42: Comparison between Certification EPNL to the INM Predictions for 777-200 35
Figure 43: Effect of 10% Derate on dBA Contour of the 747-400, Sea Level Standard Day 700,000 lbs. 36
Figure 44: Effect of 10% Derate on dBA Contour of the 747-400, Sea Level Standard Day 875,000 lbs. 36
Figure 45: Effect of 10% Derate on dBA Contour of the 747-400, Sea Level 104F Day 700,000 lbs. 36
Figure 46: Effect of 10% Derate on dBA Contour of the 747-400, Sea Level 104F Day 875,000 lbs. 37
Figure 47: Effect of 10% Derate on dBA Contour of the 747-400, 6000 Feet Standard Day 700,000 lbs. 37
Figure 48: Effect of 10% Derate on dBA Contour of the 747-400, 6000 Feet Standard Day 875,000 lbs. 37
Figure 49: Effect of 10% Derate on dBA Contour of the 747-400, 6000 Feet 104F Day 700,000 lbs. 37
Figure 50: Effect of 10% Derate on dBA Contour of the 747-400, 6000 Feet 104F Day 875,000 lbs. 37
Figure 51: Effect of 10% Derate on dBA Contour of the 737-300, Sea Level Standard Day 111,500 lbs. 38

Figure 52: Effect of 10% Derate on dBA Contour of the 737-300, Sea Level Standard Day 139,500 lbs. 38
Figure 53: Effect of 10% Derate on dBA Contour of the 737-300, Sea Level 104F Day 111,500 lbs. 38
Figure 54: Effect of 10% Derate on dBA Contour of the 737-300, Sea Level 104F Day 139,500 lbs. 38
Figure 55: Effect of 10% Derate on dBA Contour of the 737-300, 6000 Feet Standard Day 111,500 lbs. 38
Figure 56: Effect of 10% Derate on dBA Contour of the 737-300, 6000 Feet Standard Day 139,500 lbs. 38
Figure 57: Effect of 10% Derate on dBA Contour of the 737-300, 6000 Feet 104F Day 111,500 lbs. 38
Figure 58: Effect of 10% Derate on dBA Contour of the 737-300, 6000 Feet 104F Day 139,500 lbs. 38

List of Tables

Table 1: INM Spectral Class Assignments for Study Aircraft 10
Table 2 Details of Airplanes used in Study 32
Table 3 Comparison between Certification and INM EPNL Levels 32
Table 4 Effect of Thrust Split During Acceleration for 737-400 and 737-700 Aircraft 39

1 Summary

The FAA's Integrated Noise Model (INM) is widely used to estimate noise in the vicinity of airports. The model relies primarily on methods in SAE AIR-1845 "Procedure for the Calculation of Airplane Noise in the Vicinity of Airports" issued in 1986 (ref. 2). The Society of Automotive Engineering's A-21 Committee on Aircraft Noise is revising the methods to reflect more recent knowledge of acoustics, aircraft operations, and the composition of the commercial fleet.

This study addresses some of the assumptions made in selecting the representative INM aircraft for a given aircraft model. The INM database was built over time with airplane data developed using the manufacturers' judgment on how the aircraft were being used. Older aircraft submissions do not necessarily reflect present day operational reality. This study supports the development of standards by which the fleet data in the INM can be updated.

Use of flap configuration-specific noise data was studied as a method to evaluate low noise landing approach procedures. The results which include the effects of speed on the airframe noise component show noise levels to be higher at the highest speeds and lowest flap settings than would be predicted using the standard INM methods. However, data availability is limited for these "clean" configurations, and thus the conclusions should be treated with caution.

SAE AIR-1845 recommends a different atmospheric absorption standard than that used in noise certification and Boeing data typically uses the certification standard rather than that of SAE AIR-1845. The effect of this choice on dBA and SEL contours is addressed and in the process a method of adjustment using INM Spectral Classes is proposed. The effect of the change is small and relatively easy to apply to existing INM data.

A comparison of weather corrections to noise data using INM Spectral Classes is made with the Boeing integrated method. The INM spectral class method is shown to work well, capturing noise level differences due to weather especially at long distances. This was encouraging in view of the fact that previous work showed that this same method performed poorly in extrapolating from short to long ranges for constant weather conditions.

The INM was shown to be able to match noise certification data for a range of different aircraft when knowledge of the airplane state at the certification point is known.

Two studies conducted at the Denver International Airport are included in the appendices. These two studies follow earlier efforts of a similar nature performed in the year 2000. In each instance, predicted single event noise levels are compared with measurements made using the airport's noise monitoring system. The two studies adopted different approaches to modeling flight operations at the airport. Appendix A by Harris, Miller, Miller, and Hanson (HMMH) is a demonstration of what a typical INM modeler might do in modeling operations at the Denver Airport. Ground tracks were obtained from the airport's radar system. Aircraft trajectories and noise levels were predicted by several versions of the INM in the standard manner, utilizing information such as aircraft type and stage length to determine thrust and noise level. Appendix B by Wyle Laboratories is a demonstration of detailed modeling of individual events using 3-D radar data and Boeing aerodynamics data. This allows assessment of the INM acoustic propagation model and noise database, and does not rely on the INM assumptions regarding aircraft operational procedures.

When compared to the original, year 2000, results, it is apparent that changes made to the INM in terms of modeling processes and databases have resulted in improved agreement between predicted and measured noise levels. Reduced thrust takeoff (and climb) has an effect on the distribution of noise

predicted by the INM for single events, but this effect is small and was found to be of little importance in both studies.

2 Introduction

The INM calculates flight profiles using a simplified physics model from a database of engine performance and aerodynamics performance coefficients. These coefficients have been most recently developed from proprietary flight profile data for a broad range of atmospheric conditions, takeoff weights, and procedures. Previous work [1] was able to conclusively validate the FAA's regression method for calculating INM coefficients from Boeing flight profile data.

A remaining issue to be resolved is how well the theoretical profiles match actual airport operations of the fleet in service. There is no guidance on how to pick representative weights or flight procedures in the existing noise model guidance documents [2-4], the INM Database Report [5] or the INM 6.0 Users Guide [6]. This is important since the INM database was built up over time and individual airplanes were added applying operational assumptions from the time of certification. Now the fleet mix is different and load factors are higher.

The "Review of Integrated Noise Model (INM) Equations and Processes" [1] showed there were weaknesses in using Spectral Classes to extrapolate low altitude data to high altitudes using a method like the simplified procedure in Reference 2. This raised concerns as to whether Spectral Classes could be used successfully for adjustment of noise levels to different weather conditions. Two 757 variants that share the same Spectral Classes but are known to have different noise characteristics were used in a test of the method. The testing of weather correction was then expanded to include the 737-400, 737-700, 747-400, and 777-200. The Spectral Class method to correct for different weather effects at a full range of (constant) altitudes proved successful. This contrasts with the earlier study in which the method failed to correct for altitude effects at constant weather.

The INM database does not have data at idle power approach conditions, low flap settings, and high speeds necessary to model noise abatement approach procedures. An analysis was performed to examine the effect of flap setting and speed on noise contour areas. The most dramatic differences between the configuration based and standard INM occur near top of descent. This is where the airframe noise prediction is weakest due to reliance on limited data for such "clean" configurations.

A method was demonstrated to make adjustments of NPD data to different atmospheric absorption standards using spectral class spectra. The adjustments are small and result in contour area reduction of less than 2% for peak dBA and 1.5% for SEL across the seven study aircraft evaluated.

The INM was used to predict noise levels for the 717-200, 737-700, 747-400, and 777-200 aircraft when operating under certification conditions. The results of the predictions were compared with the actual noise certification data. The INM could reproduce the noise levels if the user was successful in matching the correct flight conditions.

Although the high altitude studies the use of reduced thrust was not an important factor in the noise result, the evidence from modeling the radar data from Denver showed it was being used whenever possible. The thrust levels for the 737 aircraft were lower than what is expected from the standard INM.

In the Denver Airport study by HMMH (Appendix A) eight progressive applications of the INM were run from INM 5.0 using the standard atmosphere through INM 6.2 Beta using reduced thrust, monthly average weather and new aerodynamic coefficients. HMMH was able to show improvements in the match to noise monitor data from the original study using INM 5.0.The major changes in the INM for those versions are the inclusion of adjustments to atmospheric absorption based on prevailing weather conditions (INM 6.0c) and aircraft directivity effects (INM 6.2 Beta).

No significant improvements in the results were seen due to the change from INM 5.0 to INM 5.1a. Both used the average annual weather at Denver Airport instead of Standard Atmosphere. Version 5.1a added 1dB to the noise behind takeoff.

Reduced thrust had a limited effect on the total contour area due to aircraft's limited ability to use thrust reduction at high altitude airports such as Denver.

In the Denver Airport study by Wyle Laboratories (Appendix B) flight profiles were matched to 3-D radar data. A similar pattern of improvement is seen with the change from INM 5.2a to INM 6.0c. Additional improvement is seen from INM 6.0c to INM 6.1 in the comparisons to measured data.

Improvements in the acoustic algorithms produced most of the improvement in the predictions. The remainder of the improvement resulting from updated noise tables for the 737 aircraft. The new noise tables have four approach noise power settings (increased from two) and six departure power settings (increased from four). The improved noise tables will be typical of future Boeing INM submissions.

Both studies of the Denver Airport data by Wyle Labs and HMMH showed improvements in the results from progressive versions of the INM. However, the flight paths typically flown were at lower altitude than those predicted by a standard INM procedure. The pilots typically traded reduced altitude for increased speed and thus operated the aircraft in a manner appropriate to the pressure altitude of the aircraft. The INM procedure steps operate on the basis of altitude above the runway rather than pressure altitude. As a result, profiles for high altitude airports will need adjustments to account for the difference in how the planes are operated relative to sea level.

3 Study Tasks

3.1 Standardized Modeling Assumptions

3.1.1 Standardizing Takeoff Weight vs. INM Stage Length

The INM relies on the approximate length of the mission for a given flight and the aircraft type as a proxy for takeoff gross weight. This is because the modeler has ready access to published flight schedules but does not likely have detailed knowledge of the airlines' operations engineering. Recently compiled survey data from airline operations indicate using 65% of the total payload capacity of the aircraft and the required fuel to make the required range should be used. Based on these results, the INM data for these aircraft and future submissions will be updated using the new 65% rule.

Survey data on the 737-300 fleet from Delta (DAL), United (UAL), and Lufthansa (DLH) match the 65% payload line well (Figure 1). The lower line (open squares) represents the present INM submission for the 737-300. The assumption used then and for the other airplanes in the following charts was 60% passenger load factor with no cargo.

Survey data on the 757-200 fleet from Delta (DAL), United (UAL), and Condor (CDF) match the 65% payload line well also (Figure 2). The Condor data is of note since they are known to fly at very high passenger loads. The Condor data is not far from the assumed standard loading. The lower black line (open squares) represents the present INM submission for the 757-200 (Pratt).

Survey data on the 777-200 fleet from Delta (DAL), United (UAL), and British Airways (BAB) match the 65% payload line as well (Figure 3). KLM represents the version recently delivered for this airplane. The expectation is the load factors for newer airplanes will not increase beyond the present assumed levels. The lower black line (open squares) represents the present INM submission for the 777-200 (Pratt).

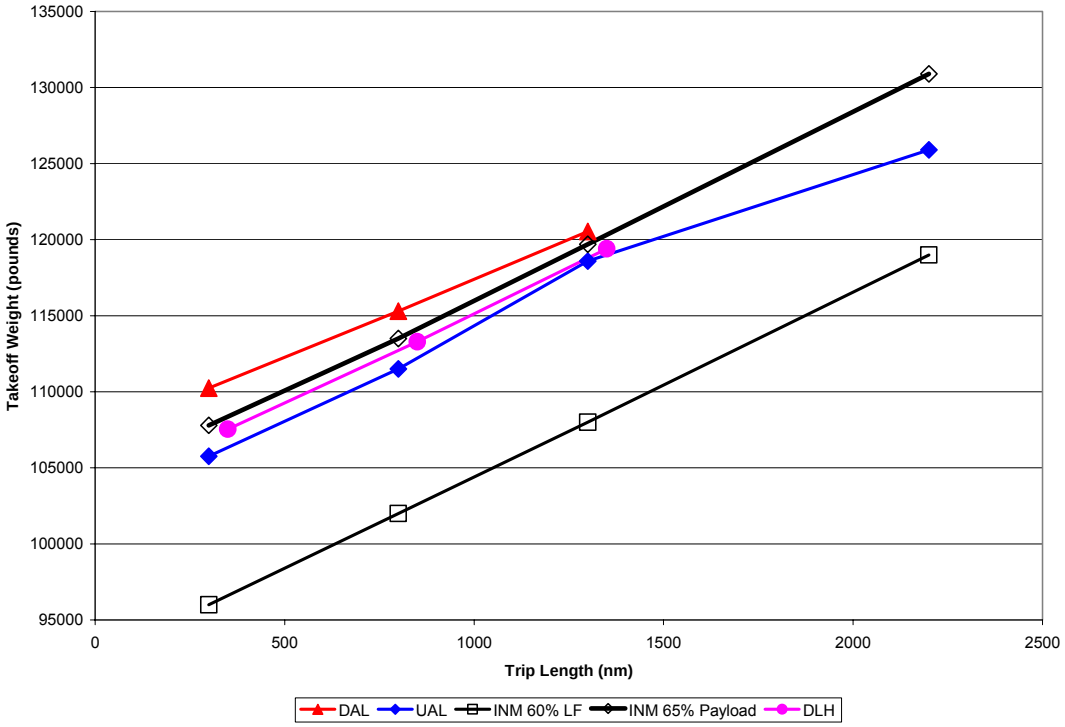


Figure 1: Takeoff Weights vs. Trip Length for 737-300s

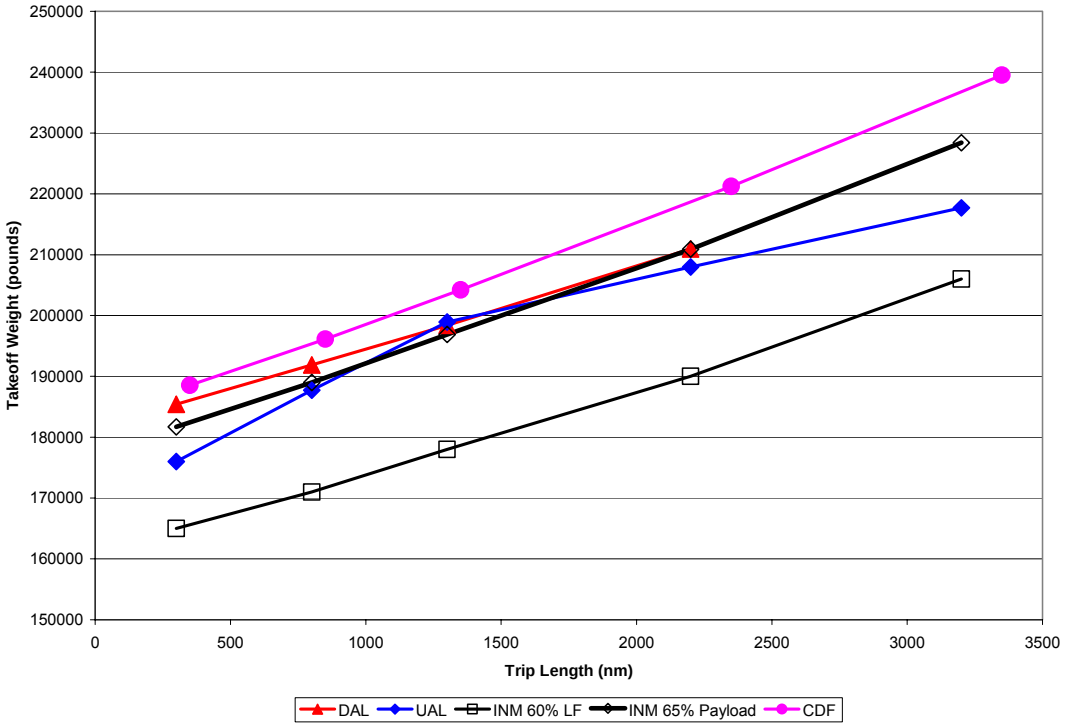


Figure 2: Takeoff Weights vs. Trip Length for 757-200s

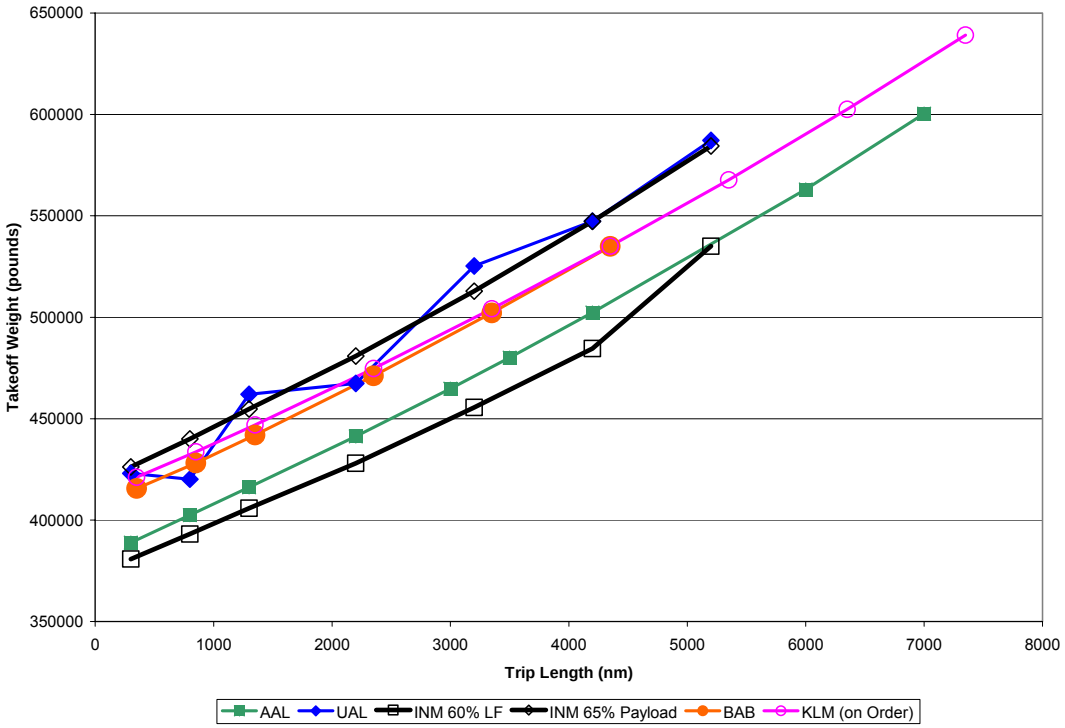


Figure 3: Takeoff Weights vs. Trip Length for 777-200s

3.1.2 Modification of NPD Data to Different Atmospheric Absorption Standard

Noise data provided to the INM for Boeing aircraft are derived from noise certification data that comply with FAR36 requirements. Full one-third octave band sound pressure level time histories are used to generate the NPD data using the SAE AIR-1845 "integrated" method. A uniform 77degF, 70% relative humidity atmosphere and the corresponding SAE ARP-866A [8] absorption coefficients are assumed.

SAE AIR-1845 specifies different atmospheric absorption coefficients than those used in the calculation of aircraft certification NPDs. The SAE AIR-1845 absorption coefficients were recommended by the ICAO Committee on Aircraft Noise (CAN) in 1983 [7] and are based on an average of values determined during aircraft noise certification tests in Europe and the USA. Because these attenuation rates are arithmetic averages, the complete set cannot be associated with a single reference atmosphere (i.e. with specific temperature and relative humidity).

Boeing certification processes allow for calculating noise for different weather conditions but not for arbitrary absorption coefficients that are not tied to some combination of temperature and relative humidity. Thus it is not possible to compute new NPDs for the "SAE AIR-1845 atmosphere" using the integrated method. Instead, a calculation based on the SAE AIR-1845 simplified method for extending noise data to higher altitudes was used to adjust Boeing NPD data to the SAE AIR-1845 absorption. This simplified method utilizes a single spectrum to represent a complete flyover. The INM spectral class spectrum was used in the following procedure. The spectral class spectrum is for an observer at 1000 feet. This spectrum is propagated back to a distance of one foot from a notional point source, thus removing effects of distance and the absorption present in a 77/70 atmosphere. This source spectrum is then propagated to all observer distances using the both the 77/70 and SAE AIR-1845 absorption coefficients. The differences in A-weighted sound pressure levels at each observer location are then applied to the original NPD's, thus creating new NPD's corrected to the SAE AIR-1845 absorption.

The INM spectral classes assigned to the study airplanes are shown in Table 1. The approach spectral classes were not evaluated in this study, but are shown for completeness.

Table 1: INM Spectral Class Assignments for Study Aircraft

INM Aircraft	INM NPD Name	Spectral Classes		Change in Takeoff Contours	
		Approach	Takeoff	65 dB SEL	65 dB LAMAX
737-300/500	CFM563	202	102	-0.0%	-0.0%
737-700	CF567B	202	104	-1.1%	-1.6%
747-400	PW4056	207	107	-1.5%	-1.9%
757-200	PW2037	203	103	-1.0%	-1.5%
777-200	GE9076	205	105	-0.0%	-0.8%
MD-83	2JT8D2	204	104	-1.4%	-1.2%

The changes in contour areas which result from the adjustment of the NPD's to the SAE AIR-1845 atmosphere are presented in Table 1. The changes are small for the aircraft chosen for this study. The figures below illustrate the largest changes in contour area from Table 1.

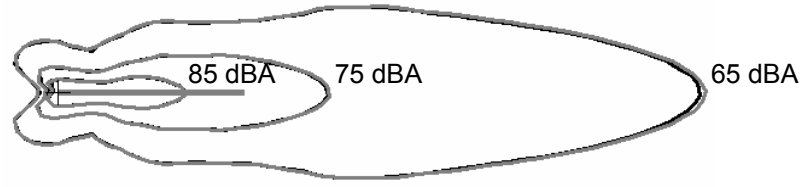


Figure 4: dBA Contours Adjusted (Black) and Unadjusted (Grey) to SAE AIR-1845 for the 737-700

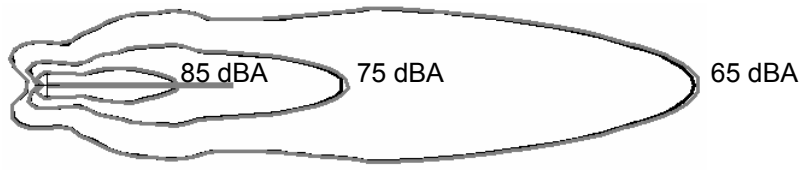


Figure 5: dBA Contours Adjusted (Black) and Unadjusted (Grey) to SAE AIR-1845 for the 757-200

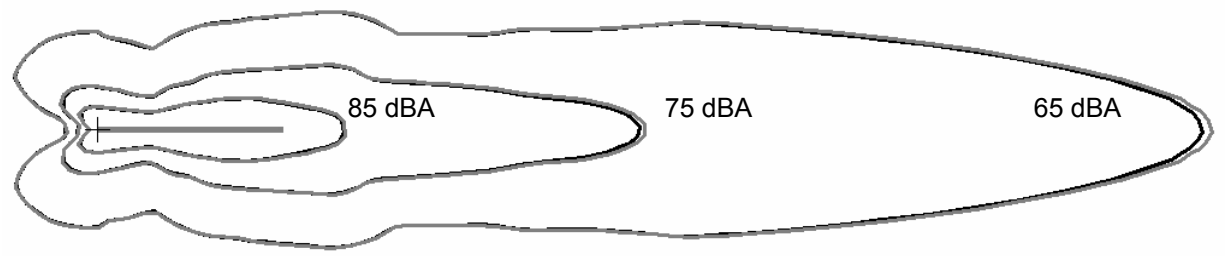


Figure 6: dBA Contours Adjusted (Black) and Unadjusted (Grey) to CAN7 SAE AIR-1845 for the 747-400

3.1.3 Adjustment of NPD Data to Account for Different Weather Conditions

A comparison of the Boeing integrated method to the INM spectral class method was made for both the Rolls-Royce and Pratt & Whitney powered 757 aircraft. Figure 7 shows the absorption coefficients for different weather using SAE ARP-866A as a function of the 1/3 octave band center frequency for the weather conditions used in the study. The temperature and relative humidity combinations used are shown in the figure and include the 77/70 noise certification condition. Also plotted is the CAN7 atmospheric absorption used in SAE AIR-1845.

The 77 degrees F 70% relative humidity condition results in the lowest absorption values for frequencies above 4000 Hz but the 59 degrees F condition has the lowest absorptions below 4000 Hz. For short propagation distances the high frequency absorption is most important, but as distances increase, the mid frequency range becomes more important. The `Dry Day' 77 degrees F 30% relative humidity and the SAE AIR-1845 atmosphere are relatively high absorption conditions. How these relationships affect weather corrections at short and long distances will be evident in the following figures.

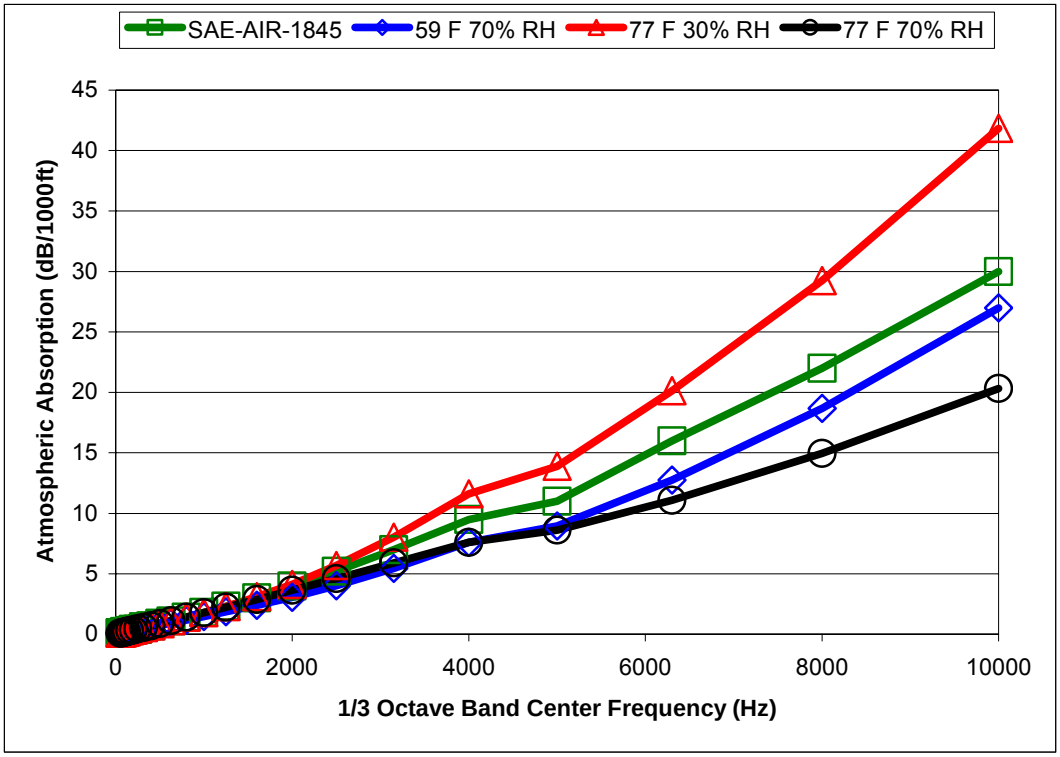


Figure 7: Atmospheric Absorptions Used in NPD Adjustment Comparisons

The integrated (full 1/3 octave band time history) method was applied to level flyovers at three power settings (approach power, cutback power and full power), all flown at 160KTAS with a take-off flap configuration. Two engine variants (RR535E4 and PW 2037) of a Boeing 757-200 are included in this analysis. The baseline atmospheric condition is 77/70% and the two other conditions are “dry day” (77/30%) and “”cool day” (59/70%). Figure 8 shows the difference between the SEL values predicted for dry day conditions and the baseline, and clearly indicates the additional absorption expected from the drier conditions. The thrust settings (9259 lbs, 25618 lbs, and 34586 lbs) are indicated in the legend. Also shown (open square symbol) is the result of applying the simplified method using spectral class 103 to the same baseline and “dry day” conditions. The simplified method shows reasonable agreement with the integrated method. The figure also shows that the CAN7 (SAE AIR-1845) atmosphere gives results similar to the dry day ones, a reflection of their similar absorption coefficients at the mid and low frequencies. Similar conclusions are evident from Figure 9 which shows results for LAmax for the same set of conditions. There is more variability between thrust conditions for LAmax than SEL which is simply due to variations in peak spectra which are smoothed out by the integration process inherent in the SEL calculation.

Differences between cool day (59/70%) and the baseline (77/70%) atmosphere are presented in Figures 10 and 11, also for the Rolls Royce engine. These cooler conditions result in less absorption than the baseline. The results for SEL in Figure 10 indicate small differences due to thrust settings. The simplified (spectral class) method shows good agreement with the integrated method. As before, more variability is evident for LAmax, Figure 11.

Figures 12-15 show the results for the Pratt and Whitney engine variant. The same general trends are observed, but there is generally more variability with thrust setting than was present for the Rolls Royce engine. At the longest distances the effects of different weather conditions show little dependence on thrust setting and indicate that the spectral class method provides a good approximation to the integrated method.

A comparison of the Boeing integrated method to the INM spectral class method was run for the 737-400 (CFM56-3), 737-700 (CFM56-7), 747-400 (PW4056), and 777-200 (GE90) in the remaining figures in the section.

Similarly those figures show the difference between the predicted Peak dBA and SEL at 77 degrees F 70% relative humidity and weather that is either cooler (59 degrees F) or dryer (30% RH) for each altitude (propagation distance) used in the standard INM NPD datasets. Each chart will show the resulting change using the Boeing integrated procedure for three power settings (approach power, cutback power and full power). All three power settings were `flown' level at 160 KTAS in the takeoff configuration. Also shown is the predicted weather effect on the spectral class spectrum associated with both airplanes for takeoff.

The weather effects for long distances line up well for both the `Dry Day' and `Cool Day' data sampled below. This suggests using spectral classes to adjust NPD data for weather effects at long range has little risk even if the same spectral class method is likely not a good way to extrapolate low altitude data to high altitude using the simplified adjustment procedure in SAE AIR-1845.

For the low altitudes where high frequency absorption is more important there is more variation. This is also the region where peculiarities of the particular engine and power state come into play. But beyond 2000 feet these effects diminish long before the noise source would be expected to devolve to a pure jet spectrum.

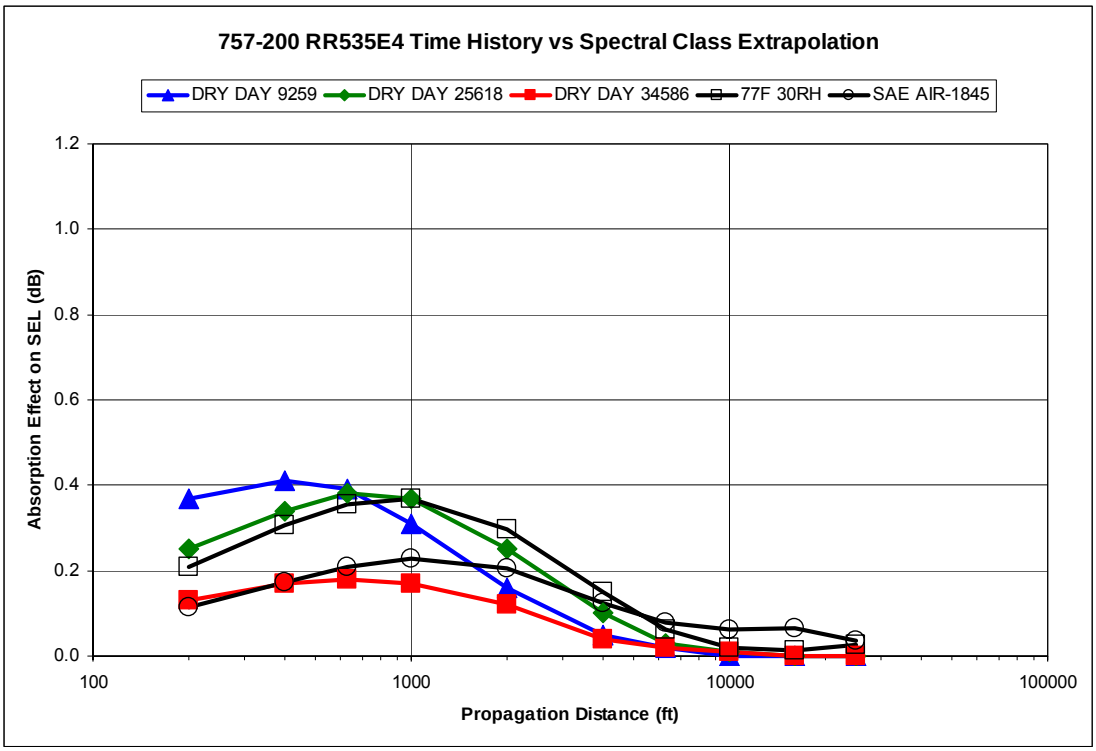


Figure 8: Difference in SEL Calculated between Baseline and Dry Day (757-200RR)

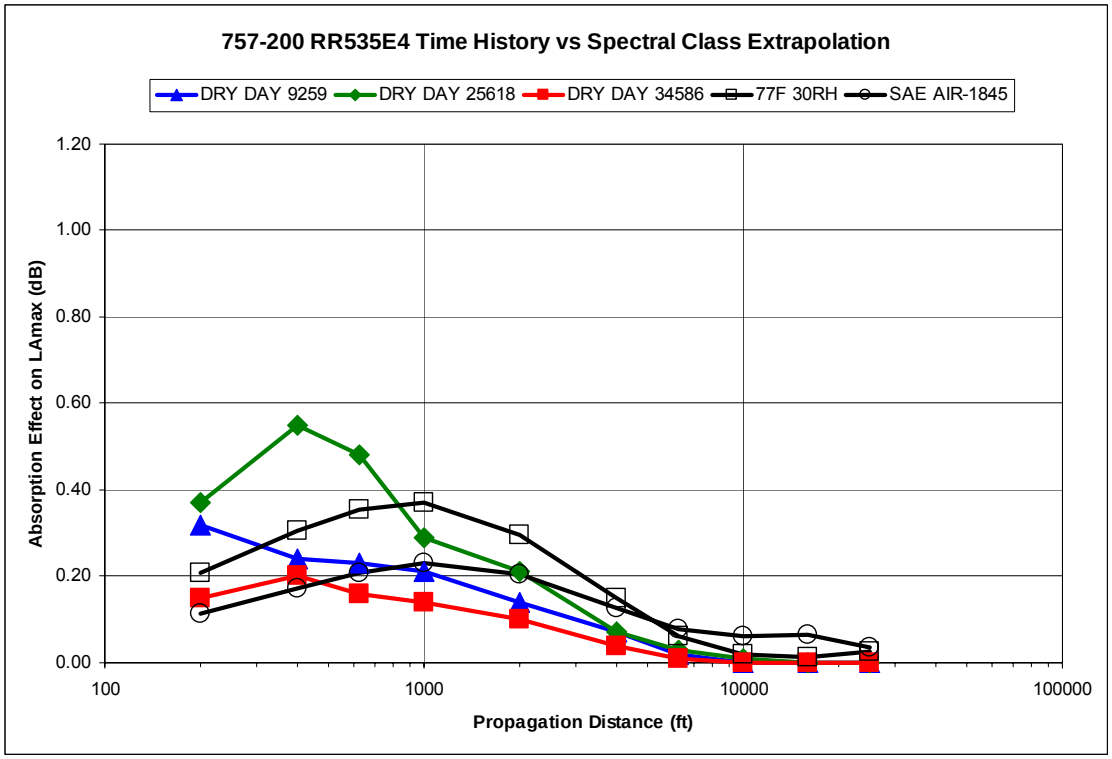


Figure 9: Difference in LAmax Calculated between Baseline and Dry Day (757-200RR)

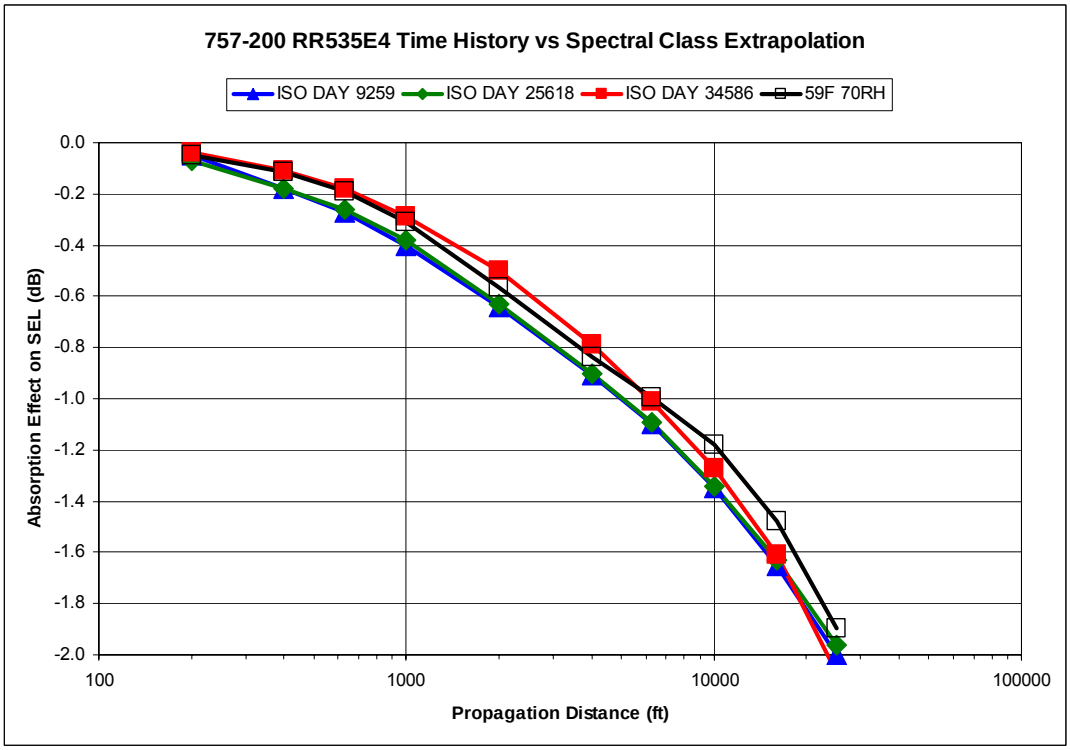


Figure 10: Difference in SEL Calculated between Baseline and Cool Day (757-200RR)

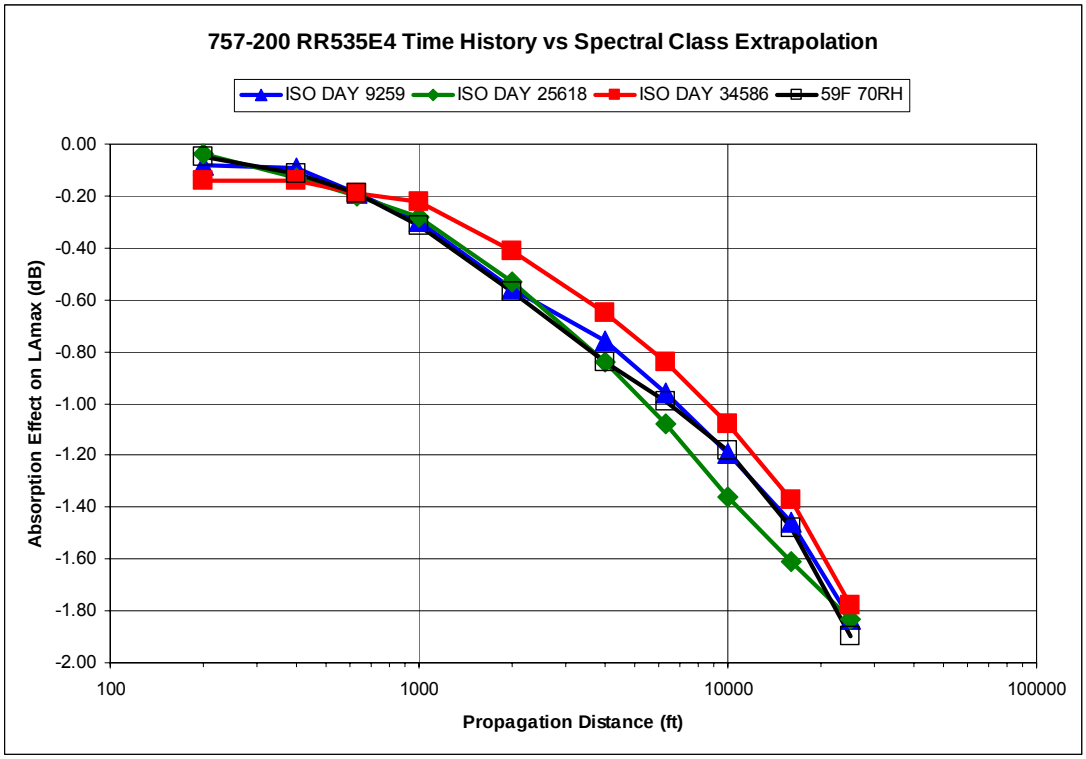


Figure 11: Difference in LAmax Calculated between Baseline and Cool Day (757-200RR)

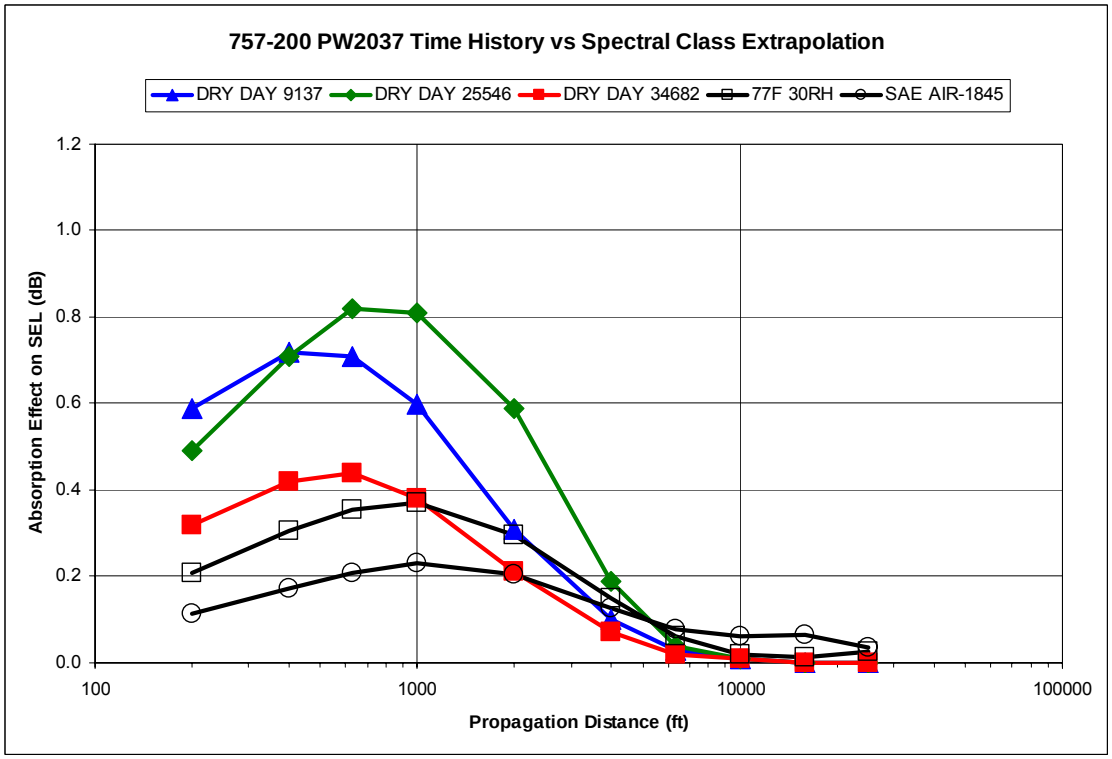


Figure 12: Difference in SEL Calculated between Baseline and Dry Day (757-200PW)

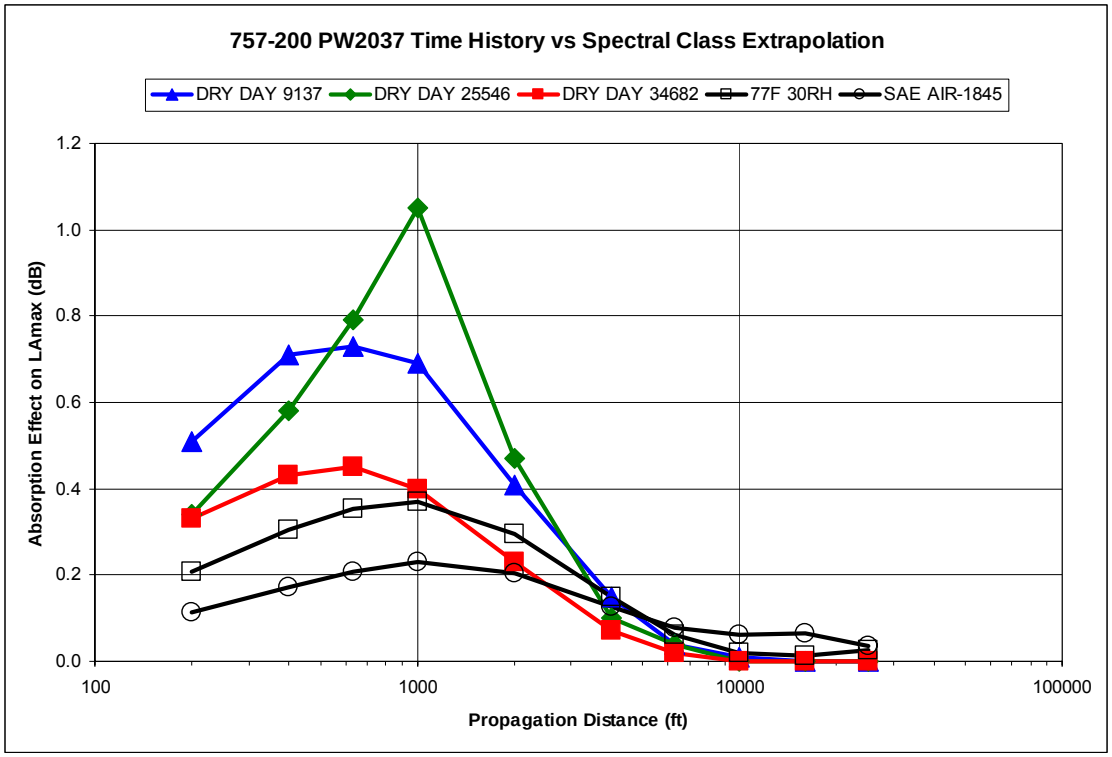


Figure 13: Difference in LAmax Calculated between Baseline and Dry Day (757-200PW)

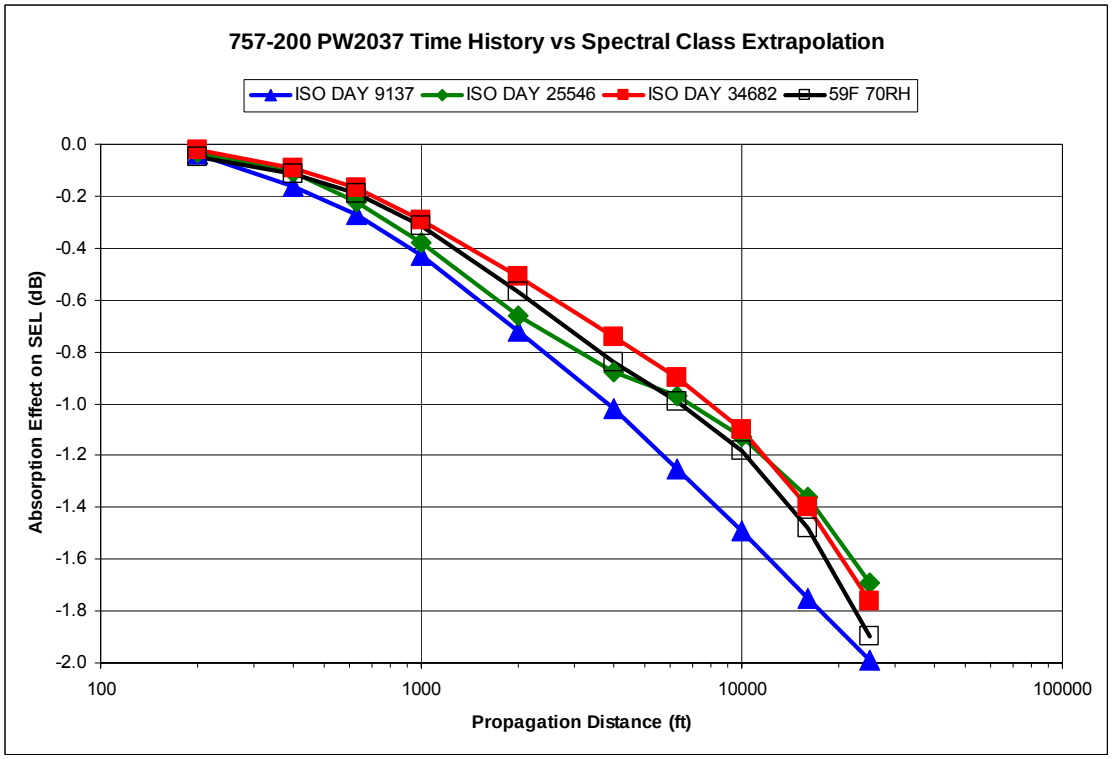


Figure 14: Difference in SEL Calculated between Baseline and Cool Day (757-200PW)

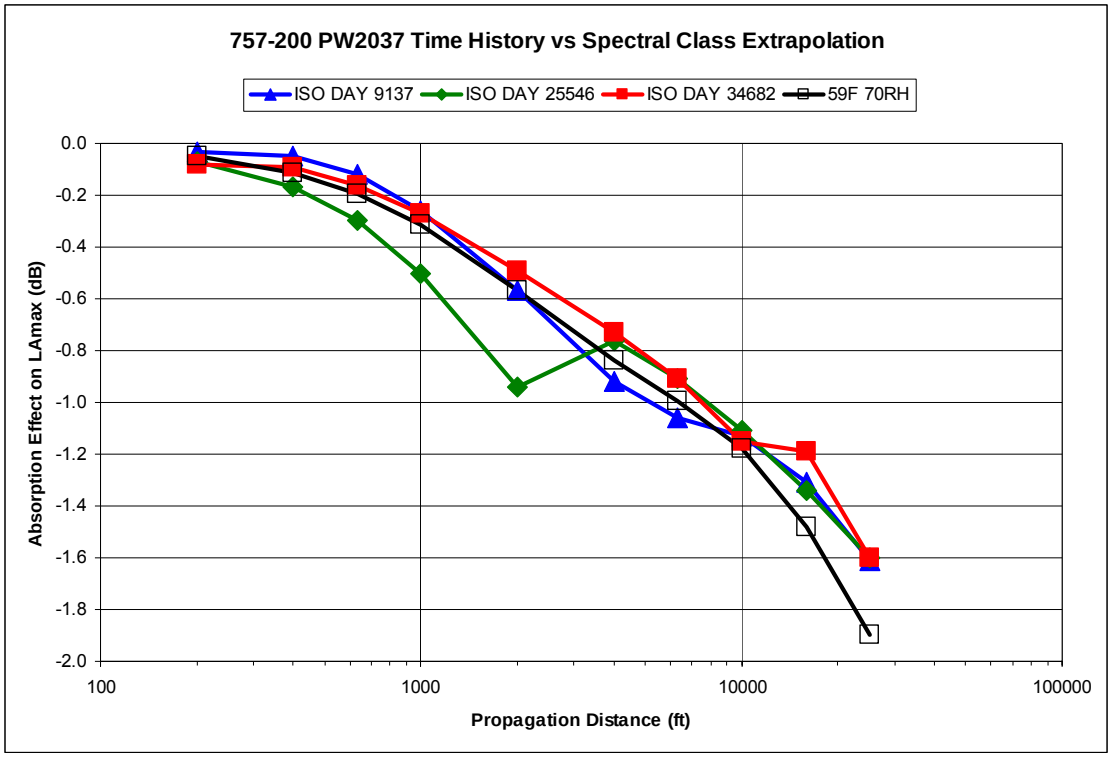


Figure 15: Difference in LAmax Calculated between Baseline and Dry Day (757-200PW)

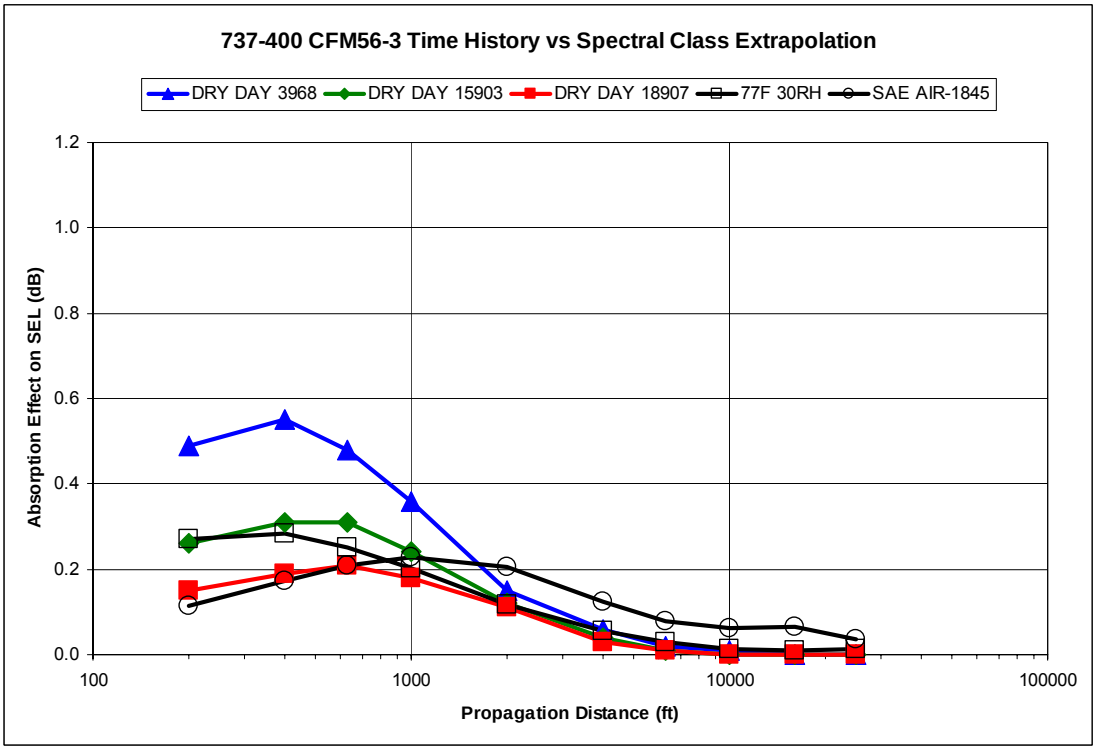


Figure 16: Difference in SEL Calculated between Baseline and Dry Day (737-400)

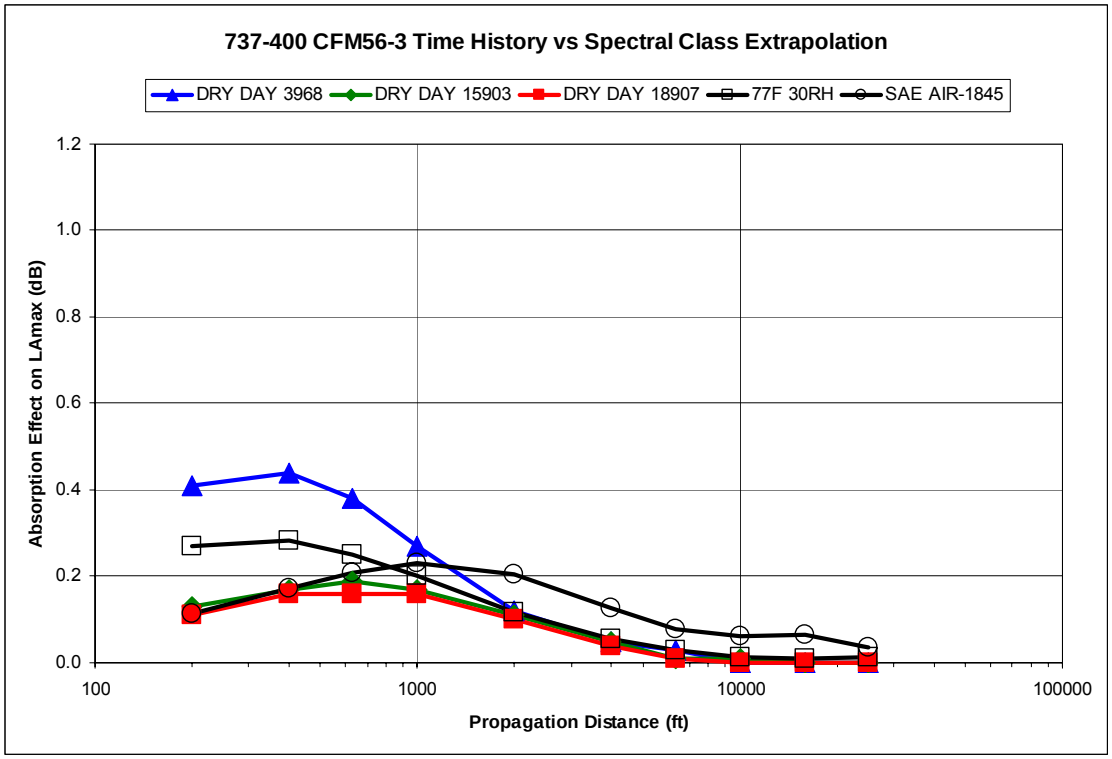


Figure 17: Difference in LAmax Calculated between Baseline and Dry Day (737-400)

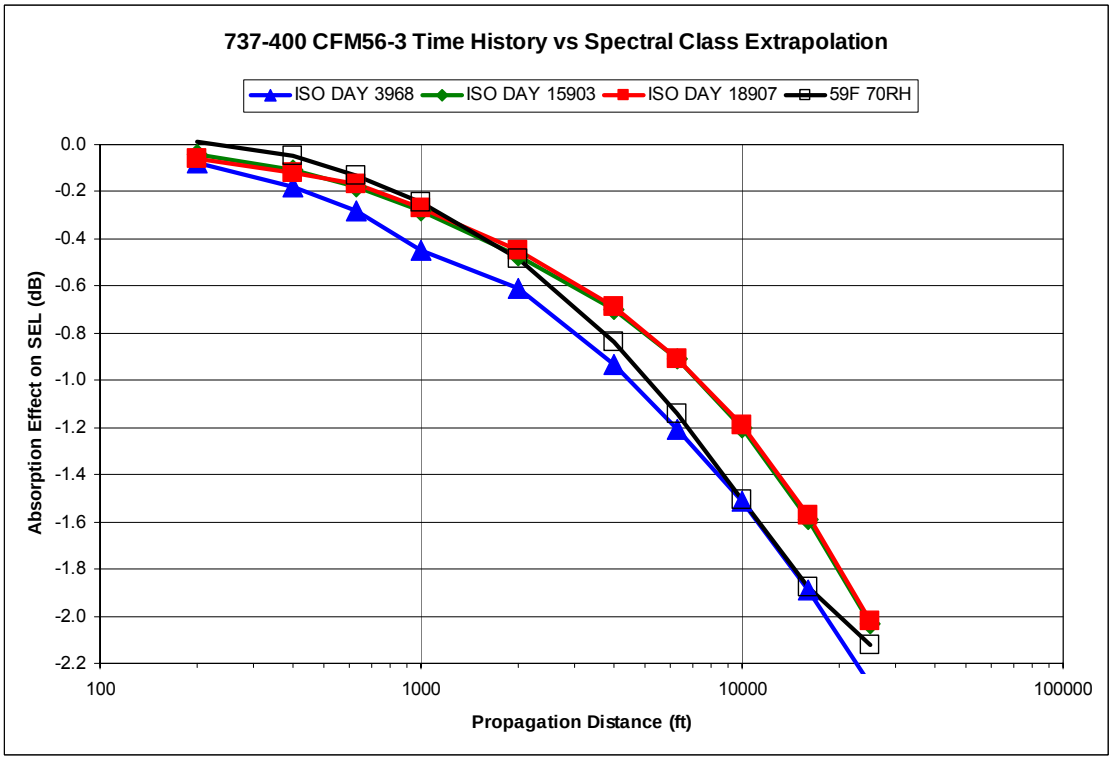


Figure 18: Difference in SEL Calculated between Baseline and Cool Day (737-400)

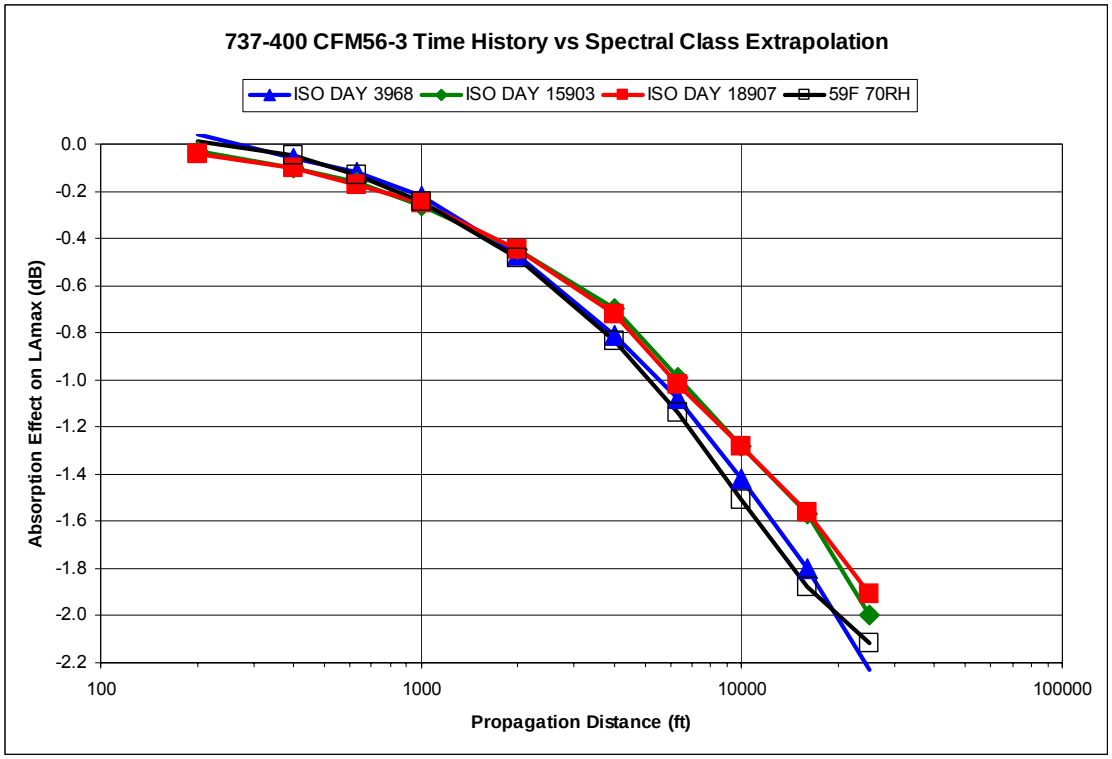


Figure 19: Difference in LAmax Calculated between Baseline and Cool Day (737-400)

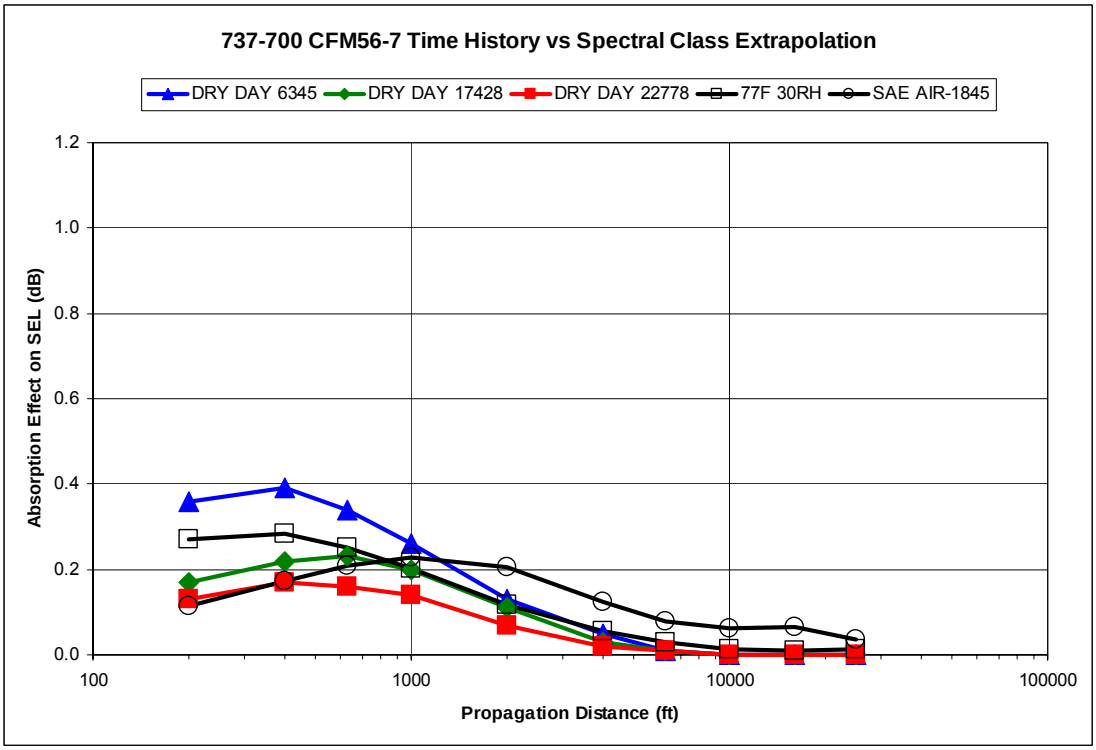


Figure 20: Difference in SEL Calculated between Baseline and Dry Day (737-700)

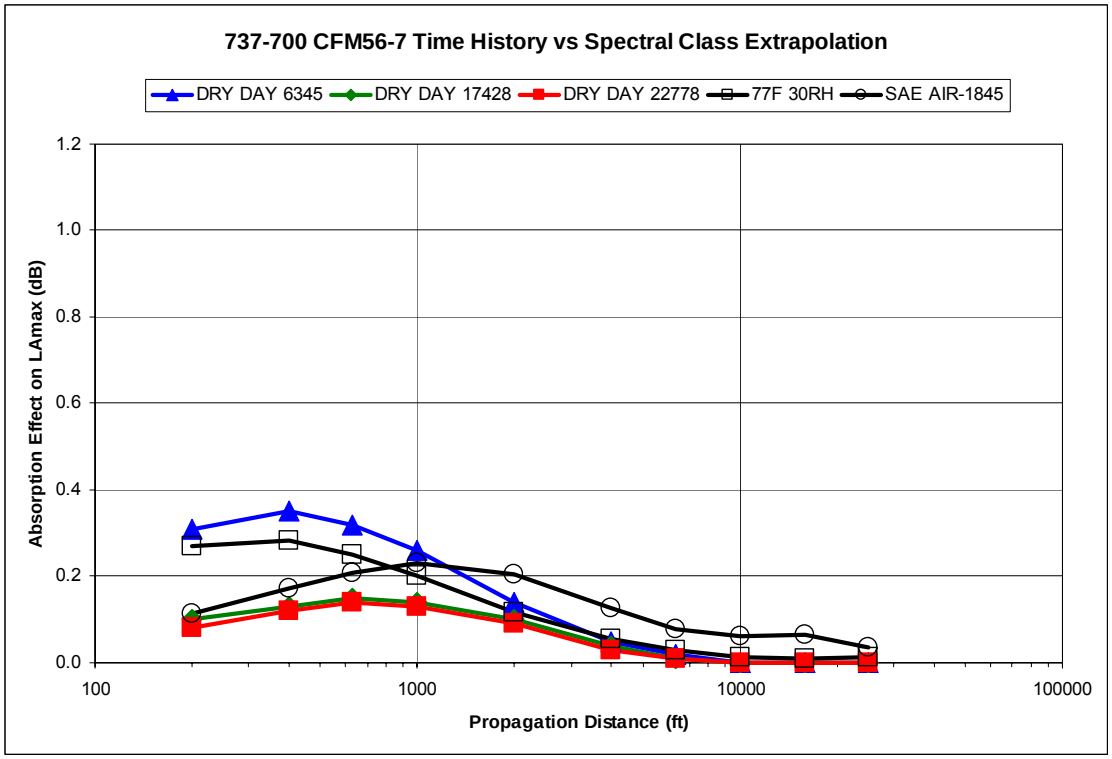


Figure 21: Difference in LAmax Calculated between Baseline and Dry Day (737-700)

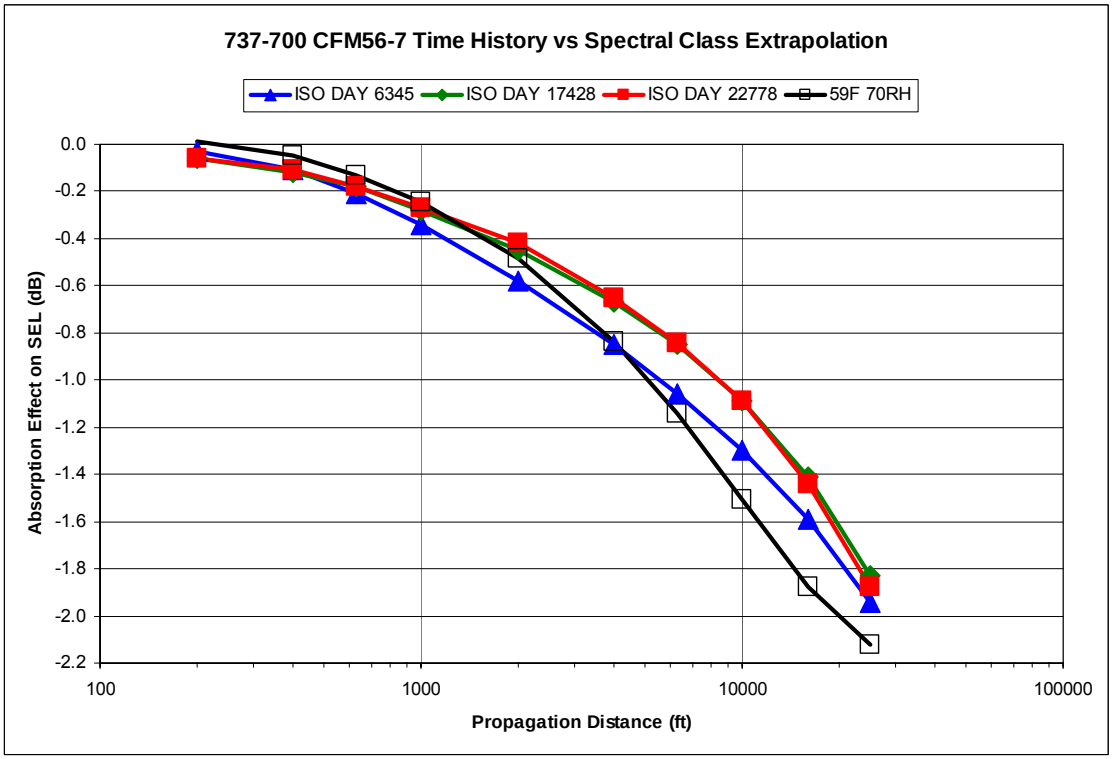


Figure 22: Difference in SEL Calculated between Baseline and Cool Day (737-700)

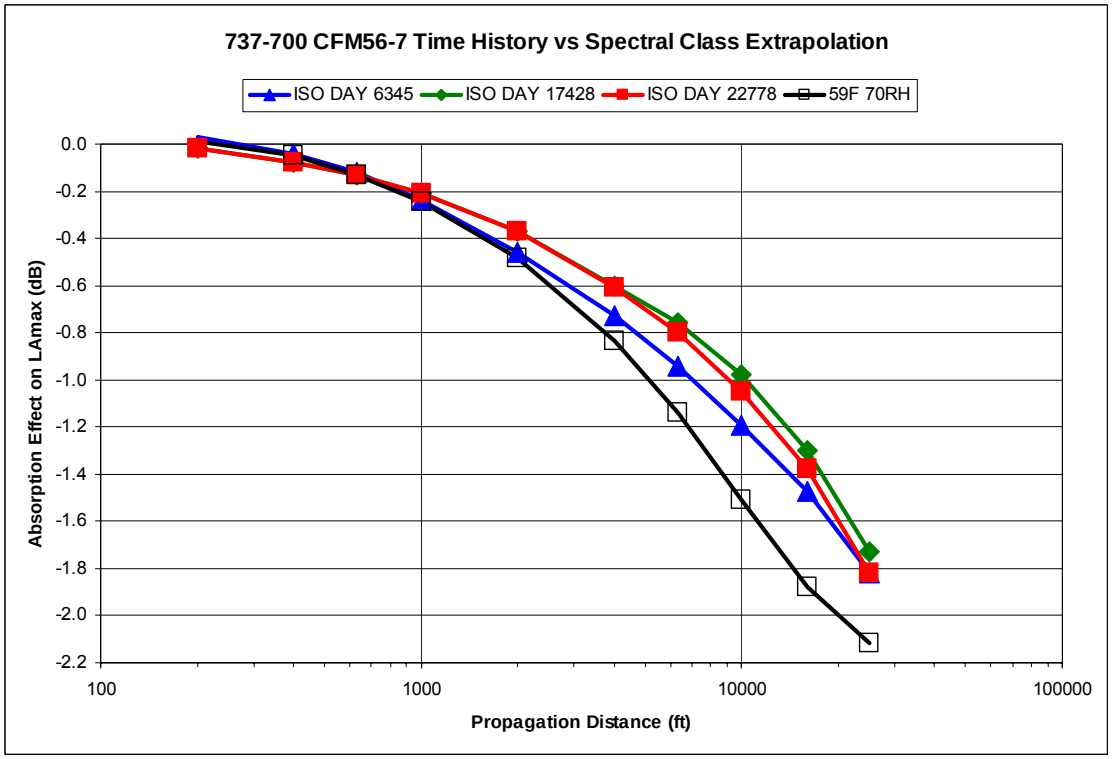


Figure 23: Difference in LAmax Calculated between Baseline and Cool Day (737-700)

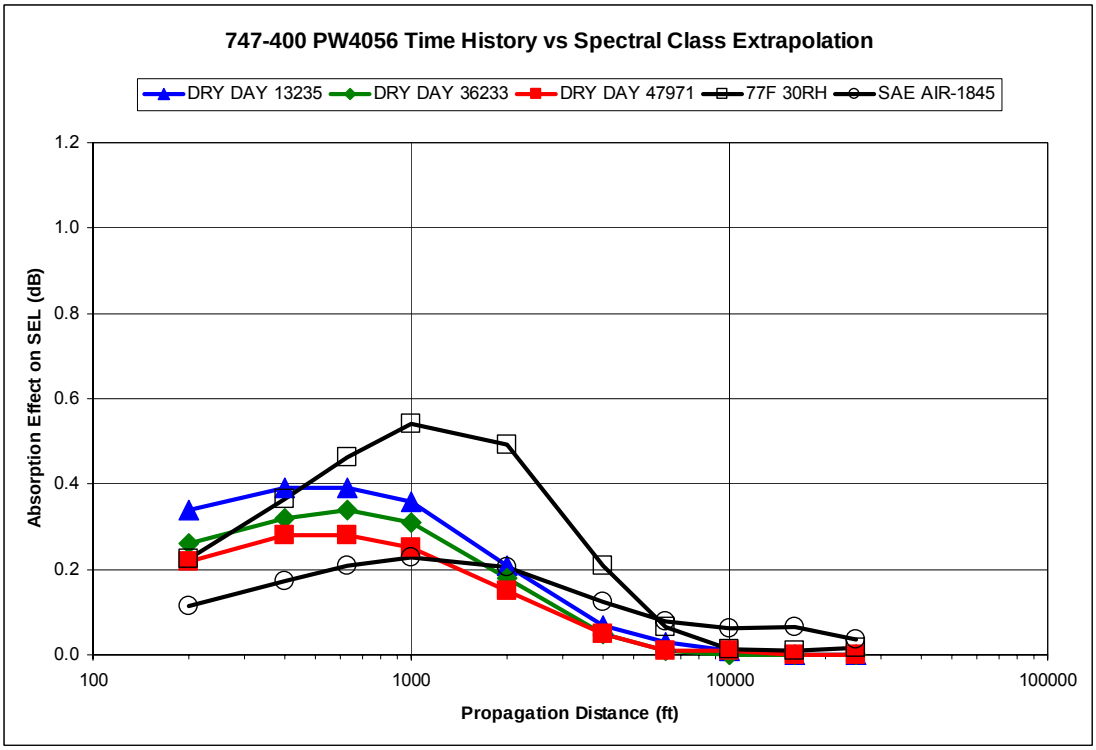


Figure 24: Difference in SEL Calculated between Baseline and Dry Day (747-400)

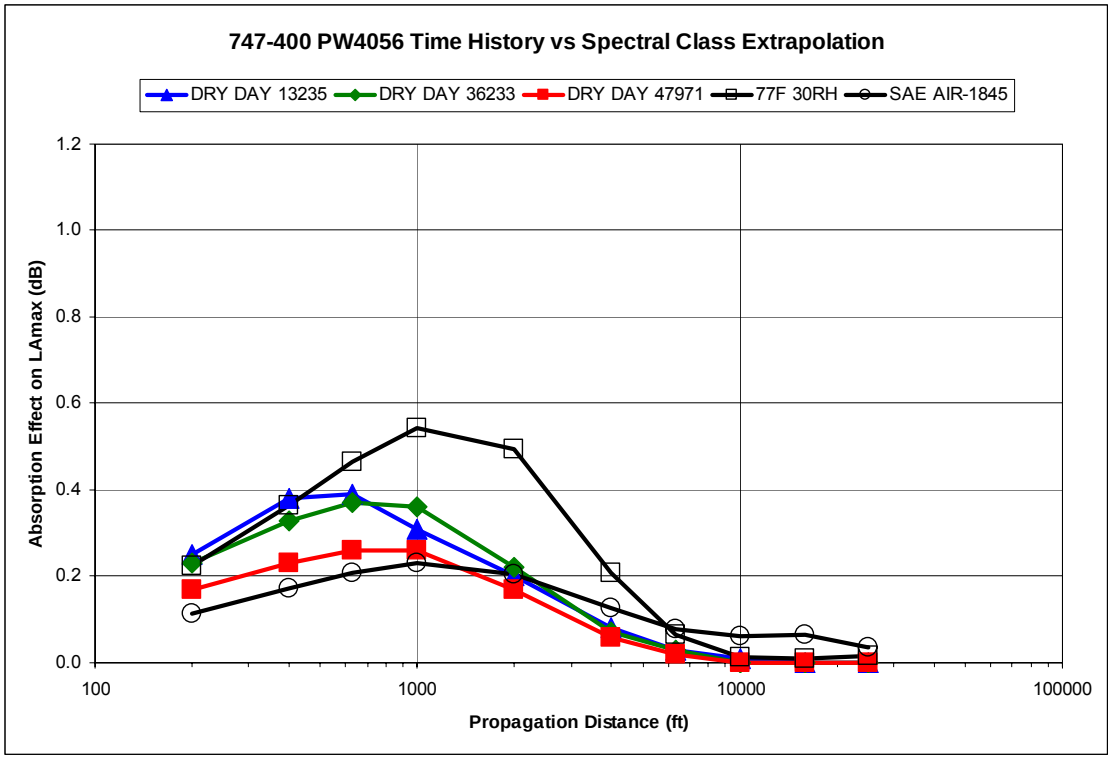


Figure 25: Difference in LAmax Calculated between Baseline and Dry Day (747-400)

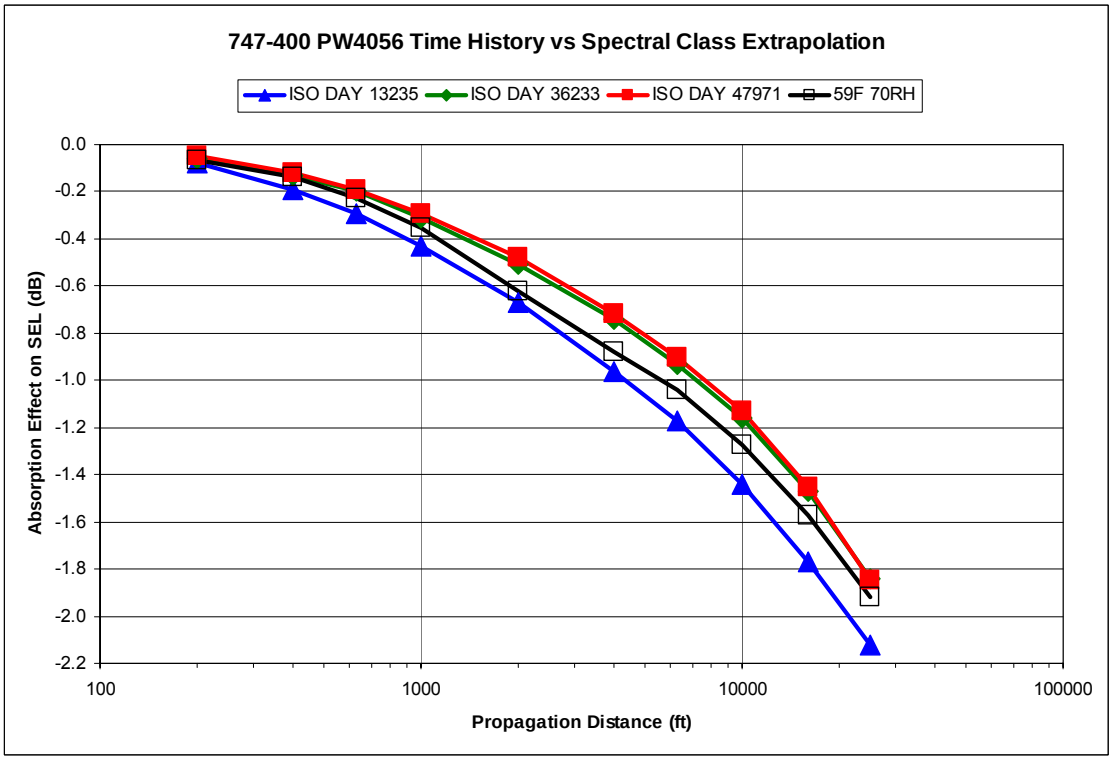


Figure 26: Difference in SEL Calculated between Baseline and Cool Day (747-400)

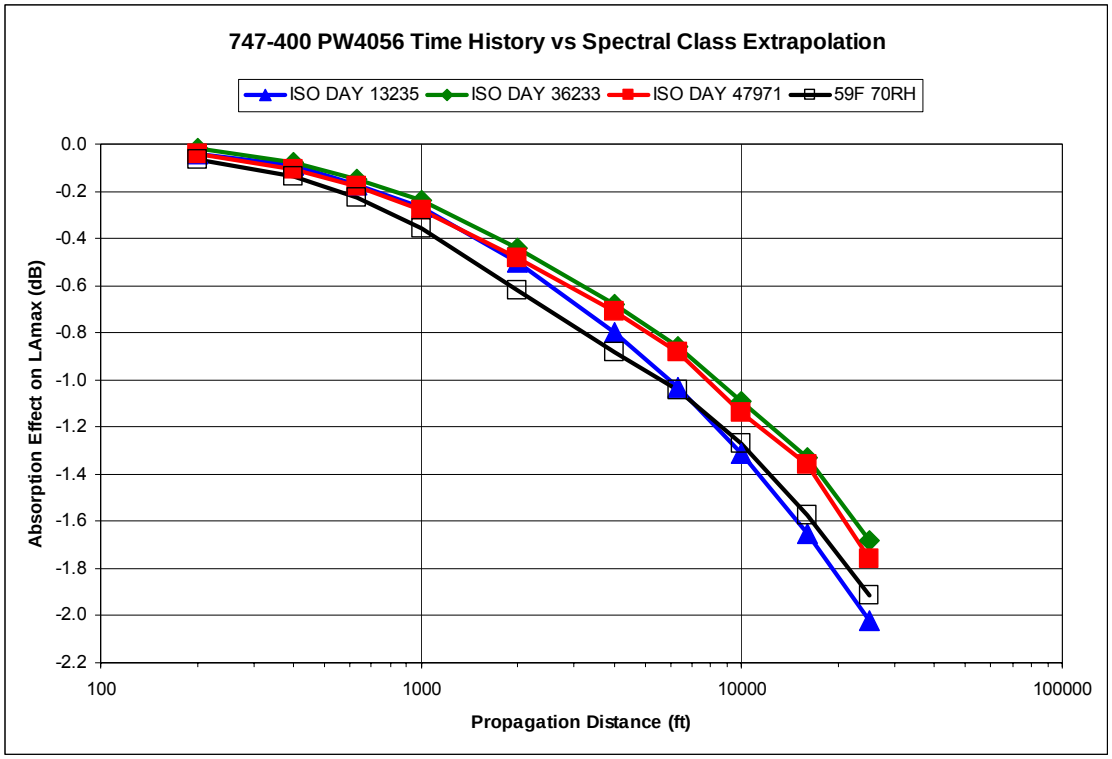


Figure 27: Difference in LAmax Calculated between Baseline and Cool Day (747-400)

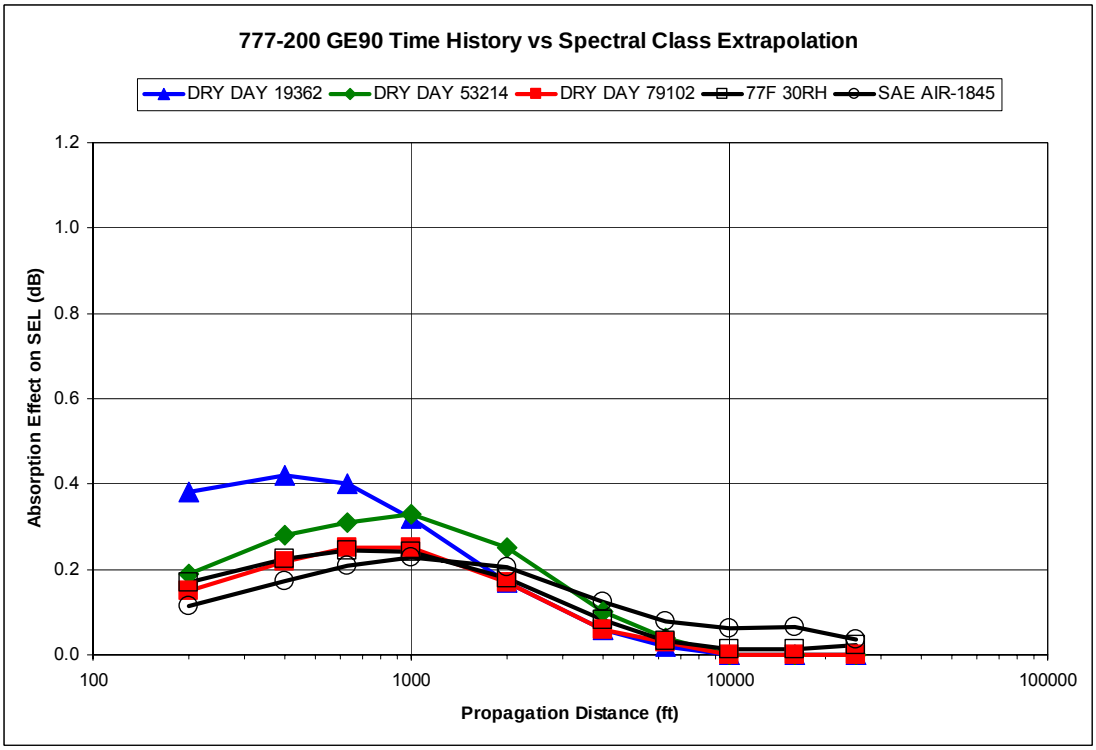


Figure 28: Difference in SEL Calculated between Baseline and Dry Day (777-200)

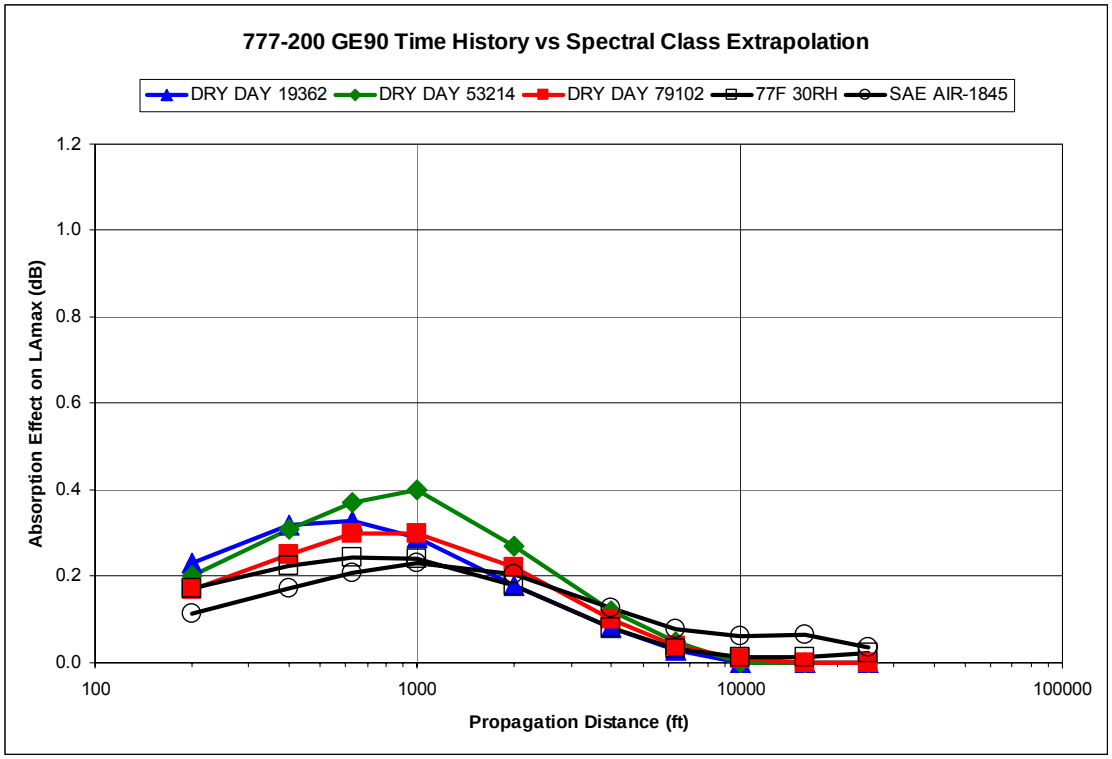


Figure 29: Difference in LAmax Calculated between Baseline and Dry Day (777-200)

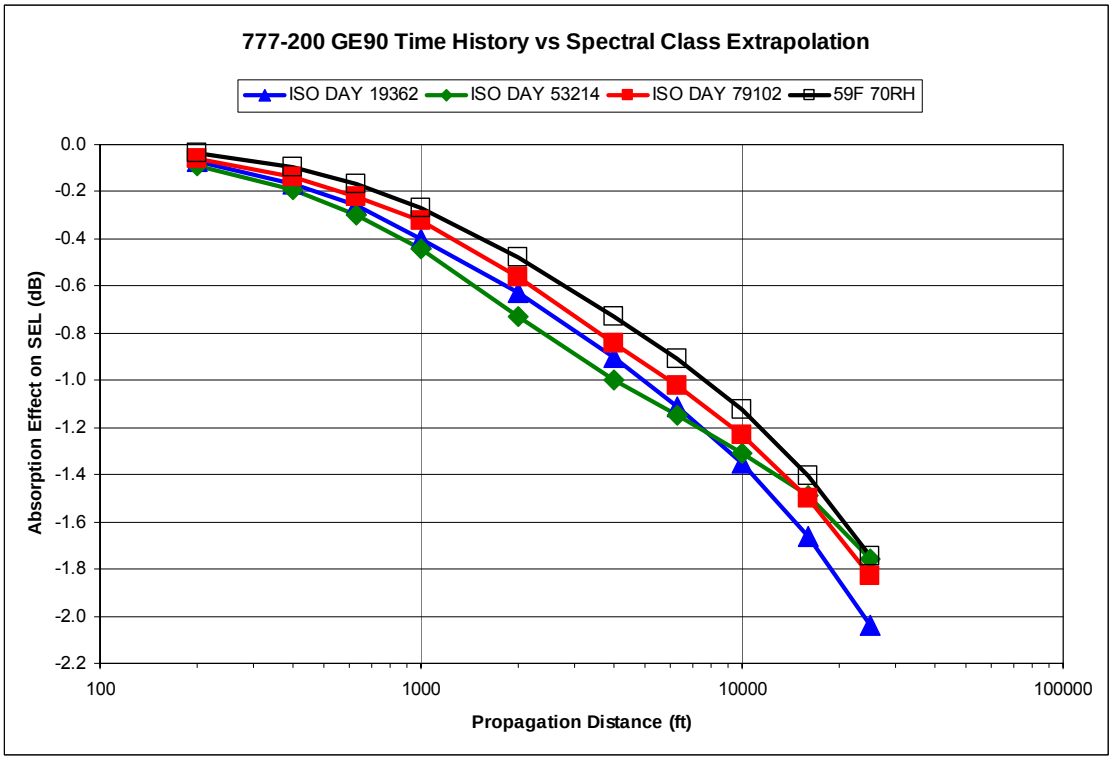


Figure 30: Difference in SEL Calculated between Baseline and Cool Day (777-200)

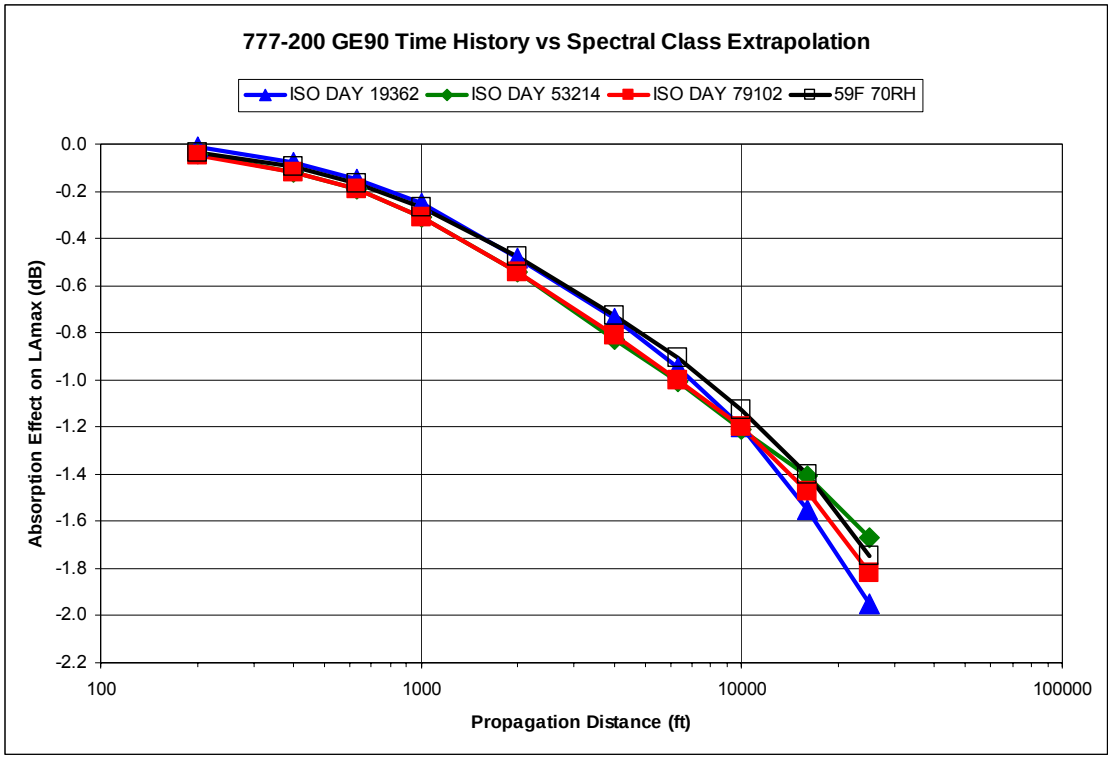


Figure 31: Difference in LAmax Calculated between Baseline and Cool Day (777-200)

3.2 Approach and Landing Noise Modeling

3.2.1 Effect of Aircraft Configuration on Approach Noise

The INM noise model uses a single approach configuration (gear down, full flaps) as representative of all approach procedures. This represents a good assumption for estimating noise levels at locations close to touchdown. However, at greater distances (e.g. gear up, less flap deflection) airframe noise will be different and will be dependent on aircraft speed. Thus, the FAA developed an experimental version of the INM with expanded noise tables allowing for speed and configuration changes to be accounted in the noise analysis.

Boeing has developed custom noise databases for this version of the INM (7.0 Proto2). These databases use a combination of flight test data and a prototype analytical model based on wind tunnel data to cover as many unique flap/gear configurations as possible. The available data is incomplete. For the clean (gear up, zero flap deflection) configuration, airframe noise was assumed to be 3dB lower than that of the next higher flap in the database. The guesswork applied to the noise modeling for the clean wing will be shown to be the primary weakness in the modeling presented here.

For the 737-700/800 and the 777-200/300 flight test airframe noise data was available for four flap states, the takeoff flap, an intermediate flap, the lower landing flap and the full landing flap. For the 737-300 and the 757-200/300 only the takeoff and full landing flap were available and other flap states had to be estimated using the prototype analytical model. In all cases, the airframe noise is adjusted for airspeed using the 5^{th} power rule up to the highest speed calculated (220kts). The lowest speed in each database is the approach speed for the particular aircraft. Databases were developed for the 737-300, 737-700/800, 757-200/300, and the 777-300. Results are shown for three of the four airplanes.

The contour plot in Figure 32 is for a standard approach (3000' level segment) of the 737-800 at 90% max landing weight. The peak dBA contours for levels 55dBA up to 65dBA do show the effects of speed and configuration. The standard INM method (black) is conservative compared to the experimental version (grey) for this example. The contours are scaled and positioned to line up with the scale of distance to threshold in the plot of aerodynamics performance parameters below. Flaps extension does not begin until 10 nm in the figure.

The contour plot in Figure 33 is for a two-segment CDA approach of the 737-800 at 90% max landing weight. The initial glide slope is 1.5 degrees before meeting the standard 3.0 degree glide slope. The peak dBA contours for 55dBA up to 65dBA do show some effect of speed and configuration. The standard version of the INM (black) is conservative compared to the experimental version (grey) for this example as well. Flap extension begins earlier at 14 nm out, but the overall contours are smaller than those of figure 32.

The contour plot in Figure 34 is for a standard approach (3000' level segment) of the 777-200 at 90% max landing weight. The peak dBA contours for levels 55dBA and 60dBA do show the effects of speed and configuration. The configuration based NPDs predict higher noise levels for the clean configuration. This is probably due to the fact that the flap setting used to estimate the noise of the clean configuration was Flaps 5, probably resulting in an overestimate of the noise for the clean configuration. This is in contrast to Flaps 1 being available for the 737-800. For the 777 profile shown flap extension begins at 10 nm.

The contour plot in Figure 35 is for a standard approach (3000' level segment) of the 757-300 at 90% max landing weight. The peak dBA contours for levels 55dBA and 60dBA show large effects of speed and configuration. The configuration based NPDs predict much higher noise for the clean configuration than the standard INM. This is probably due to the fact that the flap setting used to estimate the noise of the clean configuration was Flaps 5 instead of Flaps 1 for the 737-800 but the effect seems to be much greater than observed for the 777-200. For the 757 profile shown flap extension begins at 10.5 nm.

The contour plot in Figure 36 is for a two-segment CDA approach of the 757-300 at 90% max landing weight. The initial glide slope is 1.5 degrees before meeting the standard 3.0 degree glide slope. The clean configuration noise levels seem high, but once flap extension begins at 15 nm out, the behavior appears more realistic.

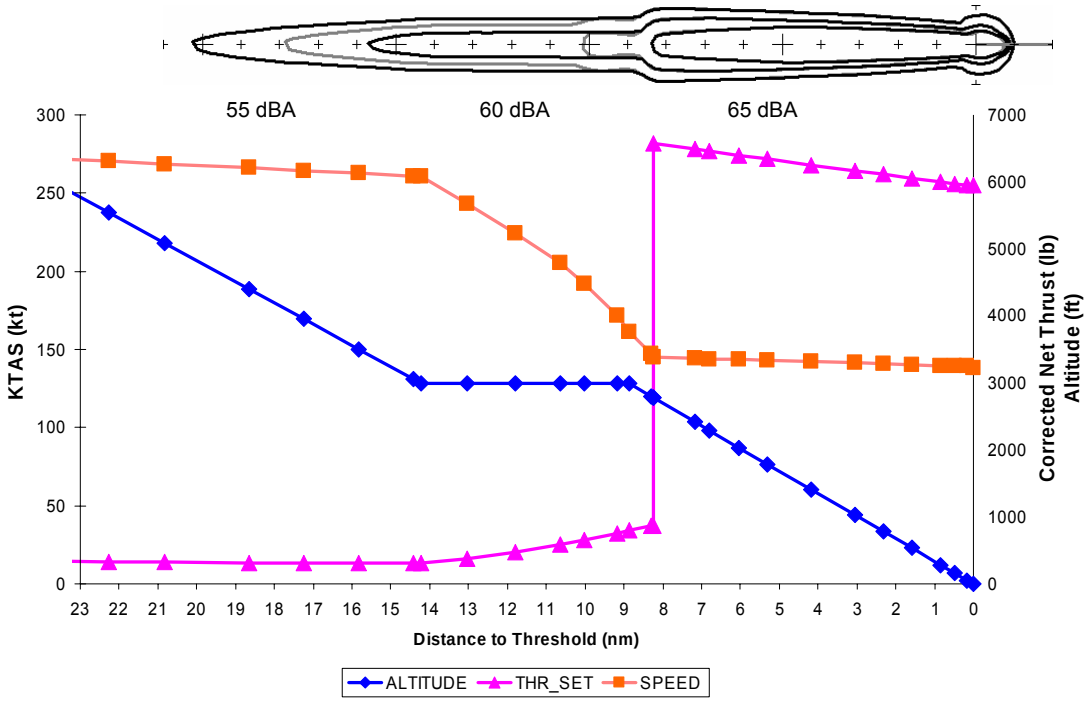


Figure 32: Effect of Configuration on dBA Contour of the 737-800 Using the Standard Approach

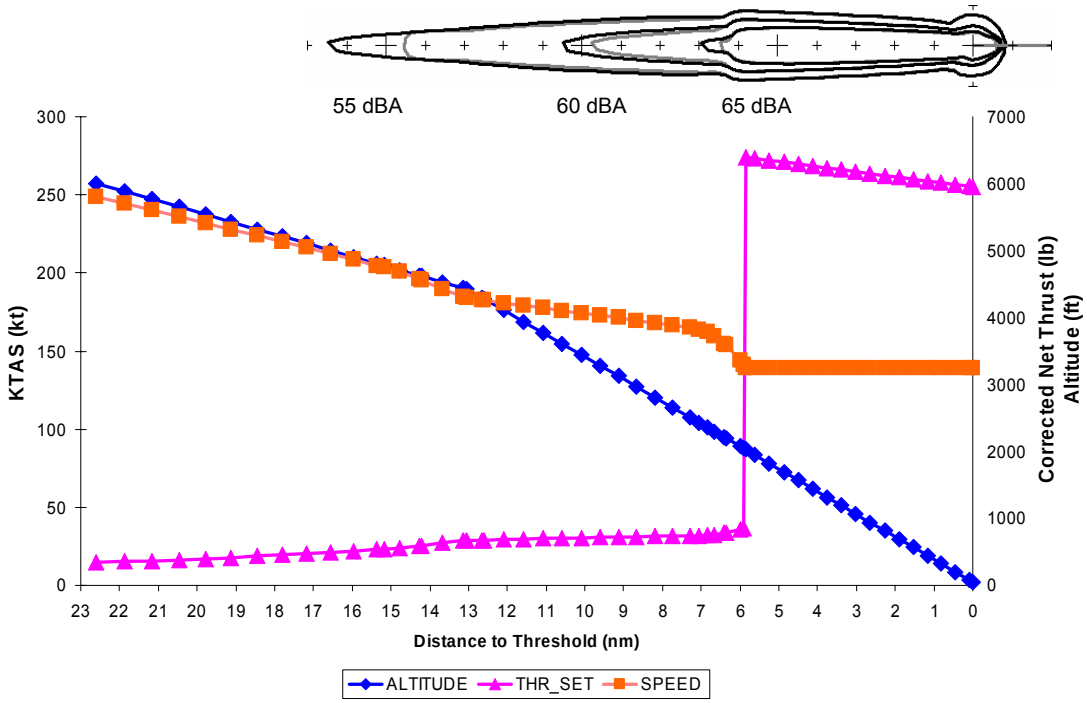


Figure 33: Effect of Configuration on dBA Contour of the 737-800 Using a CDA Type Approach

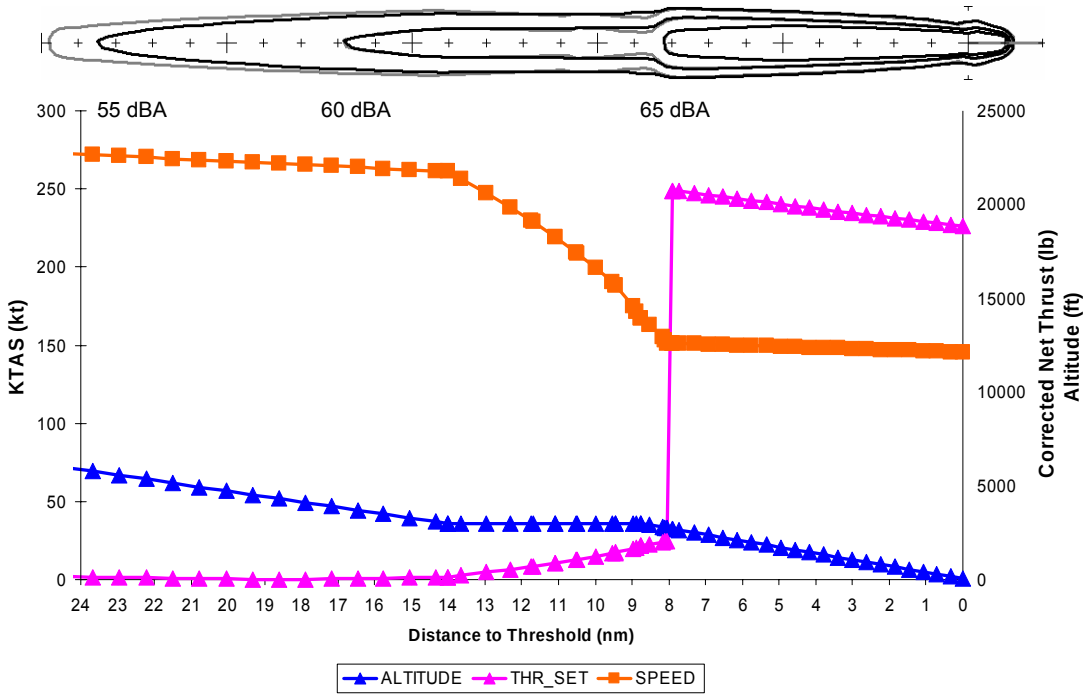


Figure 34: Effect of Configuration on dBA Contour of the 777-200 Using a Standard Approach

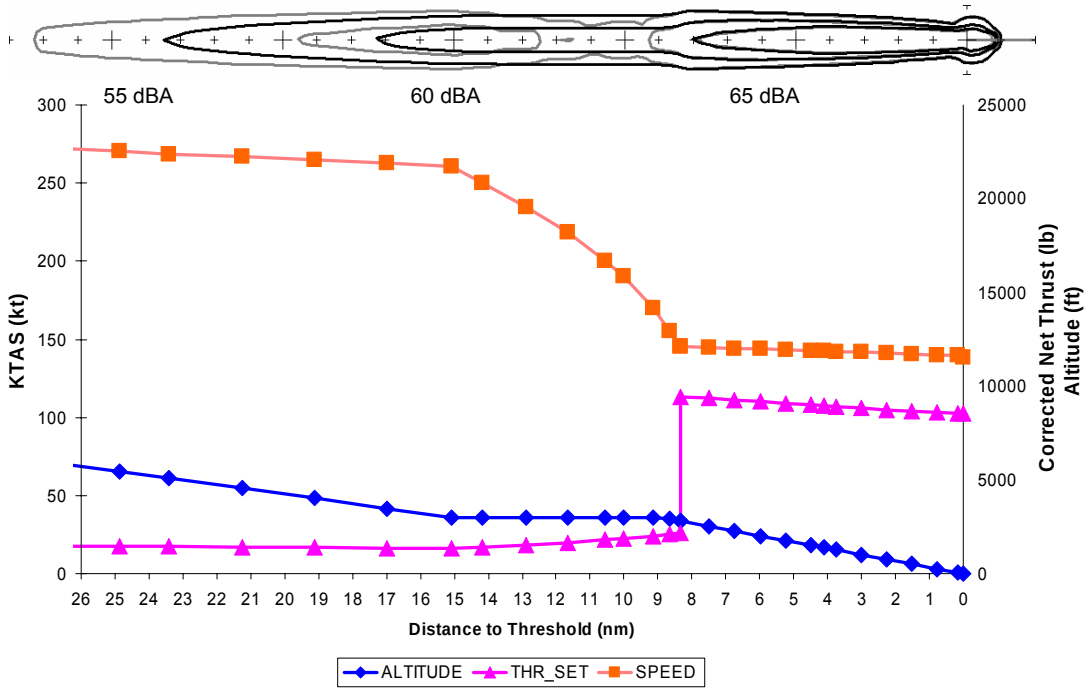


Figure 35: Effect of Configuration on dBA Contour of the 757-300 Using a Standard Approach

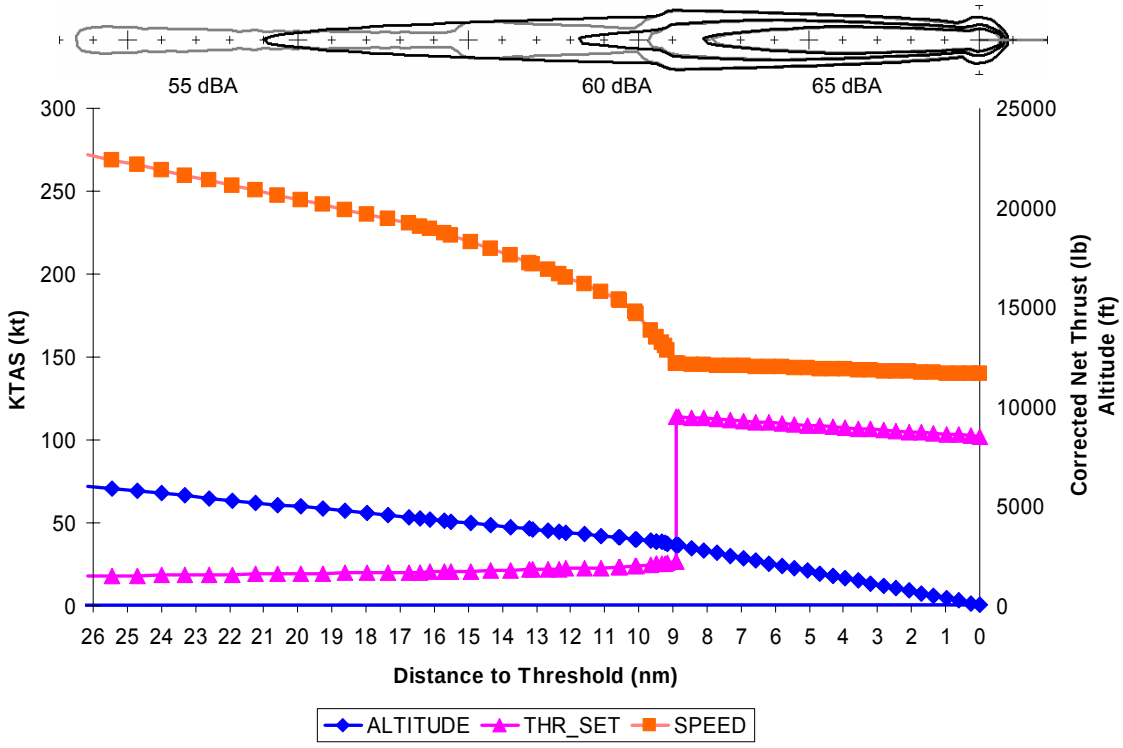


Figure 36: Effect of Configuration on dBA Contour of the 757-300 Using a CDA Approach

3.3 Comparison of INM Predictions with Certification Measurements

The Boeing optimized cutback process for computing EPNL for certification and the EPNL predicted by the Integrated Noise Model (INM) are compared. The comparison was made using the same aerodynamic flight profiles used in the optimized cutback procedure. This comparison tests the quality of the INM's NPD lookup procedure against the certification standard using a common set of Boeing generated flight profile points (thrust, speed, altitude). The Boeing aircraft evaluated were the 717-200, 737-700, 747-400, and 777-200. An additional test of the INM generated flight procedure steps was conducted against the Boeing generated flight profile points for the 737-700.

3.3.1 Certification Flight Profiles

EPNL for certification is calculated using low speed flight models based on the certified aerodynamic performance of the airplane. A certification cutback profile is defined as a full power takeoff followed by power cutback to a thrust level required to maintain a 4 percent climb gradient as the airplane approaches 31325 ft (6500 m) from brake release.

To find the optimized cutback location, flight profiles are generated for a series of cutback locations and weights. The cutback location is "optimized" to achieve the lowest EPNL. Often a thrust cutback that occurs within the 10dB down points of the EPNL calculation will produce the lowest level. Full power takeoff profiles are also generated for diagnostic purposes.

The "optimized" flight profiles for the selected aircraft were imported into the INM and used to calculate the EPNL at the takeoff certification observer point of 31325 ft (3.51 nm) from brake release. Both the "optimized" cutback profile and the full power takeoff profile for three separate weights were used for this study.

3.3.2 Boeing Noise Power Distance Curves (NPD)

The NPD is a table of noise values for a range of constant thrust levels and distances from the aircraft. The data are derived from noise values for constant corrected rotor speed that are extrapolated to a range of altitudes through a homogeneous atmosphere. The noise levels generated in the NPD are based on measured static engine and/or airplane acoustic flight data. The NPD data are normalized to 160 knots true airspeed. Exposure based metrics are adjusted to the flight path speed using a 10log velocity ratio correction.

3.3.3 Comparison of Noise Calculation Methods

The 1/3 Octave Band time history data is fully utilized in the Boeing process. This spectral data is used to compute the perceived tone corrected noise level (PNLT) time history of the aircraft as it steps through ½ second flight profile segments. The flight profiles generated by the flight performance models are based on certified airplane performance. The optimization process allows the engine spool down or cutback to occur within the 10dB down points of the PNLT time history.

INM noise databases contain NPD curves distilled from the above time integrated data along with the spectral class spectra for departure and approach. Some simplifying assumptions about the acoustic directivity of the aircraft are also made. The simplifying assumptions are required in the context of a land use planning tool that must run hundreds or thousands of varied operations with limited computing power.

To estimate the EPNL at an observer ground point, the INM uses interpolation of the NPD to compute the EPNL at each flight profile point. The interpolation is linear with thrust and with the logarithm of the altitude. The EPNL is corrected to the profile velocity using the 10log velocity correction. To account for the time history of the flight path over the point, an adjustment is made for each segment of the point flight path. In the INM, it is assumed that the time history of the flyover noise at each ground point behaves as a fourth-power 90 degree dipole. This correction is referred to as a Noise Fraction Adjustment (NFA). The NFA also takes into account the peak PNLT by performing an additional interpolation on the PNL NPDs in the INM. The Noise Fraction is applied for each flight path segment referenced to the observer ground point and the adjusted noise exposure metric (EPNL) is summed.

3.3.4 Comparison of FAR 36 Takeoff Noise Results

The results of the Integrated Noise Model are compared with certification levels produced by Boeing for the aircraft listed in Table 2. For the study, three different weights for each aircraft for a single thrust rating were evaluated.

Flight profiles from the certification data were imported into the INM. Both full power takeoff and cutback profiles are generated for the certification process and both were evaluated in the study. The INM procedure steps flight profiles are constructed using some initial information about the takeoff thrust and some intermediate altitude and thrust levels to the end of the profile.

INM then uses built-in aerodynamics (flaps coefficients) and engine performance coefficients (jet coefficients) to generate the profile from brake release to the end of the flight track. Figure 37 shows the INM built flight procedure for the cutback profile that is fitted to the certification point profile. The solid lines are the INM built profiles and the points are the Boeing profiles. It shows that there is little difference between the procedural profile and the point profile. Therefore, it is possible to build a FAR 36 profile using the INM and get them to match. However, some prior knowledge of cutback distance, and percent cutback of the engines is required to build an accurate profile.

Complex, tedious methods like those used to produce Figure 37 are the only way to get the INM procedure steps profile to match the FAR36 profile. The assumed target climb speed used to produce the INM jet and flap coefficients is V2+20kts per standard 737 operating procedure, but the target climb speed for the FAR36 profile is V2+10kts. For comparison, the 757, 767, and 777 standard target climb

speed is V2+15kts and for the 747-400 the speed is V2+10kts. Therefore attempts to model even the full power portion of the FAR36 profile will result in a lower altitude upon reaching the cutback measurement point for all airplanes except the 747. The ground roll and initial climb in all other cases will be incorrect for the FAR36 profile.

The NPD's used in the study were those included in the INM version 6.1 with the exception of the PW40NR. The PW40NR was generated from Boeing data for the PW4062A thrust rated Phase 3 NRI engine which is currently in production. The Phase 3 NRI differs from the standard INM PW4056 by having different fan blades, increased acoustic treatment and a redesigned inlet. In all cases, the INM NPD's are generated for the same engines/airframes used to compute the reported certified levels used in this study.

Comparisons of INM-predicted and actual certification noise levels are shown in Table 3 and plotted in Figures 38 through 42. In general, the INM predictions are in good agreement with the FAR 36 certified EPNL for both full power and cutback. Especially significant is the ability of the INM algorithm to accurately compute exposure metrics over the cutback region. The errors are no more significant than that of the nearly linear full power takeoff profiles.

In general, differences between INM predictions and certification levels are small, with the 777 showing the best overall agreement for all takeoff weights. Care must be taken to match flight procedures, but results indicate that the INM methodology is sound, including the noise fraction (source directivity) approximation.

Table 2 Details of Airplanes used in Study

Airplane	Engine (INM NPD) * New NPD from Boeing data	Max S.L. Static Thrust (lbs)	Study Weights (lbs)
717-200	BR 715 (BR715)	18,000	104500, 111400, 121000
737-700	CFM56-7B (CF567B)	24,000	124500, 154500, 171000
747-400	PW4056 (PW40NR*)	62,000	800000, 870000, 910000
777-200	GE90-76B (GE9076)	77,000	506000, 535000, 545000

Table 3 Comparison between Certification and INM EPNL Levels

Airplane & Engine	Takeoff Gross Weight (lbs)	Cert Full Power Takeoff EPNL	INM Full Power Takeoff EPNL	INM EPNL Error Full Power	Cert Cutback Takeoff EPNL	INM Cutback Takeoff EPNL	INM EPNL Error Cutback
717-200 BR 715	104,500	85.3	84.8	-0.5	79.6	79.5	-0.1
	111,400	86.8	86.4	-0.4	82.1	81.7	-0.4
	121,000	87.9	87.5	-0.4	84.0	83.6	-0.4
Boeing 737-700 CFM56-7B	124,500	87.8	88.9	1.1	80.6	80.7	0.1
	154,500	90.4	91.1	0.7	85.9	85.9	0.0
	171,000	91.8	92.6	0.8	88.6	89.0	0.4
	154,500*	90.4	90.7	0.3	85.9	85.5	-0.4
B747-400 PW4062A	800,000	100.5	100.9	0.4	92.7	92.7	0.0
	870,000	102.5	102.6	0.1	95.0	95.7	0.7
	910,000	103.6	103.7	0.1	96.6	97.2	0.6
Boeing 777-200 GE90-76B	506,000	90.3	90.5	0.2	86.7	86.5	-0.2
	535,000	91.3	91.5	0.2	88.3	88.0	-0.3
	545,000	91.7	91.8	0.1	88.8	88.5	-0.3
Boeing 737-700 CFM56-7B	124500	87.8	87.8	0.0	80.6	80.5	-0.1
	154500	90.4	90.5	0.1	85.9	85.7	-0.2
	171000	91.8	92.2	0.4	88.6	88.8	0.2
	154500*	90.4	90.1	-0.3	85.9	85.4	-0.5

* From INM procedure profile

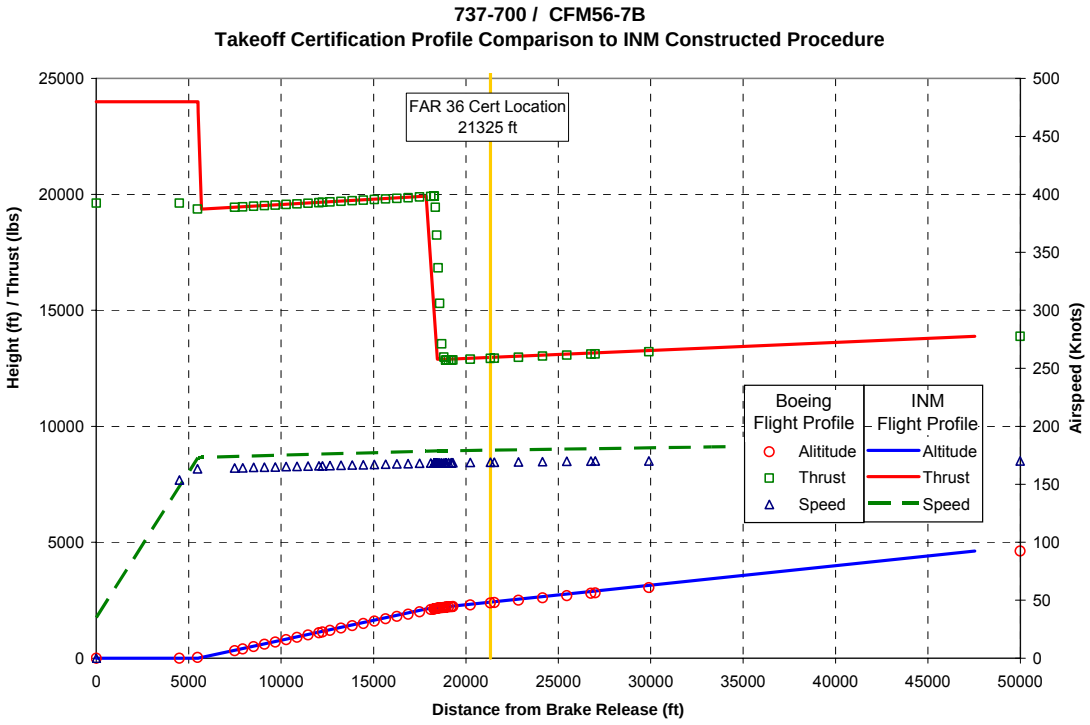


Figure 37: 737-700 Cutback Flight Profile for 154,500 lbs

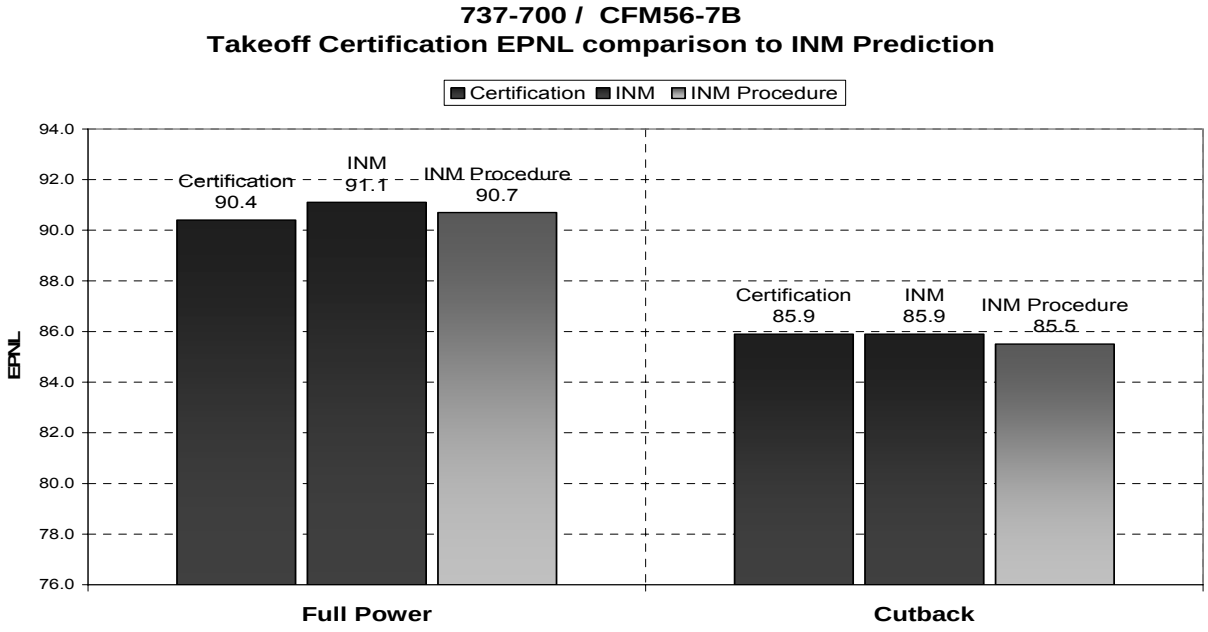


Figure 38: Comparison between Certification EPNL to the INM Predictions and INM Predictions with INM Built Procedure Profile for 737-700 at 154,500 lbs TOGW

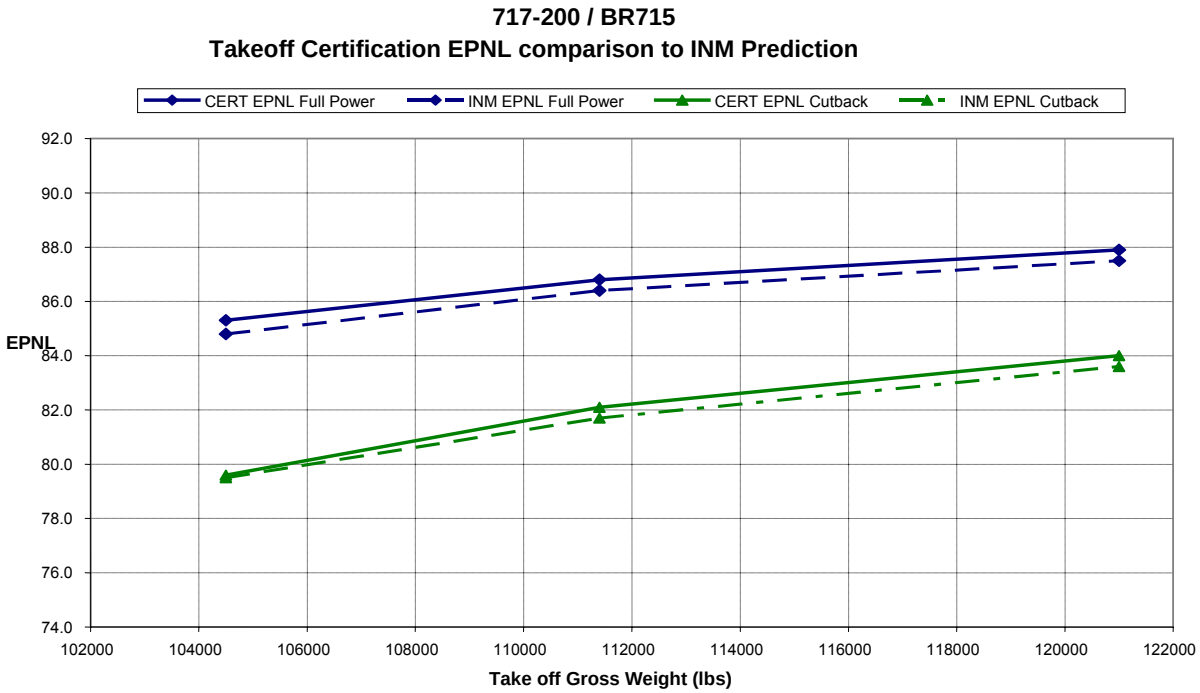


Figure 39: Comparison between Certification EPNL to the INM Predictions for 717-200

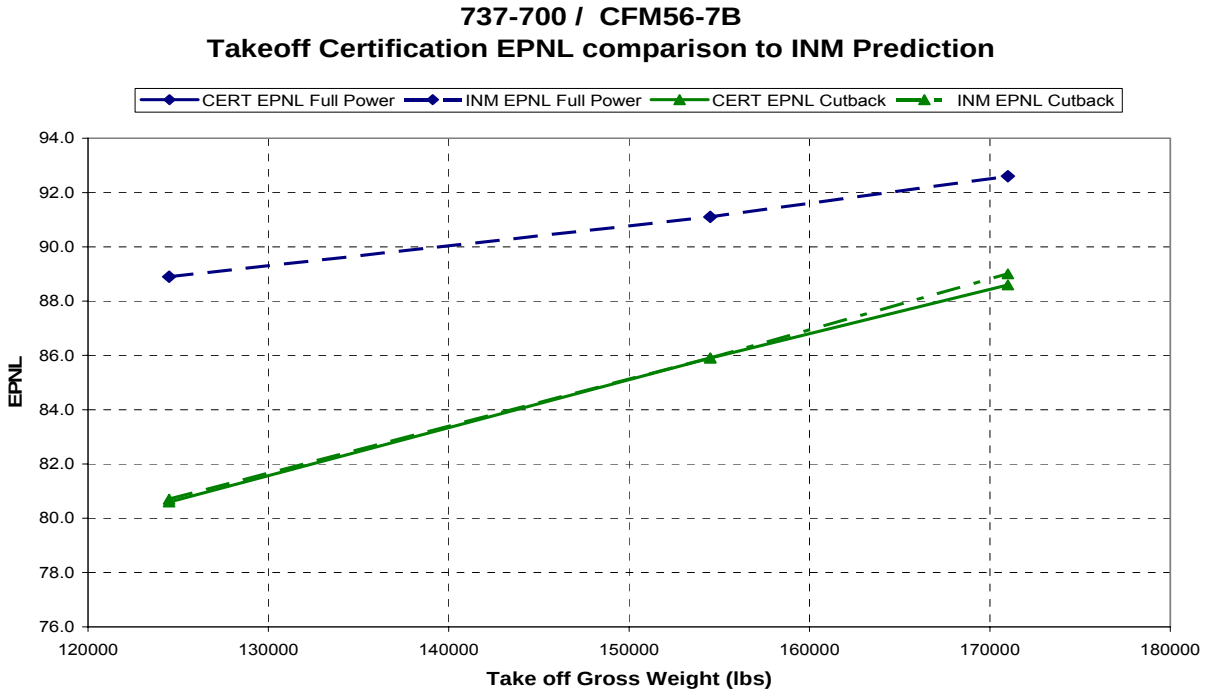


Figure 40: Comparison between Certification EPNL to the INM Predictions for 737-700

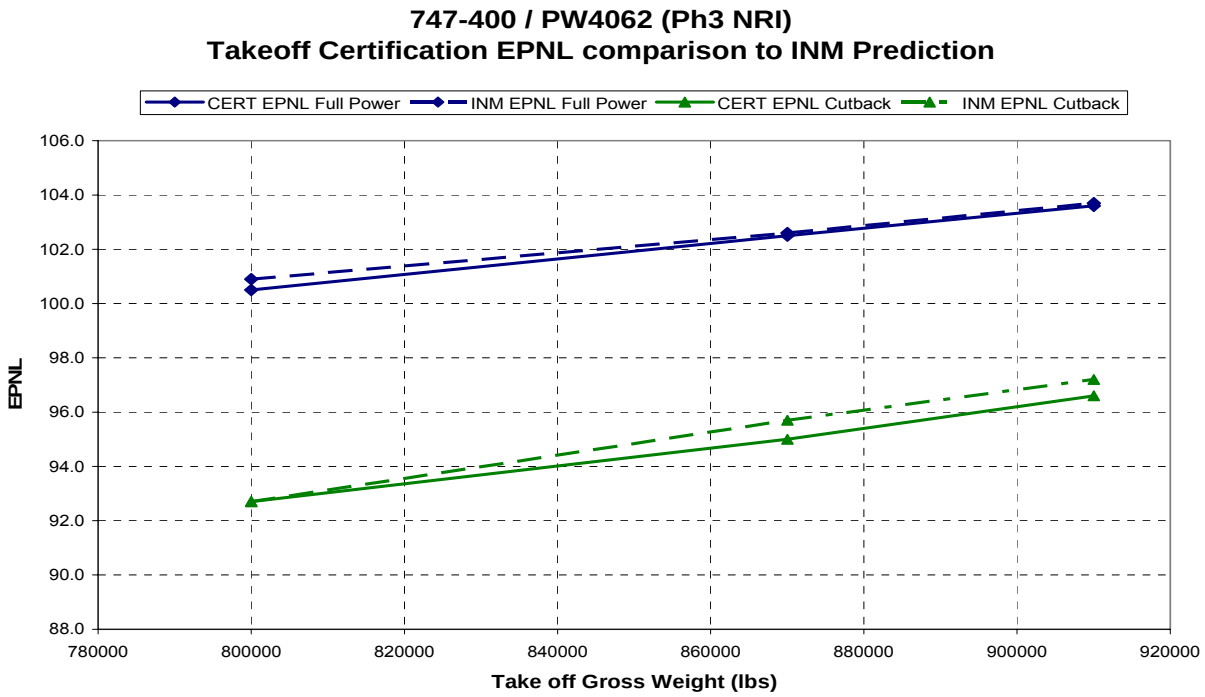


Figure 41: Comparison between Certification EPNL to the INM Predictions for 747-400

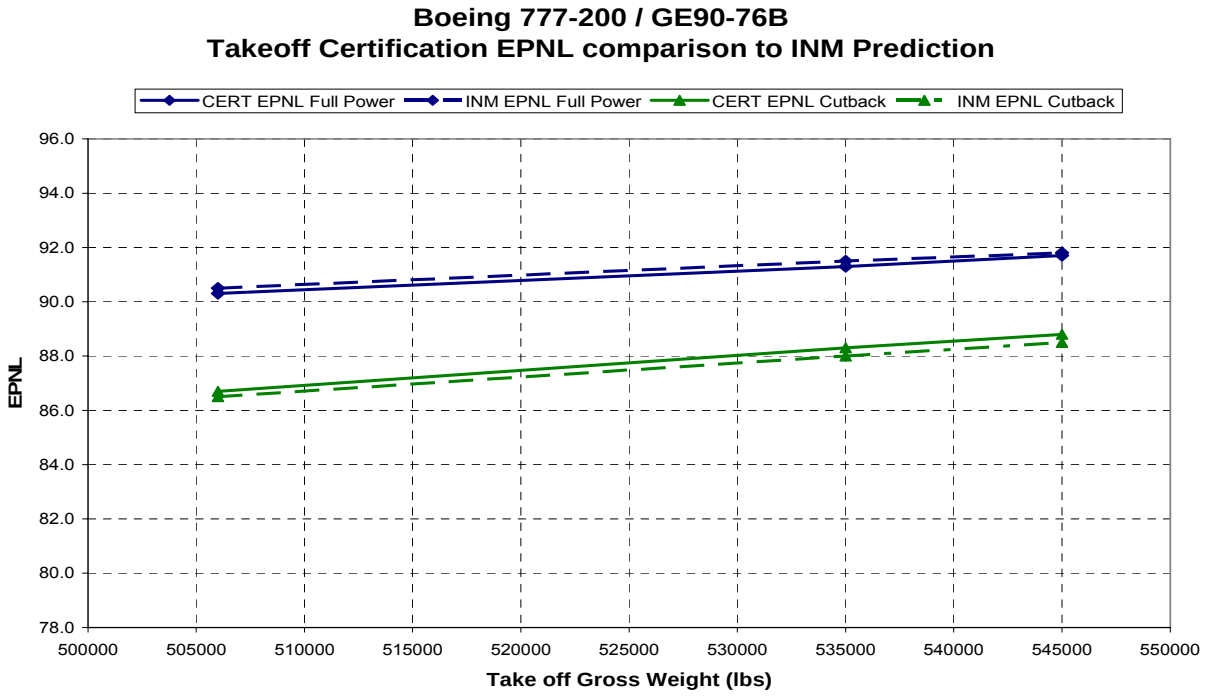


Figure 42: Comparison between Certification EPNL to the INM Predictions for 777-200

3.4 Modeling Derated Thrust Takeoffs

The INM performance coefficients are derived from a full power takeoff condition followed by cutback to maximum climb thrust for a given engine/airframe combination. It in known that operators use lower takeoff thrust (derate) when conditions permit in order to save fuel and engine wear. Typically the lower takeoff thrust setting is accompanied by a similar reduction in climb thrust. This is expected to result in differences in the level and distribution of noise from what would be predicted using the standard full-power assumption used by the INM. The effect of derate on noise contours for a range of thrust conditions will be illustrated using Boeing flight performance data. Then different approaches that an INM user might use to model derated thrust takeoffs will be evaluated.

3.4.1 Effect of Derate on Noise Contours

The Boeing Climb Out Program (BCOP) was used to calculate flight profiles for a 747-400 and a 737-300 with the first derate and contours were generated at a range of weights, temperatures and runway altitudes to see the effect on the noise contours. The 737-300 and the 747-400 were chosen to encompass a wide range of aircraft size and weight. The expected effects of using less thrust for takeoff and climb are a reduction of sideline noise combined with a possible increase in noise under the flight path due to the lower rate of climb of the aircraft. For this reason peak dBA contours are shown to illustrate the areas of noise relief and noise increase for the derated takeoffs. Each set of contours in the next eight figures show the 85dBA and 75dBA contours for the different flight conditions. In each figure the grey contour represents the derated thrust condtion.

For ten percent derated thrust conditions at low takeoff weight, real noise relief can be seen for the 747-400 under the flight path as well as on the sideline. Each set of contours in the next eight figures show the 85dBA and 75dBA contours for the different flight conditions run. This benefit persists even at the higher airport altitude of 6000 feet. However, at the high temperature (104 degrees F) the benefit under the flight path disappears. Applying the ten percent derate to the highest weight uniformly exports noise from the sideline area to the area under the flight path.



Figure 43: Effect of 10% Derate on dBA Contour of the 747-400, Sea Level Standard Day 700,000 lbs.

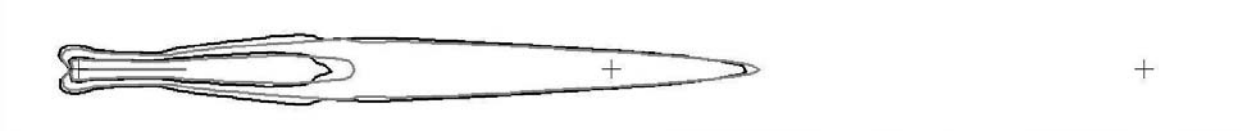


Figure 44: Effect of 10% Derate on dBA Contour of the 747-400, Sea Level Standard Day 875,000 lbs.



Figure 45: Effect of 10% Derate on dBA Contour of the 747-400, Sea Level 104F Day 700,000 lbs.



Figure 46: Effect of 10% Derate on dBA Contour of the 747-400, Sea Level 104F Day 875,000 lbs.

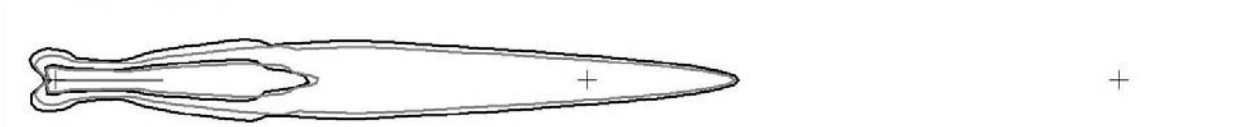


Figure 47: Effect of 10% Derate on dBA Contour of the 747-400, 6000 Feet Standard Day 700,000 lbs.

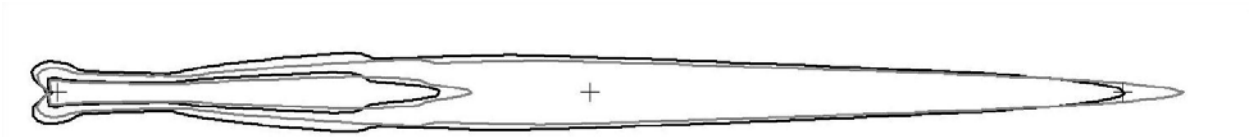


Figure 48: Effect of 10% Derate on dBA Contour of the 747-400, 6000 Feet Standard Day 875,000 lbs.



Figure 49: Effect of 10% Derate on dBA Contour of the 747-400, 6000 Feet 104F Day 700,000 lbs.

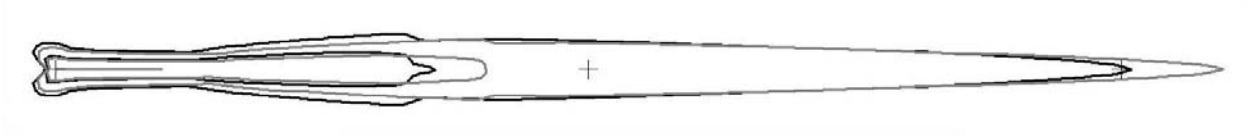


Figure 50: Effect of 10% Derate on dBA Contour of the 747-400, 6000 Feet 104F Day 875,000 lbs.

For the 737-300 reduced thrust settings for a 22K rated engine mimic the next lower engine rating of 20K. The contours compared in this series are for 65 dBA and 75dBA. Derated thrust exports noise across the weight and temperature range for the sea level airport. At 6000 foot runway altitude there are regions of the flight profile where there is an overall reduction in the contour that can be seen in the 75 dBA contours. The full power portion of the contours shows almost no change. This is due to the fact that the 20K engine rating has a thrust bump for high altitude operations that brings the thrust up to near that of the baseline 22K rating. Climb thrust for the two ratings is more noticeably different. As a result there are noise differences in the region after thrust cutback but not before.



Figure 51: Effect of 10% Derate on dBA Contour of the 737-300, Sea Level Standard Day 111,500 lbs.

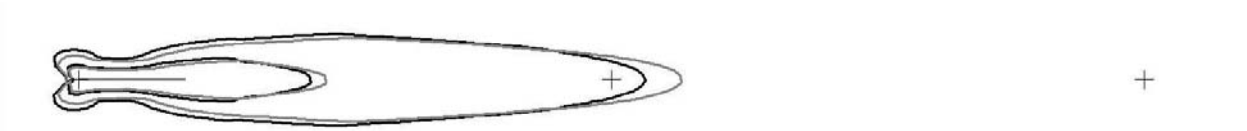


Figure 52: Effect of 10% Derate on dBA Contour of the 737-300, Sea Level Standard Day 139,500 lbs.



Figure 53: Effect of 10% Derate on dBA Contour of the 737-300, Sea Level 104F Day 111,500 lbs.

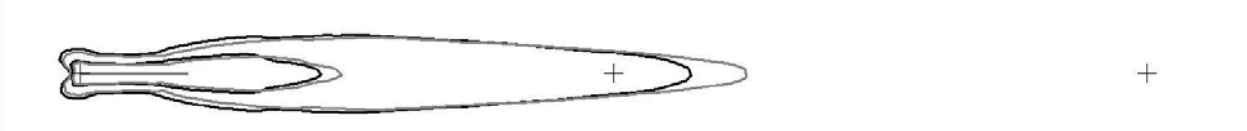


Figure 54: Effect of 10% Derate on dBA Contour of the 737-300, Sea Level 104F Day 139,500 lbs.

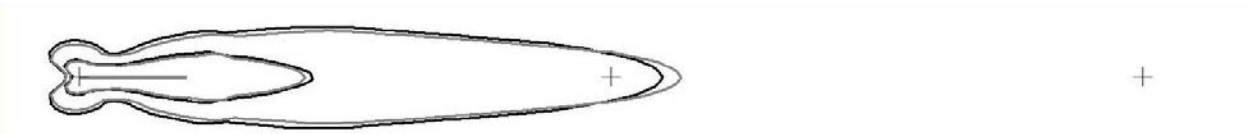


Figure 55: Effect of 10% Derate on dBA Contour of the 737-300, 6000 Feet Standard Day 111,500 lbs.

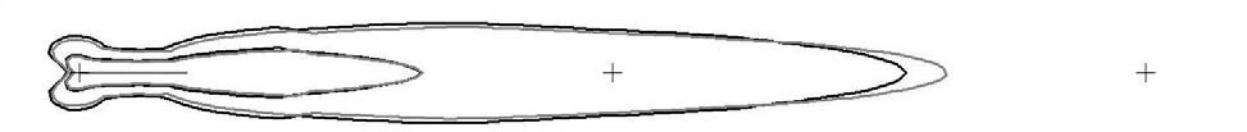


Figure 56: Effect of 10% Derate on dBA Contour of the 737-300, 6000 Feet Standard Day 139,500 lbs.

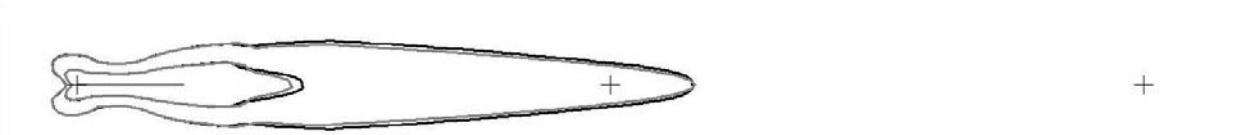


Figure 57: Effect of 10% Derate on dBA Contour of the 737-300, 6000 Feet 104F Day 111,500 lbs.

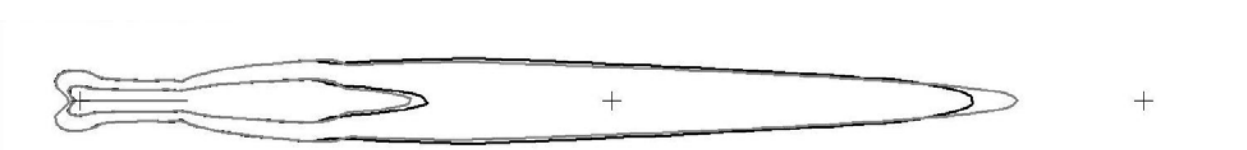


Figure 58: Effect of 10% Derate on dBA Contour of the 737-300, 6000 Feet 104F Day 139,500 lbs.

The above data were developed using Boeing performance tools to generate the flight profiles. An INM user would have to adjust the INM jet thrust coefficients to approximate the thrust reduction. In the case of the 737 family, the user could pick the next lower thrust rating where available. However, INM procedure steps have a fixed rate of climb for the acceleration portion of the flight profile. Therefore there will still be a mismatch in the thrust split of climb vs. acceleration once the thrust reduction is made to the jet thrust coefficients due to using the wrong rate of climb.

Using the same Boeing performance tools, it was possible to test the effect of that mismatch by running a range of thrust split conditions to see if the contours are affected. A ten percent change in the thrust split during the acceleration segments produces barely perceptible changes in the contour. A table is provided for two typical 737 aircraft to show the differences.

Table 4 Effect of Thrust Split During Acceleration for 737-400 and 737-700 Aircraft

Effect of Thrust Split During Acceleration for 737 Aircraft (Typical Operations are 45% Excess Climb)				
	737-400 40% Excess Climb	737-400 50% Excess Climb	737-700 40% Excess Climb	737-700 50% Excess Climb
Peak dBA Contour	Contour Area (Square mi.)	Contour Area (Square mi.)	Contour Area (Square mi.)	Contour Area (Square mi.)
55	75.283	75.562	71.000	71.200
60	41.779	41.990	39.172	39.365
65	20.501	20.614	18.697	18.779
70	10.035	10.026	8.758	8.688
75	4.691	4.634	4.072	4.028
80	2.454	2.431	2.082	2.016
85	1.067	1.048	0.875	0.860

Given the small effects of the expected mismatch to the thrust split (INM rates of climb) it should be possible to model reduced thrust operations using the INM. Maintaining constant thrust-to-weight ratio from the Maximum Takeoff Weight (MTOW) will result in ground rolls that are shorter than that for the MTOW, but how the operators use reduced thrust will vary with operator and airport. Based on what was seen in the Denver Airport studies, review of radar data is recommended in determining the best approach to applying reduced thrust to airport operations.

4 Conclusions and Recommendations

Based on the survey data collected from airlines the 65% payload assumption should be applied to future submissions and updates of Boeing aircraft to the INM. It is not expected that load factors will change in the foreseeable future.

Boeing NPD data can be adjusted to the absorption standard referenced in SAE AIR-1845 using spectral classes. The resultant errors are tolerably small.

The spectral class assumption appears to be adequate for the purposes of weather correction of an existing NPD table. Its performance is best at long range/high altitude. Even at its worst it introduces error of less than 1 dBA for lower altitude data.

Modeling advanced procedures such as Continuous Descent Approach with noise varying as a function of aircraft configuration and speed proved difficult due to the quality and availability of airframe noise data for the clean configuration and possibly for low flaps conditions at high speed. Better understanding of these conditions will be needed before a tool can be developed and verified for modeling approach noise from top of descent at idle power as is desired for Continuous Descent Approach procedures.

The INM was able to reproduce noise certification EPNLs from the Boeing certification flight profile and it was possible to force INM procedure steps to match that profile if the user had sufficient knowledge of the optimized certification flight profile.

Reduced thrust takeoffs were not found to be a factor in the Denver Airport studies. From the radar data there was ample evidence that it was being used when it was possible. For lighter takeoff weights, reduced thrust results in reduced noise at sideline locations and at positions under the flight track. For other conditions (heavy aircraft and high temperatures) sideline noise is reduced but noise under the flight track is increased.

Improvements made to the INM have resulted in improved prediction for the Denver Airport. But the model is limited to what is available in the set of procedure steps in the INM performance database. A means to adapt those procedure steps to radar data that is becoming increasingly available would make it possible to model real flight procedures in use at airports at high altitudes or with unusual weather.

Bibliography

1. **NASA, "Review of Integrated Noise Model (INM) Equations and Processes", Contractor Report NASA/CR 2003-212414, NASA Center for AeroSpace Information, 7121 Standard Drive, Hanover, MD 21076-1320, 2003.**

2. **Society of Automotive Engineers, Committee A-21, "Procedure for the Calculation of Airplane Noise in the Vicinity of Airports", Aerospace Information Report No. 1845, SAE Inc., 400 Commonwealth Drive, Warrendale, PA 15096, March 1986.**

3. **European Civil Aviation Conference, "Report on Standard Method of Computing Noise Contours around Civil Airports", ECAC Doc 29, European Civil Aviation Conference, July, 1997.**

4. **ICAO, "Recommended Method for Computing Noise Contours around Airports", Circular 205-AN/1/25, March 1987.**

5. **U.S. Department of Transportation (DOT), "Update of Aircraft Profile Data for the Integrated Noise Model Computer Program", US DOT, Volpe National Transportation Systems Center, Cambridge, MA 02142, March 1992.**

6. **Federal Aviation Administration (FAA), Office of Environment and Energy (AEE), "INM 6.0 User's Guide", Federal Aviation Administration, Noise Division, AEE-100, 800 Independence Avenue, S.W., Washington DC, 20591, September, 1999.**

7. **ICAO, "A Revision to the Definition of the Reference Atmosphere in Annex 16 to Improve Data Quality and Reliability and Ease Related Technical Problems", CAN/7-WP/19, Committee on Aircraft Noise Seventh Meeting, May 1983.**

8. **Society of Automotive Engineers, Committee A-21, "Standard Values of Atmospheric Absorption as a Function of Temperature and Humidity", Aerospace Recommended Practice No. 866A, SAE Inc., 400 Commonwealth Drive, Warrendale, PA 15096, March 1975.**

Appendix A

Comparison of INM 5.0a through 6.2 Beta Using Noise Monitoring and Radar Data Collected at Denver International Airport

Prepared for:

National Aeronautics and Space Administration
Hampton, VA

Prepared by:

Nicholas P. Miller
Grant S. Anderson
Robert C. Mentzer
Bradley L. Nicholas

HARRIS MILLER MILLER & HANSON INC.
77 South Bedford Street
Burlington, MA 01803

ACKNOWLEDGMENTS

This study was made possible by the generous support of Mike McKee at Denver International Airport. Through his agreement to make monitoring system data available, we have been able to develop the analyses presented in this report.

In addition, John Gulding at FAA and David Forsyth at Boeing have provided extensive assistance in developing modified inputs for use in the various INM versions tested.

EXECUTIVE SUMMARY

- This report documents comparisons of Integrated Noise Model (INM) computations of aircraft Sound Exposure Levels (SELs) with measured SEL values for six aircraft types (Section 1)
- Measured data were collected in 1995 and 1996 at Denver International Airport (Appendix B)
- The results of eight different INM modeling methods were compared and the results expressed as differences between the energy average INM SEL values and the energy average measured SEL values for the six aircraft types (Section 3)
- Of the eight different modeling methods, three improved the agreement of the INM with the measurements: (Sections 2 and 3)
 - INM Version 6.0c produced significant improvements compared with Version 5.1a
 - INM Version 6.2 beta produced significant improvements compared with Version 6.0c
 - New performance coefficients for the B733 and M80 further improved the agreement between the INM calculations and measured levels for those aircraft
- Graphical investigations of the results of the most complete Modeling Method revealed additional areas for improvement of the INM (Section 5)
 - INM altitudes do not well match measured altitudes
 - INM altitudes for departures are generally higher than measured altitudes
 - At these higher altitudes, INM computed SEL values are generally lower than measured values
 - Lowering the INM altitudes is sufficient to bring INM departure SEL values for several aircraft types into better agreement with measured levels
- Further improvement of INM computations should include: (Section 2)
 - Detailed analysis of the INM departure algorithms that relate power, weight and climb rate
 - New modeling method for arrivals
 - Acquisition of a new measurement database that better reflects the current fleet mix collected at airports located closer to sea level

TABLE OF CONTENTS

1 INTRODUCTION A-1
1.1 Background – FAA Continuously Improves INM A-1
1.2 Purpose – Compare INM Results with Measured Sound Levels A-2
1.3 Assessment Metric is INM SEL minus Measured SEL, by Aircraft A-3
1.4 Important Note – Denver is a High-Altitude Airport A-4
1.5 Overview of the Study - Figure 1 A-4
1.6 Remainder of this Report A-7

2 CONCLUSIONS AND RECOMMENDATIONS A-9
2.1 Three of the Modeling Methods Provide Significant Improvements A-9
2.2 Other Modeling Methods Produced No Significant Changes in INM Offsets: A-10
2.3 Graphical Investigations Suggest Incorrect INM Altitudes as Possible Target for Improvements A-10
2.4 Recommend Detailed Investigations A-11

3 INM OFFSETS A-13
3.1 Number of INM Offsets That Were Determined A-13
3.2 Full Set of INM Offsets and Confidence Ranges Summarized A-14
3.3 Tabular Summary of All "Confidently Large" INM Offsets A-17
3.4 Other Sections of this Report that Examine the Offsets A-18

4 OFFSET COMPARISONS AMONG THE MODELING METHODS A-19
4.1 Summary of All Modeling-Method Changes Shown in Table 7 A-19
4.2 Resulting Changes in INM Offset A-21
4.3 Additional Details A-23

5 GRAPHICAL INVESTIGATION OF OFFSETS FOR MODELING METHOD 8 A-25
5.1 The Starting Point: INM Offsets that Result from Modeling Method 8 A-25
5.2 Graphical Investigations of B733, B757 and M80 Aircraft, for Elevation Angles Above 60 Degrees A-26
5.3 INM Offsets, After Adjustment for Proper Aircraft Altitude A-41
5.4 Influence of Other Factors on INM Offset A-43
5.5 Limitations of These Graphical Investigations A-47

APPENDIX A DETAILED TABULATIONS/GRAPHS OF INM OFFSETS A-49
A.1 Tables A-49
A.2 Graphs A-59

APPENDIX B MEASURED DATA A-63
B.1 The DIA Monitoring System A-63
B.2 Sampled Days of the Full Year A-65
B.3 The Measured Variables A-67

APPENDIX C COMPUTED DATA A-69

C.1 Computations Common to All Modeling Methods A-69
C.2 Computations Specific to Some Modeling Methods A-72
C.3 Track Distance A-78

APPENDIX D PRELIMINARY ANALYSIS A-81
D.1 Data Cleaning A-81
D.2 Data Filtering A-83
D.3 Data Regimes A-84
D.4 Number of Data Points by Aircraft Type A-86

APPENDIX E DETERMINATION OF INM OFFSETS A-89
E.1 Data Summary A-89
E.2 Analysis Equations A-91
E.3 Additional Details A-95

APPENDIX F DERIVATION OF PROPAGATION UNCERTAINTY A-97
F.1 Repeated from Section E.2.2, Above A-97
F.2 Derivation of Eq. (15) from Eq. (14) A-98

LIST OF FIGURES

Figure 1. Overview of the study and its products A-5
Figure 2. Conclusions and recommendations within the study A-9
Figure 3. Resulting INM Offsets within the study A-13
Figure 4. INM Offsets: Elevation angles below 60 degrees A-15
Figure 5. INM Offsets: Elevation angles above 60 degrees A-16
Figure 6. Offset comparisons within the study A-19
Figure 7. Graphical investigation of offsets within the study A-25
Figure 8. INM under-computes SELs at moderate-to-high track distances: B733 A-27
Figure 9. INM under-computes SELs at moderate-to-high track distances: B757 A-28
Figure 10. INM both under- and over-computes SELs for arrivals and departures, respectively: M80 A-29
Figure 11. INM over-computes altitudes at high track distances: B733 A-30
Figure 12. INM over-computes altitudes at high track distances: B757 A-30
Figure 13. INM over-computes altitudes at high track distances: M80 A-31
Figure 14. Incorrect altitudes potentially explain incorrect SELs: B733 A-32
Figure 15. Incorrect altitudes potentially explain incorrect SELs: B757 A-33
Figure 16. Incorrect altitudes potentially explain incorrect SELs: M80 A-33
Figure 17. INM SELs can be adjusted for proper aircraft altitudes: B733 arrivals A-34
Figure 18. INM SELs can be adjusted for proper aircraft altitudes: B733 departures A-35
Figure 19. Slant distance adjustment tends to improve INM SELs: B733 A-36
Figure 20. Slant distance adjustment tends to improve INM SELs: B757 A-37
Figure 21. Slant distance adjustment produces little improvement in INM SELs: M80 A-38
Figure 22. Slant distance adjustment reduces INM stage-length under-computation for B733, B757 A-40
Figure 23. Altitude-adjusted INM Offsets: Elevation angles above 60 degrees A-41
Figure 24. Altitude-adjusted INM Offsets: Elevation angles below 60 degrees A-42
Figure 25. Influence of other factors on INM Offset: Elevation angles below 60 degrees A-45
Figure 26. Influence of other factors on INM Offset: Elevation angles above 60 degrees A-46
Figure 27. INM Offsets: Elevation angles below 60 degrees (emphasis on small effects) A-60
Figure 28. INM Offsets: Elevation angles above 60 degrees (emphasis on small effects) A-61
Figure 29. Measured data within the study A-63
Figure 30. Measurement locations (RMT numbers) at DIA A-64

Figure 25. Computed Data within the study A-69
Figure 26. Effect of updated NPD curves A-75
Figure 33. Importance of evaluating INM accuracy in different "SEL regimes" A-79
Figure 34. Preliminary analysis within the study A-81
Figure 35. Inconsistent data when same aircraft passes same RMT more than once A-82
Figure 36. Cumulative distribution of wind speeds in database A-83
Figure 37. Cumulative distribution of elevation angles in wind-speed-filtered database A-84
Figure 38. Preliminary (before filtering) comparison of computed and measured SELs: B733 arrivals, Modeling Method 1 A-85
Figure 39. Determination of INM Offsets within the study A-89

LIST OF TABLES

Table 1. INM Modeling Methods A-2
Table 2. Track-distance regimes by operation and aircraft type A-6
Table 3. Track-distance regime by operation and aircraft type....A-13
Table 4. INM Modeling Methods A-14
Table 5. Summary of "confidently large" INM Offsets: Elevation angles below 60 degrees....A-17
Table 6. Summary of "confidently large" INM Offsets: Elevation angles above 60 degrees....A-18
Table 7. Detailed changes between modeling methods A-20
Table 8. Confidently large changes in INM Offset produced by Modeling Method 4 A-22
Table 9. Confidently large changes in INM Offset produced by Modeling Method 5 A-22
Table 10. Confidently large changes in INM Offset produced by Modeling Method 7 A-23
Table 11. Confidently large INM Offsets for Modeling Method 8 A-26
Table 12. Dependence of SEL Offset upon other factors....A-43
Table 13. Apparent association of SEL Offset with concurrently measured factors A-47
Table 14. INM Offsets: Modeling Method 1 A-50
Table 15. INM Offsets: Modeling Method 2 A-50
Table 16. INM Offsets: Modeling Method 3 A-51
Table 17. INM Offsets: Modeling Method 4 A-51
Table 18. INM Offsets: Modeling Method 5 A-52
Table 19. INM Offsets: Modeling Method 6 A-52
Table 20. INM Offsets: Modeling Method 7 A-53
Table 21. INM Offsets: Modeling Method 8 A-53
Table 22. INM Offsets: Modeling Method 8Star (8*) A-54
Table 23. Changes in INM Offsets: Modeling Method 1 to 2....A-55
Table 24. Changes in INM Offsets: Modeling Method 2 to 3....A-55
Table 25. Changes in INM Offsets: Modeling Method 3 to 4....A-56
Table 26. Changes in INM Offsets: Modeling Method 4 to 5....A-56
Table 27. Changes in INM Offsets: Modeling Method 5 to 6....A-57
Table 28. Changes in INM Offsets: Modeling Method 6 to 7....A-57
Table 29. Changes in INM Offsets: Modeling Method 7 to 8....A-58
Table 30. Changes in INM Offsets: Modeling Method 8 to 8Star (8*) A-58

Table 31. Number of arrivals/departures....A-66
Table 32. Monthly Average Weather Conditions Used in the INM Modeling....A-73
Table 33. User defined data for Modeling Method 7....A-77
Table 34. User defined data for Modeling Method 8....A-77
Table 35. Aircraft and Thrust Values Used in Modeling Method 8....A-78
Table 36. INM types and Stage lengths Capable of Using De-rate....A-78
Table 37. Track-distance regimes by operation and aircraft type....A-86
Table 38. Study aircraft types: Number for each ARTS and INM aircraft type....A-86
Table 39. Study aircraft types: Number at each RMT....A-87
Table 40. Number of data points (Modeling Method 8)....A-87
Table 41. Measured variables for each aircraft noise event....A-90
Table 42. Corresponding computed variables for the same aircraft noise event....A-91

1 INTRODUCTION

This section introduces the study and this report:

- Section 1.1 discusses the study's background.
- Section 1.2 states the study's purpose.
- Section 1.3 discusses the study's assessment metric for INM accuracy.
- Section 1.4 contains an important note about generalizing the study's results.
- Section 1.5 overviews this study.
- Section 1.6 overviews the remainder of this report.

1.1 Background – FAA Continuously Improves INM

The Federal Aviation Administration (FAA) has continually refined and made improvements to the Integrated Noise Model (INM) over the past several decades. The INM includes carefully developed and officially standardized algorithms that compute:

- Each individual-aircraft altitude profile along its flight track—based on the aircraft's specific performance capabilities, its specific operating procedures, and weather
- Individual-aircraft Sound Exposure Levels (SELs) at any location on the ground—based on the aircraft's location in the sky, its certified noise-source data, standard sound propagation algorithms, and weather
- Integrated metrics of sound exposure from all aircraft, combined—typically, the Day-Night Average Sound Level (DNL).

Until recently, studies to determine INM accuracy used aircraft-noise data that were specially collected during the course of each individual study.[1,2,3,4,5] Such specially collected data have two drawbacks. First, they are limited in time duration to the length of the study's measurement program—generally several months, at most. Second, they often measure aircraft flown specially for the study, by pilots using well-defined flight procedures. Those aircraft, pilots and flight procedures may not be typical of conditions around commercial airports. Most importantly, non-typical flight procedures can result in noise levels on the ground that may differ considerably from those produced by the usual flight procedures used at the airport.

Over the past several decades, airports have installed permanent monitoring systems that measure aircraft noise continuously, over extended time periods. These systems capture aircraft noise over many years of airport operation, from in-service aircraft flown by commercial pilots under their air-carrier's specific flight procedures. Moreover, these monitoring systems capture aircraft noise at a large number of permanent monitor stations around the airport. In addition, they capture concurrent flight-tracking data from nearby FAA radar installations. These monitoring systems then match, in an automated manner, each captured sound-level event with a specific aircraft operation, to construct a database of measured sound levels and "matched" aircraft flights—for essentially all aircraft operations at all monitors, continuously throughout the year.

Such databases present a new opportunity to determine INM accuracy, by comparing measured sound levels with corresponding INM computations over extended periods of time, under typical operating conditions.

1.2 Purpose – Compare INM Results with Measured Sound Levels

- Previous Study Examined INM Version 5.0

This study takes advantage of installed monitoring systems. In particular, this study determines INM accuracy for Denver International Airport (DIA), by comparing INM computations with one year of aircraft sound levels, measured and matched by DIA's permanent monitoring system (ANOMS). A prior study determined this accuracy for INM Version 5.0.[6] This current study repeats that analysis for later INM versions, to examine the progress made in improving INM accuracy.

- Current Study Examines 4 Versions of INM and Additional Specific Modeling Variations

More specifically, this current study determines INM accuracy for the eight INM modeling methods in Table 1. As the table shows, these modeling methods differ by INM version, atmospheric input, performance coefficients used within INM, and inclusion of the effects of de-rated thrust.

Table 1. INM Modeling Methods

Modeling Method	INM Version	Atmospheric input	Performance coefficients	De-rated thrust
1 (prior study)	5.0	Standard atmosphere	As built into INM	No
2	5.0	Annual average	As built into INM	No
3	5.1a	Annual average	As built into INM	No
4	6.0c	Annual average	As built into INM	No
5	6.2 beta	Annual average	As built into INM	No
6	6.2 beta	Monthly averages	As built into INM	No
7	6.2 beta	Monthly averages	Modified	No
8	6.2 beta	Monthly averages	Modified	Maximum d-rate for the maximum number of departures anticipated

In typical use, INM flies each aircraft along a ground track that is either (1) determined individually by radar or (2) estimated by the noise analyst from dispersed, "core" ground tracks. The first of these methods (radar tracks) was used in this study—to avoid apparent INM inaccuracies actually caused by poor estimation of ground track location.

- Standard INM Methods Used, Except Radar Tracking Data Used for Each Aircraft Operation

However, radar data were not used to determine each aircraft's altitude profile along its track. Instead, INM's built-in algorithms were used for this purpose—the most common modeling practice. As a result, this study tests these "performance" algorithms within INM, which determine that altitude profile from built-in performance procedures and weather input.

In all, the comparisons in this study employ "standard" INM computations. Each aircraft operation was computed from the power, speed and altitude profiles that are built into the INM. No input modifications were made for altitudes or speeds reported by radar. Avoidance of using radar speed and altitude determines INM accuracy when only the flight track, aircraft type and stage length are available as input to INM. In other words, the modeling done here can be considered as the most rigorous modeling possible without developing unique flight profiles for each aircraft type or flight.

- Six aircraft types examined

Sufficient data were available to examine

- B727
- B733 (733, 734, 735)
- B73S
- B757
- DC10
- MD80

1.3 Assessment Metric is INM SEL minus Measured SEL, by Aircraft

This study uses the same assessment metric for INM performance that was used in the previous study.[6] That metric:

- Quantifies the difference between calculated and measured aircraft noise, separately for each aircraft type, and separately for arrivals and departures
- Is relevant to the computation of INM's integrated metrics: Day-Night Average Sound Level (DNL) and its California substitute, the Community Noise Equivalent Level (CNEL).

To satisfy this objective, this study assesses INM accuracy with the so-called INM Offset, defined as:

$$\text{INM Offset} \equiv \left(\text{Energy-average SEL}\right)_{\text{INM}} - \left(\text{Energy-average SEL}\right)_{\text{measured}}, \quad (1)$$

computed separately for each aircraft type and separately for arrivals and departures.

The following sections discuss the components of this equation.

1.3.1 The basic metric: SEL is the Building Block of DNL, CNEL

The basic metric within INM Offset is aircraft Sound Exposure Level (SEL). This SEL metric was chosen because it is the fundamental building block of DNL and CNEL, the most important integrated metrics computed by INM. If computed and measured SELs agree for a given aircraft type/operation, then computed DNL and CNEL contours will agree, as well.

By examining SEL, rather than DNL, comparisons can be made without regard to any specific mix and number of aircraft in the measured noise database. While DNL depends upon the number and type of aircraft, the runways used and flight tracks flown during the year, SEL is independent of these parameters. Therefore, by using SEL the analysis is independent of these parameters and hence can more easily identify and analyze specific computation problems of INM.

In addition, the DNL metric adds all aircraft types and operations together, in proportion to their "energy" contributions. For that reason, only the aircraft types/operations that dominate DNL would contribute to a DNL assessment of INM accuracy. Thus, if only computed and measured DNL were compared, quieter aircraft (or aircraft flying further from monitors) would be ignored in the assessment. These quieter aircraft may well dominate sound levels in the future as louder aircraft types are retired from the fleet. The analysis here of SEL allows assessment of these quieter aircraft types, as well.

1.3.2 The averaged-metric: Examine Energy-average SEL by Aircraft Type

The overall goal is to improve the INM computations of such metrics as DNL and CNEL. Both these metrics are determined by the *energy average* SELs for each aircraft type. Hence, this study assesses INM accuracy by comparing energy average SELs computed by the INM with the energy average SELs measured for each aircraft type.

Note that different aircraft types/operations are not averaged together, as they are for DNL and CNEL, however. Instead, separate energy averages are computed for each aircraft type and each operation type, to allow separate reporting of INM accuracy in these separate categories.

1.3.3 The assessment metric: "INM Offset" – Difference in Energy Average SEL's

Finally, the obvious way to compare the *computed* energy-average SEL with its corresponding *measured* energy-average SEL is to take their difference. By subtracting the measured from the computed values, the INM Offset is then:

- Positive when INM over computes
- Negative when INM under computes.

This subtraction (computed minus measured) appears in Eq. (1), above.

1.4 Important Note – Denver is a High-Altitude Airport

DIA is a high-altitude airport (5431 feet above mean sea level) and therefore is not a typical airport for INM modeling. For that reason, the results of this study should be generalized to airports at lower altitudes with great care. In particular, such generalizations should fully utilize the study's graphical investigations of remaining INM discrepancies in Modeling Method 8. Those investigations indicate to what extent the remaining discrepancies depend upon parameters that are sensitive to airport altitude.

1.5 Overview of the Study - Figure 1

1.5.1 Measured data: Aircraft Sound Levels and Radar Position, Aircraft Type

As shown in the top box of Figure 1, Remote Monitoring Terminal (RMT) data, including one-second equivalent levels (Leq) were combined by ANOMS software with FAA radar data, to identify aircraft noise events in the measurements and to pair each noise event with a specific aircraft flight. For this purpose, the ANOMS software contains sophisticated logic that examines the time-history shape of the one-second Leq's with knowledge of nearby aircraft flights at the time, plus knowledge of source strength by aircraft type and of sound-level reduction due to propagation.

Each event yielded a measured SEL for that flight/RMT pairing. All measured data, plus matching stage lengths from the Official Airline Guide (OAG data), were then stored in the project database. For any aircraft departure, stage length is the distance from DIA to the flight's first destination airport.

A primary assumption of the study is that the measured values of SEL are accurate and representative of the specific aircraft's sound level for the specific operation. The Denver ANOMS system has been previously validated by comparison of its automated results with simultaneous on-

site observations and measurements. During validation testing, these comparisons were used to adjust the parameters that ANOMS uses to identify aircraft noise events and to associate events with specific operations. In addition, acoustic and electronic checks are done automatically four times per day, and each microphone is manually checked each year. Further, all microphones are sent to a laboratory for full calibration every other year.

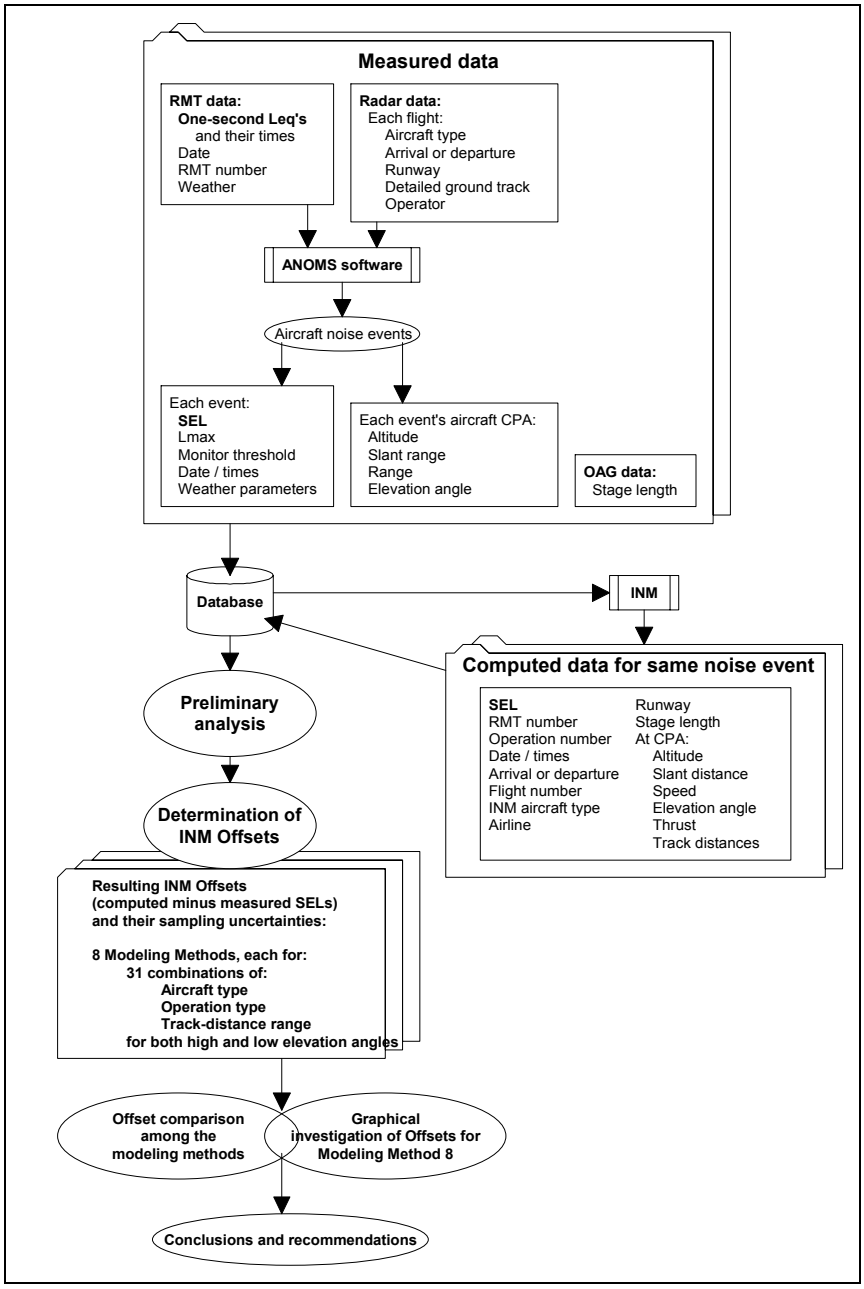


Figure 1. Overview of the study and its products

These validation tests demonstrated that the system works well at matching noise events produced by aircraft with the proper specific aircraft flights. Weaknesses appear, however, in occasionally associating non-aircraft noise events (community noise levels and wind induced noise levels) with aircraft operations. As a result, some incorrect SEL values may be present in the ANOMS database, especially for monitors far from the airport.

1.5.2 Radar Data Used in INM to Compute Individual Aircraft SEL at Each Noise Monitor

As shown center/right in Figure 1, the INM used the collected measured event data (flight track location, aircraft type, arrival / departure, stage length) to compute a matching SEL for each noise event's flight/RMT pair, as well as additional concurrently computed data (such as track distance, slant distance, etc.). All computed data were then stored in the database, as well.

For this study, only operations that are associated with measured noise events were selected. Operations without a measured noise event have no measured SEL, so cannot be used to assess INM computations.

1.5.3 Preliminary analysis: Correct Association of Aircraft Operation with Flight Track

Prior to the actual computation of INM Offsets, data were explored graphically and then cleaned and filtered as required, see report of Endnote 6 and Appendix D.

1.5.4 Determination of INM Offsets: Computed minus Measured SEL by Track Distance

INM Offsets were then determined from the paired set of measured and computed SELs—separately for the eight Modeling Methods in Table 1, above, and separately for the 31 combinations of operation type, aircraft type, and track-distance regime in Table 2.

Table 2. Track-distance regimes by operation and aircraft type

Operation type	Aircraft type	Track-distance regime (000 ft)	Shorthand name
Arrival	All	0 to 20	Low
		20 to 40	Medium
		40 or more	High
Departure	B733	0 to 30	Low
		30 to 50	Medium
		50 or more	High
	B757	0 to 50	Low
		50 or more	High
	B727, B73S, DC10, M80	0 to 60	Low
		60 or more	High

1.5.5 Resulting INM Offsets: The Fundamental Analysis Metric of This Study

These INM Offsets are the main product of this study, compared and investigated in Sections 3 and 4.

1.5.6 Offset comparison among the Modeling Methods

INM Offsets were then compared among the eight INM modeling methods. This comparison indicates the progress (or lack of progress) made by successive INM refinements in improving INM

accuracy for high-altitude airports. Essential to this comparison are the calculated sampling uncertainties, which indicate which changes are likely to be real and which likely to be happenstance.

1.5.7 Graphical investigation of Offsets for Modeling Method 8

In addition, INM Offsets for the most advanced modeling method (Method 8 in Table 1, above) were investigated graphically, using the concurrently measured/computed variables as clues about when and where the largest offsets occur.

1.5.8 Conclusions and recommendations

The study provides conclusions and recommendations for investigation of further improvements to INM.

1.6 Remainder of this Report

This remainder of this report contains the following major sections:

- **Chapter 2: Conclusions and Recommendations**, which contains the results of the study.
- **Chapter 3: INM Offsets**, which graphs and tabulates the INM Offsets.
- **Chapter 4: Offset Comparisons among the modeling methods**, which describes and relates the changes in INM Offset to each INM modeling method, relative to the prior method.
- **Chapter 5: Graphical Investigation of Offsets for Modeling Method 8**, which investigates the INM Offsets that the most advanced modeling method (Modeling Method 8) was unable to resolve—using plots of SEL Offsets (differences between the INM and the measured SEL for each aircraft operation) against the many concurrently measured/computed variables.

Supplementing these major sections are the following appendices:

- **Appendix A: Detailed Tabulations/Graphs of INM Offsets** supplements Section 3.
- **Appendix B: Measured Data** documents the assembly process used for measured sound levels, including a description of monitoring-system operations at DIA and the resulting measured SEL database—its data-collection methods, summary tabulations, and all concurrently measured variables for the analysis.
- **Appendix C: Computed Data** documents INM computation methods and assumptions for the eight modeling methods and for the resulting computed SEL database—including all concurrently computed variables for the analysis.
- **Appendix D: Preliminary Analysis** documents the analysis prior to the actual computation of INM Offsets—required cleaning/filtering of the data.
- **Appendix E: Determination of INM Offsets** documents and discusses the determination of INM Offsets (computed minus measured) and their sampling uncertainties.
- **Appendix F**: Derivation of Propagation Uncertainty, which supplements Appendix E.

2 CONCLUSIONS AND RECOMMENDATIONS

This section contains the study's conclusions and recommendations:

- Section 2.1 identifies improvements provided by three of the modeling methods
- Section 2.2 identifies modeling methods that provided no improvements
- Section 2.3 presents additional conclusions suggested by graphical investigations
- Section 2.4 offers general recommendations for further improvements to INM

Figure 2 locates Conclusions and Recommendations within the study.

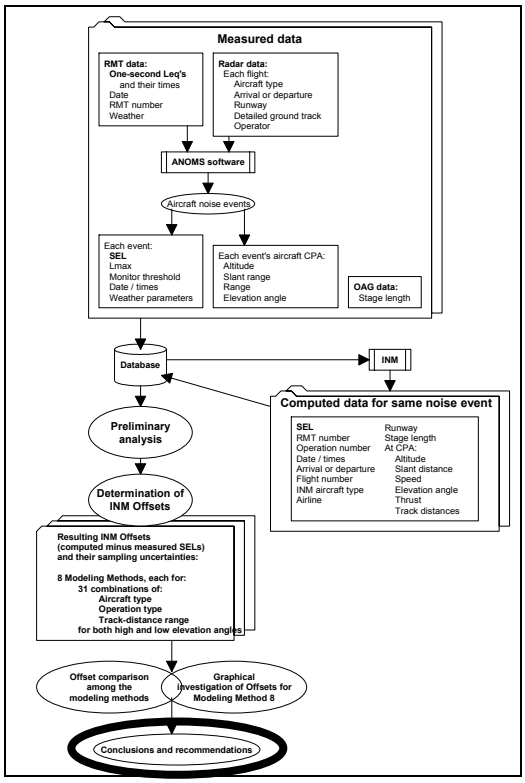


Figure 2. Conclusions and recommendations within the study

2.1 Three of the Modeling Methods Provide Significant Improvements

2.1.1 INM 6.0c (Modeling Method 4) Provides Improvements at High Track Distances

For track distances greater than 50,000 to 60,000 feet from brake release for departures and greater than 40,000 feet from touch-down for arrivals, the INM values are increased and, for all but the B727 resulted in closer agreement with measurements. Fewer significant changes resulted at lower track distances and at these lower distances B727 and B73S INM levels are now higher than measured values for departures. Figure 4 and Figure 5, pages 15 and 16, respectively plot the INM Offsets for each modeling method.

2.1.2 Modeling Method 5 (Accounting for Effects of Wing Mounted Engines and Changes to 757 for Weight and Noise-Power-Distance Relations) Adds Further Improvement

Modeling Method 5 improved the agreement of INM values with measured values at high track distances, (INM Offsets became less negative) for aircraft with wing mounted engines (B733, B73S, B757, DC10). Some minor changes in departure INM Offsets also occurred at lower track distances for elevation angles less than 60 degrees, Figure 4.

2.1.3 Additional Improvements Result from Changes to B733 (CFM563 engine) and M80 (2JT8D2 engine) Performance Coefficients (Modeling Method 7)

At high track distances, for all elevation angles, INM results are significantly improved for both the B733 and M80 departures. The B733 INM departure values for low track distances are now within

±1 dB of the measured values, with 95% confidence, for all elevation angles, Figure 5. See also Figure 26, page 75.

2.2 Other Modeling Methods Produced No Significant Changes in INM Offsets:

- Change from Standard Atmosphere to DIA Annual Average, Model Method 2
- Change from of INM Versions from 5.0 to 5.1a, Modeling Method 3
- Use of Monthly DIA Average Atmospheric Data, Modeling Method 6
- Use of De-rated Takeoff Thrusts for B733, M80, Model Method 8

 Derated thrusts were modeled for aircraft that could use reduced thrust for the given atmospheric conditions. Hence, only a fraction of the departures could use de-rate for any given month. Though the noise effects may have been significant for a single departure, the entire mix of departures of each aircraft type, B733 and M80, showed no significant change in INM Offset, Figure 4, page 15 and Figure 5, page 16.

2.3 Graphical Investigations Suggest Incorrect INM Altitudes as Possible Target for Improvements

2.3.1 Graphical Investigation of Modeling Method 8 Results Showed INM SEL Too Low and INM Altitudes too High Compared with Measurements, Especially at Higher Track Distances

Detailed graphical investigation of Modeling Method 8 results for B733, B757 and M80 confirmed that:

- INM SEL values were generally lower than the measured SEL and became more so for higher track distances ("SEL offset" – INM SEL minus measured SEL - less than zero), see Figure 8, Figure 9 and Figure 10, pages 27, 28 and 29
- INM altitudes were different from the radar altitudes and generally higher. This difference was explored using the ratio of the INM altitude to the radar altitude, called "altitude ratio", see Figure 11, Figure 12 and Figure 13 pages 30 and 31

2.3.2 INM SEL Values a Better Match with Measured Levels when INM Altitudes / Slant Distances Match Measured Altitudes / Slant Distances

- INM SEL values tend to better match measured SEL when the altitude ratio is one.

 When SEL offset is plotted *versus* altitude ratio, for several combinations of aircraft type, track distance and arrival or departure operation, the SEL offset tends toward zero for altitude ratios of one (where INM altitude equals the measured altitude), see Figure 14, Figure 15 and Figure 16, pages 32 and 33.
- INM SEL values "corrected" for altitude / distance, generally compare more closely with measured SEL values

The INM was run to yield SEL drop-off with distance curves; see for example Figure 17 on page 34. These relationships were then use to compute a "distance corrected SEL offset" as plotted in Figure 19, Figure 20 and Figure 21 on pages 36, 37 and 38, respectively.

- Improved agreement of INM SEL and measured SEL is also apparent for different departure stage lengths

 Plotting of "distance corrected SEL offset" by stage length for the B733, B757 and M80 departures shows marked improvement across all stage lengths for the B733 and B757. See Figure 22, page 40.

- Application of "distance correction" to all aircraft INM SEL shows improvement of INM offset at high track distances for departures, but mixed results for other track distances and for arrivals

 The full set of INM offsets were determined for Modeling Method 8 and plotted as Modeling Method 8* in Figure 23 and Figure 24 on pages 41 and 42.

2.4 Recommend Detailed Investigations

2.4.1 Departures – INM Considerably Improved but Has Departure Climbs Too Rapid

The different modeling methods have resulted in significant improvements of INM computed SEL in comparison with measured SEL. However, additional improvement appears possible. Graphical investigations show that increases in INM SEL comparable to the increases that would be produced by lower climb rates may reduce or eliminate many differences between INM computed and measured values of SEL. Further investigation should include at least:

- Clear identification of all INM algorithms that determine climb rate and associated variables
- Acquisition of a new database with current fleet mixes at sea-level airports
- Collection of gate-weight of aircraft and other variables needed by INM
- Statistical testing of new database to identify which variables have most influence on climb rates and resultant SEL values; examination of theoretical basis for influential variables and modification of assumptions, as appropriate to correct remaining non-zero INM offsets
- Development of "energy-average" departure profiles that minimize altitude error

 Because aircraft altitudes are widely distributed, the lower, louder flight tracks will strongly influence levels on the ground and arithmetic averages cannot account for this influence.

2.4.2 Arrivals – New Modeling Method Needed

None of the modeling methods provided significant improvement in the INM Offsets for arrivals. The adjustments for altitude / slant distance suggested by the graphical investigation also had little effect. The highly variable altitudes and variable use of thrust on approach mean that the current modeling method of continuous approach is too simplistic. New approaches to analysis of approach measurement data and to approach modeling are necessary.

3 INM OFFSETS

This section contains the INM Offsets that were determined with the methods of Appendix E and Appendix F, below:

- Section 3.1summarizes the number of INM Offsets that were determined.
- Section 3.2 graphs and tabulates the full set of INM Offsets.
- Section 3.3 summarizes all "confidently large" INM Offsets.
- Section 3.4 introduces the other sections of this report.

Figure 3 locates Resulting INM Offsets within the study.

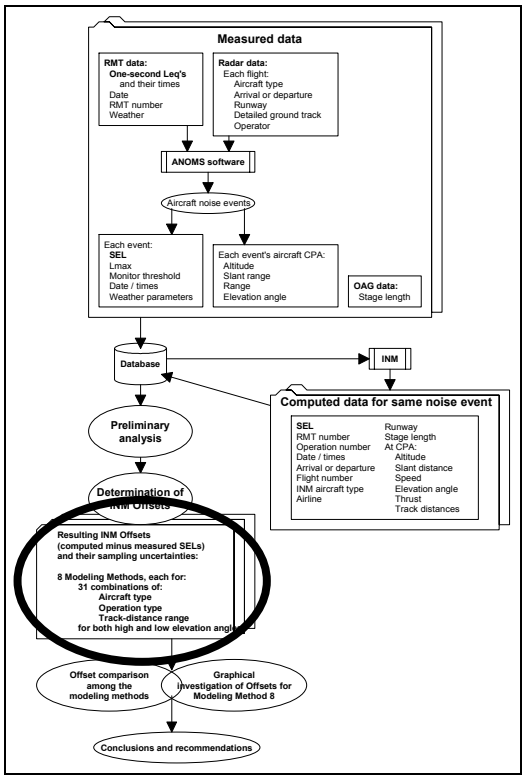


Figure 3. Resulting INM Offsets within the study

3.1 Number of INM Offsets That Were Determined

INM Offsets were separately determined for two elevation-angle intervals (below and above 60 degrees), combined with two operation types (arrivals and departures), combined with six aircraft types (B727, B733, B73S, B757, DC10, M80), combined with three track-distance regimes (low, medium and high), for each of eight modeling methods—for a total of 496 offset values.

Table 3 defines the track-distance regimes, while Table 4 defines the modeling methods.

Table 3. Track-distance regime by operation and aircraft type

Operation	Aircraft type	Track-distance regime (000 ft)	Shorthand name
Arrival	All	0 to 20	Low
		20 to 40	Medium
		40 or more	High
Departure	B733	0 to 30	Low
		30 to 50	Medium
		50 or more	High
	B757	0 to 50	Low
		50 or more	High
	B727, B73S, DC10, M80	0 to 60	Low
		60 or more	High

Table 4. INM Modeling Methods

Modeling Method	INM Version	Atmospheric input	Performance coefficients	De-rated thrust
1 (prior study)	5.0	Standard atmosphere	As built into INM	No
2	5.0	Annual average	As built into INM	No
3	5.1a	Annual average	As built into INM	No
4	6.0c	Annual average	As built into INM	No
5	6.2 beta	Annual average	As built into INM	No
6	6.2 beta	Monthly averages	As built into INM	No
7	6.2 beta	Monthly averages	Modified	No
8	6.2 beta	Monthly averages	Modified	Maximum d-rate for the maximum number of departures anticipated

3.2 Full Set of INM Offsets and Confidence Ranges Summarized

Figure 4 and Figure 5 graph the full set of all INM Offsets—for elevation angles below and above 60 degrees, respectively.

These two figures are organized as follows:

- **Frames.** Arrivals appear in the upper frame of each figure, while departures appear in the lower frame.
- **Track distances.** In each frame, track-distance regimes (low, medium and high) are grouped from left to right across the page. See Table 3, above, for definitions of these track-distance regimes.
- **INM modeling methods.** Within each track-distance regime, results appear separately for the eight INM modeling methods of this study. See Table 4, above, for definitions of these modeling methods.
- **Aircraft types.** The figure's key distinguishes among the study's six aircraft types.
- **Emphasized symbols.** For this study, "small" effects are those that lie in the region between –1dB and +1dB—in other words, "within one decibel of zero." In contrast, "confidently large" effects are those that are outside this small-effect region, with 95% confidence.
 - **Doubled symbols.** Doubled symbols show "confidently large" values of INM Offset.

 For example, in the upper frame of Figure 4, the lowest right-most point (high track distance) has a doubled symbol, showing that INM Offset to be "confidently large." Numerically, that offset's value and 95% confidence range is (–8.8 ± 1.7) dB. Clearly this offset and range lies outside the small-effect region of (0 ±1) dB.

 As is apparent from the figure, most points that lie far above or far below the zero line have doubled symbols. But exceptions do exist. For example, in the same frame of the same figure, the lowest left-most point (low track distance) *does not* have a doubled symbol. Numerically, that offset's value and 95% confidence range is (–2.3 ± 3.7) dB, which *does not* lie totally outside the small-effect region of (0 ±1) dB. In fact, it even encompassed zero. That offset of –2.3dB is therefore only "apparently large," not "confidently large."

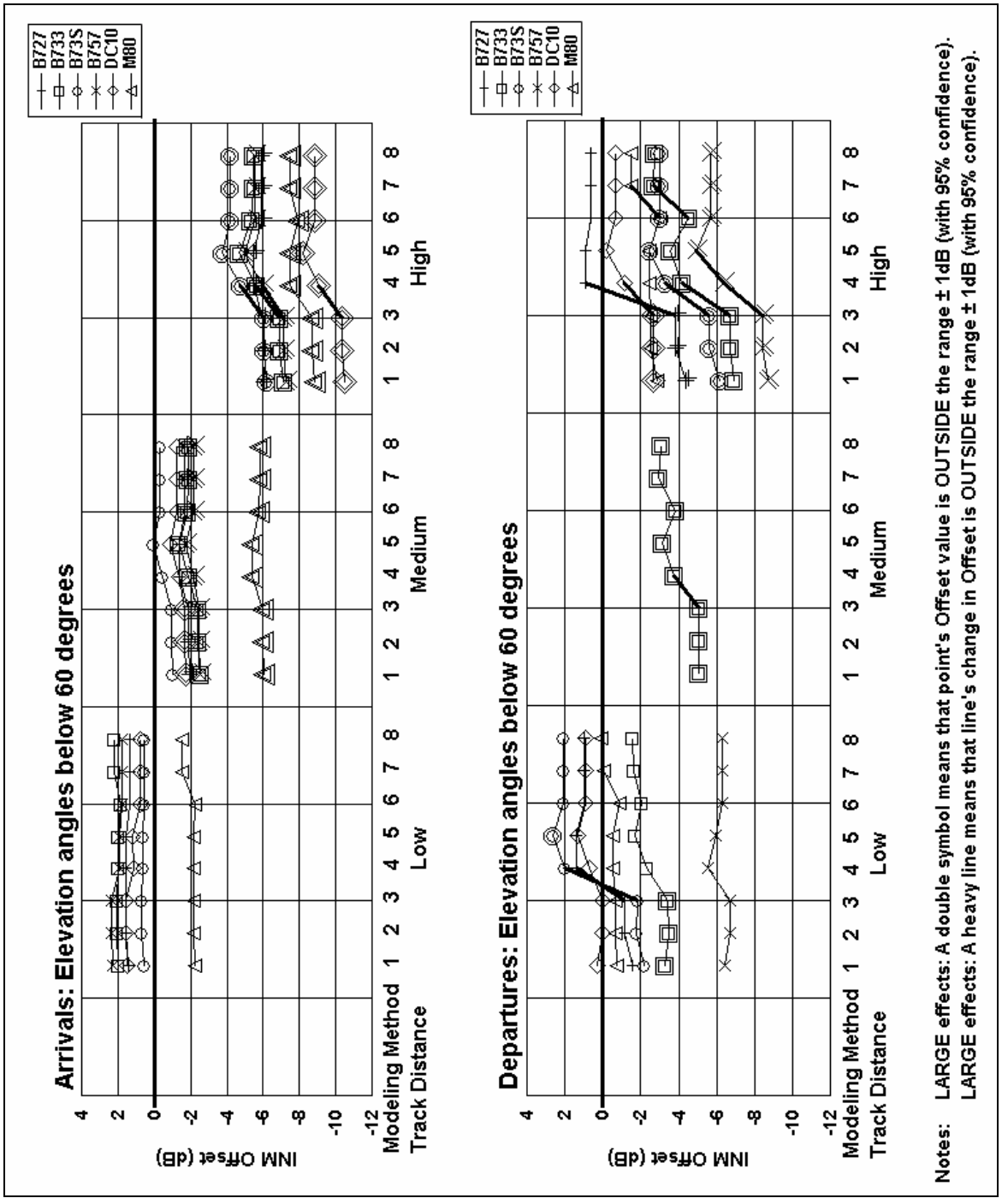


Figure 4. INM Offsets: Elevation angles below 60 degrees

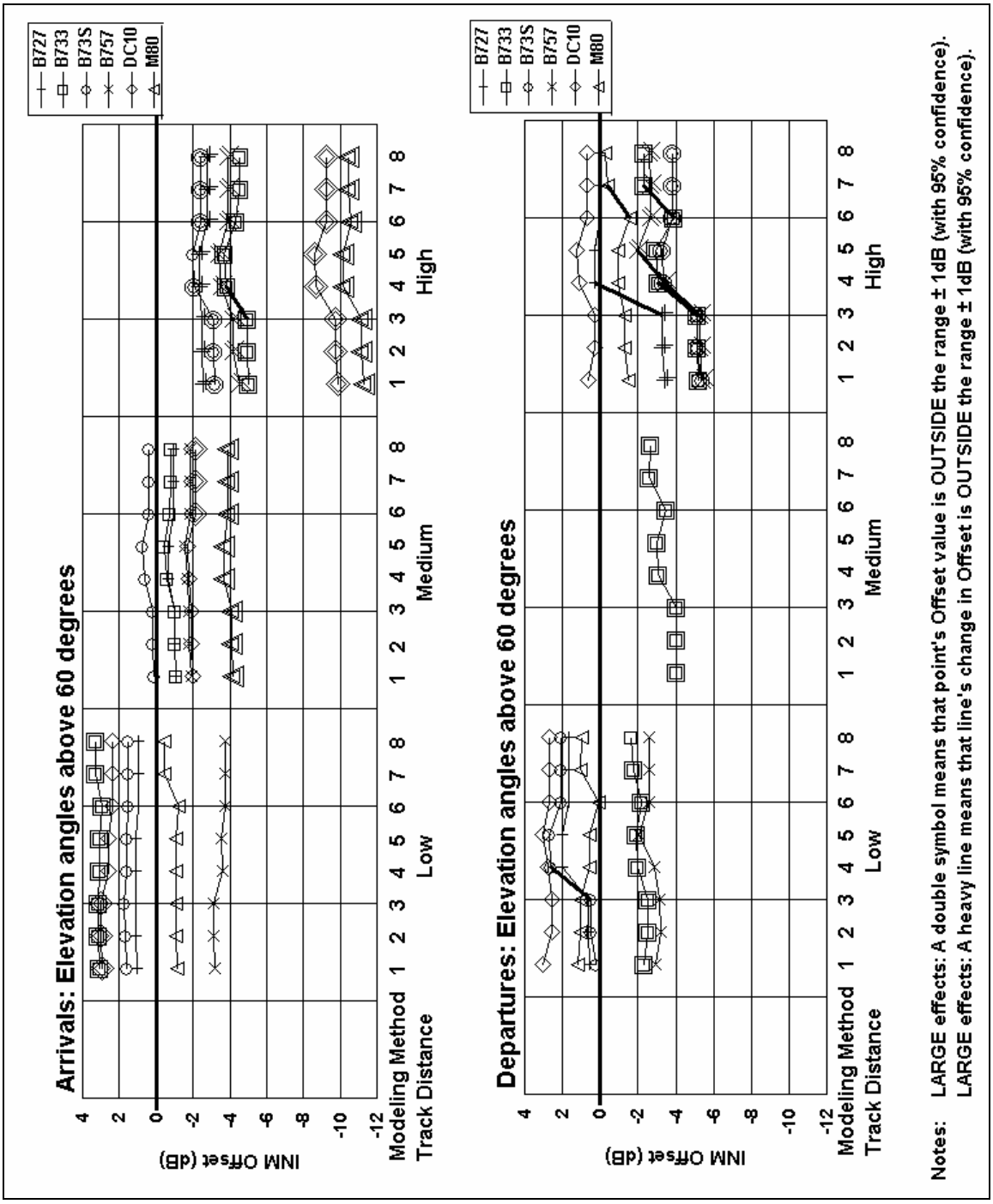


Figure 5. INM Offsets: Elevation angles above 60 degrees

- **Heavy line segments.** Heavy line segments show "confidently large" *changes* between modeling methods. For example, in the same figure and frame, the lower-right set of points contains one heavy line segment, showing that change in offset (Modeling Method 3 to Modeling Method 4) to be "confidently large." Numerically, that change's value and 95%

confidence range is (+1.33 ± 0.30)dB, which lies totally outside the small-effect region of change, (0 ±1) dB.

In contrast, the line segment just above that one is *not* heavy. Numerically, that change's 95% confidence range is (+1.3 ± 0.4) dB, which *does not* lie totally outside the small-effect region of change (0 ±1) dB.

These two figures are repeated in Appendix A, but with emphasized symbols for "confidently small" effects—that is, effects that lie *inside* the region between –1dB and +1dB, with 95% confidence.

3.3 Tabular Summary of All "Confidently Large" INM Offsets

Table 5 and Table 6 summarize all "confidently large" INM Offsets, separately by elevation angle.

Table 5. Summary of "confidently large" INM Offsets: Elevation angles below 60 degrees

Operation	Track distance regime	Aircraft type						INM Offsets + means INM over-computes – means INM under-computes		Comments (MM means Modeling Method)
		B727	B733	B73S	B757	DC10	M80	Modeling Method	INM Offset	
Arrivals	Low							————	————	No large effects
	Medium	x	x		x			All	–2 dB	————
						x		1, 2, 3	–2 dB	No large effects for other MMs
							x	All	–6 dB	————
	High	x	x	x	x			1, 2, 3 4, 5, 6, 7, 8	–6 to –7 dB –4 to –6 dB	MM4 improved 1-to-2dB
						x		1, 2, 3 4, 5, 6, 7, 8	–11 dB –9 dB	MM4 improved more than 1dB
							x	1, 2, 3 4, 5, 6, 7, 8	–9 dB –8 dB	MM4 improved ≈1dB
Departures	Low	x						————	————	MM4 swapped from ≈ –1dB to ≈+1dB, for no net improvement
			x					1, 2, 3	–3 to –4 dB	————
				x				4, 5, 6	+2 dB	MM4 swapped from ≈ –2dB to ≈+2dB, for no net improvement
	Medium		x					1, 2, 3 4, 5, 6, 7, 8	–5 dB –3 to –4 dB	MM4 improved more than 1dB
	High	x						1, 2, 3 4, 5, 6, 7, 8	–4 dB ≈ 0 to +1 dB	MM4 improved 5dB, of which 4dB is an improvement
			x	x				1, 2, 3 4, 5, 6 7, 8	–6 to –7 dB –3 to –4 dB –2 to –3 dB	MM4 improved 3dB MM7 improved 1-to-2dB
					x			1, 2, 3 4 5, 6, 7, 8	–8 to –9 dB –6 to –7 dB –5 to –6 dB	MM4 improved 2dB MM5 improved 1-to-2dB
						x		1, 2, 3 4, 5, 6, 7, 8	–3 dB ≈ –1 dB	MM4 improved 1-to-2dB
							x	1, 2, 3, 4, 5, 6 7, 8	≈ –3 dB ≈ –2 to ≈ –1 dB	MM7 improved 1-to-2dB

Table 6. Summary of "confidently large" INM Offsets: Elevation angles above 60 degrees

Operation	Track distance regime	Aircraft type						INM Offsets + means INM over-computes – means INM under-computes		Comments (MM means Modeling Method)
		B727	B733	B73S	B757	DC10	M80	Modeling Method	INM Offset	
Arrivals	Low		x					All	+3 dB	————
						x		1, 2, 3	+3 dB	Higher MMs not confidently above +1dB
	Medium					x		6, 7, 8	–2 dB	Lower MMs not confidently below –1dB
							x	All	–4 dB	————
	High	x		x				All	–2 to –3 dB	————
			x		x			All	–4 to –5 dB	MM4 improved 1dB for B733
						x	x	All	–9 to –11 dB	————
Departures	Low		x					All	–2 dB	————
				x				————	————	MM4 degraded 2dB
	Medium		x					All	–3 to –4 dB	————
	High	x						1, 2, 3 4, 5, 6, 7, 8	–3 dB ≈ 0 dB	MM4 improved 3dB
			x					1, 2, 3 4, 5, 6 7, 8	–5 dB –3 dB –2 dB	MM4 improved 2dB MM7 improved 1dB
				x				1, 2, 3 4, 5, 6, 7 8	–5 dB –4 dB	MM4 improved 1dB
					x			1, 2, 3 4, 5, 6 7, 8	–5 dB –3 dB –2 dB	MM4 improved 2dB MM5 improved 1dB
							x	————	————	MM7 improved 1dB

These two tables contain mainly "confidently large" effects. Some smaller values are included, however, when they are needed to complete an entry. These less-confident values are tagged with the "approximately equal" symbol (≈).

3.4 Other Sections of this Report that Examine the Offsets

- Section 4: Offset comparisons among the modeling methods
- Section 5: Graphical investigation of Offsets for Modeling Method 8 (the most advanced method).

4 OFFSET COMPARISONS AMONG THE MODELING METHODS

This section links modeling-method changes to the resulting changes in INM Offsets.

- Section 4.1 summarizes all modeling-method changes.
- Section 4.2 shows the resulting changes in INM Offset that are produced by Modeling Methods 2 through 8.
- Section 4.3 leads into other sections of this report.

Figure 6 locates Offset Comparisons within the study.

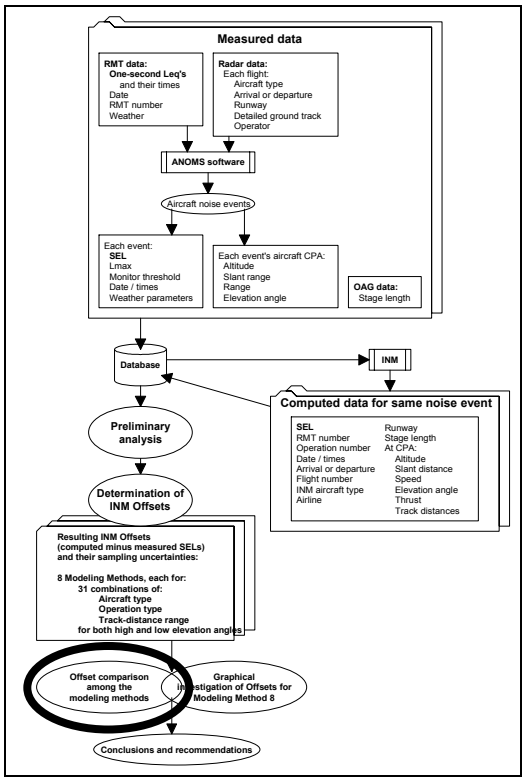


Figure 6. Offset comparisons within the study

4.1 Summary of All Modeling-Method Changes Shown in Table 7

Table 7 details all the modeling-method changes that might affect this study's INM computations, including internal changes to INM.

The first two columns of the table identify the specific change in modeling method—for example, from 1 to 2. The next three columns summarize the changes in atmospheric input, performance coefficients and de-rated thrust. These changes match the entries in Table 4, above.

The last column summarizes the internal changes to INM—but only those that would likely affect the INM computations of this study. As is obvious, most of these internal INM changes occurred with Modeling Method 4, which switched INM versions from 5.1a to 6.0c.

The following INM changes had no likelihood of affecting this study's INM computations. For this reason, these changes do not appear in Table 7:

- Incorporation of terrain—because terrain input was not used in this study.
- NPD curves separately interpolated/extrapolated for approach vs departure, with (1) reverse thrust linked to departure NPDs, and (2) level/descending/decelerating segments linked to approach NPDs—because none of the NPD curves for the selected aircraft have changed between INM versions used in this study.
- New coefficient for high temperature max-climb and max-takeoff. This new coefficient was only added to the 727Q15 and is only used above 86 degrees F—because no months in this study have an average temperature this high.

Table 7. Detailed changes between modeling methods

Change in modeling method		Change in atmospheric input	Change in performance coefficients	Change in de-rated thrust	Internal changes to INM (only those that affect this study's INM computations) Note: Numbers link with Table 8 through Table 10.
From	To				
1	2	Changed from standard atmosphere to annual DIA average	————	————	————
2	3	————	————	————	**Changed from 5.0 to 5.1a**, with this relevant revision: 1. Noise level behind take off up approx. 1dB
3	4	————	————	————	**Changed to 6.0c**, with these relevant revisions: **Affects Arrivals and Departures** 2. Spectral classes now included. 3. NPD curves now account for input atmospherics, 4. Non-standard pressure ratio revised. 5. Noise exposure fraction algorithm revised. **Affects Departures only** 6. Altitude profiles now account for each runway's specific headwind. 7. Departure thrust now has temperature break point and reduced thrust at high altitudes and temps. 8. Climb and acceleration algorithms revised. **Affects Specific Aircraft, Specific Operations** 9. Altitude profiles for 727s now use procedure steps. 10. Flap coefficients changed for some 727s, some 757s. 11. Jet coefficients changed for some 727s, some 737s. 12. Takeoff roll now subdivided into 6 segments, and first-climb portion into 3 segments.
4	5	————	————	————	**Changed to 6.2 beta**, with these relevant revisions: 13. Lateral attenuation changed for jets with wing-mounted engines. 14. B757 departure and approach changes, to account for increased allowable takeoff weight. 15. B757 NPDs updated.
5	6	Changed to monthly DIA averages	————	————	————
6	7	————	Modified for: B733, M80	————	————
7	8	————	————	Added for: B733, M80	————

- All changes that affect only SEL values near runway: Speeds revised for start-of-takeoff-roll, NPD upper extrapolation limit removed near the start-of-takeoff-roll, approaches no longer have ground-based directivity adjustment during the landing-roll segment.

4.2 Resulting Changes in INM Offset

The following subsections discuss the effects of these modeling changes on INM Offset. These effects appear graphically in Figure 4 and Figure 5, above, and in detail in Appendix Section A.1.2, page 54 below. All numerical values are from the appendix.

4.2.1 No Significant Changes produced by Modeling Method 2, Annual Ave. Atmosphere

Modeling Method 2 substituted annual-average atmospherics at DIA for the standard-atmosphere values used in the prior method. This substitution resulted in no changes in INM Offset that were confidently larger than 1 decibel. Numerically, the largest change was (+0.6 ± 0.0) dB—for B727 departures, low elevation angles, track distances of 60,000 ft or more.

4.2.2 No Significant Changes produced by Modeling Method 3, Version 5.0 to 5.1a

Modeling Method 3 changed INM versions from 5.0 to 5.1a, which increased noise levels behind take off by approximately 1dB. That change resulted in no changes in INM Offset confidently larger than 1 decibel. Numerically, all computed changes equaled 0.0 dB, to the nearest one-tenth decibel.

4.2.3 Many Significant Changes produced by Modeling Method 4, Version 5.1a to 6.0c

Table 8 contains the "confidently large" changes in INM Offset produced by Modeling Method 4.

The first four columns of the table show the specific modeling conditions: elevation angle, operation, aircraft type, and track-distance regime. The three right columns document the resulting changes in INM Offset, plus comments on those changes.

For example, the fifth row of the table pertains to:

- Elevation angles below 60 degrees
- Departures
- B727 aircraft
- Low track distances (0 to 60,000 feet, per Table 3, above).

For these modeling conditions, the table shows a change of (+2.5 ± 0.2) dB. However, this change did not make the INM offset "better," as the comment column shows. Instead, this change shifted the INM Offset from under-computation to over-computation—that is, from negative to positive. Numerically, the offset shifted from (–1.2 ± 0.7) dB to (+1.4 ± 0.8) dB.[7] This same "shifting" occurs one other place in the table, as well.

The sixth column of the table shows that nearly all the changes made INM better – the computed results are closer to the measured levels and the INM offsets closer to zero.

The right-most column of Table 8 links specific INM-offset changes to their potential causes—to specific changes in the modeling method. For example, the first four table entries link to potential causes two through five in Table 7. These INM changes are potential causes of the improvements introduced by Modeling Method 4.

These linkages between INM changes and specific improvements in INM Offsets are only speculative. They denote those changes within INM that might possibly cause the INM-offset changes. This study, however, has not determined these potential cause-and-effect relations to be a certainty.

Table 8. Confidently large changes in INM Offset produced by Modeling Method 4

1 Elevation angle	2 Operation	3 Aircraft type	4 Track-distance regime	Confidently large changes in INM Offset		
				5 Change ± 95% confidence	6 Better or worse	7 Potential causes (item numbers in Table 7, right column)
Below 60 degrees	Arrivals	B733	High	+1.4 ± 0.1	Better	2–5
		B73S	High	+1.3 ± 0.1	Better	
		B757	High	+1.2 ± 0.2	Better	
		DC10	High	+1.3 ± 0.3	Better	
	Departures	B727	Low	+2.5 ± 0.2	Shifted from under- to over-computation	2–12
			High	+4.8 ± 0.2	Better	2–11
		B733	Low	+1.3 ± 0.0	Better	2–8, 12
			High	+2.5 ± 0.0	Better	2–8
		B73S	Low	+3.8 ± 0.9	Shifted from under- to over-computation	2–8, 12
			High	+2.4 ± 0.0	Better	2–8
		B757	High	+2.1 ± 0.0	Better	
		DC10	High	+1.5 ± 0.1	Better	
Above 60 degrees	Arrivals	B733	High	+1.1 ± 0.0	Better	2–5
	Departures	B727	High	+3.6 ± 0.2	Better	2–11
		B733	High	+2.1 ± 0.0	Better	2–8
		B73S	Low	+2.1 ± 0.6	Worse (increased the over-computation)	2–8, 12
			High	+1.8 ± 0.0	Better	2–8
		B757	High	+1.8 ± 0.0	Better	

4.2.4 Limited Changes produced by Modeling Method 5, Version 6.0c to 6.2 Beta

Modeling Method 5 produced a relatively small list of internal changes to INM (Table 7, above). Table 9 contains the confidently large changes in INM Offset produced by Modeling Method 5.

Table 9. Confidently large changes in INM Offset produced by Modeling Method 5

1 Elevation angle	2 Operation	3 Aircraft type	4 Track-distance regime	Change in INM Offset		
				5 Change ± 95% confidence	6 Better or worse	7 Potential Causes (item numbers in Table 7, right column)
Below 60 degrees	Departures	B757	High	+1.5 ± 0.0	Better	13–15
Above 60 degrees	Departures	B757	High	+1.4 ± 0.0	Better	14–15

The first four columns of the table show the specific modeling conditions: elevation angle, operation, aircraft type, and track-distance regime. The three right columns document the resulting changes in INM Offset, plus comments on those changes.

In the sixth column of the table, note that all the changes made INM better—specifically, the INM Offset started out negative and shifted upwards (closer to zero) by more than 1 decibel.

The right-most column of Table 9 links specific INM-offset changes to their causes—that is, to specific changes in the modeling method. For this modeling method, these linkages are quite certain.

4.2.5 Little Change produced by Modeling Method 6, Use of Monthly Ave. Atmospherics

Modeling Method 6 changed from annual-average to monthly average DIA atmospherics. That change resulted in no changes in INM Offset that were confidently greater than 1 decibel. The largest change was (–1.0 ± 0.1) dB—for B757 departures, both low and high elevation angles, track distances of 50,000 ft or more.

4.2.6 Significant Changes produced by Modeling Method 7, New B733, MD80 Coefficients

Table 10 contains the confidently large changes in INM Offset produced by Modeling Method 7.

Table 10. Confidently large changes in INM Offset produced by Modeling Method 7

1 Elevation angle	2 Operation	3 Aircraft type	4 Track-distance regime	Change in INM Offset		
				5 Change ± 95% confidence	6 Better or worse	7 Cause
Below 60 degrees	Departures	B733	High	+1.9 ± 0.1	Better	Modified performance coefficients
		M80	High	+1.6 ± 0.2	Better	
Above 60 degrees	Departures	B733	High	+1.6 ± 0.0	Better	
		M80	High	+1.2 ± 0.1	Better	

The new performance coefficients for the two aircraft types clearly produced improvements in the computed levels *versus* the measured levels.

4.2.7 No Changes produced by Modeling Method 8, Maximum use of De-rated Thrust

Modeling Method 8 added the effects of de-rated takeoff thrust for B733 and M80 aircraft. That new INM capability resulted in no changes in INM Offset that were confidently greater than 1 decibel. All changes were between +0.1 dB and –0.1 dB.

Note that the percentages of aircraft using de-rated thrust was limited to those aircraft weights that could safely use de-rate for the given atmospheric conditions. Thus, not all aircraft of either type would use de-rate on any particular day.

4.3 Additional Details

Additional details concerning INM Offsets appear in:

- Section 5: Graphical investigations of Offsets for Modeling Method 8 (the most advanced method).

5 GRAPHICAL INVESTIGATION OF OFFSETS FOR MODELING METHOD 8

This section graphically investigates the remaining INM Offsets for Modeling Method 8, the most advanced method in this study. In particular:

- Section 5.1 repeats INM Offsets for Modeling Method 8, as a starting point for the graphical investigation.
- Section 5.2 graphically investigates INM Offsets for B733, B757 and M80 aircraft—those aircraft that are both widely used and the modeling of which has been most modified for this study. This investigation focuses on elevation angles above 60 degrees—those conditions affected least by wind direction/speed and temperature gradients. In brief, this section shows that:
 - INM under-computes SELs at high track distances.
 - INM over-computes altitudes at these same track distances.
 - Incorrect altitudes potentially explain incorrect SELs.
 - INM SELs can be adjusted by spreadsheet to "correct" all aircraft altitudes.
 - Such adjustments significantly improve INM SELs.
 - The same adjustments eliminate apparent stage-length effects.
- Section 5.3 documents INM Offsets, after adjustment for proper aircraft altitude—for all study aircraft, all track distances, and all elevation angles.
- Section 5.4 documents factors with no apparent effect on INM Offset.
- Section 5.5 suggests limitations of these graphical investigations

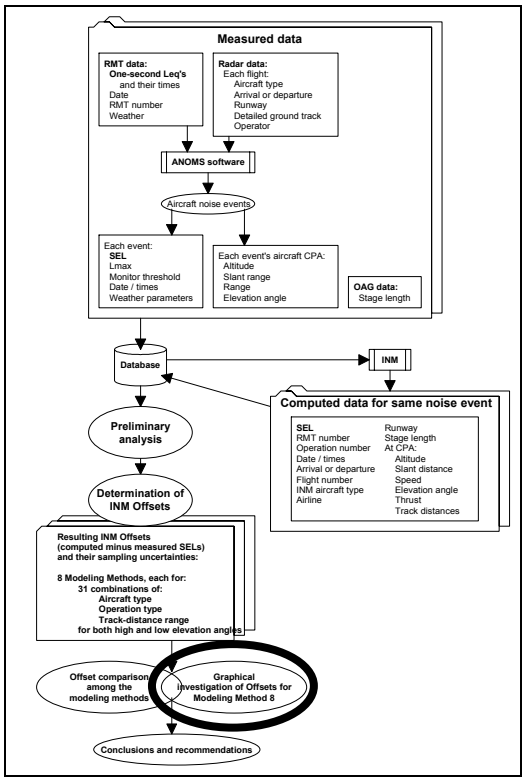


Figure 7. Graphical investigation of offsets within the study

Figure 7 locates graphical investigation of offsets within the study.

5.1 The Starting Point: INM Offsets that Result from Modeling Method 8

Table 11 contains all the confidently large INM Offsets for Modeling Method 8, including their 95% confidence regions. This table is the starting point for the graphical investigations of this section. With one exception, these offsets are all negative—ranging from –10.4 to +3.3 dB, and averaging –4.1 dB.

Table 11. Confidently large INM Offsets for Modeling Method 8

Elevation angles	Operation	Track distance regime	Aircraft type						INM Offsets (dB) ± 95% confidence + means INM over-computes – means INM under-computes
			B727	B733	B73S	B757	DC10	M80	
Above 60 degrees	Arrivals	Low		x					+3.3 ± 0.4
		Medium					x		–2.1 ± 1.1
								x	–3.9 ± 0.5
		High	x						–2.8 ± 1.0
				x					–4.5 ± 2.5
					x				–2.4 ± 1.0
						x			–3.9 ± 1.3
							x		–9.2 ± 1.5
								x	–10.4 ± 5.2
	Departures	Medium		x					–2.7 ± 0.9
		High		x					–2.3 ± 0.3
					x				–3.8 ± 0.5
						x			–2.6 ± 0.5
Below 60 degrees	Arrivals	Medium	x						–1.7 ± 0.5
				x					–1.9 ± 0.3
						x			–2.1 ± 0.6
								x	–5.8 ± 2.1
		High	x						–5.9 ± 2.1
				x					–5.5 ± 1.1
					x				–4.2 ± 1.3
						x			–5.6 ± 1.6
							x		–8.8 ± 1.7
								x	–7.5 ± 3.0
	Departures	Medium		x					–3.1 ± 0.6
		High		x					–2.7 ± 1.2
					x				–3.0 ± 0.6
						x			–5.7 ± 3.0

These values and confidence ranges derive from detailed tables in Appendix A. Values that are not "confidently large" appear in that appendix, as well.

5.2 Graphical Investigations of B733, B757 and M80 Aircraft, for Elevation Angles Above 60 Degrees

Although the computation of INM Offsets is analytical, the investigations here are graphical. In the sections that follow, these investigations show that:

- INM under-computes SELs at high track distances.
- INM over-computes altitudes at these same track distances.
- Incorrect altitudes potentially explain incorrect SELs.
- INM SELs can be adjusted by spreadsheet to "correct" all aircraft altitudes.

- Such adjustments significantly improve INM SELs.
- The same adjustments eliminate apparent stage-length effects.

5.2.1 INM under-computes SELs at high track distances

Table 11 shows that most INM Offsets for Modeling Method 8 are negative for high track distances. Figure 8 shows this pattern graphically for B733 aircraft. In the figure, each point represents a single noise event—that is, a single aircraft flyover at a single RMT. The distance along the aircraft ground track to the aircraft's point of closest approach to the RMT is plotted horizontally. The "SEL offset" for that noise event is plotted vertically:

$$\text{SEL offset} \equiv (\text{SEL})_{\text{INM}} - (\text{SEL})_{\text{measured}} \quad \text{for each noise event.} \tag{2}$$

With this order of subtraction:

- SEL offset is positive when INM over-computes.
- SEL offset is negative when INM under-computes.

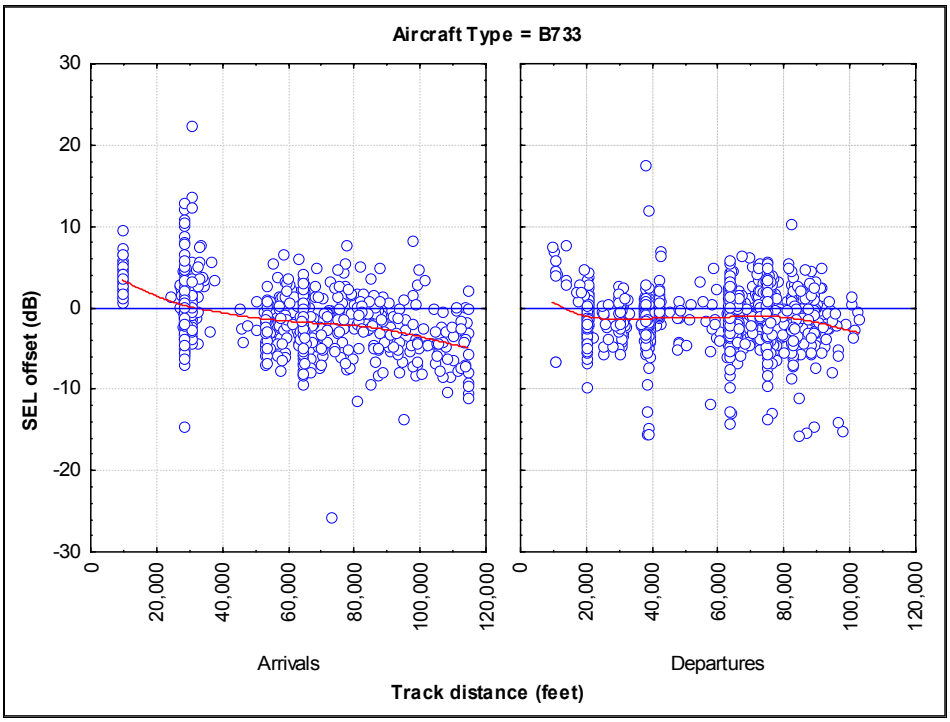


Figure 8. INM under-computes SELs at moderate-to-high track distances: B733

Note that SEL offset pertains to just one noise event, whereas INM Offset—Eq. (1), above—is energy averaged over all noise events.

In each frame of this figure, the curve through the data points follows the general pattern of points—"falling" downward to the right—especially for arrivals in the left frame. For arrivals, the curve falls from an SEL offset of +4 dB at the left, to –5dB at the right.

Figure 9 and Figure 10 are the same as Figure 8, except they are for B757 and M80 aircraft. The same falling pattern is apparent in these additional figures, as well. Again, the pattern is stronger for arrivals than for departures. Moreover, similar patterns appear on comparable graphs for B727, B73S and DC10 aircraft.

In summary, INM under-computes SELs at high track distances for all aircraft types in the study, except for M80 departures. This is apparent from the individual-aircraft data points of these figures and also apparent from the INM Offset values (

Table 11), which are energy averaged over all these data points.

Can INM under-computation be graphically associated with other parameters? The next two sections show that it can.

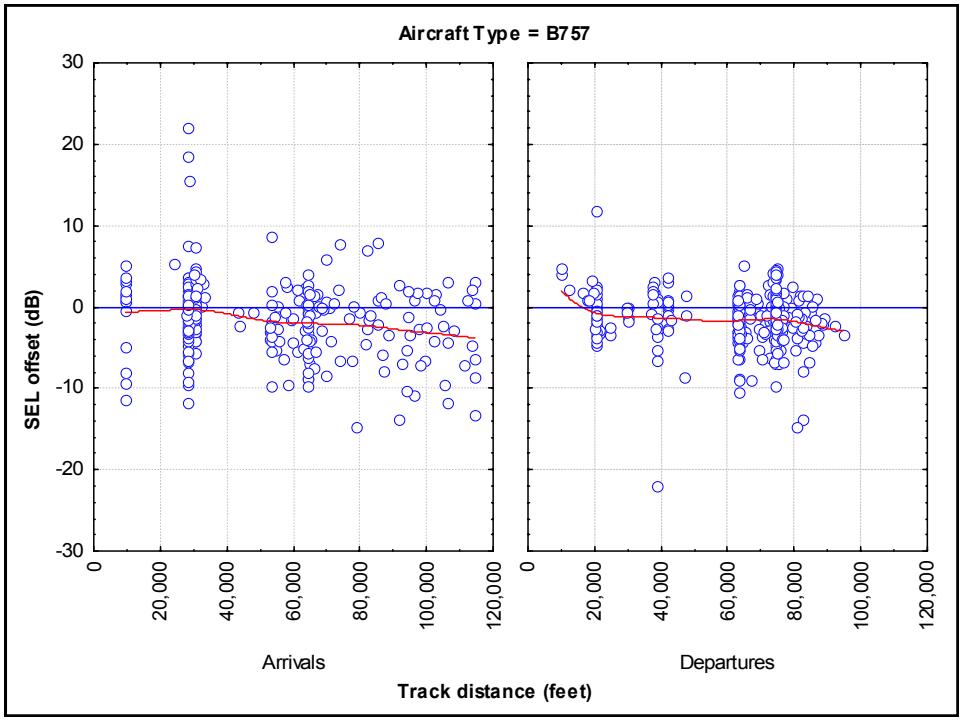


Figure 9. INM under-computes SELs at moderate-to-high track distances: B757

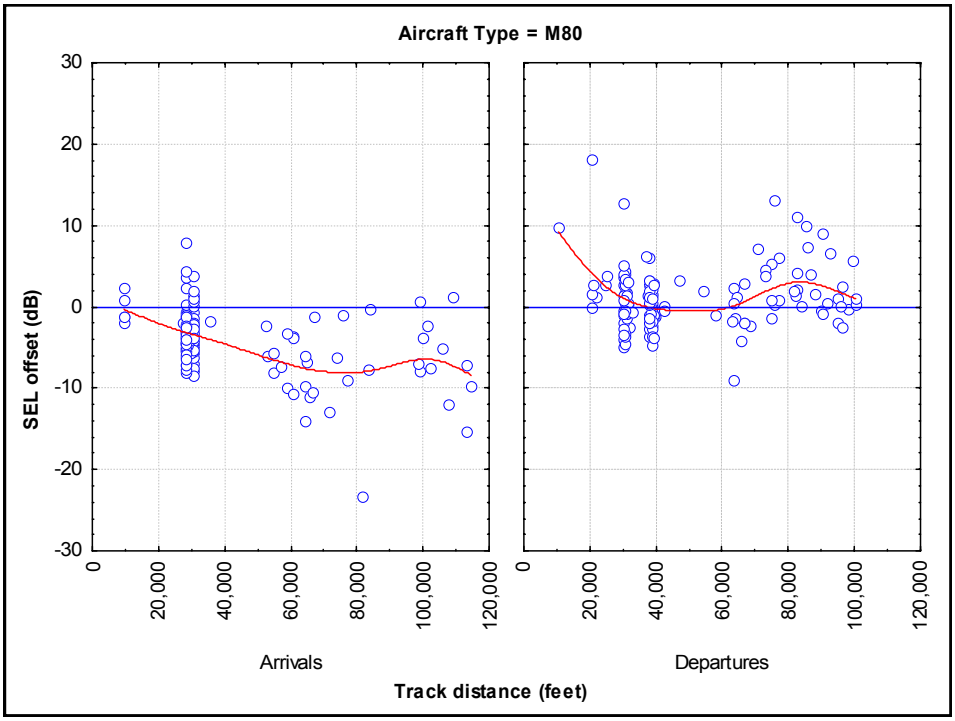


Figure 10. INM both under- and over-computes SELs for arrivals and departures, respectively: M80

5.2.2 INM over-computes altitudes at these same track distances

The next set of graphs, Figure 11 through Figure 13, mimic the preceding graphs except they plot "altitude ratio" vertically, instead of SEL offset:[8]

$$\text{Altitude ratio} \equiv \frac{(\text{Altitude})_{\text{INM}}}{(\text{Altitude})_{\text{measured}}} \quad (3)$$

for each noise event.

With this order of division:

- Altitude ratio is > 1 when INM over-computes the altitude.
- Altitude ratio is < 1 when INM under-computes the altitude.

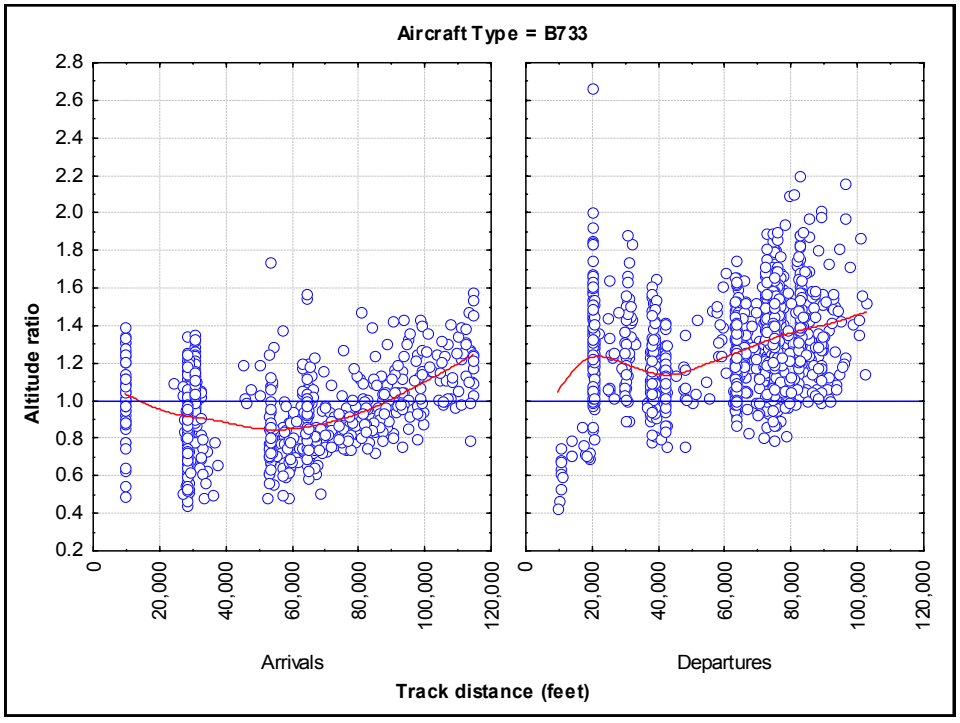


Figure 11. INM over-computes altitudes at high track distances: B733

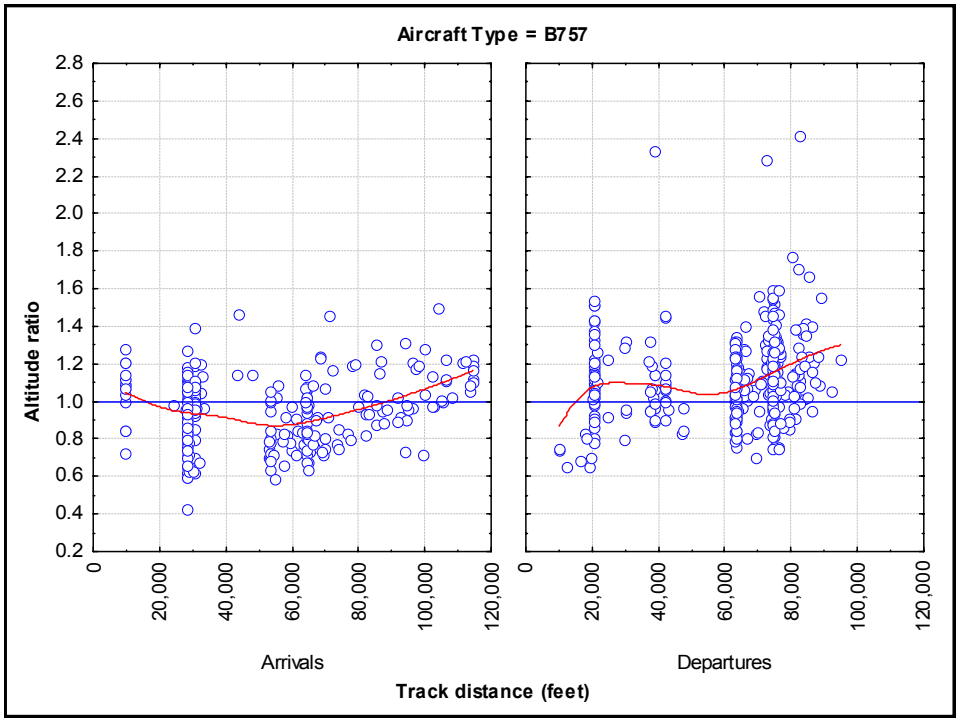


Figure 12. INM over-computes altitudes at high track distances: B757

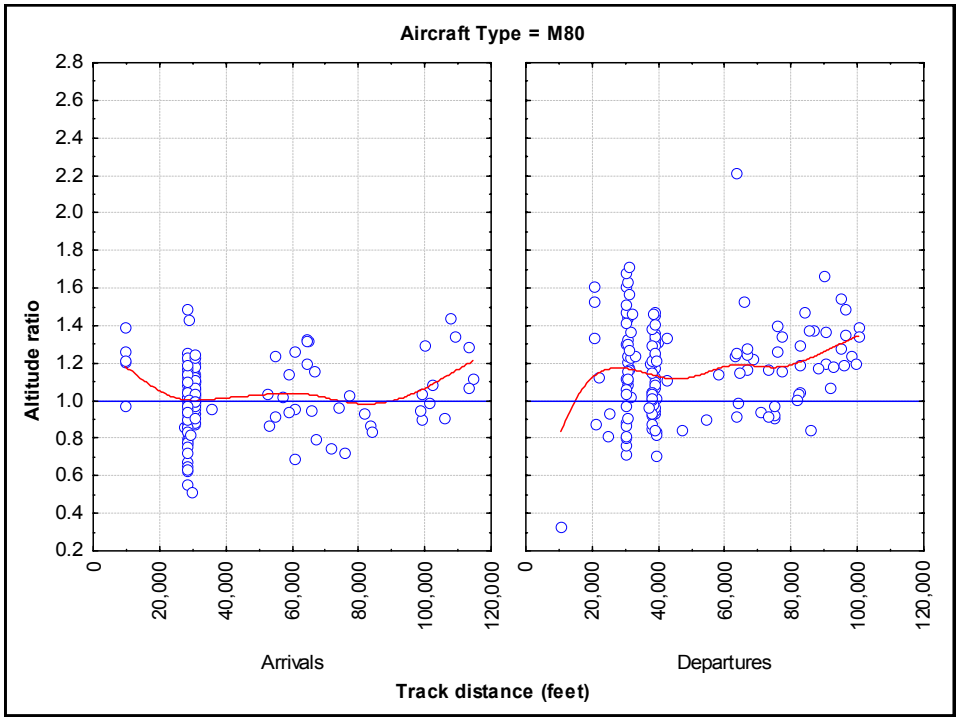


Figure 13. INM over-computes altitudes at high track distances: M80

In these figures, the curves through the data points are "rising" upward to the right, especially for departures. Arrivals have a more "sagging" shape, instead. Moreover, similar patterns appear on comparable graphs for B727, B73S and DC10 aircraft.

To a first approximation, the altitude-ratio patterns are the opposite of the SEL-offset patterns in the three previous graphs. The INM tends to under-compute SELs when it tends to over-compute altitudes.

Can the relation between SEL offset and altitude ratio be graphically shown in a more explicit way? The next section contains more explicit graphs.

5.2.3 Over-computation of altitudes potentially explain under-computation of SELs

The next three graphs, Figure 14 through Figure 16, show directly the relation between too high altitudes and too low SELs—again for B733, B757 and M80 aircraft. Each of these figures contains six frames: separate rows for arrivals and departures, and separate columns for the three track intervals. Each noise-event's point is plotted horizontally at its altitude ratio, and vertically at its SEL offset. The straight lines show the general pattern of the points in each frame.

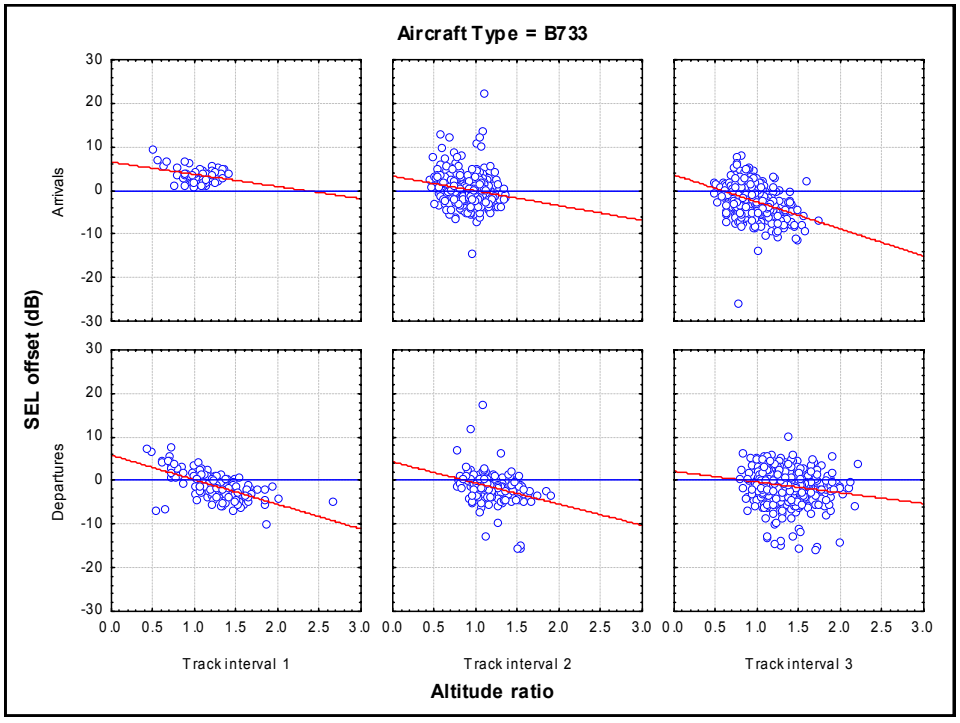


Figure 14. Incorrect altitudes potentially explain incorrect SELs: B733

These graphs have several strong messages about INM performance:

- **The more INM over-computes altitude, the more it under-computes SEL.** This tendency appears in the graph as a negative slope on the regression line. Points to the lower right have altitudes too high and SELs too low. And vice versa: points to the upper left have altitudes too low and SELs too high.
- This result is not surprising. When distances are too high, sound levels are too low.

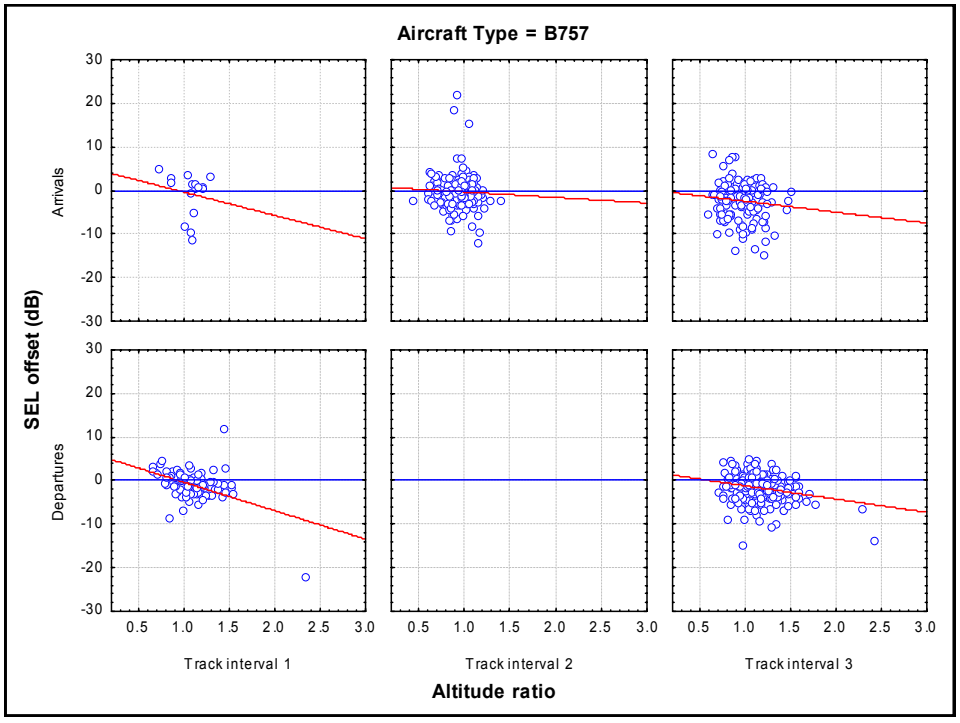


Figure 15. Incorrect altitudes potentially explain incorrect SELs: B757

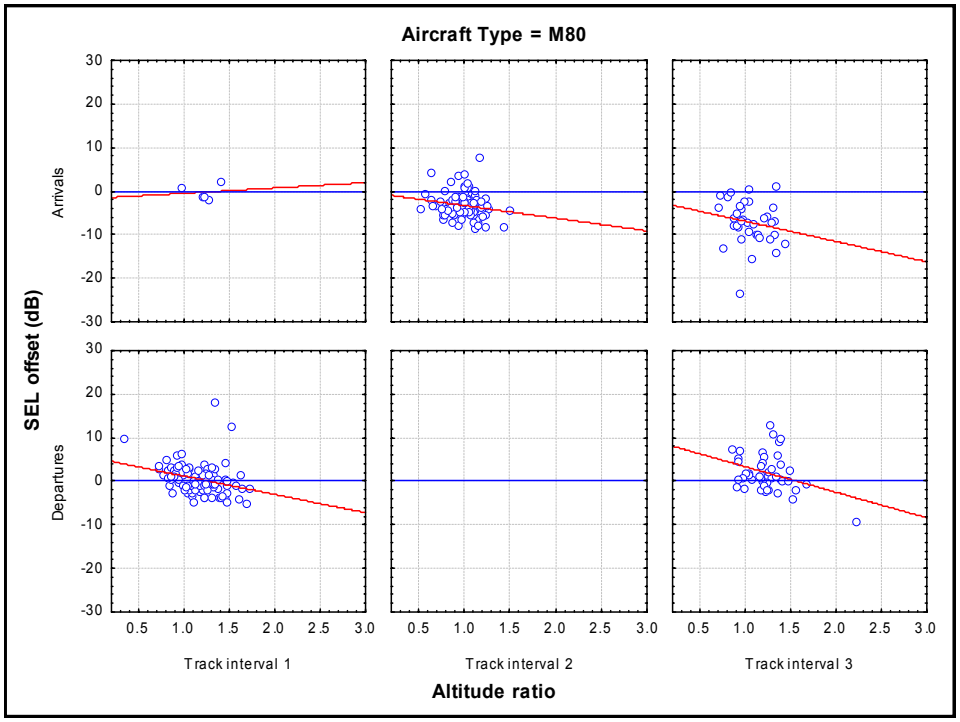


Figure 16. Incorrect altitudes potentially explain incorrect SELs: M80

- **Correct altitude generally matches correct SEL.** In many of these figure frames, the regression line passes very closely through the "correct" point—altitude ratio equals 1, SEL offset equals zero.
- This is highly encouraging. It suggests that INM altitude computations are the main cause of incorrect INM SELs.

Can the SEL values in this study be adjusted to "correct" all aircraft altitudes? The next section provides the method for such an adjustment.

5.2.4 INM SELs can be adjusted by spreadsheet to "correct" all aircraft altitudes

At the point of closest approach to the RMT, each noise event in the study has two aircraft altitudes: one computed by INM and the other determined by radar. From these two altitudes, INM SELs can be adjusted to account for the discrepancy between these two. To do that, the SEL dependence on distance must be known.

Figure 17 and Figure 18 show that distance dependence for B733 arrivals and departures. Each of these figures plots the calculated slant distance at PCA to the calculated SEL. This plot shows INM's view of how SEL depends upon distance.

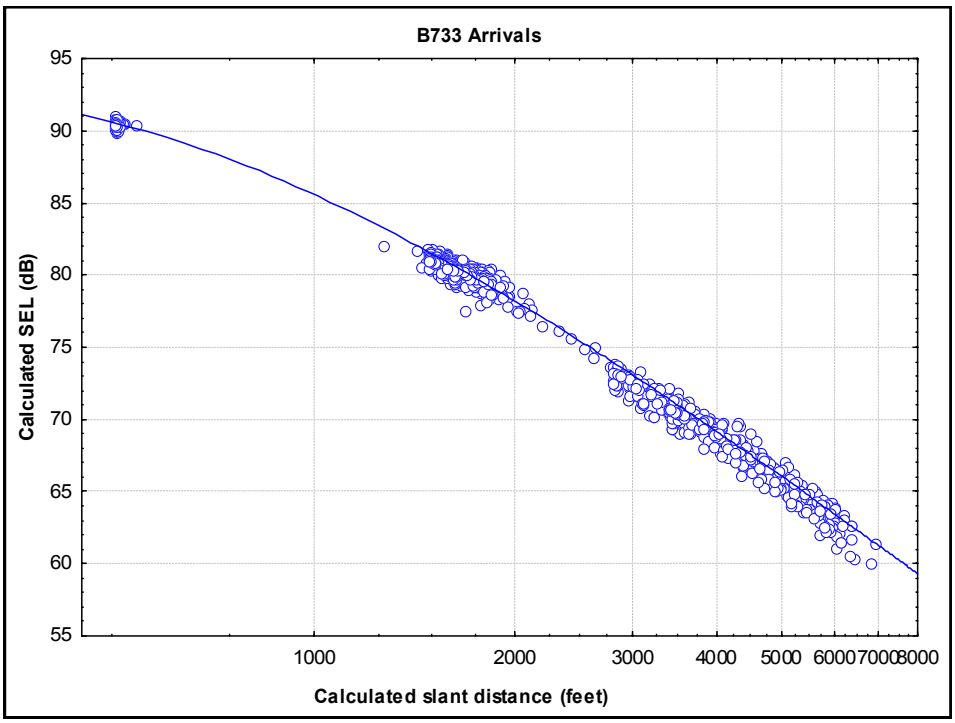


Figure 17. INM SELs can be adjusted for proper aircraft altitudes: B733 arrivals

The figures show this dependence to scatter somewhat around a regression line determined from the data points. This scatter derives from different engine thrusts for the various aircraft, as well as other influences such flight-track curvature, atmospheric propagation conditions, and so forth. In spite of this scatter, the distance dependence is well determined from plots of this type.

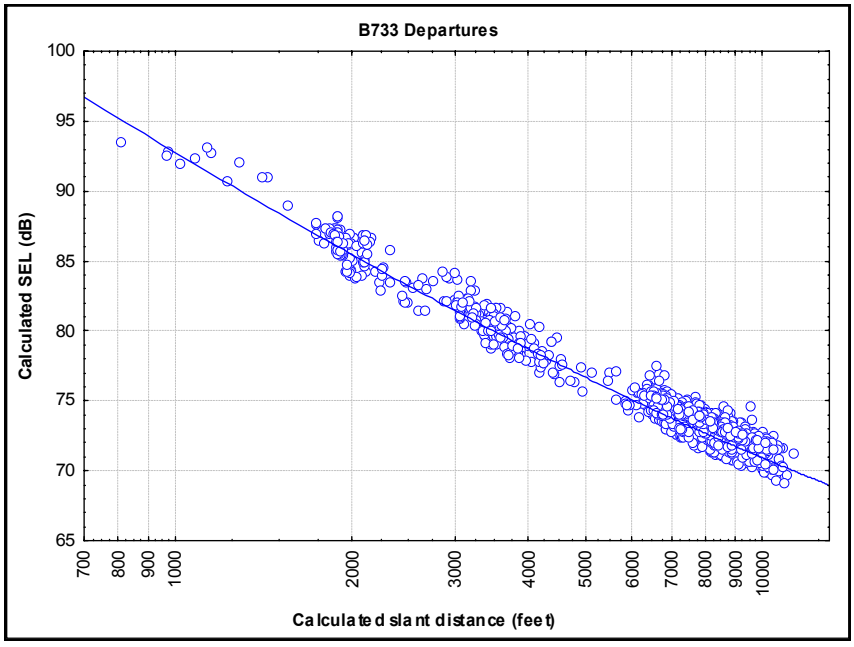


Figure 18. INM SELs can be adjusted for proper aircraft altitudes: B733 departures

Similar regressions were used to determine average SEL distance dependence within the INM, separately for each aircraft type and separately for arrivals and departures. Then these distance functions were used to convert INM's computed SEL from the slant distance thought true by INM to the slant distance known to be true from radar.

Does this SEL adjustment significantly improve the match between computed and measured SELs? The next section shows that it does.

5.2.5 Adjustments to correct slant distance significantly improves agreement of INM SELs with measured SELs

Figure 19 through Figure 21 show the resulting improvement in SEL versus track distance, separately by aircraft type. In each of these figures, the bottom frames plot distance-corrected SEL offset vertically. For comparison, the top frames are duplicates of prior figures, before adjustment (SEL offset, vertically).

Comparison of the regression line in each upper frame, with its companion in the frame below it, is the graphic measure of the adjustment's effect. In detail:

- In Figure 19 (B733 aircraft), the adjustment has flattened out the regression line for arrivals (the lower-left regression is flatter than the upper-left regression). This is especially true at moderate-to-high track distances. The adjustment has thereby reduced the distance dependence of SEL offset, except at low track distances. Notice, however, that the total under-computation for B733 aircraft arrivals is made somewhat worse by the adjustment (the lower-left regression line lies further below zero, overall).
- For departures, the distance dependence is eliminated by this adjustment (the lower-right regression is essentially independent of track distance).

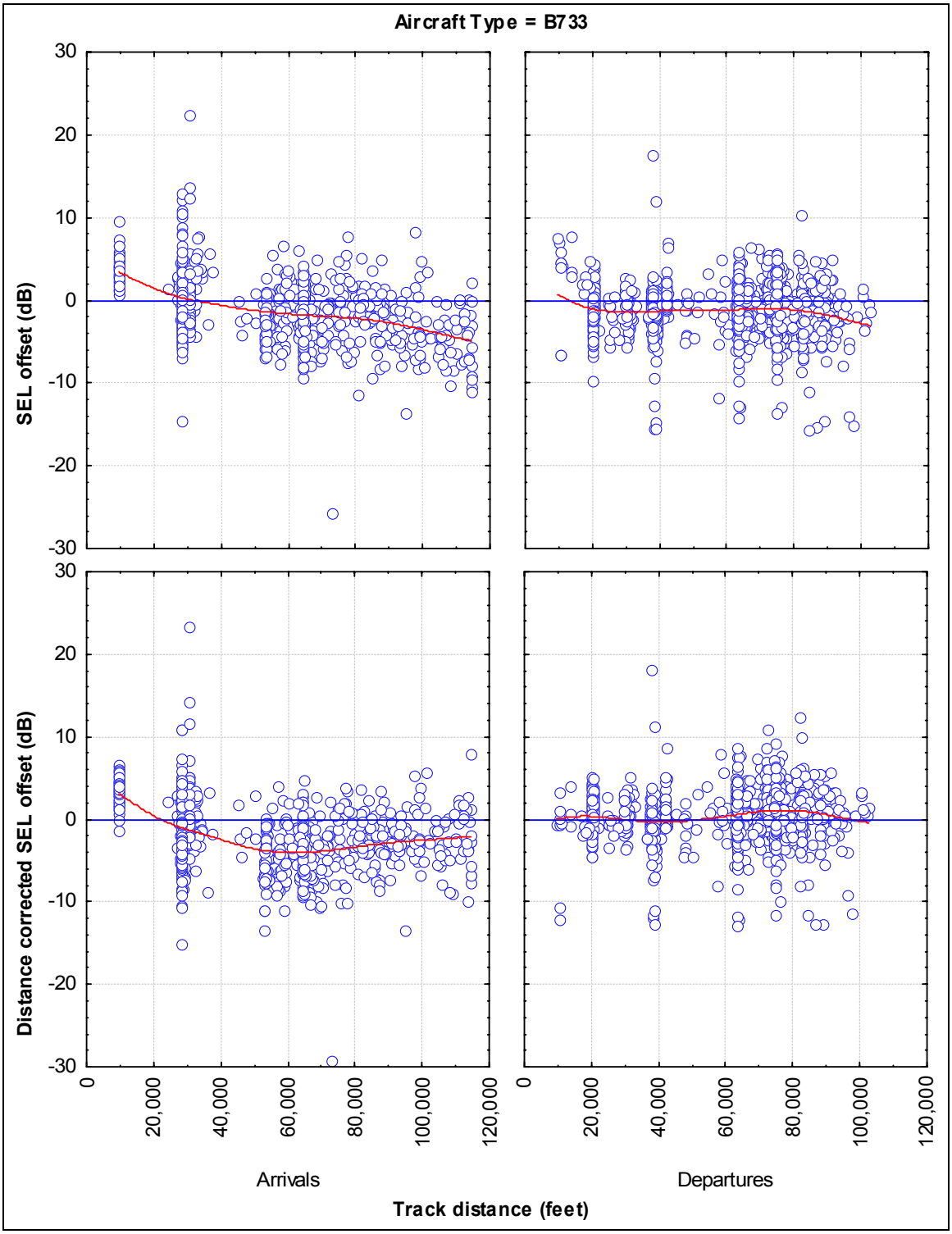


Figure 19. Slant distance adjustment tends to improve INM SELs: B733

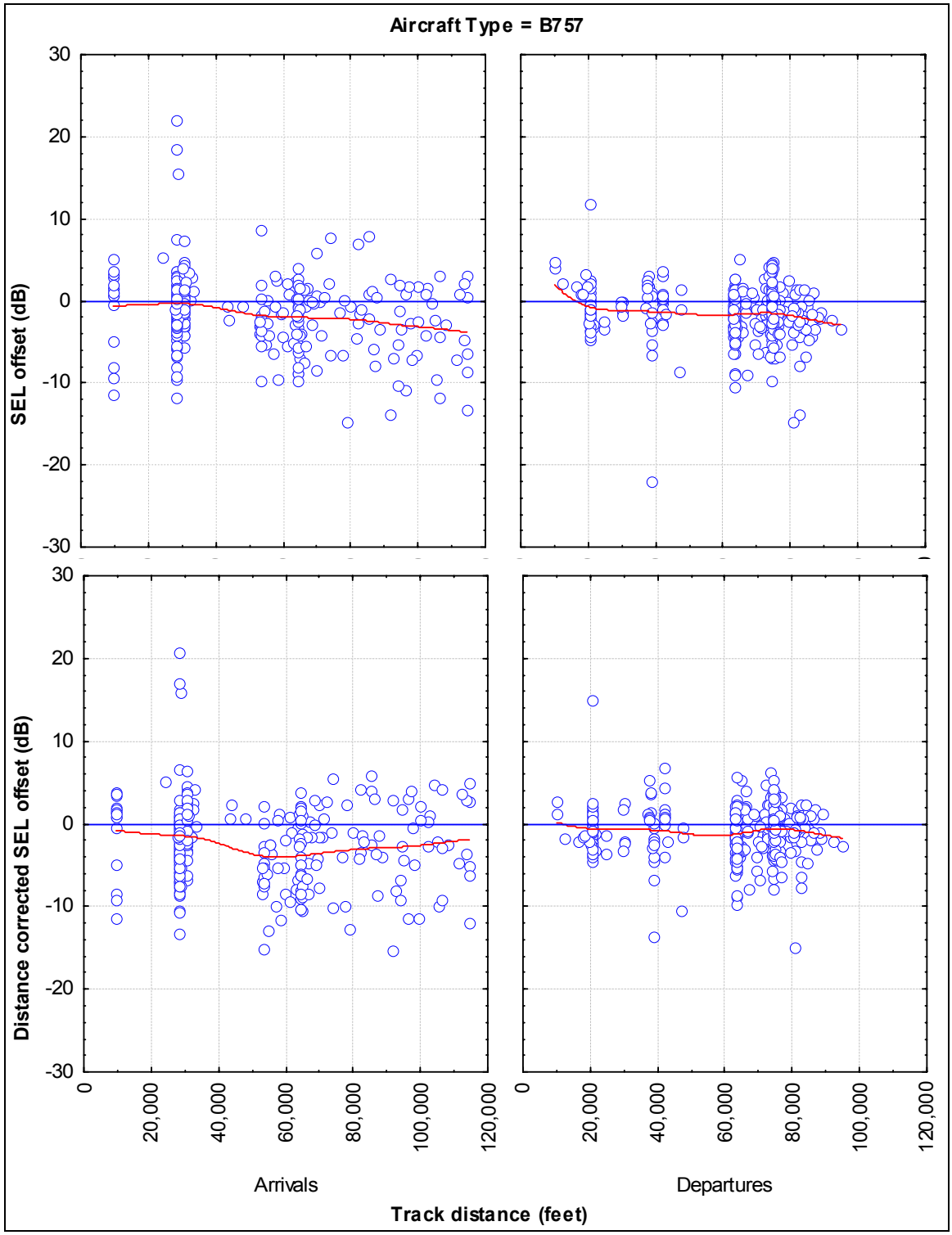


Figure 20. Slant distance adjustment tends to improve INM SELs: B757

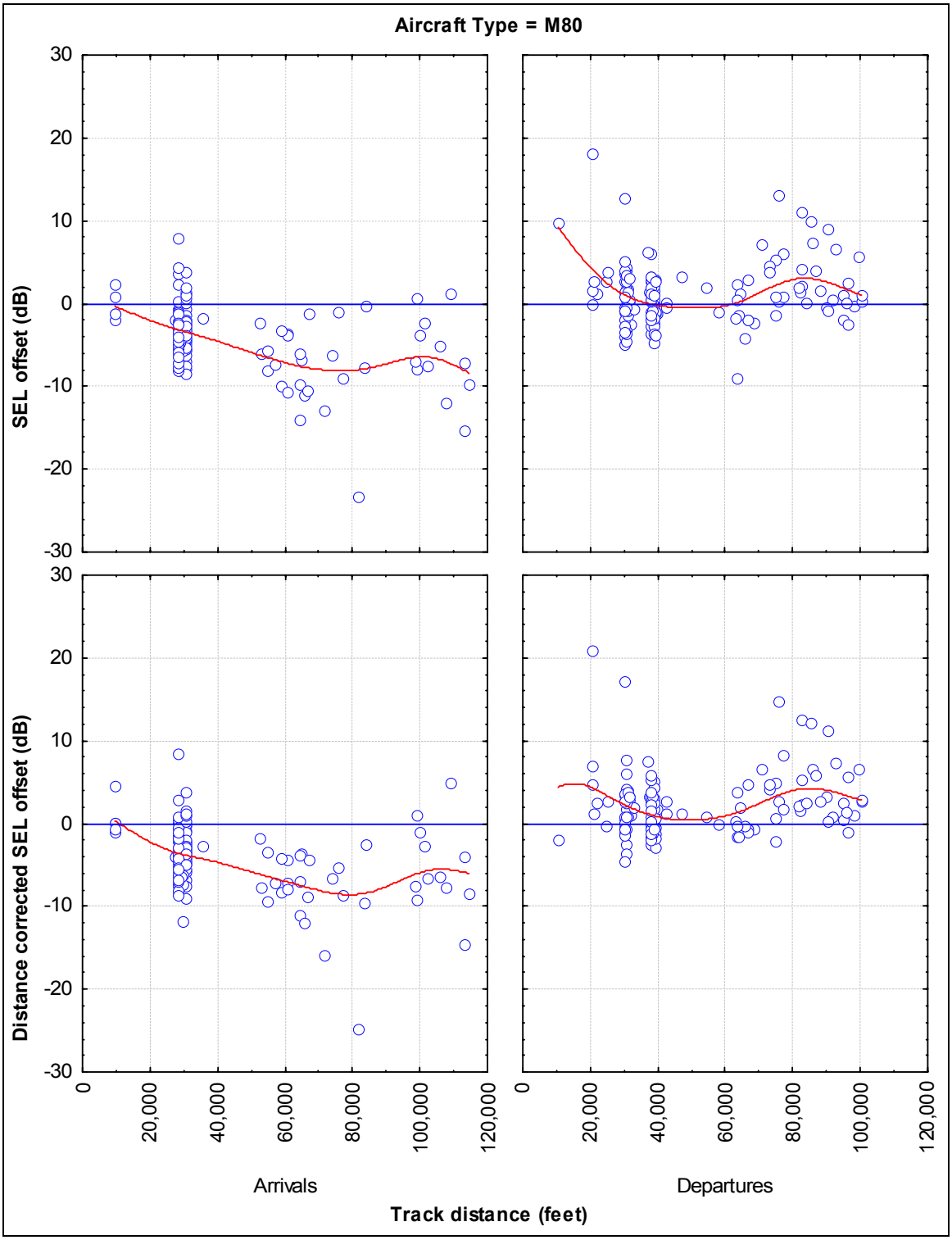


Figure 21. Slant distance adjustment produces little improvement in INM SELs: M80

- In Figure 20 (B757 aircraft), the adjustment has approximately the same effect as in the prior figure—except somewhat less.
- In Figure 21 (M80 aircraft), the adjustment has no effect on arrivals (left frames), and a slight effect on departures (right frames). For departures, note that the effect on the left tail of the regression line is due to only one point, so is not very significant.

5.2.6 The slant distance adjustments tend to eliminate apparent stage-length effects

Figure 22 shows that this same distance adjustment also tends to eliminate the apparent dependence of SEL offset upon "stage length" for departing aircraft.

Each frame in the figure contains four "box plots" of data points, separately for each stage length, one through four. In each box plot:

- All the noise-event points are plotted vertically at their offset value. The sideways scatter has no meaning. It serves only to minimize overlap among the points.
- Outliers and extreme points appear with different symbols from the more-centrally located points (the triangles). "Outliers" and "extremes" are defined in a complicated manner, as is standard for box plots.
- The gray box shows the central fifty percent of the data points.
- The dark horizontal line connects the median of each box plot with its neighbors. Half the points lie above the median and half lie below it.

The median lines in this figure show improvement for the B733 and B757 from "before" the adjustment (top frames) to "after" the adjustment (bottom frames), though only slight improvement (a flattening with stage length) for the M80.

- For B733 aircraft (left two frames), the upward slope of the median line in the top frame has been flattened in the bottom frame. In addition, the entire line has been elevated by 1-to-2 decibels, thereby adjusting out a slight negative SEL offset.
- For B757 (central two frames), the upward slope has been reduced by the adjustment.
- Prior to the adjustment, B757 aircraft of stage length one (SL1) had a large negative SEL offset (–3 dB), while the opposite was true for SL4 aircraft (+2 dB). Prior to adjustment, this seemed to indicate an INM difficulty with stage-length assignments during input. An input difficulty with INM is preferred to a difficulty with its algorithms, because input is generally easier to fix (or to work around).
- However, the B757 stage-length dependence is reduced (lower frame) when INM output is adjusted for proper aircraft altitude (or slant distance).
- For M80 aircraft (right two frames), the horizontal median line is flattened somewhat by the distance adjustment, though over-computation still is evident.

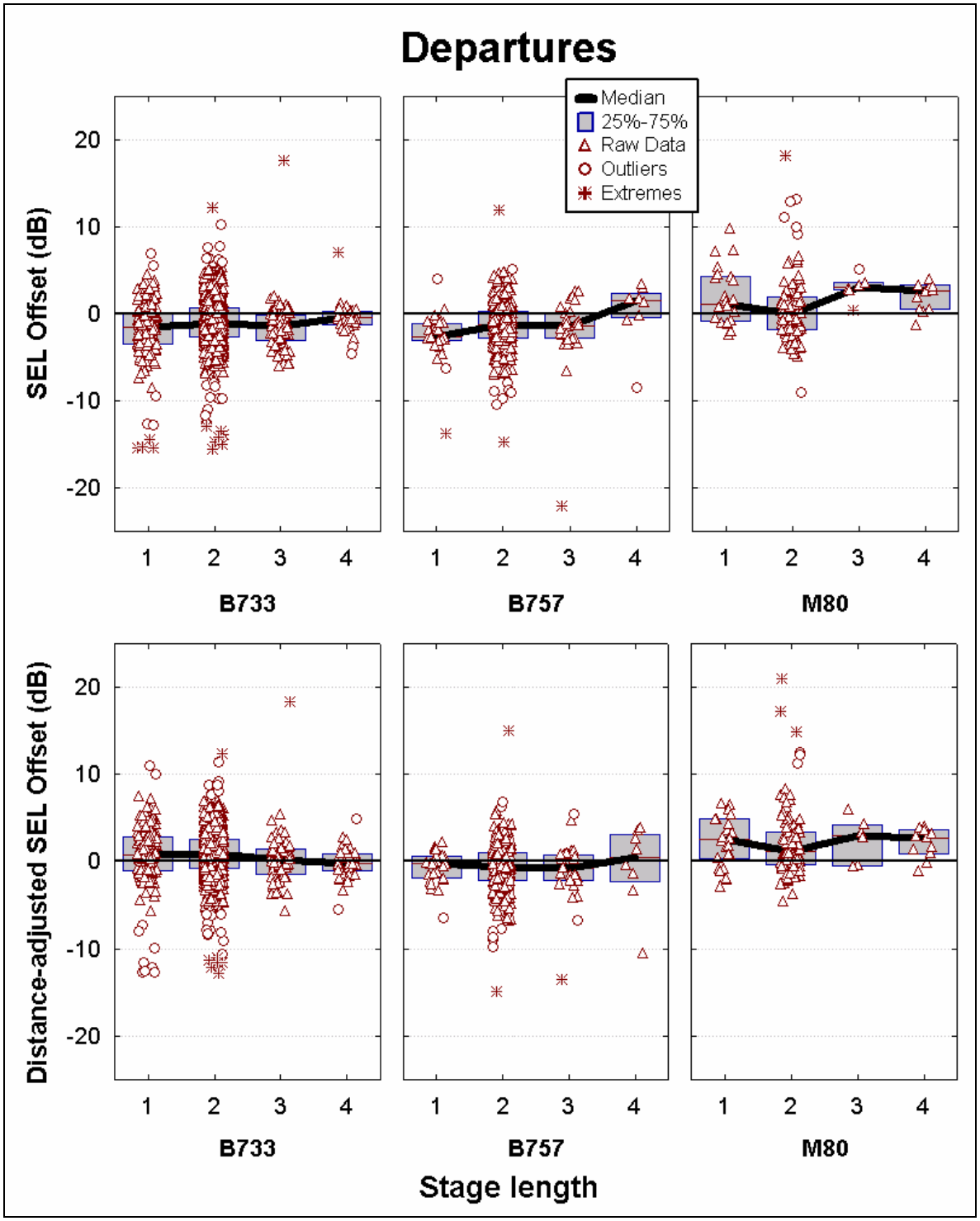


Figure 22. Slant distance adjustment reduces INM stage-length under-computation for B733, B757

5.3 INM Offsets, After Adjustment for Proper Aircraft Altitude

Figure 23 and Figure 24 repeat those from Section 5.2, above. Added to those prior figures is a new modeling method, given the label "8Star" (8*). This method is identical to Modeling Method 8, except that the INM SELs have been adjusted for proper (radar) altitude / slant distance, as discussed above in Section 5.2. The INM Offsets for Modeling Method 8star appear at the right end of each string of points in the figures.

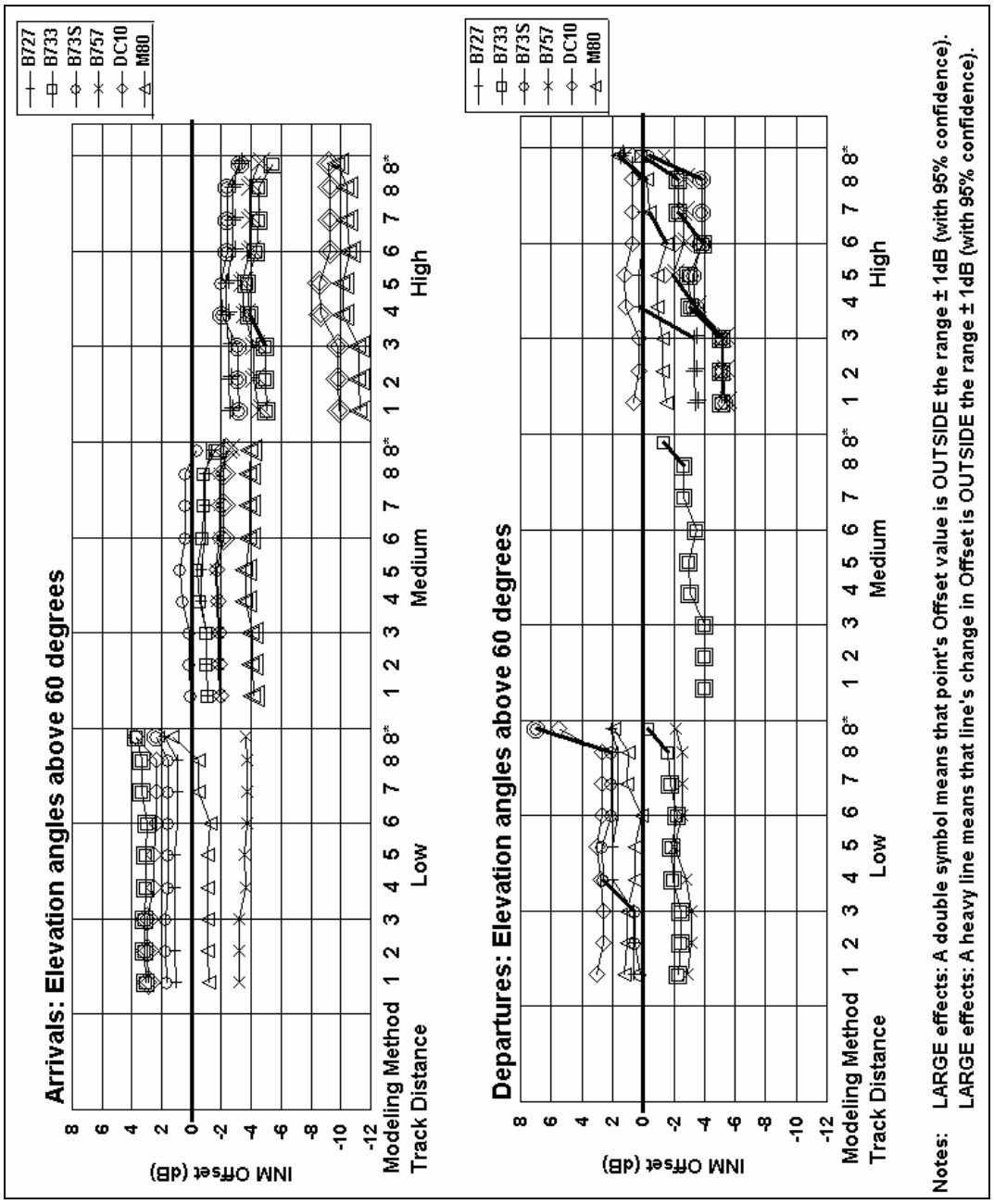


Figure 23. Altitude-adjusted INM Offsets: Elevation angles above 60 degrees

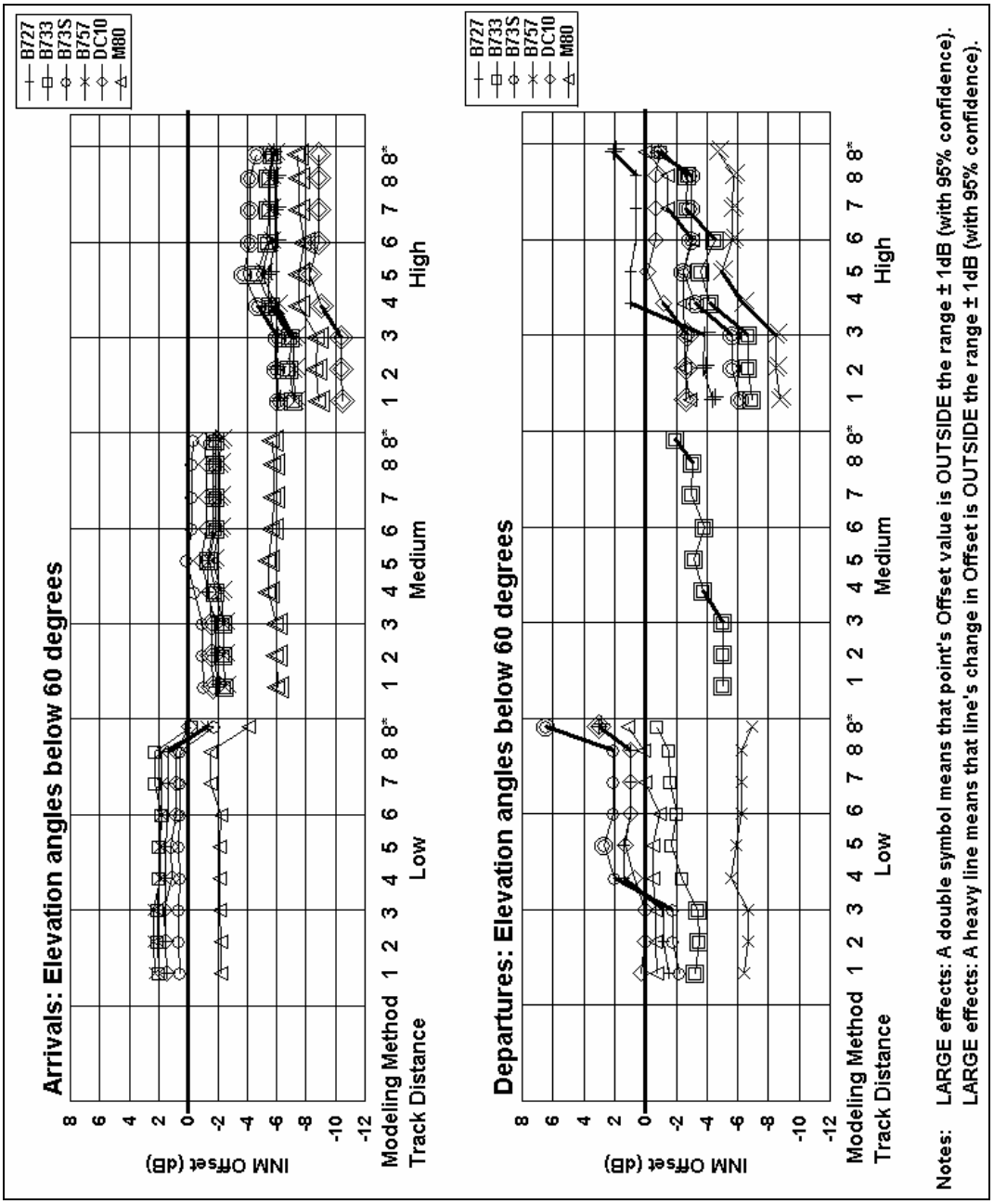


Figure 24. Altitude-adjusted INM Offsets: Elevation angles below 60 degrees

These two figures show the effects of the distance adjustment on INM Offset, rather than on the SEL offset that was graphically analyzed in the preceding section. INM Offset is the energy-average metric, which is most relevant to computation of Day Night Average Sound Level.

In the figures, the emphasized lines between Modeling Methods 8 and 8Star show changes that are confidently large (greater than 1 dB, with 95% confidence). Only these changes are discussed below.

In summary of these two figures (8Star compared with 8):

- **2-to-4dB improvement.** Most improvement due to proper INM altitudes would occur at elevation angles above 60 degrees (first figure), for departures (lower frame), at medium and high track distances—all for B733, B73S and M80 aircraft. For these conditions, improved INM altitude computations have the potential to improve INM Offsets as much as 4 dB.
- **1-to-2 dB improvement**. Moderate improvement occurs in the other figure (elevation angle below 60 degrees), again for departures at medium-to-high track distances—for B733 and B73S aircraft.
- **Worse after adjustment.** Adjustment makes INM Offset worse for departures at low track distances, at all elevation angles—for several aircraft types.
- This result indicates that the method chosen to improve INM altitudes will be important. Most likely, a different method is needed early in the flight track than later on along the track.

These two figures are repeated in Appendix A, but with emphasized symbols for "confidently small" effects—that is, effects that lie *inside* the region between –1dB and +1dB, with 95% confidence.

5.4 Influence of Other Factors on INM Offset

5.4.1 Correlations

During diagnostic investigations, other concurrently measured factors showed less effect on INM Offset than discussed above. Table 12 contains correlation coefficients between SEL Offset for each noise event and these other currently determined factors.

Table 12. Dependence of SEL Offset upon other factors

Concurrent factor		Correlation coefficient	
		Elevation angle: Below 60 degrees	Elevation angle: Above 60 degrees
Atmospherics factors	Wind speed	+0.00	–0.02
	Wind direction	+0.03	+0.04
	Temperature	+0.02	–0.02
	Relative humidity	–0.13	–0.11
Location factors	RMT	–0.01	–0.11
	Elevation angle	–0.04	+0.02
	Runway	+0.19	–0.04
	Waypoint	–0.01	+0.09
Time and aircraft factors	Time of year	+0.00	+0.00
	Time of day	+0.03	+0.02
	Speed	+0.06	–0.16
	Thrust	+0.21	+0.07
Noise-event factors	Duration	–0.04	–0.15
	Lmax	–0.05	–0.14
	Monitor threshold	–0.11	–0.10
	Event protrusion	+0.01	–0.07

In the table, shading refers to Table 13, below.

As the table shows, none of these factors are highly correlated with SEL Offset. In particular, the following factors have no apparent association with noise-event SEL Offset, and therefore none with (energy-average) INM Offset, this study's measure of INM inaccuracy:

- For elevation angles below 60 degrees:
 - Wind speed and direction
 - Temperature
 - RMT
 - Elevation angle
 - Waypoint
 - Time of year or time of day
 - Event protrusion
- For elevation angles above 60 degrees:
 - Wind speed and direction
 - Temperature
 - Elevation angle
 - Runway
 - Time of year or time of day.

5.4.2 Corresponding graphs

Figure 25 and Figure 26 plot SEL Offset against these same factors, one point per noise event - for elevation angles below and above 60 degrees, respectively.

In each figure, SEL Offset is plotted vertically in each sub-graph. The various sub-graphs have differing factors plotted horizontally, as shown. Each subplot contains one point for each aircraft/RMT noise event, for a total of 22,531 points in each sub-graph of Figure 25 and 6,361 points in each sub-graph of Figure 26.

Within each figure, the four rows of sub-graphs contain these types of factors:

- Row 1: Atmospheric factors
- Row 2: Location factors
- Row 3: Time and aircraft factors
- Row 4: Noise-event factors.

In these figures, the linear-regression line in many of the sub-graphs is very nearly flat. For these factors, these graphs clearly show no apparent association with SEL Offset—and therefore none with (energy-average) INM Offset, either. The flat regression lines in these figures correspond to correlations that are very nearly equal to zero (not shaded) in Table 12.

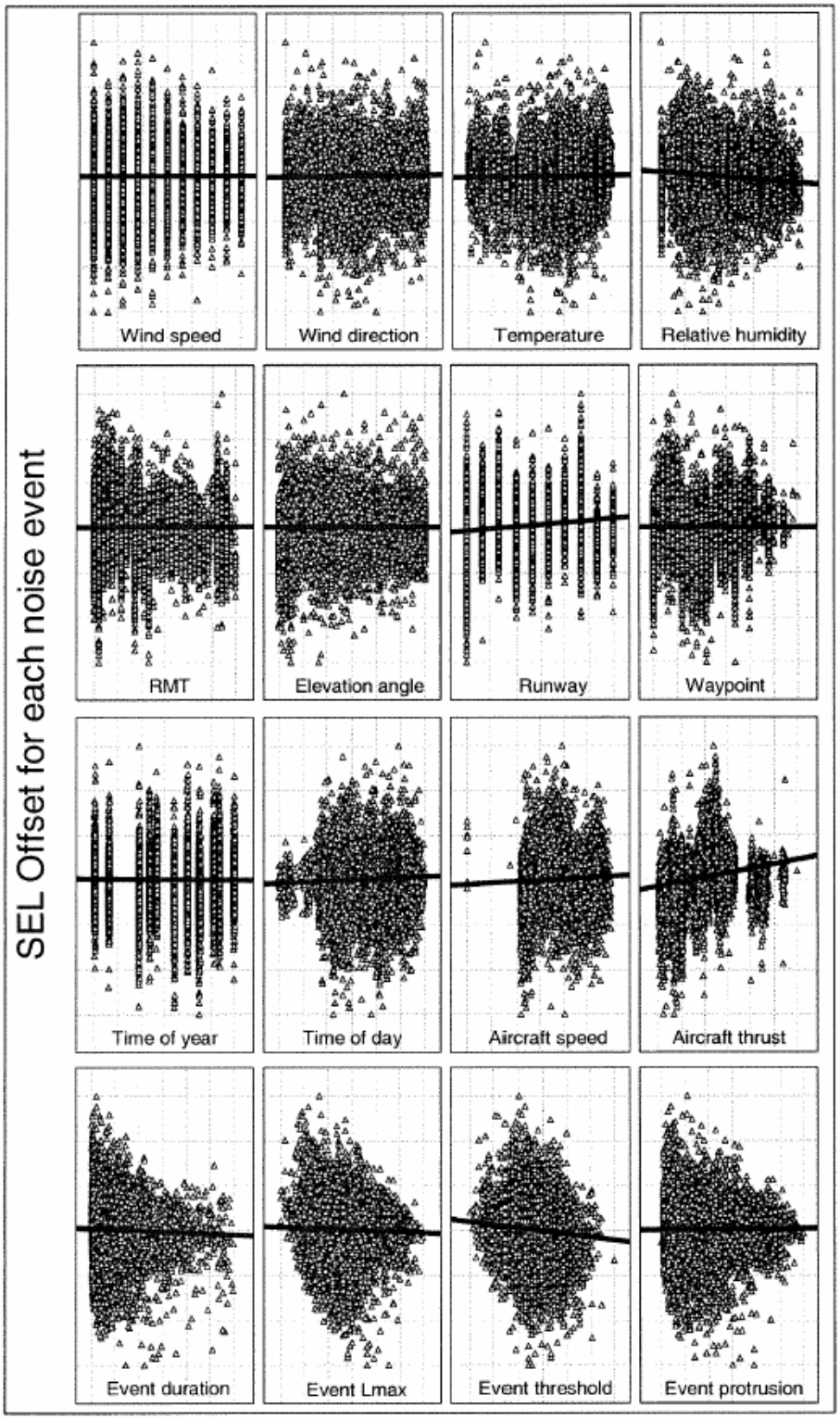


Figure 25. Influence of other factors on INM Offset: Elevation angles below 60 degrees

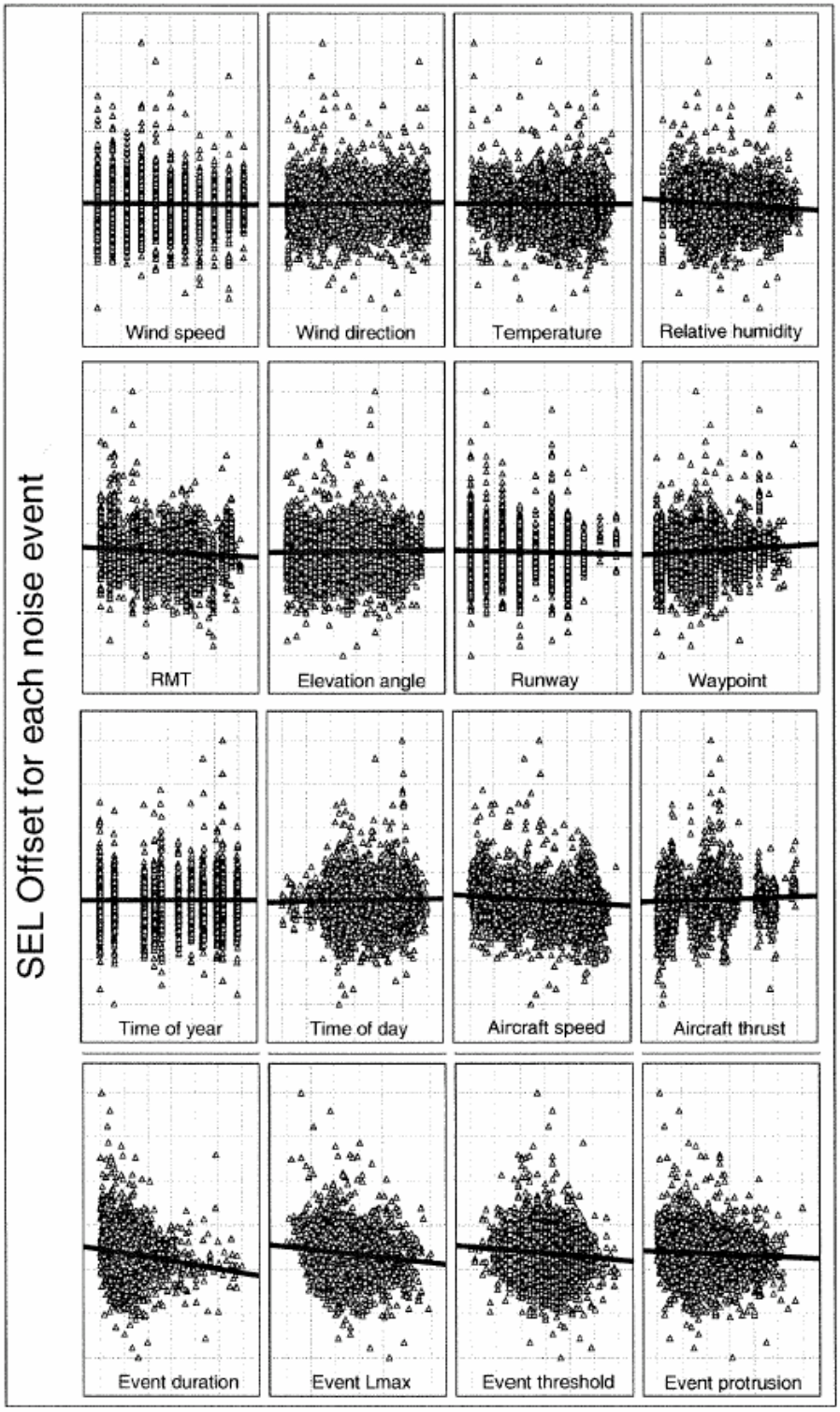


Figure 26. Influence of other factors on INM Offset: Elevation angles above 60 degrees

Table 13 tabulates and discusses the exceptions—that is, the non-flat correlation lines. These generally correspond, as well, to correlation coefficients greater than +0.05 or less than –0.05 in the prior table.

Table 13. Apparent association of SEL Offset with concurrently measured factors

Concurrent factor	Elevation angle		Discussion
	Below 60 degrees	Above 60 degrees	
Relative humidity	x	x	SEL Offset gets slightly more negative for larger values of relative humidity (RH). RH is the only atmospheric factor that shows any apparent association with SEL Offset, however.
RMT		x	The apparent association with RMT most likely happens because the higher-numbered RMTs are further from the airport. Negative SEL Offsets at higher track distances therefore will cause negative values at higher RMTs, as well.
Runway	x		The apparent associations with runway and waypoint are artifacts of how these two factors are numbered.
Waypoint		x	
Aircraft speed	x	x	The associations of SEL Offset with aircraft speed and thrust are most likely linked to its association with aircraft altitude. Future modifications of INM to correct its computation of aircraft altitude will invariable involve changes in aircraft speed and thrust, thereby changing these apparent associations, as well.
Aircraft thrust	x	x	
Noise-event duration	x	x	Very high event durations are likely to capture ambient noise along with aircraft noise, thereby over-measuring the reported aircraft SEL. In this study, such an occurrence would look like an under-computation by INM, as the graphs show. Subsequent re-analysis might delete the relatively few points of extreme duration (5% of durations are longer than 2 minutes).
Noise-event Lmax	x	x	When low Lmax combines with a high monitor threshold, then the aircraft noise event does not protrude very much above the threshold. Noise-event protrusion measures that protrusion and therefore combines the effect of Lmax and threshold. Very low event protrusions run the risk of missing some of the noise-event's energy, thereby under-measuring the noise event. In this study, under-measuring would look like an over-computation by INM, as the graphs show. The effect is small, however, for these data.
Noise-event threshold	x	x	
Noise-event protrusion		x	

This table discusses only those sub-graphs of Figure 25 and Figure 26 that contain apparent factor dependence (sloped regression lines).

5.5 Limitations of These Graphical Investigations

Note that these investigations are not definitive. First, they focus on just three aircraft types, rather than all six types of this study. Second, they focus on elevation angles above 60 degrees, and therefore bypass complexities with INM's lateral-attenuation algorithm. Third, these investigations are graphical rather than analytical. They produce graphs with a strong message, but do not analytically justify or qualify these graphs.

Missing completely from this investigation are multi-variable, non-linear regressions—aided by such considerations as cluster analysis, factor analysis, principal components analysis, and discriminant analysis. Such multivariate analyses might well uncover multi-variable interrelations that do not appear on these two-dimensional graphs.

APPENDIX A DETAILED TABULATIONS/GRAPHS OF INM OFFSETS

This appendix tabulates and graphs:

- All INM Offsets
- All changes in INM Offsets, produced by improvements in INM Modeling Methods.

A.1 Tables

A.1.1 INM Offsets

Table 14 through Table 22 contain all INM Offsets, for Modeling Methods 1 through 8Star, respectively.

Each table consists of two major sections: Low elevation angles (below 60 degrees), and high elevation angles (above 60 degrees). Within each major section:

- The first four columns contain the aircraft type, operation type, track-distance regime, and the corresponding track-distance interval.
- The fifth column contains the number of data points for that combination of conditions.
- The final column contains the resulting INM Offset, plus its 95% confidence interval.

Table 14. INM Offsets: Modeling Method 1

Aircraft type	Operation	Track-distance regime	Track-distance interval	Number of data points	INM Offset ± 95% confidence
B727	Arrival	1	0 to 20k	1,273	1.4 ± 1.9
B727	Arrival	2	20k to 40k	1,860	-1.9 ± 0.5
B727	Arrival	3	40k or more	604	-6.1 ± 2.1
B727	Departure	1	0 to 60k	2,818	-1.6 ± 0.7
B727	Departure	2	60k or more	1,312	-4.4 ± 0.4
B733	Arrival	1	0 to 20k	581	2.0 ± 1.8
B733	Arrival	2	20k to 40k	2,272	-2.5 ± 0.3
B733	Arrival	3	40k or more	687	-7.1 ± 1.1
B733	Departure	1	0 to 30k	281	-3.3 ± 1.8
B733	Departure	2	30k to 50k	626	-5.1 ± 0.6
B733	Departure	3	50k or more	1,462	-6.9 ± 1.2
B73S	Arrival	1	0 to 20k	424	0.6 ± 3.1
B73S	Arrival	2	20k to 40k	1,073	-1.0 ± 0.6
B73S	Arrival	3	40k or more	380	-6.2 ± 1.3
B73S	Departure	1	0 to 60k	1,704	-2.2 ± 1.7
B73S	Departure	2	60k or more	849	-6.1 ± 0.6
B757	Arrival	1	0 to 20k	190	2.3 ± 2.6
B757	Arrival	2	20k to 40k	706	-2.5 ± 0.6
B757	Arrival	3	40k or more	203	-7.3 ± 1.8
B757	Departure	1	0 to 50k	132	-6.4 ± 7.4
B757	Departure	2	50k or more	320	-8.7 ± 2.9
DC10	Arrival	1	0 to 20k	187	1.5 ± 3.7
DC10	Arrival	2	20k to 40k	447	-1.7 ± 0.6
DC10	Arrival	3	40k or more	132	-10.5 ± 1.9
DC10	Departure	1	0 to 60k	230	0.3 ± 1.7
DC10	Departure	2	60k or more	304	-2.7 ± 0.9
M80	Arrival	1	0 to 20k	207	-2.3 ± 3.7
M80	Arrival	2	20k to 40k	398	-6.1 ± 2.1
M80	Arrival	3	40k or more	35	-8.9 ± 3.1
M80	Departure	1	0 to 60k	713	-0.8 ± 0.9
M80	Departure	2	60k or more	144	-2.9 ± 4.2
			Sum:	22,554	
			Maximum:		2.3 7.4
			Average:		-3.4 1.9
			Minimum:		-10.5 0.3

Low elevation angles

Aircraft type	Operation	Track-distance regime	Track-distance interval	Number of data points	INM Offset ± 95% confidence
B727	Arrival	1	0 to 20k	34	1.0 ± 1.5
B727	Arrival	2	20k to 40k	409	-1.1 ± 0.6
B727	Arrival	3	40k or more	272	-2.6 ± 1.2
B727	Departure	1	0 to 60k	167	0.6 ± 2.6
B727	Departure	2	60k or more	466	-3.4 ± 0.5
B733	Arrival	1	0 to 20k	64	3.1 ± 0.4
B733	Arrival	2	20k to 40k	536	-1.1 ± 0.4
B733	Arrival	3	40k or more	427	-5.0 ± 2.5
B733	Departure	1	0 to 30k	161	-2.3 ± 0.8
B733	Departure	2	30k to 50k	244	-4.0 ± 0.9
B733	Departure	3	50k or more	947	-5.2 ± 0.3
B73S	Arrival	1	0 to 20k	57	1.6 ± 0.9
B73S	Arrival	2	20k to 40k	270	0.1 ± 0.7
B73S	Arrival	3	40k or more	259	-3.2 ± 1.1
B73S	Departure	1	0 to 60k	241	0.2 ± 1.9
B73S	Departure	2	60k or more	434	-5.3 ± 0.5
B757	Arrival	1	0 to 20k	16	-3.2 ± 4.5
B757	Arrival	2	20k to 40k	160	-1.9 ± 1.0
B757	Arrival	3	40k or more	139	-4.5 ± 1.4
B757	Departure	1	0 to 50k	93	-2.9 ± 3.3
B757	Departure	2	50k or more	305	-5.4 ± 0.5
DC10	Arrival	1	0 to 20k	4	2.9 ± 1.8
DC10	Arrival	2	20k to 40k	63	-2.0 ± 1.1
DC10	Arrival	3	40k or more	82	-9.9 ± 1.5
DC10	Departure	1	0 to 60k	54	3.1 ± 1.5
DC10	Departure	2	60k or more	165	0.6 ± 0.8
M80	Arrival	1	0 to 20k	5	-1.1 ± 2.2
M80	Arrival	2	20k to 40k	119	-4.2 ± 0.5
M80	Arrival	3	40k or more	36	-11.3 ± 5.3
M80	Departure	1	0 to 60k	100	1.2 ± 0.9
M80	Departure	2	60k or more	45	-1.5 ± 2.5
			Sum:	6,374	
			Maximum:		3.1 5.3
			Average:		-2.2 1.5
			Minimum:		-11.3 0.3

High elevation angles

Table 15. INM Offsets: Modeling Method 2

Aircraft type	Operation	Track-distance regime	Track-distance interval	Number of data points	INM Offset ± 95% confidence
B727	Arrival	1	0 to 20k	1,179	1.6 ± 1.9
B727	Arrival	2	20k to 40k	1,854	-1.9 ± 0.5
B727	Arrival	3	40k or more	601	-5.9 ± 2.1
B727	Departure	1	0 to 60k	2,817	-1.1 ± 0.7
B727	Departure	2	60k or more	1,312	-3.8 ± 0.4
B733	Arrival	1	0 to 20k	570	2.0 ± 1.8
B733	Arrival	2	20k to 40k	2,257	-2.4 ± 0.3
B733	Arrival	3	40k or more	672	-6.9 ± 1.1
B733	Departure	1	0 to 30k	270	-3.5 ± 1.7
B733	Departure	2	30k to 50k	607	-5.1 ± 0.6
B733	Departure	3	50k or more	1,458	-6.7 ± 1.2
B73S	Arrival	1	0 to 20k	416	0.7 ± 3.2
B73S	Arrival	2	20k to 40k	1,068	-0.9 ± 0.6
B73S	Arrival	3	40k or more	373	-6.0 ± 1.3
B73S	Departure	1	0 to 60k	1,695	-1.8 ± 1.7
B73S	Departure	2	60k or more	848	-5.6 ± 0.6
B757	Arrival	1	0 to 20k	186	2.3 ± 2.6
B757	Arrival	2	20k to 40k	704	-2.4 ± 0.6
B757	Arrival	3	40k or more	202	-7.1 ± 1.7
B757	Departure	1	0 to 50k	128	-6.7 ± 7.3
B757	Departure	2	50k or more	315	-8.5 ± 3.0
DC10	Arrival	1	0 to 20k	186	1.6 ± 3.7
DC10	Arrival	2	20k to 40k	446	-1.6 ± 0.6
DC10	Arrival	3	40k or more	126	-10.4 ± 1.8
DC10	Departure	1	0 to 60k	229	0.0 ± 1.6
DC10	Departure	2	60k or more	303	-2.7 ± 0.8
M80	Arrival	1	0 to 20k	199	-2.2 ± 3.9
M80	Arrival	2	20k to 40k	396	-6.0 ± 2.1
M80	Arrival	3	40k or more	33	-8.7 ± 3.2
M80	Departure	1	0 to 60k	710	-0.7 ± 0.9
M80	Departure	2	60k or more	144	-2.5 ± 4.2
			Sum:	22,304	
			Maximum:		2.3 7.3
			Average:		-3.3 1.9
			Minimum:		-10.4 0.3

Low elevation angles

Aircraft type	Operation	Track-distance regime	Track-distance interval	Number of data points	INM Offset ± 95% confidence
B727	Arrival	1	0 to 20k	34	1.1 ± 1.5
B727	Arrival	2	20k to 40k	408	-1.0 ± 0.6
B727	Arrival	3	40k or more	272	-2.5 ± 1.1
B727	Departure	1	0 to 60k	167	0.7 ± 2.7
B727	Departure	2	60k or more	466	-3.3 ± 0.5
B733	Arrival	1	0 to 20k	64	3.2 ± 0.4
B733	Arrival	2	20k to 40k	536	-1.0 ± 0.4
B733	Arrival	3	40k or more	427	-4.9 ± 2.5
B733	Departure	1	0 to 30k	160	-2.5 ± 0.8
B733	Departure	2	30k to 50k	237	-4.0 ± 0.9
B733	Departure	3	50k or more	947	-5.1 ± 0.3
B73S	Arrival	1	0 to 20k	57	1.7 ± 0.9
B73S	Arrival	2	20k to 40k	270	0.2 ± 0.7
B73S	Arrival	3	40k or more	259	-3.1 ± 1.0
B73S	Departure	1	0 to 60k	241	0.5 ± 2.0
B73S	Departure	2	60k or more	434	-5.2 ± 0.5
B757	Arrival	1	0 to 20k	16	-3.1 ± 4.5
B757	Arrival	2	20k to 40k	160	-1.8 ± 1.0
B757	Arrival	3	40k or more	138	-4.2 ± 1.3
B757	Departure	1	0 to 50k	91	-3.2 ± 3.4
B757	Departure	2	50k or more	305	-5.2 ± 0.5
DC10	Arrival	1	0 to 20k	4	3.0 ± 1.8
DC10	Arrival	2	20k to 40k	63	-1.9 ± 1.1
DC10	Arrival	3	40k or more	82	-9.8 ± 1.5
DC10	Departure	1	0 to 60k	54	2.6 ± 1.6
DC10	Departure	2	60k or more	165	0.3 ± 0.8
M80	Arrival	1	0 to 20k	5	-1.0 ± 2.2
M80	Arrival	2	20k to 40k	119	-4.1 ± 0.5
M80	Arrival	3	40k or more	36	-11.2 ± 5.2
M80	Departure	1	0 to 60k	100	1.0 ± 0.9
M80	Departure	2	60k or more	45	-1.3 ± 2.4
			Sum:	6,362	
			Maximum:		3.2 5.2
			Average:		-2.1 1.5
			Minimum:		-11.2 0.3

High elevation angles

Table 16. INM Offsets: Modeling Method 3

Aircraft type	Operation	Track-distance regime	Track-distance interval	Number of data points	INM Offset ± 95% confidence
B727	Arrival	1	0 to 20k	1,083	1.6 ± 2.0
B727	Arrival	2	20k to 40k	1,848	-1.9 ± 0.5
B727	Arrival	3	40k or more	598	-5.9 ± 2.1
B727	Departure	1	0 to 60k	2,817	-1.2 ± 0.7
B727	Departure	2	60k or more	1,312	-3.8 ± 0.4
B733	Arrival	1	0 to 20k	567	2.1 ± 1.8
B733	Arrival	2	20k to 40k	2,258	-2.4 ± 0.3
B733	Arrival	3	40k or more	672	-6.9 ± 1.1
B733	Departure	1	0 to 30k	266	-3.4 ± 1.7
B733	Departure	2	30k to 50k	609	-5.1 ± 0.6
B733	Departure	3	50k or more	1,460	-6.7 ± 1.2
B73S	Arrival	1	0 to 20k	409	0.7 ± 3.2
B73S	Arrival	2	20k to 40k	1,068	-0.9 ± 0.6
B73S	Arrival	3	40k or more	374	-6.0 ± 1.3
B73S	Departure	1	0 to 60k	1,697	-1.8 ± 1.7
B73S	Departure	2	60k or more	848	-5.6 ± 0.6
B757	Arrival	1	0 to 20k	184	2.3 ± 2.7
B757	Arrival	2	20k to 40k	705	-2.4 ± 0.6
B757	Arrival	3	40k or more	199	-7.1 ± 1.7
B757	Departure	1	0 to 50k	128	-6.7 ± 7.4
B757	Departure	2	50k or more	316	-8.5 ± 2.9
DC10	Arrival	1	0 to 20k	167	1.6 ± 3.5
DC10	Arrival	2	20k to 40k	446	-1.6 ± 0.6
DC10	Arrival	3	40k or more	125	-10.4 ± 1.8
DC10	Departure	1	0 to 60k	228	0.0 ± 1.6
DC10	Departure	2	60k or more	303	-2.7 ± 0.8
M80	Arrival	1	0 to 20k	190	-2.2 ± 3.7
M80	Arrival	2	20k to 40k	396	-6.0 ± 2.1
M80	Arrival	3	40k or more	33	-8.7 ± 3.2
M80	Departure	1	0 to 60k	709	-0.7 ± 0.9
M80	Departure	2	60k or more	144	-2.5 ± 4.2
			Sum:	22,159	
			Maximum:		2.3 7.4
			Average:		-3.3 1.9
			Minimum:		-10.4 0.3

Low elevation angles

Aircraft type	Operation	Track-distance regime	Track-distance interval	Number of data points	INM Offset ± 95% confidence
B727	Arrival	1	0 to 20k	34	1.1 ± 1.5
B727	Arrival	2	20k to 40k	408	-1.0 ± 0.6
B727	Arrival	3	40k or more	272	-2.5 ± 1.1
B727	Departure	1	0 to 60k	167	0.7 ± 2.7
B727	Departure	2	60k or more	466	-3.3 ± 0.5
B733	Arrival	1	0 to 20k	64	3.2 ± 0.4
B733	Arrival	2	20k to 40k	536	-1.0 ± 0.4
B733	Arrival	3	40k or more	427	-4.9 ± 2.5
B733	Departure	1	0 to 30k	160	-2.5 ± 0.8
B733	Departure	2	30k to 50k	239	-4.0 ± 0.9
B733	Departure	3	50k or more	947	-5.1 ± 0.3
B73S	Arrival	1	0 to 20k	57	1.7 ± 0.9
B73S	Arrival	2	20k to 40k	270	0.2 ± 0.7
B73S	Arrival	3	40k or more	259	-3.1 ± 1.0
B73S	Departure	1	0 to 60k	241	0.5 ± 2.0
B73S	Departure	2	60k or more	434	-5.2 ± 0.5
B757	Arrival	1	0 to 20k	16	-3.1 ± 4.5
B757	Arrival	2	20k to 40k	160	-1.8 ± 1.0
B757	Arrival	3	40k or more	138	-4.2 ± 1.3
B757	Departure	1	0 to 50k	92	-3.2 ± 3.3
B757	Departure	2	50k or more	305	-5.2 ± 0.5
DC10	Arrival	1	0 to 20k	4	3.0 ± 1.8
DC10	Arrival	2	20k to 40k	63	-1.9 ± 1.1
DC10	Arrival	3	40k or more	82	-9.8 ± 1.5
DC10	Departure	1	0 to 60k	54	2.6 ± 1.6
DC10	Departure	2	60k or more	165	0.3 ± 0.8
M80	Arrival	1	0 to 20k	5	-1.0 ± 2.2
M80	Arrival	2	20k to 40k	119	-4.1 ± 0.5
M80	Arrival	3	40k or more	36	-11.2 ± 5.2
M80	Departure	1	0 to 60k	100	1.0 ± 0.9
M80	Departure	2	60k or more	45	-1.3 ± 2.4
			Sum:	6,365	
			Maximum:		3.2 5.2
			Average:		-2.1 1.5
			Minimum:		-11.2 0.3

High elevation angles

Table 17. INM Offsets: Modeling Method 4

Aircraft type	Operation	Track-distance regime	Track-distance interval	Number of data points	INM Offset ± 95% confidence
B727	Arrival	1	0 to 20k	1,273	1.6 ± 1.9
B727	Arrival	2	20k to 40k	1,860	-1.4 ± 0.5
B727	Arrival	3	40k or more	604	-5.5 ± 2.1
B727	Departure	1	0 to 60k	2,818	1.4 ± 0.8
B727	Departure	2	60k or more	1,312	0.9 ± 0.4
B733	Arrival	1	0 to 20k	581	2.0 ± 1.7
B733	Arrival	2	20k to 40k	2,272	-1.9 ± 0.3
B733	Arrival	3	40k or more	687	-5.6 ± 1.1
B733	Departure	1	0 to 30k	281	-2.3 ± 1.6
B733	Departure	2	30k to 50k	626	-3.8 ± 0.6
B733	Departure	3	50k or more	1,462	-4.2 ± 1.2
B73S	Arrival	1	0 to 20k	424	0.6 ± 3.1
B73S	Arrival	2	20k to 40k	1,073	-0.4 ± 0.6
B73S	Arrival	3	40k or more	380	-4.7 ± 1.3
B73S	Departure	1	0 to 60k	1,704	2.0 ± 1.2
B73S	Departure	2	60k or more	849	-3.3 ± 0.5
B757	Arrival	1	0 to 20k	190	1.9 ± 2.5
B757	Arrival	2	20k to 40k	706	-2.2 ± 0.6
B757	Arrival	3	40k or more	203	-6.0 ± 1.6
B757	Departure	1	0 to 50k	132	-5.5 ± 7.2
B757	Departure	2	50k or more	320	-6.3 ± 2.9
DC10	Arrival	1	0 to 20k	187	1.1 ± 3.5
DC10	Arrival	2	20k to 40k	447	-1.4 ± 0.6
DC10	Arrival	3	40k or more	132	-9.0 ± 1.7
DC10	Departure	1	0 to 60k	230	0.7 ± 1.3
DC10	Departure	2	60k or more	304	-1.2 ± 0.8
M80	Arrival	1	0 to 20k	207	-2.1 ± 3.6
M80	Arrival	2	20k to 40k	398	-5.4 ± 2.1
M80	Arrival	3	40k or more	35	-7.5 ± 3.0
M80	Departure	1	0 to 60k	713	-0.5 ± 0.9
M80	Departure	2	60k or more	144	-2.4 ± 4.2
			Sum:	22,554	
			Maximum:		2.0 7.2
			Average:		-2.3 1.8
			Minimum:		-9.0 0.3

Low elevation angles

Aircraft type	Operation	Track-distance regime	Track-distance interval	Number of data points	INM Offset ± 95% confidence
B727	Arrival	1	0 to 20k	34	1.1 ± 1.5
B727	Arrival	2	20k to 40k	409	-0.6 ± 0.6
B727	Arrival	3	40k or more	272	-2.3 ± 1.0
B727	Departure	1	0 to 60k	167	2.0 ± 2.9
B727	Departure	2	60k or more	466	0.3 ± 0.4
B733	Arrival	1	0 to 20k	64	3.1 ± 0.4
B733	Arrival	2	20k to 40k	536	-0.6 ± 0.4
B733	Arrival	3	40k or more	427	-3.9 ± 2.5
B733	Departure	1	0 to 30k	161	-2.0 ± 0.8
B733	Departure	2	30k to 50k	244	-3.1 ± 0.9
B733	Departure	3	50k or more	947	-3.1 ± 0.3
B73S	Arrival	1	0 to 20k	57	1.6 ± 0.9
B73S	Arrival	2	20k to 40k	270	0.6 ± 0.7
B73S	Arrival	3	40k or more	259	-2.1 ± 1.0
B73S	Departure	1	0 to 60k	241	2.6 ± 1.9
B73S	Departure	2	60k or more	434	-3.4 ± 0.5
B757	Arrival	1	0 to 20k	16	-3.6 ± 4.5
B757	Arrival	2	20k to 40k	160	-1.7 ± 1.0
B757	Arrival	3	40k or more	139	-3.5 ± 1.3
B757	Departure	1	0 to 50k	93	-2.8 ± 3.3
B757	Departure	2	50k or more	305	-3.4 ± 0.5
DC10	Arrival	1	0 to 20k	4	2.6 ± 1.8
DC10	Arrival	2	20k to 40k	63	-1.8 ± 1.1
DC10	Arrival	3	40k or more	82	-8.7 ± 1.5
DC10	Departure	1	0 to 60k	54	2.8 ± 1.6
DC10	Departure	2	60k or more	165	1.1 ± 0.7
M80	Arrival	1	0 to 20k	5	-1.1 ± 2.2
M80	Arrival	2	20k to 40k	119	-3.6 ± 0.5
M80	Arrival	3	40k or more	36	-10.2 ± 5.2
M80	Departure	1	0 to 60k	100	0.5 ± 1.1
M80	Departure	2	60k or more	45	-0.9 ± 2.4
			Sum:	6,374	
			Maximum:		3.1 5.2
			Average:		-1.4 1.5
			Minimum:		-10.2 0.3

High elevation angles

Table 18. INM Offsets: Modeling Method 5

Aircraft type	Operation	Track-distance regime	Track-distance interval	Number of data points	INM Offset ± 95% confidence
B727	Arrival	1	0 to 20k	1,273	1.6 ± 1.9
B727	Arrival	2	20k to 40k	1,860	-1.4 ± 0.5
B727	Arrival	3	40k or more	604	-5.5 ± 2.1
B727	Departure	1	0 to 60k	2,818	1.4 ± 0.8
B727	Departure	2	60k or more	1,312	0.9 ± 0.4
B733	Arrival	1	0 to 20k	581	2.0 ± 1.7
B733	Arrival	2	20k to 40k	2,272	-1.4 ± 0.3
B733	Arrival	3	40k or more	687	-4.7 ± 1.1
B733	Departure	1	0 to 30k	281	-1.7 ± 1.7
B733	Departure	2	30k to 50k	626	-3.2 ± 0.6
B733	Departure	3	50k or more	1,462	-3.6 ± 1.2
B73S	Arrival	1	0 to 20k	424	0.6 ± 3.1
B73S	Arrival	2	20k to 40k	1,073	0.1 ± 0.6
B73S	Arrival	3	40k or more	380	-3.7 ± 1.3
B73S	Departure	1	0 to 60k	1,704	2.6 ± 1.2
B73S	Departure	2	60k or more	849	-2.5 ± 0.6
B757	Arrival	1	0 to 20k	190	1.9 ± 2.5
B757	Arrival	2	20k to 40k	706	-1.7 ± 0.6
B757	Arrival	3	40k or more	203	-5.0 ± 1.6
B757	Departure	1	0 to 50k	132	-5.9 ± 6.4
B757	Departure	2	50k or more	320	-5.0 ± 2.9
DC10	Arrival	1	0 to 20k	187	1.2 ± 3.5
DC10	Arrival	2	20k to 40k	447	-0.9 ± 0.6
DC10	Arrival	3	40k or more	132	-8.2 ± 1.7
DC10	Departure	1	0 to 60k	230	1.3 ± 1.3
DC10	Departure	2	60k or more	304	-0.2 ± 0.8
M80	Arrival	1	0 to 20k	207	-2.1 ± 3.6
M80	Arrival	2	20k to 40k	398	-5.4 ± 2.1
M80	Arrival	3	40k or more	35	-7.5 ± 3.0
M80	Departure	1	0 to 60k	713	-0.5 ± 0.9
M80	Departure	2	60k or more	144	-2.4 ± 4.2
			Sum:	22,554	
			Maximum:		2.6 6.4
			Average:		-1.9 1.8
			Minimum:		-8.2 0.3

Low elevation angles

Aircraft type	Operation	Track-distance regime	Track-distance interval	Number of data points	INM Offset ± 95% confidence
B727	Arrival	1	0 to 20k	34	1.1 ± 1.5
B727	Arrival	2	20k to 40k	409	-0.6 ± 0.6
B727	Arrival	3	40k or more	272	-2.3 ± 1.0
B727	Departure	1	0 to 60k	167	2.0 ± 2.9
B727	Departure	2	60k or more	466	0.3 ± 0.4
B733	Arrival	1	0 to 20k	64	3.1 ± 0.4
B733	Arrival	2	20k to 40k	536	-0.4 ± 0.4
B733	Arrival	3	40k or more	427	-3.7 ± 2.5
B733	Departure	1	0 to 30k	161	-1.9 ± 0.8
B733	Departure	2	30k to 50k	244	-3.0 ± 0.9
B733	Departure	3	50k or more	947	-3.0 ± 0.3
B73S	Arrival	1	0 to 20k	57	1.6 ± 0.9
B73S	Arrival	2	20k to 40k	270	0.7 ± 0.7
B73S	Arrival	3	40k or more	259	-2.0 ± 1.0
B73S	Departure	1	0 to 60k	241	2.7 ± 1.9
B73S	Departure	2	60k or more	434	-3.3 ± 0.5
B757	Arrival	1	0 to 20k	16	-3.6 ± 4.5
B757	Arrival	2	20k to 40k	160	-1.6 ± 1.0
B757	Arrival	3	40k or more	139	-3.4 ± 1.3
B757	Departure	1	0 to 50k	93	-2.0 ± 3.1
B757	Departure	2	50k or more	305	-2.0 ± 0.5
DC10	Arrival	1	0 to 20k	4	2.6 ± 1.8
DC10	Arrival	2	20k to 40k	63	-1.7 ± 1.1
DC10	Arrival	3	40k or more	82	-8.6 ± 1.5
DC10	Departure	1	0 to 60k	54	3.0 ± 1.6
DC10	Departure	2	60k or more	165	1.3 ± 0.7
M80	Arrival	1	0 to 20k	5	-1.1 ± 2.2
M80	Arrival	2	20k to 40k	119	-3.6 ± 0.5
M80	Arrival	3	40k or more	36	-10.2 ± 5.2
M80	Departure	1	0 to 60k	100	0.5 ± 1.1
M80	Departure	2	60k or more	45	-0.9 ± 2.4
			Sum:	6,374	
			Maximum:		3.1 5.2
			Average:		-1.3 1.5
			Minimum:		-10.2 0.3

High elevation angles

Table 19. INM Offsets: Modeling Method 6

Aircraft type	Operation	Track-distance regime	Track-distance interval	Number of data points	INM Offset ± 95% confidence
B727	Arrival	1	0 to 20k	1,273	1.4 ± 1.9
B727	Arrival	2	20k to 40k	1,860	-1.7 ± 0.5
B727	Arrival	3	40k or more	604	-5.9 ± 2.1
B727	Departure	1	0 to 60k	2,818	1.0 ± 0.8
B727	Departure	2	60k or more	1,312	0.6 ± 0.4
B733	Arrival	1	0 to 20k	581	1.8 ± 1.8
B733	Arrival	2	20k to 40k	2,272	-1.8 ± 0.3
B733	Arrival	3	40k or more	687	-5.3 ± 1.1
B733	Departure	1	0 to 30k	281	-2.0 ± 1.7
B733	Departure	2	30k to 50k	626	-3.8 ± 0.6
B733	Departure	3	50k or more	1,462	-4.5 ± 1.2
B73S	Arrival	1	0 to 20k	424	0.5 ± 3.1
B73S	Arrival	2	20k to 40k	1,073	-0.3 ± 0.6
B73S	Arrival	3	40k or more	380	-4.2 ± 1.3
B73S	Departure	1	0 to 60k	1,704	2.1 ± 1.2
B73S	Departure	2	60k or more	849	-3.0 ± 0.6
B757	Arrival	1	0 to 20k	190	1.8 ± 2.5
B757	Arrival	2	20k to 40k	706	-2.1 ± 0.6
B757	Arrival	3	40k or more	203	-5.6 ± 1.6
B757	Departure	1	0 to 50k	132	-6.3 ± 6.7
B757	Departure	2	50k or more	320	-5.7 ± 2.9
DC10	Arrival	1	0 to 20k	187	0.8 ± 3.5
DC10	Arrival	2	20k to 40k	447	-1.3 ± 0.6
DC10	Arrival	3	40k or more	132	-8.8 ± 1.7
DC10	Departure	1	0 to 60k	230	0.9 ± 1.3
DC10	Departure	2	60k or more	304	-0.7 ± 0.8
M80	Arrival	1	0 to 20k	207	-2.2 ± 3.7
M80	Arrival	2	20k to 40k	398	-5.8 ± 2.1
M80	Arrival	3	40k or more	35	-7.9 ± 3.1
M80	Departure	1	0 to 60k	713	-0.9 ± 0.9
M80	Departure	2	60k or more	144	-3.0 ± 4.3
			Sum:	22,554	
			Maximum:		2.1 6.7
			Average:		-2.3 1.8
			Minimum:		-8.8 0.3

Low elevation angles

Aircraft type	Operation	Track-distance regime	Track-distance interval	Number of data points	INM Offset ± 95% confidence
B727	Arrival	1	0 to 20k	34	1.0 ± 1.5
B727	Arrival	2	20k to 40k	409	-0.9 ± 0.6
B727	Arrival	3	40k or more	272	-2.8 ± 1.0
B727	Departure	1	0 to 60k	167	1.6 ± 3.0
B727	Departure	2	60k or more	466	0.0 ± 0.4
B733	Arrival	1	0 to 20k	64	2.9 ± 0.4
B733	Arrival	2	20k to 40k	536	-0.7 ± 0.4
B733	Arrival	3	40k or more	427	-4.3 ± 2.5
B733	Departure	1	0 to 30k	161	-2.2 ± 0.8
B733	Departure	2	30k to 50k	244	-3.5 ± 0.9
B733	Departure	3	50k or more	947	-3.9 ± 0.3
B73S	Arrival	1	0 to 20k	57	1.5 ± 0.9
B73S	Arrival	2	20k to 40k	270	0.4 ± 0.7
B73S	Arrival	3	40k or more	259	-2.4 ± 1.0
B73S	Departure	1	0 to 60k	241	2.1 ± 1.9
B73S	Departure	2	60k or more	434	-3.8 ± 0.5
B757	Arrival	1	0 to 20k	16	-3.8 ± 4.6
B757	Arrival	2	20k to 40k	160	-1.8 ± 1.0
B757	Arrival	3	40k or more	139	-3.9 ± 1.3
B757	Departure	1	0 to 50k	93	-2.6 ± 3.1
B757	Departure	2	50k or more	305	-2.6 ± 0.5
DC10	Arrival	1	0 to 20k	4	2.4 ± 2.9
DC10	Arrival	2	20k to 40k	63	-2.1 ± 1.1
DC10	Arrival	3	40k or more	82	-9.2 ± 1.5
DC10	Departure	1	0 to 60k	54	2.7 ± 1.7
DC10	Departure	2	60k or more	165	0.7 ± 0.7
M80	Arrival	1	0 to 20k	5	-1.2 ± 2.1
M80	Arrival	2	20k to 40k	119	-3.9 ± 0.5
M80	Arrival	3	40k or more	36	-10.6 ± 5.2
M80	Departure	1	0 to 60k	100	0.1 ± 1.1
M80	Departure	2	60k or more	45	-1.6 ± 2.5
			Sum:	6,374	
			Maximum:		2.9 5.2
			Average:		-1.7 1.5
			Minimum:		-10.6 0.3

High elevation angles

Table 20. INM Offsets: Modeling Method 7

Aircraft type	Operation	Track-distance regime	Track-distance interval	Number of data points	INM Offset ± 95% confidence
B727	Arrival	1	0 to 20k	1,273	1.4 ± 1.9
B727	Arrival	2	20k to 40k	1,860	-1.7 ± 0.5
B727	Arrival	3	40k or more	604	-5.9 ± 2.1
B727	Departure	1	0 to 60k	2,818	1.0 ± 0.8
B727	Departure	2	60k or more	1,312	0.6 ± 0.4
B733	Arrival	1	0 to 20k	581	2.2 ± 1.8
B733	Arrival	2	20k to 40k	2,272	-1.9 ± 0.3
B733	Arrival	3	40k or more	687	-5.5 ± 1.1
B733	Departure	1	0 to 30k	281	-1.6 ± 1.5
B733	Departure	2	30k to 50k	626	-3.0 ± 0.6
B733	Departure	3	50k or more	1,462	-2.7 ± 1.2
B73S	Arrival	1	0 to 20k	424	0.5 ± 3.1
B73S	Arrival	2	20k to 40k	1,073	-0.3 ± 0.6
B73S	Arrival	3	40k or more	380	-4.2 ± 1.3
B73S	Departure	1	0 to 60k	1,704	2.1 ± 1.2
B73S	Departure	2	60k or more	849	-3.0 ± 0.6
B757	Arrival	1	0 to 20k	190	1.8 ± 2.5
B757	Arrival	2	20k to 40k	706	-2.1 ± 0.6
B757	Arrival	3	40k or more	203	-5.6 ± 1.6
B757	Departure	1	0 to 50k	132	-6.3 ± 6.7
B757	Departure	2	50k or more	320	-5.7 ± 2.9
DC10	Arrival	1	0 to 20k	187	0.8 ± 3.5
DC10	Arrival	2	20k to 40k	447	-1.3 ± 0.6
DC10	Arrival	3	40k or more	132	-8.8 ± 1.7
DC10	Departure	1	0 to 60k	230	0.9 ± 1.3
DC10	Departure	2	60k or more	304	-0.7 ± 0.8
M80	Arrival	1	0 to 20k	207	-1.5 ± 3.6
M80	Arrival	2	20k to 40k	398	-5.8 ± 2.1
M80	Arrival	3	40k or more	35	-7.5 ± 3.0
M80	Departure	1	0 to 60k	713	0.0 ± 1.0
M80	Departure	2	60k or more	144	-1.5 ± 4.3
			Sum:	22,554	
			Maximum:		2.2 6.7
			Average:		-2.1 1.8
			Minimum:		-8.8 0.3

Low elevation angles

Aircraft type	Operation	Track-distance regime	Track-distance interval	Number of data points	INM Offset ± 95% confidence
B727	Arrival	1	0 to 20k	34	1.0 ± 1.5
B727	Arrival	2	20k to 40k	409	-0.9 ± 0.6
B727	Arrival	3	40k or more	272	-2.8 ± 1.0
B727	Departure	1	0 to 60k	167	1.6 ± 3.0
B727	Departure	2	60k or more	466	0.0 ± 0.4
B733	Arrival	1	0 to 20k	64	3.3 ± 0.4
B733	Arrival	2	20k to 40k	536	-0.8 ± 0.4
B733	Arrival	3	40k or more	427	-4.5 ± 2.5
B733	Departure	1	0 to 30k	161	-1.8 ± 0.8
B733	Departure	2	30k to 50k	244	-2.6 ± 0.9
B733	Departure	3	50k or more	947	-2.3 ± 0.3
B73S	Arrival	1	0 to 20k	57	1.5 ± 0.9
B73S	Arrival	2	20k to 40k	270	0.4 ± 0.7
B73S	Arrival	3	40k or more	259	-2.4 ± 1.0
B73S	Departure	1	0 to 60k	241	2.1 ± 1.9
B73S	Departure	2	60k or more	434	-3.8 ± 0.5
B757	Arrival	1	0 to 20k	16	-3.8 ± 4.6
B757	Arrival	2	20k to 40k	160	-1.8 ± 1.0
B757	Arrival	3	40k or more	139	-3.9 ± 1.3
B757	Departure	1	0 to 50k	93	-2.6 ± 3.1
B757	Departure	2	50k or more	305	-2.6 ± 0.5
DC10	Arrival	1	0 to 20k	4	2.4 ± 2.9
DC10	Arrival	2	20k to 40k	63	-2.1 ± 1.1
DC10	Arrival	3	40k or more	82	-9.2 ± 1.5
DC10	Departure	1	0 to 60k	54	2.7 ± 1.7
DC10	Departure	2	60k or more	165	0.7 ± 0.7
M80	Arrival	1	0 to 20k	5	-0.5 ± 2.1
M80	Arrival	2	20k to 40k	119	-3.9 ± 0.5
M80	Arrival	3	40k or more	36	-10.4 ± 5.2
M80	Departure	1	0 to 60k	100	1.0 ± 1.2
M80	Departure	2	60k or more	45	-0.4 ± 2.5
			Sum:	6,374	
			Maximum:		3.3 5.2
			Average:		-1.5 1.5
			Minimum:		-10.4 0.3

High elevation angles

Table 21. INM Offsets: Modeling Method 8

Aircraft type	Operation	Track-distance regime	Track-distance interval	Number of data points	INM Offset ± 95% confidence
B727	Arrival	1	0 to 20k	1,273	1.4 ± 1.9
B727	Arrival	2	20k to 40k	1,860	-1.7 ± 0.5
B727	Arrival	3	40k or more	604	-5.9 ± 2.1
B727	Departure	1	0 to 60k	2,818	1.0 ± 0.8
B727	Departure	2	60k or more	1,312	0.6 ± 0.4
B733	Arrival	1	0 to 20k	581	2.2 ± 1.8
B733	Arrival	2	20k to 40k	2,272	-1.9 ± 0.3
B733	Arrival	3	40k or more	687	-5.5 ± 1.1
B733	Departure	1	0 to 30k	281	-1.6 ± 1.5
B733	Departure	2	30k to 50k	626	-3.1 ± 0.6
B733	Departure	3	50k or more	1,447	-2.7 ± 1.2
B73S	Arrival	1	0 to 20k	424	0.5 ± 3.1
B73S	Arrival	2	20k to 40k	1,073	-0.3 ± 0.6
B73S	Arrival	3	40k or more	380	-4.2 ± 1.3
B73S	Departure	1	0 to 60k	1,704	2.1 ± 1.2
B73S	Departure	2	60k or more	848	-3.0 ± 0.6
B757	Arrival	1	0 to 20k	190	1.8 ± 2.5
B757	Arrival	2	20k to 40k	706	-2.1 ± 0.6
B757	Arrival	3	40k or more	203	-5.6 ± 1.6
B757	Departure	1	0 to 50k	132	-6.3 ± 6.7
B757	Departure	2	50k or more	315	-5.7 ± 3.0
DC10	Arrival	1	0 to 20k	187	0.8 ± 3.5
DC10	Arrival	2	20k to 40k	447	-1.3 ± 0.6
DC10	Arrival	3	40k or more	132	-8.8 ± 1.7
DC10	Departure	1	0 to 60k	230	0.9 ± 1.3
DC10	Departure	2	60k or more	302	-0.7 ± 0.8
M80	Arrival	1	0 to 20k	207	-1.5 ± 3.6
M80	Arrival	2	20k to 40k	398	-5.8 ± 2.1
M80	Arrival	3	40k or more	35	-7.5 ± 3.0
M80	Departure	1	0 to 60k	713	0.1 ± 0.9
M80	Departure	2	60k or more	144	-1.5 ± 4.3
			Sum:	22,531	
			Maximum:		2.2 6.7
			Average:		-2.1 1.8
			Minimum:		-8.8 0.3

Low elevation angles

Aircraft type	Operation	Track-distance regime	Track-distance interval	Number of data points	INM Offset ± 95% confidence
B727	Arrival	1	0 to 20k	34	1.0 ± 1.5
B727	Arrival	2	20k to 40k	409	-0.9 ± 0.6
B727	Arrival	3	40k or more	272	-2.8 ± 1.0
B727	Departure	1	0 to 60k	167	1.6 ± 3.0
B727	Departure	2	60k or more	466	0.0 ± 0.4
B733	Arrival	1	0 to 20k	64	3.3 ± 0.4
B733	Arrival	2	20k to 40k	536	-0.8 ± 0.4
B733	Arrival	3	40k or more	427	-4.5 ± 2.5
B733	Departure	1	0 to 30k	161	-1.6 ± 0.8
B733	Departure	2	30k to 50k	244	-2.7 ± 0.9
B733	Departure	3	50k or more	938	-2.3 ± 0.3
B73S	Arrival	1	0 to 20k	57	1.5 ± 0.9
B73S	Arrival	2	20k to 40k	270	0.4 ± 0.7
B73S	Arrival	3	40k or more	259	-2.4 ± 1.0
B73S	Departure	1	0 to 60k	241	2.1 ± 1.9
B73S	Departure	2	60k or more	434	-3.8 ± 0.5
B757	Arrival	1	0 to 20k	16	-3.8 ± 4.6
B757	Arrival	2	20k to 40k	160	-1.8 ± 1.0
B757	Arrival	3	40k or more	139	-3.9 ± 1.3
B757	Departure	1	0 to 50k	93	-2.6 ± 3.1
B757	Departure	2	50k or more	301	-2.6 ± 0.5
DC10	Arrival	1	0 to 20k	4	2.4 ± 2.9
DC10	Arrival	2	20k to 40k	63	-2.1 ± 1.1
DC10	Arrival	3	40k or more	82	-9.2 ± 1.5
DC10	Departure	1	0 to 60k	54	2.7 ± 1.7
DC10	Departure	2	60k or more	165	0.7 ± 0.7
M80	Arrival	1	0 to 20k	5	-0.5 ± 2.1
M80	Arrival	2	20k to 40k	119	-3.9 ± 0.5
M80	Arrival	3	40k or more	36	-10.4 ± 5.2
M80	Departure	1	0 to 60k	100	1.0 ± 1.2
M80	Departure	2	60k or more	45	-0.3 ± 2.5
			Sum:	6,361	
			Maximum:		3.3 5.2
			Average:		-1.5 1.5
			Minimum:		-10.4 0.3

High elevation angles

Table 22. INM Offsets: Modeling Method 8Star (8*)

Aircraft type	Operation	Track-distance regime	Track-distance interval	Number of data points	INM Offset ± 95% confidence
B727	Arrival	1	0 to 20k	1,273	-1.3 ± 1.9
B727	Arrival	2	20k to 40k	1,860	-1.7 ± 0.5
B727	Arrival	3	40k or more	604	-5.7 ± 2.0
B727	Departure	1	0 to 60k	2,818	3.1 ± 1.1
B727	Departure	2	60k or more	1,312	2.1 ± 0.5
B733	Arrival	1	0 to 20k	581	-0.3 ± 1.9
B733	Arrival	2	20k to 40k	2,272	-1.9 ± 0.3
B733	Arrival	3	40k or more	687	-5.7 ± 1.1
B733	Departure	1	0 to 30k	281	-0.7 ± 1.3
B733	Departure	2	30k to 50k	626	-1.9 ± 0.6
B733	Departure	3	50k or more	1,447	-1.0 ± 1.2
B73S	Arrival	1	0 to 20k	424	-1.8 ± 3.1
B73S	Arrival	2	20k to 40k	1,073	-0.4 ± 0.6
B73S	Arrival	3	40k or more	380	-4.6 ± 1.3
B73S	Departure	1	0 to 60k	1,704	6.4 ± 1.4
B73S	Departure	2	60k or more	848	-0.8 ± 0.6
B757	Arrival	1	0 to 20k	190	-1.2 ± 2.9
B757	Arrival	2	20k to 40k	706	-2.2 ± 0.6
B757	Arrival	3	40k or more	203	-5.8 ± 1.6
B757	Departure	1	0 to 50k	132	-6.9 ± 6.0
B757	Departure	2	50k or more	315	-4.7 ± 3.0
DC10	Arrival	1	0 to 20k	187	-0.1 ± 5.0
DC10	Arrival	2	20k to 40k	447	-1.1 ± 0.6
DC10	Arrival	3	40k or more	132	-8.9 ± 1.8
DC10	Departure	1	0 to 60k	230	3.0 ± 1.6
DC10	Departure	2	60k or more	302	-0.9 ± 0.8
M80	Arrival	1	0 to 20k	207	-4.1 ± 3.4
M80	Arrival	2	20k to 40k	398	-5.7 ± 2.1
M80	Arrival	3	40k or more	35	-7.5 ± 3.0
M80	Departure	1	0 to 60k	713	1.1 ± 0.9
M80	Departure	2	60k or more	144	0.0 ± 4.3
			Sum:	22,531	
			Maximum:		6.4 6.0
			Average:		-2.0 1.8
			Minimum:		-8.9 0.3

Low elevation angles

Aircraft type	Operation	Track-distance regime	Track-distance interval	Number of data points	INM Offset ± 95% confidence
B727	Arrival	1	0 to 20k	34	1.8 ± 1.2
B727	Arrival	2	20k to 40k	409	-1.3 ± 0.6
B727	Arrival	3	40k or more	272	-3.2 ± 1.0
B727	Departure	1	0 to 60k	167	2.1 ± 2.0
B727	Departure	2	60k or more	466	1.5 ± 0.4
B733	Arrival	1	0 to 20k	64	3.6 ± 0.7
B733	Arrival	2	20k to 40k	536	-1.6 ± 0.4
B733	Arrival	3	40k or more	427	-5.4 ± 2.5
B733	Departure	1	0 to 30k	161	-0.4 ± 0.7
B733	Departure	2	30k to 50k	244	-1.3 ± 0.9
B733	Departure	3	50k or more	938	0.1 ± 0.4
B73S	Arrival	1	0 to 20k	57	2.3 ± 0.9
B73S	Arrival	2	20k to 40k	270	-0.4 ± 0.7
B73S	Arrival	3	40k or more	259	-3.3 ± 1.0
B73S	Departure	1	0 to 60k	241	7.0 ± 2.0
B73S	Departure	2	60k or more	434	-0.4 ± 0.6
B757	Arrival	1	0 to 20k	16	-3.6 ± 4.6
B757	Arrival	2	20k to 40k	160	-2.5 ± 1.1
B757	Arrival	3	40k or more	139	-4.5 ± 1.5
B757	Departure	1	0 to 50k	93	-2.1 ± 3.0
B757	Departure	2	50k or more	301	-1.3 ± 0.5
DC10	Arrival	1	0 to 20k	4	3.7 ± 5.5
DC10	Arrival	2	20k to 40k	63	-2.3 ± 1.2
DC10	Arrival	3	40k or more	82	-9.1 ± 1.8
DC10	Departure	1	0 to 60k	54	5.5 ± 1.5
DC10	Departure	2	60k or more	165	0.7 ± 0.7
M80	Arrival	1	0 to 20k	5	1.3 ± 3.4
M80	Arrival	2	20k to 40k	119	-4.0 ± 0.6
M80	Arrival	3	40k or more	36	-9.8 ± 5.3
M80	Departure	1	0 to 60k	100	1.9 ± 1.0
M80	Departure	2	60k or more	45	1.6 ± 2.4
			Sum:	6,361	
			Maximum:		7.0 5.5
			Average:		-0.8 1.6
			Minimum:		-9.8 0.4

High elevation angles

A.1.2 Changes in INM Offsets from One Modeling Method to the Next

Table 23 through Table 30 contain all changes in INM Offsets, from each modeling method to the next.

Each table consists of two major sections: Low elevation angles (below 60 degrees), and high elevation angles (above 60 degrees). Within each major section:

- The first four columns contain the aircraft type, operation type, track-distance regime, and the corresponding track-distance interval.
- The fifth column contains the number of data points for that combination of conditions.
- The final column contains the resulting change in INM Offset, plus its 95% confidence interval.

Table 23. Changes in INM Offsets: Modeling Method 1 to 2

Aircraft type	Operation	Track-distance regime	Track-distance interval	Number of data points	Change in INM Offset ± 95% confidence
B727	Arrival	1	0 to 20k	1,179	0.1 ± 0.0
B727	Arrival	2	20k to 40k	1,854	0.1 ± 0.0
B727	Arrival	3	40k or more	601	0.1 ± 0.2
B727	Departure	1	0 to 60k	2,817	0.4 ± 0.2
B727	Departure	2	60k or more	1,312	0.6 ± 0.0
B733	Arrival	1	0 to 20k	570	0.1 ± 0.0
B733	Arrival	2	20k to 40k	2,257	0.1 ± 0.0
B733	Arrival	3	40k or more	672	0.1 ± 0.2
B733	Departure	1	0 to 30k	270	0.0 ± 0.1
B733	Departure	2	30k to 50k	607	0.0 ± 0.0
B733	Departure	3	50k or more	1,458	0.2 ± 0.0
B73S	Arrival	1	0 to 20k	416	0.1 ± 0.0
B73S	Arrival	2	20k to 40k	1,068	0.1 ± 0.0
B73S	Arrival	3	40k or more	373	0.1 ± 0.2
B73S	Departure	1	0 to 60k	1,695	0.4 ± 0.3
B73S	Departure	2	60k or more	848	0.5 ± 0.0
B757	Arrival	1	0 to 20k	186	0.1 ± 0.0
B757	Arrival	2	20k to 40k	704	0.1 ± 0.0
B757	Arrival	3	40k or more	202	0.1 ± 0.4
B757	Departure	1	0 to 50k	128	-0.2 ± 0.5
B757	Departure	2	50k or more	315	0.3 ± 0.1
DC10	Arrival	1	0 to 20k	186	0.1 ± 0.1
DC10	Arrival	2	20k to 40k	446	0.1 ± 0.0
DC10	Arrival	3	40k or more	126	0.1 ± 0.3
DC10	Departure	1	0 to 60k	229	-0.3 ± 0.2
DC10	Departure	2	60k or more	303	0.0 ± 0.1
M80	Arrival	1	0 to 20k	199	0.1 ± 0.0
M80	Arrival	2	20k to 40k	396	0.1 ± 0.0
M80	Arrival	3	40k or more	33	0.1 ± 0.5
M80	Departure	1	0 to 60k	710	0.1 ± 0.0
M80	Departure	2	60k or more	144	0.4 ± 0.1
			Sum:	22,304	
			Maximum:		0.6 0.5
			Average:		0.1 0.1
			Minimum:		-0.3 0.0

Low elevation angles

Aircraft type	Operation	Track-distance regime	Track-distance interval	Number of data points	Change in INM Offset ± 95% confidence
B727	Arrival	1	0 to 20k	34	0.1 ± 0.0
B727	Arrival	2	20k to 40k	408	0.1 ± 0.0
B727	Arrival	3	40k or more	272	0.1 ± 0.4
B727	Departure	1	0 to 60k	167	0.1 ± 0.5
B727	Departure	2	60k or more	466	0.1 ± 0.0
B733	Arrival	1	0 to 20k	64	0.1 ± 0.0
B733	Arrival	2	20k to 40k	536	0.1 ± 0.0
B733	Arrival	3	40k or more	427	0.1 ± 0.1
B733	Departure	1	0 to 30k	160	-0.2 ± 0.0
B733	Departure	2	30k to 50k	237	-0.1 ± 0.0
B733	Departure	3	50k or more	947	0.0 ± 0.0
B73S	Arrival	1	0 to 20k	57	0.1 ± 0.0
B73S	Arrival	2	20k to 40k	270	0.1 ± 0.0
B73S	Arrival	3	40k or more	259	0.1 ± 0.2
B73S	Departure	1	0 to 60k	241	0.3 ± 0.2
B73S	Departure	2	60k or more	434	0.2 ± 0.0
B757	Arrival	1	0 to 20k	16	0.1 ± 0.0
B757	Arrival	2	20k to 40k	160	0.1 ± 0.0
B757	Arrival	3	40k or more	138	0.1 ± 0.4
B757	Departure	1	0 to 50k	91	-0.2 ± 0.1
B757	Departure	2	50k or more	305	0.1 ± 0.0
DC10	Arrival	1	0 to 20k	4	0.1 ± 0.1
DC10	Arrival	2	20k to 40k	63	0.1 ± 0.0
DC10	Arrival	3	40k or more	82	0.1 ± 0.1
DC10	Departure	1	0 to 60k	54	-0.5 ± 0.1
DC10	Departure	2	60k or more	165	-0.4 ± 0.0
M80	Arrival	1	0 to 20k	5	0.1 ± 0.0
M80	Arrival	2	20k to 40k	119	0.1 ± 0.0
M80	Arrival	3	40k or more	36	0.1 ± 0.5
M80	Departure	1	0 to 60k	100	-0.2 ± 0.1
M80	Departure	2	60k or more	45	0.2 ± 0.3
			Sum:	6,362	
			Maximum:		0.3 0.5
			Average:		0.0 0.1
			Minimum:		-0.5 0.0

High elevation angles

Table 24. Changes in INM Offsets: Modeling Method 2 to 3

Aircraft type	Operation	Track-distance regime	Track-distance interval	Number of data points	Change in INM Offset ± 95% confidence
B727	Arrival	1	0 to 20k	1,080	0.0 ± 0.1
B727	Arrival	2	20k to 40k	1,847	0.0 ± 0.0
B727	Arrival	3	40k or more	598	0.0 ± 0.0
B727	Departure	1	0 to 60k	2,817	0.0 ± 0.0
B727	Departure	2	60k or more	1,312	0.0 ± 0.0
B733	Arrival	1	0 to 20k	565	0.0 ± 0.0
B733	Arrival	2	20k to 40k	2,254	0.0 ± 0.0
B733	Arrival	3	40k or more	669	0.0 ± 0.0
B733	Departure	1	0 to 30k	266	0.0 ± 0.0
B733	Departure	2	30k to 50k	606	0.0 ± 0.0
B733	Departure	3	50k or more	1,458	0.0 ± 0.0
B73S	Arrival	1	0 to 20k	409	0.0 ± 0.2
B73S	Arrival	2	20k to 40k	1,067	0.0 ± 0.0
B73S	Arrival	3	40k or more	373	0.0 ± 0.0
B73S	Departure	1	0 to 60k	1,695	0.0 ± 0.0
B73S	Departure	2	60k or more	848	0.0 ± 0.0
B757	Arrival	1	0 to 20k	184	0.0 ± 0.0
B757	Arrival	2	20k to 40k	704	0.0 ± 0.0
B757	Arrival	3	40k or more	199	0.0 ± 0.0
B757	Departure	1	0 to 50k	128	0.0 ± 0.0
B757	Departure	2	50k or more	315	0.0 ± 0.0
DC10	Arrival	1	0 to 20k	167	0.0 ± 0.1
DC10	Arrival	2	20k to 40k	446	0.0 ± 0.0
DC10	Arrival	3	40k or more	125	0.0 ± 0.0
DC10	Departure	1	0 to 60k	228	0.0 ± 0.0
DC10	Departure	2	60k or more	303	0.0 ± 0.0
M80	Arrival	1	0 to 20k	190	0.0 ± 0.2
M80	Arrival	2	20k to 40k	395	0.0 ± 0.0
M80	Arrival	3	40k or more	33	0.0 ± 0.0
M80	Departure	1	0 to 60k	708	0.0 ± 0.0
M80	Departure	2	60k or more	144	0.0 ± 0.0
			Sum:	22,133	
			Maximum:		0.0 0.2
			Average:		0.0 0.0
			Minimum:		0.0 0.0

Low elevation angles

Aircraft type	Operation	Track-distance regime	Track-distance interval	Number of data points	Change in INM Offset ± 95% confidence
B727	Arrival	1	0 to 20k	34	0.0 ± 0.0
B727	Arrival	2	20k to 40k	408	0.0 ± 0.0
B727	Arrival	3	40k or more	272	0.0 ± 0.0
B727	Departure	1	0 to 60k	167	0.0 ± 0.0
B727	Departure	2	60k or more	466	0.0 ± 0.0
B733	Arrival	1	0 to 20k	64	0.0 ± 0.0
B733	Arrival	2	20k to 40k	536	0.0 ± 0.0
B733	Arrival	3	40k or more	427	0.0 ± 0.0
B733	Departure	1	0 to 30k	160	0.0 ± 0.0
B733	Departure	2	30k to 50k	237	0.0 ± 0.0
B733	Departure	3	50k or more	947	0.0 ± 0.0
B73S	Arrival	1	0 to 20k	57	0.0 ± 0.0
B73S	Arrival	2	20k to 40k	270	0.0 ± 0.0
B73S	Arrival	3	40k or more	259	0.0 ± 0.0
B73S	Departure	1	0 to 60k	241	0.0 ± 0.0
B73S	Departure	2	60k or more	434	0.0 ± 0.0
B757	Arrival	1	0 to 20k	16	0.0 ± 0.0
B757	Arrival	2	20k to 40k	160	0.0 ± 0.0
B757	Arrival	3	40k or more	138	0.0 ± 0.0
B757	Departure	1	0 to 50k	91	0.0 ± 0.0
B757	Departure	2	50k or more	305	0.0 ± 0.0
DC10	Arrival	1	0 to 20k	4	0.0 ± 0.0
DC10	Arrival	2	20k to 40k	63	0.0 ± 0.0
DC10	Arrival	3	40k or more	82	0.0 ± 0.0
DC10	Departure	1	0 to 60k	54	0.0 ± 0.0
DC10	Departure	2	60k or more	165	0.0 ± 0.0
M80	Arrival	1	0 to 20k	5	0.0 ± 0.0
M80	Arrival	2	20k to 40k	119	0.0 ± 0.0
M80	Arrival	3	40k or more	36	0.0 ± 0.0
M80	Departure	1	0 to 60k	100	0.0 ± 0.0
M80	Departure	2	60k or more	45	0.0 ± 0.0
			Sum:	6,362	
			Maximum:		0.0 0.0
			Average:		0.0 0.0
			Minimum:		0.0 0.0

High elevation angles

Table 25. Changes in INM Offsets: Modeling Method 3 to 4

Aircraft type	Operation	Track-distance regime	Track-distance interval	Number of data points	Change in INM Offset ± 95% confidence
B727	Arrival	1	0 to 20k	1,083	0.1 ± 0.2
B727	Arrival	2	20k to 40k	1,848	0.5 ± 0.0
B727	Arrival	3	40k or more	598	0.5 ± 0.1
B727	Departure	1	0 to 60k	2,817	2.5 ± 0.2
B727	Departure	2	60k or more	1,312	4.8 ± 0.2
B733	Arrival	1	0 to 20k	567	-0.1 ± 0.2
B733	Arrival	2	20k to 40k	2,258	0.5 ± 0.0
B733	Arrival	3	40k or more	672	1.4 ± 0.1
B733	Departure	1	0 to 30k	266	0.9 ± 0.3
B733	Departure	2	30k to 50k	609	1.3 ± 0.0
B733	Departure	3	50k or more	1,460	2.5 ± 0.0
B73S	Arrival	1	0 to 20k	409	-0.1 ± 0.2
B73S	Arrival	2	20k to 40k	1,068	0.5 ± 0.0
B73S	Arrival	3	40k or more	374	1.3 ± 0.1
B73S	Departure	1	0 to 60k	1,697	3.8 ± 0.9
B73S	Departure	2	60k or more	848	2.4 ± 0.0
B757	Arrival	1	0 to 20k	184	-0.4 ± 0.3
B757	Arrival	2	20k to 40k	705	0.2 ± 0.1
B757	Arrival	3	40k or more	199	1.2 ± 0.2
B757	Departure	1	0 to 50k	128	1.1 ± 0.5
B757	Departure	2	50k or more	316	2.1 ± 0.0
DC10	Arrival	1	0 to 20k	167	-0.4 ± 0.5
DC10	Arrival	2	20k to 40k	446	0.3 ± 0.1
DC10	Arrival	3	40k or more	125	1.3 ± 0.3
DC10	Departure	1	0 to 60k	228	0.7 ± 0.6
DC10	Departure	2	60k or more	303	1.5 ± 0.1
M80	Arrival	1	0 to 20k	190	0.0 ± 0.4
M80	Arrival	2	20k to 40k	396	0.6 ± 0.1
M80	Arrival	3	40k or more	33	1.3 ± 0.4
M80	Departure	1	0 to 60k	709	0.2 ± 0.2
M80	Departure	2	60k or more	144	0.1 ± 0.1
			Sum:	22,159	
			Maximum:		4.8 ± 0.9
			Average:		1.0 ± 0.2
			Minimum:		-0.4 ± 0.0

Low elevation angles

Aircraft type	Operation	Track-distance regime	Track-distance interval	Number of data points	Change in INM Offset ± 95% confidence
B727	Arrival	1	0 to 20k	34	0.0 ± 0.0
B727	Arrival	2	20k to 40k	408	0.3 ± 0.0
B727	Arrival	3	40k or more	272	0.1 ± 0.1
B727	Departure	1	0 to 60k	167	1.3 ± 0.6
B727	Departure	2	60k or more	466	3.6 ± 0.2
B733	Arrival	1	0 to 20k	64	-0.1 ± 0.0
B733	Arrival	2	20k to 40k	536	0.4 ± 0.0
B733	Arrival	3	40k or more	427	1.1 ± 0.0
B733	Departure	1	0 to 30k	160	0.5 ± 0.1
B733	Departure	2	30k to 50k	239	1.0 ± 0.0
B733	Departure	3	50k or more	947	2.1 ± 0.0
B73S	Arrival	1	0 to 20k	57	-0.1 ± 0.0
B73S	Arrival	2	20k to 40k	270	0.4 ± 0.0
B73S	Arrival	3	40k or more	259	1.0 ± 0.1
B73S	Departure	1	0 to 60k	241	2.1 ± 0.6
B73S	Departure	2	60k or more	434	1.8 ± 0.0
B757	Arrival	1	0 to 20k	16	-0.5 ± 0.0
B757	Arrival	2	20k to 40k	160	0.1 ± 0.0
B757	Arrival	3	40k or more	138	0.9 ± 0.1
B757	Departure	1	0 to 50k	92	0.3 ± 0.1
B757	Departure	2	50k or more	305	1.8 ± 0.0
DC10	Arrival	1	0 to 20k	4	-0.4 ± 0.1
DC10	Arrival	2	20k to 40k	63	0.1 ± 0.0
DC10	Arrival	3	40k or more	82	1.1 ± 0.2
DC10	Departure	1	0 to 60k	54	0.2 ± 0.3
DC10	Departure	2	60k or more	165	0.9 ± 0.0
M80	Arrival	1	0 to 20k	5	0.0 ± 0.1
M80	Arrival	2	20k to 40k	119	0.5 ± 0.0
M80	Arrival	3	40k or more	36	1.0 ± 0.1
M80	Departure	1	0 to 60k	100	-0.5 ± 0.3
M80	Departure	2	60k or more	45	0.3 ± 0.1
			Sum:	6,365	
			Maximum:		3.6 ± 0.6
			Average:		0.7 ± 0.1
			Minimum:		-0.5 ± 0.0

High elevation angles

Table 26. Changes in INM Offsets: Modeling Method 4 to 5

Aircraft type	Operation	Track-distance regime	Track-distance interval	Number of data points	Change in INM Offset ± 95% confidence
B727	Arrival	1	0 to 20k	1,273	0.0 ± 0.0
B727	Arrival	2	20k to 40k	1,860	0.0 ± 0.0
B727	Arrival	3	40k or more	604	0.0 ± 0.0
B727	Departure	1	0 to 60k	2,818	0.0 ± 0.0
B727	Departure	2	60k or more	1,312	0.0 ± 0.0
B733	Arrival	1	0 to 20k	581	0.0 ± 0.0
B733	Arrival	2	20k to 40k	2,272	0.5 ± 0.0
B733	Arrival	3	40k or more	687	1.0 ± 0.1
B733	Departure	1	0 to 30k	281	0.7 ± 0.2
B733	Departure	2	30k to 50k	626	0.6 ± 0.1
B733	Departure	3	50k or more	1,462	0.6 ± 0.0
B73S	Arrival	1	0 to 20k	424	0.0 ± 0.1
B73S	Arrival	2	20k to 40k	1,073	0.5 ± 0.0
B73S	Arrival	3	40k or more	380	1.0 ± 0.1
B73S	Departure	1	0 to 60k	1,704	0.6 ± 0.2
B73S	Departure	2	60k or more	849	0.8 ± 0.1
B757	Arrival	1	0 to 20k	190	0.0 ± 0.1
B757	Arrival	2	20k to 40k	706	0.5 ± 0.0
B757	Arrival	3	40k or more	203	1.0 ± 0.2
B757	Departure	1	0 to 50k	132	-0.4 ± 1.9
B757	Departure	2	50k or more	320	1.4 ± 0.0
DC10	Arrival	1	0 to 20k	187	0.0 ± 0.1
DC10	Arrival	2	20k to 40k	447	0.5 ± 0.1
DC10	Arrival	3	40k or more	132	0.8 ± 0.2
DC10	Departure	1	0 to 60k	230	0.6 ± 0.3
DC10	Departure	2	60k or more	304	1.0 ± 0.1
M80	Arrival	1	0 to 20k	207	0.0 ± 0.0
M80	Arrival	2	20k to 40k	398	0.0 ± 0.0
M80	Arrival	3	40k or more	35	0.0 ± 0.0
M80	Departure	1	0 to 60k	713	0.0 ± 0.0
M80	Departure	2	60k or more	144	0.0 ± 0.0
			Sum:	22,554	
			Maximum:		1.4 ± 1.9
			Average:		0.4 ± 0.1
			Minimum:		-0.4 ± 0.0

Low elevation angles

Aircraft type	Operation	Track-distance regime	Track-distance interval	Number of data points	Change in INM Offset ± 95% confidence
B727	Arrival	1	0 to 20k	34	0.0 ± 0.0
B727	Arrival	2	20k to 40k	409	0.0 ± 0.0
B727	Arrival	3	40k or more	272	0.0 ± 0.0
B727	Departure	1	0 to 60k	167	0.0 ± 0.0
B727	Departure	2	60k or more	466	0.0 ± 0.0
B733	Arrival	1	0 to 20k	64	0.0 ± 0.0
B733	Arrival	2	20k to 40k	536	0.2 ± 0.0
B733	Arrival	3	40k or more	427	0.2 ± 0.0
B733	Departure	1	0 to 30k	161	0.1 ± 0.0
B733	Departure	2	30k to 50k	244	0.1 ± 0.0
B733	Departure	3	50k or more	947	0.1 ± 0.0
B73S	Arrival	1	0 to 20k	57	0.0 ± 0.0
B73S	Arrival	2	20k to 40k	270	0.1 ± 0.0
B73S	Arrival	3	40k or more	259	0.1 ± 0.0
B73S	Departure	1	0 to 60k	241	0.1 ± 0.0
B73S	Departure	2	60k or more	434	0.1 ± 0.0
B757	Arrival	1	0 to 20k	16	0.0 ± 0.1
B757	Arrival	2	20k to 40k	160	0.2 ± 0.0
B757	Arrival	3	40k or more	139	0.1 ± 0.0
B757	Departure	1	0 to 50k	93	0.8 ± 0.7
B757	Departure	2	50k or more	305	1.5 ± 0.0
DC10	Arrival	1	0 to 20k	4	0.0 ± 0.0
DC10	Arrival	2	20k to 40k	63	0.1 ± 0.0
DC10	Arrival	3	40k or more	82	0.1 ± 0.0
DC10	Departure	1	0 to 60k	54	0.2 ± 0.1
DC10	Departure	2	60k or more	165	0.1 ± 0.0
M80	Arrival	1	0 to 20k	5	0.0 ± 0.0
M80	Arrival	2	20k to 40k	119	0.0 ± 0.0
M80	Arrival	3	40k or more	36	0.0 ± 0.0
M80	Departure	1	0 to 60k	100	0.0 ± 0.0
M80	Departure	2	60k or more	45	0.0 ± 0.0
			Sum:	6,374	
			Maximum:		1.5 ± 0.7
			Average:		0.1 ± 0.0
			Minimum:		0.0 ± 0.0

High elevation angles

Table 27. Changes in INM Offsets: Modeling Method 5 to 6

Aircraft type	Operation	Track-distance regime	Track-distance interval	Number of data points	Change in INM Offset ± 95% confidence
B727	Arrival	1	0 to 20k	1,273	-0.2 ± 0.2
B727	Arrival	2	20k to 40k	1,860	-0.3 ± 0.0
B727	Arrival	3	40k or more	604	-0.4 ± 0.1
B727	Departure	1	0 to 60k	2,818	-0.4 ± 0.2
B727	Departure	2	60k or more	1,312	-0.3 ± 0.2
B733	Arrival	1	0 to 20k	581	-0.2 ± 0.2
B733	Arrival	2	20k to 40k	2,272	-0.4 ± 0.0
B733	Arrival	3	40k or more	687	-0.7 ± 0.1
B733	Departure	1	0 to 30k	281	-0.3 ± 0.3
B733	Departure	2	30k to 50k	626	-0.7 ± 0.1
B733	Departure	3	50k or more	1,462	-1.0 ± 0.1
B73S	Arrival	1	0 to 20k	424	-0.1 ± 0.2
B73S	Arrival	2	20k to 40k	1,073	-0.4 ± 0.1
B73S	Arrival	3	40k or more	380	-0.5 ± 0.1
B73S	Departure	1	0 to 60k	1,704	-0.6 ± 0.2
B73S	Departure	2	60k or more	849	-0.5 ± 0.1
B757	Arrival	1	0 to 20k	190	-0.2 ± 0.7
B757	Arrival	2	20k to 40k	706	-0.4 ± 0.1
B757	Arrival	3	40k or more	203	-0.6 ± 0.2
B757	Departure	1	0 to 50k	132	-0.4 ± 1.1
B757	Departure	2	50k or more	320	-0.7 ± 0.1
DC10	Arrival	1	0 to 20k	187	-0.4 ± 1.1
DC10	Arrival	2	20k to 40k	447	-0.4 ± 0.1
DC10	Arrival	3	40k or more	132	-0.6 ± 0.2
DC10	Departure	1	0 to 60k	230	-0.4 ± 0.2
DC10	Departure	2	60k or more	304	-0.5 ± 0.1
M80	Arrival	1	0 to 20k	207	-0.1 ± 0.3
M80	Arrival	2	20k to 40k	398	-0.3 ± 0.1
M80	Arrival	3	40k or more	35	-0.4 ± 0.4
M80	Departure	1	0 to 60k	713	-0.4 ± 0.2
M80	Departure	2	60k or more	144	-0.6 ± 0.3
			Sum:	22,554	
			Maximum:		-0.1 1.1
			Average:		-0.4 0.2
			Minimum:		-1.0 0.0

Low elevation angles

Aircraft type	Operation	Track-distance regime	Track-distance interval	Number of data points	Change in INM Offset ± 95% confidence
B727	Arrival	1	0 to 20k	34	-0.1 ± 0.1
B727	Arrival	2	20k to 40k	409	-0.3 ± 0.0
B727	Arrival	3	40k or more	272	-0.5 ± 0.1
B727	Departure	1	0 to 60k	167	-0.3 ± 0.7
B727	Departure	2	60k or more	466	-0.3 ± 0.1
B733	Arrival	1	0 to 20k	64	-0.2 ± 0.1
B733	Arrival	2	20k to 40k	536	-0.3 ± 0.0
B733	Arrival	3	40k or more	427	-0.6 ± 0.1
B733	Departure	1	0 to 30k	161	-0.3 ± 0.2
B733	Departure	2	30k to 50k	244	-0.5 ± 0.1
B733	Departure	3	50k or more	947	-1.0 ± 0.1
B73S	Arrival	1	0 to 20k	57	-0.1 ± 0.1
B73S	Arrival	2	20k to 40k	270	-0.3 ± 0.1
B73S	Arrival	3	40k or more	259	-0.4 ± 0.1
B73S	Departure	1	0 to 60k	241	-0.6 ± 0.3
B73S	Departure	2	60k or more	434	-0.6 ± 0.1
B757	Arrival	1	0 to 20k	16	-0.2 ± 0.3
B757	Arrival	2	20k to 40k	160	-0.3 ± 0.1
B757	Arrival	3	40k or more	139	-0.5 ± 0.2
B757	Departure	1	0 to 50k	93	-0.6 ± 0.3
B757	Departure	2	50k or more	305	-0.6 ± 0.1
DC10	Arrival	1	0 to 20k	4	-0.2 ± 1.5
DC10	Arrival	2	20k to 40k	63	-0.4 ± 0.2
DC10	Arrival	3	40k or more	82	-0.6 ± 0.2
DC10	Departure	1	0 to 60k	54	-0.4 ± 0.2
DC10	Departure	2	60k or more	165	-0.5 ± 0.1
M80	Arrival	1	0 to 20k	5	-0.1 ± 0.2
M80	Arrival	2	20k to 40k	119	-0.3 ± 0.0
M80	Arrival	3	40k or more	36	-0.5 ± 0.2
M80	Departure	1	0 to 60k	100	-0.4 ± 0.3
M80	Departure	2	60k or more	45	-0.6 ± 0.2
			Sum:	6,374	
			Maximum:		-0.1 1.5
			Average:		-0.4 0.2
			Minimum:		-1.0 0.0

High elevation angles

Table 28. Changes in INM Offsets: Modeling Method 6 to 7

Aircraft type	Operation	Track-distance regime	Track-distance interval	Number of data points	Change in INM Offset ± 95% confidence
B727	Arrival	1	0 to 20k	1,273	0.0 ± 0.0
B727	Arrival	2	20k to 40k	1,860	0.0 ± 0.0
B727	Arrival	3	40k or more	604	0.0 ± 0.0
B727	Departure	1	0 to 60k	2,818	0.0 ± 0.0
B727	Departure	2	60k or more	1,312	0.0 ± 0.0
B733	Arrival	1	0 to 20k	581	0.4 ± 0.1
B733	Arrival	2	20k to 40k	2,272	-0.1 ± 0.0
B733	Arrival	3	40k or more	687	-0.1 ± 0.1
B733	Departure	1	0 to 30k	281	0.4 ± 0.3
B733	Departure	2	30k to 50k	626	0.9 ± 0.1
B733	Departure	3	50k or more	1,462	1.9 ± 0.1
B73S	Arrival	1	0 to 20k	424	0.0 ± 0.0
B73S	Arrival	2	20k to 40k	1,073	0.0 ± 0.0
B73S	Arrival	3	40k or more	380	0.0 ± 0.0
B73S	Departure	1	0 to 60k	1,704	0.0 ± 0.0
B73S	Departure	2	60k or more	849	0.0 ± 0.0
B757	Arrival	1	0 to 20k	190	0.0 ± 0.0
B757	Arrival	2	20k to 40k	706	0.0 ± 0.0
B757	Arrival	3	40k or more	203	0.0 ± 0.0
B757	Departure	1	0 to 50k	132	0.0 ± 0.0
B757	Departure	2	50k or more	320	0.0 ± 0.0
DC10	Arrival	1	0 to 20k	187	0.0 ± 0.0
DC10	Arrival	2	20k to 40k	447	0.0 ± 0.0
DC10	Arrival	3	40k or more	132	0.0 ± 0.0
DC10	Departure	1	0 to 60k	230	0.0 ± 0.0
DC10	Departure	2	60k or more	304	0.0 ± 0.0
M80	Arrival	1	0 to 20k	207	0.7 ± 0.3
M80	Arrival	2	20k to 40k	398	0.0 ± 0.0
M80	Arrival	3	40k or more	35	0.4 ± 0.3
M80	Departure	1	0 to 60k	713	0.9 ± 0.2
M80	Departure	2	60k or more	144	1.6 ± 0.2
			Sum:	22,554	
			Maximum:		1.9 0.3
			Average:		0.2 0.1
			Minimum:		-0.1 0.0

Low elevation angles

Aircraft type	Operation	Track-distance regime	Track-distance interval	Number of data points	Change in INM Offset ± 95% confidence
B727	Arrival	1	0 to 20k	34	0.0 ± 0.0
B727	Arrival	2	20k to 40k	409	0.0 ± 0.0
B727	Arrival	3	40k or more	272	0.0 ± 0.0
B727	Departure	1	0 to 60k	167	0.0 ± 0.0
B727	Departure	2	60k or more	466	0.0 ± 0.0
B733	Arrival	1	0 to 20k	64	0.4 ± 0.0
B733	Arrival	2	20k to 40k	536	0.0 ± 0.0
B733	Arrival	3	40k or more	427	-0.2 ± 0.0
B733	Departure	1	0 to 30k	161	0.4 ± 0.1
B733	Departure	2	30k to 50k	244	0.9 ± 0.0
B733	Departure	3	50k or more	947	1.6 ± 0.0
B73S	Arrival	1	0 to 20k	57	0.0 ± 0.0
B73S	Arrival	2	20k to 40k	270	0.0 ± 0.0
B73S	Arrival	3	40k or more	259	0.0 ± 0.0
B73S	Departure	1	0 to 60k	241	0.0 ± 0.0
B73S	Departure	2	60k or more	434	0.0 ± 0.0
B757	Arrival	1	0 to 20k	16	0.0 ± 0.0
B757	Arrival	2	20k to 40k	160	0.0 ± 0.0
B757	Arrival	3	40k or more	139	0.0 ± 0.0
B757	Departure	1	0 to 50k	93	0.0 ± 0.0
B757	Departure	2	50k or more	305	0.0 ± 0.0
DC10	Arrival	1	0 to 20k	4	0.0 ± 0.0
DC10	Arrival	2	20k to 40k	63	0.0 ± 0.0
DC10	Arrival	3	40k or more	82	0.0 ± 0.0
DC10	Departure	1	0 to 60k	54	0.0 ± 0.0
DC10	Departure	2	60k or more	165	0.0 ± 0.0
M80	Arrival	1	0 to 20k	5	0.7 ± 0.1
M80	Arrival	2	20k to 40k	119	0.0 ± 0.0
M80	Arrival	3	40k or more	36	0.2 ± 0.1
M80	Departure	1	0 to 60k	100	0.9 ± 0.3
M80	Departure	2	60k or more	45	1.2 ± 0.1
			Sum:	6,374	
			Maximum:		1.6 0.3
			Average:		0.2 0.0
			Minimum:		-0.2 0.0

High elevation angles

Table 29. Changes in INM Offsets: Modeling Method 7 to 8

Aircraft type	Operation	Track-distance regime	Track-distance interval	Number of data points	Change in INM Offset ± 95% confidence
B727	Arrival	1	0 to 20k	1,273	0.0 ± 0.0
B727	Arrival	2	20k to 40k	1,860	0.0 ± 0.0
B727	Arrival	3	40k or more	604	0.0 ± 0.0
B727	Departure	1	0 to 60k	2,818	0.0 ± 0.0
B727	Departure	2	60k or more	1,312	0.0 ± 0.0
B733	Arrival	1	0 to 20k	581	0.0 ± 0.0
B733	Arrival	2	20k to 40k	2,272	0.0 ± 0.0
B733	Arrival	3	40k or more	687	0.0 ± 0.0
B733	Departure	1	0 to 30k	281	0.0 ± 0.3
B733	Departure	2	30k to 50k	626	-0.1 ± 0.0
B733	Departure	3	50k or more	1,447	-0.1 ± 0.0
B73S	Arrival	1	0 to 20k	424	0.0 ± 0.0
B73S	Arrival	2	20k to 40k	1,073	0.0 ± 0.0
B73S	Arrival	3	40k or more	380	0.0 ± 0.0
B73S	Departure	1	0 to 60k	1,704	0.0 ± 0.0
B73S	Departure	2	60k or more	848	0.0 ± 0.0
B757	Arrival	1	0 to 20k	190	0.0 ± 0.0
B757	Arrival	2	20k to 40k	706	0.0 ± 0.0
B757	Arrival	3	40k or more	203	0.0 ± 0.0
B757	Departure	1	0 to 50k	132	0.0 ± 0.0
B757	Departure	2	50k or more	315	0.0 ± 0.0
DC10	Arrival	1	0 to 20k	187	0.0 ± 0.0
DC10	Arrival	2	20k to 40k	447	0.0 ± 0.0
DC10	Arrival	3	40k or more	132	0.0 ± 0.0
DC10	Departure	1	0 to 60k	230	0.0 ± 0.0
DC10	Departure	2	60k or more	302	0.0 ± 0.0
M80	Arrival	1	0 to 20k	207	0.0 ± 0.0
M80	Arrival	2	20k to 40k	398	0.0 ± 0.0
M80	Arrival	3	40k or more	35	0.0 ± 0.0
M80	Departure	1	0 to 60k	713	0.1 ± 0.2
M80	Departure	2	60k or more	144	0.0 ± 0.1
			Sum:	22,531	
			Maximum:		0.1 ± 0.3
			Average:		0.0 ± 0.0
			Minimum:		-0.1 ± 0.0

Low elevation angles

Aircraft type	Operation	Track-distance regime	Track-distance interval	Number of data points	Change in INM Offset ± 95% confidence
B727	Arrival	1	0 to 20k	34	0.0 ± 0.0
B727	Arrival	2	20k to 40k	409	0.0 ± 0.0
B727	Arrival	3	40k or more	272	0.0 ± 0.0
B727	Departure	1	0 to 60k	167	0.0 ± 0.0
B727	Departure	2	60k or more	466	0.0 ± 0.0
B733	Arrival	1	0 to 20k	64	0.0 ± 0.0
B733	Arrival	2	20k to 40k	536	0.0 ± 0.0
B733	Arrival	3	40k or more	427	0.0 ± 0.0
B733	Departure	1	0 to 30k	161	0.1 ± 0.1
B733	Departure	2	30k to 50k	244	-0.1 ± 0.0
B733	Departure	3	50k or more	938	0.0 ± 0.0
B73S	Arrival	1	0 to 20k	57	0.0 ± 0.0
B73S	Arrival	2	20k to 40k	270	0.0 ± 0.0
B73S	Arrival	3	40k or more	259	0.0 ± 0.0
B73S	Departure	1	0 to 60k	241	0.0 ± 0.0
B73S	Departure	2	60k or more	434	0.0 ± 0.0
B757	Arrival	1	0 to 20k	16	0.0 ± 0.0
B757	Arrival	2	20k to 40k	160	0.0 ± 0.0
B757	Arrival	3	40k or more	139	0.0 ± 0.0
B757	Departure	1	0 to 50k	93	0.0 ± 0.0
B757	Departure	2	50k or more	301	0.0 ± 0.0
DC10	Arrival	1	0 to 20k	4	0.0 ± 0.0
DC10	Arrival	2	20k to 40k	63	0.0 ± 0.0
DC10	Arrival	3	40k or more	82	0.0 ± 0.0
DC10	Departure	1	0 to 60k	54	0.0 ± 0.0
DC10	Departure	2	60k or more	165	0.0 ± 0.0
M80	Arrival	1	0 to 20k	5	0.0 ± 0.0
M80	Arrival	2	20k to 40k	119	0.0 ± 0.0
M80	Arrival	3	40k or more	36	0.0 ± 0.0
M80	Departure	1	0 to 60k	100	0.0 ± 0.3
M80	Departure	2	60k or more	45	0.1 ± 0.1
			Sum:	6,361	
			Maximum:		0.1 ± 0.3
			Average:		0.0 ± 0.0
			Minimum:		-0.1 ± 0.0

High elevation angles

Table 30. Changes in INM Offsets: Modeling Method 8 to 8Star (8*)

Aircraft type	Operation	Track-distance regime	Track-distance interval	Number of data points	INM Offset ± 95% confidence
B727	Arrival	1	0 to 20k	34	0.4 ± 0.5
B727	Arrival	2	20k to 40k	409	-0.5 ± 0.2
B727	Arrival	3	40k or more	272	-0.4 ± 0.6
B727	Departure	1	0 to 60k	167	0.5 ± 2.8
B727	Departure	2	60k or more	466	1.5 ± 0.2
B733	Arrival	1	0 to 20k	64	-0.1 ± 0.3
B733	Arrival	2	20k to 40k	536	-0.8 ± 0.2
B733	Arrival	3	40k or more	427	-1.0 ± 0.4
B733	Departure	1	0 to 30k	161	1.6 ± 0.6
B733	Departure	2	30k to 50k	244	1.5 ± 0.3
B733	Departure	3	50k or more	938	2.2 ± 0.1
B73S	Arrival	1	0 to 20k	57	-0.1 ± 0.3
B73S	Arrival	2	20k to 40k	270	-0.9 ± 0.3
B73S	Arrival	3	40k or more	259	-0.9 ± 0.6
B73S	Departure	1	0 to 60k	241	4.6 ± 1.9
B73S	Departure	2	60k or more	434	3.0 ± 0.3
B757	Arrival	1	0 to 20k	16	-0.1 ± 0.3
B757	Arrival	2	20k to 40k	160	-0.7 ± 0.3
B757	Arrival	3	40k or more	139	-0.7 ± 0.9
B757	Departure	1	0 to 50k	93	0.5 ± 0.7
B757	Departure	2	50k or more	301	1.0 ± 0.2
DC10	Arrival	1	0 to 20k	4	-0.4 ± 1.4
DC10	Arrival	2	20k to 40k	63	-0.3 ± 0.6
DC10	Arrival	3	40k or more	82	0.2 ± 1.3
DC10	Departure	1	0 to 60k	54	2.3 ± 1.8
DC10	Departure	2	60k or more	165	0.0 ± 0.3
M80	Arrival	1	0 to 20k	5	1.0 ± 1.3
M80	Arrival	2	20k to 40k	119	-0.1 ± 0.3
M80	Arrival	3	40k or more	36	0.7 ± 1.1
M80	Departure	1	0 to 60k	100	1.3 ± 1.3
M80	Departure	2	60k or more	45	1.7 ± 0.7
			Sum:	6,361	
			Maximum:		4.6 ± 2.8
			Average:		0.6 ± 0.7
			Minimum:		-1.0 ± 0.1

Low elevation angles

Aircraft type	Operation	Track-distance regime	Track-distance interval	Number of data points	INM Offset ± 95% confidence
B727	Arrival	1	0 to 20k	1,273	-1.9 ± 0.5
B727	Arrival	2	20k to 40k	1,860	0.0 ± 0.1
B727	Arrival	3	40k or more	604	0.2 ± 0.4
B727	Departure	1	0 to 60k	2,818	2.7 ± 1.7
B727	Departure	2	60k or more	1,312	1.4 ± 0.2
B733	Arrival	1	0 to 20k	581	-1.1 ± 0.5
B733	Arrival	2	20k to 40k	2,272	0.0 ± 0.1
B733	Arrival	3	40k or more	687	-0.2 ± 0.3
B733	Departure	1	0 to 30k	281	1.1 ± 1.4
B733	Departure	2	30k to 50k	626	1.2 ± 0.1
B733	Departure	3	50k or more	1,447	1.7 ± 0.1
B73S	Arrival	1	0 to 20k	424	-0.9 ± 0.4
B73S	Arrival	2	20k to 40k	1,073	-0.1 ± 0.1
B73S	Arrival	3	40k or more	380	-0.4 ± 0.4
B73S	Departure	1	0 to 60k	1,704	3.8 ± 1.2
B73S	Departure	2	60k or more	848	2.3 ± 0.2
B757	Arrival	1	0 to 20k	190	-1.3 ± 0.9
B757	Arrival	2	20k to 40k	706	-0.1 ± 0.1
B757	Arrival	3	40k or more	203	-0.3 ± 0.6
B757	Departure	1	0 to 50k	132	-0.8 ± 2.3
B757	Departure	2	50k or more	315	0.9 ± 0.1
DC10	Arrival	1	0 to 20k	187	-0.5 ± 0.9
DC10	Arrival	2	20k to 40k	447	0.1 ± 0.2
DC10	Arrival	3	40k or more	132	0.0 ± 0.7
DC10	Departure	1	0 to 60k	230	1.8 ± 0.7
DC10	Departure	2	60k or more	302	-0.2 ± 0.2
M80	Arrival	1	0 to 20k	207	-1.8 ± 0.9
M80	Arrival	2	20k to 40k	398	0.1 ± 0.2
M80	Arrival	3	40k or more	35	0.0 ± 0.5
M80	Departure	1	0 to 60k	713	1.2 ± 0.6
M80	Departure	2	60k or more	144	1.5 ± 0.6
			Sum:	22,531	
			Maximum:		3.8 ± 2.3
			Average:		0.3 ± 0.6
			Minimum:		-1.9 ± 0.1

High elevation angles

A.2 Graphs

Graphs of INM Offsets appear in Section 3.2, above (Figure 4 and Figure 5). In those figures, all confidently large offsets appear as emphasized symbols. In addition, all confidently large changes between modeling methods appear as emphasized line segments connecting the respective symbols. For this study, "confidently large" means outside the range –1dB to +1dB, with 95% confidence.

Figure 27 and Figure 28 repeat those graphs from above, but with emphasis upon values and changes that are confidently *small*.

Comparison of the two sets of figures shows that some symbols and some line segments are neither confidently large nor confidently small—that is, they are not emphasized in either set of figures. These un-emphasized values might be large or they might be small. For example:

- An INM offset of (3.0 ± 2.8) dB might be as small as 0.2dB, or it might be as large as 5.8dB. Its relation to the range –1dB to +1dB is not certain.
- Similarly, a change in INM Offset of (–0.2 ± 1.2) dB might be as small as 0 dB, or it might be as large as –1.4 dB. Its relation to the range –1dB to +1dB is not certain, either.

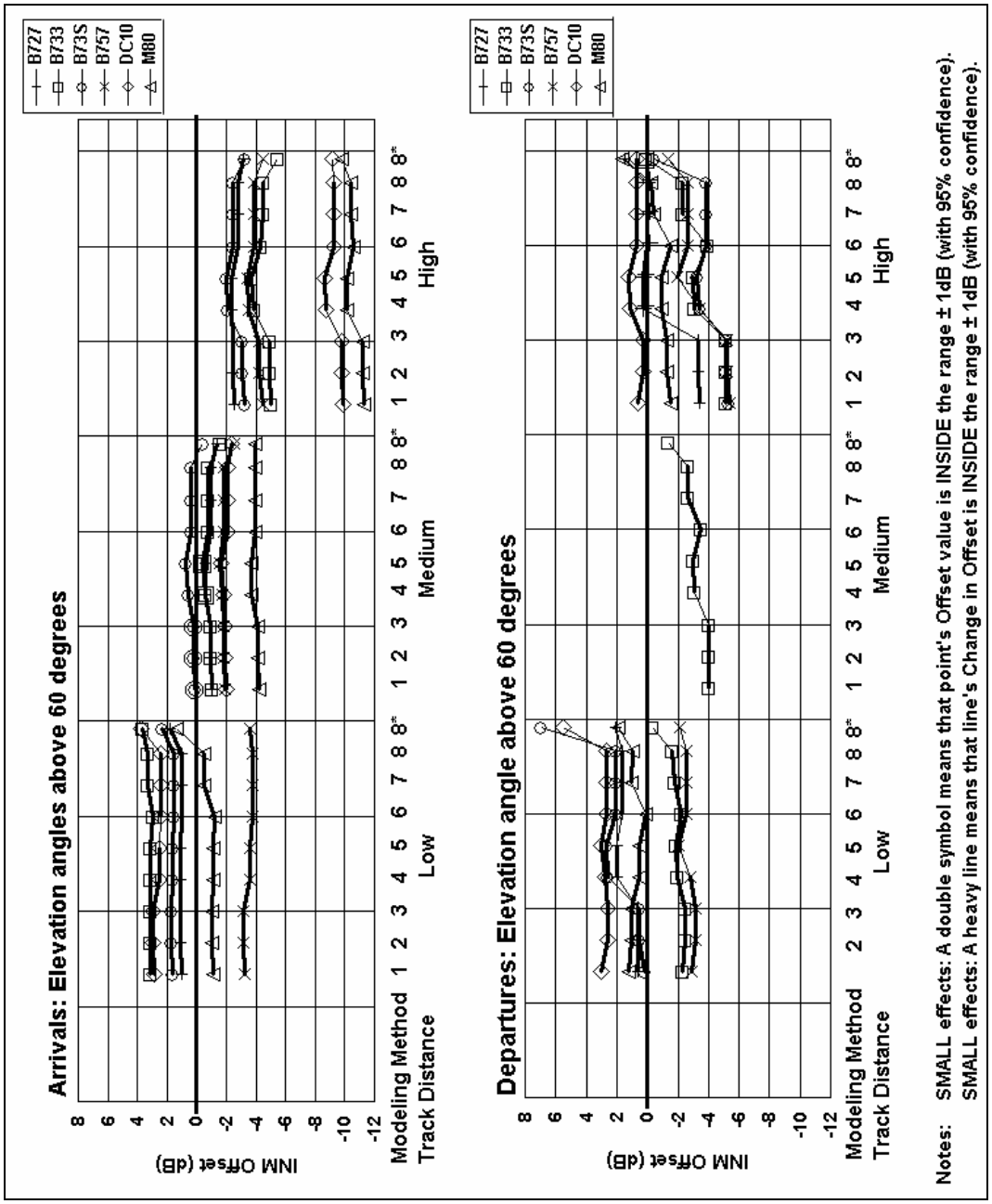


Figure 27. INM Offsets: Elevation angles below 60 degrees (emphasis on small effects)

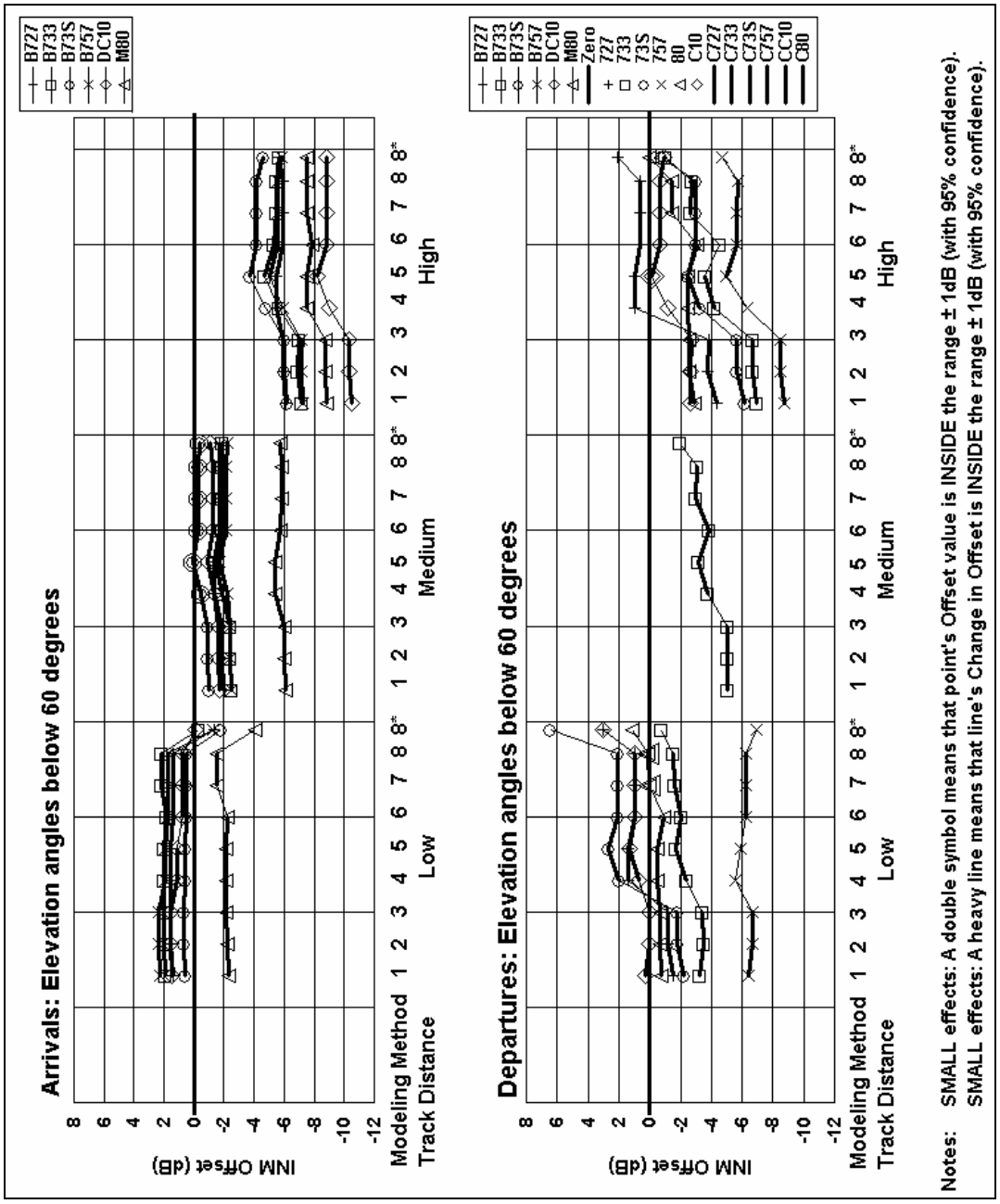


Figure 28. INM Offsets: Elevation angles above 60 degrees (emphasis on small effects)

APPENDIX B MEASURED DATA

This section describes the study's measured data:

- Section B.1 contains a brief description of the DIA monitoring system.
- Section B.2 lists the sampled measurement days (from a full year of data).
- Section B.3 lists and describes the measured variables.

Figure 29 locates Measured Data within the study.

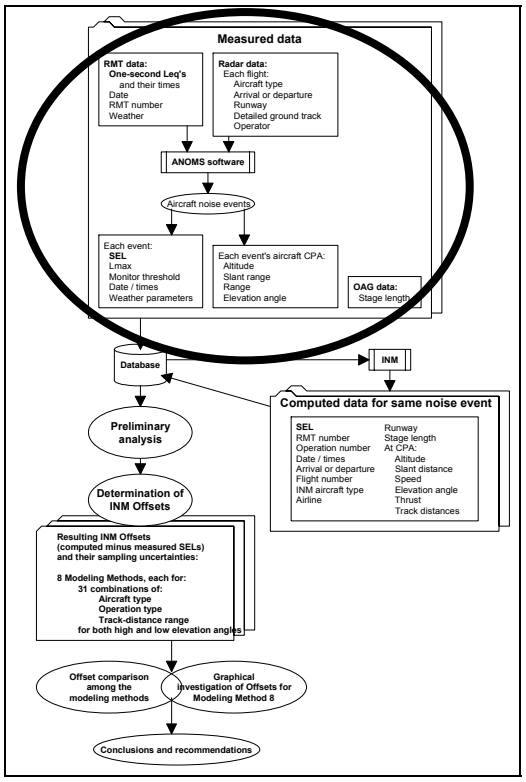


Figure 29. Measured data within the study

B.1 The DIA Monitoring System

The Denver ANOMS monitoring system has an unusually large number of RMTs (32 at the time of data collection), exceeded in number by only one or two other installations. These RMTs range from one to 10 miles from the airport (see Figure 30), thereby extending well beyond RMT distances at most airports and well beyond DIA's 65 DNL contours. The 26 original RMTs have collected data since before the airport was opened in February 1995.

At each RMT, a sound-level time history of one-second A-weighted L_{eq}'s is measured and stored for daily download to the ANOMS computer. Each one-second Leq is time-stamped and tagged with the RMT number. In addition, weather sensors at three RMTs (11, 18 and 26 in Figure 30) continuously measure and download the wind speed/direction, temperature, humidity and atmospheric pressure.

ANOMS also acquires daily radar ARTS data (Automatic Radar Terminal System) from the FAA. These radar data include aircraft type, arrival/departure and runway data from the aircraft's flight plan, plus continuous aircraft position over the ground as a function of time (ground tracks). Continuous altitude data is also stored, but was not used as INM input for this study. The ground-position data is time stamped and recorded by ARTS at each antenna rotation (approximately once every 4½ seconds).

ANOMS then combines the RMT sound-level history with the radar ground-track data (both time stamped) to match one or more aircraft flights with each noise event. Sophisticated matching algorithms use such parameters as time of event and time of operation, aircraft type, location, orientation, rate of climb and speed.

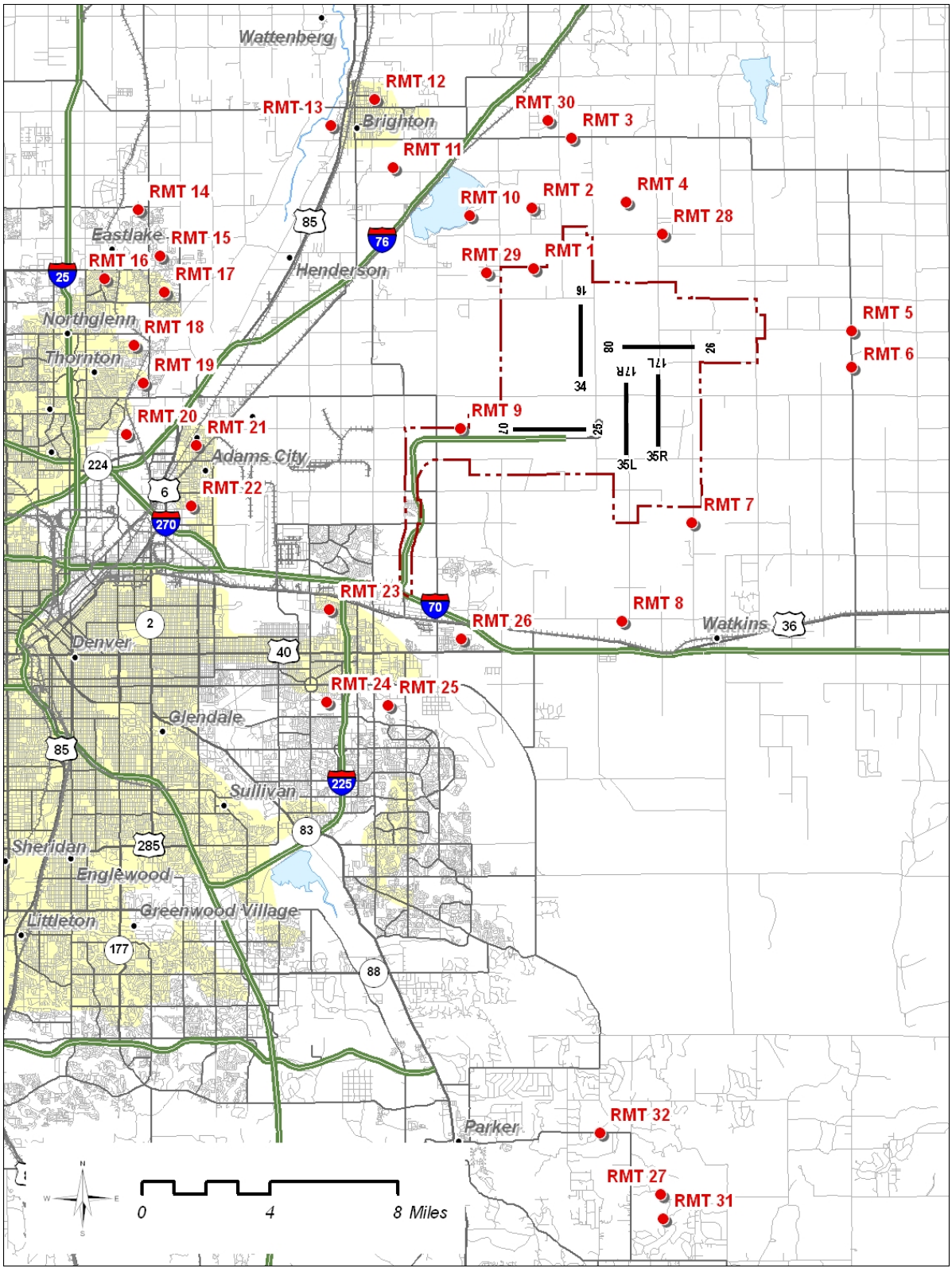


Figure 30. Measurement locations (RMT numbers) at DIA

As a last step, the Official Airline Guide (AOG) provides corresponding "stage length" for each departure. Stage length for each departure depends upon the distance that an aircraft will fly to its next destination. As such, stage length is a standby parameter for aircraft weight, which depends mostly upon fuel load.

Once an aircraft flight is thereby associated with each noise event, that flight's "point of closest approach" (PCA) to the noise-event's monitor is calculated. The PCA is approximated as the aircraft position for which the "radar return" has the shortest distance to the RMT.

PCA parameters include aircraft altitude, slant range and horizontal range (distance) from the aircraft to the RMT, plus elevation angle at the RMT of the aircraft above the horizon.

B.2 Sampled Days of the Full Year

For this study, measured data were obtained for three days each month, for the twelve-month period of April 1995 through March 1996. Table 31 shows the days selected and the number of acceptable aircraft operations each day. Acceptable operations are those (1) that ANOMS associated with at least one measured SEL, at one RMT, and (2) that included sufficient concurrent data to be modeled by INM.

Days were selected randomly, in contiguous groupings of three days, with each grouping including one weekend day. This selection method ensured a ratio of week days to weekend days of 2:1 (close to the true ratio of 2½:1). June data were excluded because they did not sufficiently designate which flights were arrivals and which were departures. Instead of June, two other months were randomly selected—December 1995 (one day) and March 1996 (two days). Contiguous days were used to simplify data extraction.

Table 32 shows the resulting number of arrivals and departures for the study, separately by aircraft type. Only aircraft types with more than 100 operations are listed, because only these were included in the study. For this reason, this table contains fewer operations than does the previous table.

Where justified, the study grouped several ARTS aircraft types into one "study" aircraft type, as shown in the table. For example, 72S and B727 are both ARTS designations for Boeing 727 aircraft, so they were combined into the B727 study aircraft type. Also, all INM-type 737-300, -400 and -500 aircraft were treated as one study type (B733), since they have very similar engines and since they produce very similar sound levels per INM (within about 1 dB). These ARTS aircraft types were converted to INM types for modeling.

Note that the table includes more arrivals than departures. Most likely, this happened because DIA's particular RMT locations, combined with flight-track locations, make ANOMS event/aircraft matching easier for arrivals than for departures. In addition, arriving aircraft are spaced more uniformly and fly lower than departing aircraft. For both these reason, RMTs in line with runways will naturally measure more arrivals than departures.

Table 31 Measurement dates, days of week, and number of operations

Date	Day of week	Number of acceptable operations
April 6, 1995	Thursday	1339
April 7, 1995	Friday	1347
April 8, 1995	Saturday	1232
May 11, 1995	Thursday	718
May 12 1995	Friday	1359
May 13, 1995	Saturday	1130
July 23, 1995	Sunday	1598
July 24, 1995	Monday	1344
July 25, 1995	Tuesday	1398
August 17, 1995	Thursday	1534
August 18, 1995	Friday	1419
August 19, 1995	Saturday	1422
September 3, 1995	Sunday	1125
September 4, 1995	Monday	1279
September 5, 1995	Tuesday	1506
October 15, 1995	Sunday	1717
October 16, 1995	Monday	1212
October 17, 1995	Tuesday	1897
November 16, 1995	Thursday	1100
November 17, 1995	Friday	1578
November 18, 1995	Saturday	887
December 14, 1995	Thursday	1274
December 15, 1995	Friday	1246
December 16, 1995	Saturday	929
December 17, 1995	Sunday	1036
December 18, 1995	Monday	1038
January 18, 1995	Thursday	1667
January 19, 1995	Friday	1331
January 20, 1995	Saturday	1308
February 1, 1996	Thursday	1468
February 2, 1996	Friday	1349
February 3, 1996	Saturday	1370
March 7, 1996	Thursday	1217
March 8, 1996	Friday	1318
March 9, 1996	Saturday	1115
March 10, 1996	Sunday	980
Total operations		**46787**

Table 32. Number of arrivals/departures

Study aircraft type	ARTS aircraft type	Number of arrivals	Number of departures	TOTAL
B727	72S, B727	5693	6286	**11979**
B733	733, 734, 735	6188	4718	**10906**
B73S	B73S, 73S, B737	3401	4277	**7678**
B757	757, B757	1896	1038	**2934**
DC10	D10	1120	962	**2082**
MD80	M80	1085	1534	**2619**
TOTAL		**19383**	**18815**	**38198**

B.3 The Measured Variables

The following measured data were obtained for these aircraft operations. In this list, each variable is tagged with its variable name from either the ARTS system or the ANOMS system:

- OPNUM. A unique operation number assigned by ANOMS to each radar tracked operation. It is used in this study to match ANOMS data with data generated for each operation by the INM. When the INM is run for the specific flight track, the flight track name is derived from this number, so that the INM results that appear in the DBF file (GRID_DTL) can be matched by this variable with ANOMS data for the same operation. Of great importance is the variable TRK_ID1, which uniquely identifies an operation and permits the measured data to be associated with the correct INM output.
- ACTUALTI. The day/month/year of the start of the noise event.
- STAGE. The certification stage of the aircraft.
- RMTID. The number of the remote monitoring terminal (RMT) at which the noise event was measured.
- SEL_M, NUMOFSEL, and MAXSEL. A single aircraft flight can sometimes produce more than one noise event at a single RMT—because of sound-level fluctuations due to atmospherics, for example. When it does, it obtains several component SELs for the match. When this happens, ANOMS reports three parameters for these "component" SELs—the energy-sum (SEL_M), their number (NUMOFSEL), and their maximum (MAXSEL). For this study, SEL_M is the measured SEL.

 In total, the database has very few matched events with more than one SEL component. Exceptions usually involved only two SELs. Moreover, the maximum SEL was generally only a few tenths of a decibel less than the sum.
- WINDS. The wind speed at the nearest weather station (RMT 11, 18 or 26), in miles per hour, at the time of aircraft PCA. Wind speed and direction were sampled once per second and averaged over a minute for this study.
- WINDD. The direction at the nearest weather station (RMT 11, 18 or 26), in degrees relative to true north, from which the wind was blowing at the time of aircraft PCA.
- TEMP. The temperature (at RMT 26), in degrees Fahrenheit, at the time of aircraft PCA. Temperature was sampled once per minute and averaged over an hour.
- HUMIDITY. The relative humidity (at RMT 26) at the time of aircraft PCA. Relative humidity was sampled once per minute and averaged over an hour.
- PRESSURE. The pressure (at RMT 26), in inches of mercury, at the time of aircraft PCA. Pressure was sampled once per minute and averaged over an hour.
- OP_TYPE. The type of operation (arrival or departure).
- RWY_ID. The runway for this aircraft operation.
- OPER. The three-letter code for the operator of the aircraft (usually an airline).
- TYPE. The ARTS aircraft type.
- STAGELEN. The INM stage length, obtained from the Official Airline Guide for the specific flight.

- STARTS. The start time of the noise event, as hour:minute:second.
- END. The end time of the noise event, as hour:minute:second.
- DURATION. The difference between END and STARTS, in seconds.
- MAXLEVEL. The maximum A-weighted level for the noise event.
- THRESHOL. The threshold level, in A-weighted decibels, that existed at the time the noise event was determined by the ANOMS software to commence. At DIA, ANOMS uses a variable-threshold level based on ambient levels, to maximize the probability of capturing low-level events.
- PCADISTA. The slant distance, in feet, from the RMT to the point of closest approach (PCA) of the aircraft's flight track. The PCA is determined by computing the vector lengths from each radar return along the track to the RMT location, and then selecting the return with the shortest vector. That vector is the PCADIST. All PCA calculations use the elevation of the specific RMT and the relative altitude of the track points.
- PCAALTIT. The ARTS altitude of the aircraft above the RMT elevation at the PCA.
- PCARANGE. The horizontal distance from the RMT to the PCA.
- PCAELEVA. The angle of the PCA above the horizon, in degrees, as seen from the RMT.

APPENDIX C COMPUTED DATA

This section describes the study's computed data:

- Section C.1 summarizes the computations common to all INM modeling methods.
- Section C.2 supplements this with the computations specific to some modeling methods.
- Section C.3 discusses track distance—the distance from runway to RMT.

Figure 25 locates Computed Data within the study.

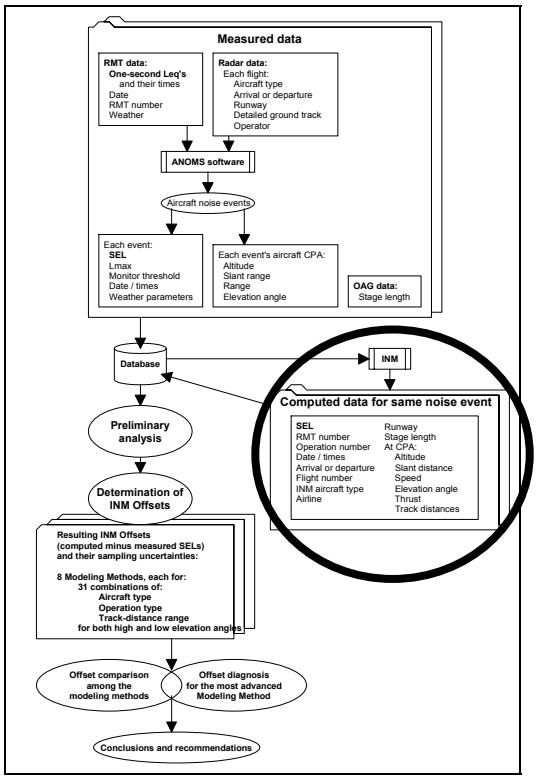


Figure 31. Computed Data within the study

C.1 Computations Common to All Modeling Methods

The FAA's standard noise model INM has had many updates since the original INM accuracy study was done. Fortunately the majority of the input data to the model has remained the same. This study uses relevant updates to the model to asses the performance of those changes. Because the INM accomplishes all calculations through the use of various input and output files (in a standard data base format), it was possible to construct the input files from the study's database of measured variables.

In summary:

- The ANOMS-identified noise events and their matching flights identified which flights were relevant.
- The corresponding radar data provided the ground tracks for each relevant flight. Flights were not combined for INM input; each was modeled separately with its actual ground track.
- Corresponding OAG data provided stage lengths for each flight. In turn, INM used these stage lengths to choose its "performance" coefficients, which determine that flight's altitude profile (altitude as a function of distance along the track) and corresponding thrust profile. No ARTS altitude data were used.

In more detail, basic information for DIA was used to create an INM study. Some data were entered manually using the INM user interface, while other data were fed directly into the appropriate file format and designation. Airport origin, elevation and all INM aircraft types were entered into the file study.inm. The actual elevation of DIA was used in all INM runs. DIA's Remote Monitoring Terminal (RMT) locations were entered into file loc_pts.dbf in latitude and longitude units, along with the elevation of each RMT in feet. To compute SEL values for each flight at each RMT, the coordinates of each RMT were transformed into nautical miles, relative to the airport "origin" and

then were entered manually into the file grid.dbf. Each RMT assumes the airfield elevation for the SEL computations. Terrain data for the RMT sites were not used in this study. The coordinate transformation was checked by plotting before/after positions on the screen at the same time.

Other specific files and their parameters consisted of the following:

- RUNWAY—This file is a list of the Runway Identification codes and the width of each runway.
- RWY_END—This file consists of the information needed to define each runway in the INM. The coordinates of each runway end along with the threshold crossing height (TCH), glide slope angle, runway end elevation and displaced threshold information determine where each flight track arrives and departs from DIA.
- TRACK—This file contains information about each modeled track—including its runway, whether the operation is an arrival or departure, a track identifier, and the percentage use of the track. ANOMS data for one day of operations were fed automatically to the appropriate fields in this file (roughly 1000 tracks). Each track was input with one operation (100% use), so that each single operation had its own track. This file also identifies the track as a "points type"(P) track.
 - Actual radar ground tracks were used to model each operation. Therefore, the study accounts for all variables so that any differences between measured-calculated data are a result of as few additional variables as possible.
 - Some prior studies of INM accuracy have used nominal flight tracks, instead of individual tracks. However, use of nominal tracks adds random error to the analysis, in proportion to how well the nominal track duplicates the actual track. Some of the apparent INM inaccuracy may therefore result from incorrect track location along the ground. Use of actual ground tracks removes track location as a source of error.
 - Of particular importance is the track identifier, TRK_ID1. This parameter uniquely identifies an operation and permits the output of the INM to be associated with the correct ANOMS data (see OPNUM in Appendix B.3 above).
- TRK_SEGS—This file, in addition to carrying most of the same information as given in TRACK, contains the entire set of x and y coordinates (nmi) for the tracks. Correct translation of the flight tracks from ANOMS to INM format was verified by plotting sample tracks at the same scale from both ANOMS and INM.
- OPS_FLT—The number of flights on each track is identified in this file. Each modeled track contained only one operation, since each track was the actual one flown by a single arrival or departure. Note that the profile stage identifier (PROF_ID2) for departures was the stage length provided by the ANOMS data base for each departure operation (stage length is determined by the number of miles from departure to next destination, see STAGELEN in Appendix B.3).
 - This file associates a specific INM aircraft type with each modeled track. The ANOMS data base does not supply the INM aircraft type, but rather the three-letter code assigned to the aircraft in ARTS. This ARTS type was converted to INM aircraft type by a statistical assignment process. For DIA, each airline's fleet mix was used to quasi-randomly associate an INM type with each operation. For example, if United Airlines flies 25% B727-200 / JT8D-15QN and 75% B727-200 / JT8D-17 to DIA, then 25% of all UAL 727 operations reported by ARTS were randomly assigned to INM type 727Q15, and 75% were assigned to 727D17. For airlines whose DIA fleet mix was not known, that airline's total fleet mix was used. In turn, for airlines whose total fleet mix was not known, the overall DIA fleet mix was used.

 - To the extent that different models, combined with different engine types, produce different sound levels, this random assignment would increase the scatter of the data and degraded the reported INM accuracy somewhat.
 - The INM aircraft assignments and stage lengths that were prepared for the INM 5.0 model runs were not modified with improvements in the model. They remained the same for each set of model runs.
- OPS_CALC—Because no sub-tracks are used, this file provides basically the same information as OPS_FLT.
- GRID_DTL—All INM output of interest to this study is contained in this file. In particular, for each modeled operation, this file contains:
 - SEL. The INM-computed SEL for this flight at each RMT
 - ACFT_ID. INM aircraft type used to model the computed SEL
 - OP_TYPE. Type of operations used to model the computed SEL
 - PROF_ID2. Stage length used to model the computed SEL
 - RWY_ID. Runway used to model the computed SEL
 - TRK_ID1. Used to match the computed SEL with the corresponding operation (OPNUM) in the ANOMS data base
 - DISTANCE. The INM-computed slant distance from RMT to the aircraft point of closest approach (PCA)
 - ALTITUDE. The INM-computed altitude of the aircraft at the aircraft PCA above the RMT elevation (equal to the Airfield elevation)
 - ELEV_ANG. The INM-computed angle of the aircraft above the horizon at aircraft PCA, as viewed from the RMT
 - SPEED. The INM-computed speed of the aircraft at PCA,
 - THR_SET. The INM-computed thrust setting at aircraft PCA.

C.1.1 Aircraft performance profiles

The INM uses a set of built in "profiles" which allow the INM to "fly" each aircraft. These profiles can be defined in two ways.

- Profile points—A set of points defining where the aircraft is and how it is performing along a given track distance
- Procedure steps—A set of procedures and coefficients which allow the INM to calculate where the aircraft is and how it is performing along a given track distance

Aircraft using profile points perform the same whether they are flying at a sea level airport or at Denver at 5431' above sea level. Aircraft performance with profile points is also independent of meteorological conditions.

Aircraft using procedure steps have performance characteristics which are related to the airport elevation, runway gradient and meteorological conditions. The majority of the aircraft types analyzed in this report use procedure steps.

INM departure profiles end at 10,000 feet above the airfield elevation and arrival profiles begin at 6000 feet above the airfield elevation. No noise is produced above these altitudes. A departure model track may pass over an RMT site but if the aircraft is above 10,000 feet the SEL is calculated from the PCA which is where the aircraft reached 10,000 feet. These profiles are sufficient for most contour and specific point calculations done by the INM. For this study, many of the RMT sites are far from the airport so the INM standard profiles were extended to 10,000 feet for arrivals and to 18,000 feet for departures.

Only procedure step profiles were extended. For the departure procedure step profile an additional step was added at the end of the INM standard profile. This step is the same as the final step of the standard profile with the final altitude changed to 18,000 feet.

The last step of a standard INM departure profile is:

> *Climb to 10000 feet using MaxClimb thrust and Zero flaps*

The final step added is:

> *Climb to 18000 feet using MaxClimb thrust and Zero flaps*

For the arrival procedure step profile an additional step was added at the beginning of the INM standard profile. This step is the same as the first step of the standard profile with the final altitude changed to 10,000 feet.

The first step of a standard INM arrival profile is:

> *Descend from 6000 feet at 3 degrees using Zero flaps and terminal-area entrance speed*

This step is pushed to being the second step and a new first step is added:

> *Descend* from 10000 feet at 3 degrees using Zero flaps and a speed extrapolated from the standard INM profile.

These adjusted profiles were used in all modeling methods except for modeling method 1 which is from the prior study.

C.2 Computations Specific to Some Modeling Methods

For this study, the majority of the input data did not change between modeling methods. Modeling Methods 1 thru 6 all used the same input data information. In some input files the format of the file changed but not the data (i.e. Track names are only 4 characters in INM 5.01 but changed to a maximum of 8 characters by INM 6.0c) in order to give the user more flexibility. Between Methods 2 thru 6 the only changes to the input data were the meteorological conditions listed below.

C.2.1 Weather data

The INM uses several atmospheric inputs to compute aircraft performance and noise propagation effects. Modeling method 1 (INM 5.01) used the standard atmosphere inputs for all 36 days of model runs.

- Temperature = 59 degrees F
- Atmospheric pressure = 29.92 inches-Hg
- Default average headwind = 8 knots

Modeling methods 2 (INM 5.01) & 3(INM 5.1a) used the annual average atmospheric conditions for the modeling period. Meteorological data was obtained from the National Climatic Data Center (NCDC) for the 12 month period beginning April 1995 thru March 1996. Averages of the meteorological data were computed from this data set for the 12 month period and for each month. The annual averages for the period are listed below:

- Temperature = 48.9 degrees F
- Atmospheric pressure = 29.93 inches-Hg
- Default average headwind = 8 knots

Modeling Method 4 (INM 6.0c) & 5 (INM 6.2B3) use the annual average conditions listed above but also use the annual average Relative Humidity. This additional input allows the model to adjust the noise levels due to the density of the air.

- Relative Humidity = 55.9%

Modeling methods 6 thru 8 (all INM6.2B3) use the monthly average weather conditions

The monthly averages appear in Table 33.

Table 33. Monthly Average Weather Conditions Used in the INM Modeling

Year	Month	Number_of Records	Temp (F)	Pressure (in-Hg)	%RH
1995	4	30	43.17	29.84	62.87
1995	5	31	50.26	29.84	72.79
1995	6	30	62.43	29.88	63.43
1995	7	31	71.00	29.91	50.73
1995	8	31	75.48	29.83	47.31
1995	9	30	62.00	29.98	55.57
1995	10	31	48.71	29.94	49.19
1995	11	30	42.13	30.00	54.17
1995	12	30	33.35	30.03	53.48
1996	1	31	27.39	29.95	55.08
1996	2	29	34.17	29.98	49.26
1996	3	31	36.19	29.96	57.00

C.2.2 Modeling Methods 2 and 3

Modeling methods 2 and 3 all used the same input data and standard INM database tables. The only changes made for each modeling method was the version of the INM used. They all used annual average weather conditions. In comparing results for these modeling methods, the SEL's and associated data from the detail grid files were used to evaluate the results. In the interest of reducing file sizes the INM only reports operations which contribute to the top 97% of the metric. Because of this feature some operations which were near this cutoff were either not included or were newly include when comparing results between Modeling methods 1, 2 or 3. These differences have a negligible effect on the results.

C.2.3 Modeling Methods 4 and 5

Modeling methods 4 and 5 all used the same input data and standard INM database tables. The only changes made for each modeling method was the version of the INM used. They all used annual

average weather conditions. The INM was updated in INM 6.0 to include an option to include all 100% of the contributors to the selected metric. This option was used for the remaining model runs. Methods 4 and 5 were also able to use the annual average Relative humidity term and the "Modify NPD" option was selected. This option allows the INM to compute the effects of air density and elevation on the propagation of noise through the air using SAE-ARP-866A

C.2.4 Modeling Method 6

Modeling Method 6 uses the same version of the INM and the same input data as modeling method 5 except for the meteorological inputs. For Method 6, monthly average data was used, all other input data and options remained the same as method 5.

C.2.5 Updated Noise Curves

The INM contains a set of Noise-Power-Distance (NPD) curves for each engine type. These curves are identified by a code that is relative to the engine type. For example, 737-300, 737-3B23, 737-400 and 737-500 aircraft (737 classic series) all have CFM56-3 engines and each aircraft type has a slight variation of that engine. In the INM there are NPD curves supplied for that engine with the code CFM563. All four 737 INM types use these NPD curves. Boeing and FAA have supplied updated NPD curves for the CFM563 engines and the MD-80 engine type (2JT8D2).

The updated curves include more thrust values for each noise type and operation type. The previous data had only two curves for arrival operations now there are four. For departures the number of curves increased from four to six curves. These new curves should result in better and more consistent results for these aircraft types. The changes to the MD-80 curves are similar. See Figure 26.

The new NPD curves were used in both modeling methods 7 and modeling method 8. The figure below demonstrates the effect of the new NPD curves. In this case the 737-300 is louder with the new noise data for a departure out of DIA for that day. The effect is primarily seen as the aircraft increases altitude away from the airport.

C.2.6 Performance adjustments

Each version of the INM used in this study contains aircraft database and computational algorithm updates designed to improve the modeled results of the model. These improvements are considered part of the standard model release. The performance adjustments described here are adjustments added to the input data for each of the model runs and are considered "user-defined" data. These user-defined adjustments only apply to modeling methods 7 and 8 which are both INM 6.2B3 and only affect certain aircraft using procedure step profiles.

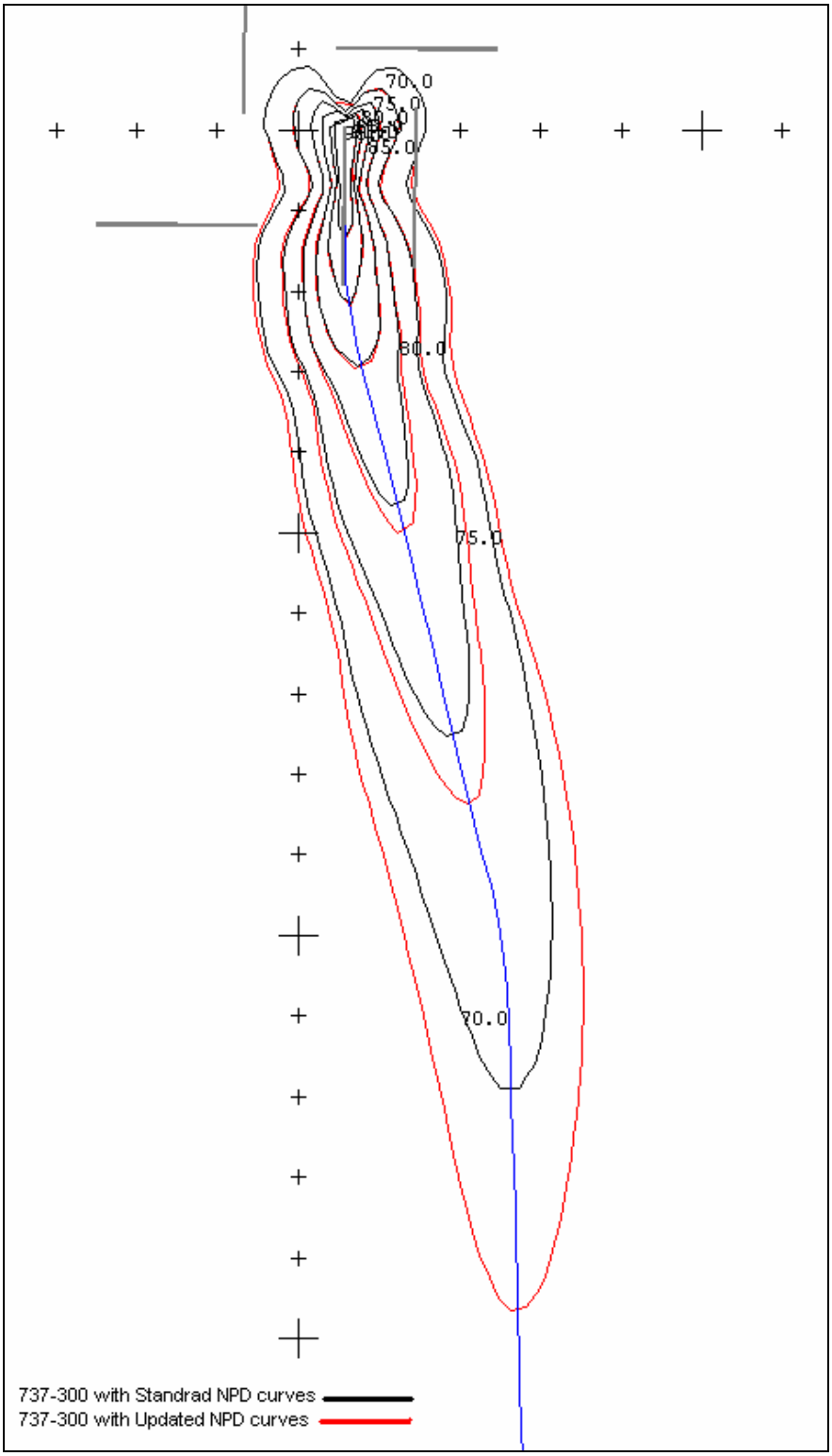


Figure 32. Effect of updated NPD curves

The INM uses the information in several files to compute the aircraft flight profile.

- PROFILE—This file lists the profiles available for each INM aircraft type and the weight of the aircraft associated with that profile
- PROCEDUR—This file contains the steps used by each profile to describe the flight profile of each aircraft. There are three typical steps for departures.
 - The takeoff step with flap and thrust values
 - The climb step with flap, thrust and a final altitude value
 - The accelerate step with flap, thrust, climb rate and a final speed value

 There are three typical steps for arrivals.
 - The descend step with flap setting, starting altitude, starting speed and decent angle
 - The landing step with flap setting and landing roll distance
 - The decelerate step with distance, speed and thrust values
- FLAPS—These are the aerodynamic coefficients associated with each flap setting
- THR_JET—These are the engine coefficients associated with each thrust setting

All of the data supplied in the files above allow the INM to compute where the aircraft is and how the aircraft is performing at a given track distance.

Modeling Method 7 and 8 use a set of modified performance coefficients supplied by Boeing and FAA for use in the model. The new coefficients were added to the THR_JET file as user-defined data for the B733 and MD80 series aircraft.

C.2.7 Modeling Method 7

This modeling method uses the same version of the model as methods 5 and 6 and all of the same input data including the monthly average data used in method 6. Method 7 includes updates to the NPD curves for the 737 classic series and MD-80 style aircraft. This method also includes modified coefficients for the same aircraft types. See Table 34.

C.2.8 Modeling Method 8

Modeling method 8 is the same as method 7 except certain aircraft types and stage lengths use derated thrust for there departure profiles. The derated thrusts were only created for the 737 classic series, MD-82 and MD-83 aircraft. See Table 35.

For the 737 classic series, the profiles using derated thrusts used the engine coefficients for the next lowest thrust level as shown in Table 36. Boeing and FAA supplied an additional set of engine coefficients to be used for the MD82 and MD83 de-rate conditions.

Since using a derated thrust will affect the performance of the aircraft, it can only be used when conditions are safe for its use. For the aircraft capable of using de-rate, Boeing supplied information as to which stage lengths could use a de-rate procedure at DIA. Each month was evaluated using the average temperature for that month. See Table 33.

Table 34. User defined data for Modeling Method 7

Study aircraft type	INM type	Modified coefficients	Updated NPD curves	Derated thrust
B727	727Q15	No	No	No
	727D17	No	No	No
	727Q9	No	No	No
B733	737300	Yes	Yes	No
	7373B2	Yes	Yes	No
	737400	Yes	Yes	No
	737500	Yes	Yes	No
B73S	737D17	No	No	No
	737QN	No	No	No
B757	757PW	No	No	No
	757RR	No	No	No
DC10	DC1010	No	No	No
MD80	MD81	Yes	Yes	No
	MD82	Yes	Yes	No
	MD83	Yes	Yes	No

Table 37 lists the heaviest stage length which can be used at DIA for each month. Any stage lengths lighter than and including the one listed in the table were assigned to use a de-rate thrust departure for each day. So for April 6th, 1995, all 737-500 departures which have a stage length of 1 or 2 used a derated thrust procedure. On the same day, only stage length 1 737-300 aircraft could use the de-rate thrust procedure.

Table 35. User defined data for Modeling Method 8

Study aircraft type	INM type	Modified coefficients	Updated NPD curves	Derated thrust
B727	727Q15	No	No	No
	727D17	No	No	No
	727Q9	No	No	No
B733	737300	Yes	Yes	Yes
	7373B2	Yes	Yes	Yes
	737400	Yes	Yes	Yes
	737500	Yes	Yes	Yes
B73S	737D17	No	No	No
	737QN	No	No	No
B757	757PW	No	No	No
	757RR	No	No	No
DC10	DC1010	No	No	No
MD80	MD81	Yes	Yes	No
	MD82	Yes	Yes	Yes
	MD83	Yes	Yes	Yes

Table 36. Aircraft and Thrust Values Used in Modeling Method 8

INM type	Aircraft description	Thrust	Derate thrust
737300	Boeing 737-300/CFM56-3B-1	20K	18.5K
7373B2	Boeing 737-300/CFM56-3B-2	22K	20K
737400	Boeing 737-400/CFM56-3C-1	23.5K	22K
737500	Boeing 737-500/CFM56-3B-1	20K	18.5K
MD82	MD-82/JT8D-217A	20.9K	MD82 5% derate
MD83	MD-83/JT8D-219	21.7K	MD83 5% derate

Table 37. INM types and Stage lengths Capable of Using De-rate

		Heaviest INM stage to use derate					
Year	Month	737-500	737--300	737—3B2	737-400	MD-82	MD-83
1995	4	2	1	2	2	1	2
1995	5	2	1	2	2	1	2
1995	6	2	1	2	1	1	1
1995	7	1	0	1	1	1	1
1995	8	1	0	1	1	1	1
1995	9	2	1	2	1	1	1
1995	10	2	1	2	2	1	2
1995	11	2	1	2	2	1	2
1995	12	2	1	2	2	1	2
1996	1	2	1	2	2	1	2
1996	2	2	1	2	2	1	2
1996	3	2	1	2	2	1	2

C.3 Track Distance

C.3.1 Importance

Figure 33 shows an initial comparison between computed and measured SELs—for one aircraft and one operation type. In that figure, each point is the difference between INM and measured SEL values for a single aircraft noise event, for a specific aircraft flight at a specific RMT. Each noise event is located vertically at the difference between INM minus measured (ANOMS) SEL and horizontally at the distance along the flight track from the RMT to the runway.

Multiple plots of this type indicated that INM accuracy tends to depend upon track length – distance from the runway. For most of the plots, INM accuracy appeared better for shorter track lengthes (generally higher SELs) than for greater track lengths. For many of the aircraft types under study, this effect was more pronounced than in the figure, especially for arrivals. These many plots suggested that INM accuracy be separately determined for different track distances.

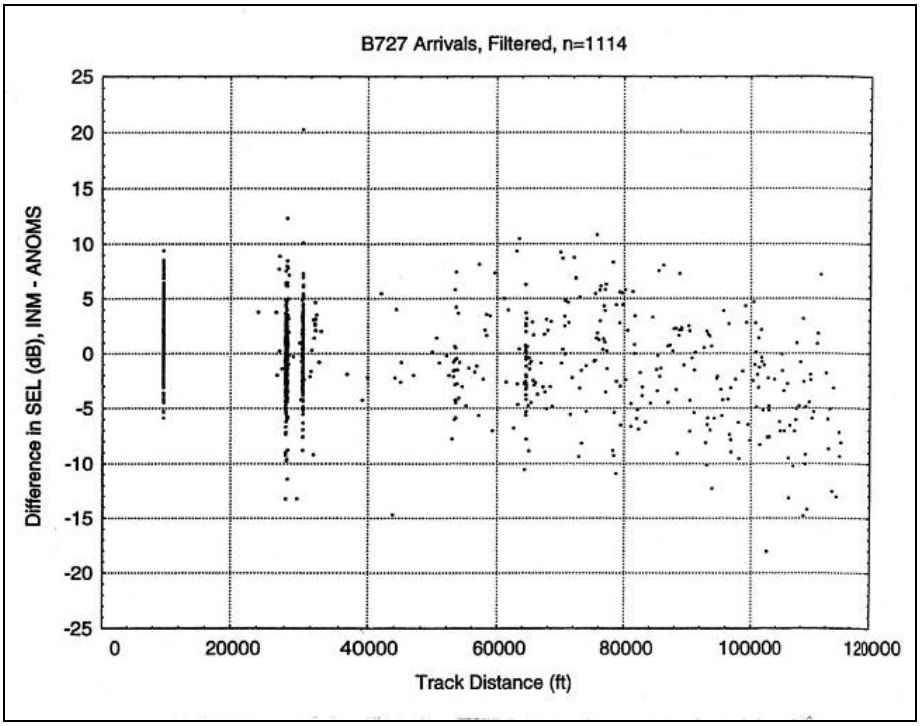


Figure 33. Importance of evaluating INM accuracy for different track lengths

C.3.2 Computation

For each aircraft noise event, track distance at PCA was not directly available from either the ANOMS system or INM output. Instead, it was determined from:

- The INM altitude at that PCA
- The relevant INM altitude profile for that flight, unique to that flight's "stage length" from the Official Airline Guide.

INM internally determines the track distance to PCA, from knowledge of the radar flight track and the RMT location. Then INM converts that track distance to the flight's altitude at PCA, using its built-in altitude profile for that "stage length." Then INM reports that altitude at PCA for that noise event. In short, from the altitude profile INM converts track distance (horizontal axis) to altitude (vertical axis).

For the analysis, this process was reversed. The reported INM altitude at PCA (vertical axis) was simply converted back to track distance (horizontal axis), by a spreadsheet that contained the same altitude profile.

APPENDIX D PRELIMINARY ANALYSIS

This section describes several preliminary analyses, undertaken prior to the computation of INM Offsets:

- Section D.1 discusses data cleaning.
- Section D.2 discusses data filtering for excessive wind speeds.
- Section D.3 discusses how the separate data-analysis regimes were based upon elevation angle and track distance.
- Section D.4 summarizes the number of data points by aircraft type.

Figure 34 locates Preliminary Analysis within the study.

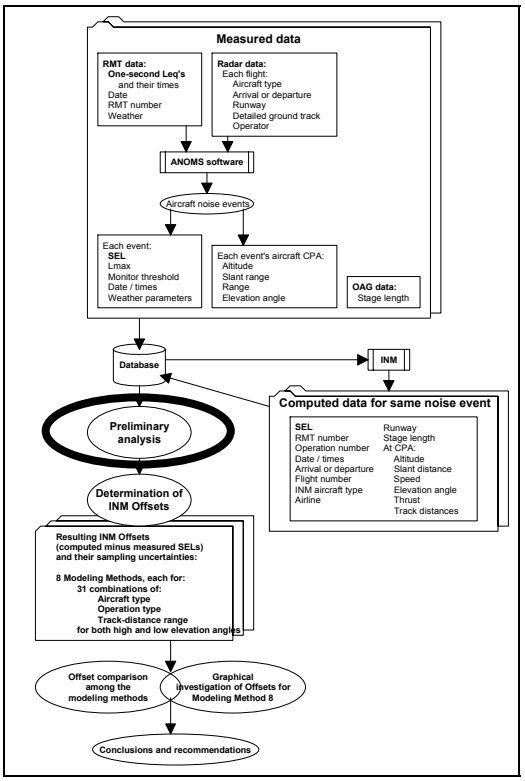


Figure 34. Preliminary analysis within the study

D.1 Data Cleaning

As mentioned above, the ANOMS software contains algorithms that identify aircraft noise events and match each with specific aircraft operation. Detailed examination of the airspace and sound-level time histories of seven departures and 20 arrivals showed that some matching anomalies do occur—anomalies such as a noise-event match to more than one aircraft operation, or an under-measurement of SEL due to noise-event truncation.

Data-cleaning methods were therefore used to reduce or eliminate these anomalies. This current section describes the most important of these: the removal of anomalous data for aircraft that pass the same RMT more than once.

D.1.1 Aircraft that pass the same RMT more than once

Figure 35 shows several anomalous points at track distances less than 50,000 feet but altitudes greater than 5000 feet. These anomalous points occur when the same aircraft passes the same RMT more than once—often on its downwind approach and again on its final approach towards the runway. When this occurs, ANOMS and INM sometimes report data for different passbys, causing their data to be inherently inconsistent.

This inconsistency is easily identified in plots where X-coordinates derive from INM but Y-coordinates derive from ANOMS. This is the case in the figure, where track distance derives from INM and ANOMS altitude derives from ANOMS. For the anomalous points in the figure, INM reported data for the final approach leg (very small track distance on the X-axis), but ANOMS

reported for an earlier RMT passby of the same aircraft flight, when the aircraft's track distance was truly much larger than plotted and the aircraft's altitude (Y axis) was corresponding higher, as well.

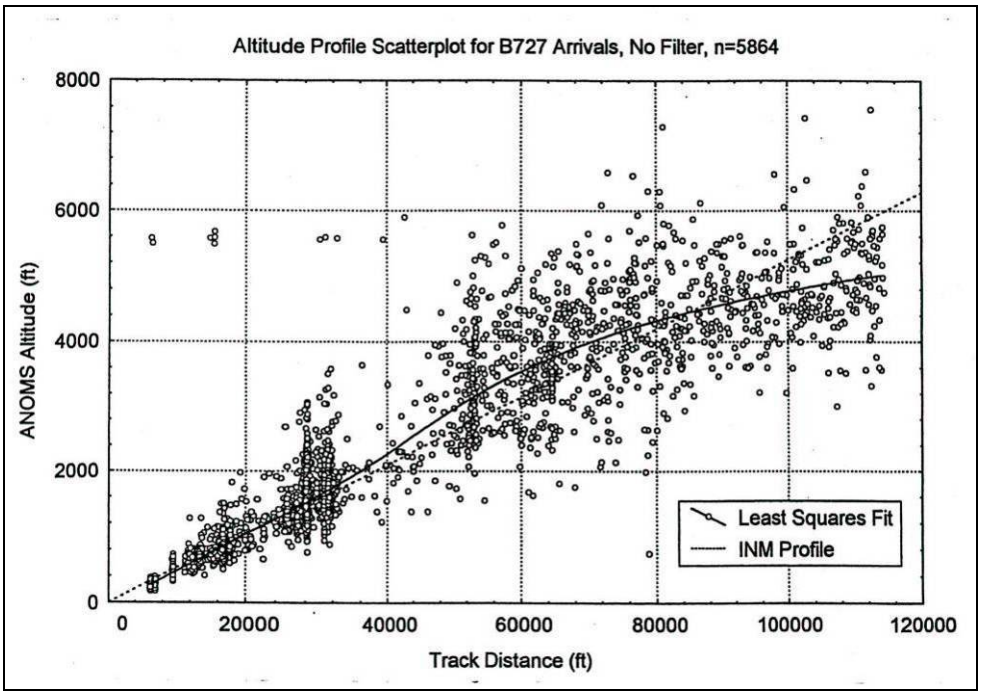


Figure 35. Inconsistent data when same aircraft passes same RMT more than once

Similar figures for all aircraft types, separately for arrivals and departures were used to identify these anomalous points—in all, fewer than 50 data points during arrivals and several during departures. These data points were deleted from the analysis during preliminary analysis, before computation of INM Offsets.

D.1.2 Data outliers

In the previous study (reference in endnote 6) data outliers were removed before computation of INM accuracy. In particular, points were removed when their computed and measured SELs disagreed significantly.

In that prior study, it did not seem appropriate to use the energy average of all data points, because a few significantly high outliers might heavily influence INM Offset. It was thought then that these outliers might be caused by inaccurate measurements or incorrectly identified aircraft or flight tracks—particularly at very large track distances. Of particular concern were measured SELs that might contain local-street noise in addition to aircraft noise. Such aircraft SELs would be "over-measured"—that is, their measured values would be improperly high, due to local-street contributions.

On the other hand, local-street noise might also improperly truncate a measured noise event—by delaying its proper onset, or by prematurely ending the event, or both. Such aircraft SELs would be "under-measured" due to local-street noise, thereby counter-balancing the other local-street effect. In addition, outlier points might also be caused by INM-computation anomalies. In particular, INM

might position some aircraft improperly low in the sky, thereby improperly increasing their computed SEL.

For this current study, outliers were not excluded. INM difficulties of this type are what this study intends to find. In short, the prior study's method of removing outliers is now considered too arbitrary. For this current study, therefore, data outliers were not removed from the analysis.

D.2 Data Filtering

D.2.1 Wind speed

Wind gusts can produce monitored sound events that mimic aircraft sound events. To be conservative, data were therefore filtered out whenever wind speeds were greater than 10 miles per hour.

Figure 36 shows the cumulative distribution of wind speeds in the database. As shown in the figure, approximately 76 percent of the data have acceptable wind speeds of 10 miles per hour or less. The remaining 24 percent were filtered out, which reduced the total number of data points from 38,138 to 28,945.

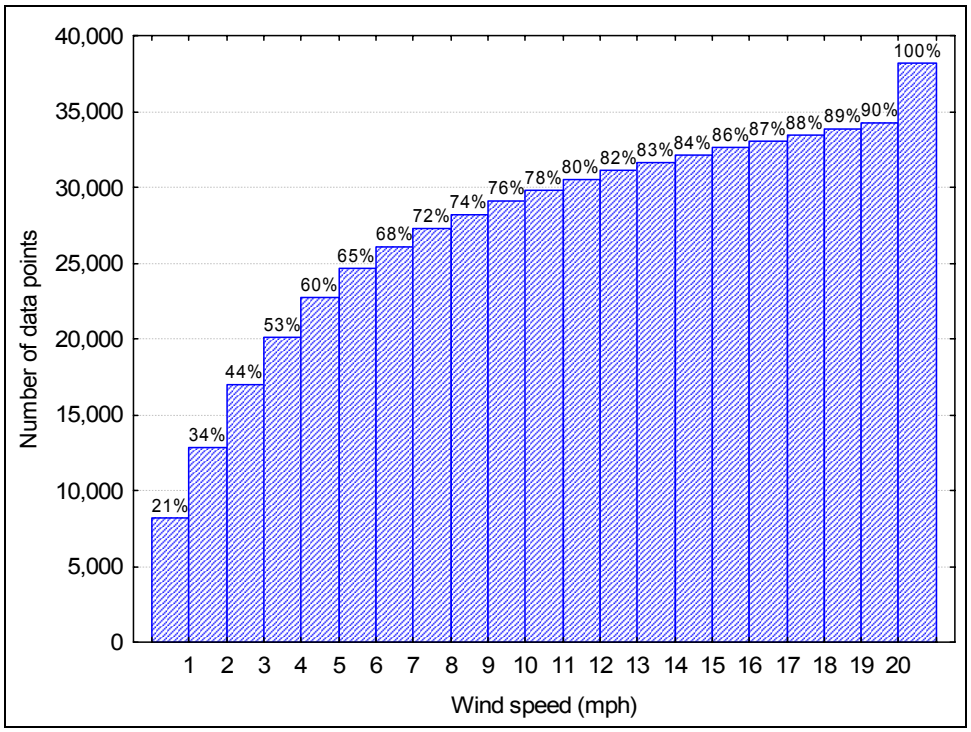


Figure 36. Cumulative distribution of wind speeds in database

D.2.2 Rejected variables

The following additional variables were considered, but then rejected, for filtering:

- Temperature

- Slant range

D.3 Data Regimes

D.3.1 Elevation angle

For elevation angles below 60 degrees, INM uses its "lateral attenuation" algorithm to compute the effect of the ground, combined with atmospherics. To separately determine possible INM inaccuracies due to that algorithm, data were separately analyzed in two elevation-angle regimes:

- Elevation angle less than 60 degrees (with lateral attenuation)
- Elevation angle equal to or greater than 60 degrees (no lateral attenuation).

Figure 37 shows the cumulative distribution of elevation angles in the database, after filtered by wind speed. As shown in the figure, 79 percent of the remaining data have have elevation angles less than 60 degrees, while the remaining 21 percent have angles larger than 60 degrees.[9]

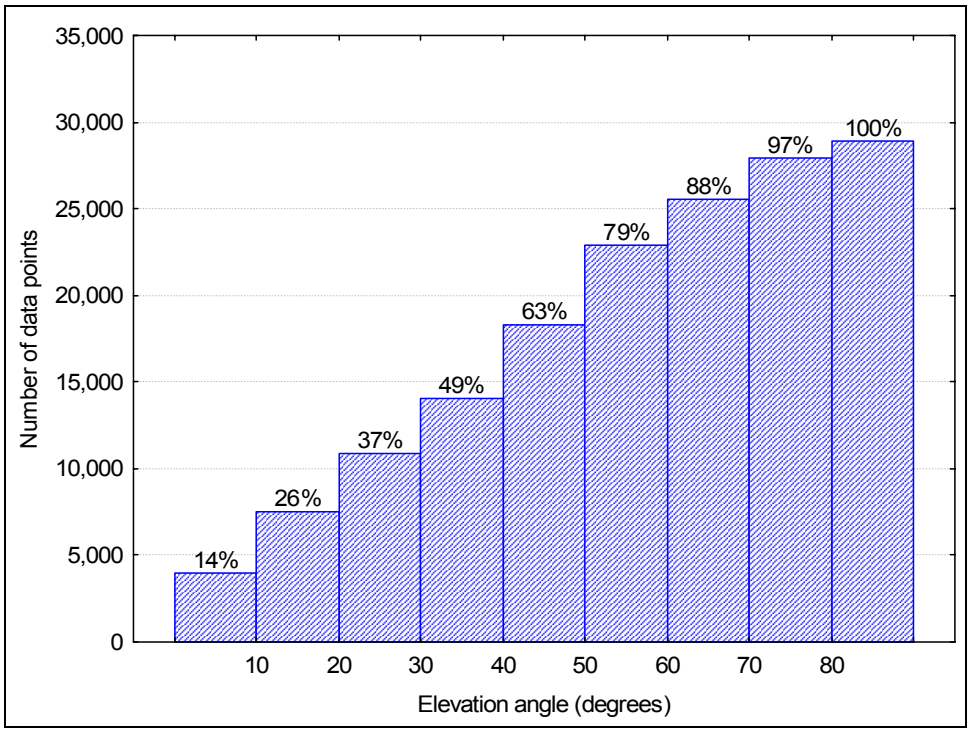


Figure 37. Cumulative distribution of elevation angles in wind-speed-filtered database

D.3.2 Track distance

Figure 35 (above) shows an altitude-profile plot for B727s on arrival (plotted prior to data filtering). Each aircraft noise event (flight track passing an RMT) contributes one point to the plot. That point is plotted vertically at the aircraft altitude at PCA (measured by radar) and horizontally at the event's track distance at PCA (from INM output).

The solid line in the figure is a least-squares regression fit through the points, mathematically following their general trend. This is the best estimate of the average, measured altitude profile for the approaching aircraft type. For comparison, the dashed line is the corresponding INM altitude profile (standard 3-degree approach).

Plots of this type show where measured and computed aircraft altitudes agree or disagree—a useful indicator of potential INM accuracy. Therefore, rather than combine all track distances into a single measure of INM accuracy, INM Offset was determined separately for three track-range intervals: low, medium and high. Plots of this type suggest reasonable boundaries between these three regions.

Even more useful in determining those boundaries were plots similar to Figure 38, which shows a preliminary comparison between computed and measured SELs. In the figure, each data point is located vertically at the difference between computed and measured SEL (called over-calculation in the figure, but INM Offset in this report), and horizontally at that flight/RMT track distance to PCA. The data points in this figure also suggest that INM accuracy is different for low, medium and high track distances (for B733 arrivals). Plots of this type also suggest reasonable boundaries between three track-distance regions: low medium and high.

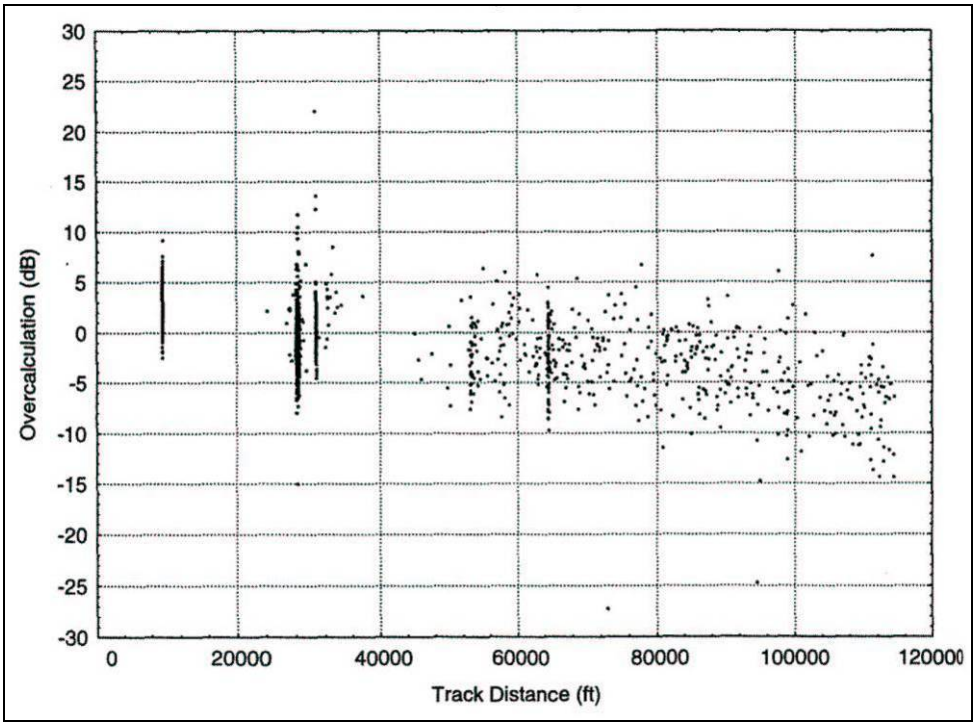


Figure 38. Preliminary (before filtering) comparison of computed and measured SELs: B733 arrivals, Modeling Method 1

Table 38 shows the resulting track-distance regimes and their shorthand names. As shown, track distance regimes differ by operation and aircraft type.

Table 38. Track-distance regimes by operation and aircraft type

Operation type	Aircraft type	Track-distance regime (000 ft)	Shorthand name
Arrival	All	0 to 20	Low
		20 to 40	Medium
		40 or more	High
Departure	B733	0 to 30	Low
		30 to 50	Medium
		50 or more	High
	B757	0 to 50	Low
		50 or more	High
	B727, B73S, DC10, M80	0 to 60	Low
		60 or more	High

D.4 Number of Data Points by Aircraft Type

The study aircraft types were combined out of similar-performance aircraft (1) within the ARTS radar system and (2) within INM. Table 39 distributes the six study aircraft (across the top) among the 26 combinations of ARTS and INM aircraft types (down the left). In addition, Table 40 distributes these same aircraft among the 32 RMTs, while Table 41 distributes them among the various combinations of elevation-angle interval, track-distance regime, and operation.

Table 39. Study aircraft types: Number for each ARTS and INM aircraft type

ARTS aircraft type	INM aircraft type	B727	B733	B73S	B757	DC10	M80	Row Totals
72S	727Q15	8,148	0	0	0	0	0	8,148
72S	727L17	477	0	0	0	0	0	477
B727	727Q15	265	0	0	0	0	0	265
B727	727Q9	185	0	0	0	0	0	185
72S	727Q9	116	0	0	0	0	0	116
B727	727L17	24	0	0	0	0	0	24
733	737300	0	3,770	0	0	0	0	3,770
735	737500	0	2,504	0	0	0	0	2,504
733	7373B2	0	1,561	0	0	0	0	1,561
734	737400	0	429	0	0	0	0	429
73S	737L17	0	0	3,255	0	0	0	3,255
73S	737QN	0	0	2,412	0	0	0	2,412
B737	737L17	0	0	12	0	0	0	12
B737	737QN	0	0	11	0	0	0	11
757	757PW	0	0	0	2,198	0	0	2,198
757	757RR	0	0	0	30	0	0	30
B757	757PW	0	0	0	25	0	0	25
B757	757RR	0	0	0	2	0	0	2
D10	DC1010	0	0	0	0	1,623	0	1,623
DC10	DC1010	0	0	0	0	41	0	41
DC10	DC1030	0	0	0	0	2	0	2
M80	MD82	0	0	0	0	0	1,154	1,154
M80	MD83	0	0	0	0	0	607	607
M80	MD81	0	0	0	0	0	21	21
MD80	MD82	0	0	0	0	0	15	15
MD80	MD83	0	0	0	0	0	5	5
Column Totals		9,215	8,264	5,690	2,255	1,666	1,802	28,892

Table 40. Study aircraft types: Number at each RMT

RMT	B727	B733	B73S	B757	DC10	M80	Row Totals
1	313	103	257	39	21	49	782
2	1,145	496	543	154	161	200	2,699
3	1,125	1,519	725	467	278	309	4,423
4	551	252	198	68	66	146	1,281
5	994	645	371	50	103	292	2,455
6	320	19	126	1	9	89	564
7	206	113	157	17	20	83	596
8	331	387	293	117	42	95	1,265
9	113	323	119	91	51	40	737
10	392	113	305	22	29	48	909
11	290	300	236	76	51	32	985
12	115	162	97	46	36	8	464
13	111	115	74	40	35	4	379
14	104	77	64	20	17	11	293
15	175	164	120	30	27	14	530
16	203	152	145	21	25	10	556
17	211	193	161	30	29	17	641
18	249	250	175	43	28	18	763
19	237	394	169	105	67	18	990
20	194	466	154	160	116	10	1,100
21	310	540	246	209	126	32	1,463
22	216	393	170	115	101	49	1,044
23	51	62	50	9	2	18	192
24	31	41	19	7	2	6	106
25	35	47	19	11	5	3	120
26	38	37	20	17	6	8	126
27	13	0	14	0	0	0	27
28	329	146	126	37	37	73	748
29	195	36	158	13	17	20	439
30	588	703	365	233	158	100	2,147
31	19	6	8	2	1	0	36
32	11	10	6	5	0	0	32
Column totals	9,215	8,264	5,690	2,255	1,666	1,802	28,892

Table 41. Number of data points (Modeling Method 8)

Elevation-angle interval	Track-distance regime	Operation	B727	B733	B73S	B757	DC10	M80	Row Totals
Below 60 degrees	Low	Arrivals	1273	581	424	190	187	207	2862
Below 60 degrees	Low	Departures	2818	281	1704	132	230	713	5878
Below 60 degrees	Medium	Arrivals	1860	2272	1073	706	447	398	6756
Below 60 degrees	Medium	Departures	1312	626	848	315	302	144	3547
Below 60 degrees	High	Arrivals	604	687	380	203	132	35	2041
Below 60 degrees	High	Departures	0	1447	0	0	0	0	1447
Above 60 degrees	Low	Arrivals	34	64	57	16	4	5	180
Above 60 degrees	Low	Departures	167	161	241	93	54	100	816
Above 60 degrees	Medium	Arrivals	409	536	270	160	63	119	1557
Above 60 degrees	Medium	Departures	466	244	434	301	165	45	1655
Above 60 degrees	High	Arrivals	272	427	259	139	82	36	1215
Above 60 degrees	High	Departures	0	938	0	0	0	0	938
Column Totals			9215	8264	5690	2255	1666	1802	28892

APPENDIX E DETERMINATION OF INM OFFSETS

This section describes how INM Offsets were determined:

- Section E.1 summarizes the data that underlie INM Offsets.
- Section E.2 summarizes the analysis equations for INM Offsets.
- Section E.3 provides additional details.

Figure 6 locates Determination of INM Offsets within the study. Actual offset values appear in Section A.1.1.

The INM Offsets in this section are single-number measures, in decibels with 95% sampling-uncertainty ranges. They permit rank ordering of INM accuracy by aircraft type, operation type, and track-distance ranges. Because they are based upon energy averages, they relate directly to INM computation of DNL (Day-Night Average Sound Level), used for aircraft-noise assessment in the U.S.

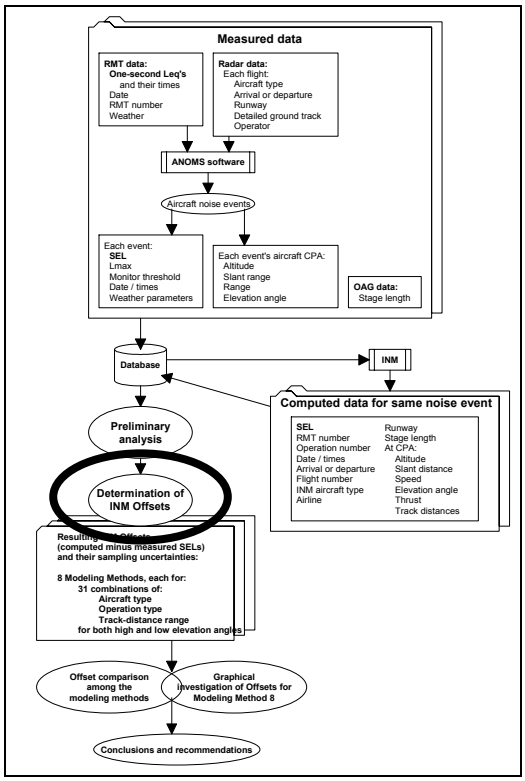


Figure 39. Determination of INM Offsets within the study

E.1 Data Summary

This section summarizes the data that underlie INM Offsets.

Analysis data consist of the following variables:

- Table 42. Measured variables for each aircraft noise event, at each RMT
- Table 43. Corresponding computed variables for that same noise event, same RMT.

Each table includes the variable name used for analysis, plus an abridged definition of the variable. More-complete definitions appear in Sections Appendix A and Appendix C, above.

Table 42. Measured variables for each aircraft noise event

Variable	Details
MOpNum	Operation number assigned by the monitor system
MRmt	RMT (monitor) number
MOpNumRmt	Combination of MOpNum and MRmt (used during merge with computed variables)
MAcStage	Aircraft stage length
MArrDep	Type of operation (arrival or departure)
MSel	SEL of this aircraft at this monitor—measured at monitor
MWindSpeed	Wind speed (mph) at nearest weather station, at time of aircraft PCA
MWindDir	Wind direction (blowing from, clockwise from true north, deg) at nearest weather station, at time of aircraft PCA
MTemp	Temperature (degrees F) at RMT26, at time of aircraft PCA
MHumidity	Humidity (%) at closest weather station, at time of aircraft PCA
MPressure	Pressure (inches Hg) at closest weather station, at time of aircraft PCA
MRunway	Runway for this aircraft operation
MOperator	Operator (carrier) of this aircraft
MArtsAcType	Aircraft type, per the ARTS monitor system
MAcType	Aircraft type for this study (specific grouping from among MArtsAcType)
MStageLength	INM stage length, per OAG for that flight
MStartTime	Start time of noise event
MEndTime	End time of noise event
MDuration	Duration (sec) of noise event
MLmax	Lmax of noise event
MThreshold	ANOMS-derived floating threshold at start of noise event
MSlantDistance	Slant distance (ft) from monitor to aircraft, at aircraft PCA—per ARTS
MAltitude	Altitude (ft) of aircraft at PCA—per ARTS
MRange	Range (horizontal distance, ft) to aircraft at PCA—per ARTS
MElevAngle	Elevation angle (above the horizontal, deg) to aircraft at PCA—per ARTS
MWaypoint	Waypoint per flight plan in the ARTS data
MAngle	Angle (deg) subtended at the monitor by the full noise event
MTrackDist	Distance (ft) along the flight track to the aircraft PCA (computed from ARTS track along the ground)
MTrackInt	Track interval (low, medium, high), based upon MTrackDist

Table 43. Corresponding computed variables for the same aircraft noise event

Variable	Details	Name in INM-generated database
COpNum	Operation number assigned by the monitor system	Operation.OperationID
CRmt	RMT (monitor) number	Site.SiteCode
COpNumRmt	Combination of COpNum and CRmt (used during merge with measured variables)	————
CInmAcType	INM aircraft type	Operation.RepAircraftCode
CAcType	Aircraft type for this study (specific grouping from among CInmAcType)	
CArrDep	Type of operation (arrival or departure)	Operation.FF2
CDate	Date of start of flight operation	Operation.ActualTime
CEndTime		Operation.TrackEnd
CAirline	Airline	Operation.RepAirlineCode
CRunway	Runway	Operation.RepRunway
CFlightNum	Flight number	Operation.FlightNumber
CStageLength	INM stage length	Operation.StageLength
CSlantDistance	Slant distance (ft) from monitor to aircraft, at aircraft PCA—per INM	NoiseMonitorEvent.StantDist
CElevAngle	Elevation angle (above the horizontal, deg) to aircraft at PCA—per INM	NoiseMonitorEvent.ElevAngleDeg
CSpeed	Range (horizontal distance, ft) to aircraft at PCA—per INM	NoiseMonitorEvent.Speed
CThrust	Aircraft thrust at PCA—per INM	NoiseMonitorEvent.ThrustSet
CStartTime		Operation.TrackStart
CAltitude	Altitude (ft) of aircraft at PCA—per INM	NoiseMonitorEvent.AltitudeMSL (Note 1)
CSel	SEL of this aircraft at this monitor—computed by INM	NoiseMonitorEvent.SEL

Note 1. Erroneously named MSL in the database. Actual altitudes are those above the airport elevation.

E.2 Analysis Equations

As discussed above in Section 1.3, this study assesses INM accuracy with the so-called INM Offset, defined as:

$$\text{INM Offset} \equiv \left(\text{Energy-average SEL}\right)_{\text{INM}} - \left(\text{Energy-average SEL}\right)_{\text{measured}}. \quad (4)$$

This assessment metric is computed separately for every combination of:

- Two elevation-angle regimes (above and below 60 degrees)
- Two types of operations (arrivals and departures)
- Six aircraft types
- Two or three track-distance regimes, depending upon aircraft type
- Eight INM modeling methods,

for a total of 496 INM Offset values.

This section summarizes equations to determine these INM Offsets and their sampling uncertainties, in these major subsections:

- Energy-average SEL: Computed and measured. The standard equations for energy averages of decibel-like quantities—used separately for (1) INM-computed SELs and (2) their corresponding measured SELs.
- INM Offset: Computed minus measured. Equations for the difference between INM energy-average SEL and its corresponding energy-average measured SEL, plus the sampling uncertainty of each INM Offset.
- Change in INM offset: Equations for the change (better or worse) in INM Offset due to each successive improvement in modeling method, plus the sampling uncertainty of each change in INM Offset.

E.2.1 Energy-average SEL

This study uses the standard equation for the energy average of decibel-like quantities—separately for the INM-computed SELs and for their corresponding measured SELs:

$$\begin{aligned}\left(L_{E\text{avg}}\right)_{\text{comp}} &= 10\log_{10}\left(\frac{1}{\text{C}}\sum_{c=1}^{\text{C}}10^{0.1\left(L_c\right)}\right)\\ \left(L_{E\text{avg}}\right)_{\text{meas}} &= 10\log_{10}\left(\frac{1}{\text{M}}\sum_{m=1}^{\text{M}}10^{0.1\left(L_m\right)}\right).\end{aligned} \tag{5}$$

In these equations:

- L_{Eavg} is the energy average of a collection of SELs.
- comp means computed (by INM).
- meas means measured.
- c = 1,...,C = the number of computed SELs.
- m = 1,...,M = the number of measured SELs.
- L is a single-character abbreviation for Sound Exposure Level (SEL)—either L_c or L_m.

In words, these equations first convert each SEL (L_c or L_m) to an energy-like term, through multiplication by 0.1 and then raising 10 to that power. Then these energy-like terms are averaged in the normal manner, by adding them up and dividing by their "quantity" (C or M). Finally, 10 times the common logarithm of the result yields the "energy average" of the SELs.

Note that C = M in this study, because each computed SEL is paired with a corresponding measured SEL (same aircraft, same monitor).

E.2.2 INM Offset (computed minus measured) and its uncertainty

From these two energy-average SELs, the INM Offset (Ω) is determined as follows:

$$\begin{aligned}\text{INM Offset} \equiv \Omega\\ &= \left(L_{E\text{avg}}\right)_{\text{comp}} - \left(L_{E\text{avg}}\right)_{\text{meas}}\\ &= 10\log_{10}\left(\frac{1}{\text{C}}\sum_{c=1}^{\text{C}}10^{0.1\left(L_c\right)}\right) - 10\log_{10}\left(\frac{1}{\text{M}}\sum_{m=1}^{\text{M}}10^{0.1\left(L_m\right)}\right).\end{aligned} \tag{6}$$

Each SEL (L_c or L_m) in Eq. (6) contains sampling uncertainty, because it was sampled from the population of all possible SELs—all locations within the community (not just RMT locations), combined with all aircraft during the year (not just on the sampled days in the year).

Eq. (6) indirectly determines how the sampling uncertainty of each individual SEL "propagates" (combines, or coalesces) into the resulting sampling uncertainty of INM Offset on the left. For this study, computation of uncertainty propagation through Eq. (6) used the "law of propagation of uncertainty" in the ISO *Guide to the Expression of Uncertainty in Measurement*.[10]

Sampling variance

Details of this computation, which involve partial derivatives of Eq.(6), appear in Appendix F. The resulting uncertainty-propagation equation from that section is:

$$\mathrm{Var}_{\Omega} = \frac{\mathrm{Var}_{L_c}}{\mathrm{S}}\left(\frac{\overline{E_c^{\,2}}}{\left(\overline{E_c}\right)^2}\right) + \frac{\mathrm{Var}_{L_m}}{\mathrm{S}}\left(\frac{\overline{E_m^{\,2}}}{\left(\overline{E_m}\right)^2}\right) - \frac{2\ \mathrm{Cov}_{L_c L_m}}{\mathrm{S}}\left(\frac{\overline{E_c E_m}}{\overline{E_c}\ \overline{E_m}}\right). \qquad (7)$$

In this equation:

- "Var" is an abbreviation for "variance," a measure of variability and sampling uncertainty for this study. On the equation's right side, the variance of *Lc* and the variance of *Lm* are computed from the measured values of *Lc* and *Lm* , using the standard equation (or Excel function) for variance. The equation's output (on the left side), is the resulting sampling uncertainty in INM Offset (Ω), which is later converted to confidence limits for Ω.
- "Cov" is an abbreviation for "covariance," a measure of the correlation between the computed and measured values of SEL. This covariance is computed from the measured values of *Lc* and *Lm*, using the standard equation (or Excel function) for covariance.
- $E_c \equiv 10^{0.1 L_c}$, used here only for compactness.
- The bar over *Ec* —yielding $\overline{E_c}$ —indicates an "arithmetic average" of all the values of *Ec*. The overhead bar denotes this arithmetic average wherever it appears in the equation. For example, $\left(\overline{E_c}\right)^2$ is computed by first averaging all the *Ec* and then squaring the result. In contrast, $\overline{E_c^{\,2}}$ is computed by first squaring all the *Ec* and then averaging the result. The same is true for the overhead bar for terms involving E_m .
- S (= C = M) is the number of paired samples.

In words, Eq. (7) says that the sampling uncertainty of INM Offset increases with the underlying variability $\left(\mathrm{Var}_{L_c}\text{ and }\mathrm{Var}_{L_m}\right)$ of the SELs. In contrast, the sampling uncertainty of INM Offset decreases with the number of samples (S) and the covariance $\left(\mathrm{Cov}_{L_c L_m}\right)$ between the computed and measured SELs. In addition, the sampling uncertainty of INM Offset depends in a very specific way upon the various energy-like quantities within it $\left(\text{all the } E_c \text{ and } E_m\right)$.

Almost certainly the covariance (correlation) between computed and measured SELs will be positive. Therefore, the third term will reduce the variance of Ω, compared to the situation when the SELs are not paired.

95% sampling uncertainty

As the final step in computing sampling uncertainty, the sampling "variance" of Eq. (7) is converted to a 95% sampling uncertainty. To do that, INM Offset (Ω) and its 95% confidence interval computes as:

$$\begin{aligned} &\Omega \pm \mathrm{Conf}_{95\%} \\ &\Omega \pm t_{\mathrm{S};0.975}\sqrt{\mathrm{Var}_{\Omega}}, \end{aligned} \tag{8}$$

where

$$t_{\mathrm{S};1-\alpha/2} = \begin{array}{l}\text{cumulative Student-t distribution} \\ \text{for S degrees of freedom} \\ \text{at a } 100(1-\alpha)\% \text{ confidence level.}\end{array} \tag{9}$$

E.2.3 Change in INM Offset and its uncertainty

This study involves eight different modeling methods, each an improvement over the prior one—either improved input or improved algorithms.

The change in INM Offset between Modeling Method "A" and Modeling Method "B: is then:

$$\begin{aligned} \left(\Delta\Omega\right)_{\mathrm{AB}} &= \Omega_{\mathrm{B}} - \Omega_{\mathrm{A}} \\ &= \left[\left(L_{E\mathrm{avg}}\right)_{\mathrm{comp}} - \left(L_{E\mathrm{avg}}\right)_{\mathrm{meas}}\right]_{\mathrm{B}} - \left[\left(L_{E\mathrm{avg}}\right)_{\mathrm{comp}} - \left(L_{E\mathrm{avg}}\right)_{\mathrm{meas}}\right]_{\mathrm{A}} \\ &= \left(L_{E\mathrm{avg}}\right)_{\mathrm{comp,B}} - \left(L_{E\mathrm{avg}}\right)_{\mathrm{meas,B}} - \left(L_{E\mathrm{avg}}\right)_{\mathrm{comp,A}} - \left(L_{E\mathrm{avg}}\right)_{\mathrm{meas,A}} \\ &= \left(L_{E\mathrm{avg}}\right)_{\mathrm{comp,B}} - \left(L_{E\mathrm{avg}}\right)_{\mathrm{comp,A}}. \end{aligned} \tag{10}$$

Note that the measured values have dropped out of this equation, because the measured SELs are the same for both modeling methods.

Sampling variance

The mathematical form of Eq. (10) is the same as of Eq. (6)—the difference between two energy averages. In addition, all aircraft in Modeling Method B are paired with the very same aircraft in Modeling Method A—identical to Eq. (6), as well. As a result, Eq. (7) for sampling uncertainty applies here, as well, with changes only in the subscripts:

$$\mathrm{Var}_{(\Omega)_{\mathrm{AB}}} = \frac{\mathrm{Var}_{L_{c\mathrm{B}}}}{\mathrm{S}}\left(\frac{\overline{E_{\mathrm{C_B}}^{\,2}}}{\left(\overline{E_{\mathrm{C_B}}}\right)^2}\right) + \frac{\mathrm{Var}_{L_{c\mathrm{A}}}}{\mathrm{S}}\left(\frac{\overline{E_{\mathrm{C_A}}^{\,2}}}{\left(\overline{E_{\mathrm{C_A}}}\right)^2}\right) - \frac{2\ \mathrm{Cov}_{L_{c\mathrm{B}}L_{c\mathrm{A}}}}{\mathrm{S}}\left(\frac{\overline{E_{\mathrm{C_B}}E_{\mathrm{C_A}}}}{\overline{E_{\mathrm{C_B}}}\ \overline{E_{\mathrm{C_A}}}}\right). \tag{11}$$

Note that the sampling uncertainty here (for change in INM Offset) might be smaller than the sampling uncertainty for each modeling method's offset, alone. This would occur if INM Offset

uncertainty for each modeling method is dominated by the variability in measured SELs. The measured variability subtracts out when one modeling method is compared to another one.

95% sampling uncertainty

As above, the change in INM Offset, $(\Delta\Omega)_{AB}$, and its 95% confidence interval computes as:

$$\begin{aligned}&(\Delta\Omega)_{AB} \pm \mathrm{Conf}_{95\%} \\ &(\Delta\Omega)_{AB} \pm t_{S;0.975}\sqrt{\mathrm{Var}_{(\Omega)_{AB}}},\end{aligned} \tag{12}$$

where

$$t_{S;1-\alpha/2} = \begin{array}{l}\text{cumulative Student-t distribution} \\ \text{for S degrees of freedom} \\ \text{at a } 100(1-\alpha)\% \text{ confidence level.}\end{array} \tag{13}$$

E.3 Additional Details

Additional details concerning INM Offsets appear in:

- Section 3: Graphs and tabulations of the resulting INM Offsets
- Section 4 Offset comparisons among the modeling methods
- Section 5: Graphical investigations of Offsets for Modeling Method 8 (the most advanced method)
- Appendix F: Derivation of the sampling uncertainty equation in this current section.
- Appendix A: Detailed tabulations and further graphs of INM Offsets, including their 95% confidence ranges—including figures identical to Figure 4 and Figure 5, except emphasizing SMALL effects (those within ±1dB) instead of LARGE effects.

APPENDIX F DERIVATION OF PROPAGATION UNCERTAINTY

F.1 Repeated from Section E.2.2, Above

The INM Offset (Ω) is determined as follows:

$$\begin{aligned}\text{INM Offset} \equiv \Omega \\ &= \left(L_{E\text{avg}}\right)_{\text{comp}} - \left(L_{E\text{avg}}\right)_{\text{meas}} \\ &= 10\log_{10}\left(\frac{1}{\text{C}}\sum_{c=1}^{\text{C}} 10^{0.1\,(L_c)}\right) - 10\log_{10}\left(\frac{1}{\text{M}}\sum_{m=1}^{\text{M}} 10^{0.1\,(L_m)}\right).\end{aligned} \tag{14}$$

Each SEL (L_c or L_m) in Eq. (14) contains sampling uncertainty, because it was sampled from the population of all possible SELs—all locations within the community (not just RMT locations), combined with all aircraft during the year (not just on the sampled days in the year).

Eq. (14) indirectly determines how the sampling uncertainty of each individual SEL "propagates" (combines, or coalesces) into the resulting sampling uncertainty of INM Offset on the left. For this study, computation of uncertainty propagation through Eq. (14) used the "law of propagation of uncertainty" in the ISO *Guide to the Expression of Uncertainty in Measurement*. In the remainder of this appendix, that document is abbreviated as the "ISO Guide."

The resulting uncertainty-propagation equation is:

$$\text{Var}_{\Omega} = \frac{\text{Var}_{L_c}}{\text{S}}\left(\frac{\overline{E_c^{\,2}}}{\left(\overline{E_c}\right)^2}\right) + \frac{\text{Var}_{L_m}}{\text{S}}\left(\frac{\overline{E_m^{\,2}}}{\left(\overline{E_m}\right)^2}\right) - \frac{2\ \text{Cov}_{L_c L_m}}{\text{S}}\left(\frac{\overline{E_c E_m}}{\overline{E_c}\ \overline{E_m}}\right). \tag{15}$$

In this equation:

- "Var" is an abbreviation for "Variance," a measure of variability and uncertainty (due to sampling) for this study. On the equation's right side, the variance of *Lc* and the variance of *Lm* are computed from the measured values of *Lc* and *Lm* , using the standard equation (or Excel function) for variance. The equation's output (on the left side), is the resulting sampling uncertainty in INM Offset (Ω), which is later converted to confidence limits for Ω.
- $E_c \equiv 10^{0.1 L_c}$, used here only for compactness.
- The bar over *Ec* —yielding $\overline{E_c}$ —indicates an "arithmetic average" of all the values of *Ec.* The overhead bar denotes this arithmetic average wherever it appears in the equation. For example, $\left(\overline{E_c}\right)^2$ is computed by first averaging all the *Ec* and then squaring the result. In contrast, $\overline{E_c^{\,2}}$ is computed by first squaring all the *Ec* and then averaging the result. The same is true for the overhead bar for terms involving E_m .

- The subscript in *Ec* shows that this value is for one specific SEL (one specific aircraft-monitor combination), indexed by *c*. In contrast, the subscript in $\overline{E_c}$ is just a reminder that the arithmetic average, which involves all SELs, concerns "computed" SELs rather than "measured" ones.

F.2 Derivation of Eq. (15) from Eq. (14)

F.2.1 Parameters, subscripts, and nomenclature

Eq. (14) contains C+M random parameters, one for each of the computed and measured SELs. The sampling uncertainty in these parameters propagates through that equation into a resulting uncertainty in INM Offset, Ω. More mathematically, the sampling variances of all the parameters (plus the covariances between their sampling uncertainties) propagates through the equation into a resulting sampling-uncertainty variance in Ω.

We renumber the subscripts to simplify future notation—that is, we adopt a common subscript, $i = 1,...,\text{C+M}$—and similarly for *j*.

F.2.2 The "law of propagation of uncertainty" in the ISO Guide

With these parameters, subscripts, and nomenclature, Eq. (13) of the ISO Guide (page 21) becomes:

$$\text{Var}_\Omega = \sum_{i=1}^{\text{C+M}} \sum_{j=1}^{\text{C+M}} \frac{\partial \Omega}{\partial L_i} \frac{\partial \Omega}{\partial L_j} \text{Cov}_{L_i L_j}. \tag{16}$$

In this equation, both *i* and *j* range from 1 to C+M, the total number of random parameters. In other words, the double summation includes every combination of these parameters, two at a time. In particular, it includes combination pairs of *c* values with *c* values, of *m* values with *m* values, and also the "cross" pairs of *c* values with *m* values. In all, the double sum has $(\text{C+M})^2$ terms.

F.2.3 Manipulation of various terms

It is common practice to separate this double summation into two separate summations: (1) a summation for cases when *i* equals *j*, and (2) a second summation when *i* and *j* are not equal:

$$\text{Var}_\Omega = \sum_{i=1}^{\text{C+M}} \left(\frac{\partial \Omega}{\partial L_i} \right)^2 \text{Var}_{L_i} + 2 \sum_{i=1}^{\text{C+M}} \sum_{j=i+1}^{\text{C+M}} \frac{\partial \Omega}{\partial L_i} \frac{\partial \Omega}{\partial L_j} \text{Cov}_{L_i L_j}. \tag{17}$$

Note that $\text{Cov}_{ii} = \text{Var}_i$ when *i* equals *j*, as usual. The first summation of this equation further separates into two summations of its own—one for C and one for M—to yield:

$$\text{Var}_\Omega = \sum_{c=1}^{\text{C}} \left(\frac{\partial \Omega}{\partial L_c} \right)^2 \text{Var}_{L_c} + \sum_{m=1}^{\text{M}} \left(\frac{\partial \Omega}{\partial L_m} \right)^2 \text{Var}_{L_m} + 2 \sum_{i=1}^{\text{C+M}} \sum_{j=i+1}^{\text{C+M}} \frac{\partial \Omega}{\partial L_i} \frac{\partial \Omega}{\partial L_j} \text{Cov}_{L_i L_j}. \tag{18}$$

In this rearrangement of Eq.(16), the first summation contains C number of terms, the second summation contains M number of terms and the third summation contains $(\text{C+M})(\text{C+M}-1)/2$ number of terms. In the third summation, each term is symmetrical in *i* and *j*, so that the

multiplication by two (2) accounts for the symmetric terms. As a result, the third summation (multiplied by two) accounts for $(C+M)(C+M-1)$ terms, altogether. Then the total number of terms equals:

$$\begin{aligned} & C+M+(C+M)(C+M-1) \\ &= C+M+C^2+M^2+2CM-C-M \\ &= (C+M)^2, \end{aligned} \tag{19}$$

as expected.

Now the various L_c are all mutually independent, as are the various L_m. In fact, the only statistically dependent pairs in the third term of this equation are the pairs for which L_c is for the same aircraft-monitor combination as L_m. This happens for exactly C (= M) terms in the double sum. Hence Eq.(18) can be written:

$$\mathrm{Var}_\Omega = \sum_{c=1}^{S}\left(\frac{\partial\Omega}{\partial L_c}\right)^2 \mathrm{Var}_{L_c} + \sum_{m=1}^{S}\left(\frac{\partial\Omega}{\partial L_m}\right)^2 \mathrm{Var}_{L_m} + 2\sum_{c=m=1}^{S}\frac{\partial\Omega}{\partial L_c}\frac{\partial\Omega}{\partial L_m}\mathrm{Cov}_{L_cL_m}, \tag{20}$$

where S = 1,...,C (=M) is the number of paired samples. In the third term, here, the statistically independent terms have dropped out, because their covariances equal zero.

In summary, Eq. (20) is the final propagation-of-uncertainty equation for Eq. (14). Through it, the SEL sampling uncertainties (the variance and covariance terms) propagate into the uncertainty in INM Offset, Ω. The resulting uncertainty in Ω depends not only upon these variances and covariances, but also upon the partial derivatives of Ω, which depend upon the explicit functional form of Eq. (6).

F.2.4 The partial derivatives

As required by Eq. (20), we next take the partial derivatives of Ω with respect to all the SEL variables, L_c and L_m, as follows:

$$\begin{aligned}
\frac{\partial \Omega}{\partial L_c} &= \left(\frac{10}{\ln 10}\right)\left(\frac{1}{\mathrm{C}}\sum_{c=1}^{\mathrm{C}} e^{(\ln 10/10)L_c}\right)^{-1} \frac{1}{\mathrm{C}} e^{(\ln 10/10)L_c}\left(\frac{\ln 10}{10}\right) \\
&= \left(\frac{1}{\mathrm{C}}\sum_{c=1}^{\mathrm{C}} e^{(\ln 10/10)L_c}\right)^{-1} \frac{1}{\mathrm{C}} e^{(\ln 10/10)L_c} \\
&= \frac{\frac{1}{\mathrm{C}} e^{(\ln 10/10)L_c}}{\left(\frac{1}{\mathrm{C}}\sum_{c=1}^{\mathrm{C}} e^{(\ln 10/10)L_c}\right)} \\
&= \frac{\frac{1}{\mathrm{C}} 10^{0.1 L_c}}{\left(\frac{1}{\mathrm{C}}\sum_{c=1}^{\mathrm{C}} 10^{0.1 L_c}\right)} \\
&= \frac{1}{\mathrm{C}}\left(E_c / \overline{E_c}\right) \quad \text{for } c = 1,...,\mathrm{C}.
\end{aligned} \tag{21}$$

The partial derivative with respect to L_m is the same, except for the change in subscript and the minus sign in front of the second term (the "M" term) in Eq. (6). In particular:

$$\frac{\partial \Omega}{\partial L_m} = -\frac{1}{\mathrm{M}}\left(E_m / \overline{E_m}\right) \quad \text{for } m = 1,...,\mathrm{M}. \tag{22}$$

F.2.5 Substitution of partial derivatives

Next we substitute from Eqs.(21) and (22) into Eq.(20):

$$\begin{aligned}
\mathrm{Var}_\Omega &= \sum_{c=1}^{\mathrm{S}}\left(\frac{\partial \Omega}{\partial L_c}\right)^2 \mathrm{Var}_{L_c} + \sum_{m=1}^{\mathrm{S}}\left(\frac{\partial \Omega}{\partial L_m}\right)^2 \mathrm{Var}_{L_m} + 2\sum_{c=m=1}^{\mathrm{S}} \frac{\partial \Omega}{\partial L_c}\frac{\partial \Omega}{\partial L_m}\mathrm{Cov}_{L_c L_m} \\
&= \sum_{c=1}^{\mathrm{S}}\left(\frac{1}{\mathrm{S}}\left(E_c / \overline{E_c}\right)\right)^2 \mathrm{Var}_{L_c} + \sum_{m=1}^{\mathrm{S}}\left(-\frac{1}{\mathrm{S}}\left(E_m / \overline{E_m}\right)\right)^2 \mathrm{Var}_{L_m} \\
&\qquad + 2\sum_{c=m=1}^{\mathrm{S}}\left(\frac{1}{\mathrm{S}}\left(E_c / \overline{E_c}\right)\right)\left(-\frac{1}{\mathrm{S}}\left(E_m / \overline{E_m}\right)\right)\mathrm{Cov}_{L_c L_m} \\
&= \frac{\mathrm{Var}_{L_c}}{\mathrm{S}^2}\sum_{c=1}^{\mathrm{S}}\left(E_c / \overline{E_c}\right)^2 + \frac{\mathrm{Var}_{L_m}}{\mathrm{S}^2}\sum_{m=1}^{\mathrm{S}}\left(E_m / \overline{E_m}\right)^2 - \frac{2\,\mathrm{Cov}_{L_c L_m}}{\mathrm{S}^2}\sum_{c=m=1}^{\mathrm{S}}\left(E_c / \overline{E_c}\right)\left(E_m / \overline{E_m}\right).
\end{aligned} \tag{23}$$

In this algebraic manipulation, note that each of the L_c terms has the same sampling variance, so it can be brought outside the summation. The same is true for each of the L_m terms. In addition, the covariance between c and m is the same for each cm pair, so it can be brought outside its summation, as well.

F.2.6 Final equation

Next we note that the denominators within the summations are independent of the summation variable—because those averages have already been summed over all values of their indexes. Hence:

$$\begin{aligned}
\mathrm{Var}_{\Omega} &= \frac{\mathrm{Var}_{L_c}}{\mathrm{S}^2\left(\overline{E_c}\right)^2}\sum_{c=1}^{\mathrm{S}} {E_c}^2 + \frac{\mathrm{Var}_{L_m}}{\mathrm{S}^2\left(\overline{E_m}\right)^2}\sum_{m=1}^{\mathrm{S}} {E_m}^2 - \frac{2\ \mathrm{Cov}_{L_c L_m}}{\mathrm{S}^2\ \overline{E_c}\ \overline{E_m}}\sum_{c=m=1}^{\mathrm{S}} E_c E_m \\
&= \frac{\mathrm{Var}_{L_c}}{\mathrm{S}\left(\overline{E_c}\right)^2}\left(\frac{1}{\mathrm{S}}\sum_{c=1}^{\mathrm{S}} {E_c}^2\right) + \frac{\mathrm{Var}_{L_m}}{\mathrm{S}\left(\overline{E_m}\right)^2}\left(\frac{1}{\mathrm{S}}\sum_{m=1}^{\mathrm{S}} {E_m}^2\right) - \frac{2\ \mathrm{Cov}_{L_c L_m}}{\mathrm{S}\ \overline{E_c}\ \overline{E_m}}\left(\frac{1}{\mathrm{S}}\sum_{c=m=1}^{\mathrm{S}} E_c E_m\right) \\
&= \frac{\mathrm{Var}_{L_c}}{\mathrm{S}}\left(\frac{\overline{{E_c}^2}}{\left(\overline{E_c}\right)^2}\right) + \frac{\mathrm{Var}_{L_m}}{\mathrm{S}}\left(\frac{\overline{{E_m}^2}}{\left(\overline{E_m}\right)^2}\right) - \frac{2\ \mathrm{Cov}_{L_c L_m}}{\mathrm{S}}\left(\frac{\overline{E_c E_m}}{\overline{E_c}\ \overline{E_m}}\right).
\end{aligned} \tag{24}$$

In words, Eq. (24) says that:

- The sampling uncertainty of INM Offset increases with the underlying variability $\left(\mathrm{Var}_{L_c}\text{ and }\mathrm{Var}_{L_m}\right)$ of the SELs.
- In contrast, the sampling uncertainty of INM Offset decreases with:
 - The number of samples (S)
 - The covariance $\left(\mathrm{Cov}_{L_c L_m}\right)$ between the computed and measured SELs.
- In addition, the sampling uncertainty of INM Offset depends in a very specific way upon the various energy-like quantities within it $\left(\text{all the } E_c \text{ and } E_m\right)$.

F.2.7 Comparison without energy averages

Eq. (24) is very similar to the well-known equation for the sampling uncertainty in the comparable case when regular arithmetic averages are involved, instead of energy averages. More specifically, if the INM Offset were just the difference in *arithmetic* averages, instead of the difference in energy-averages, then:

$$\begin{aligned}
\left(L_{\mathrm{avg}}\right)_{\mathrm{comp}} &= \frac{1}{\mathrm{C}}\sum_{c=1}^{\mathrm{C}} L_c \\
\left(L_{\mathrm{avg}}\right)_{\mathrm{meas}} &= \frac{1}{\mathrm{M}}\sum_{m=1}^{\mathrm{M}} L_m \\
\Omega &= \frac{1}{\mathrm{C}}\sum_{c=1}^{\mathrm{C}} L_c - \frac{1}{\mathrm{M}}\sum_{m=1}^{\mathrm{M}} L_m \\
\mathrm{Var}_{\Omega} &= \frac{\mathrm{Var}_{L_c}}{\mathrm{S}} + \frac{\mathrm{Var}_{L_m}}{\mathrm{S}} - \frac{2\ \mathrm{Cov}_{L_c L_m}}{\mathrm{S}}.
\end{aligned} \tag{25}$$

As seen, the resulting equation for Var_Ω is the same here as in Eq. (24), except for the former equation's three factors in parentheses. Those three factors modify the more familiar Eq. (25) to its energy-average equivalent, Eq. (24).

F.2.8 Summary

In summary, Eq. (24) relates the sampling variances and covariances of the SELs to the resulting sampling variance of the INM Offset, Ω. Almost certainly the covariance between computed and measured SELs will be positive. Therefore, the third term will reduce the variance of Ω, compared to the situation when the SELs are not paired.

Note in the extreme case that the correlation might equal unity. This would happen if the level difference between each pair of computed and measured SELs is exactly the same—that is, if the computed-measured offset is exactly the same for each and every aircraft. Unity correlation would then reduce the variance of Ω to zero through this equation, as expected.

Although this is not apparent, the additional factors in parentheses will always produce an energy-average sampling variance that is larger than the comparable arithmetic-average one. Intuitively, energy-averages depend very strongly upon just a few of the largest values being averaged. The small values are completely inconsequential to the energy average. This has the effect of throwing these small values out, completely. In effect, this reduces the number of values being averaged, thereby increasing the sampling uncertainty. The factors in parenthesis in Eq. (24) account for this effective reduction in sample size, S.

[1] Gados, R. G., and Aldred, J. M., *FAA Integrated Noise Model Phase I: Analysis of Integrated Noise Model Calculations for Air Carrier Flyovers*, MITRE Report MTR-79W00095, December 1979 (also FAA Report FAA-EE-80-4).

[2] Gados, R. G., *Comparison of FAA Integrated Noise Model Flight Profiles with Observed Altitudes and Velocities at Dulles Airport*, MITRE Report MTR-80W00119, March 1980.

[3] Flathers, G. W., *A Comparison of FAA Integrated Noise Model Flight Profiles with Profiles Observed at Seattle-Tacoma Airport*, MITRE Report MTR-81W288, December 1981 (also FAA Report FAA-EE-82-10).

[4] Flathers, G. W., *FAA Integrated Noise Model Validation: Analysis of Air Carrier Flyovers at Seattle-Tacoma Airport*, MITRE Report MTR-82W162 (also FAA Report FAA-EE-82-19).

[5] Page, J. A., *et al*, *Validation of Aircraft Noise Models at Lower Levels of Exposure* (draft), Wyle Research Report WR 96-11, February 1996.

[6] Miller, N. P. *et al*, *Examining INM Accuracy Using Empirical Sound Monitoring and Radar Data*, Harris Miller Miller & Hanson Inc. (HMMH) Report 294520.03, October 1999.

[7] Note that +2.5 does not exactly match the change from –1.2 to +1.4, due to rounding.

[8] For these graphs, the altitude ratio was used because aircraft sound levels on the ground are approximately proportional to this ratio. This is not true for an "altitude difference."

[9] The prior report included only elevation angles greater than 60 degrees.

[10] Equation (13) in International Standards Organization, *Guide to the Expression of Uncertainty in Measurement*, Switzerland, 1995 (corrected and reprinted).

Prepared for:

Boeing Phantom Works
9725 East Marginal Way South
Building 9-51 (Mail Room)
Mail Stop 45-83
Seattle, WA 98108

Appendix B

WR 05-28

Reduced Thrust Departures from a High Altitude Airport Using Procedure Steps with the Integrated Noise Model

Contract No. NAS1-00086

Prepared by:
Juliet Page
Scott Usdrowski

WYLE LABORATORIES, INC.
WYLE RESEARCH AND CONSULTING
2001 JEFFERSON DAVIS HIGHWAY
SUITE 701
ARLINGTON, VA 22202
TEL: 703 415 4550
FAX: 703 415 4556
WWW.WYLELABS.COM

Table of Contents

1.0 Introduction 1-1

2.0 Measurement Program and Data Acquisition 2-1
2.1 Denver Measurement Program Overview 2-1
2.2 Noise Measurement Sites 2-1
2.3 Flight Operations Radar Data Analysis 2-4
2.4 Noise Event Extraction 2-5

3.0 Flight Operation Modeling 3-1
3.1 Creation of Flight Profiles using INM Procedure Steps 3-1
3-2 Tailoring the Ground Roll to Match Measured Radar Trajectories 3-6
3-3 Analysis of Liftoff Speed and Takeoff Field Length using the Video Data from the 1997 Lateral Attenuation Study at Denver 3-10
3.4 Automated Profile Generator 3-14
3.5 Comparison of Profile Generation Optimization Techniques 3-25

4.0 Acoustic Analysis 4-1
4.1 Full Acoustic Analysis Dataset Description 4-1
4.2 Selected INM Results and the Thrust Rating Selection Process 4-3
4-3 Operations Not Modeled with INM 4-31

5.0 Acoustic Results 5-1

6.0 Conclusions and Recommendations 6-1

References R-1

Appendix A: Summary of the CATS (Climb and Throttle Scheduler) Code Thrust Calculation Procedure A-1

List of Figures

Figure No.

2-1 Noise Monitoring Locations at Denver International Airport 2-2
2-2 DIA Departure Operations and Noise Monitoring Locations Considered in the Current INM Noise Study 2-5
3-1 Comparison of Radar Altitude with INM Stage Length 4 Profile 3-3
3-2 Comparison of Radar Altitude with INM Stage Length 4 Profile (Close-up) 3-4
3-3 Comparison of Radar Velocity with INM Stage Length 4 Profile (Close-up) 3-4
3-4 Comparison of Radar Altitude with INM Standard Profiles 3-5
3-5 Comparison of Radar Altitude with INM Standard Profiles (Close-up) 3-5
3-6 Comparison of Radar Velocity with INM Standard Profiles (Close-up) 3-6
3-7 INM User Defined Flight Altitude Profile Development UAL1684.523 3-8
3-8 INM User Defined Flight Velocity Profile Development UAL1684.523 3-9
3-9 INM User Defined Flight Power Profile Development UAL1684.52 3-9
3-10 Layout of Lateral Attenuation Study Measurement Site and Video Surveillance System 3-10
3-11 Example Analysis of Video Tracking Data 3-11
3-12 Sample B737 Liftoff Speeds at DIA 3-13
3-13 Sample B737 Takeoff Ground Roll Distances at DIA 3-13
3-14 Typical Radar Flight Profile Initial Segment (a) Altitude and (b) Speed 3-16
3-15 UAL1102.524 Altitude Profile, INM vs. Radar for Several Thrust Ratings 3-19
3-16 UAL1102.524 Velocity Profile, INM vs. Radar for Several Thrust Ratings 3-19
3-17 UAL1102.524 Thrust Profile, INM vs. Radar for Several Thrust Ratings 3-20
3-18 UAL1080.531 Altitude Profile, INM vs. Radar for Several Thrust Ratings 3-20
3-19 UAL1080.531 Velocity Profile, INM vs. Radar for Several Thrust Ratings 3-21
3-20 UAL1080.531 Thrust Profile, INM vs. Radar for Several Thrust Ratings 3-21
3-21 UAL1406.527 Altitude Profile, INM vs. Radar for Several Thrust Ratings 3-22
3-22 UAL1406.527 Velocity Profile, INM vs. Radar for Several Thrust Ratings 3-22
3-23 UAL1406.527 Thrust Profile, INM vs. Radar for Several Thrust Ratings 3-23
3-24 UAL1280.527 Altitude Profile, INM vs. Radar for Several Thrust Ratings 3-23
3-25 UAL1280.527 Velocity Profile, INM vs. Radar for Several Thrust Ratings 3-24
3-26 UAL 1280.527 Thrust Profile, INM vs. Radar for Several Thrust Ratings 3-24
3-27 R1 Step Refinement (Every Radar Point) UAL1035.521 (M1R1TN5) 3-27
3-28 R2 Step Refinement (Every Other Radar Point) UAL1035.521 (M1R2TN5) 3-27
3-29 R3 Step Refinement (Every Third Radar Point) UAL1035.521 (M1R3TN5) 3-28
3-30 R4 Step Refinement (Every Fourth Radar Point) UAL1035.521 (M1R4TN5) 3-28
3-31 R5 Step Refinement (Every Fifth Radar Point) UAL1035.521 (M1R5TN5) 3-29
3-32 Minimization Method M1 (%-Speed and %-Altitude) UAL1035.521 (M1R2TN5) 3-29
3-33 Minimization Method M2 (Potential and Kinetic Energy) UAL1035.521 (M2R2TN5) 3-30
3-34 Minimization Method M3 (Velocity Match, Adjust Climb Rate) UAL1035.521 (M3R2TN5) 3-30

3-35 Minimization Method M4 (Altitude Match, Adjust Climb Rate) UAL1035.521 (M4R2TN5) ... 3-31
3-36 Minimization Method M5 (Velocity Match, Adjust Ending Speed) UAL1035.521 (M5R2TN5) ... 3-31
3-37 Minimization Method M6 (Altitude Match, Adjust Ending Speed) UAL1035.521 (M6R2TN5) ... 3-32
3-38 Threshold N5 (All Accelerate Steps), UAL1035.521 (M2R2TN5) Duplicate of Figure 3-33 for Clarity ... 3-33
3-39 Threshold N01 (dv/dz>.01 for Climb Step) UAL1035.521 (M2R2T01) ... 3-33
3-40 Threshold N02 (dv/dz>.02 for Climb Step) UAL1035.521 (M2R2T02) ... 3-34
3-41 Threshold N04 (dv/dz>.04 for Climb Step) UAL 1035.521 (M2R2T04) ... 3-34
4-1a 1280.521 Ground Track ... 4-5
4-1b 1280.521 Altitude Profile ... 4-5
4-1c 1280.521 Velocity Profile ... 4-6
4-1d 1280.521 Power Profile ... 4-6
4-2a 1685.528 Ground Track ... 4-7
4-2b 1685.528 Altitude Profile ... 4-7
4-2c 1685.528 Velocity Profile ... 4-8
4-2d 1685.528 Power Profile ... 4-8
4-3a 1845.522 Ground Track ... 4-9
4-3b 1845.522 Altitude Profile ... 4-9
4-3c 1845.522 Velocity Profile ... 4-10
4-3d 1845.522 Power Profile ... 4-11
4-4a 1132.530 Ground Track ... 4-11
4-4b 1132.530 Altitude Profile ... 4-11
4-4c 1132.530 Velocity Profile ... 4-12
4-4d 1132.530 Power Profile ... 4-12
4-5a 484.527 Ground Track ... 4-13
4-5b 484.527 Altitude Profile ... 4-13
4-5c 484.527 Velocity Profile ... 4-14
4-5d 484.527 Power Profile ... 4-14
4-6a 588.528 Ground Track ... 4-15
4-6b 588.528 Altitude Profile ... 4-15
4-6c 588.528 Velocity Profile ... 4-16
4-6d 588.528 Power Profile ... 4-16
4-7a 1227.531 Ground Track ... 4-17
4-7b 1227.531 Altitude Profile ... 4-17
4-7c 1227.531 Velocity Profile ... 4-18
4-7d 1227.531 Power Profile ... 4-18
4-8a 1430.527 Ground Track ... 4-19
4-8b 1430.527 Altitude Profile ... 4-19
4-8c 1430.527 Velocity Profile ... 4-20
4-8d 1430.527 Power Profile ... 4-20
4-9a 1604.523 Ground Track ... 4-21
4-9b 1604.523 Altitude Profile ... 4-21

4-9c 1604.523 Velocity Profile 4-22
4-9d 1604.523 Power Profile 4-22
4-10a 1111.524 Ground Track 4-23
4-10b 1111.524 Altitude Profile 4-23
4-10c 1111.524 Velocity Profile 4-24
4-10d 1111.524 Power Profile 4-24
4-11a 484.522 Ground Track 4-25
4-11b 484.522 Altitude Profile 4-25
4-11c 484.522 Velocity Profile 4-26
4-11d 484.522 Power Profile 4-26
4-12a 226.527 Ground Track 4-27
4-12b 226.527 Altitude Profile 4-27
4-12c 226.527 Velocity Profile 4-28
4-12d 226.527 Power Profile 4-28
4-13a 1801.523 Ground Track 4-29
4-13b 1801.523 Altitude Profile 4-29
4-13c 1801.523 Velocity Profile 4-30
4-13d 1801.523 Power Profile 4-30
4-14a Ground Track 385.528 4-32
4-14b Altitude Profile 385.528 Not Handled by the Automated Profile Builder 4-32
4-14c Speed Profile 385.528 Not Handled by the Automated Profile Builder 4-33
4-14d Power Profile 385.528 Not Handled by the Automated Profile Builder 4-33
4-15a 1845.525 Ground Track 4-34
4-15b Climb Profile 1845.525 Not Handled by the Automated Profile Builder 4-34
4-15c Velocity Profile 1845.525 Not Handled by the Automated Profile Builder 4-35
4-15d Power Profile 1845.525 Not Handled by the Automated Profile Builder 4-35
5-1 Prediction Accuracy – Altitude at the Point of Closest Approach 5-3
5-2 Prediction Accuracy – Ground Track Distance at the Point of Closest Approach 5-4
5-3 Prediction Accuracy – Radar Speed at the Point of Closest Approach 5-4
5-4 Prediction Accuracy – Slant Range to Radar Point of Closest Approach 5-5
5-5 Prediction Accuracy – Measured SEL (dB) 5-5
5-6 Prediction Accuracy – Measured L_{max} (dB) 5-6
5-7 Prediction Accuracy – Elevation Angle (degrees) 5-6
5-8 Prediction Accuracy – Takeoff Gross Weight (lbs) 5-7
5-9 Prediction Accuracy – Outside Air Temperature at PCA (°F) 5-7
5-10 Prediction Accuracy – Relative Humidity at the Airport (%) 5-8
5-11 Prediction Accuracy – INM Thrust at the PCA (Fn/δ lbs) 5-8
5-12 Prediction Accuracy – INM Altitude – Radar Altitude at PCA (Ft) 5-9
5-13 Prediction Accuracy – INM Speed – Radar Speed at PCA (TAS kts) 5-9
5-14 Prediction Accuracy – INM Thrust – 1998 CATS Thrust at PCA (lbs) 5-10
5-15 Prediction Accuracy – Flight Speed – 160 kt Reference Airspeed 5-10
5-16 Prediction Accuracy – Mach Number at the Point of Closest Approach 5-11

List of Tables

Table No.

2-1 DIA (S) and Wyle (W) Noise Monitor Site Distances 2-3
2-2 Noise Monitor Site Coordinates and Elevations 2-4
3-1 INM Standard Departure Procedure for a B737-300 3-2
3-2 INM Standard Aircraft Flap and Jet Coefficients for B737-300 3-2
3-3 INM Custom Procedure Steps to Simulate a Flight UAL 1684.523 3-7
3-4 Modified Custom INM B737 Flap and Jet Coefficients to Match UAL 1684.523 3-7
3-4A Sample of B737 Takeoff Field Length Historical Data Obtained from a Video Surveillance System 3-12
3-5 B737 Mean and Standard Deviation Takeoff Field Lengths for Video Recorded Operations at DIA 3-14
3-6 INM Climb Segment 3-15
3-7 INM Accelerated Segment 3-15
3-8 INM Boeing 737 Reduced Thrust Jet Coefficients 3-18
4-1 Summary of Flight Operation Noise Events – INM Aircraft Types 4-1
4-2 Summary of Flight Operation Noise Events by Day 4-2
4-3 Summary of Flight Operation Noise Events by Runway 4-2
4-4 Summary of Noise Monitoring Events 4-2
4-5 New NPD Curves Analyzed in INM 4-3
4-6 Sample Flight Operation List for in Depth Review Using INM6.1 4-4
5-1 Acoustic Summary 5-2
5-2 Aircraft Types Modeled in the Various Studies 5-3
6-1 Acoustic Summary 6-2
A-1 Takeoff Thrust Prediction Methodology Flowchart A-1
A-2 Maximum Allowable Takeoff Weight, B737-500, Flaps 5, Bleeds ON A-3
A-3 Maximum Takeoff Thrust – 737-300 (B1/C1-20k) A-5
A-4 Reduced Takeoff Thrust %N1 Adjustment A-6
A-5 Maximum Climb Thrust Table A-7

1.0 Introduction

Prior studies[1] comparing measured noise levels at Denver International Airport with predictions made using Version 5 of the Integrated Noise Model[2] (INM) indicated that noise was under predicted by approximately 4.4 dB with a standard deviation of 3.3 dB. Furthermore, that study[1] showed that prediction errors increased as the aircraft moved further from the airport and gained altitude. Candidate explanations for the source of this discrepancy include errors in aircraft performance modeling, errors in predicted thrust settings, propagation issues, and changes in engine source noise characteristics when operating at higher altitudes. In the period since the earlier studies were performed there have been advances in both the acoustic and performance modeling capabilities of INM. Improvements have been made to the noise – power – distance (NPD) curves, revised lateral attenuation algorithms have been incorporated into INM, and a spectrally based relative-humidity absorption model has been incorporated into INM. The advances in aircraft performance modeling are due to both the inclusion of a procedure step modeling capability in INM[3] and the development of additional aircraft performance coefficients for INM[4], allowing one to model reduced thrust departure procedures in INM. The intent of the study documented in this report is to reevaluate the aircraft noise predictions using the expanded INM flight profile predictive capabilities and revised acoustical algorithms, and compare INM noise predictions with previously obtained noise measurements[1].

2.0 Measurement Program and Data Acquisition

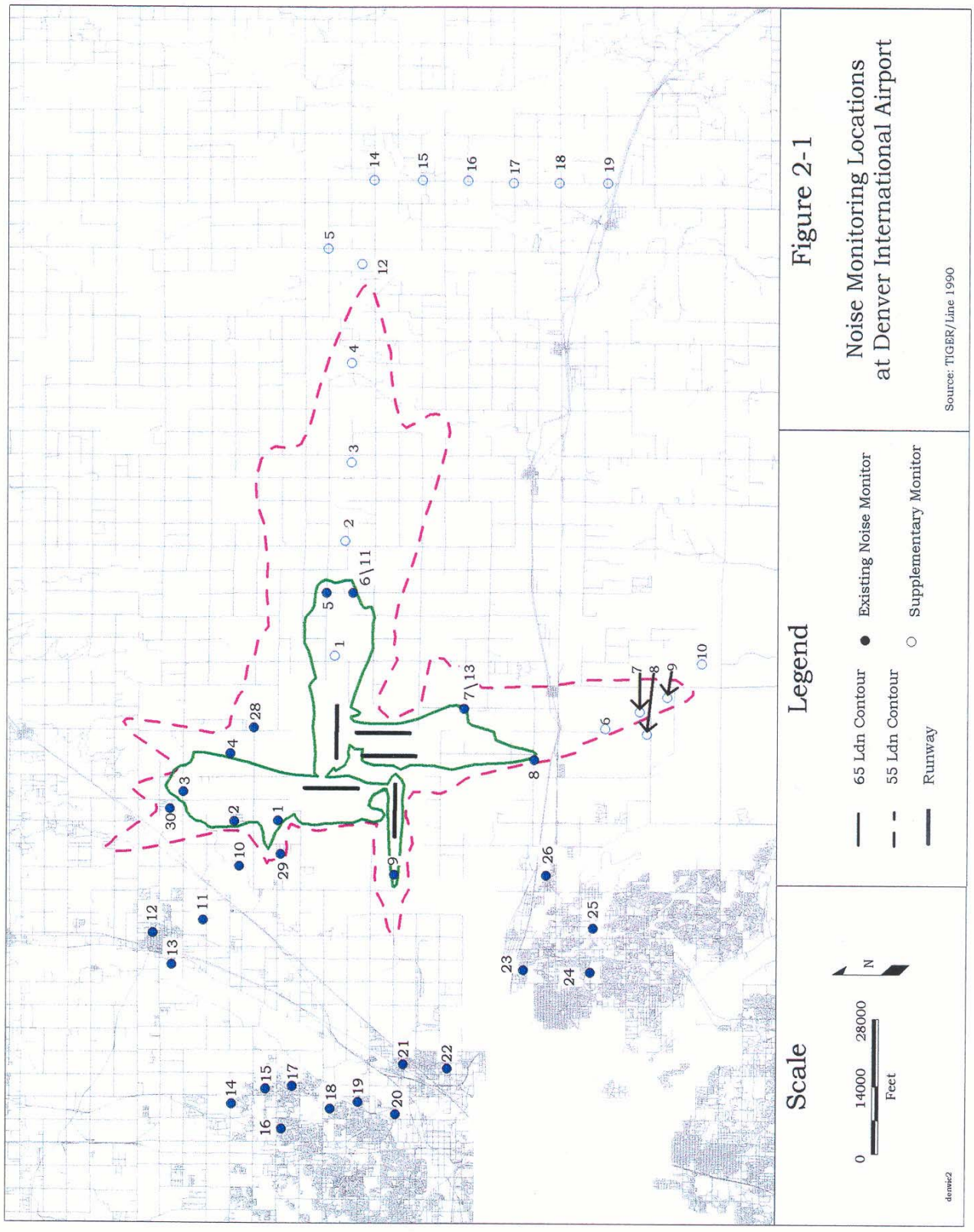
2.1 Denver Measurement Program Overview

Noise monitoring was conducted at Denver International Airport during the period from May 13, 1997 through June 13, 1997. Noise monitoring stations included the 31 permanently installed monitors operated by the DIA noise abatement office, as well as 19 additional temporary noise monitors installed by Wyle Laboratories. Additional details about the monitoring-site selection process, the equipment used to gather data, and other procedural details are presented in "Validation of Aircraft Noise Prediction Models at Low Levels of Exposure."[1]

During this monitoring time period, additional operational flight and atmospheric information was gathered. Takeoff gross-weight data was obtained from United and Delta Airlines. Exact equipment usage including vehicle nose number and hence airframe model and engine model, was provided by United Airlines. Hourly surface airport weather data was obtained from the local airport weather station. Upper air and atmospheric profile information was recorded twice daily by the NOAA operating at the Denver-Stapleton Airport facility.

2.2 Noise Measurement Sites

The DIA Noise Abatement Office provided to Wyle Laboratories a series of official L_{dn} contours surrounding the airport (Figure 2-1). Several days of sample radar tracking data were also provided to aid in the monitor-location selection process. As can be seen in Figure 2-1, DIA has in place an extensive noise monitoring system, to which access was granted for obtaining noise measurement data. Additional temporary monitoring stations were selected to supplement the DIA permanent monitoring system.


Figure 2-1
Noise Monitoring Locations
at Denver International Airport
Source: TIGER/Line 1990
Legend
65 Ldn Contour
55 Ldn Contour
Existing Noise Monitor
Supplementary Monitor
Runway
Scale
0
14000
28000
Feet
N
denvic2

All supplementary sites were located outside or near the 65 dB L_{dn} contour except for one. The monitors installed by Wyle were located east of Runway 08/26 and south of the airport. Using flight tracks as a guide, the noise monitors were located under the densest air traffic. The distances between the airport origin and the noise monitoring sites are listed in Table 2-1.

Table 2-1. DIA (S) and Wyle (W) Noise Monitor Site Distances

Monitor Site	Distance, nmi	Monitor Site	Distance, nmi	Monitor Site	Distance, nmi
S01	3.51	S18	10.81	W04	18.49
S02	5.14	S19	10.46	W05	22.39
S03	7.14	S20	10.95	W06	9.36
S04	5.96	S21	9.09	W07	10.86
S05	9.02	S22	9.60	W08	11.03
S06	8.89	S23	7.87	W09	12.21
S07	5.63	S24	9.88	W10	13.91
S08	6.58	S25	9.15	W11	8.89
S09	2.00	S26	6.78	W12	21.88
S10	5.18	S27	21.90	W13	5.63
S11	7.22	S28	5.77	W14	24.49
S12	9.10	S29	3.56	W15	24.55
S13	9.12	S30	7.55	W16	24.70
S14	11.74	S31	22.57	W17	24.98
S15	10.70	W01	6.58	W18	25.36
S16	11.95	W02	10.68	W19	25.89
S17	10.28	W03	14.34		

Coordinates for the monitor locations are shown in Table 2-2. The coordinates for the Denver sites (denoted with an S) were given to us by the DIA officials. The Wyle sites (denoted with a W) were determined by locating the site on 7.5 x 7.5 minute maps and verifying in the field with a global positioning system. The margin of error is 150 feet in the horizontal plane and 20 feet in the vertical direction.

Table 2-2. Noise Monitor Site Coordinates and Elevations

Site	Latitude	Longitude	Elevation	Site	Latitude	Longitude	Elevation
S01	39.913417	-104.71386	5,243	W01	39.86975	-104.57708	5,380
S02	39.940714	-104.71449	5,158	W02	39.87658	-104.48877	5,238
S03	39.972091	-104.69054	5,112	W03	39.868474	-104.40838	5,233
S04	39.943126	-104.65899	5,279	W04	39.869266	-104.31845	5,140
S05	39.88391	-104.52659	5,266	W05	39.883978	-104.23518	5,095
S06	39.867579	-104.52661	5,299	W06	39.710779	-104.64083	5,711
S07	39.797821	-104.62164	5,423	W07	39.690147	-104.62097	5,772
S08	39.753662	-104.66348	5,604	W08	39.682132	-104.63654	5,810
S09	39.841317	-104.75777	5,292	W09	39.667582	-104.6151	5,870
S10	39.937485	-104.75127	5,098	W10	39.647203	-104.58455	5,970
S11	39.959605	-104.79585	5,046	W11	39.867946	-104.5267	5,306
S12	39.990732	-104.80629	4,977	W12	39.852291	-104.24486	5,110
S13	39.979036	-104.83249	4,967	W13	39.797821	-104.62164	5,423
S14	39.941792	-104.9463	5,338	W14	39.855233	-104.18819	4,979
S15	39.920678	-104.93377	5,171	W15	39.826166	-104.18839	5,021
S16	39.910657	-104.96674	5,325	W16	39.797211	-104.18929	5,056
S17	39.904312	-104.93136	5,203	W17	39.768049	-104.1913	5,101
S18	39.880582	-104.94985	5,249	W18	39.739084	-104.19081	5,163
S19	39.863181	-104.94443	5,121	W19	39.710338	-104.19086	5,225
S20	39.839967	-104.95437	5,125	ASR	39.854986	-104.7183	5,431
S21	39.834983	-104.91327	5,151				
S22	39.807386	-104.91656	5,181				
S23	39.759972	-104.83585	5,335				
S24	39.718379	-104.8378	5,459				
S25	39.716632	-104.80171	5,450				
S26	39.746086	-104.75819	5,459				
S27	39.494244	-104.6437	5,900				
S28	39.928624	-104.63775	5,200				
S29	39.911728	-104.74136	5,243				
S30	39.980388	-104.70447	5,112				
S31	39.483224	-104.64222	5,900				

It should be noted that use of the current L_{dn} contours in this report was for the purpose of providing a reference noise environment to aid in the selection of the noise monitoring locations. The L_{dn} contours shown in Figure 2-1 are an interpretation of the official contours in that they were digitized from the original exhibit and registered in a geographic information system (GIS). These modified contours are a good representation of the originals so far as the shape and extent of the footprint; however, due to the digitization process, the contour lines are not as smooth as the originals. These contours should not be considered the official L_{dn} contours for Denver International Airport nor should they be used for any land-use planning purposes. As Figure 2-1 indicates, most of the noise monitoring sites span and exceed the space between the 55 and 65 dB contours.

2.3 Flight Operations Radar Data Analysis

FAA ARTS5 radar data was obtained from DIA for the duration of the noise monitoring period in the form of Dimensions International REL files[6]. This data was processed into ASCII flight trajectories during the previous Denver noise study[1].

INM Version 5[7] ground tracks were developed in 1999 and used again in the current analysis. The INM import function was applied to convert the tracks into INM Version 6[3]-compatible flight tracks. Figure 2-2 is a graphic from the NDADS radar analysis tool depicting all of the flight operations considered in the current study.

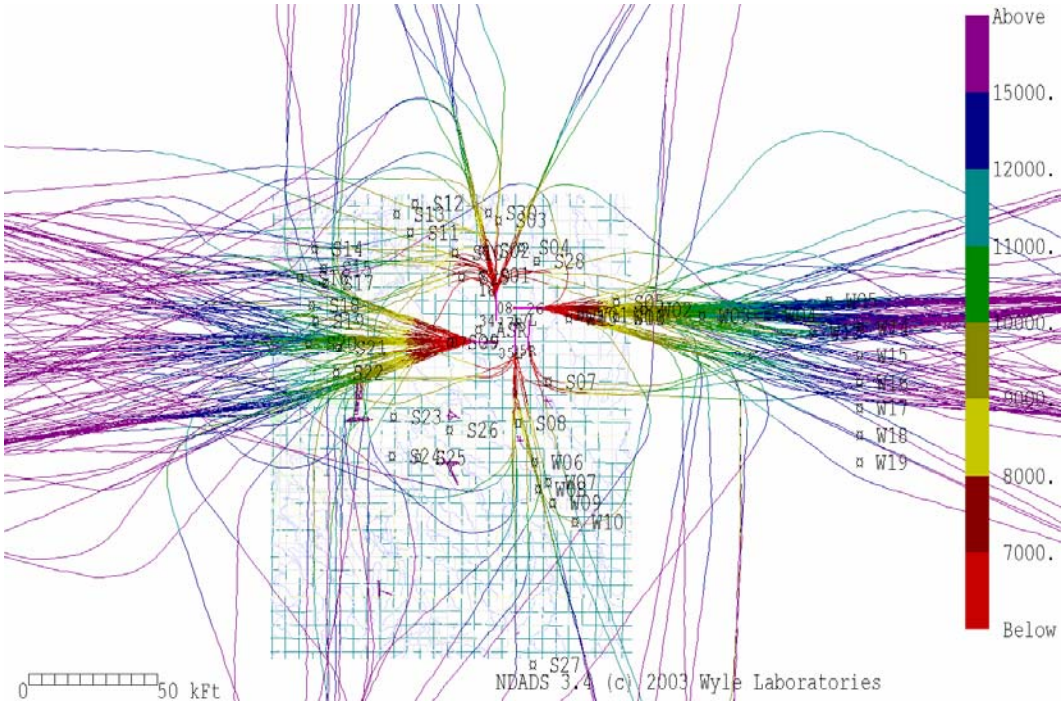


Figure 2-2. DIA Departure Operations and Noise Monitoring Locations Considered in the Current INM Noise Study

2.4 Noise Event Extraction

Wyle Laboratories applies a "track first" approach for associating particular noise measurement events with flight operations. This methodology begins with a radar flight track and based on synchronized monitor and radar times and the geometric point of closest approach, predicts sound event arrival times at the noise monitors. The noise monitoring data is then searched at the appropriate arrival times and the event selected and associated with the given flight operation. This method was employed during the previous study[1] and the corresponding measured SEL data associated with the flight operations is utilized for the current analysis.

3.0 Flight Operation Modeling

The ground rules for this project were to utilize the aerodynamic flight performance capabilities within three versions of INM (6.0c, 6.1, and 6.2) and develop sequences of procedure steps that most closely match the measured radar climb profiles. These procedure step sequences were developed separately for each individual flight trajectory. The automated procedure used a batch version of the flight module. Since only Version 6.1 was available, the procedure steps were used for all versions of INM. The details of the procedure step modeling process are described in this chapter.

3.1 Creation of Flight Profiles using INM Procedure Steps

The first step toward modeling the flight operations was to check if any of the standard departure procedures based on stage length are sufficient for the recorded flight profile. Since the trajectory is an integration of all the procedure steps in succession, the takeoff roll and initial climb need to be matched first. This section documents using the INM procedure steps with the standard aircraft jet coefficient data and flap coefficient data distributed with INM Version 6.1 and compares those profiles with measured radar flights. For this analysis, an examination was performed using 14 Denver flight departures of B737-300 aircraft equipped with CFM-56-3B1 engines. These 14 operations were selected from departures off runway 08, which headed in a nominal eastward direction without any significant turns over the monitoring area. Operations with a straight out departure were selected in order to more easily match the physics with an effectively two-dimensional departure without the consideration of any energy going toward turning operations. This procedure was employed for the entire analysis presented in this report.

The standard INM departure profile based on vehicle stage length was examined as the first part of this process. The NDADS radar analysis system[8] was used to determine the statistical geometric information based on the recorded radar flight tracks. The mean aircraft takeoff gross weight for these fourteen B737 flight operations was 116,626 lbs., with a standard deviation of 8137 lbs. This mean weight corresponds to a stage length 4 departure according to the INM6 database (stage length = 4, takeoff gross weight = 119000 lbs).

The standard INM departure procedure steps were modeled and the flight profiles, extracted from INM using the Flight Path feature, were compared with the measured radar profiles in order to determine the applicability of using INM stage lengths to simulate flight profiles. Table 3-1 shows the standard INM procedure steps for a B737.

Table 3-1. INM Standard Departure Procedure for a B737-300

Step	Type	Flaps	Thrust	Final Alt AFE	Climb Rate FPM	Final Speed CAS (kt)
1	Takeoff	5	Max Takeoff			
2	Climb	5	Max Takeoff	1000		
3	Accelerate	5	Max Takeoff		1544	185
4	Accelerate	1	Max Takeoff		1544	190
5	Accelerate	0	Max Climb		1000	220
6	Climb	0	Max Climb	3000		
7	Accelerate	0	Max Climb		1000	250
8	Climb	0	Max Climb	5500		
9	Climb	0	Max Climb	7500		
10	Climb	0	Max Climb	10000		

Table 3-2. INM Standard Aircraft Flap and Jet Coefficients for a B737-300

INM Standard 1 degree Flap Coefficients:
D/L = .076100 (L/D=13.1406)
Takeoff C = .4958
Takeoff Roll B = .01260

INM Standard Max Takeoff Thrust Coefficients
E = 18745 lbs.
F = -20.12 (lb/kt)
Ga = 4.043e-01
Gb = 0
H = 0

INM Standard Max Climb Thrust Coefficients
E = 17448 lbs.
F = -17.32 (lb/kt)
Ga = 1.557e-01
Gb = 0
H = 0

A comparison of the INM stage length 4 standard flight profiles with radar data is given in Figures 3-1 and 3-2. Included in this graphic is a nominal flight profile in heavy black with red squares, calculated using NDADS, which is based on statistical analysis of the measured radar profile data. The standard departure profile for stage length 4 in INM is shown in heavy blue with black diamonds. For detailed analysis it is appropriate to select one radar flight profile, which closely approximates the nominal profile in the region of interest. The reason for doing this is to ensure a representative energy state of the flight vehicle. If one were to simply attempt to approximate the mean profile the throttle setting from point to point could be varying, depending on the different weights of each operation or throttle setting of each different operation and how the nominal profiles average out. Selecting a single representative flight profile, using the nominal profile as guidance, ensures a consistent energy state along the length of the operation. This nominal flight profile is illustrated in Figures 3-1 and 3-2 as a heavy broken green line. Figure 3-2 is a close up of the first part of the departure profile. One can clearly see the large difference between the INM standard stage length 4 profile and the recorded radar

profile. The position at which the vehicle leaves the ground is too close to the start of the takeoff roll, the changes in speed and altitude are modeled too abruptly, and the second segment climb out has a significantly higher climb rate and acceleration than the recorded radar data. The other INM Stage length departure profiles are even less representative of Denver operations due to the reduce weight and max thrust departures which yields very high acceleration and climb rates as can be seen in Figures 3-1 and 3-2.

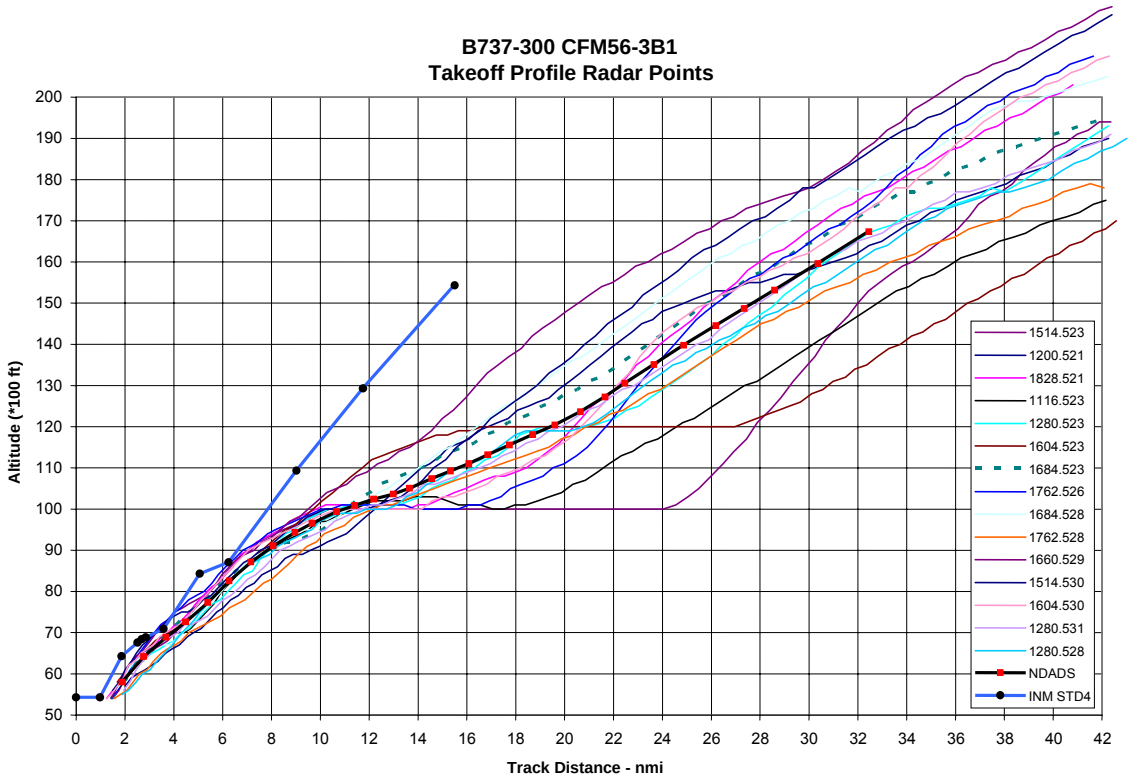


Figure 3-1. Comparison of Radar Altitude with INM Stage Length 4 Profile

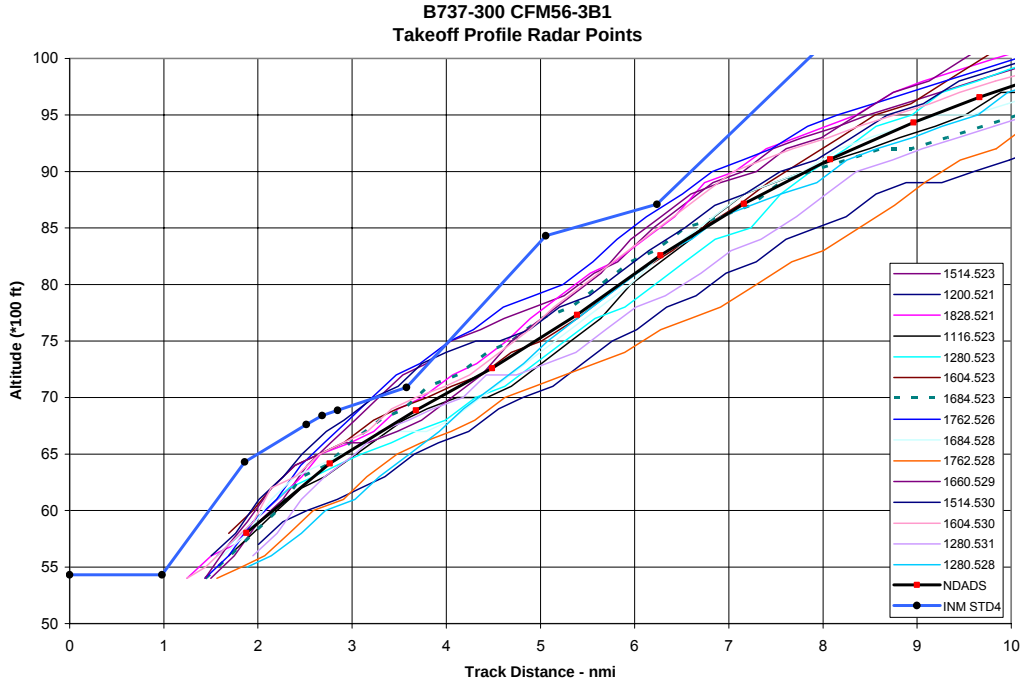


Figure 3-2. Comparison of Radar Altitude with INM Stage Length 4 Profile (Close-up)

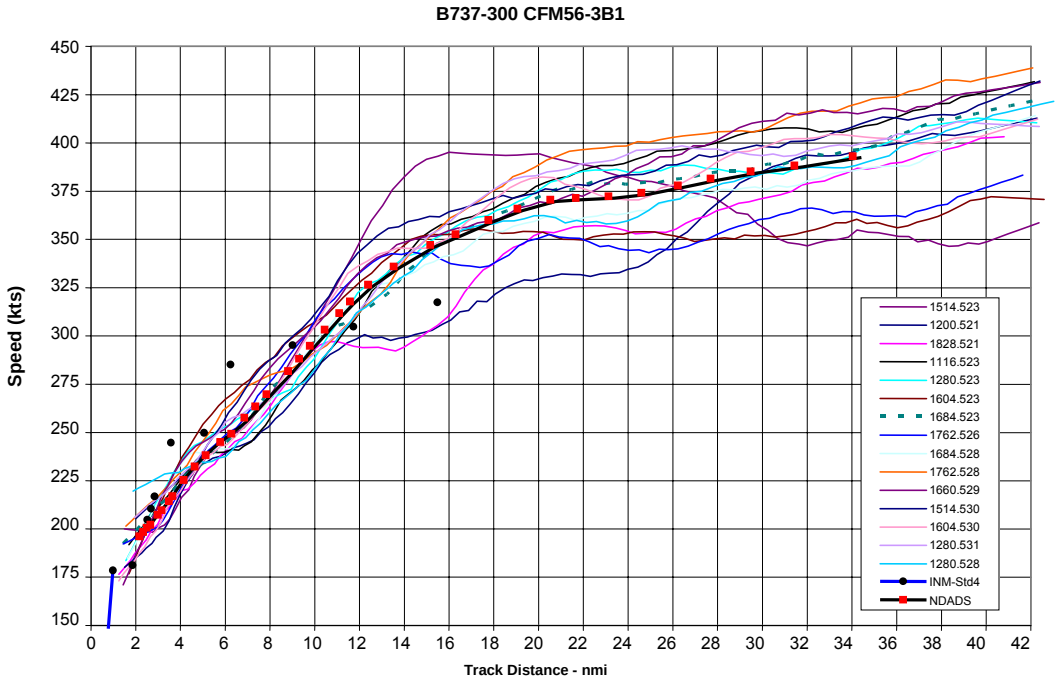


Figure 3-3. Comparison of Radar Velocity with INM Stage Length 4 Profile (Close-up)

For completeness, the profiles were also compared with other stage length standard departure procedures in INM. These results are shown in Figures 3-4, 3-5 and 3-6.

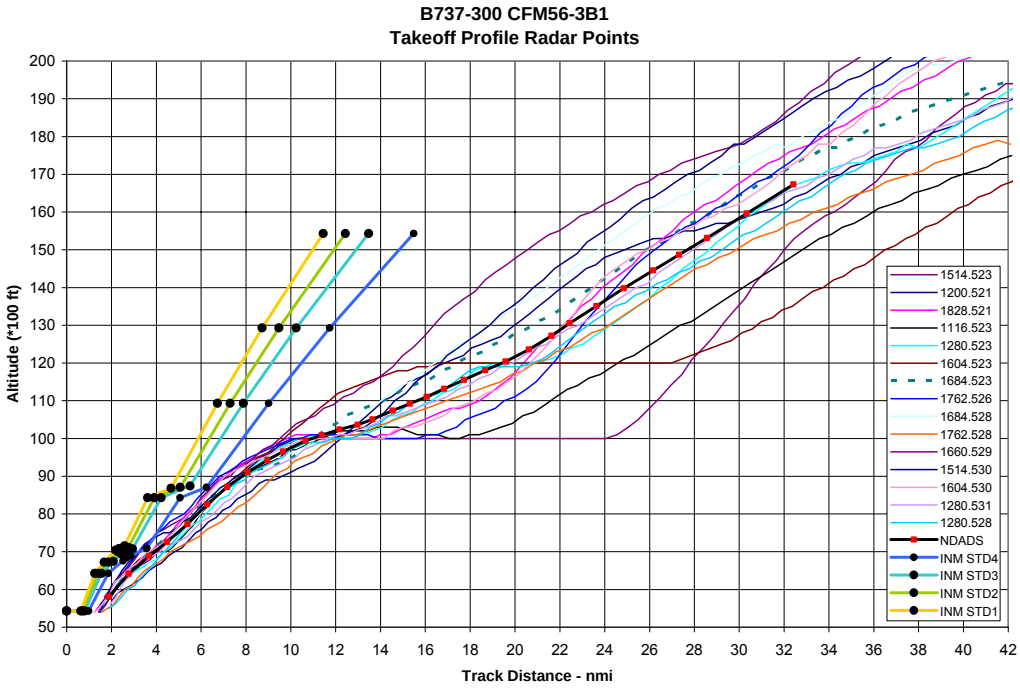


Figure 3-4. Comparison of Radar Altitude with INM Standard Profiles

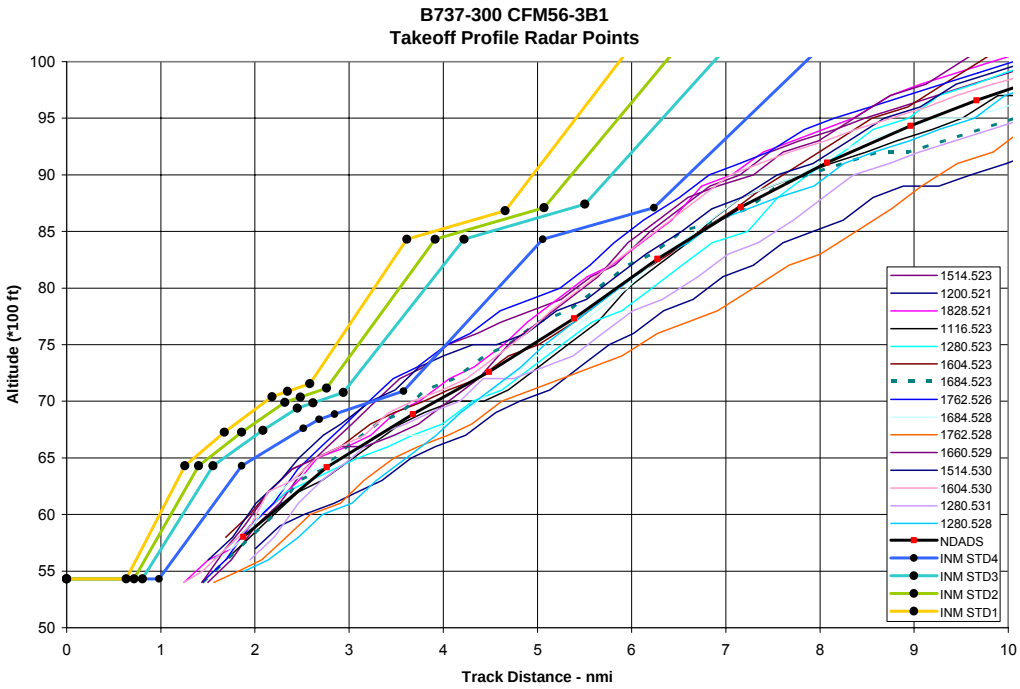


Figure 3-5. Comparison of Radar Altitude with INM Standard Profiles (Close-up)

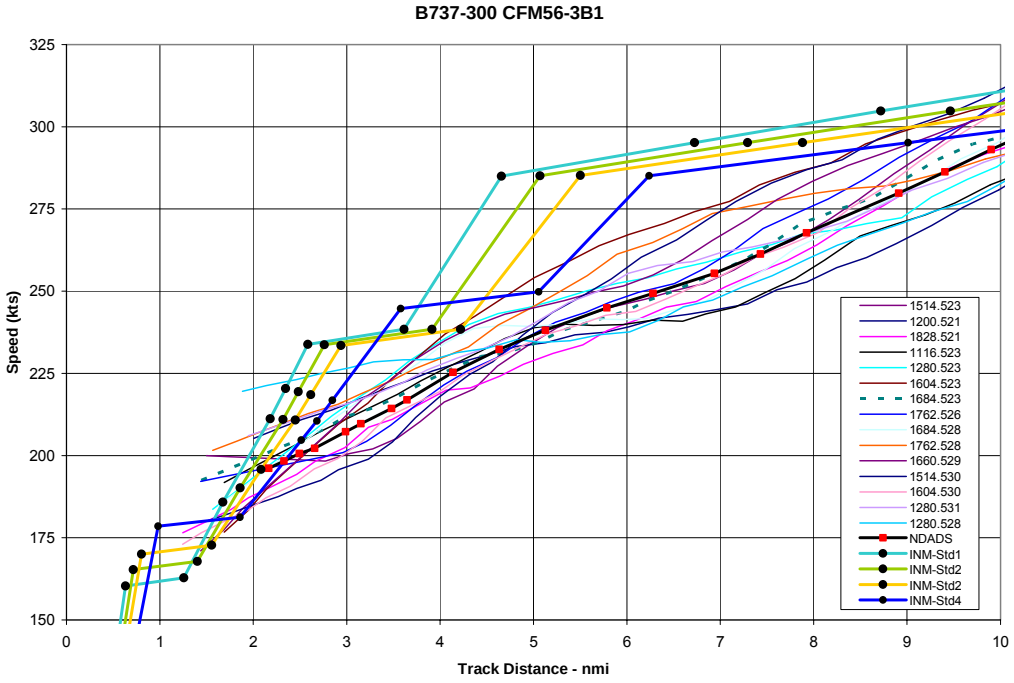


Figure 3-6. Comparison of Radar Velocity with INM Standard Profiles (Close-up)

As can been observed in Figures 3-4, 3-5 and 3-6, modifying the stage length in INM (a surrogate for aircraft takeoff weight) does not achieve the required increased runway takeoff ground roll, increased liftoff speed or lower climb rate as seen in the radar data. The fundamental reason is because the departing aircraft from Denver are performing reduced thrust departures and the standard INM departure procedures use full thrust.

3.2 Tailoring the Ground Roll to Match Measured Radar Trajectories

The next step was to interactively, via the INM graphical user interface, design a series of procedure steps that puts the aircraft along the recorded radar flight altitude profile, while matching the recorded radar flight speeds profile. The objective is to determine what kinds of changes need to be made to the procedure steps or aircraft coefficients. Again, a representative flight profile that closely matches the nominal radar flight trajectory was selected: UAL1684 on May 23, 1997 (UAL1684.523) with a reported takeoff gross weight of 123,000 lbs.

In developing a new INM set of procedure steps, aircraft operational procedure knowledge obtained during the previous DIA noise study[1] was used. The power profile calculated using the CATS code during the pervious Denver study[1] was extracted for this particular flight trajectory in order to have a point of reference for comparing the INM predicted power data. A summary of the aircraft operational procedures employed by United Airlines, as modeled by the CATS code are presented in Appendix A.

The salient United Airlines historical operational features learned in the prior study and applied here in order to develop a custom set of procedure steps are:

- Most operations perform a reduced thrust takeoff
- B737s primarily utilize a 1°-improved wing high-lift flap setting
 - employs a higher liftoff speed and
 - allows the aircraft to use additional runway length
- Most operations perform a reduced thrust climb

Since the vehicle trajectory is integrated using the procedure steps, one must begin with the takeoff segment. The fundamental parameter in the INM flap coefficients which controls the liftoff speed is the C_f parameter. The ground roll coefficient B_f has a significant effect on the takeoff ground roll distance. The user defined profile is given in Table 3-3 and uses modified flap coefficients corresponding to the 1-imp flap setting as shown in Table 3-4.

Table 3-3. INM Custom Procedure Steps to Simulate a Flight UAL1684.523

Step	Type	Flaps	Thrust	Final Alt AFE	Climb Rate FPM	Final Speed CAS (kt)
1	Takeoff	1-imp	Max Takeoff			
2	Accelerate	1-imp	Max Takeoff		2200	185
3	Accelerate	1-imp	Max Takeoff		2200	200
4	Accelerate	0	Max Climb		1500	210
5	Climb	0	Max Climb	3000		
6	Accelerate	0	Max Climb		1500	250
7	Climb	0	Max Climb	5500		
8	Climb	0	Max Climb	7500		
9	Climb	0	Max Climb	10000		

Note that it was not possible to use a "Climb" step for segment 2 and have the both the flight speed and segment length match radar, while keeping the take off field length and liftoff speeds close to the radar data.

Table 3-4. Modified Custom INM B737 Flap and Jet Coefficients to Match UAL1684.523

Flap Coefficients:
Aircraft: 737300
Flaps ID 1_IMP
R (D/L) = .0715
Takeoff C = 0.5100
TO Roll B = .0160

The result of this new "cookbook recipe" for this departure based on the INM calculated flight trajectory (labeled User-INM) is compared with the radar trajectory (labeled 1684.523), nominal profile (labeled NDADS) and INM stage length 4 standard departure profile (labeled INMSTD4) in Figures 3-7, 3-8 and 3-9. Some of the steps taken to develop the trajectory are shown and labeled. Step 1 reduced the takeoff flap setting from 5° to 1°. Step 2 modified the aircraft R, C and B coefficients to those shown in Table 3-4. Finally Step 3 illustrates the effect of modifying the

segments, specifically changing segment 2 from climb to accelerate in order to better match the radar profile.

It can be seen, by visually extrapolating the recorded radar trajectory down to the ground, that one can indeed match the takeoff ground roll and velocity for the first two segments by using INM procedure steps. This does however require changing the aircraft coefficients, which in the case of UAL departures for DIA was justified due to the documented frequent use of the 1°-improved flap setting by UAL. Also note from Figures 3-7 to 3-10 that the aircraft is accelerating and climbing faster than the radar starting in segment 4. This is due to excess thrust. For this particular example, only the flap coefficients were modified to match the takeoff segment. Clearly the thrust must be changed to match subsequent segments. This typical result was in support of the Boeing and the FAA development of alternate reduced thrust coefficients for INM. These will be discussed later in the report.

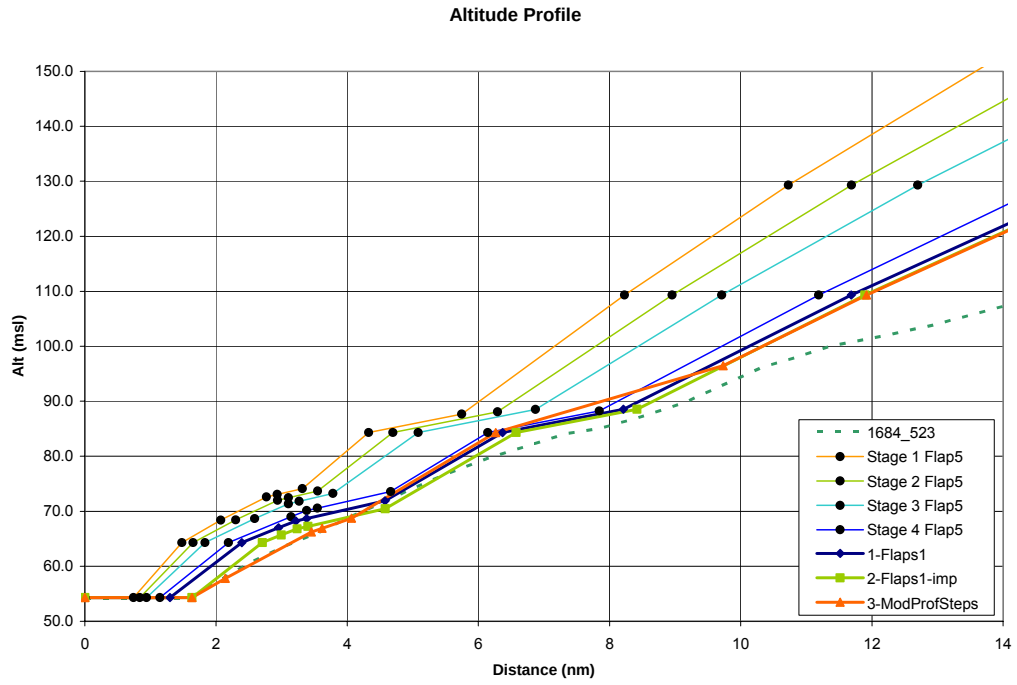


Figure 3-7. INM User Defined Flight Altitude Profile Development UAL1684.523

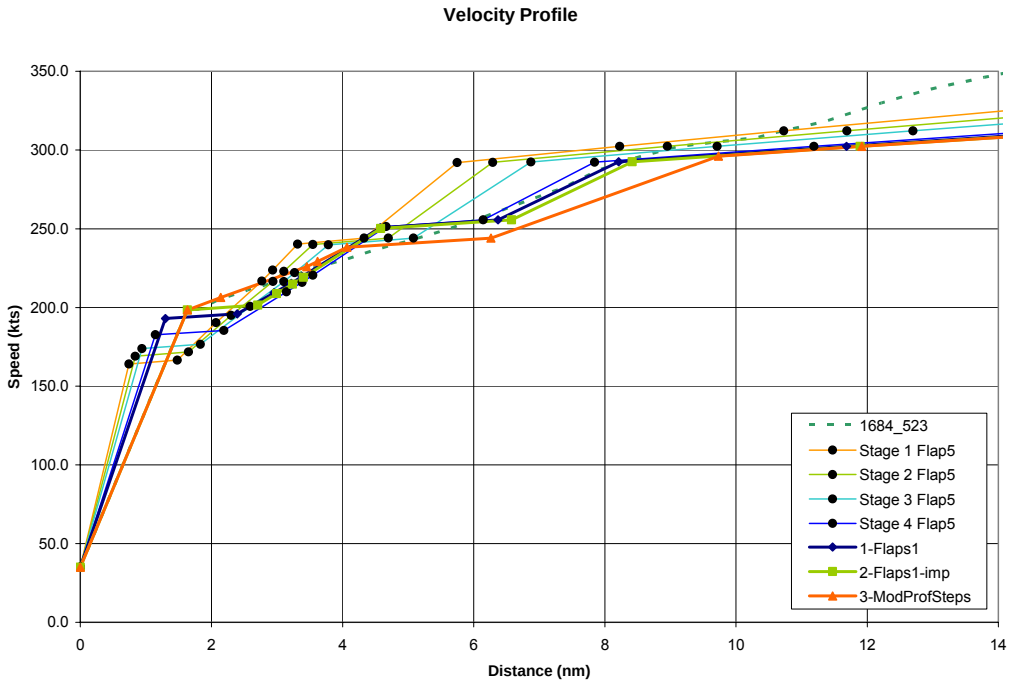


Figure 3-8. INM User Defined Flight Velocity Profile Development UAL1684.523

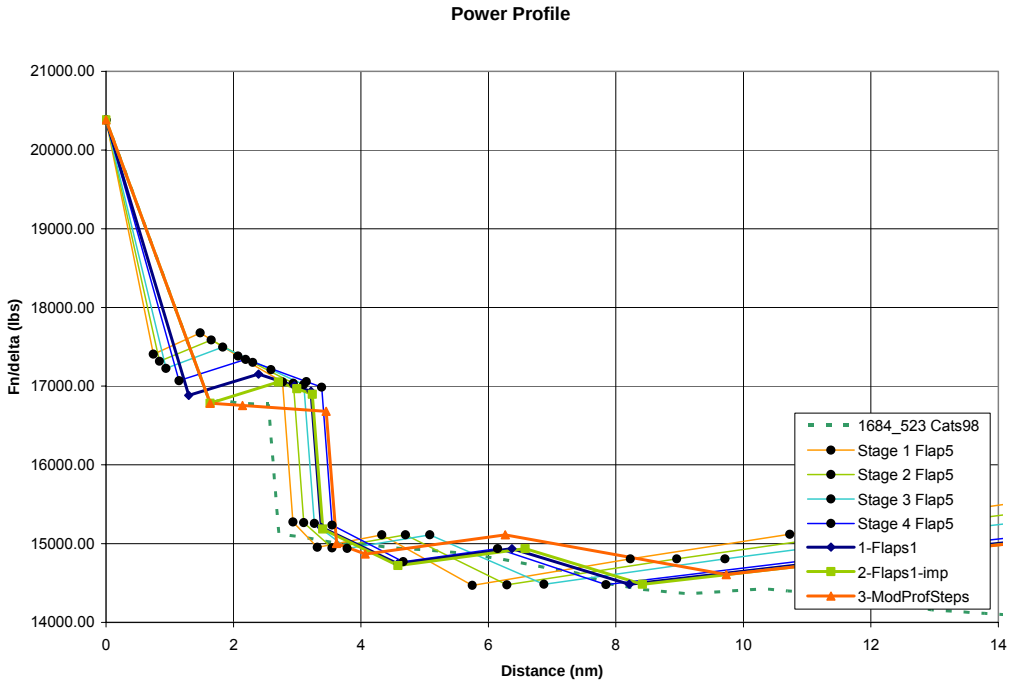


Figure 3-9. INM User Defined Flight Power Profile Development UAL1684.52

When examining the feasibility of performing a takeoff roll model, the sparse radar data in the vicinity of the takeoff roll made such a derivation of appropriate performance coefficients from radar data impossible. As a result, the development of an automated system to simulate the ground roll and first-segment takeoff flight procedure steps was problematic. A companion study of lateral attenuation[9], recorded on video, Aircraft departures from Runway 08. Section 3.4 will discuss a study that was performed using the video data in order to evaluate the feasibility of determining a nominal ground roll or liftoff speed.

3.3 Analysis of Liftoff Speed and Takeoff Field Length using the Video Data from the 1997 Lateral Attenuation Study at Denver

The recorded ARTS data did not reliably include any aircraft positional data until the aircraft was several hundred feet above the field elevation. This lack of radar average precluded the evaluation of the takeoff field length using the radar data. In Figures 3-1, 3-2 and 3-3 one can clearly see the point at which the ARTS radar system started to record the aircraft position. Very little information can be directly gleaned from these plots as to the aircraft takeoff field length or liftoff speed without extrapolation of aircraft trajectories.

A video measurement system was set up to record exact aircraft position for the DIA Lateral Attenuation Study in 1997[9]. Examination of the lateral attenuation study video tracking data provided some indication of the takeoff field lengths and liftoff speeds. Figure 3-10 shows the measurement site layout, including the runway and video camera location. Figure 3-11 shows an example analysis of the video tracking data.

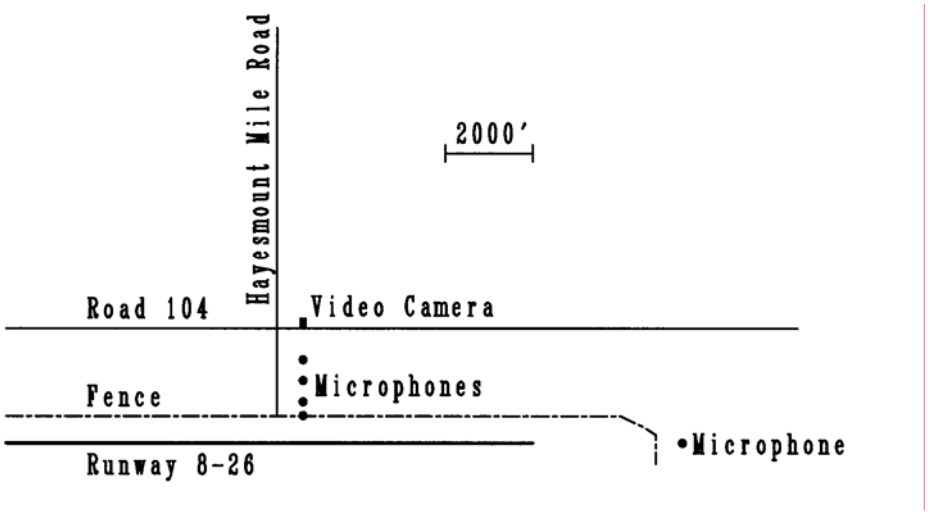


Figure 3-10. Layout of Lateral Attenuation Study Measurement Site and Video Surveillance System

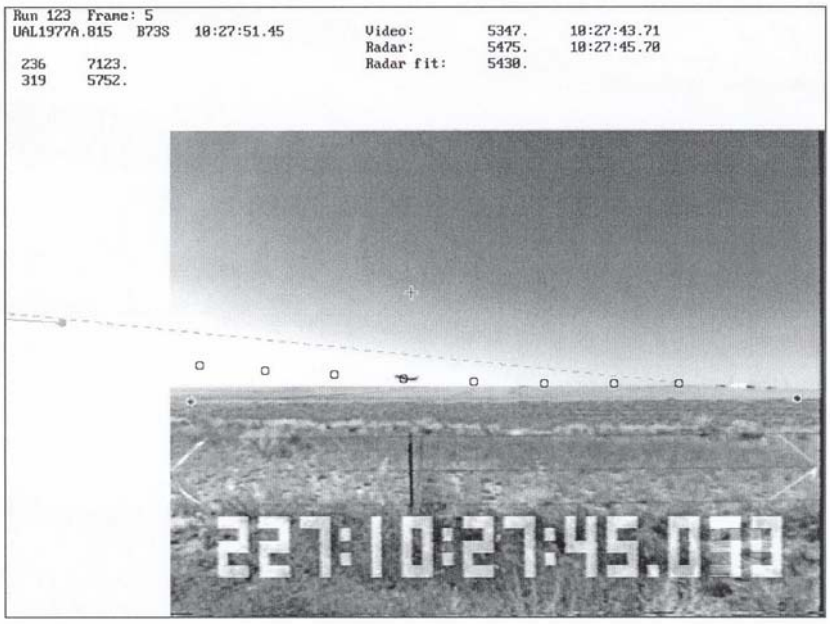


Figure 3-11. Example Analysis of Video Tracking Data

During the video measurement period approximately 800 departures were observed. Of these, approximately 200 were recorded and processed for video analysis during the Lateral Attenuation study. The 200 selections represented virtually all of the aircraft that were airborne and some that were still on the ground as they passed the microphone and video position. These 200 were filtered by day, by airframe/engine type, and by airline. Takeoff weight data was available from United and Delta Airlines. This resulted in at total of 33 data points. Of these, the distribution was 6 operations of 737-300 CFM56-3B1, 21 operations of 737-500 CFM56-3B1 and 5 operations of 737-300 CFM56-3B2 and 1 operation of 737-200 JT8D-19. Data is given in Table 3-4. The fields separated at the bottom of Table 3-4 are operations which were not airborne when passing the video field of view. It is important to note that there were aircraft which were already airborne before passing the video recorder. These 600 takeoffs, out of the approximately 800 observed departures, were not recorded nor included in this study.

Analysis of these 33 operations (Table 3-4A) gave some insight into some common 737 takeoff flight speeds and field lengths for Denver operations. The results calculated here were of interest in terms of the ability of INM to replicate alternate takeoff field lengths and liftoff speeds. Given the position of the video surveillance system (optimized for a different noise study), a large number of operations were airborne before entering the video field of view. This precluded the ability to calculate without introducing bias a nominal takeoff field length and liftoff flight speed which could be used for the full set of monitoring data. The recorded data is presented in Figures 3-12 through 3-13 and Table 3-5.

Table 3-4A. Sample of B737 Takeoff Field Length Historical Data Obtained from a Video Surveillance System

RUN	FLIGHT	DATE	TIME	AC TYPE	Z msl	TO Dist	AC Weight	Feet/ Sec	L/O (KTS)	AC Index	AC Tail #	Temp deg F	RH %	Wind KTS	Wind Dir deg	Airframe	Engine
218A	UAL1124	16-Aug	12.38	**B73S**	5357	5984	113958	303	179.5	8	N359UA	70	62	4	VRB	737-322	CFM56-3-B1 or -3-C1
369	UAL1124	19-Aug	12.28	**B73S**	5345	5702	106960	288	170.6	8	N304UA	72	49	15	40	737-322	CFM56-3-B1 or -3-C1
383	UAL1622	19-Aug	12.54	**B73S**	5347	6206	110217	288	170.6	8	N392UA	72	49	15	40	737-322	CFM56-3-B1 or -3-C1
367	UAL8877	19-Aug	12.11	**B73S**	5354	5908	104481	304	180.1	8	N399UA	72	49	15	40	737-322	CFM56-3-B1 or -3-C1
458	UA1124	20-Aug	12.39	**B73S**	5359	5936	103260	307	181.9	8	N359UA	73	45	0	0	737-322	CFM56-3-B1 or -3-C1
534A	UAL484	22-Aug	8.25	**B73S**	5350	5768	101592	294	174.2	8	N369UA	63	66	3	140	737-322	CFM56-3-B1 or -3-C1
195B	UAL1274	16-Aug	10.47	**B73J**	5359	6250	106182	285	168.9	9	N903UA	63	77	3	VRB	737-522	CFM56-3-B1 or -3-C1
170	UAL1491	16-Aug	8.33	**B73J**	5352	5935	102031	290	171.8	9	N944UA	57	87	7	360	737-522	CFM56-3-B1 or -3-C1
241	UAL1606	16-Aug	13.50	**B73J**	5354	6572	110291	302	178.9	9	N916UA	70	62	6	360	737-522	CFM56-3-B1 or -3-C1
175	UAL1660	16-Aug	8.53	**B73J**	5352	6795	116200	304	180.1	9	N932UA	57	87	7	360	737-522	CFM56-3-B1 or -3-C1
172	UAL484	16-Aug	8.41	**B73J**	5357	6121	109742	300	177.7	9	N955UA	57	87	7	360	737-522	CFM56-3-B1 or -3-C1
395	UAL1168	19-Aug	13.46	**B73J**	5356	5977	102403	293	173.6	9	N907UA	72	49	15	40	737-522	CFM56-3-B1 or -3-C1
339	UAL1184	19-Aug	10.34	**B73J**	5345	5921	108951	284	168.3	9	N913UA	73	39	3	250	737-522	CFM56-3-B1 or -3-C1
467B	UAL1043	20-Aug	12.54	**B73J**	5347	5936	102150	293	173.6	9	N936UA	75	42	0	0	737-522	CFM56-3-B1 or -3-C1
460	UAL1146	20-Aug	12.42	**B73J**	5345	6875	120166	298	176.6	9	N913UA	73	45	0	0	737-522	CFM56-3-B1 or -3-C1
426B	UAL1184	20-Aug	10.42	**B73J**	5340	6024	100682	298	176.6	9	N905UA	66	63	7	300	737-522	CFM56-3-B1 or -3-C1
402A	UAL1491	20-Aug	8.47	**B73J**	5349	5936	94470	298	176.6	9	N941UA	61	77	7	260	737-522	CFM56-3-B1 or -3-C1
418	UAL1500	20-Aug	10.22	**B73J**	5359	6007	99802	251	148.7	9	N917UA	66	63	7	300	737-522	CFM56-3-B1 or -3-C1
472	UAL1802	20-Aug	13.04	**B73J**	5350	6620	117183	298	176.6	9	N950UA	75	42	0	0	737-522	CFM56-3-B1 or -3-C1
461	UAL586	20-Aug	12.44	**B73J**	5336	5950	105438	288	170.6	9	N932UA	73	45	0	0	737-522	CFM56-3-B1 or -3-C1
524A	UAL1606	21-Aug	13.39	**B73J**	5345	6430	110467	302	178.9	9	N914UA	86	22	3	270	737-522	CFM56-3-B1 or -3-C1
506	UAL586	21-Aug	12.45	**B73J**	5349	6069	110952	298	176.6	9	N925UA	82	30	7	270	737-522	CFM56-3-B1 or -3-C1
613A	UAL1168	22-Aug	13.39	**B73J**	5354	5644	99391	275	162.9	9	N909UA	82	26	4	VRB	737-522	CFM56-3-B1 or -3-C1
561	UAL1184	22-Aug	10.28	**B73J**	5382	5575	97305	276	163.5	9	N919UA	75	36	3	VRB	737-522	CFM56-3-B1 or -3-C1
612B	UAL1606	22-Aug	13.38	**B73J**	5350	5883	103589	289	176.6	9	N914UA	82	26	4	VRB	737-522	CFM56-3-B1 or -3-C1
601A	UAL1610	22-Aug	12.50	**B73J**	5345	5685	113510	276	163.5	9	N945UA	81	28	6	50	737-522	CFM56-3-B1 or -3-C1
535	UAL1726	22-Aug	8.27	**B73J**	5354	5575	99166	271	160.6	9	N914UA	63	66	3	140	737-522	CFM56-3-B1 or -3-C1
123	UAL1977	15-Aug	10.27	**B73S**	5350	6843	116881	290	171.8	20	N340UA	75	30	9	200	737-322	CFM56-3-B2 or -3C-1
384	UAL1688	19-Aug	12.56	**B73S**	5347	6827	122482	303	179.5	20	N341UA	72	49	15	40	737-322	CFM56-3-B2 or -3C-1
335C	UAL1977	19-Aug	10.28	**B73S**	5340	5844	105472	301	178.3	20	N313UA	73	39	3	250	737-322	CFM56-3-B2 or -3C-1
439	UAL1728	20-Aug	11.21	**B73S**	5343	6554	107709	302	178.9	20	N316UA	70	54	3	340	737-322	CFM56-3-B2 or -3C-1
564A	UAL396	22-Aug	10.34	**B73S**	5350	5984	106068	285	168.9	20	N333UA	75	36	3	VRB	737-322	CFM56-3-B2 or -3C-1
167B	UAL1598	16-Aug	8.27	**B737**	5347	7821	96764	280	165.9	21	N984UA	57	87	7	360	737-291	JT8D-17

215A	UAL1043	16-Aug	12.33	**B73J**	5412	5938	102497			9	N943UA	70	62	4	VRB	737-522	CFM56-3-B1 or -3-C1
416	UAL1977	20-Aug	10.18	**B73S**	5363	6016	104276			8	N203UA	66	63	7	300	737-322	CFM56-3-B1 or -3-C1
371	UAL1043	19-Aug	12.30	**B73J**	5370	5657	95342			9	N930UA	72	49	15	40	737-522	CFM56-3-B1 or -3-C1
272	UAL1184	17-Aug	10.24	**B73J**	5400	5899	101708			9	N927UA	64	72	17	140	737-522	CFM56-3-B1 or -3-C1
168	UAL1145	16-Aug	8.30	**B73J**	5409	5914	96788			9	N927UA	57	87	7	360	737-522	CFM56-3-B1 or -3-C1

= Aircraft is Airborne before reaching the video array

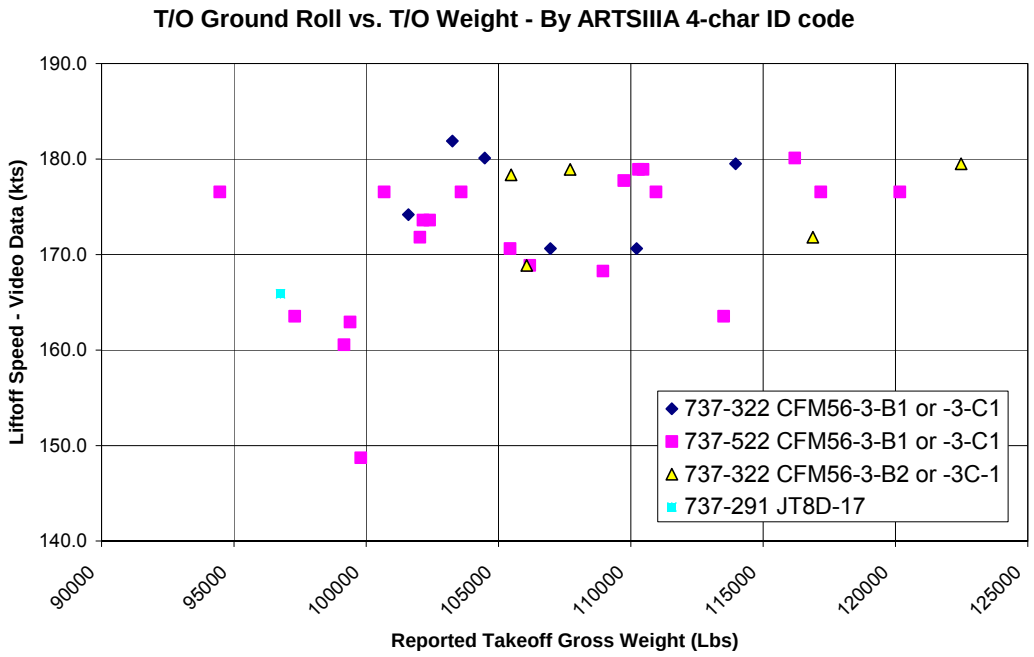


Figure 3-12. Sample B737 Liftoff Speeds at DIA

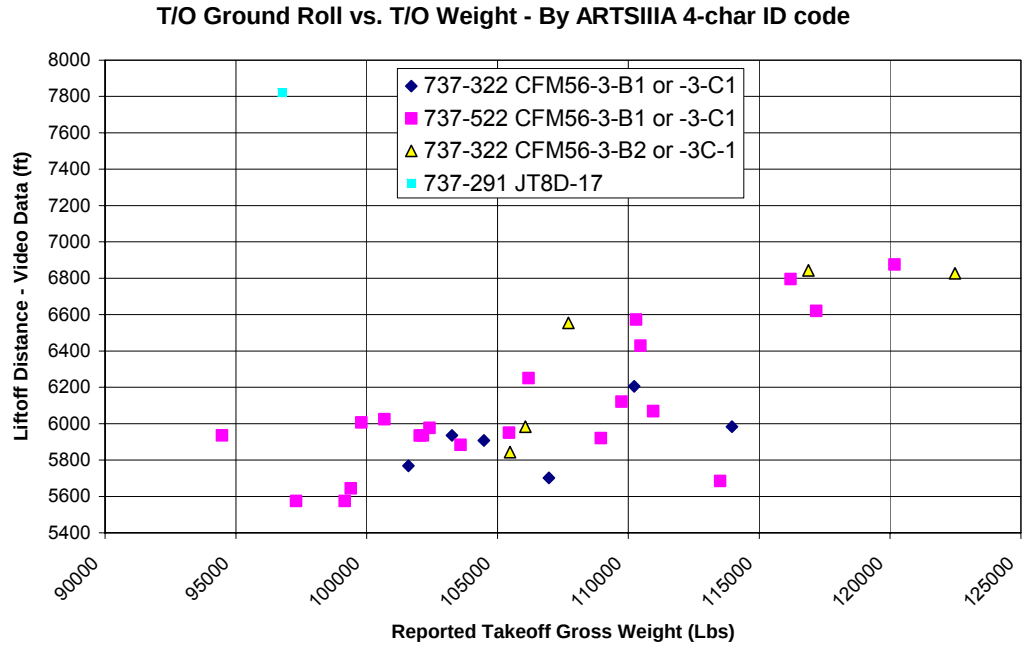


Figure 3-13. Sample B737 Takeoff Ground Roll Distances at DIA

Table 3-5. B737 Mean and Standard Deviation Takeoff Field Lengths for Video Recorded Operations at DIA

INDXX	#	Mean TOFL	STD TOFL	Airframe	Engine
8	6	5917.33	177.13	737-322	CFM56-3-B1 or -3-C1
9	21	6084.76	377.38	737-522	CFM56-3-B1 or -3-C1
20	5	6410.40	470.09	737-322	CFM56-3-B2 or -3C-1
21	1	7821.00	0.00	737-291	JT8D-17

3.4 Automated Profile Generator

Within the INM procedure step calculations, the user must string together a sequence of climb, level and/or acceleration segments. With numerous radar trajectories an automated procedure generator program was created which would iteratively determine an optimized set of profile steps, starting with the takeoff roll and initial climb, flap cleanup and continuing on to the second segment climb.

An analysis of the takeoff roll segment based on a limited amount of video data was presented in Section 3.4. The lack of a wide enough field of view to fully cover all departure liftoff points precluded the calculation of takeoff field length or liftoff speed. Given the lack of any measured information by which the aircraft takeoff field length could be determined with accuracy, and given the location of the noise monitoring equipment several miles from the rotation point, no attempts were made to automate modeling of the takeoff ground roll segment by modifying the aircraft coefficients. The standard aircraft performance coefficients were used for the initial ground roll/takeoff segment.

The procedure generator is a driver that builds INM Procedure Step DBF files and runs the batch version of INM. Once the INM flight profile portions of the calculations are run, the INM-calculated flight path is exported and compared with the recorded input radar flight trajectory. The parameters of the Procedure Steps are then modified appropriately and the batch versions of INM run again until the difference between the INM and radar trajectories are minimized.

In the prior DIA study[1], the CATS program was developed which determined, based on aircraft equipment and weight and atmospheric conditions, the takeoff and climb engine throttle settings (NI or EPR), and then using the radar trajectory determined the engine thrust (Fn/δ) at each point along the flight path. This code was compared with the United Airlines Unimatic predictions and agreed well[1]. For the current study the ground rules were that only INM performance calculations could be used to predict the flight trajectory and engine thrust settings. For comparative purposes throughout this document aircraft power graphs are presented which include thrust calculations made in the 1997 study using the CATS code.

The physics modeled by the climb and acceleration segments are documented in the INM technical manual[3] with the basic elements reiterated in Tables 3-6 and 3-7. A Climb segment is flown at constant calibrated airspeed. During an acceleration segment, the aircraft accelerates and climbs with 45 percent of the excess thrust (above that required to maintain steady level flight)

going into the climb and 55 percent going into the longitudinal acceleration. Within INM, an iterative process of updating the final altitude is used with a convergence criterion of 1 foot.

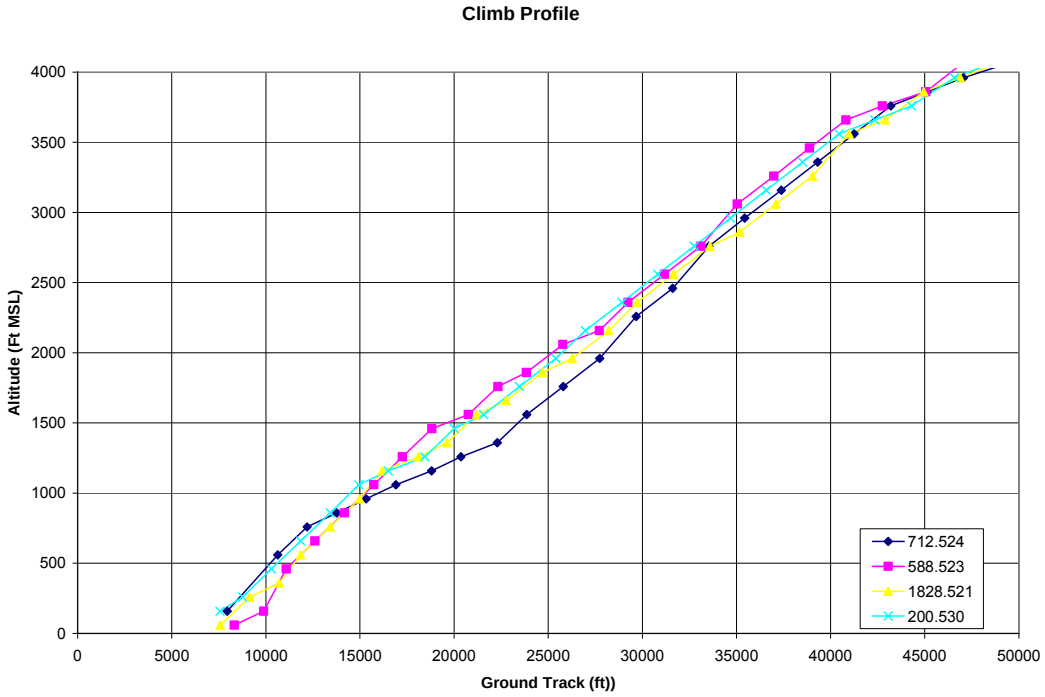
Table 3-6. INM Climb Segment

Information Obtained from the end of the prior segment:
Initial Altitude
Initial Calibrated and True Airspeeds
Initial Thrust
Final Calibrated Airspeed
Information Supplied by User Inputs
Final Altitude
Information Calculated by the Climb Segment Physics
Average Climb Angle (AIR-1845[10] equation A8)
Final Altitude
Horizontal Distance (AIR-1845[10] equation A9)
Final True Airspeed

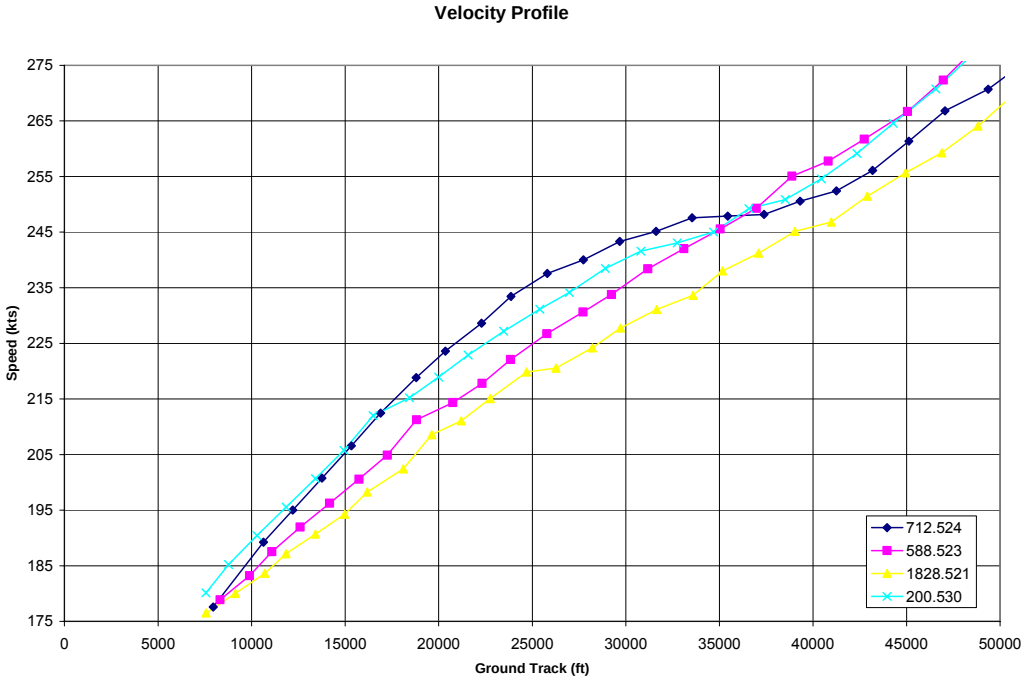
Table 3-7. INM Acceleration Segment

Information Obtained from the end of the prior segment:
Initial Altitude
Initial Calibrated and True Airspeeds
Initial Thrust
Information Supplied by User Inputs
Average Climb Rate
Final Calibrated Airspeed
Information Calculated by the Climb Segment Physics
Final Altitude
Horizontal Distance (AIR-1845[10] equation A10, A11, A18)
Final True Airspeed
Final Thrust

The procedure step calculation method is itself a tool which runs INM in batch mode iteratively, trying various profile procedure steps and comparing the INM calculated flight altitude and speed to the measured radar flight data. Procedure input parameters are tried in succession, methodically marching out along the flight profile, optimizing one procedure step at a time, until the errors between the INM flight path and radar flight paths are minimized. For this measurement study, the noise monitoring locations were are all located on the ground beneath the flight trajectory when the aircraft is in the second segment climb flight region, after the initial takeoff and climb segment and after the aircraft flap cleanup has occurred. No attempt was made to iteratively model the takeoff ground roll because the radar data were only available after the aircraft cleared approximately 300 ft. AGL. The recorded radar profiles, figure 3-14 (a) and (b), did not clearly show a level accelerating segment where flap cleanup occurred. Because the majority of the operations used the 1-improved flap setting there was a fairly rapid transition to 'clean' flight configuration and no obvious cleanup segment in the altitude profiles. Within the automated procedure step generator, a fixed flap cleanup altitude of 1500 ft. AGL was used for all flight profiles modeled. This altitude was based on the documented airline flight procedures at United Airlines.



(a)



(b)

Figure 3-14. Typical Radar Flight Profile Initial Segment (a) Altitude and (b) Speed (Concluded)

The fundamental question that this study needed to first answer was whether it was possible to discriminate different thrust ratings of an aircraft from measured radar altitude and velocity profiles. In order to illustrate that this is indeed possible, the profile optimizer was exercised and procedure steps determined using a simple minimization of the percent speed and altitude normalized to radar values. For this initial analysis five different thrust ratings were modeled for the Boeing 737 aircraft. Within INM the thrust ratings are modeled via the Jet Thrust Coefficients. These parameters (E, F, G_a, G_b, H) are coefficients to the physical equation within INM which is used to determine, for a given engine operating state, and set of physical parameters (Speed, Altitude, Temperature) the net corrected installed thrust of an aircraft based on a modified version of the methodology defined in AIR-1845[10] Equation A1. The INM modification to the original AIR-1845 equation included the incorporation of a higher order G_b polynomial coefficient for the pressure altitude as shown in Equation 3-1.

$$\frac{F_n}{\delta} = E + Fv + G_a h + G_b h^2 + HT_c$$

Equation 3-1

Within INM different thrust ratings can be modeled by varying the five jet thrust coefficients. The set of thrust coefficients were each assigned a different thrust rating level. Within the INM procedure step model, each trajectory point has associated with it a particular Fn/δ value for the thrust. This value of Fn/δ varies as the vehicle speed and altitude changes. These revised thrust rating INM coefficients were derived from Boeing data by the FAA and provided to Wyle for this study. The various reduced thrust rating departure profiles were calculated by Boeing, utilizing a detailed profile prediction aerodynamic tool, Boeing Climbout Program (BCOP)[11] containing high fidelity aerodynamic modeling and complete engine cycle decks from the engine manufacturer. BCOP has a Windows-based graphical user interface designed to produce aircraft performance and flight path information for operations in the terminal area. The application will analyze the performance of Standard Instrument Departure (SID) and Standard Arrivals (STAR) and provide both vertical and horizontal flight path data representing the given SID and STAR. Analysis of engine-out, terrain avoidance, approach, go-around, and escape procedures also can be accomplished with the application. The application takes user input gross weight, ambient conditions, airplane configuration, vertical profile definition, and horizontal profile definition and produces flight path data as a solution. This application does not solve for takeoff or landing gross weight, and it does not provide obstacle clearance analysis.

BCOP was parametrically exercised over a range of aircraft weights, temperatures, thrust ratings including several levels of reduced thrust and field elevations. The FAA subsequently performed a regression analysis of these detailed profiles in order to determine the best match performance coefficients[12]. A set of revised jet thrust coefficients, simulating reduced thrust departure ratings for five different takeoff and climb conditions for Boeing 737s, were provided to Wyle by the FAA and Boeing. Table 3-8 contains a list of the reduced thrust rating INM coefficients used in

this noise study. The thrust ratings include the following rated takeoff thrust levels for takeoff and the corresponding climb thrust at that same operating state (N1): 18,500 lbs., 20,000 lbs., 22,000 lbs., and 23,000 lbs. One "blended" thrust rating was created, namely one where the 22,000 lbs. rated takeoff and the 20,000 lbs. rated climb thrusts are used together in the same profile. Where available those regressions combined with particular airframes were used. In some instances where the matrix was lacking data, with the concurrence of Boeing, the engines were selected independently from the airframe. The jet thrust coefficients from other airframes were utilized as shown in Table 3-8.

Table 3-8. INM Boeing 737 Reduced Thrust Jet Coefficients

Thrust State	ACFT_ID	THR_TYPE	COEFF_E	COEFF_F	COEFF_GA	COEFF_GB	COEFF_H
18.5k	737300	C	17573.7	-16.19741	1.320710E-01	0.000000E+00	-2.316000E+01
	737300	T	18507.8	-25.74727	3.647020E-01	0.000000E+00	-6.778000E+00
	7373B2	C	17573.7	-16.19741	1.320710E-01	0.000000E+00	-2.316000E+01
	7373B2	T	18507.8	-25.74727	3.647020E-01	0.000000E+00	-6.778000E+00
	737500	C	17573.7	-16.19741	1.320710E-01	0.000000E+00	-2.316000E+01
	737500	T	18507.8	-25.74727	3.647020E-01	0.000000E+00	-6.778000E+00
20k	737300	C	17383.1	-15.60722	1.48043e-01	-1.00000e-06	-2.420e+01
	737300	T	19347.0	-25.86886	4.56499e-01	-1.12000e-05	-1.478e+01
	7373B2	C	17383.1	-15.60722	1.48043e-01	-1.00000e-06	-2.420e+01
	7373B2	T	19347.0	-25.86886	4.56499e-01	-1.12000e-05	-1.478e+01
	737500	C	17530.9	-16.35562	1.53997e-01	-1.30000e-06	-2.339e+01
	737500	T	19629.4	-26.75042	5.50433e-01	-2.17000e-05	-7.999e+00
22k / 20k	737300	C	17383.1	-15.60722	1.48043e-01	-1.00000e-06	-2.420e+01
	737300	T	21480.7	-25.88800	2.25791e-01	0.00000e+00	-8.441e+00
	7373B2	C	17383.1	-15.60722	1.48043e-01	-1.00000e-06	-2.420e+01
	7373B2	T	21480.7	-25.88800	2.25791e-01	0.00000e+00	-8.441e+00
	737500	C	17530.9	-16.35562	1.53997e-01	-1.30000e-06	-2.339e+01
	737500	T	21480.7	-25.88800	2.25791e-01	0.00000e+00	-8.441e+00
22k	737300	C	18623.5	-16.47974	1.69674e-01	0.00000e+00	-9.126e+00
	737300	T	21480.7	-25.88800	2.25791e-01	0.00000e+00	-8.441e+00
	7373B2	C	18623.5	-16.47974	1.69674e-01	0.00000e+00	-9.126e+00
	7373B2	T	21480.7	-25.88800	2.25791e-01	0.00000e+00	-8.441e+00
	737500	C	18623.5	-16.47974	1.69674e-01	0.00000e+00	-9.126e+00
	737500	T	21480.7	-25.88800	2.25791e-01	0.00000e+00	-8.441e+00
23k	737300	C	19662.2	-18.22095	2.07237e-01	0.00000e+00	0.000e+00
	737300	T	22116.3	-26.01745	2.59442e-01	0.00000e+00	0.000e+00
	7373B2	C	19662.2	-18.22095	2.07237e-01	0.00000e+00	0.000e+00
	7373B2	T	22116.3	-26.01745	2.59442e-01	0.00000e+00	0.000e+00
	737500	C	19662.2	-18.22095	2.07237e-01	0.00000e+00	0.000e+00
	737500	T	22116.3	-26.01745	2.59442e-01	0.00000e+00	0.000e+00

In order to illustrate the ability to select an appropriate engine thrust rating from radar, several flights were modeled in INM using a fixed set of procedure steps, varying only the jet thrust coefficients. These INM calculated profile points were then compared with measured radar data and shown in Figures 3-15 through 3-26 for four randomly selected flight operations for several variants of the B737. In the thrust profiles shown here, the "radar" profiles displayed are those calculated using the CATS code during the prior DIA study[1] and represent the engine states (N1) as listed in the legend. One can clearly see a demarcation in the altitude and velocity profile charts for the various thrust ratings. The thrust profiles, while not utilized in any way for determining procedure steps or selecting an appropriate thrust setting, are included here for comparative purposes.

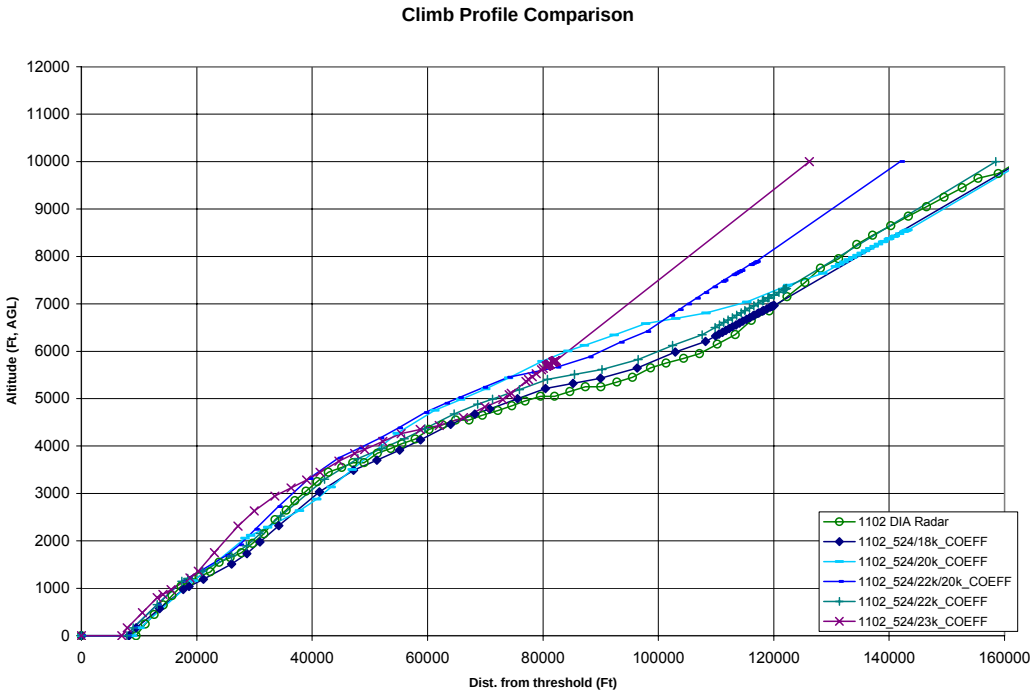


Figure 3-15. UAL1102.524 Altitude Profile, INM vs. Radar for Several Thrust Ratings

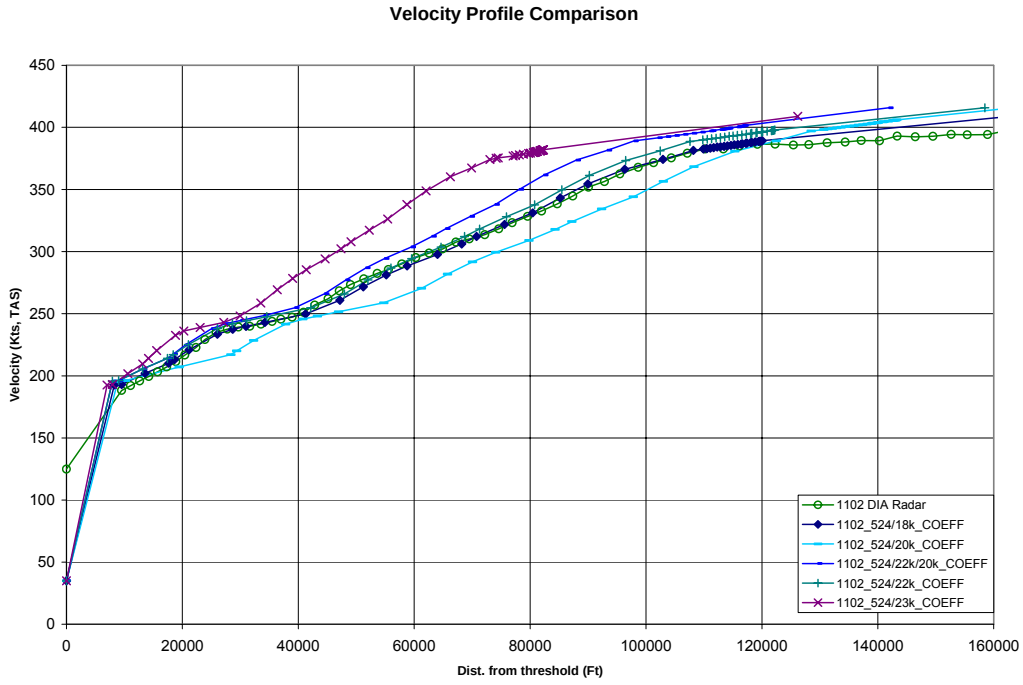


Figure 3-16. UAL1102.524 Velocity Profile, INM vs. Radar for Several Thrust Ratings

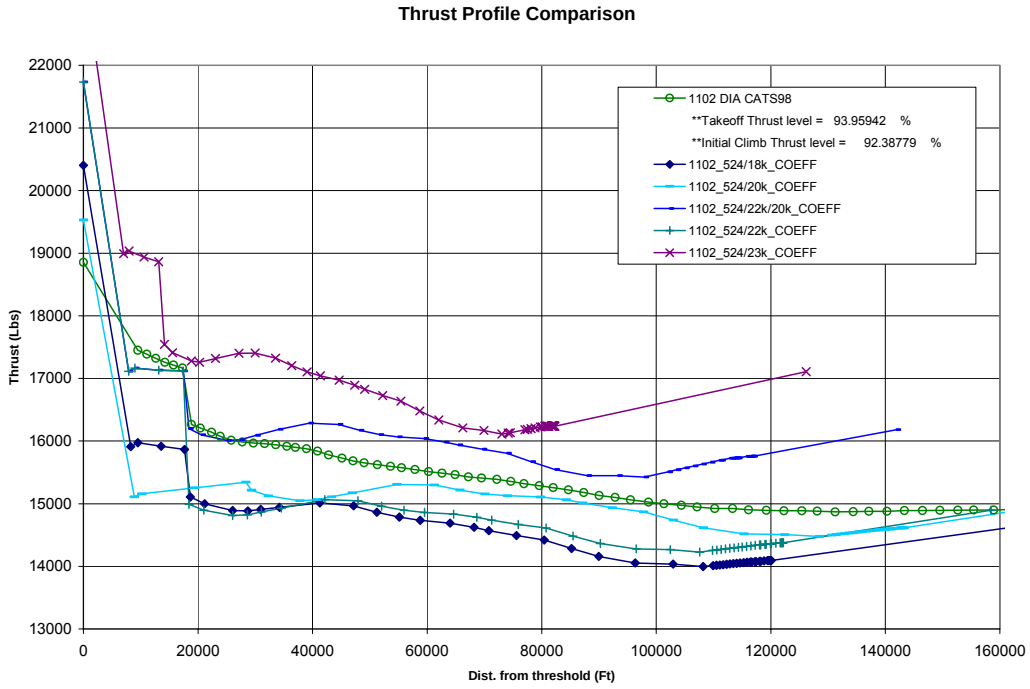


Figure 3-17. UAL1102.524 Thrust Profile, INM vs. Radar for Several Thrust Ratings

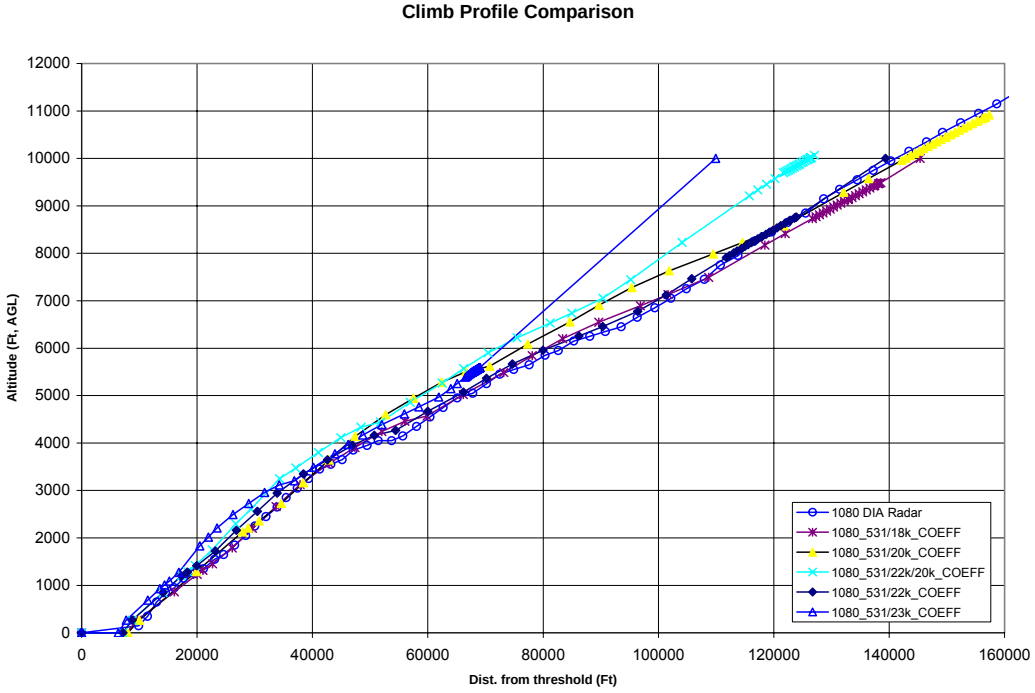


Figure 3-18. UAL1080.531 Altitude Profile, INM vs. Radar for Several Thrust Ratings

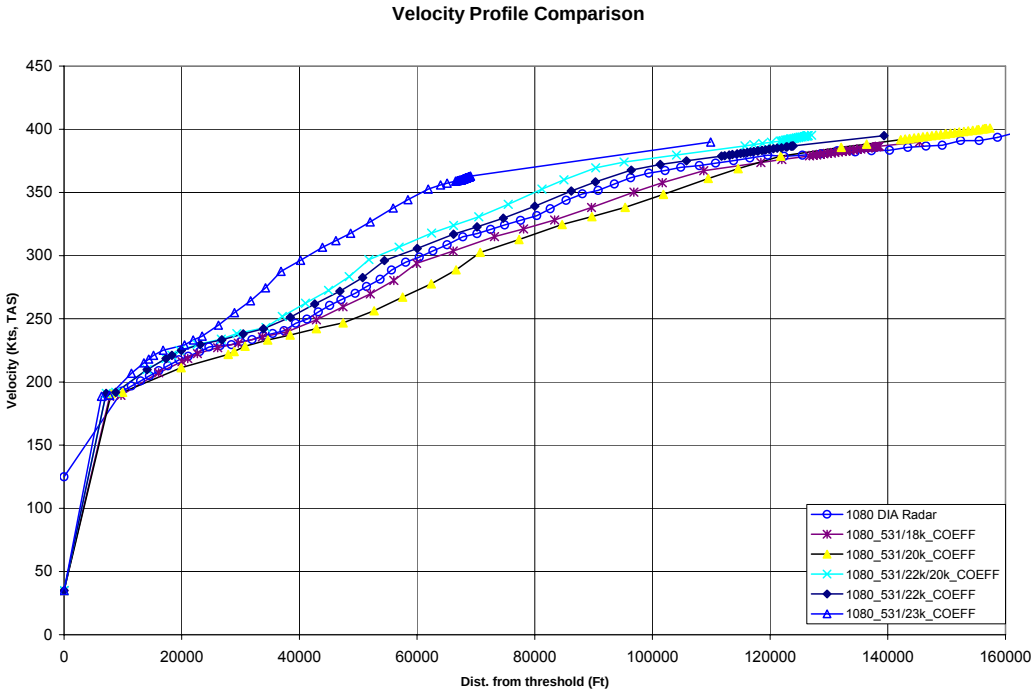


Figure 3-19. UAL1080.531 Velocity Profile, INM vs. Radar for Several Thrust Ratings

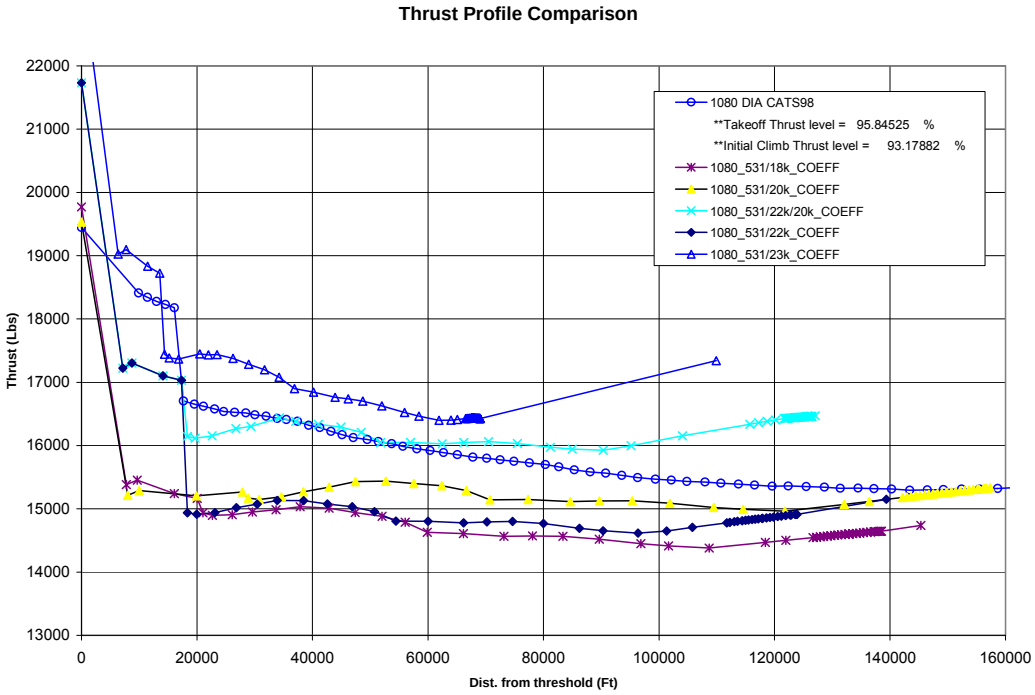


Figure 3-20. UAL1080.531 Thrust Profile, INM vs. Radar for Several Thrust Ratings

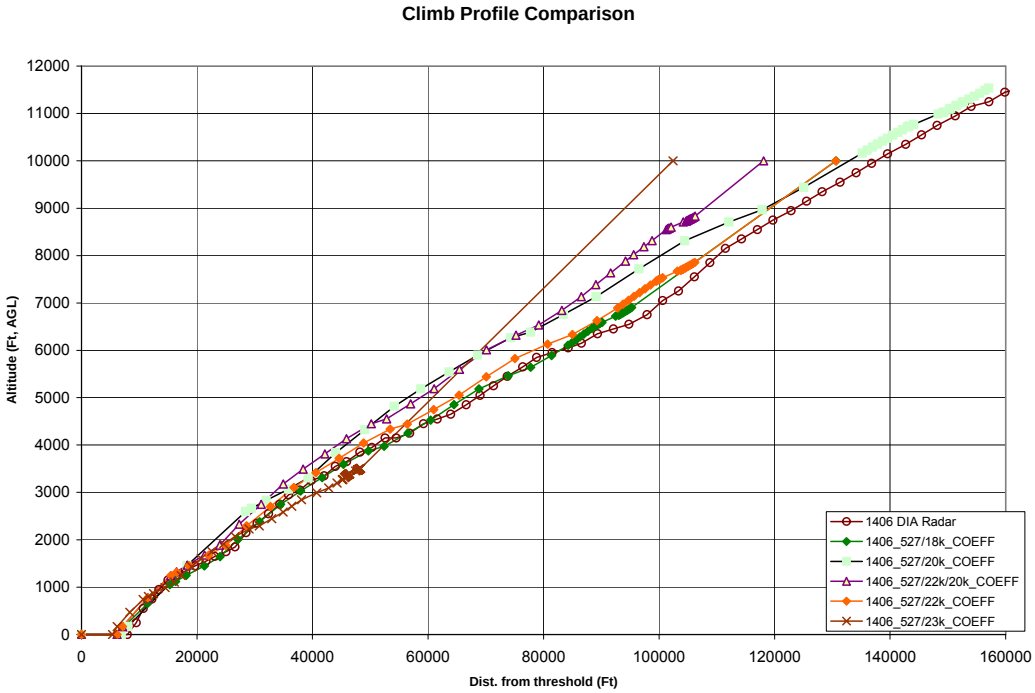


Figure 3-21. UAL1406.527 Altitude Profile, INM vs. Radar for Several Thrust Ratings

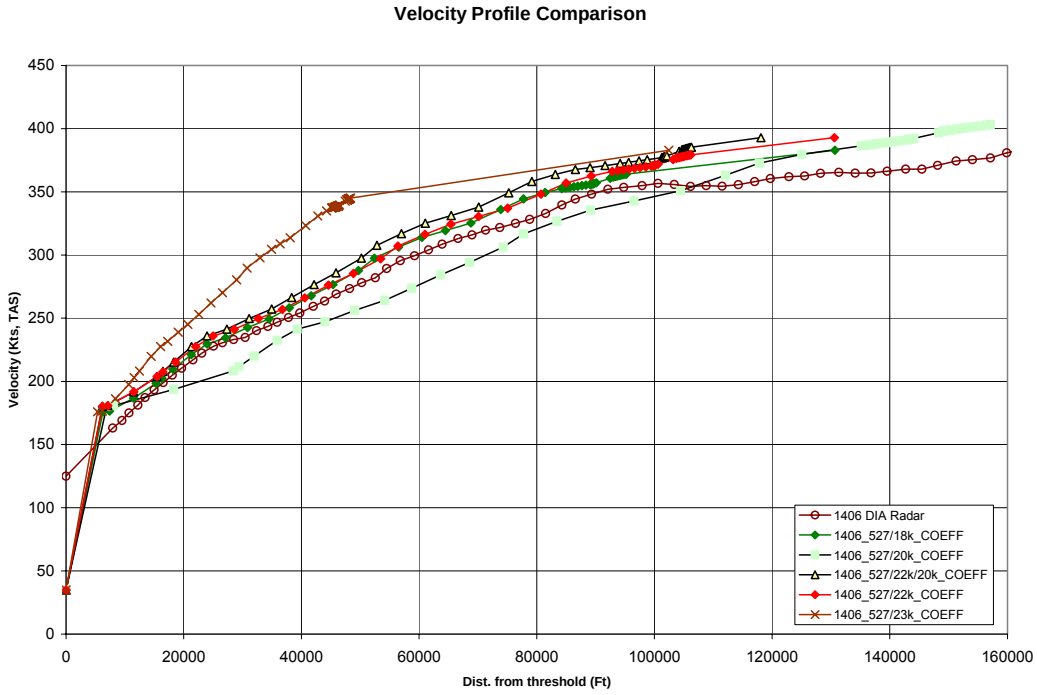


Figure 3-22. UAL1406.527 Velocity Profile, INM vs. Radar for Several Thrust Ratings

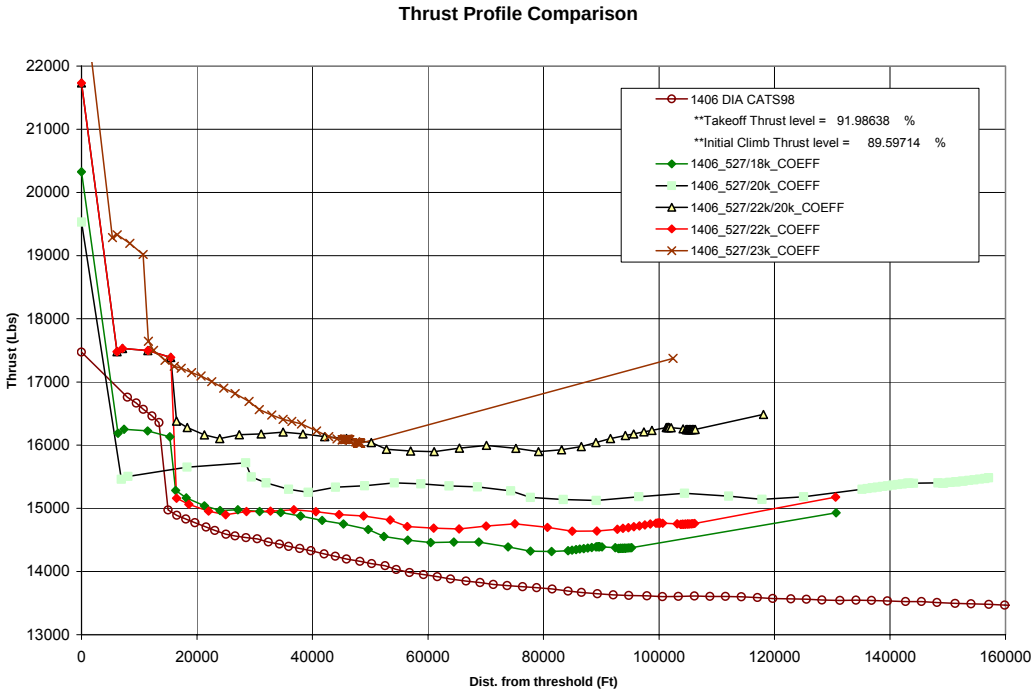


Figure 3-23. UAL1406.527 Thrust Profile, INM vs. Radar for Several Thrust Ratings

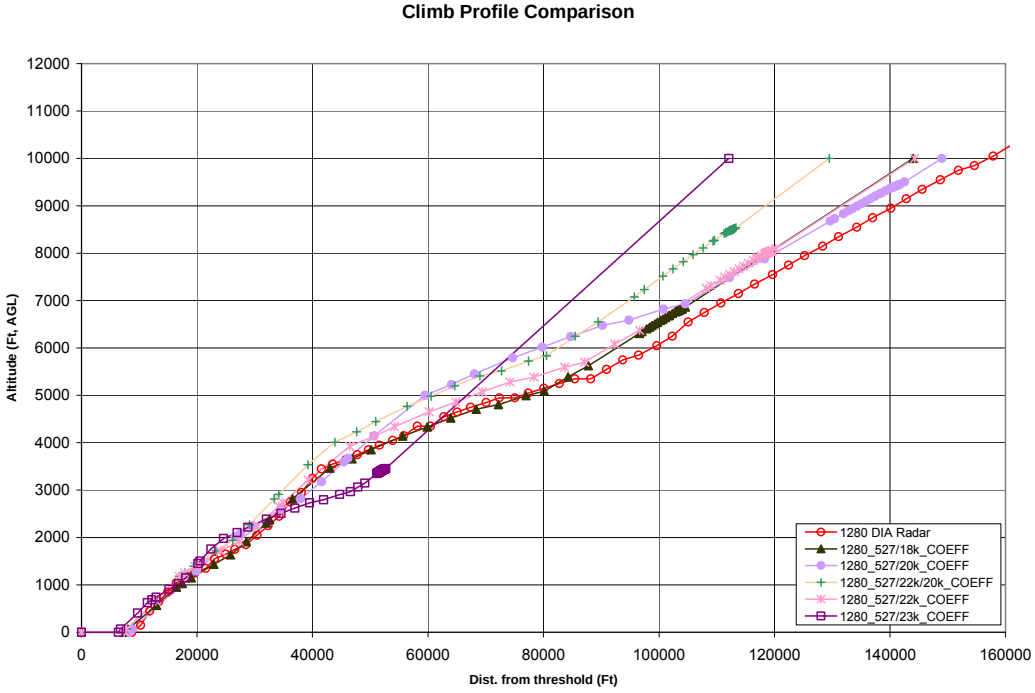


Figure 3-24. UAL1280.527 Altitude Profile, INM vs. Radar for Several Thrust Ratings

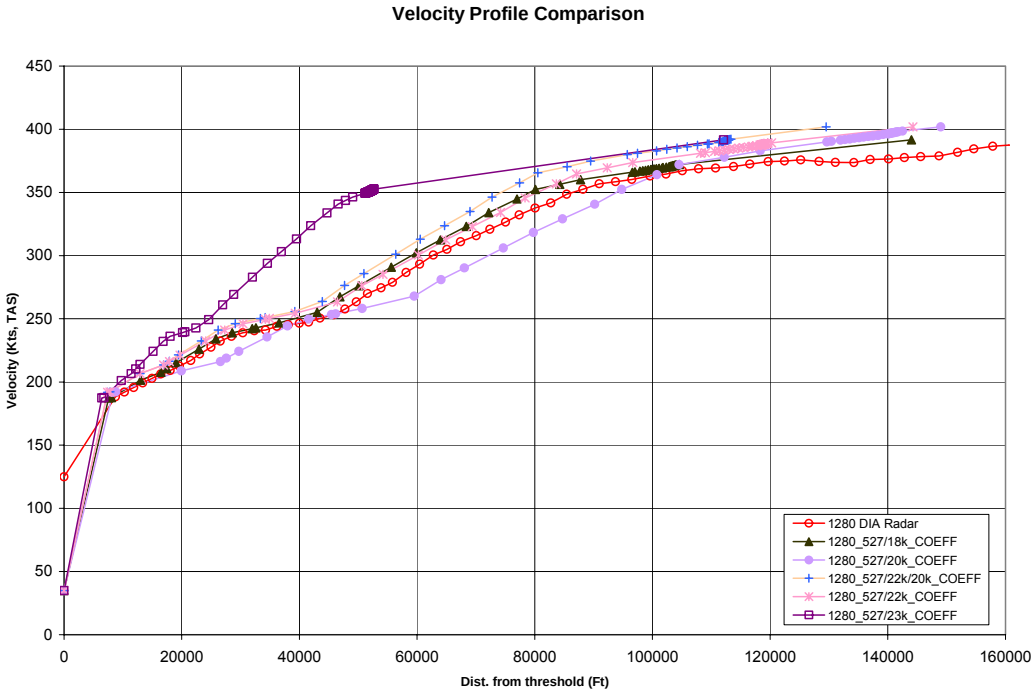


Figure 3-25. UAL1280.527 Velocity Profile, INM vs. Radar for Several Thrust Ratings

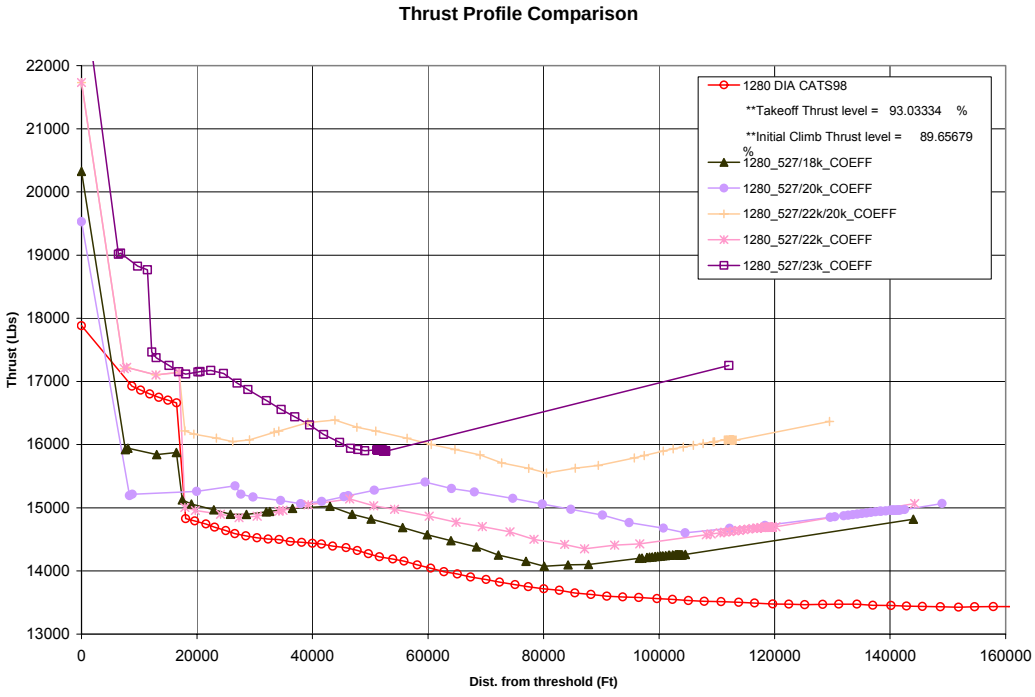


Figure 3-26. UAL1280.527 Thrust Profile, INM vs. Radar for Several Thrust Ratings

3.5 Comparison of Profile Generation Optimization Techniques

The profile generator was created with several adjustable parameters. These are the minimization method (M), the refinement (R) and the threshold (T). The effect of these parameters will be discussed in this section.

There are five different profile optimization methods (M), which are explored with the profile procedure step calculation code. These five concepts are termed methods M1–M5. In essence these five different methods use different criteria for minimizing the difference between the INM profile and the radar profile. Since the INM procedure steps are based on a physical thrust rating, and since the aircraft coefficients are fixed (lift and drag state), other than varying the sequence and types of profile procedure steps, the user has little control over the INM profile. The five methods, and the quantity minimized by each, are:

M1) Difference minimization based on percent speed and altitude normalized to the radar values.

$$\left(abs\left(\frac{INM_V}{Radar_V}-1\right)\right)+\left(abs\left(\frac{INM_Z}{Radar_Z}-1\right)\right)$$

M2) Potential (mgh) and Kinetic Energy (1/2 m v2) Minimization Error function.

$$\left(32.2\left(abs(INM_Z-Radar_Z)\right)+\frac{1}{2}abs\left(INM_V^2-Radar_V^2\right)\right)^2$$

M3) Altitude Match and change INM input climb rate iteratively.

$$\left(abs\left(\frac{INM_Z}{Radar_Z}-1\right)\right)$$

M4) Velocity Match and change INM input climb rate iteratively.

$$\left(abs\left(\frac{INM_V}{Radar_V}-1\right)\right)$$

M5) Altitude Match and change INM input velocity iteratively.

$$\left(abs\left(\frac{INM_Z}{Radar_Z}-1\right)\right)$$

M6) Slant Range match and change INM input velocity iteratively.

$$\left(INM_Z-Radar_Z\right)^2+\left(INM_S-Radar_S\right)^2$$

The refinement parameter controls the fidelity of the INM flight segments. A refinement parameter of 1 causes the optimizer to attempt to match flight segments in between each individual radar point. However within INM there is a limit of 99 flight steps in procedural profiles. Given the nominal 4.5 second spacing between radar points, the optimized flight profiles can exceed this 99 step limit.

The profile modeling threshold parameter in the optimizer may be varied in order to control whether a given radar flight segment is to be modeled within INM using an acceleration or climb step. Four different climb/accelerate step thresholds were exercised. These five threshold options are itemized here:

- TN5 – Threshold = -5. This forces each step to be an accelerate step regardless of the input radar flight profile information;
- T01 – Climb if dV / dZ > .01, otherwise an accelerate step is used;
- T02 – Climb if dV / dZ > .02, otherwise an accelerate step is used; and
- T04 – Climb if dV / dZ > .04, otherwise an accelerate step is used.

For this examination of the profile optimization techniques the 33 B737 flight trajectories on 21 May were analyzed. First the effects of the grid refinement (R1, R2, R3, R4, R5) was examined. An illustration of R1 through R5 is given in Figures 3-27 to 3-31. For these examples a flight step type threshold of -5 (N5) was used. This threshold setting forces all procedure steps to be modeled as acceleration segments. For the comparative figures shown below (Figure 3-32 to 3-37), flight UAL1035 on 21 May was highlighted. In these graphics, the abscissa for the Altitude (Feet, above ground level) is on the left, the Aircraft speed (true airspeed in knots) and the engine thrust (Corrected net thrust) is on the right. The input data from the radar installation is illustrated by the symbol X and the INM calculated flight trajectory is illustrated by the symbol □. Note that the Thrust marked by the X symbols is that which was calculated by the CATS code during the prior Denver Noise Analysis study[1] since aircraft thrust levels are not available in from the ARTS radar system. It is included on the plots for comparison with to the prior INM study thrust levels.

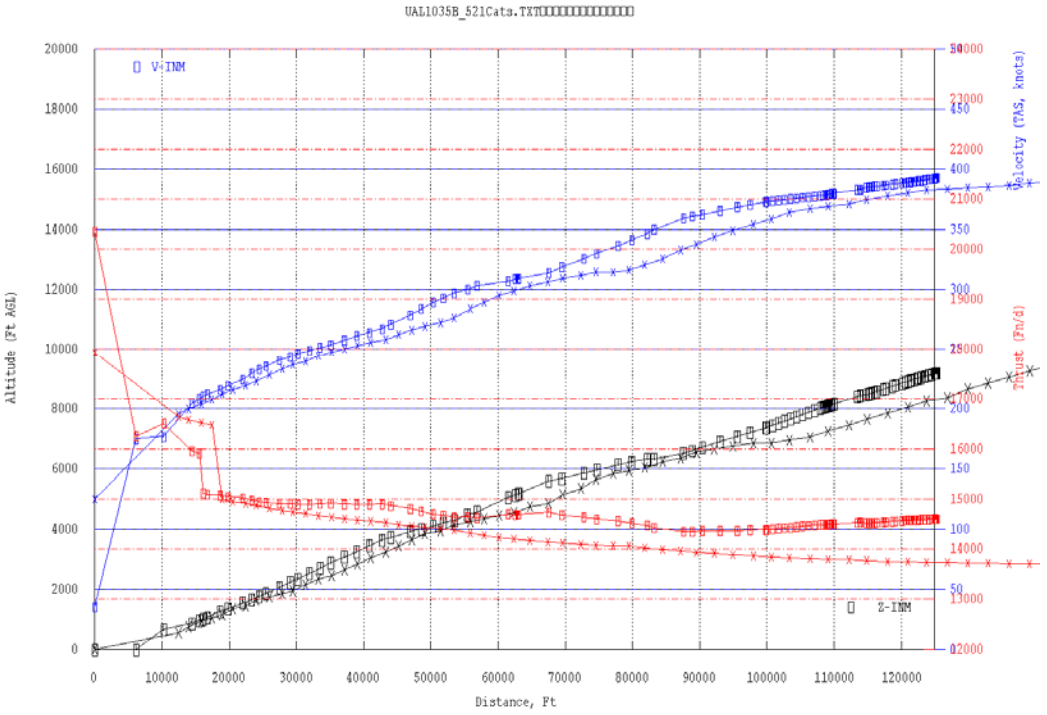


Figure 3-27. R1 Step Refinement (Every Radar Point) UAL1035.521 (M1R1TN5)

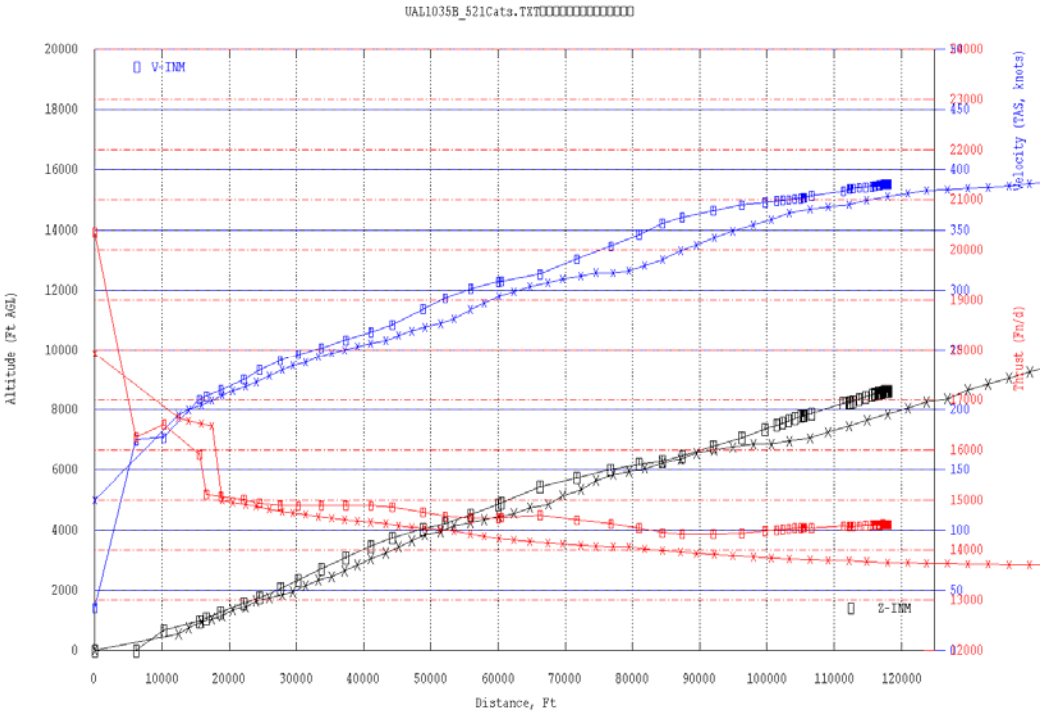


Figure 3-28. R2 Step Refinement (Every Other Radar Point) UAL1035.521 (M1R2TN5)

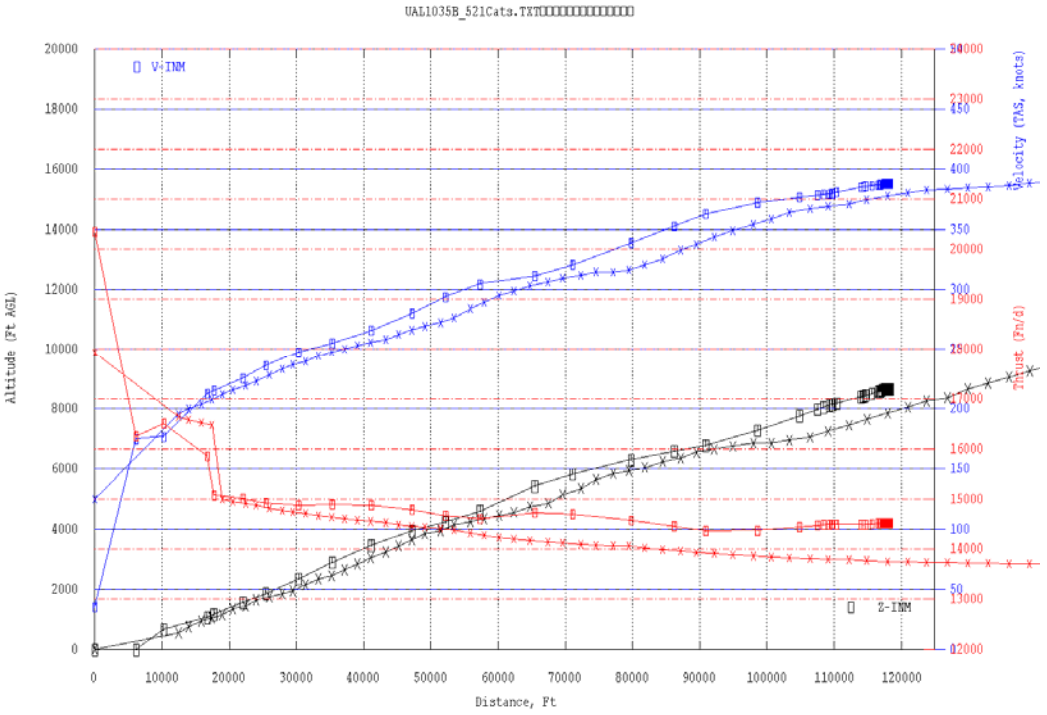


Figure 3-29. R3 Step Refinement (Every Third Radar Point) UAL1035.521 (M1R3TN5)

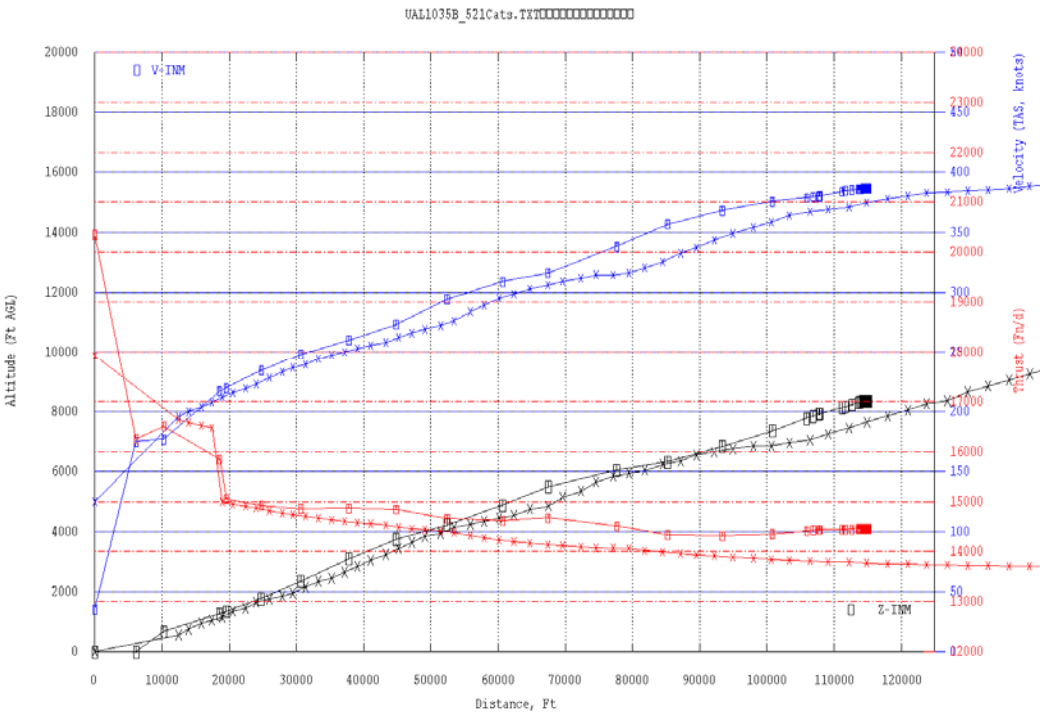


Figure 3-30. R4 Step Refinement (Every Fourth Radar Point) UAL1035.521 (M1R4TN5)

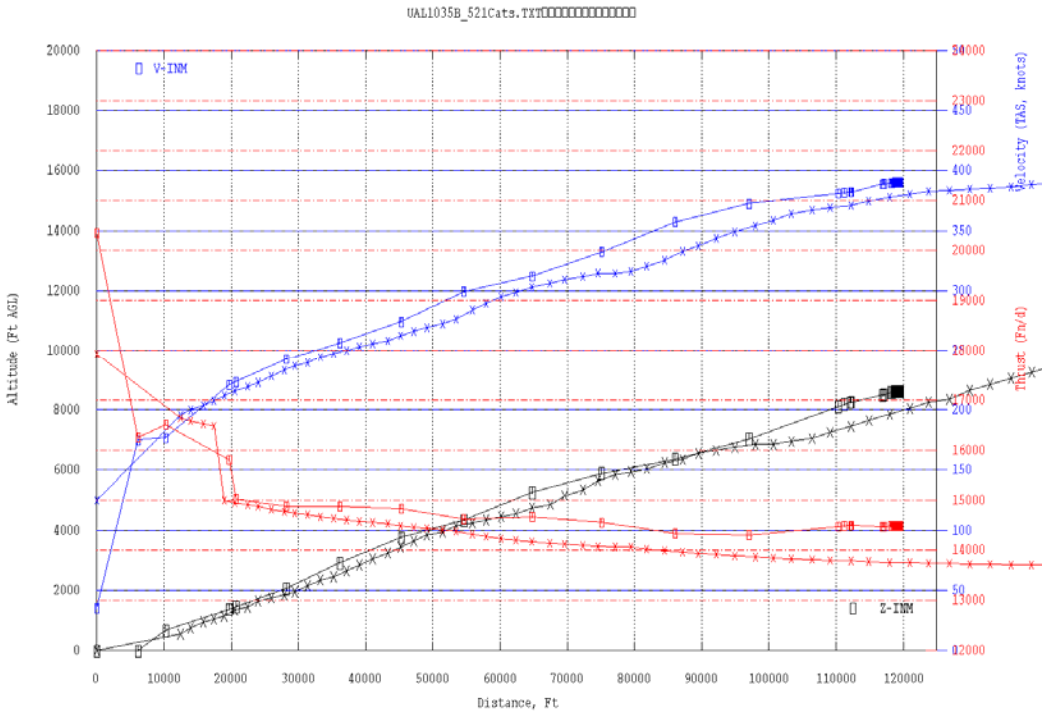


Figure 3-31. R5 Step Refinement (Every Fifth Radar Point) UAL1035.521 (M1R5TN5)

Minimization methods M1– M6 are illustrated below for one representative flight profile, Flight UAL1035 on 21 May. For these Figures 19-24 only R2 step refinement and Threshold N5 was chosen.

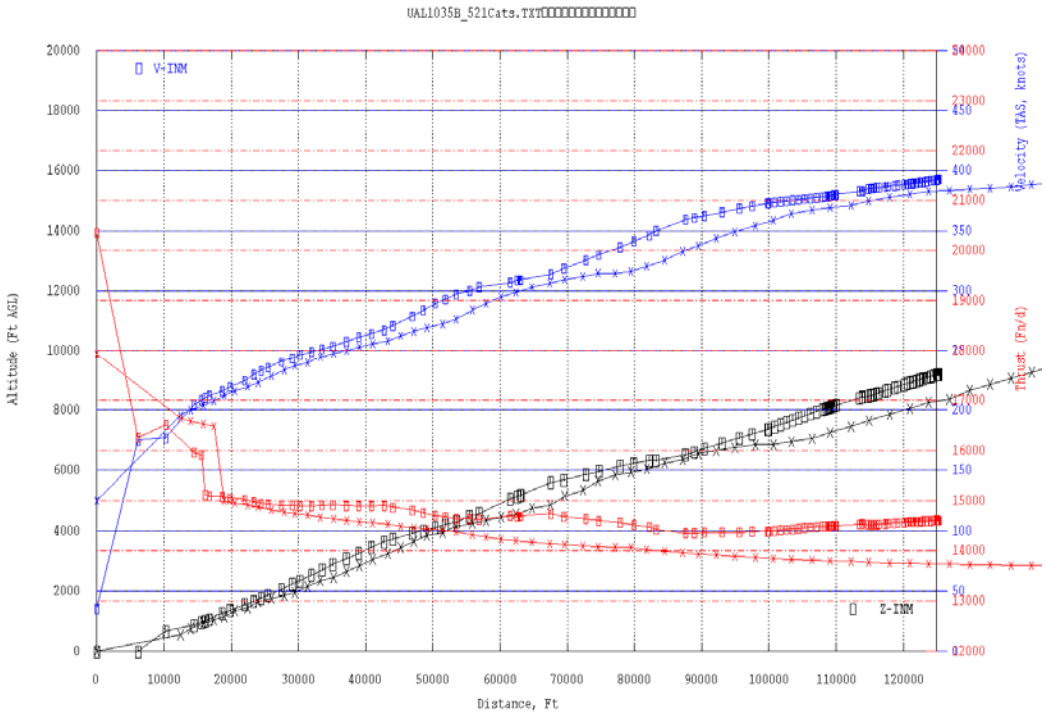


Figure 3-32. Minimization Method M1 (%-Speed and %-altitude) UAL1035.521 (M1R2TN5)

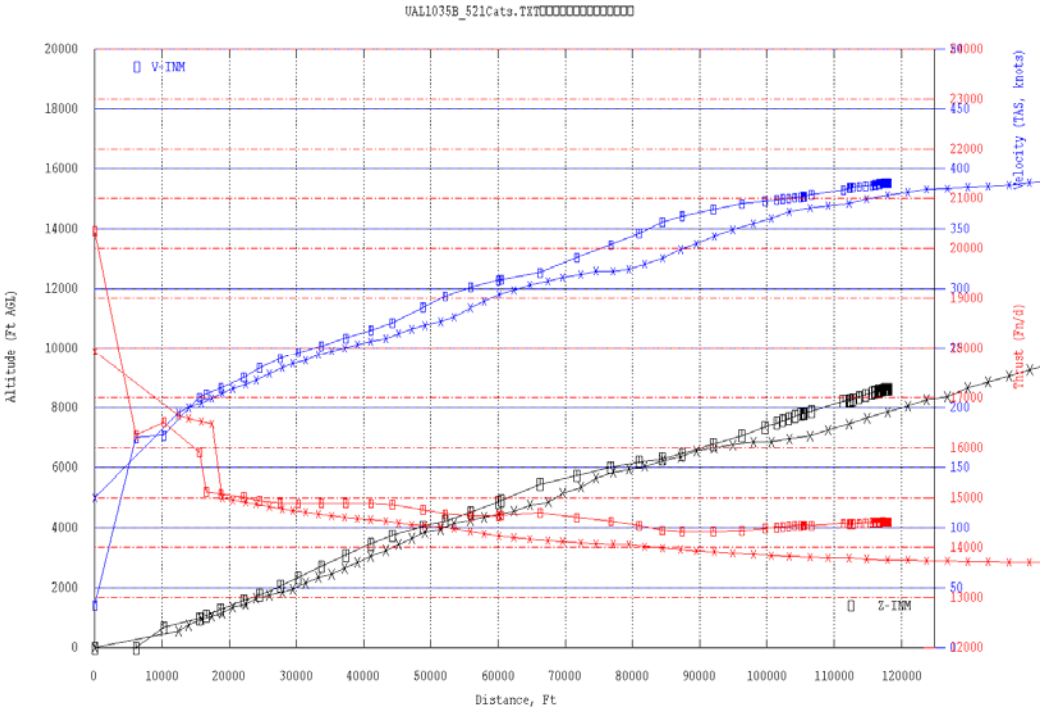


Figure 3-33. Minimization Method M2 (Potential & Kinetic Energy) UAL1035.521 (M2R2TN5)

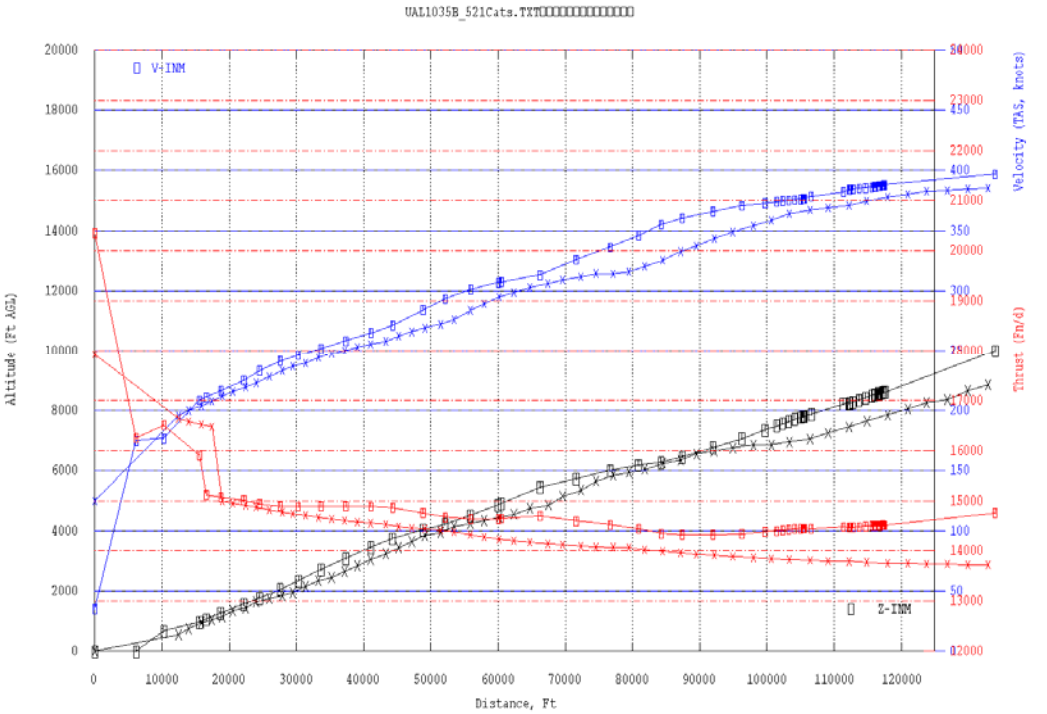


Figure 3-34. Minimization Method M3 (Velocity Match, Adjust Climb Rate) UAL1035.521 (M3R2TN5)

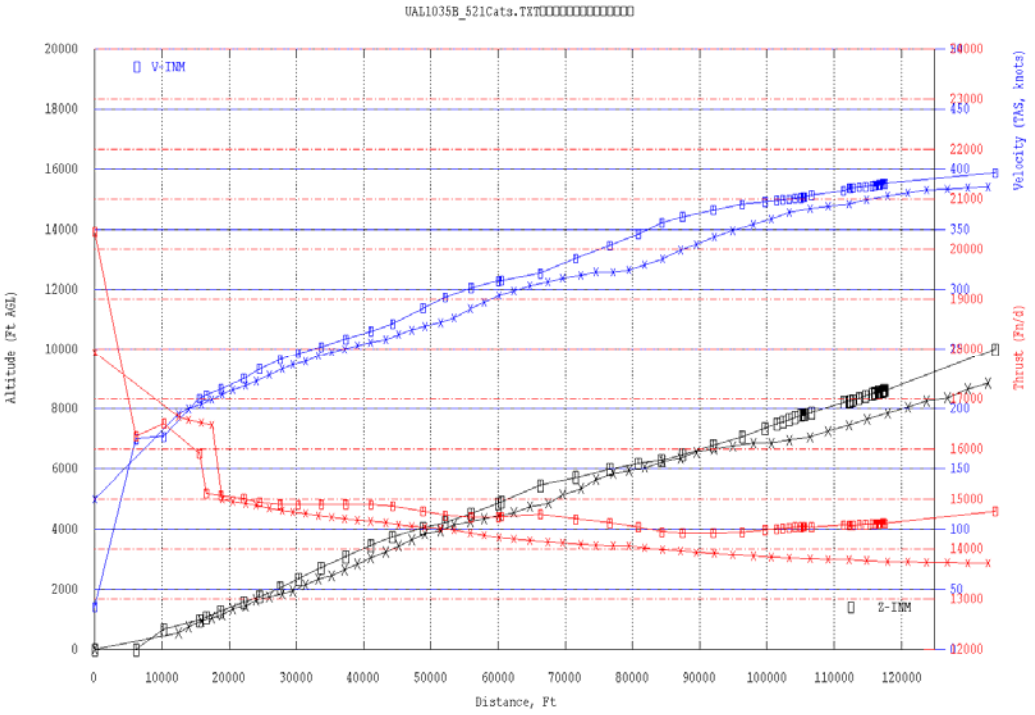


Figure 3-35. Minimization Method M4 (Altitude Match, Adjust Climb Rate) UAL1035.521 (M4R2TN5)

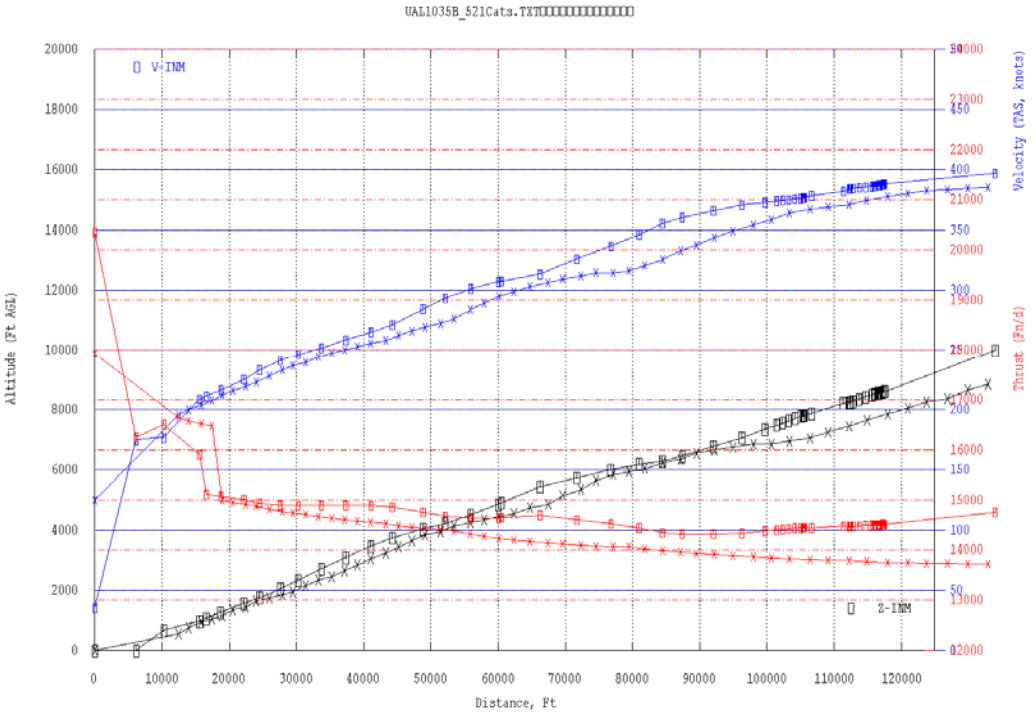


Figure 3-36. Minimization Method M5 (Velocity Match, Adjust Ending Speed) UAL1035.521 (M5R2TN5)

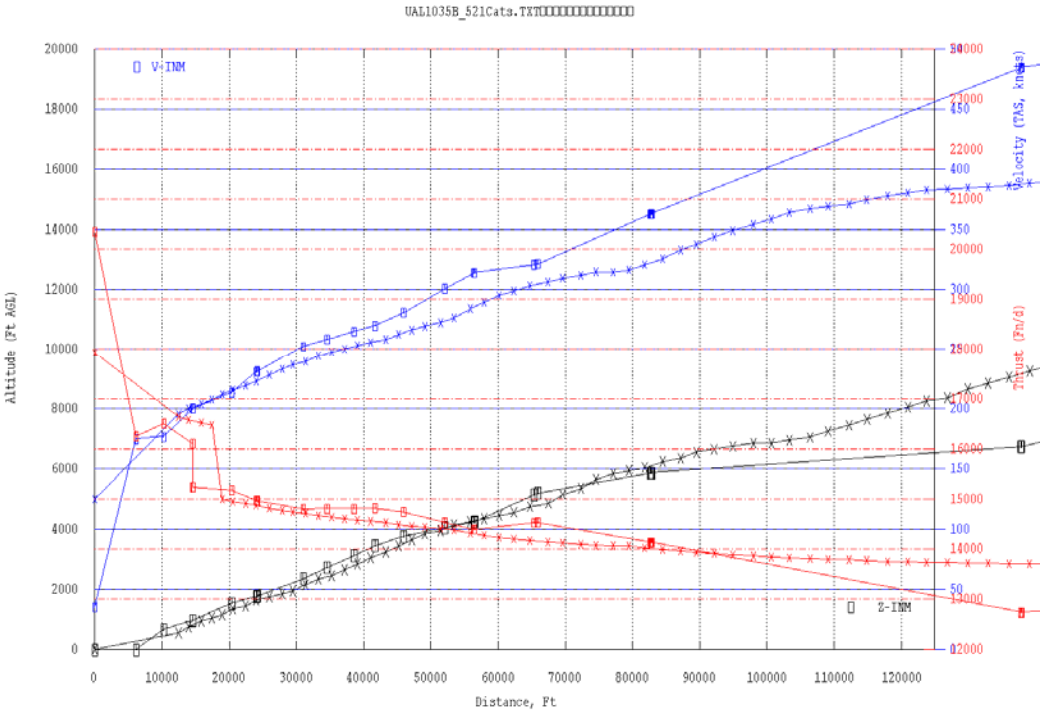


Figure 3-37. Minimization Method M6 (Altitude Match, Adjust Ending Speed) UAL1035.521 (M6R2TN5)

A look at the decision criteria whereby the automated profile generator selects an accelerate step versus a climb step follows in Figures 3-38 to 3-41. Again UAL1035 on 21 May is examined in detail. For these examples a refinement of R2 (every other radar point), minimization method M2 (Potential and Kinetic Energy Match) was utilized and the range of accelerate/climb step thresholds (TN5, T01, T02 and T04) were exercised.

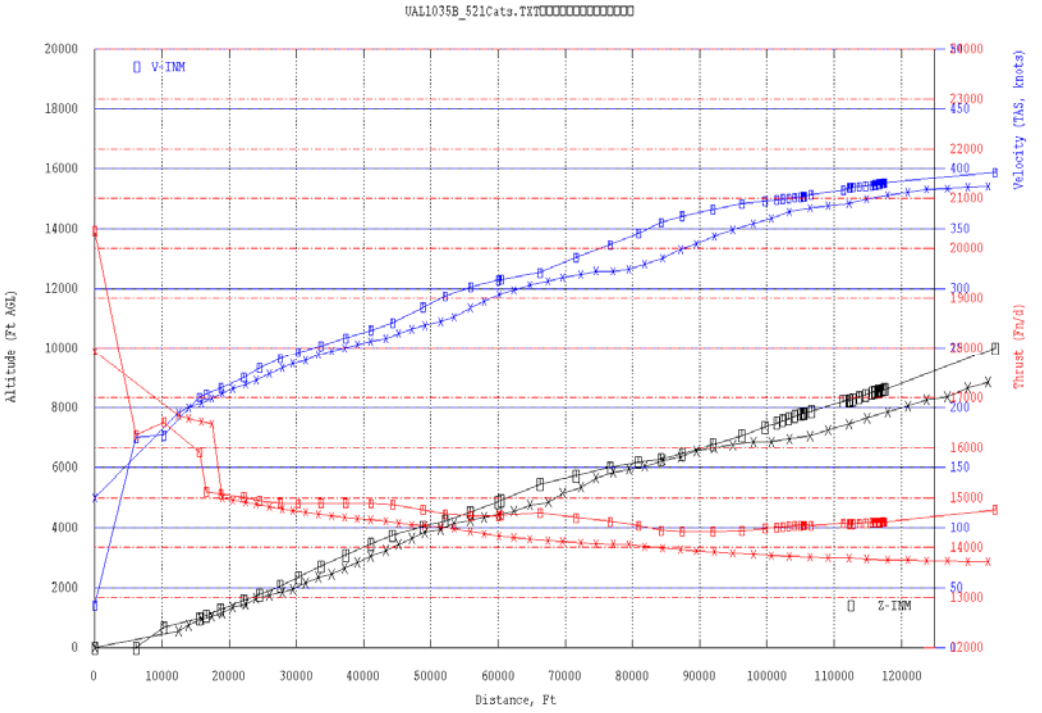


Figure 3-38. Threshold N05 (All Accelerate Steps), UAL1035.521 (M2R2TN5) Duplicate of Figure 3-33 for Clarity

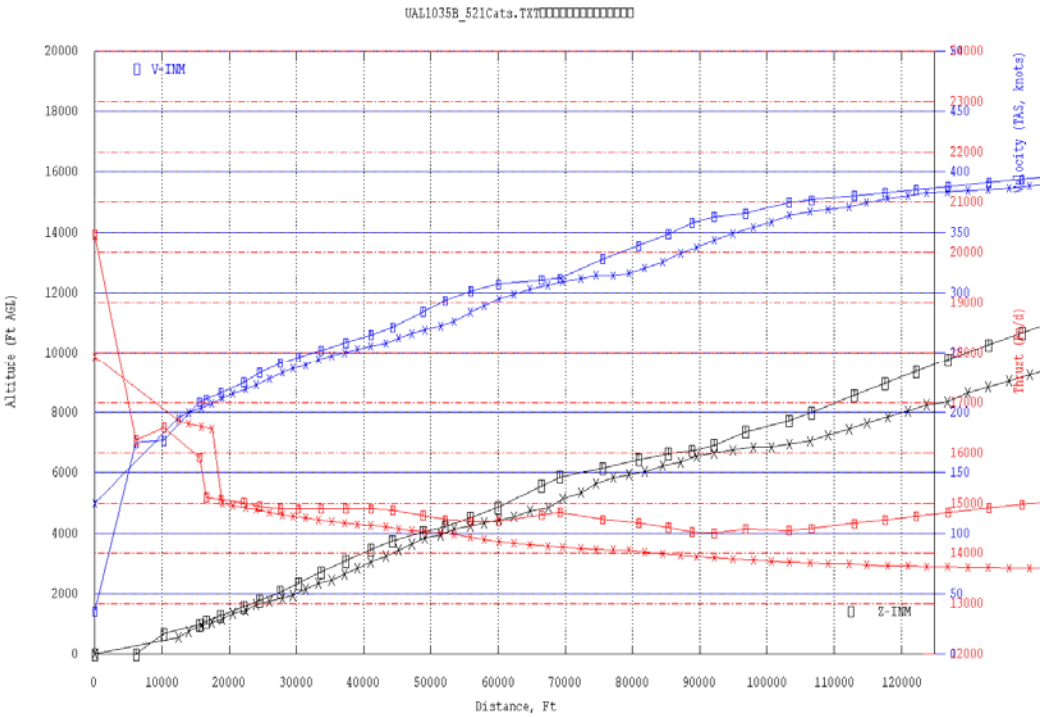


Figure 3-39. Threshold N01 (dV/dZ >.01 for Climb Step) UAL1035.521 (M2R2T01)

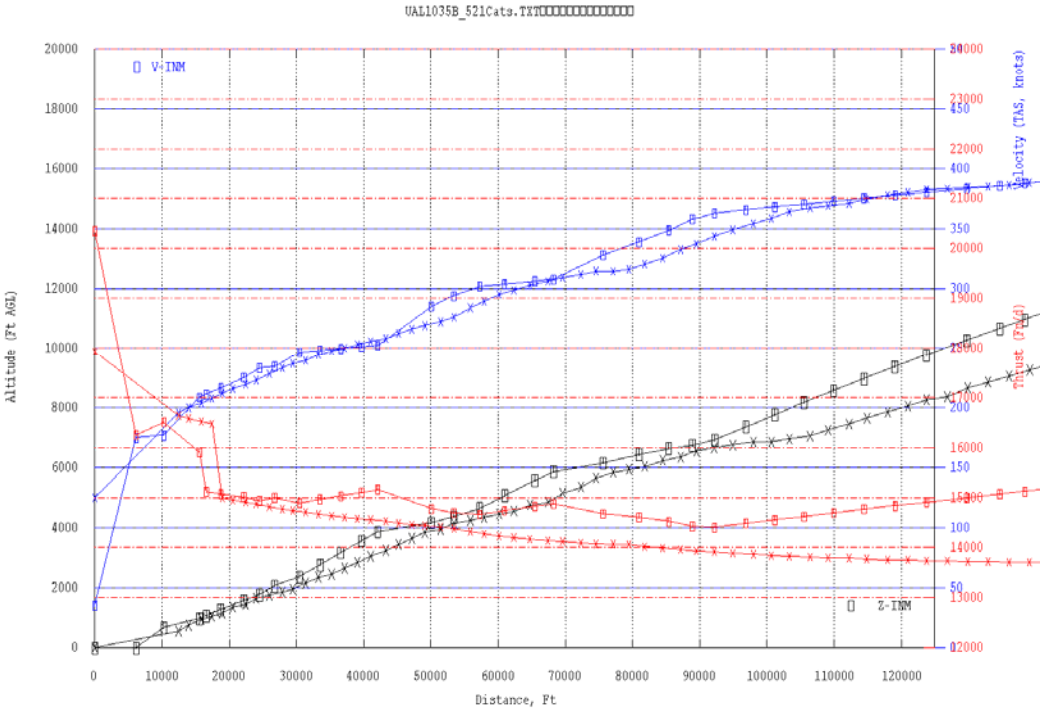


Figure 3-40. Threshold N02 (dV/dZ >.02 for Climb Step) UAL1035.521 (M2R2T02)

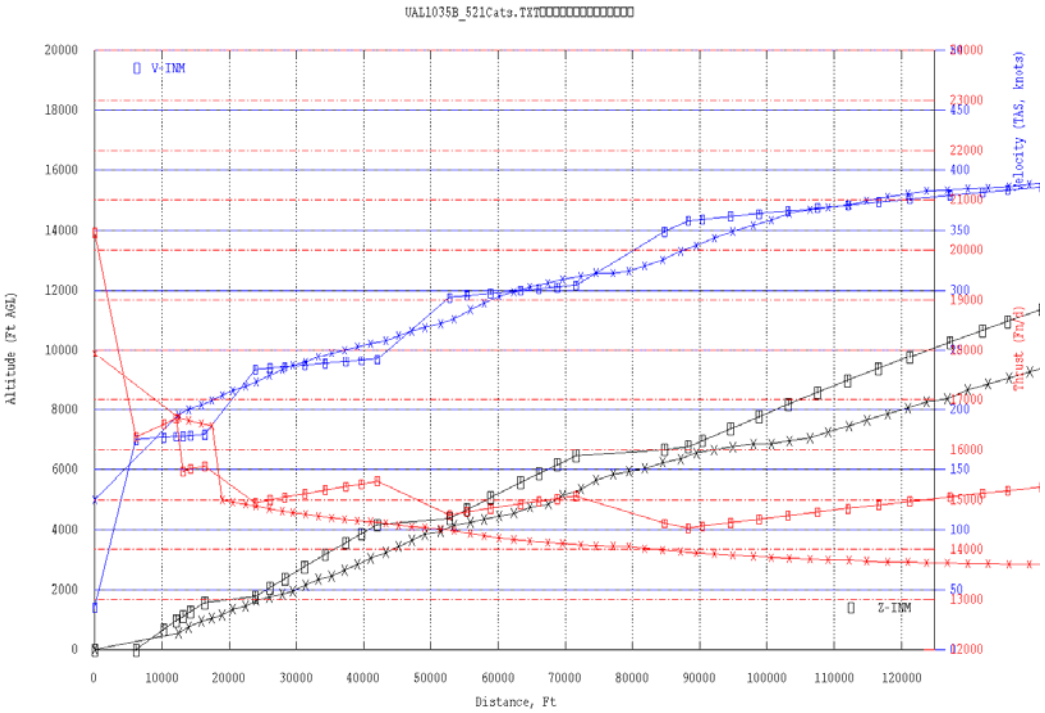


Figure 3-41. Threshold N04 (dV/dZ >.04 for Climb Step) UAL1035.521 (M2R2T04)

Based on this comparison of profile generation optimization techniques the energy match method was chosen as that seemed to give the best match to the radar data for a variety of input profiles. The percentage speed and altitude match was very similar to the energy match method, but it was decided to base the technique on a more physical interpretation of the profile modeling method, namely the determination of a thrust or energy state of the aircraft based on potential energy (altitude) and kinetic energy (velocity). Subsequent chapters which compare INM noise predictions with measured noise monitor data utilize the energy optimization method, with threshold TN5 (all segments modeled as accelerate segments) and refinement R2 (every other radar point used as input for the flight segment determination).

4.0 Acoustic Analysis

With a sequence of procedure steps determined, INM was run via the Graphical User Interface whereby acoustic levels at the noise monitoring locations were determined. Output was via the detailed grid option within INM and a separate grid was created for each noise monitor. Using this feature provided not only the noise level (SEL) but also the flight trajectory information (altitude, speed and net corrected installed thrust) at the point of closest approach to each noise monitor. Macro programs were developed which read in the detailed grid output from INM and correlated predicted SEL levels with the measured results at the noise monitoring locations. The profile optimizer was executed for each flight operation for each of the five thrust ratings. These procedure step profiles were in turn run through three versions of INM (6.0c, 6.1, and 6.2). For each noise event, the 'best' thrust rating was picked by evaluating on an energy basis (kinetic + potential energy) the aircraft speed and altitude at the point of closest approach (as reported by INM) with the measured radar speed and altitude at the point of closest approach. An energy minimization technique, consistent with the profile optimizer was used to select the optimal thrust rating. Section 4.1 summarizes the full analysis dataset. Section 4.2 describes in detail for some selected flights, the INM results, profiles for various thrust ratings and the energy minimization selection result. Section 4.3 presents the overall acoustic summaries for the three versions of INM.

4.1 Full Acoustic Analysis Dataset Description

The total dataset evaluated included only Boeing 737 operations. A summary of the operations by INM aircraft type, day and runway is given in Table 4-1, 4-2 and 4-3 respectively. These tables represent those events included in the final analysis, after those profiles which were not adequately modeled using INM procedure steps were removed from the results. A further discussion on this process is in Section 4.3. As discussed in Section 3, the study was setup with custom jet coefficients, so in this context the INM Aircraft type represents only the aircraft flap coefficients, or aerodynamic performance of the vehicle since each flight operation was optimized with five different thrust ratings. A total of 44 noise monitors recorded 742 aircraft noise events, which were modeled in this study. A distribution by site and INM aircraft type is given in Table 4-2.

Table 4-1. Summary of Flight Operation Noise Events – INM Aircraft Types

INM Aircraft Type	# Operations
737-300	176
737-3B2	369
737-500	197

Table 4-2. Summary of Flight Operation Noise Events by Day

21 May	22 May	23 May	24 May	25 May	26 May	27 May	28 May	29 May	30 May	31 May
80	92	120	80	56	14	62	84	33	66	55

Table 4-3. Summary of Flight Operation Noise Events by Runway

08	26	16	34	17L	35R	17R	35L
381	275	0	60	3	0	23	0

Table 4-4 . Summary of Noise Monitoring Events

Monitor	# Events	Monitor	# Events
S01	23	S23	2
S02	3	S24	1
S03	5	S25	1
S04	5	S26	0
S05	70	S27	0
S06	35	S28	0
S07	5	S29	0
S08	6	S30	0
S09	102	S31	0
S10	8	W01	18
S11	5	W02	73
S12	1	W03	66
S13	2	W04	57
S14	6	W05	21
S15	6	W06	5
S16	8	W07	2
S17	13	W08	4
S18	14	W09	0
S19	27	W10	1
S20	37	W11	29
S21	37	W12	13
S22	31	W13	0

In the time since the 1998 Noise study, INM has gone through several revisions to both the computational modules and to the noise source database. An updated version of noise – power – distance (NPD) curves was provided by Boeing and was analyzed in INM. An itemization of the source noise curves, referred to as "New NPD Curves" is given in Table 4-5.

Table 4-5. New NPD Curves Analyzed in INM

NOISE_ID	NOISE_TYPE	OP_MODE	THR_SET	L_200	L_400	L_630	L_1000	L_2000	L_4000	L_6300	L_10000	L_16000	L_25000
CFM563	E	A	2500.00	97.8	92.7	89.4	85.3	78.6	71.2	65.4	58.6	51.7	45.2
CFM563	E	A	3500.00	100.1	94.8	91.3	87.0	80.0	72.5	66.7	60.0	53.2	46.8
CFM563	E	A	4500.00	102.9	97.1	93.5	88.9	81.8	74.3	68.5	61.9	55.1	48.8
CFM563	E	A	5500.00	104.6	98.8	95.2	90.6	83.5	76.2	70.5	63.8	57.1	50.8
CFM563	E	D	6500.00	101.8	97.2	93.6	89.5	82.7	75.8	70.5	63.9	57.2	50.9
CFM563	E	D	9000.00	103.8	99.1	95.5	91.2	84.5	77.7	72.5	66.1	59.5	53.4
CFM563	E	D	11500.00	103.4	98.9	95.5	91.8	85.9	79.6	74.8	68.7	62.5	56.7
CFM563	E	D	14000.00	103.2	99.0	95.9	92.8	87.7	81.8	77.3	71.5	65.7	60.2
CFM563	E	D	16500.00	104.3	100.3	97.5	94.6	89.9	84.3	80.0	74.5	68.9	63.7
CFM563	E	D	19000.00	107.4	103.6	100.9	98.0	93.3	87.7	83.4	78.0	72.6	67.5
CFM563	M	A	2500.00	93.4	85.7	80.8	75.6	67.4	58.2	51.5	44.0	36.5	29.1
CFM563	M	A	3500.00	94.5	86.7	81.8	76.5	68.2	59.1	52.5	45.1	37.6	30.4
CFM563	M	A	4500.00	95.8	88.0	83.0	77.7	69.5	60.4	53.9	46.6	39.2	32.1
CFM563	M	A	5500.00	97.2	89.3	84.4	79.1	71.0	62.0	55.6	48.3	41.0	33.9
CFM563	M	D	6500.00	95.8	89.1	84.5	79.6	71.7	63.2	56.9	49.8	42.5	35.7
CFM563	M	D	9000.00	97.0	90.3	85.8	80.9	73.2	64.8	58.6	51.6	44.5	37.8
CFM563	M	D	11500.00	98.6	92.0	87.4	82.7	75.0	66.7	60.6	53.8	46.8	40.2
CFM563	M	D	14000.00	100.4	93.8	89.3	84.5	77.0	68.8	62.8	56.0	49.2	42.7
CFM563	M	D	16500.00	102.2	95.7	91.2	86.5	79.0	70.9	65.0	58.4	51.6	45.3
CFM563	M	D	19000.00	104.4	97.9	93.5	88.9	81.5	73.5	67.6	61.1	54.5	48.3
CFM563	P	A	2500.00	106.5	98.3	92.9	86.8	77.3	67.1	59.6	51.3	42.9	35.0
CFM563	P	A	3500.00	107.9	99.6	94.1	88.0	78.4	68.4	61.0	52.8	44.5	36.7
CFM563	P	A	4500.00	109.3	101.0	95.5	89.4	79.9	70.0	62.6	54.5	46.3	38.5
CFM563	P	A	5500.00	110.8	102.4	97.0	91.0	81.6	71.7	64.4	56.3	48.1	40.4
CFM563	P	D	6500.00	108.6	101.4	96.2	90.4	82.0	72.6	65.7	57.8	49.8	42.2
CFM563	P	D	9000.00	109.9	102.7	97.5	92.0	83.7	74.5	67.7	60.0	52.1	44.6
CFM563	P	D	11500.00	111.4	104.2	99.2	93.8	85.8	76.7	70.1	62.5	54.8	47.5
CFM563	P	D	14000.00	113.0	105.9	100.9	95.8	87.9	79.0	72.6	65.1	57.6	50.5
CFM563	P	D	16500.00	114.6	107.6	102.7	97.8	90.1	81.4	75.1	67.9	60.6	53.7
CFM563	P	D	19000.00	116.5	109.6	104.8	100.1	92.6	84.2	78.0	71.1	64.1	57.5
CFM563	S	A	2500.00	94.7	90.2	87.1	83.7	78.1	71.5	66.7	61.1	55.4	49.8
CFM563	S	A	3500.00	96.3	91.5	88.3	84.7	79.0	72.5	67.7	62.2	56.6	51.2
CFM563	S	A	4500.00	97.6	92.8	89.5	85.8	80.1	73.7	69.0	63.6	58.1	52.8
CFM563	S	A	5500.00	98.8	93.9	90.6	86.9	81.4	75.0	70.4	65.1	59.7	54.4
CFM563	S	D	6500.00	96.4	92.3	89.3	86.1	80.9	75.2	70.8	65.6	60.3	55.4
CFM563	S	D	9000.00	97.9	93.7	90.7	87.5	82.4	76.8	72.5	67.5	62.5	57.7
CFM563	S	D	11500.00	99.5	95.4	92.5	89.3	84.3	78.9	74.7	69.9	64.9	60.3
CFM563	S	D	14000.00	101.1	97.2	94.4	91.3	86.5	81.2	77.1	72.3	67.5	63.0
CFM563	S	D	16500.00	102.8	99.0	96.3	93.5	88.8	83.6	79.6	74.9	70.2	65.8
CFM563	S	D	19000.00	104.7	101.2	98.7	96.0	91.5	86.4	82.5	78.0	73.4	69.1

4.2 Selected INM Results and the Thrust Rating Selection Process

The flights listed in Table 4-6, as modeled using the automated flight profile builder with INM6.1, will be illustrated in detail in this section. A dozen flights were selected to give a representative overview from various runways, monitoring locations, flight altitudes at the point of closest approach (PCA) as well as for a range of differences between predicted and measured SEL levels. As discussed in Section 3, the profile builder was exercised attempting to match every other radar point using an energy minimization between the radar profile and the INM calculated profile. Each flight profile was developed and optimized for each of five possible thrust ratings. There were some flights which could not be run in INM due to insufficient thrust for the requested climb rates. For those flights, only the remaining thrust ratings were used in the selection process. The offset in potential and kinetic energy was calculated at the point of closest approach using the radar altitude and speed and the INM altitude and speed and the closest thrust rating was selected. The energy calculations and thrust selections were performed using vertical lookup functions in Excel based on the reported Radar and INM PCA values. Table 4-6 lists the selected thrust rating while Figures 4-1a through 4-13d show the corresponding altitude, velocity and

power profiles for all five thrust ratings with the measured radar data. Note that in the power curves, in the absence of radar data, the 1998 CATS thrust settings as calculated in the prior study[1] and explained in Appendix A, are shown for reference. The point in the trajectory where the energy is evaluated and the thrust decision is made is at the point of closest approach which is listed in Table 4-6. One thing to note in the profile figures which follow is that in some of the power profiles the three thrust ratings (18k, 20k, 2220k) appear the same. Thrust rating 20k and the blended 2022k are indeed almost identical because the only difference between those two jet coefficients is in the takeoff segment. Both use the same 20k thrust rating for climbing segments. The reason for the 18k rating being so similar to the 20k rating thrust curves is also due to the similarity between the jet coefficients (Table 3-8). The 18.5k thrust has a higher base thrust coefficient (E) but it also has a larger velocity correction coefficient (F), so that for the slightly different flight speeds and altitudes for the two profiles the net corrected installed thrust (F_n/δ) comes out to be about the same.

Table 4-6. Sample Flight Operation List for in Depth Review Using INM6.1

Flight	Rwy	Monitor	Alt PCA (ft MSL)	Meas SEL	Pred SEL	INM -Meas SEL	Thrust Rating Selected
1280.521	08	W02	9408	73.8	78.0	4.2	18k
1685.528	34	S01	6861	82.4	83.1	0.7	2220k
1845.522	25	S19	10697	71.6	71.6	0.0	18k
1132.530	08	S06	8289	82.2	80.4	-1.8	2220k
484.527	17L	S07	7054	87.9	85.3	-2.6	18k
588.528	08	W03	11006	77.3	74.0	-3.3	20k
1227.531	25	S09	6477	87.8	83.5	-4.3	20k
1430.527	08	W04	12179	76.9	71.7	-5.2	22k
1604.523	08	W05	12000	68.7	63.4	-5.3	18k
1111.524	25	S14	10000	65.3	59.7	-5.6	18k
484.522	08	W05	15595	72.8	67.1	-5.7	18k
226.527	08	W05	14275	74.2	68	-6.2	2220k
1801.523	25	S09	6479	91.2	84.8	-6.4	18k

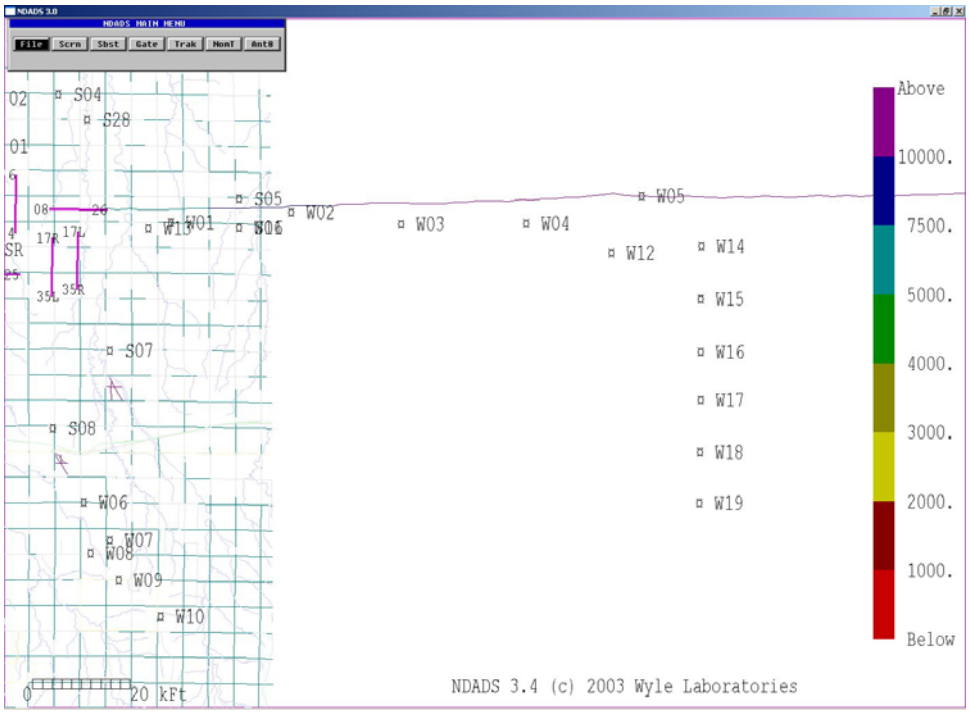


Figure 4-1a. 1280.521 Ground Track

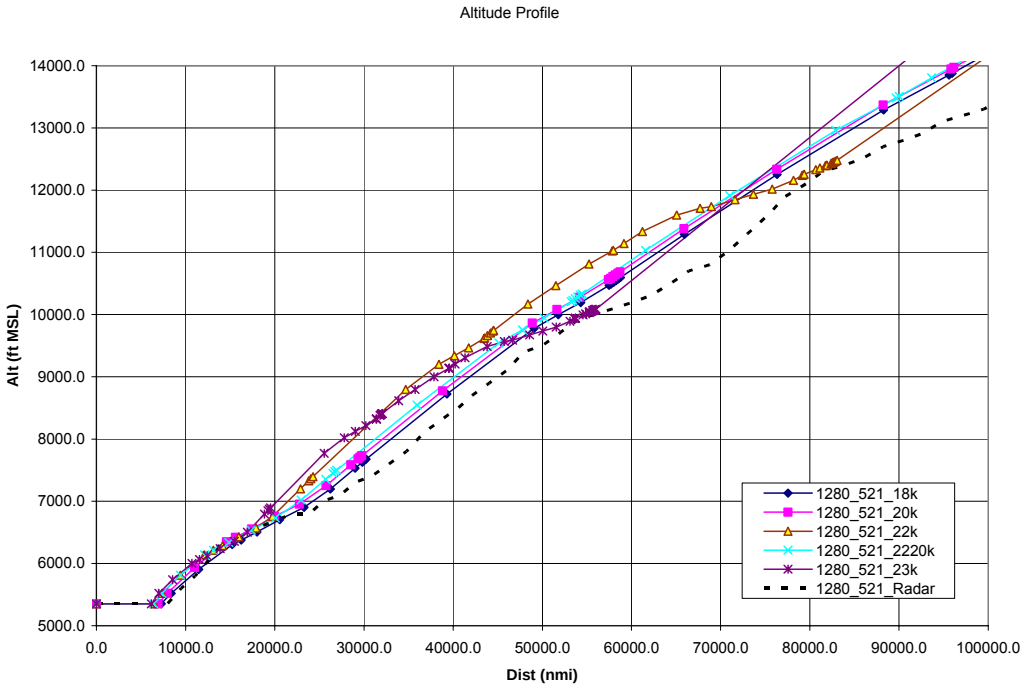


Figure 4-1b. 1280.521 Altitude Profile

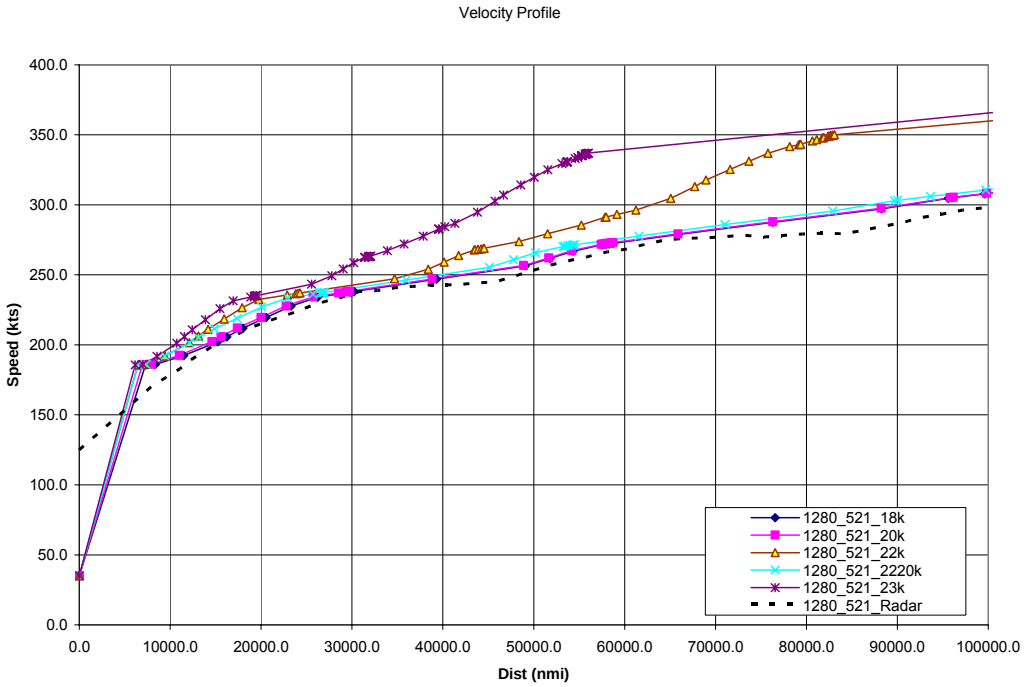


Figure 4-1c. 1280.521 Velocity Profile

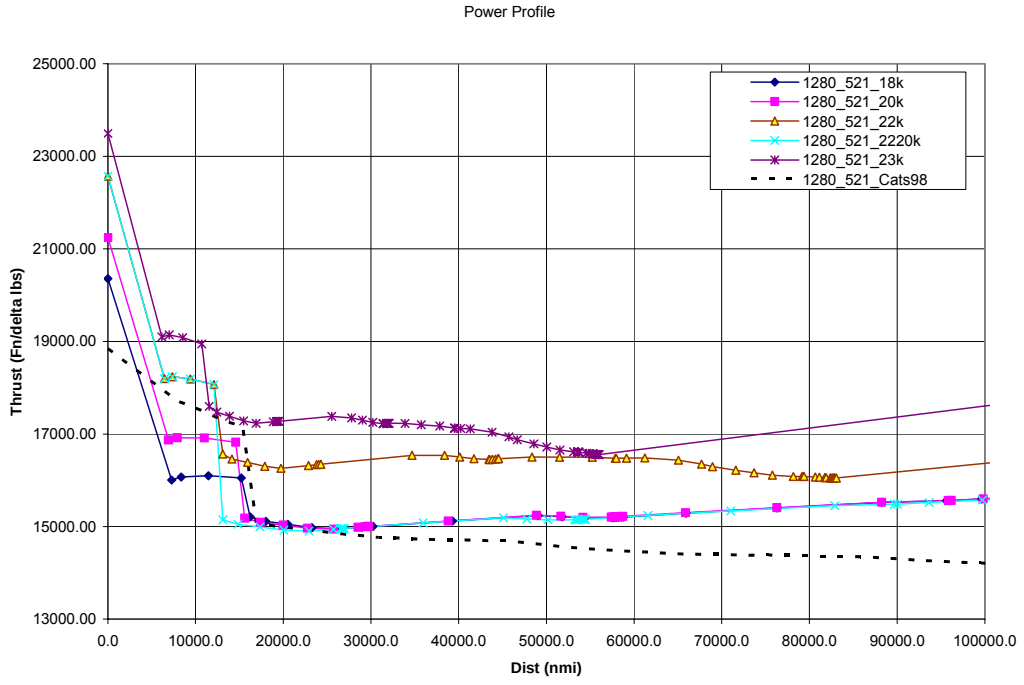


Figure 4-1d. 1280.521 Power Profile

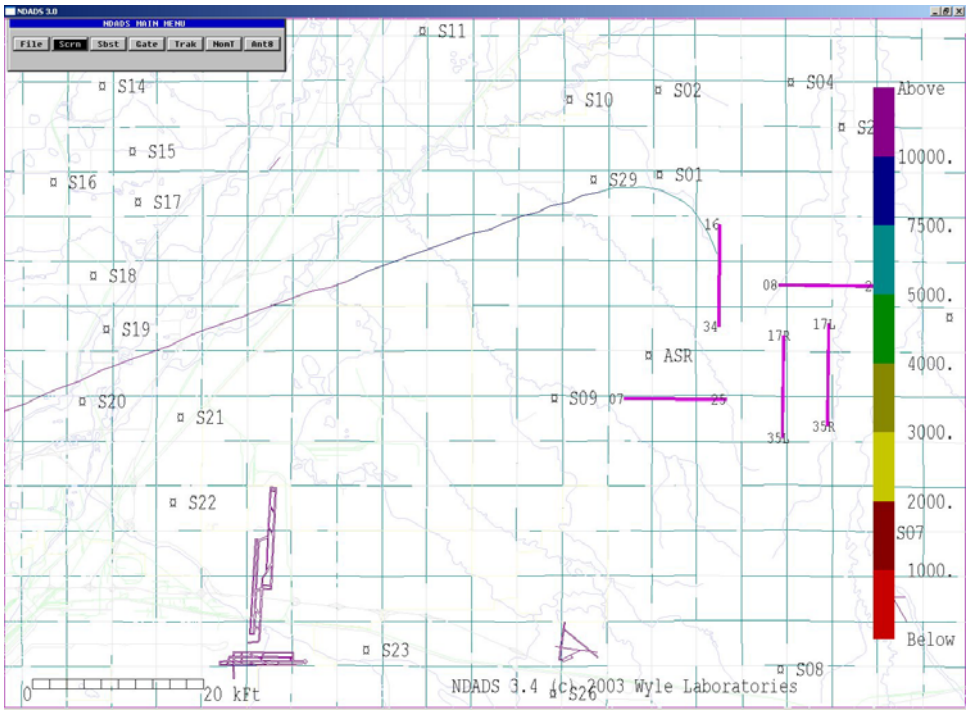


Figure 4-2a. 1685.528 Ground Track

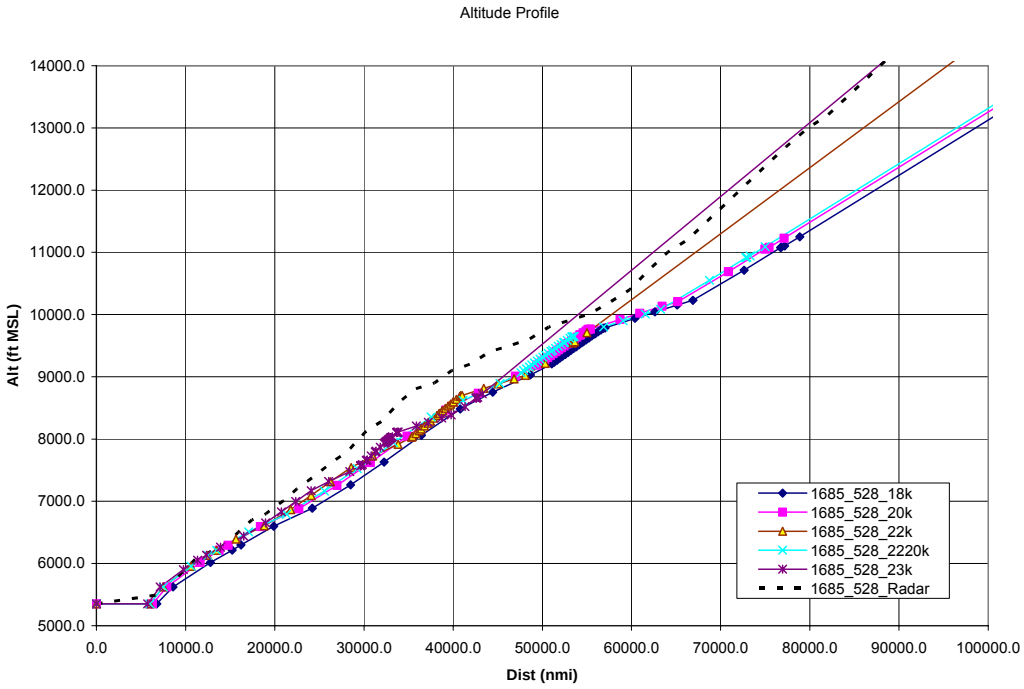


Figure 4-2b. 1685.528 Altitude Profile

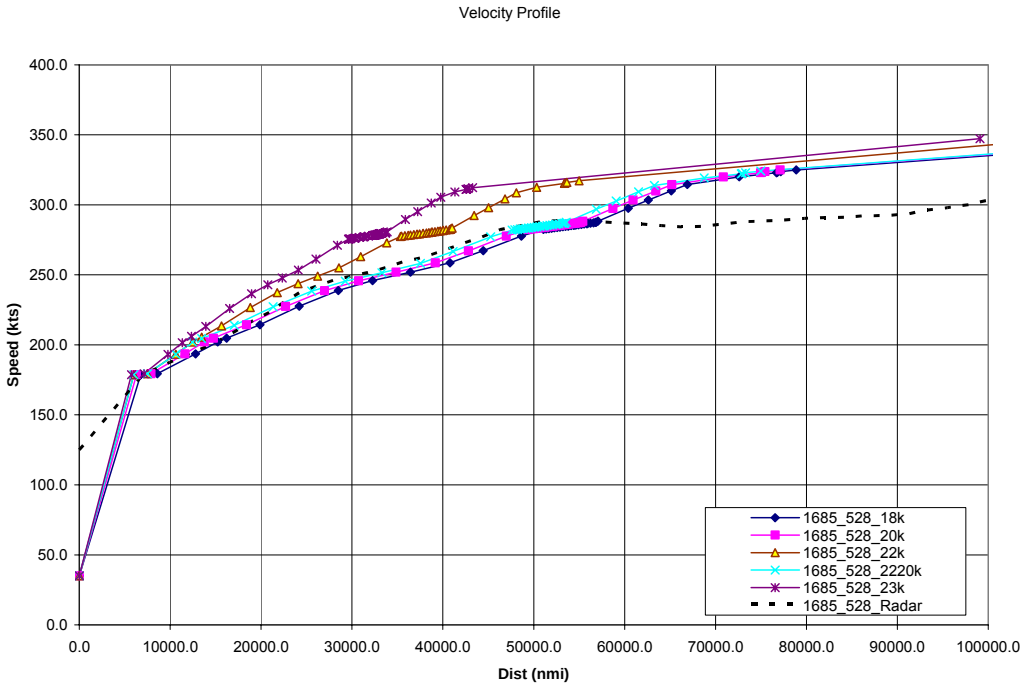


Figure 4-2c. 1685.528 Velocity Profile

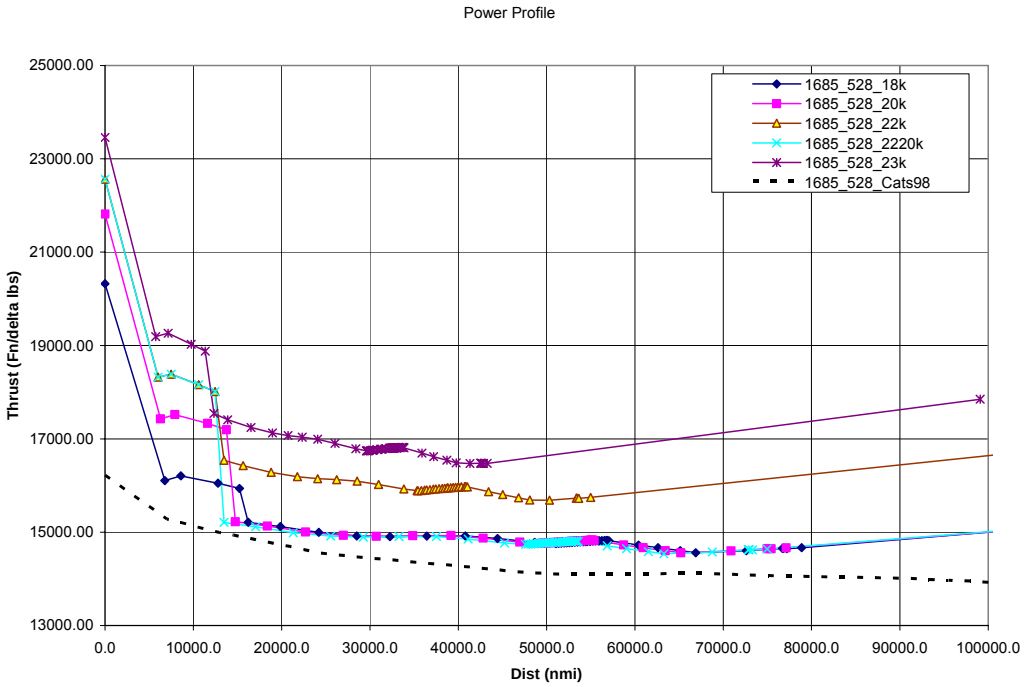


Figure 4-2d. 1685.528 Power Profile

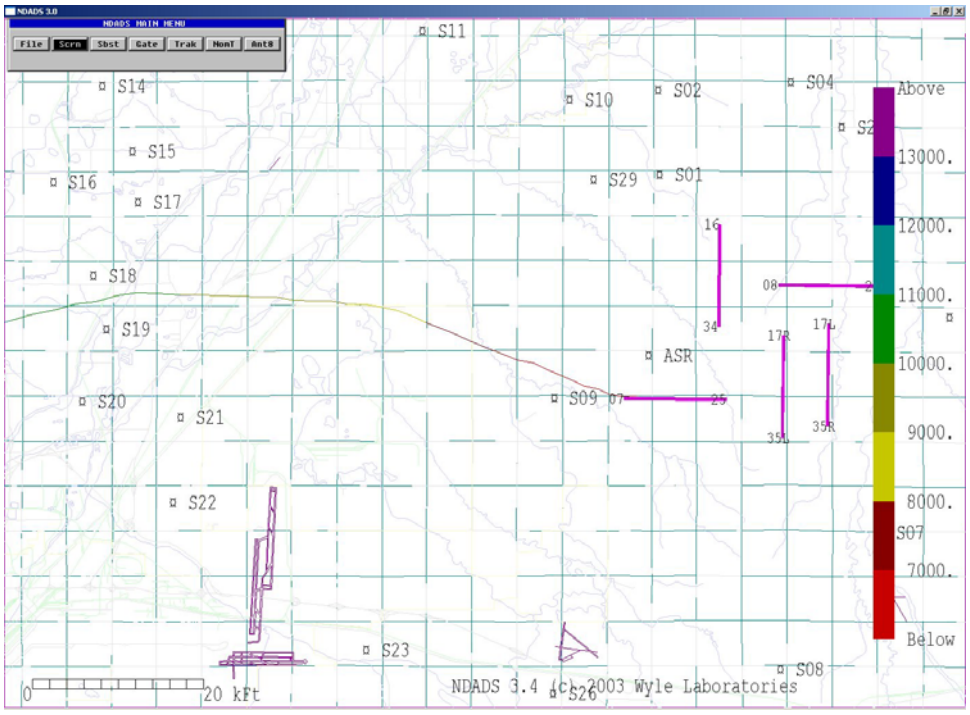


Figure 4-3a. 1845.522 Ground Track

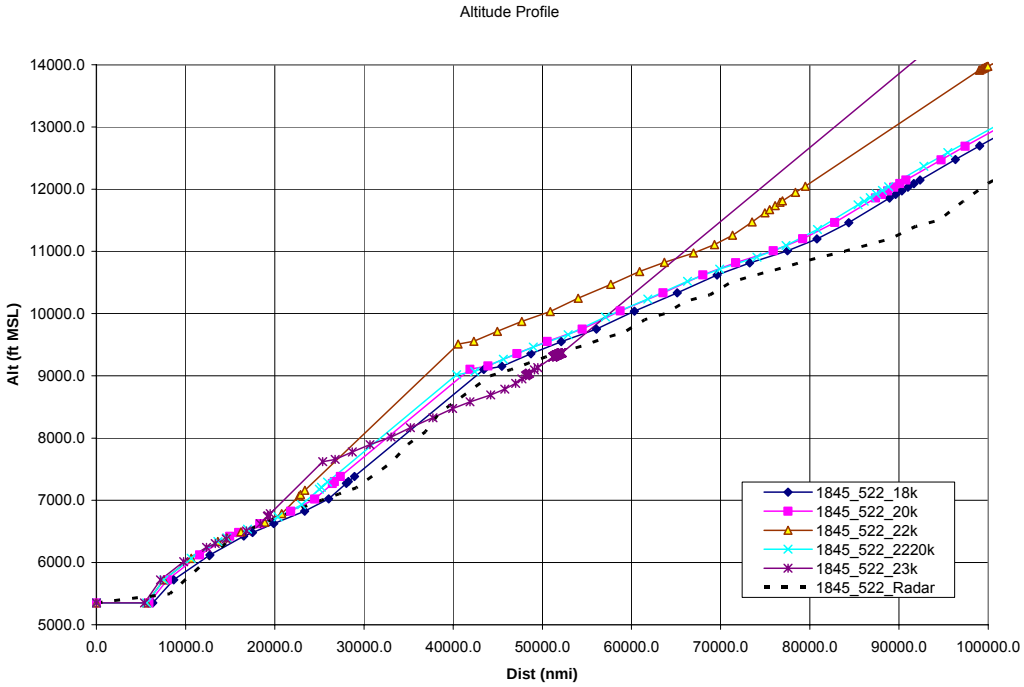


Figure 4-3b. 1845.522 Altitude Profile

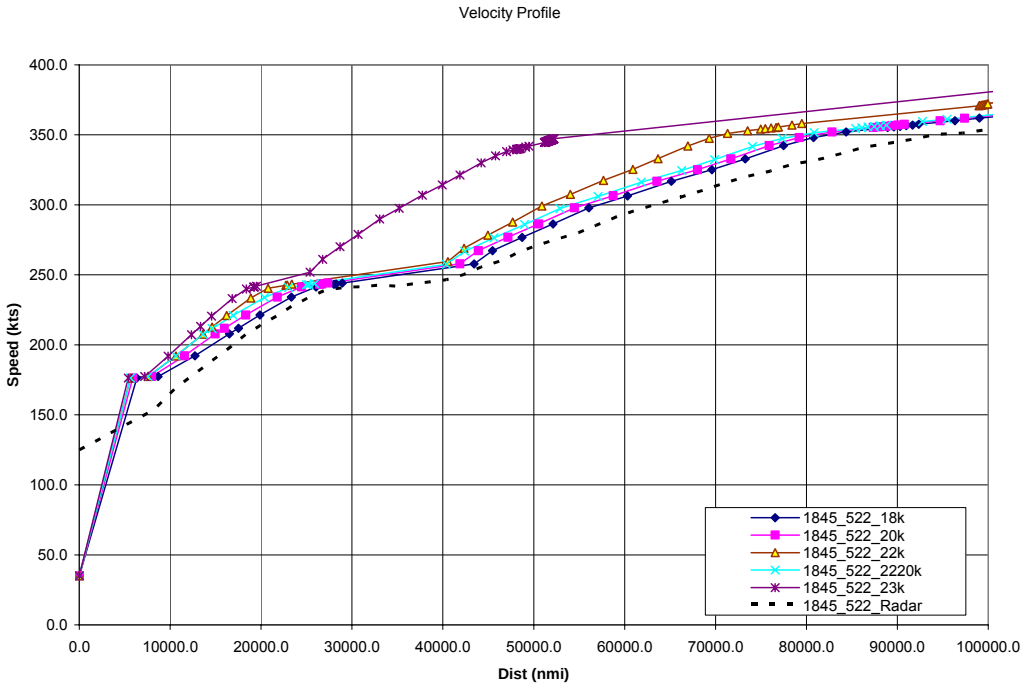


Figure 4-3c. 1845.522 Velocity Profile

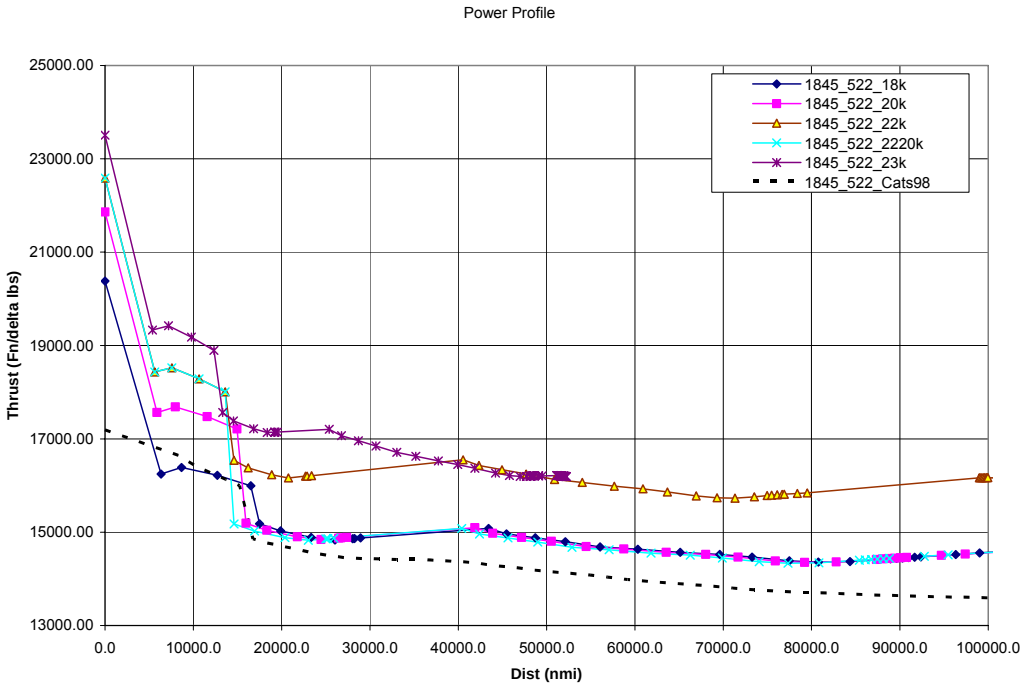


Figure 4-3d. 1845.522 Power Profile

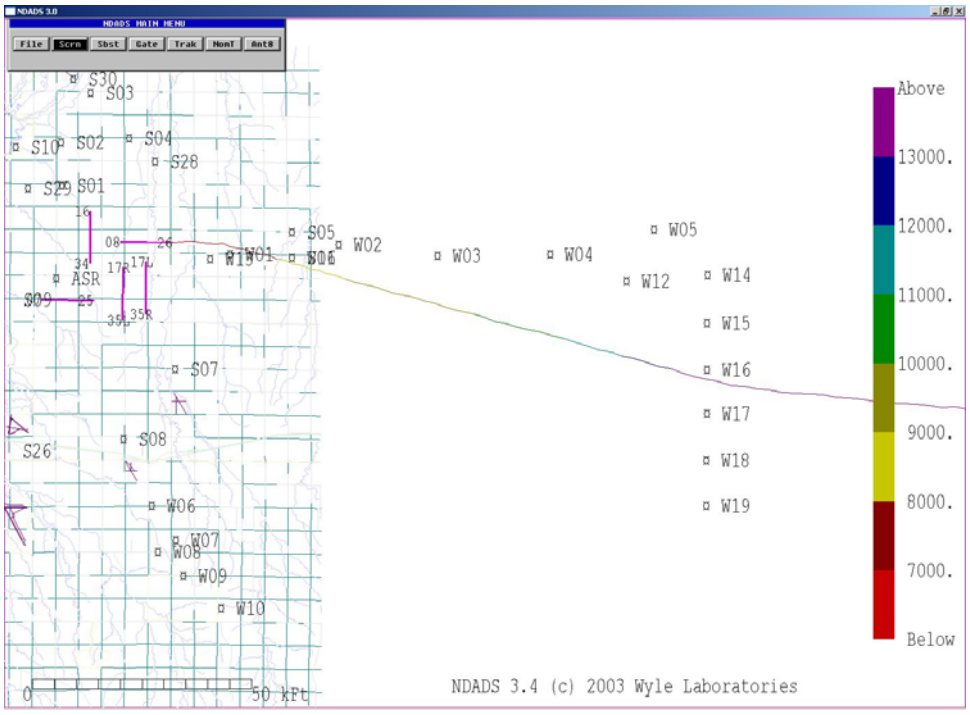


Figure 4-4a. 1132.530 Ground Track

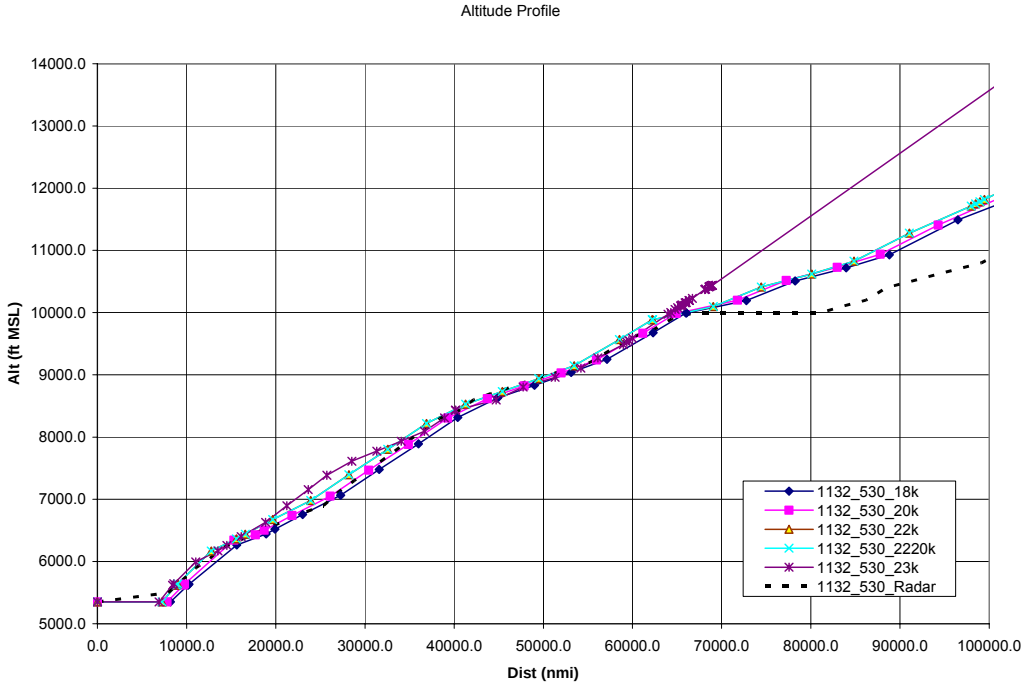


Figure 4-4b. 1132.530 Altitude Profile

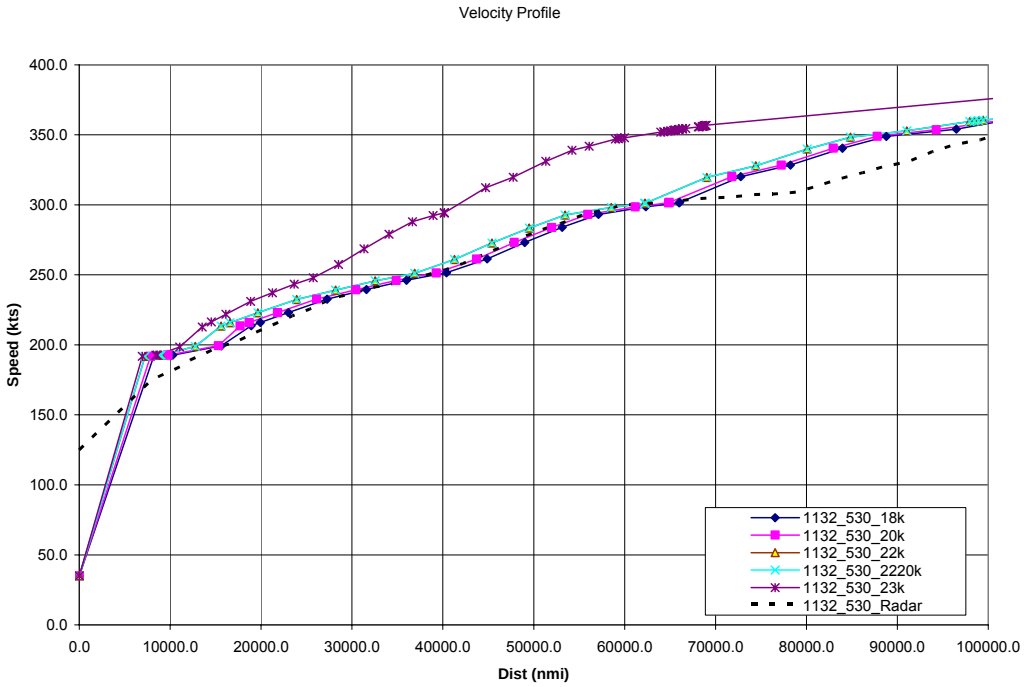


Figure 4-4c. 1132.530 Velocity Profile

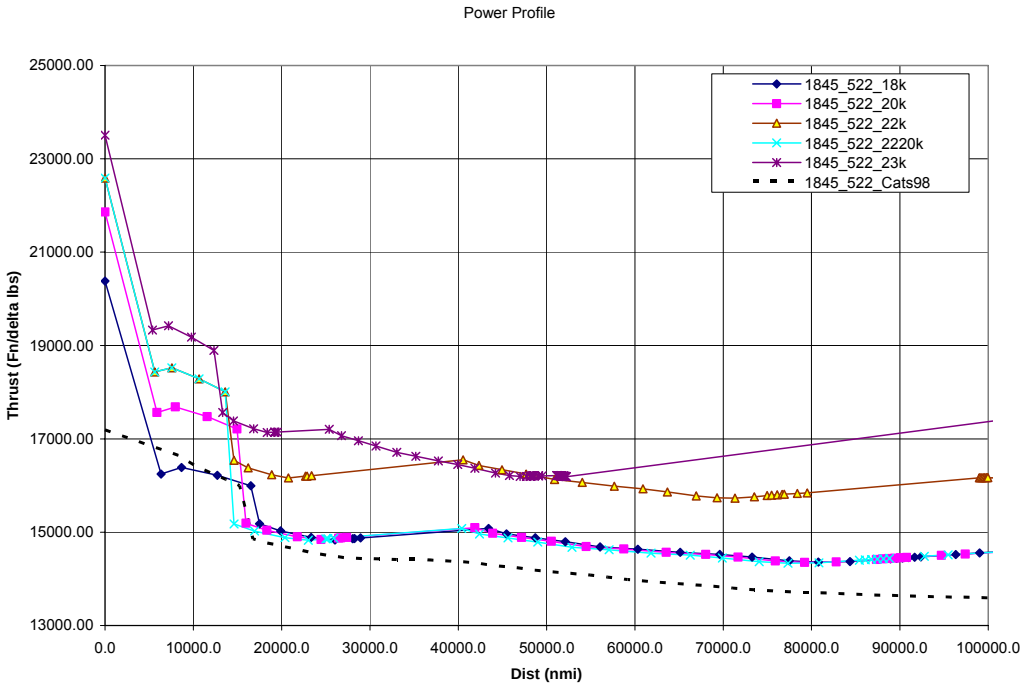


Figure 4-4d. 1132.530 Power Profile

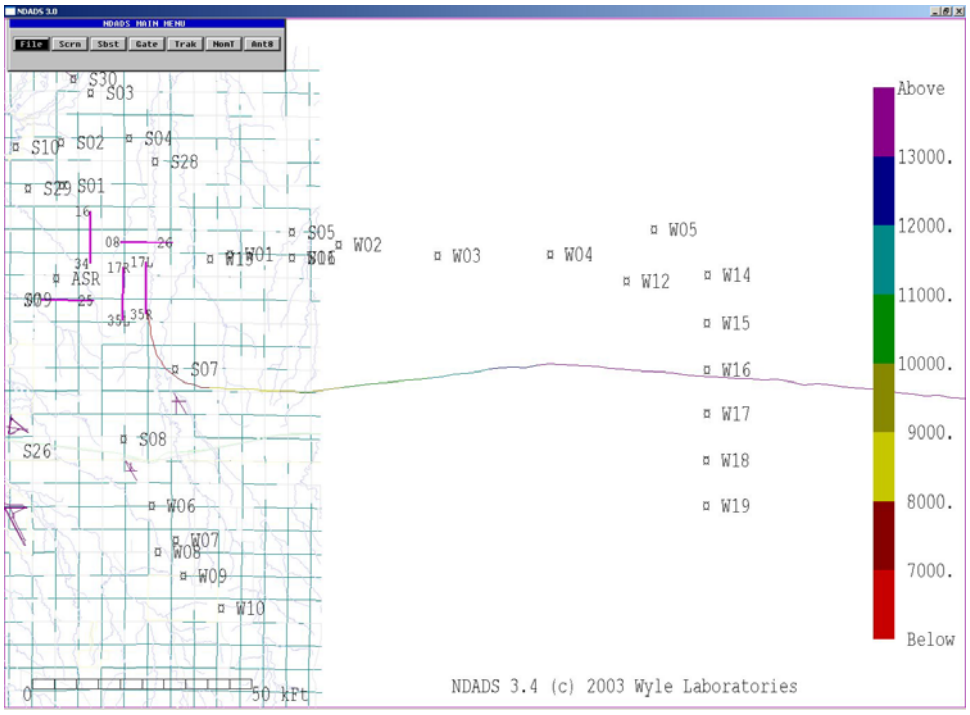


Figure 4-5a. 484.527 Ground Track

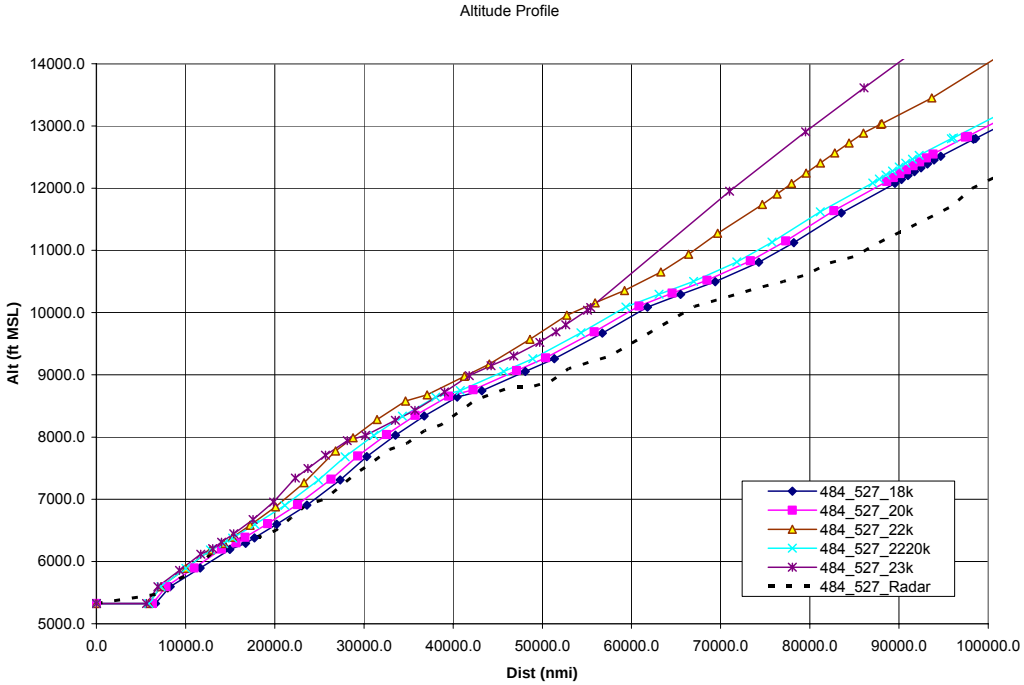


Figure 4-5b. 484.527 Altitude Profile

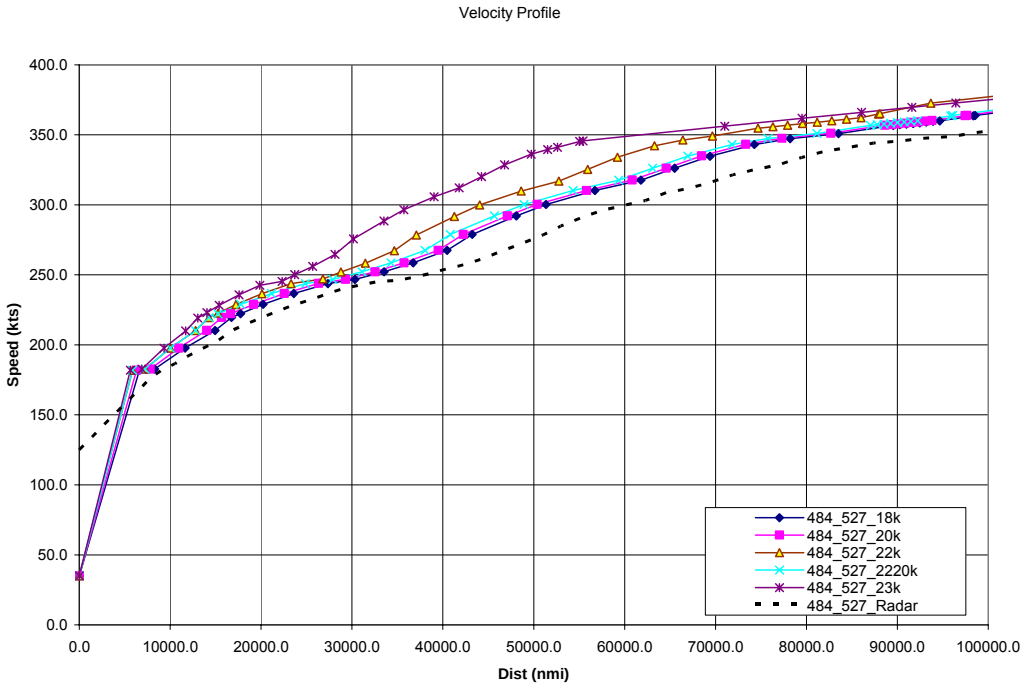


Figure 4-5c. 484.527 Velocity Profile

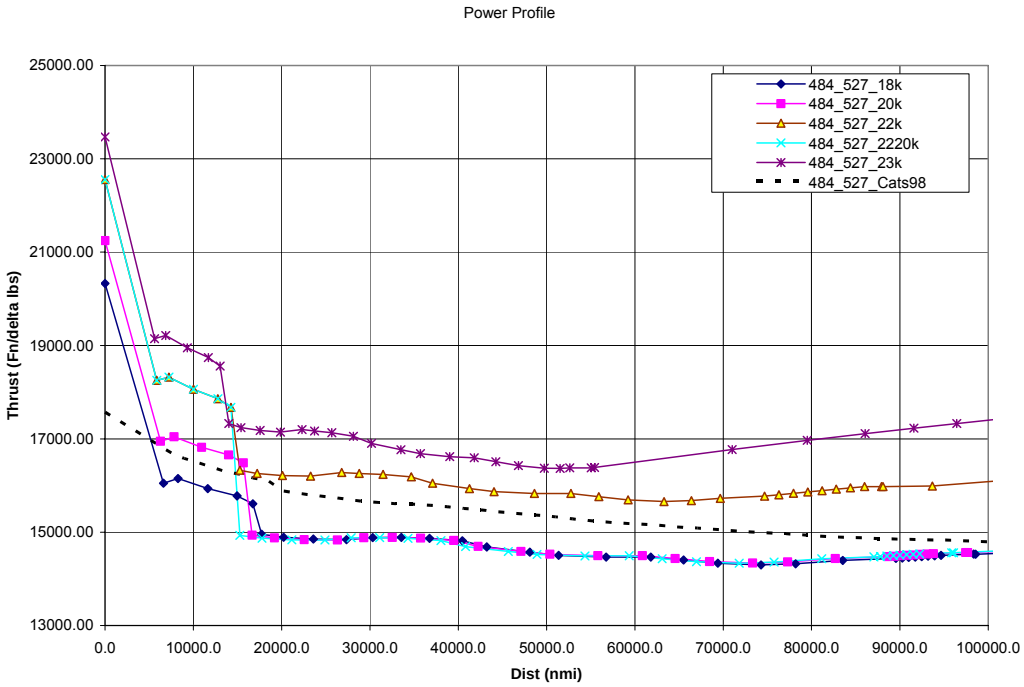


Figure 4-5d. 484.527 Power Profile

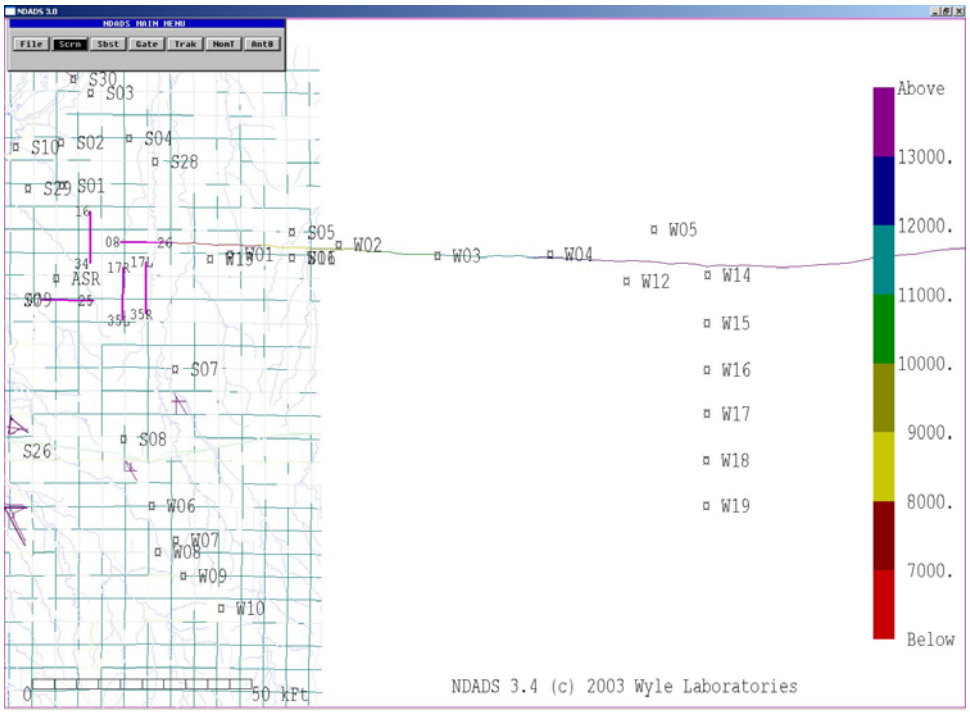


Figure 4-6a. 588.528 Ground Track

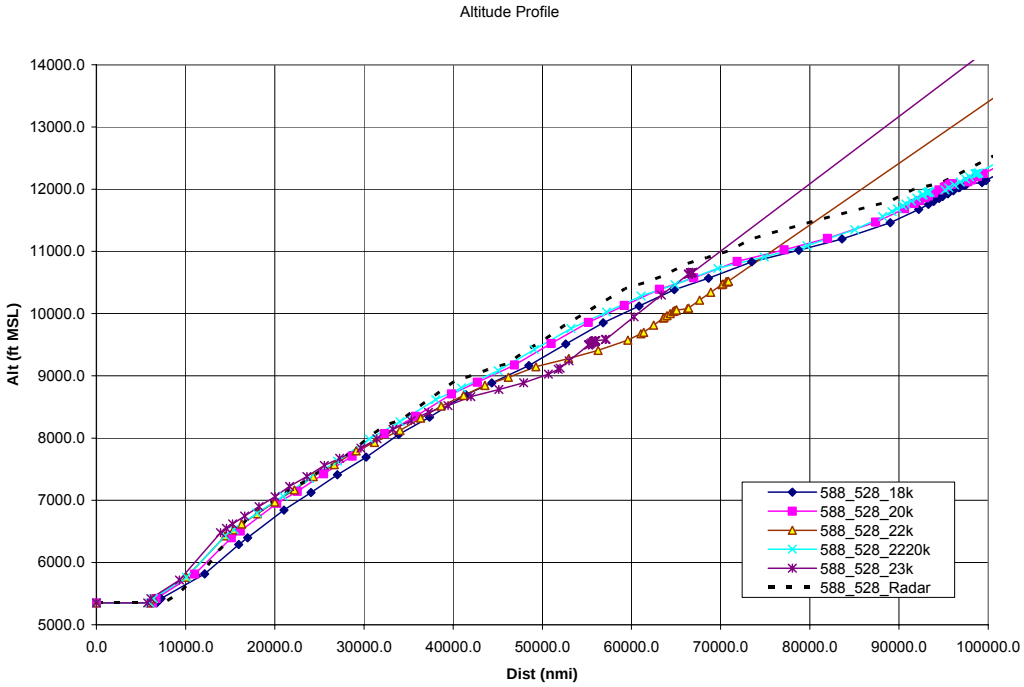


Figure 4-6b. 588.528 Altitude Profile

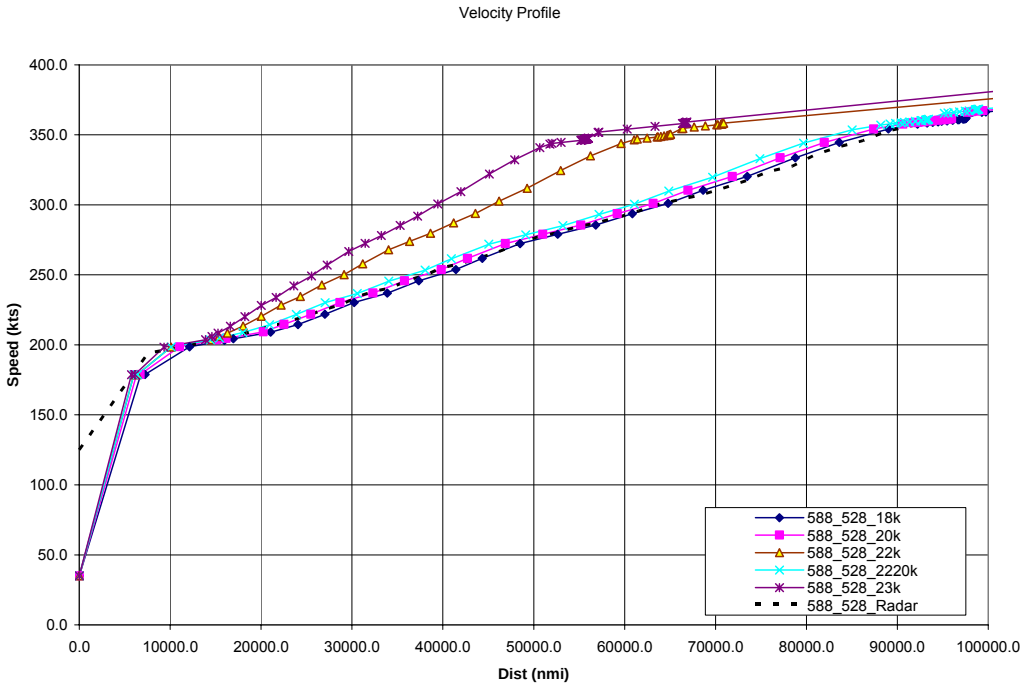


Figure 4-6c. 588.528 Velocity Profile

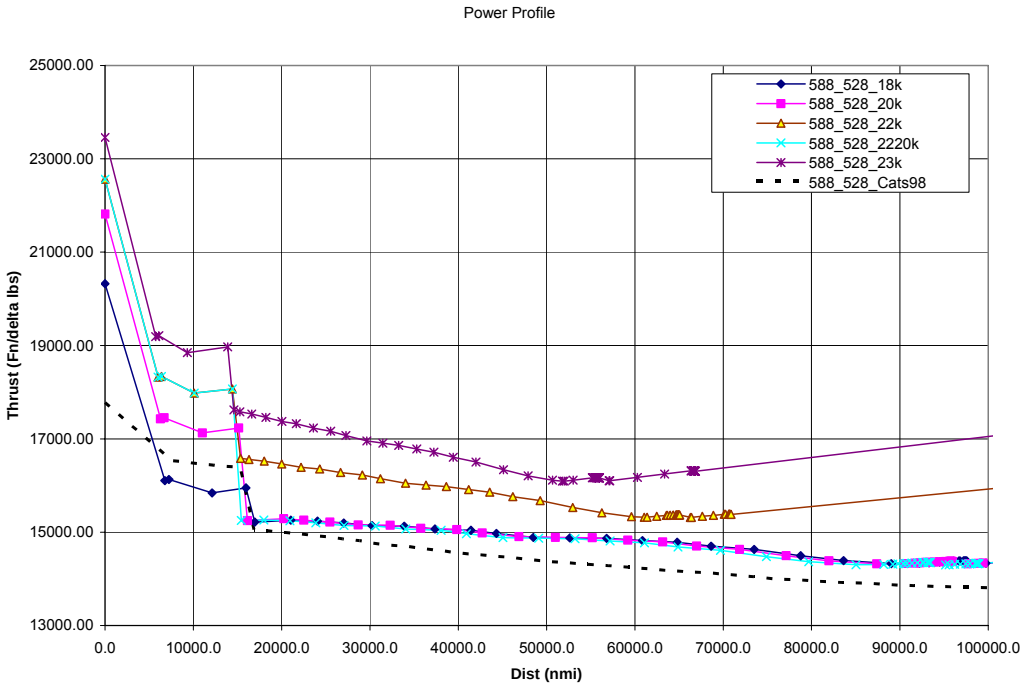


Figure 4-6d. 588.528 Power Profile

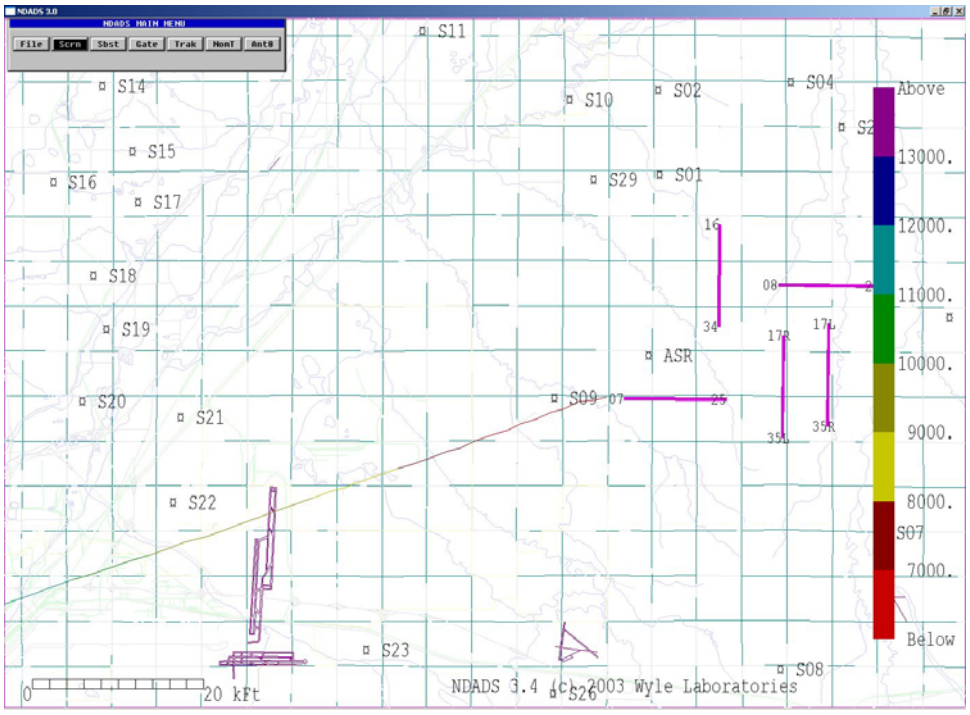


Figure 4-7a. 1227.531 Ground Track

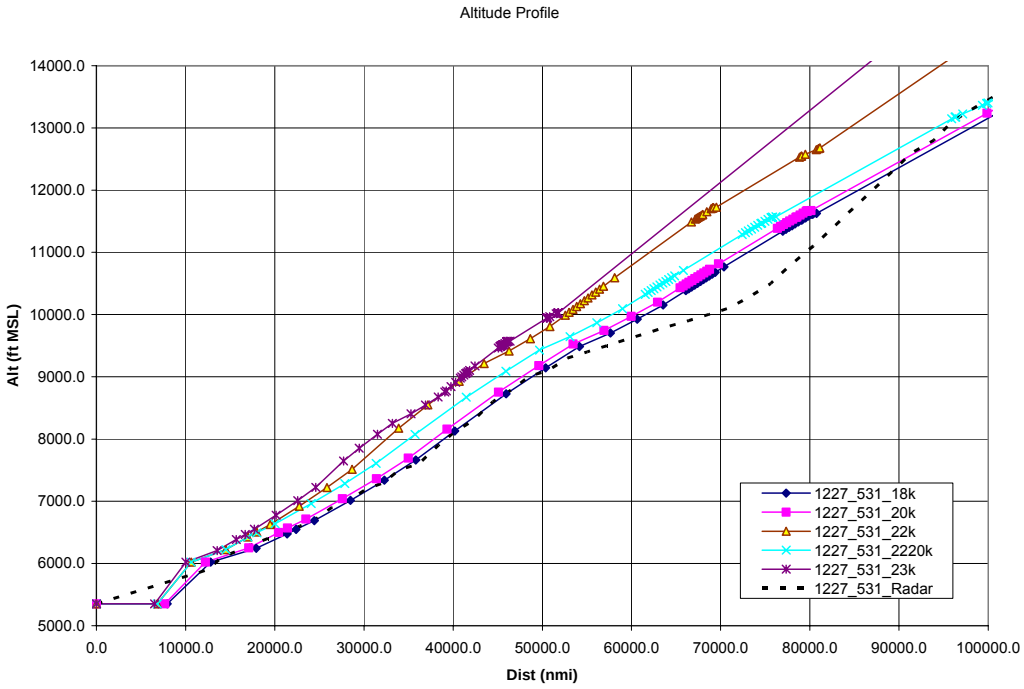


Figure 4-7b. 1227.531 Altitude Profile

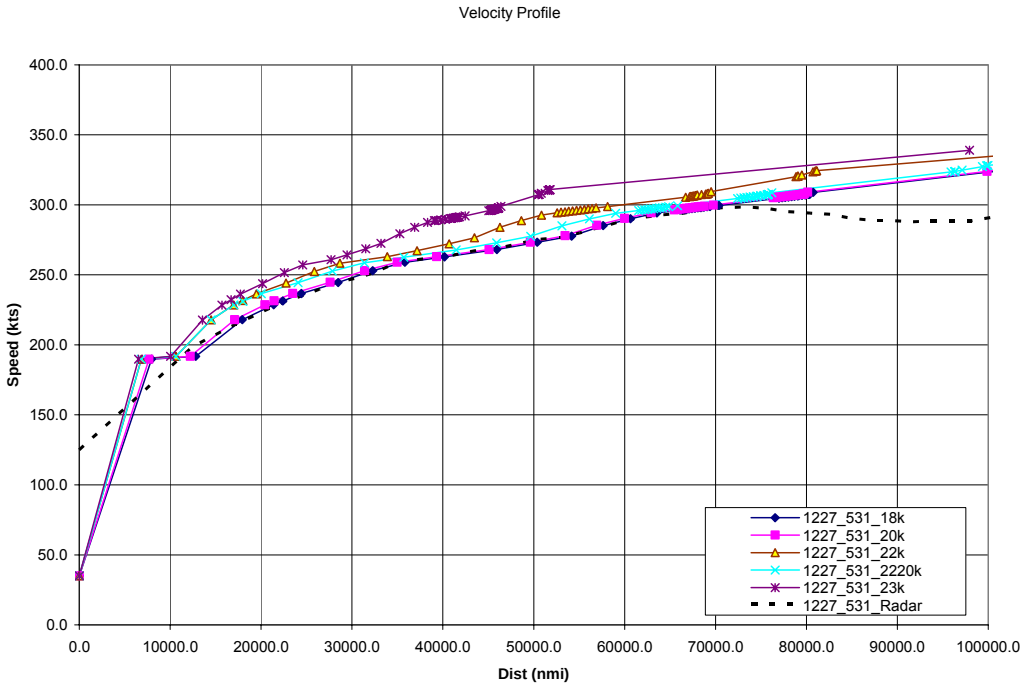


Figure 4-7c. 1227.531 Velocity Profile

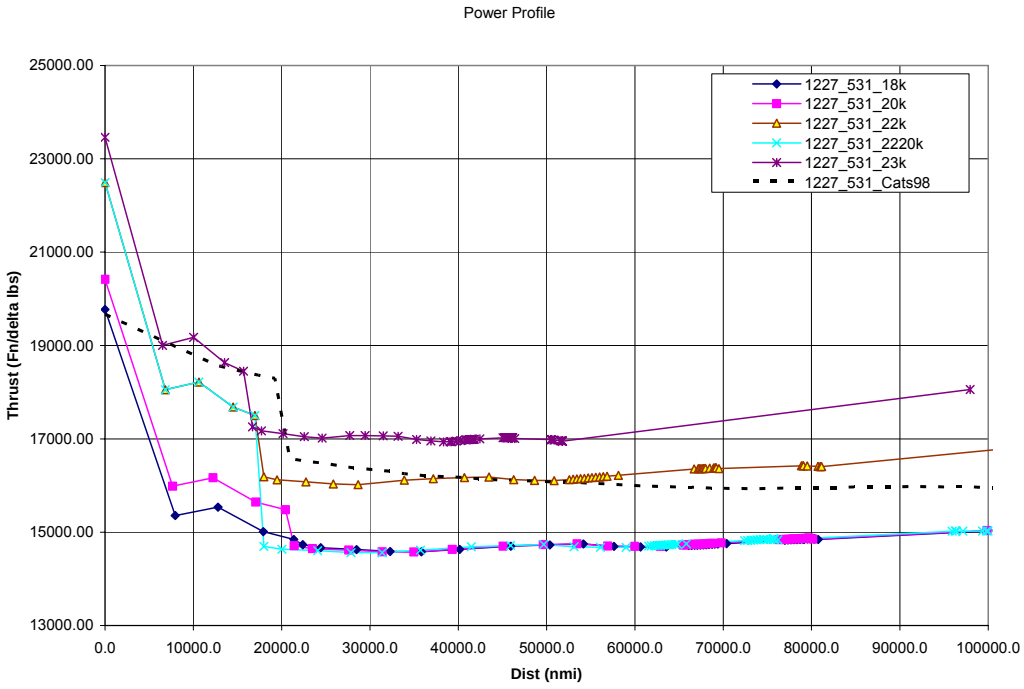


Figure 4-7d. 1227.531 Power Profile

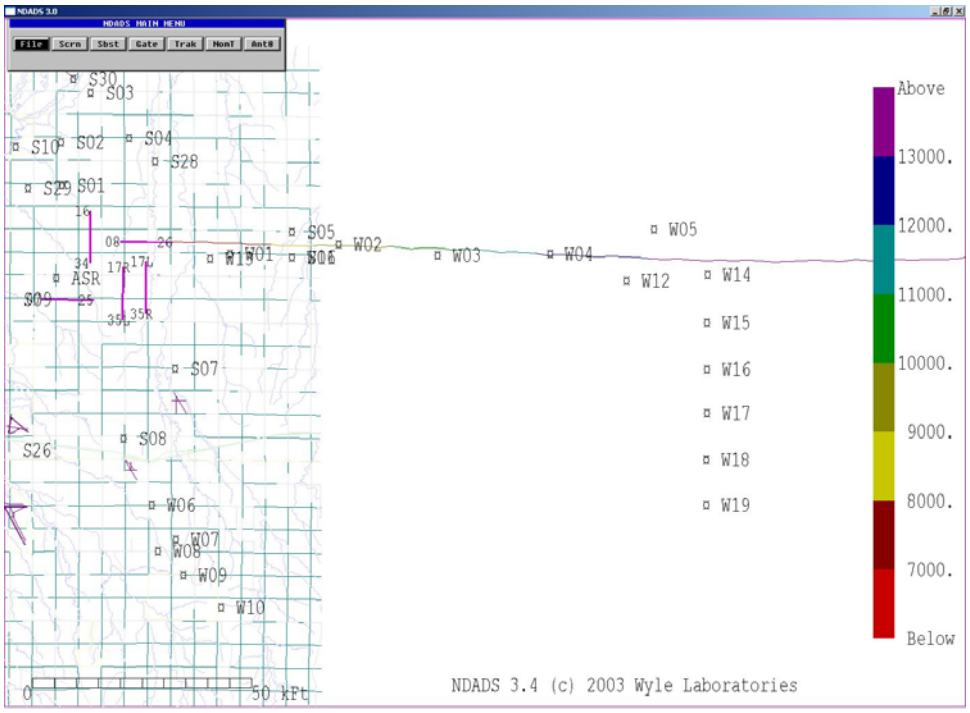


Figure 4-8a. 1430.527 Ground Track

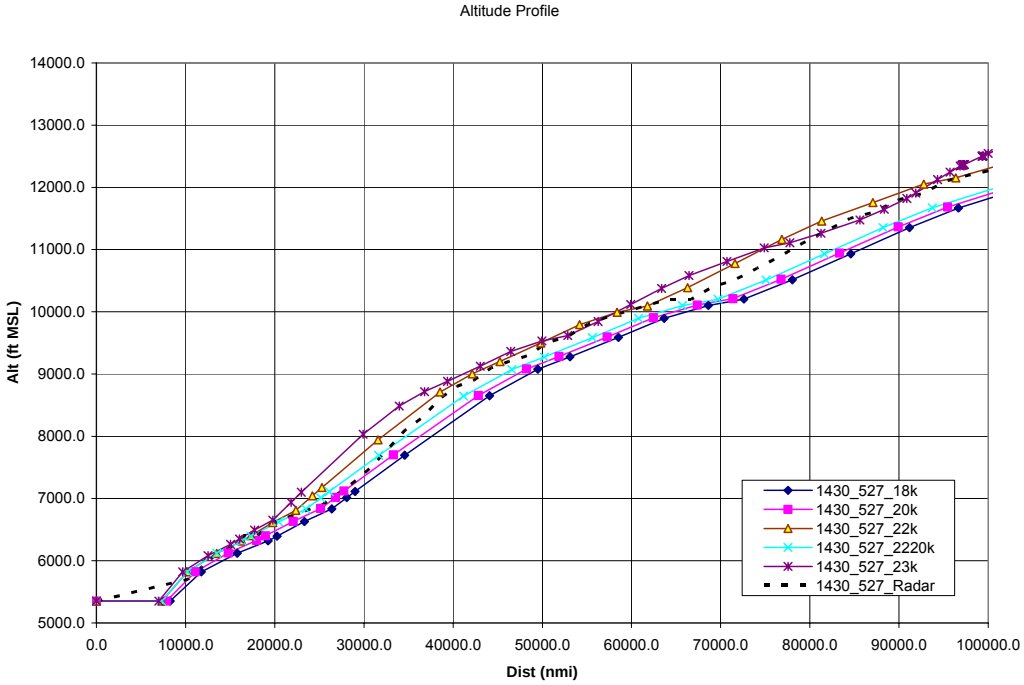


Figure 4-8b. 1430.527 Altitude Profile

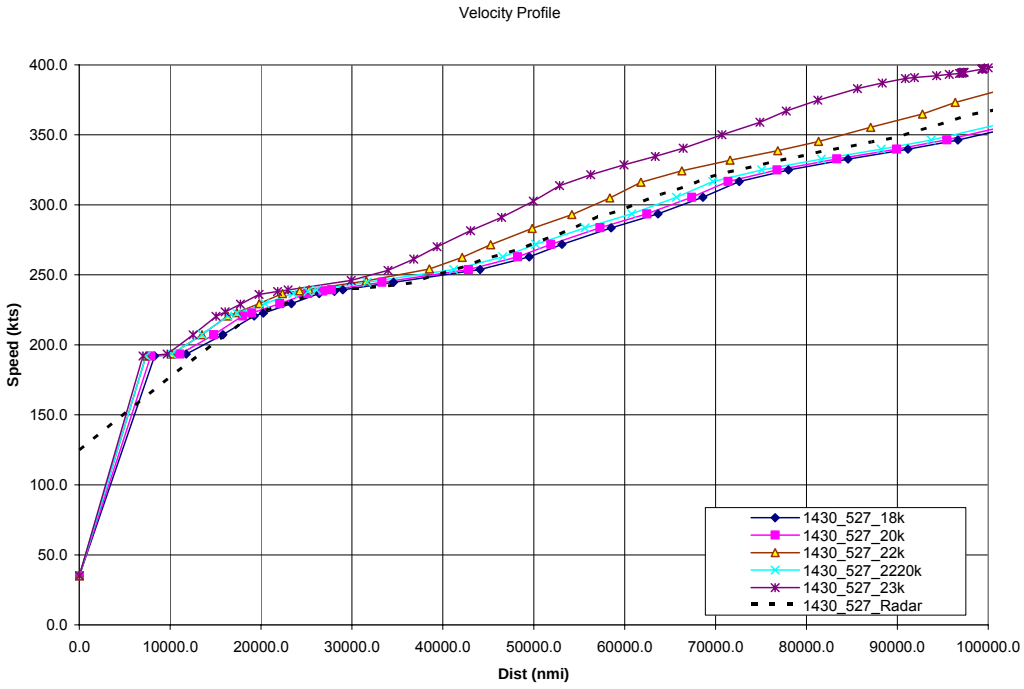


Figure 4-8c. 1430.527 Velocity Profile

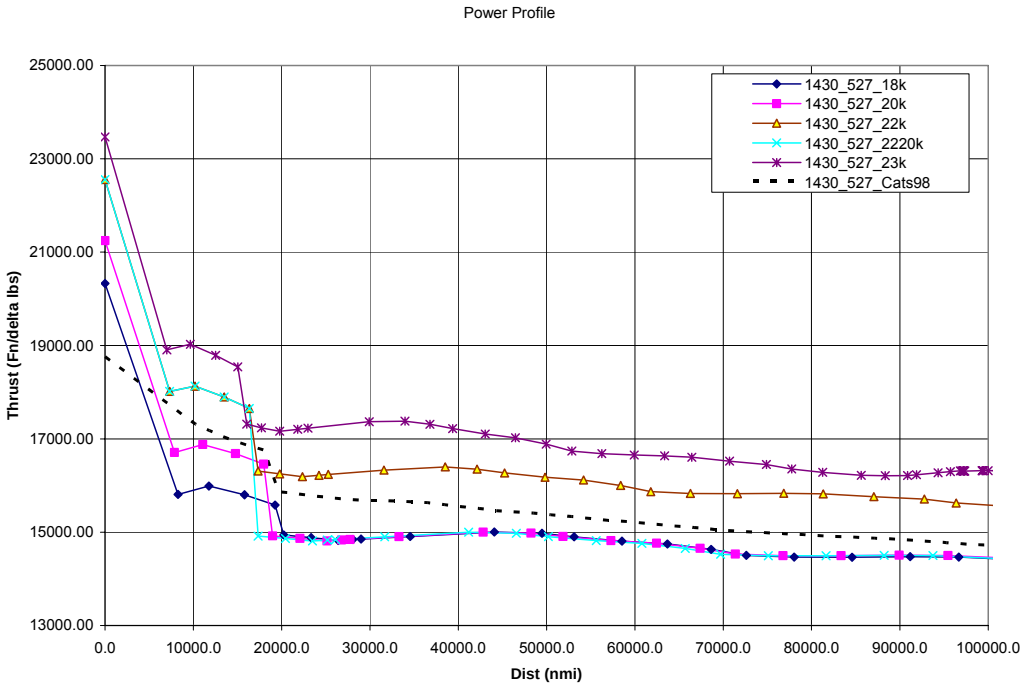


Figure 4-8d. 1430.527 Power Profile

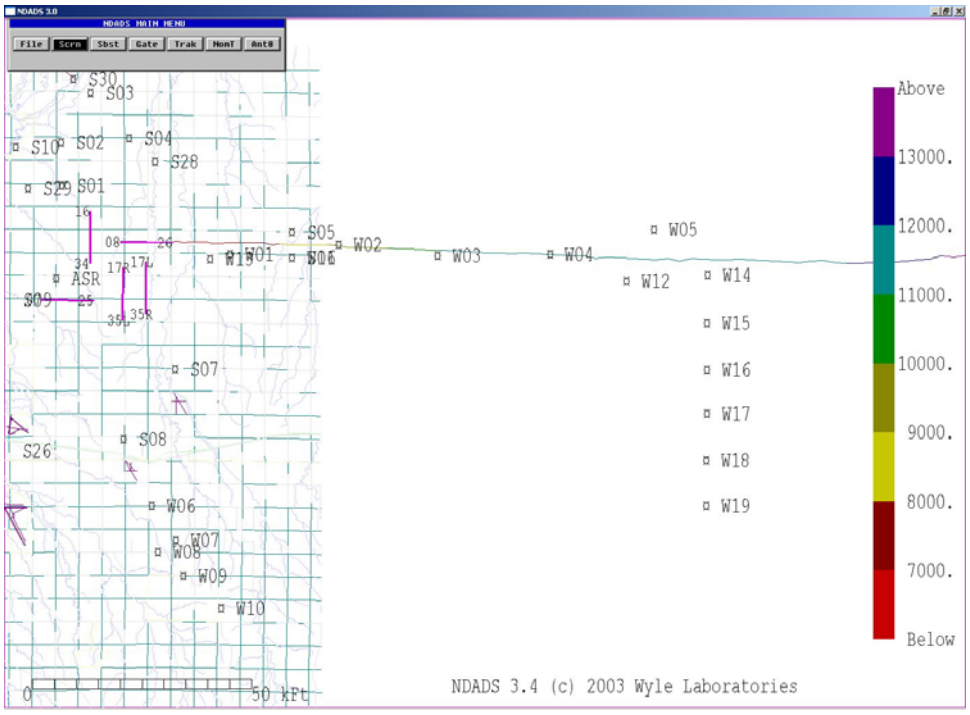


Figure 4-9a. 1604.523 Ground Track

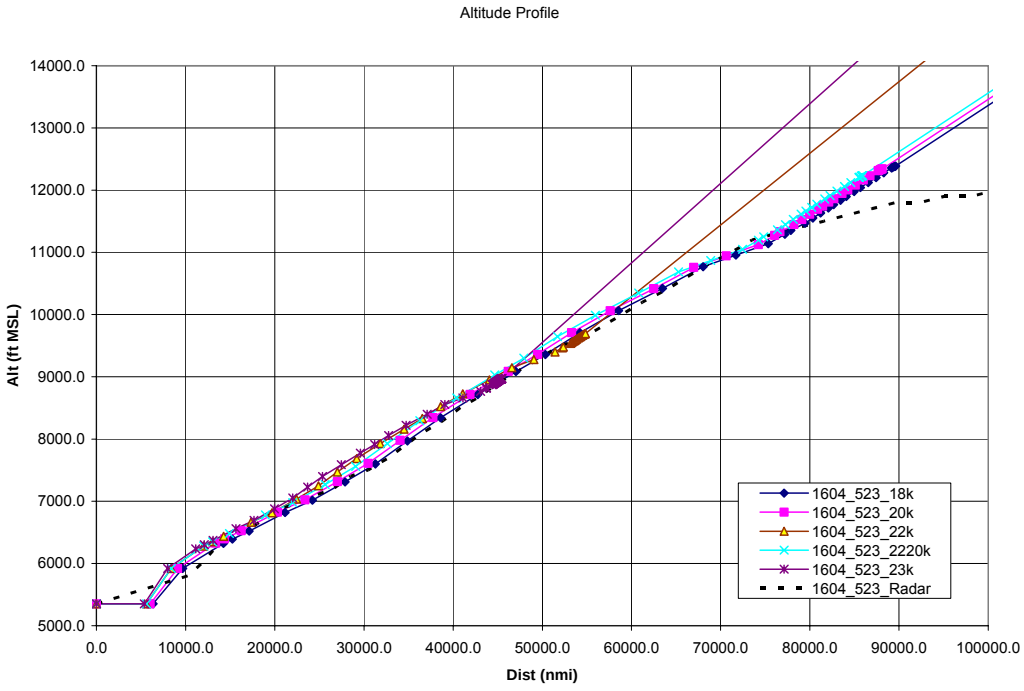


Figure 4-9b. 1604.523 Altitude Profile

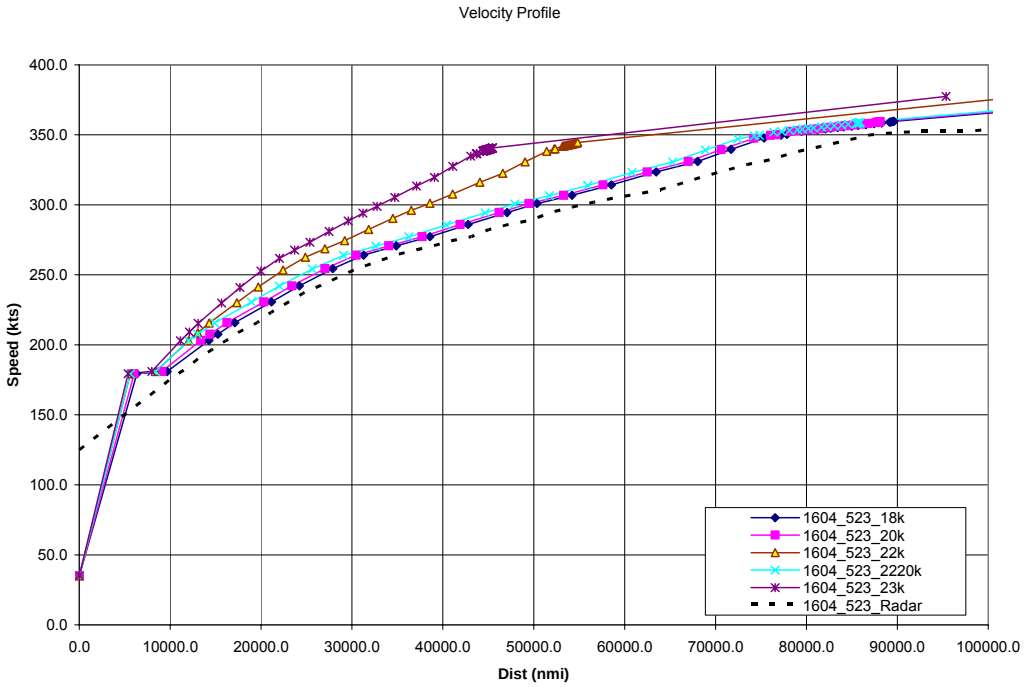


Figure 4-9c. 1604.523 Velocity Profile

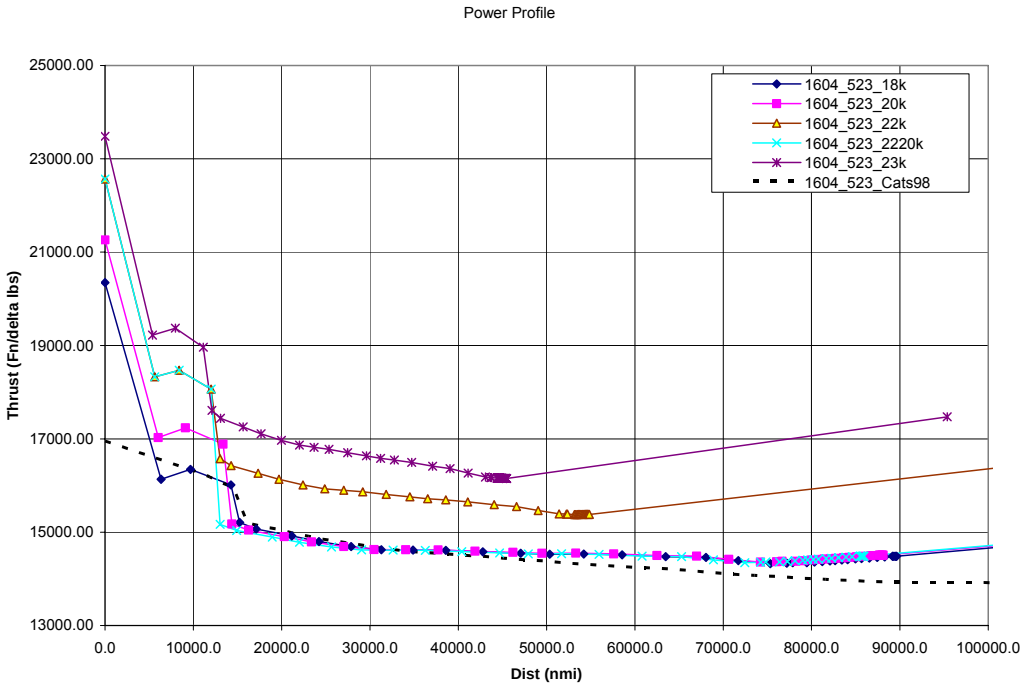


Figure 4-9d. 1604.523 Power Profile

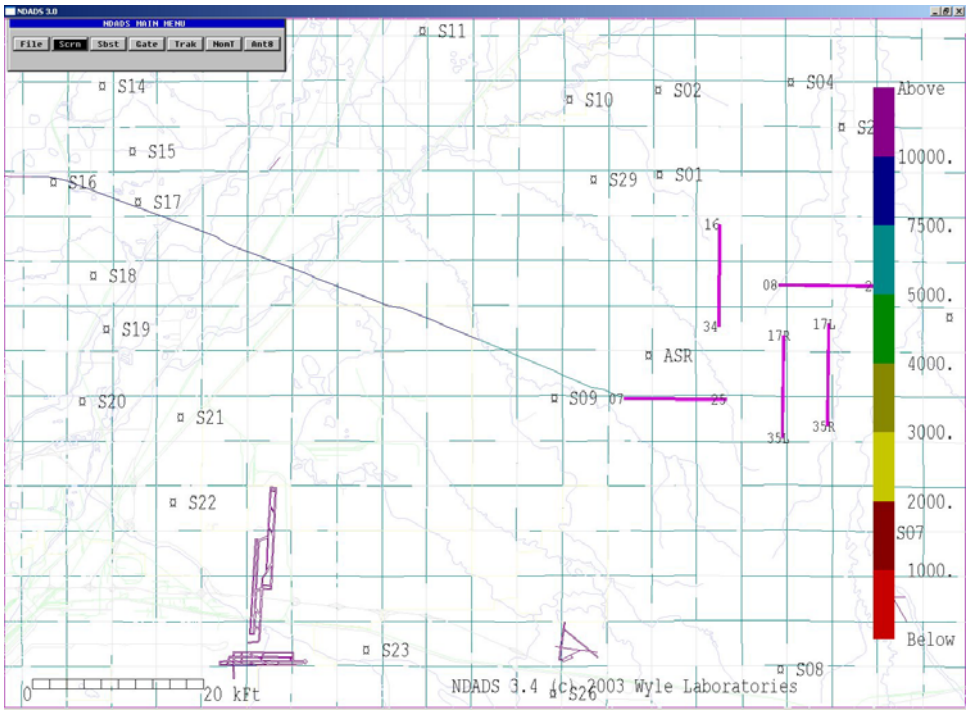


Figure 4-10a. 1111.524 Ground Track

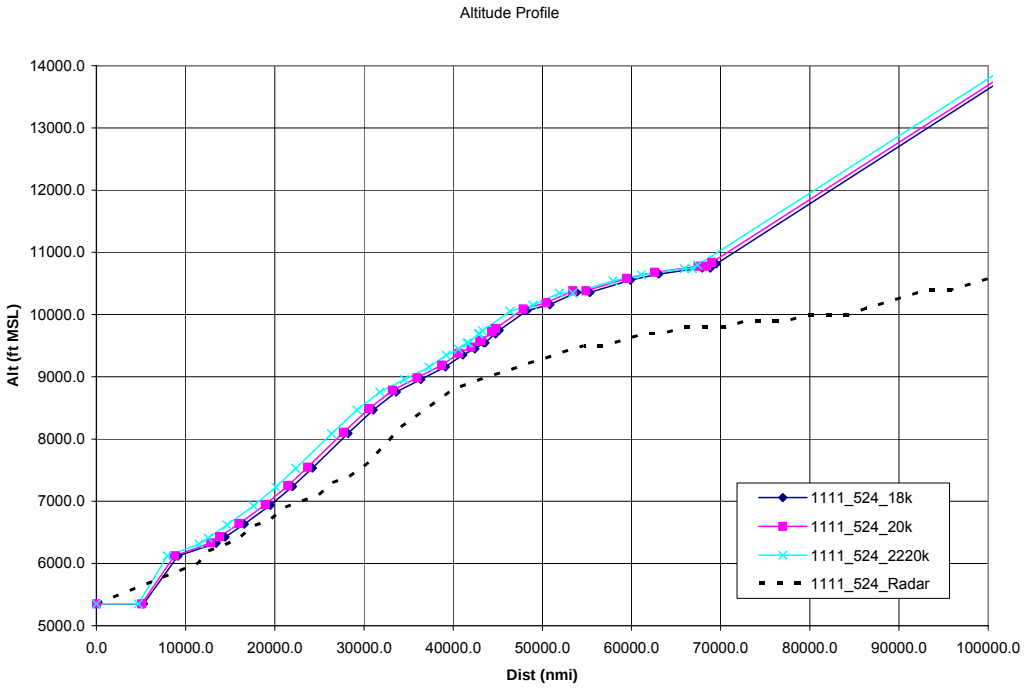


Figure 4-10b. 1111.524 Altitude Profile

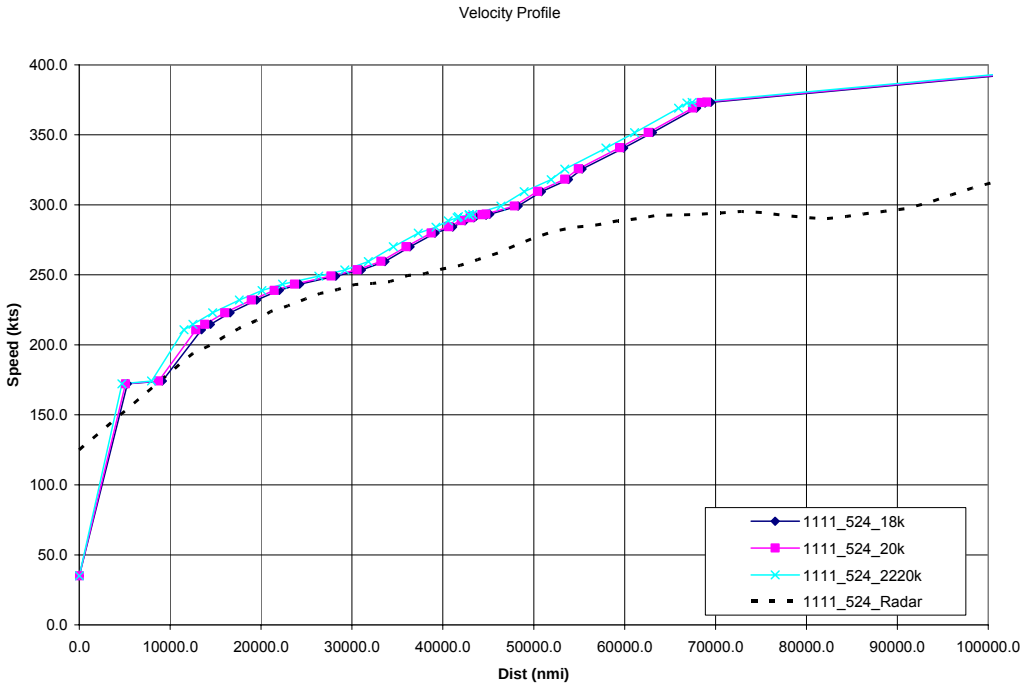


Figure 4-10c. 1111.524 Velocity Profile

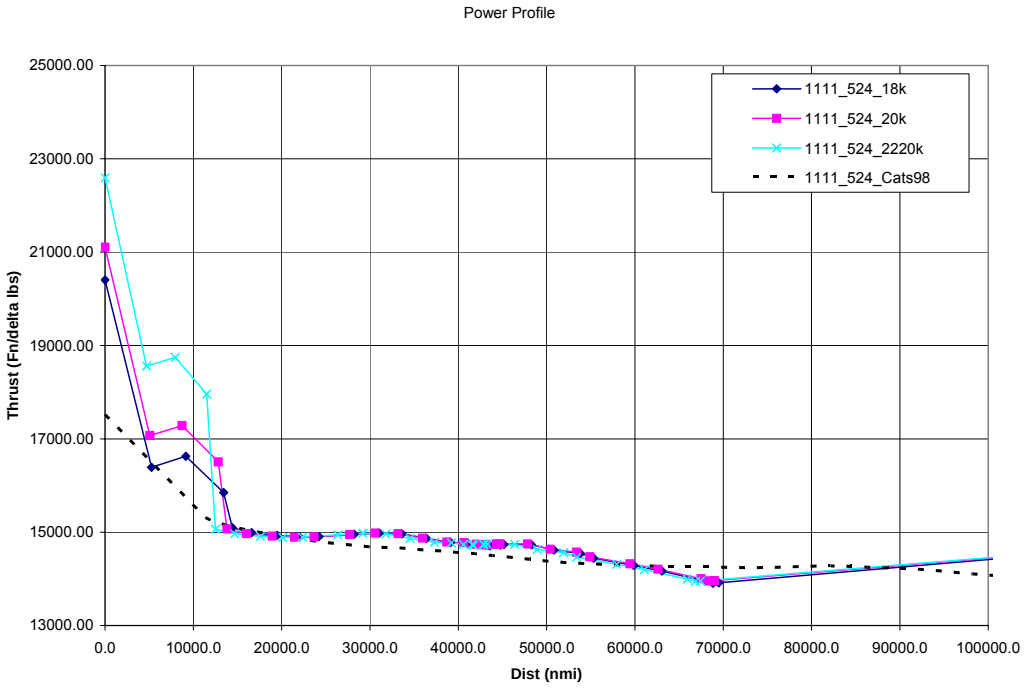


Figure 4-10d. 1111.524 Power Profile

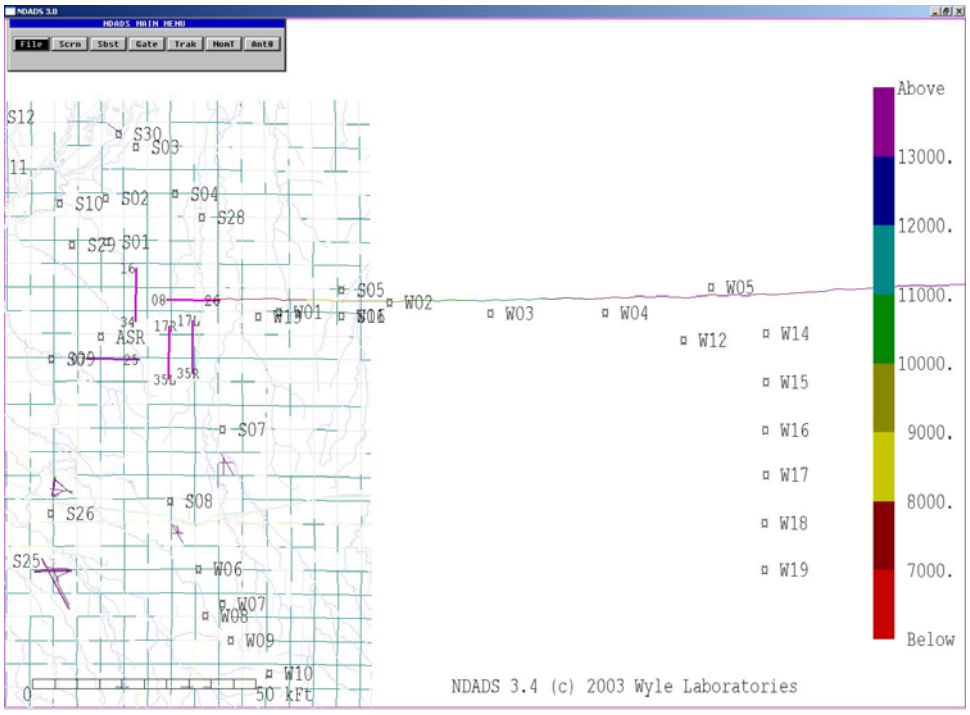


Figure 4-11a. 484.522 Ground Track

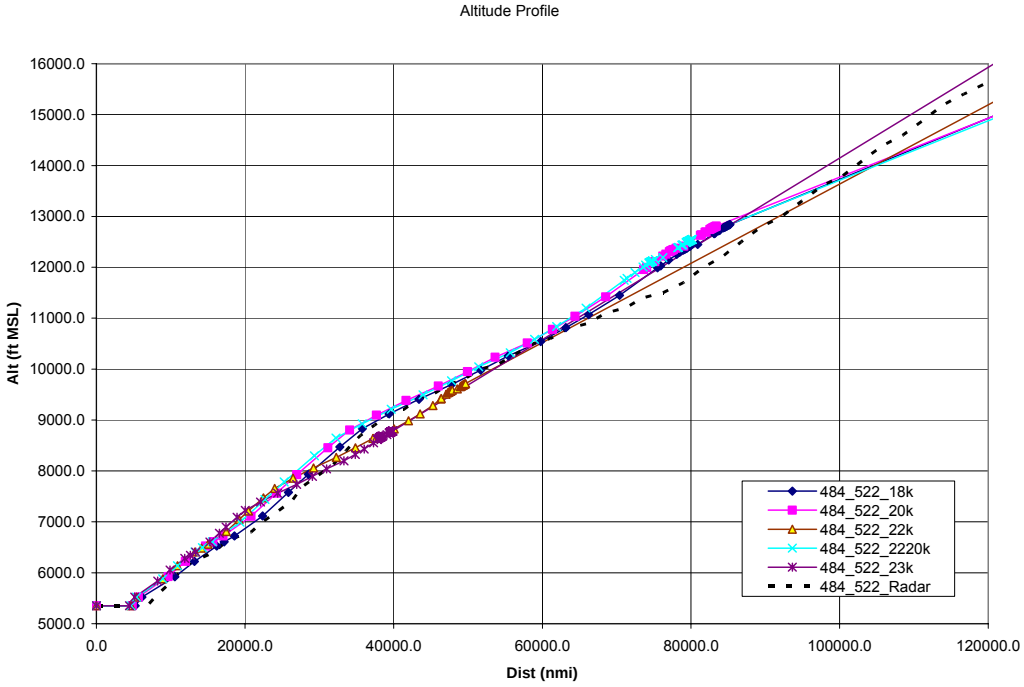


Figure 4-11b. 484.522 Altitude Profile

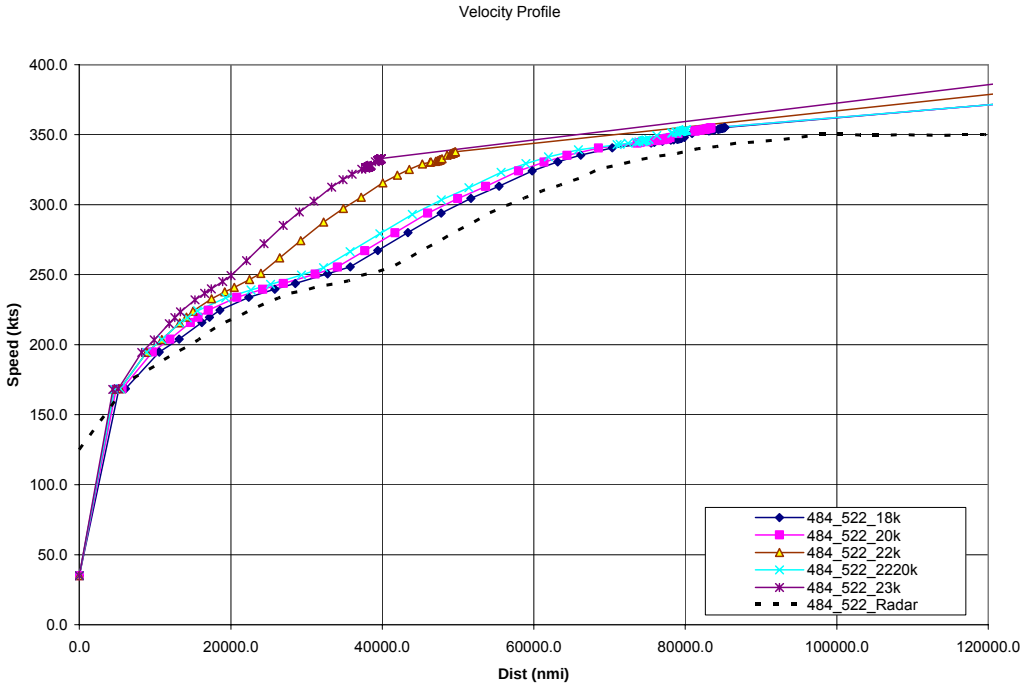


Figure 4-11c. 484.522 Velocity Profile

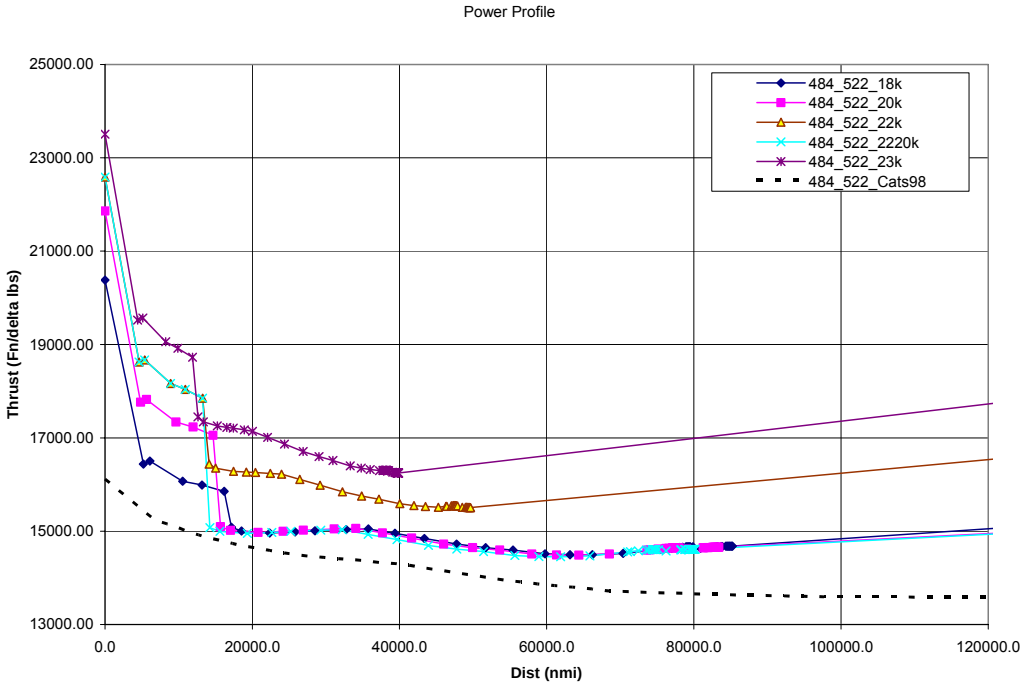


Figure 4-11d. 484.522 Power Profile

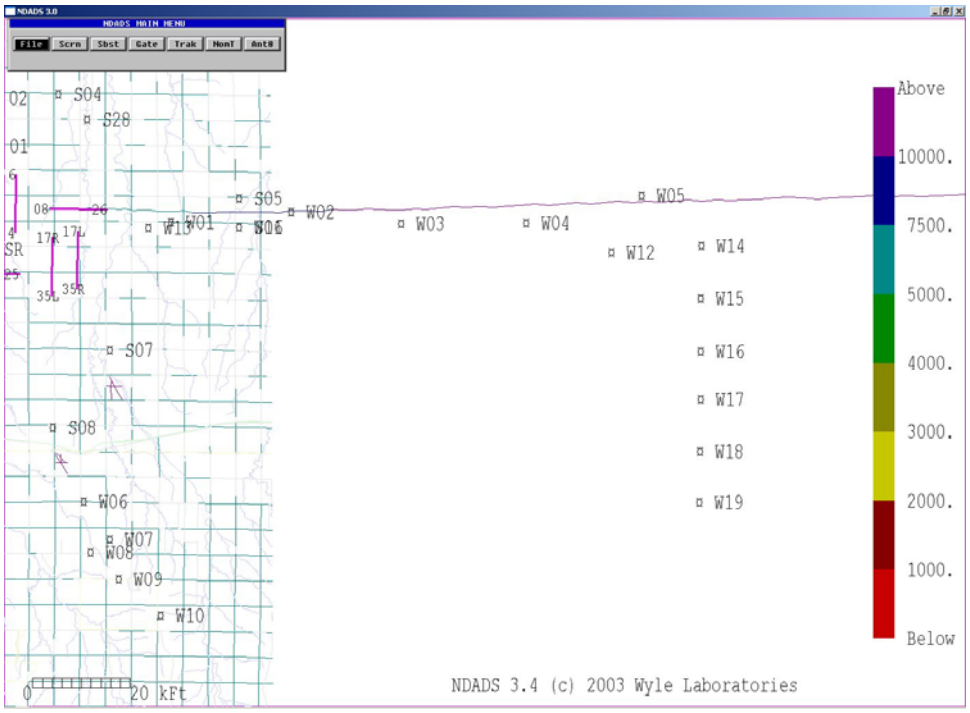


Figure 4-12a. 226.527 Ground Track

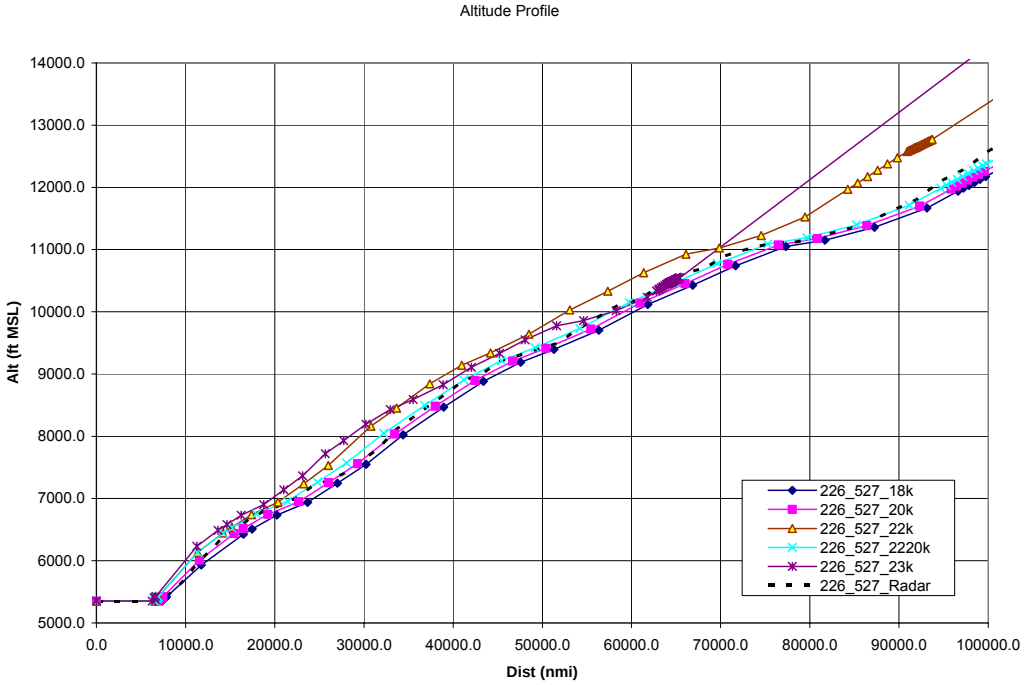


Figure 4-12b. 226.527 Altitude Profile

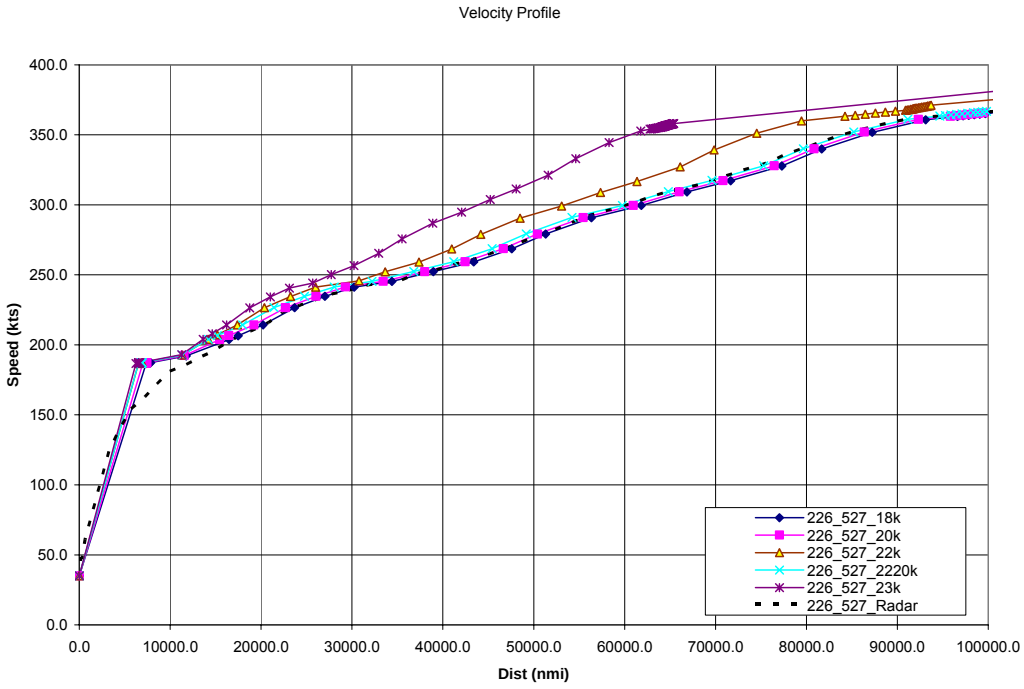


Figure 4-12c. 226.527 Velocity Profile

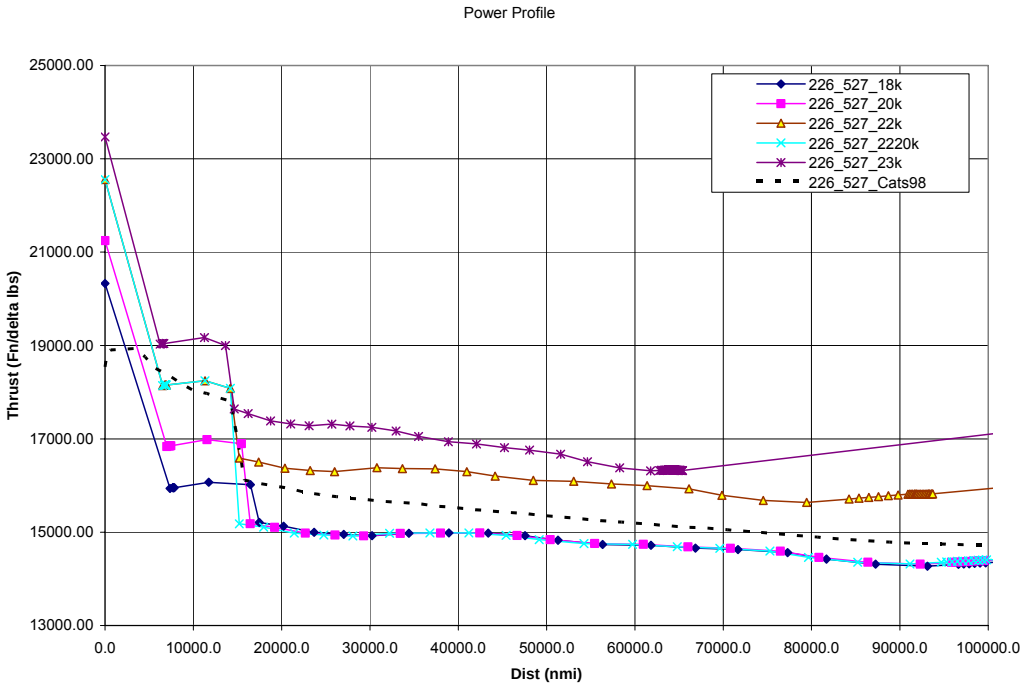


Figure 4-12d. 226.527 Power Profile

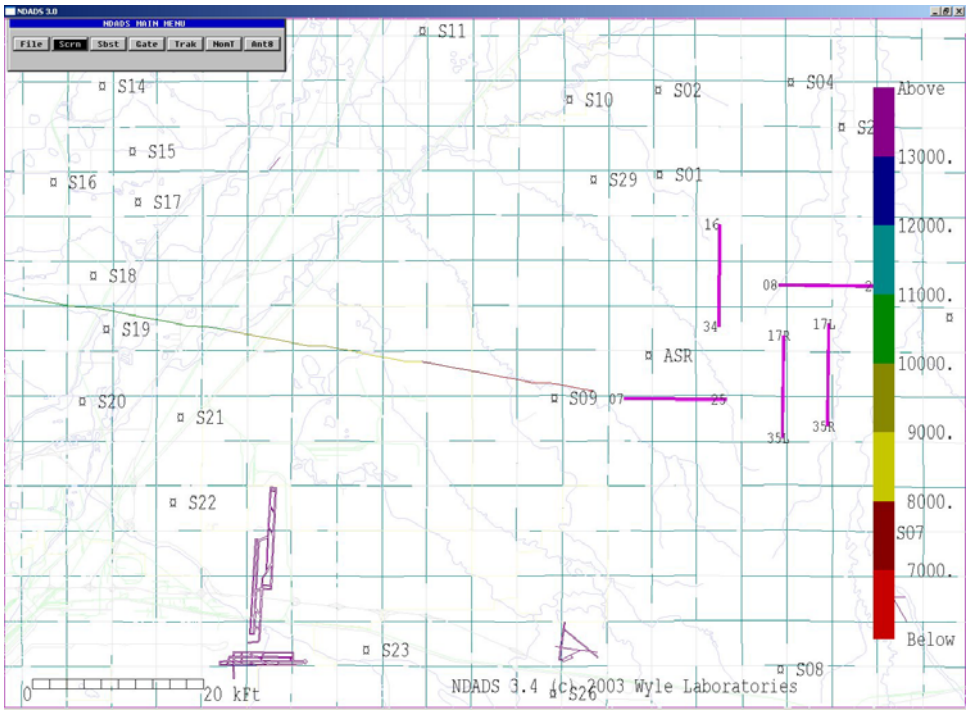


Figure 4-13a. 1801.523 Ground Track

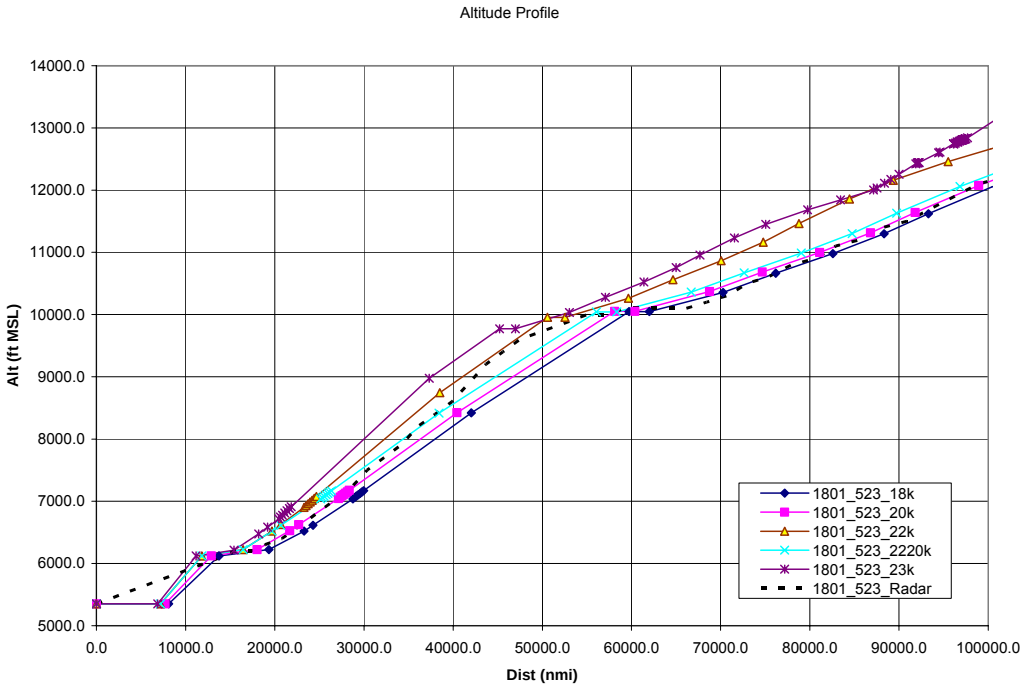


Figure 4-13b. 1801.523 Altitude Profile

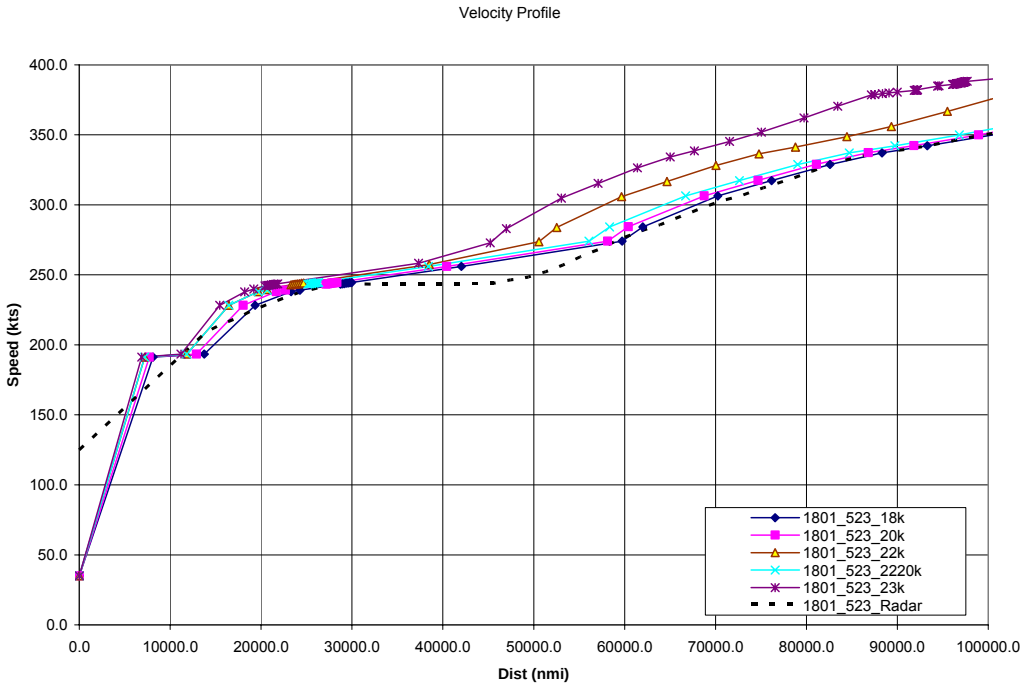


Figure 4-13c. 1801.523 Velocity Profile

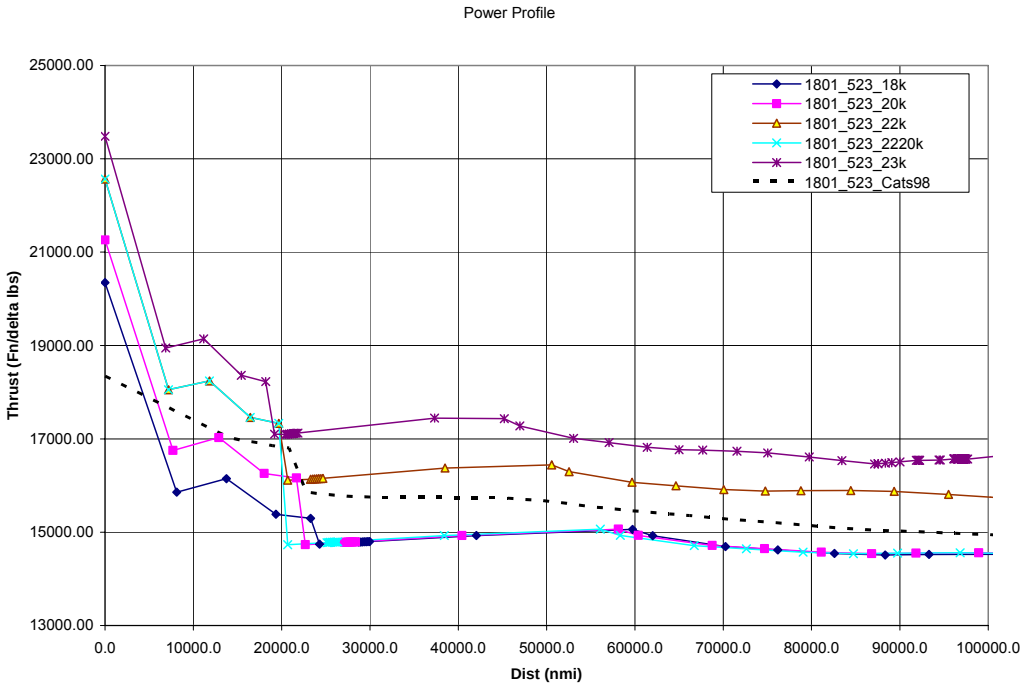


Figure 4-13d. 1801.523 Power Profile

4.3 Operations Not Modeled with INM

Some departures did not follow a typical departure trajectory for unknown reasons and included extended level flight segments or non-accelerating flight segments and even some descending and decelerating segments that could not be reasonably modeled and optimized with the automated procedure step builder. Examples of such operations were removed from the acoustic summary but some examples are shown below for illustrative purposes.

There were a total of 355 available B737 Flight tracks where a total of 910 noise monitoring events were successfully recorded. Each flight track was examined in person for each thrust rating. After viewing several hundred it became apparent that the energy error used to select the optimized thrust setting could serve to identify large discrepancies between the INM and radar profiles. The following equation was used to evaluate the potential & kinetic energy error at the point of closest approach:

$$[32.2 * abs(Z_{INM} - Z_{radar}) + 0.5 * abs((V_{INM})^2 - (V_{radar})^2)]^2$$

Equation 4-1

Of the 910 noise events, flight operations representing 78 flights (124 noise events) were removed from the study due to the inability to develop procedure steps. The mean (energy error)^2 of these removed events at the point of closest approach was 8.74 e+09. The mean (energy error)^2 of the final included noise events at the point of closest approach was 5.65 e+08. This gross difference is indicative of the fact that when the procedure steps don't match, they tend to rapidly diverge from the radar profile. Some typical examples of this are shown in Figures 4-14a to 4-15d.

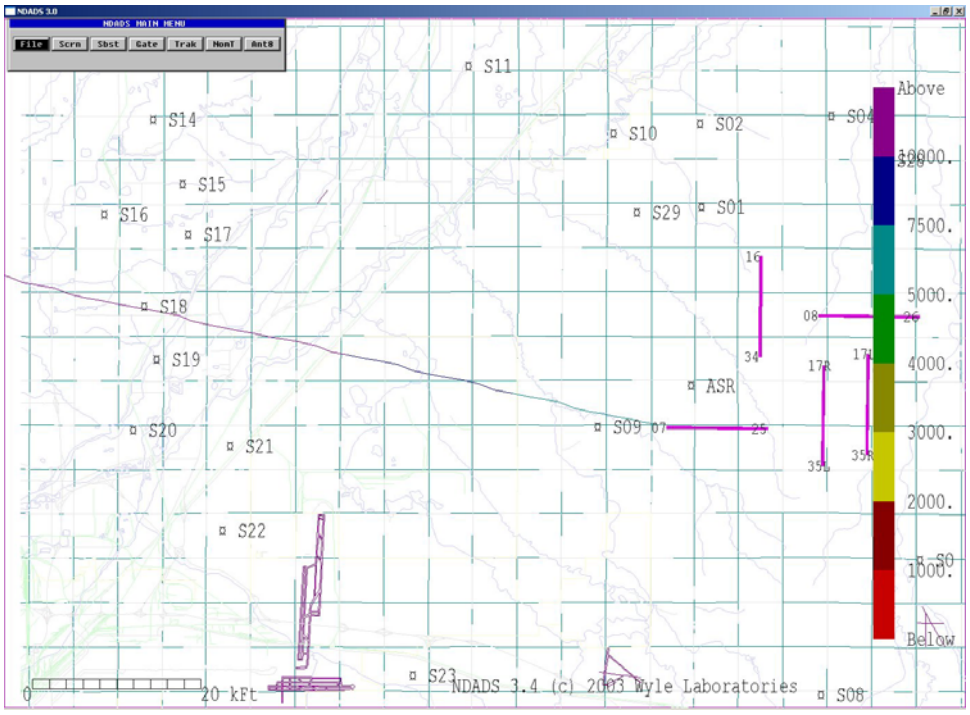


Figure 4-14a. Ground Track 385.528

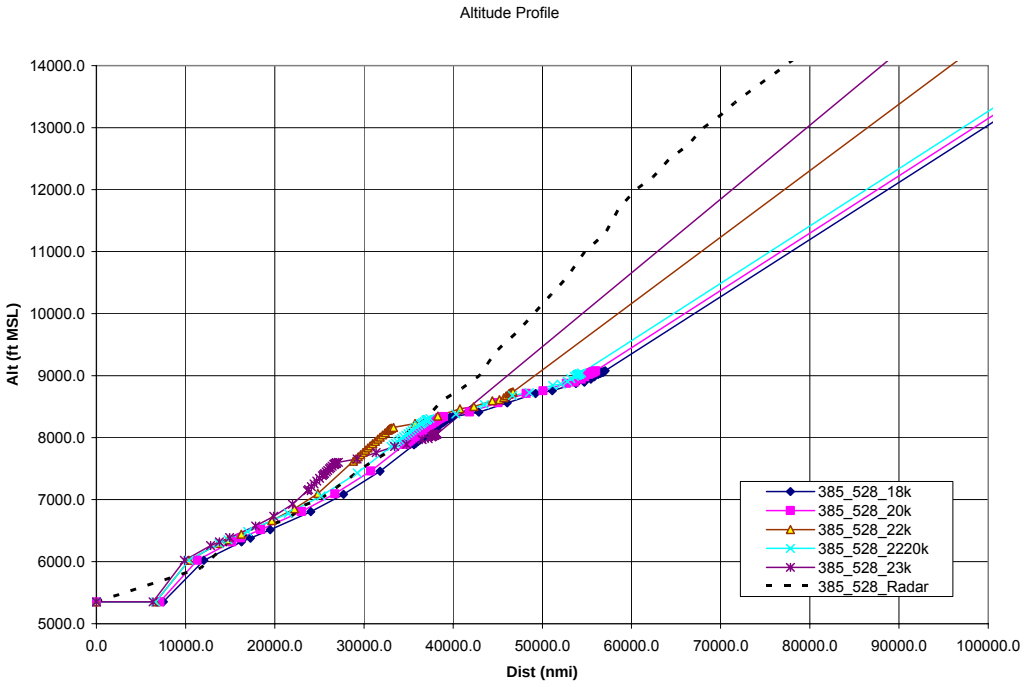


Figure 4-14b. Altitude Profile 385.528 Not Handled by the Automated Profile Builder

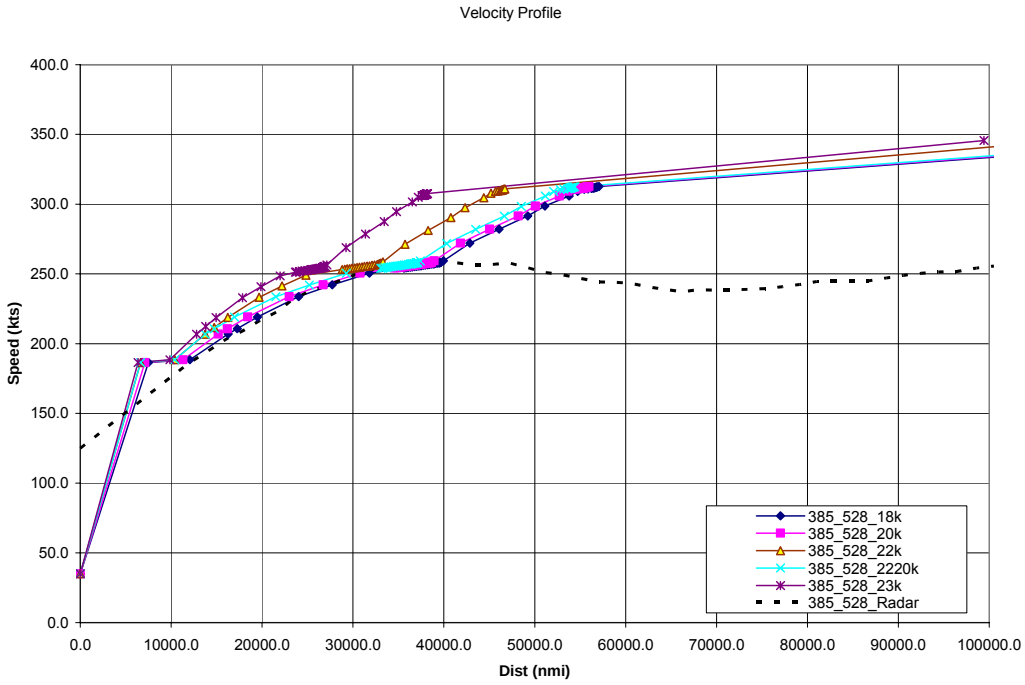


Figure 4-14c. Speed Profile 385.528 Not Handled by the Automated Profile Builder

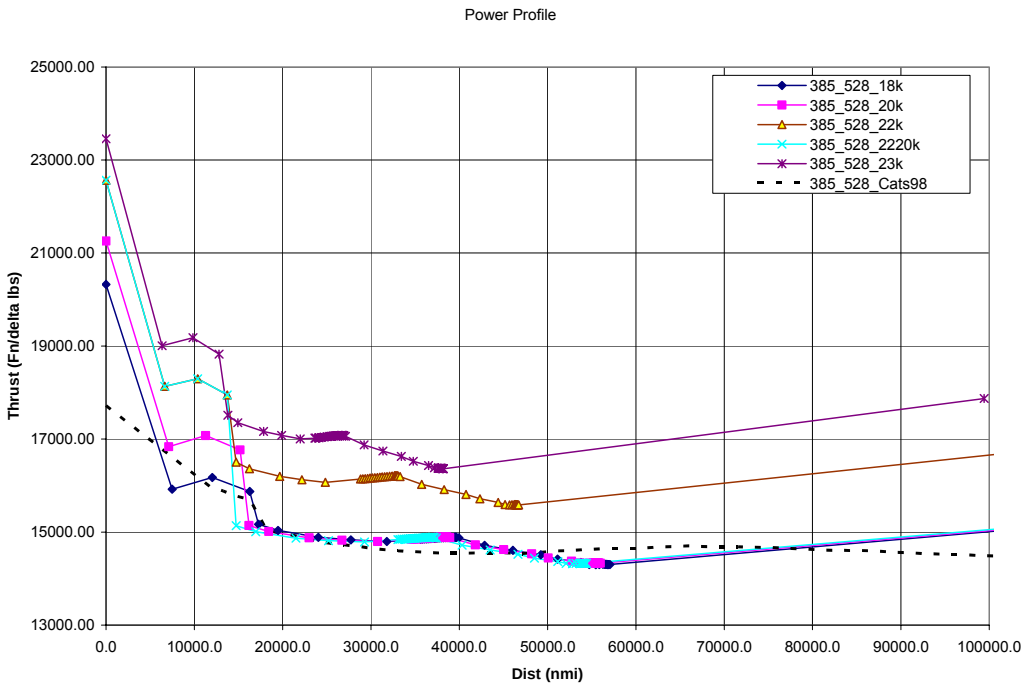


Figure 4-14d. Power Profile 385.528 Not Handled by the Automated Profile Builder

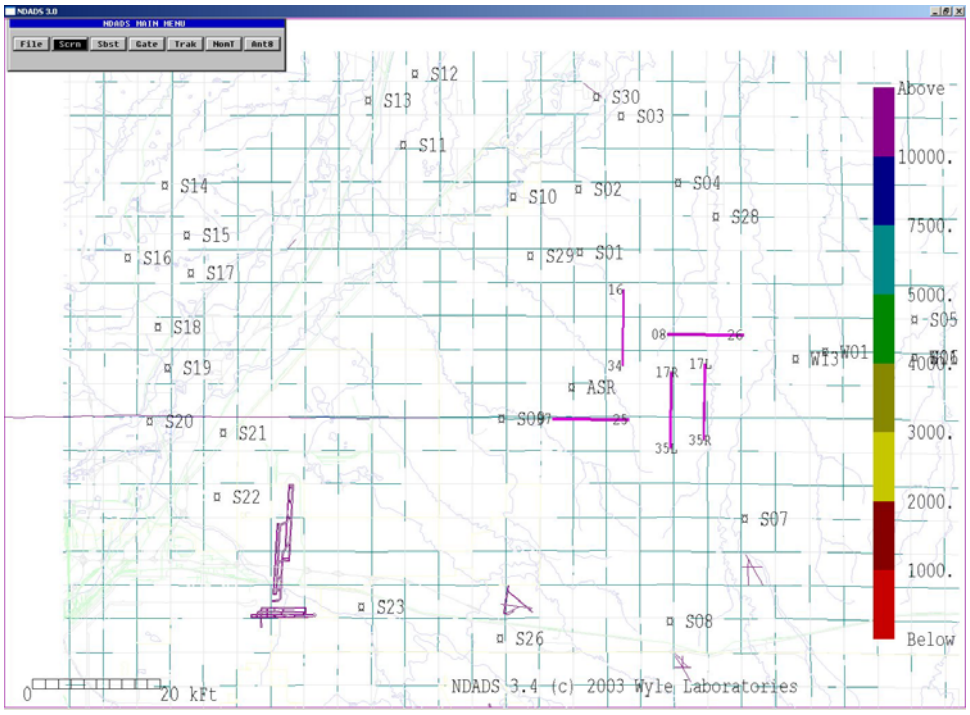


Figure 4-15a. 1845.525 Ground Track

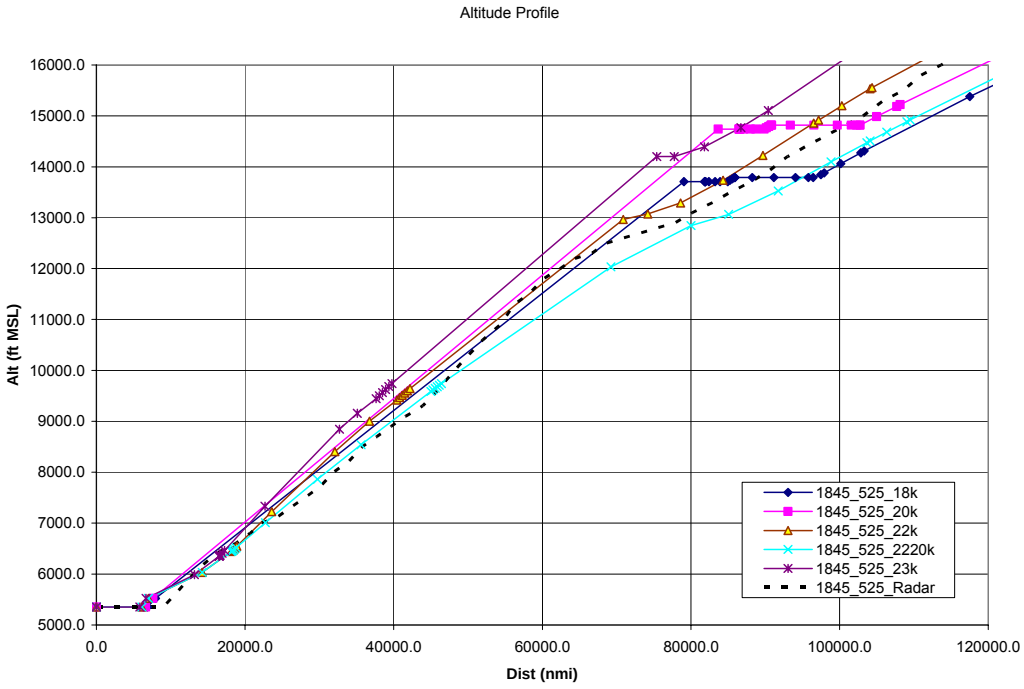


Figure 4-15b. Climb Profile 1845.525 Not Handled by the Automated Profile Builder

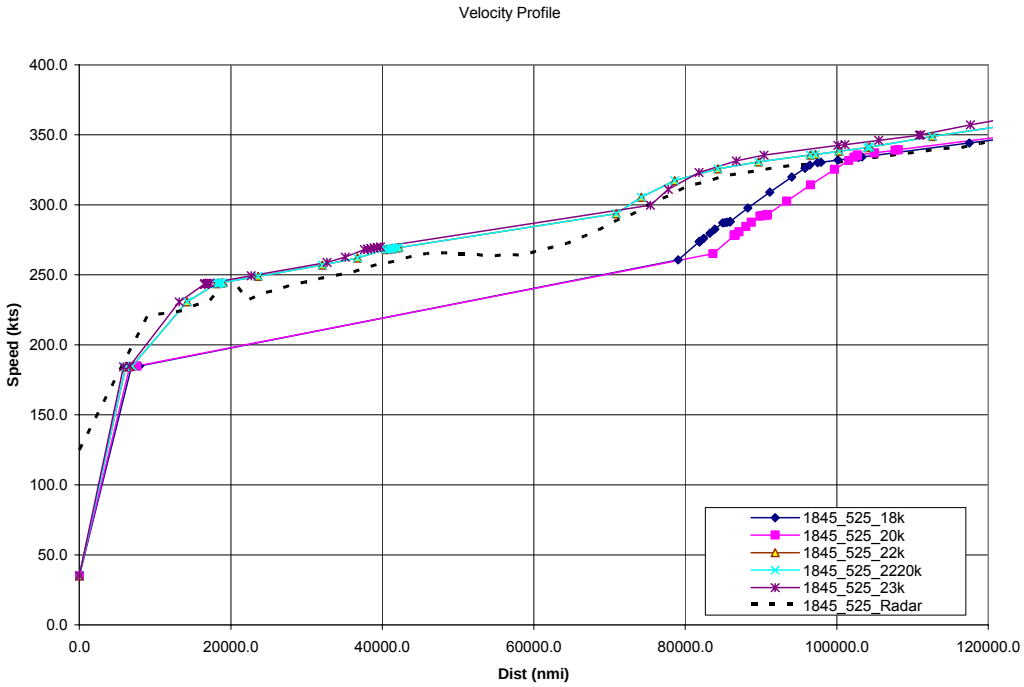


Figure 4-15c. Velocity Profile 1845.525 Not Handled by the Automated Profile Builder

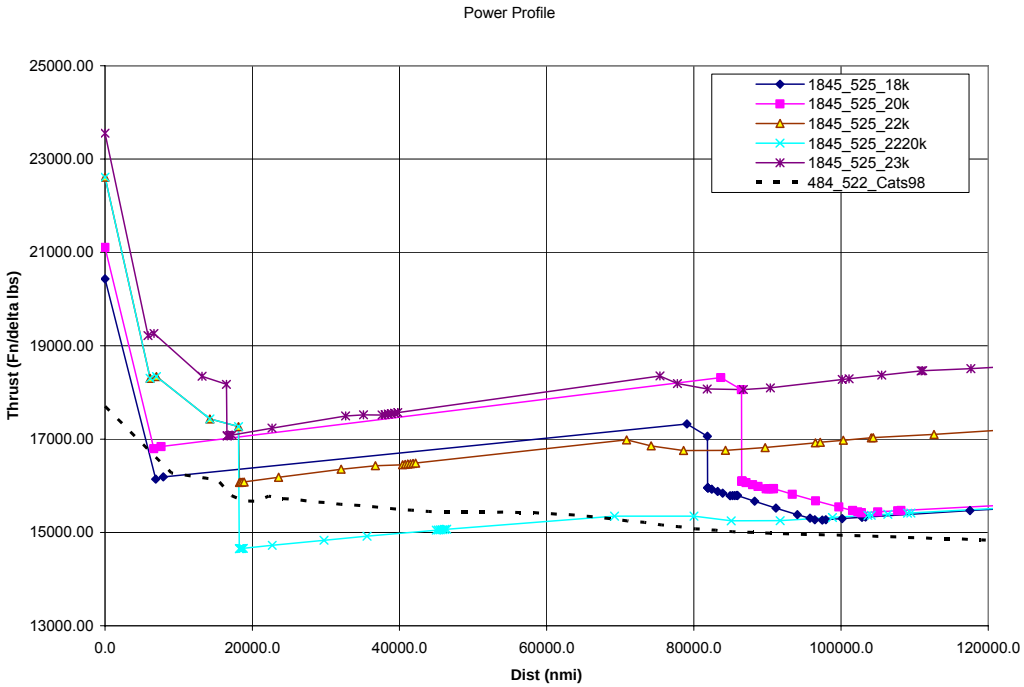


Figure 4-15d. Power Profile 1845.525 Not Handled by the Automated Profile Builder

5.0 Acoustic Results

After applying the thrust selection process described in Section 4.2, the INM predictions were made using INM 6.0c, INM 6.1, and INM 6.2. The noise results were compared with the measured SEL levels for a variety of independent variables. A summary of the overall results are given in Table 5-1. INM was executed using terrain for all analyses. Two versions of the noise–power-distance (NPD) curves were considered for all versions of INM. The procedure step profiles used were those optimized with INM 6.1. This constraint was driven by the availability of a batch version of the flight module only for INM 6.1. The new NPD curves (see Table 4-5) were also used with INM 6.0c and INM 6.2 with procedure step profiles. The 1998 study[1] modeled the profiles using point to point profiles and ground tracks based directly on the measured radar data and the thrust calculated using "power mode 6" using the CATS code (Appendix A). The full 1998 study included the aircraft types listed in Table 5-2, whereas the current study only analyzed in detail (and modeled using the automated procedure step generator) several variants of the Boeing 737. A subset of the 1998 data which included all 912 measurements from B737 aircraft was used to determine the corresponding mean prediction error and standard deviation shown in Table 5-1. A further sub-selection of the INM 5.2a and CATS results to the same 742 events is also given in Table 5-1. In the 1998 study the actual radar trajectories were input to INM. In the current study there were many profiles which could not be modeled using INM procedure steps.

Table 5-1. Acoustic Summary

INM 6.2 No SC New NPD	70% RH	INM 6.1 No SC New NPD	70% RH	INM 6.0 No SC New NPD	70% RH
AVG	-3.24	AVG	-3.24	AVG	-3.71
St. Dev	2.06	St. Dev	2.06	St. Dev	2.13
# Events	742	# Events	742	# Events	742
INM-Meas		INM-Meas		INM-Meas	
INM 6.2 SC on New NPD	RH by Flight	INM 6.1 SC on New NPD	RH by Flight	INM 6.0 SC on New NPD	RH by Flight
AVG	-2.34	AVG	-2.39	AVG	-2.81
St. Dev	2.04	St. Dev	2.05	St. Dev	2.15
# Events	742	# Events	742	# Events	742
INM-Meas		INM-Meas		INM-Meas	
INM6.2 SC on New NPD	64% RH				
AVG	-2.35				
St. Dev	2.05				
# Events	742				
INM-Meas					
INM 6.2 SC on New NPD	Day% Avg			INM 5.2 NoSC Old NPD	70% RH
AVG	-2.35			AVG	-5.83
St. Dev	2.05			St. Dev	2.55
# Events	742			# Events	742
INM-Meas				INM-Meas	
INM6.2 SC on Old NPD	RH by Flight			INM 5.2 NoSC Old NPD	70% RH
AVG	-3.43			AVG	-4.44
St. Dev	2.12			St. Dev	2.55
# Events	742			# Events	742
INM-Meas				INM-Meas	

Table 5-2. Aircraft Types Modeled in the Various Studies

Airframe	Engine	2005 Study Procedure Steps	1998 Study[1] CATS Mode 6
A319-100	V2522		●
A320-200	V2527		●
B727-Advanced	JT8D-15		●
B737-200	ADV-9A JT8D-9A		●
B737-200	ADV-17 JT8D-17		●
B737-222	STR-7 JT8D-7 & 7B		●
B737-300	(CFM 56-3 B1/C1-20K)	●	●
B737-300N	(CFM 56-3 B2-22K)	●	●
B737-500	(CFM 56-3 B1/C1-20K)	●	●
B757-200	PW2037		●
B767-200	JT9D-7R4D		●
B767-300ER	PW 4060		●
B777-200	PW4077		●
B777-200B	PW 4090		●
DC10-10	CF6-6D		●
DC10-30	CF6-50C2		●
DC10-30F	CF6-50C2		●

Linear regression analyses were performed on various independent variables and are presented in Figures 5-1 to 5-14.

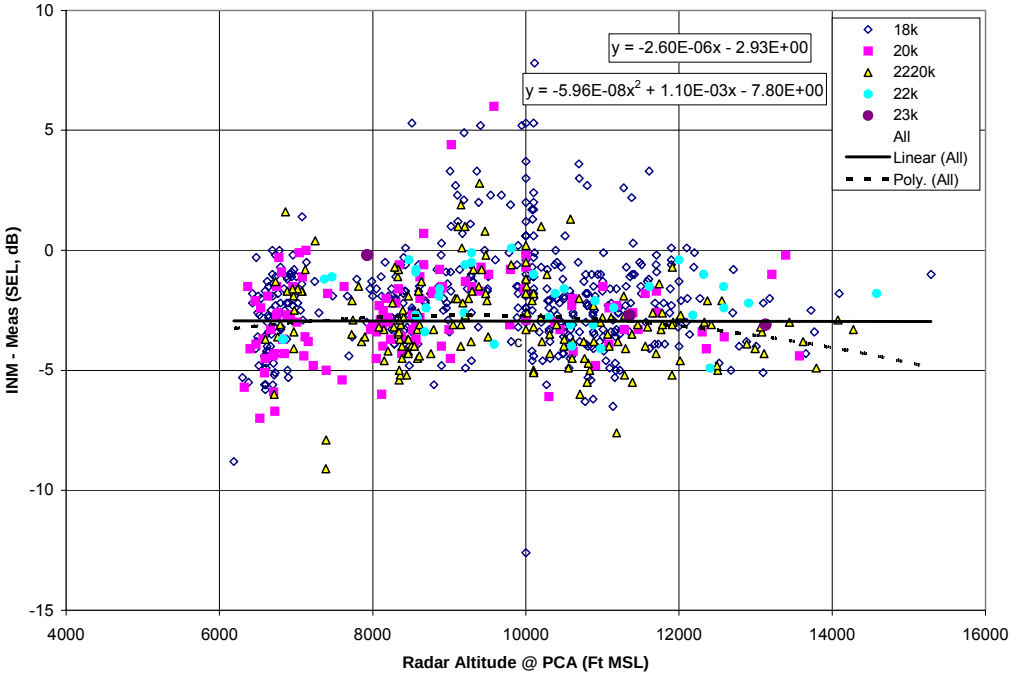


Figure 5-1. Prediction Accuracy – Altitude at the Point of Closest Approach

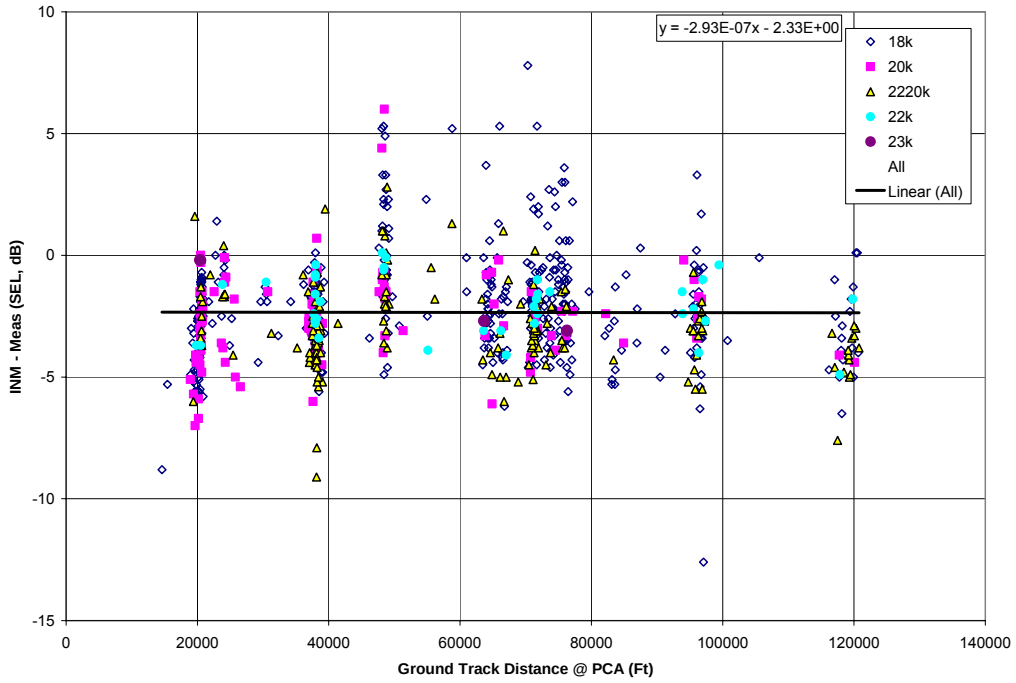


Figure 5-2. Prediction Accuracy – Ground Track Distance at the Point of Closest Approach

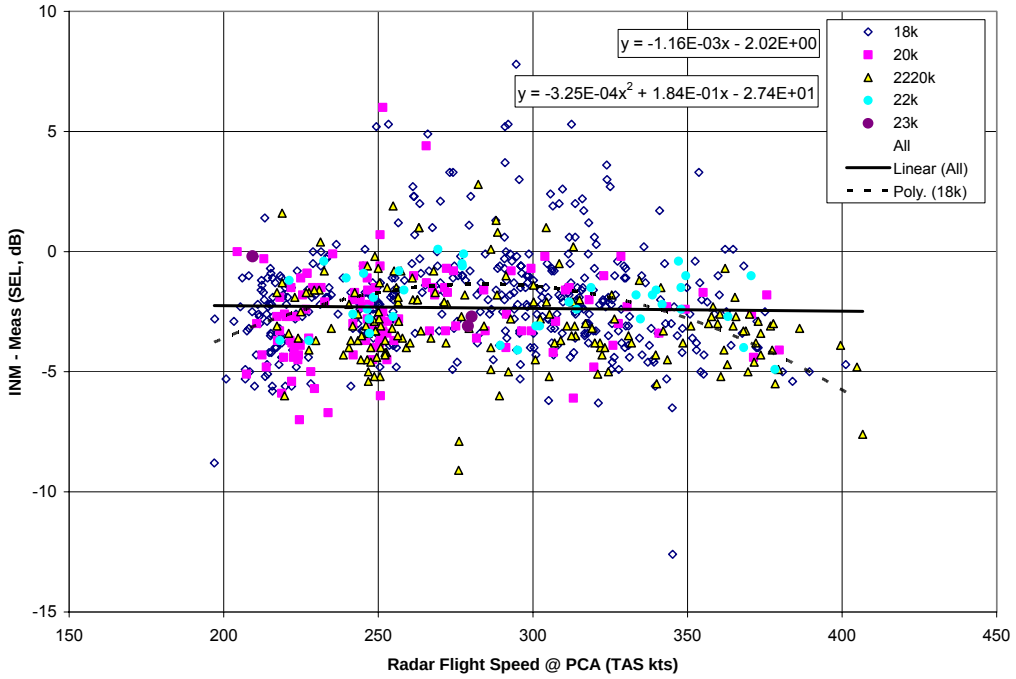


Figure 5-3. Prediction Accuracy – Radar Speed at the Point of Closest Approach

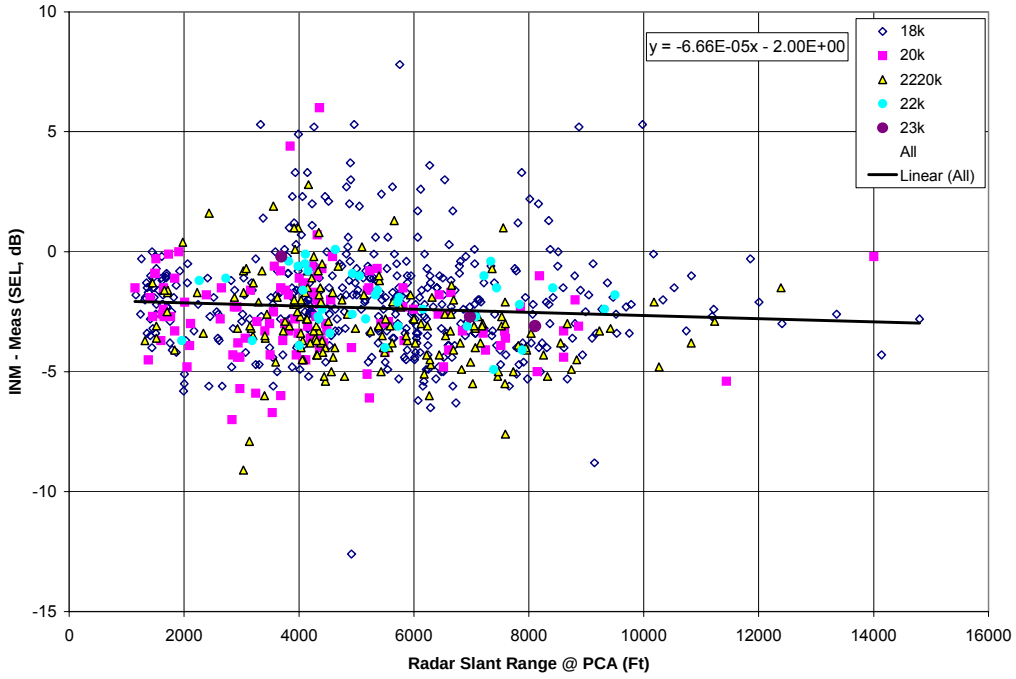


Figure 5-4. Prediction Accuracy – Slant Range to Radar Point of Closest Approach

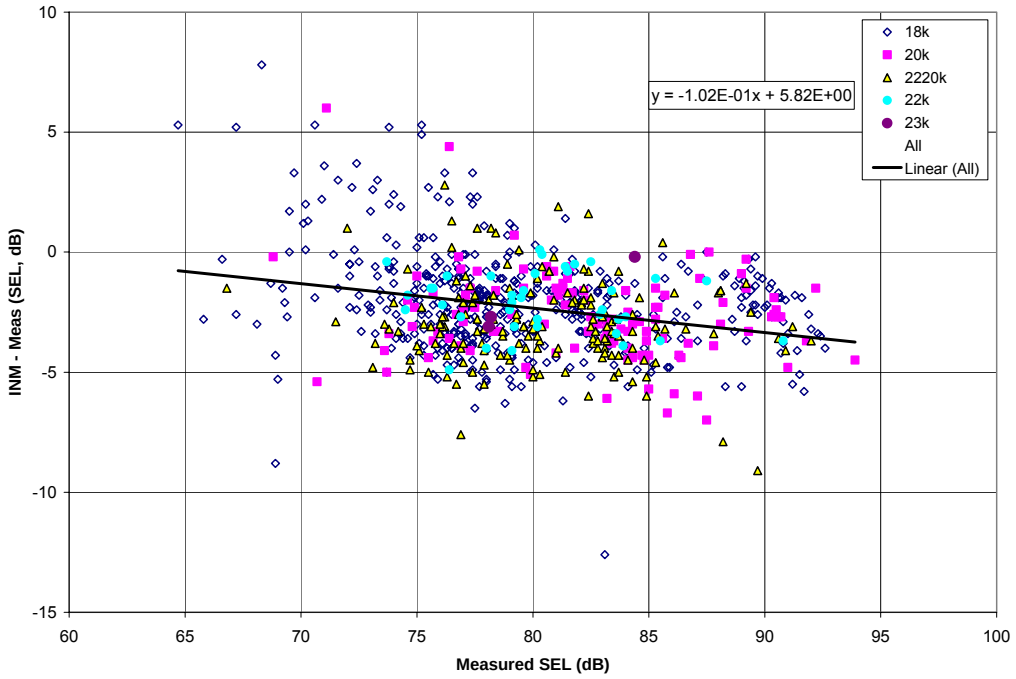


Figure 5-5. Prediction Accuracy – Measured SEL (dB)

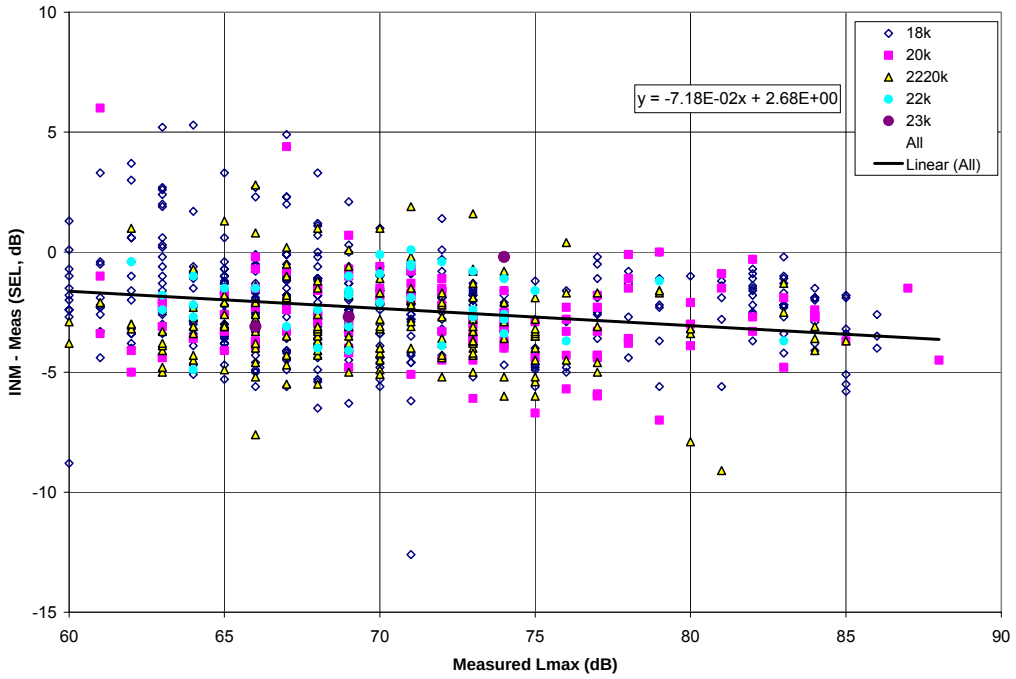


Figure 5-6. Prediction Accuracy – Measured L_{max} (dB)

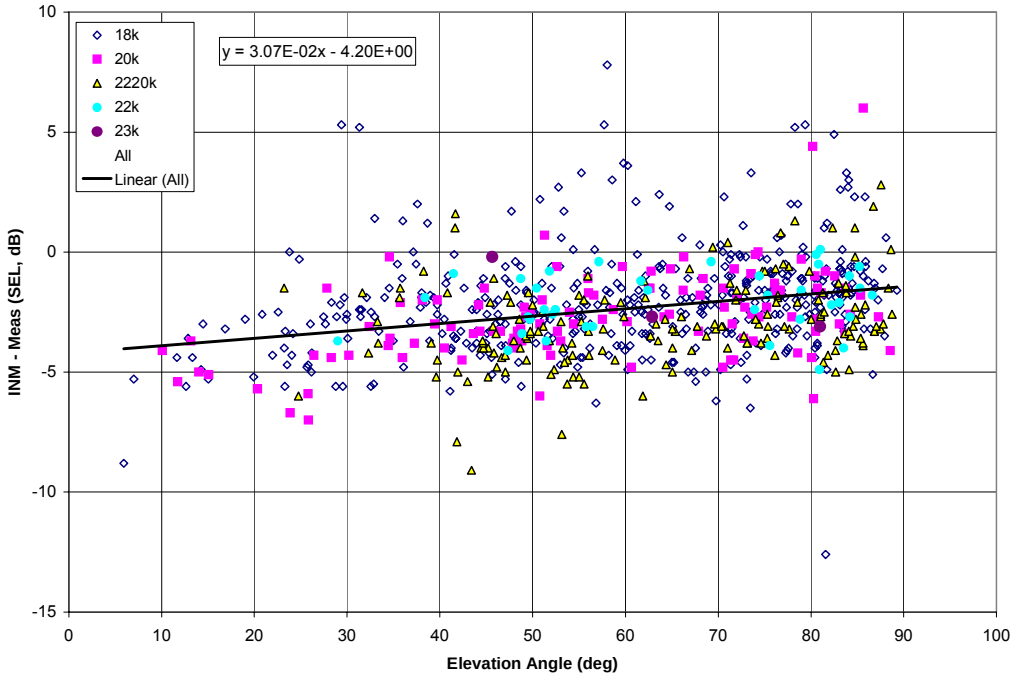


Figure 5-7. Prediction Accuracy – Elevation Angle (deg)

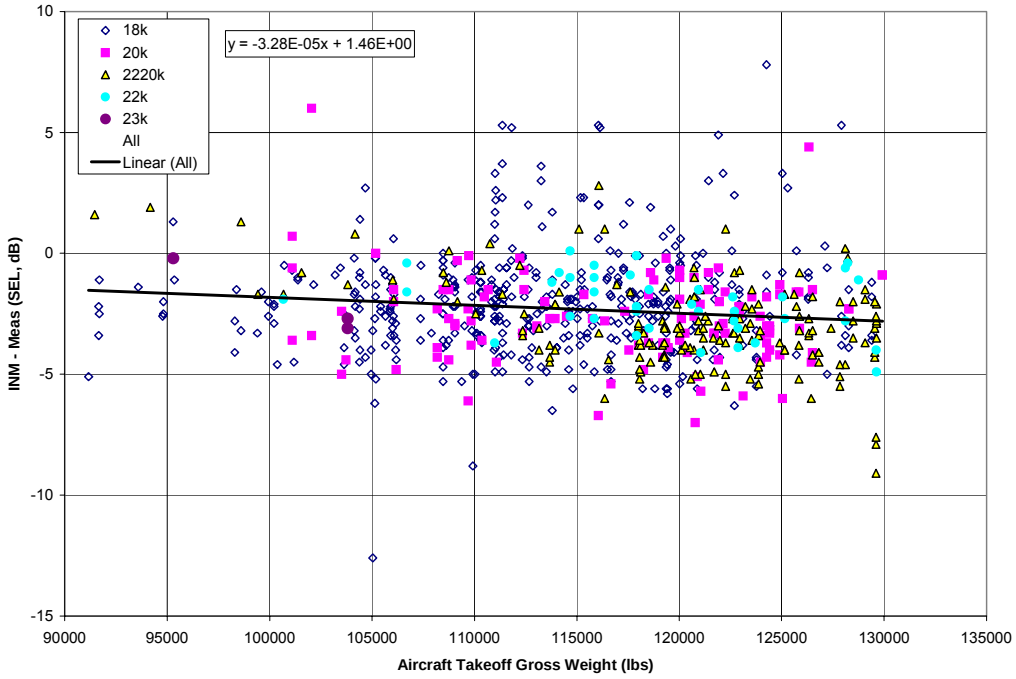


Figure 5-8. Prediction Accuracy – Takeoff Gross Weight (lbs)

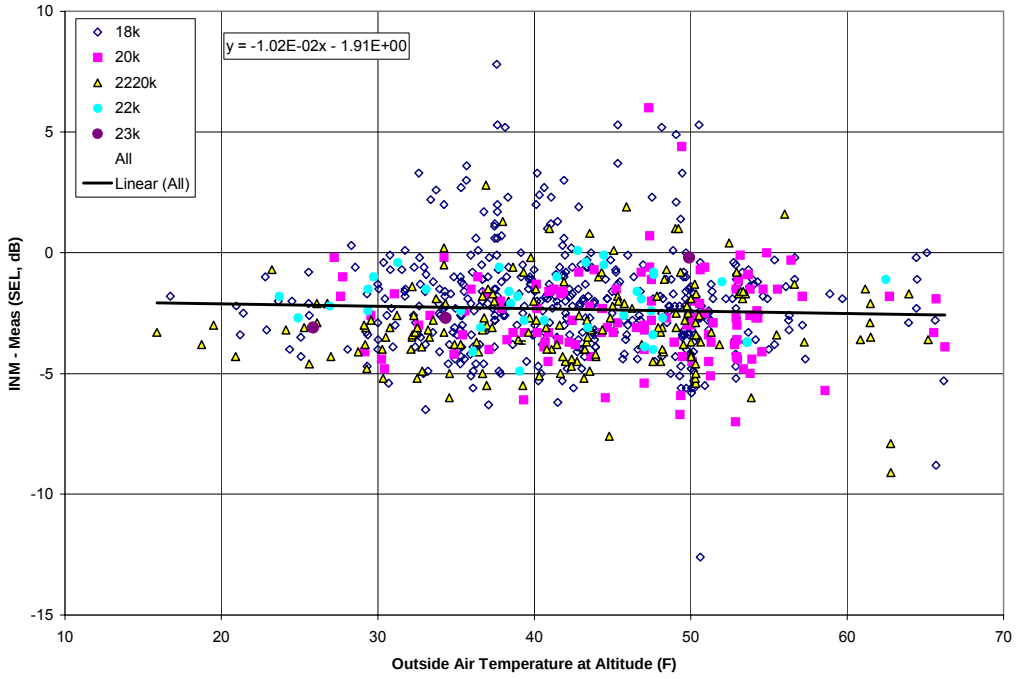


Figure 5-9. Prediction Accuracy – Outside Air Temperature at PCA (°F)

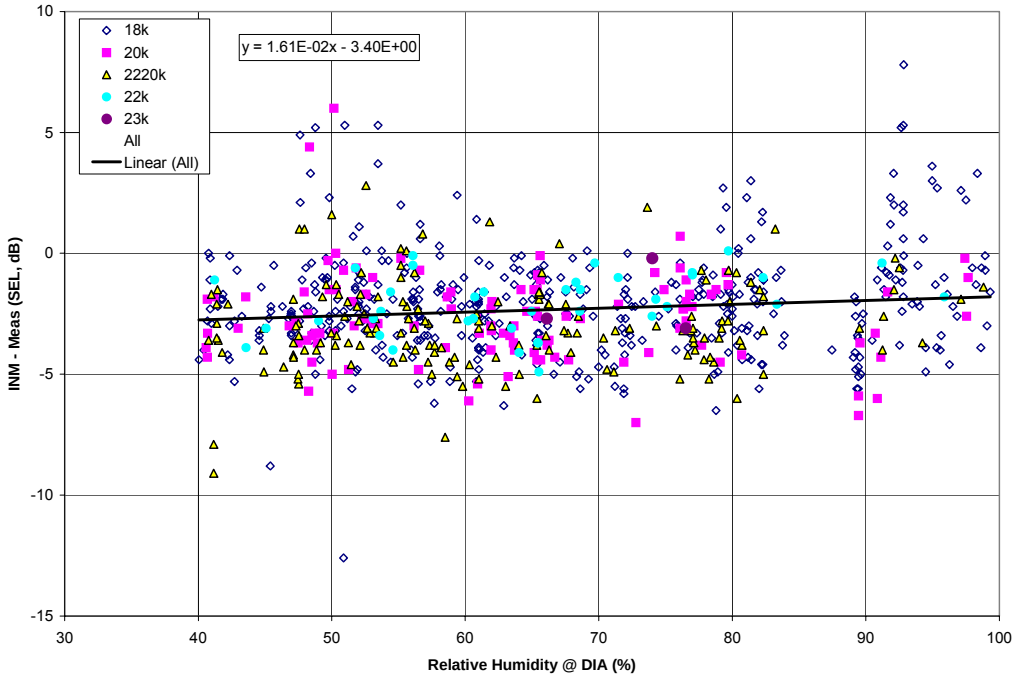


Figure 5-10. Prediction Accuracy – Relative Humidity at the Airport (%)

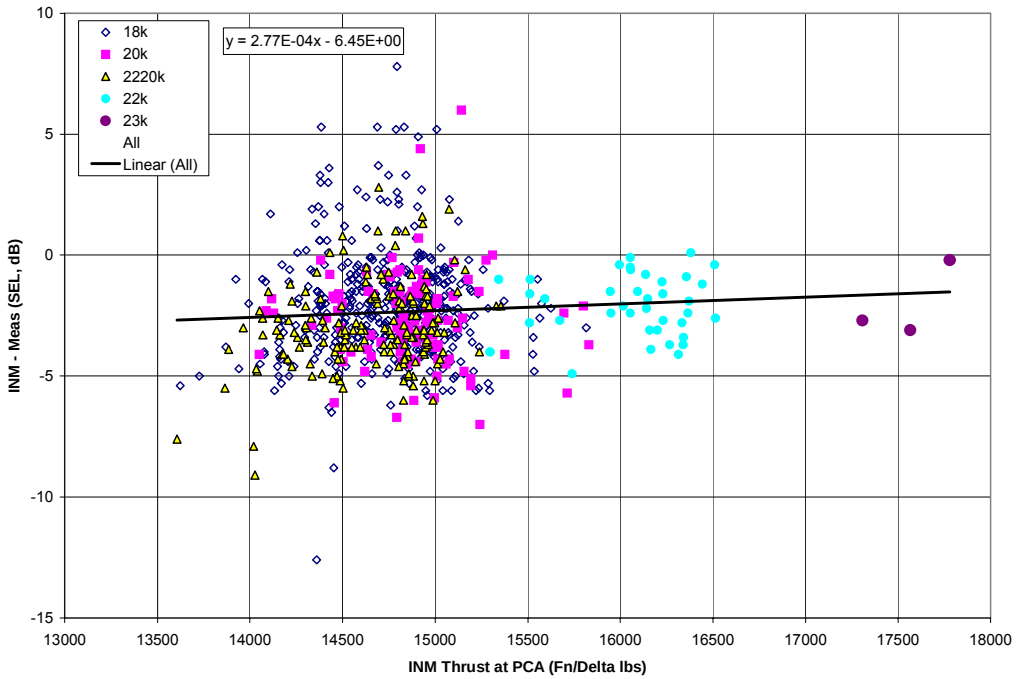


Figure 5-11. Prediction Accuracy – INM Thrust at the PCA (Fn/delta lbs)

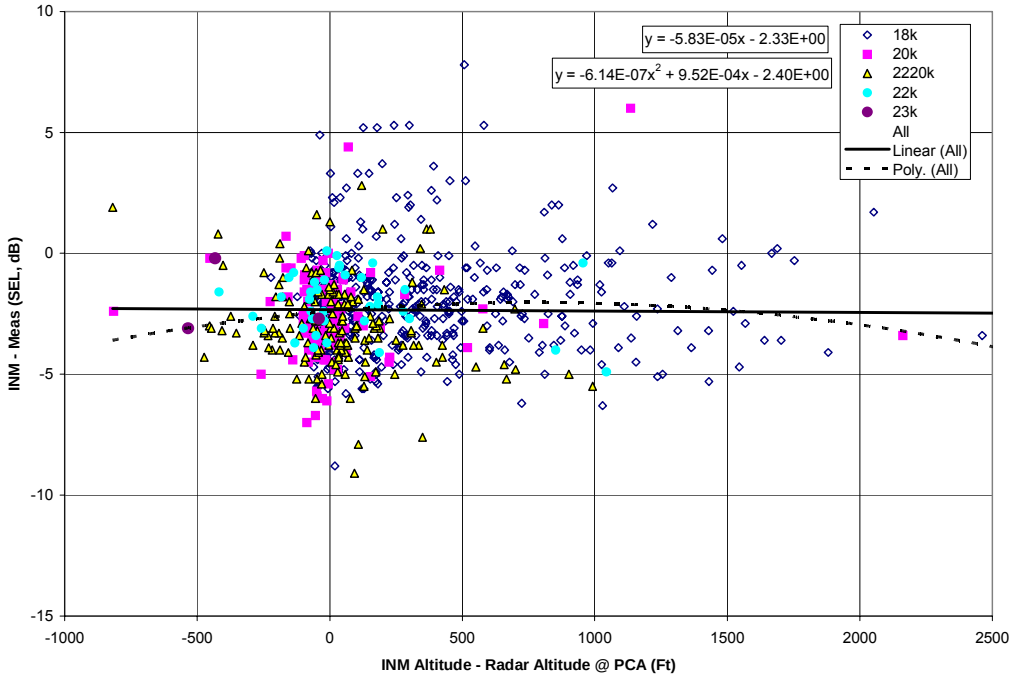


Figure 5-12. Prediction Accuracy – INM Altitude – Radar Altitude at PCA (Ft)

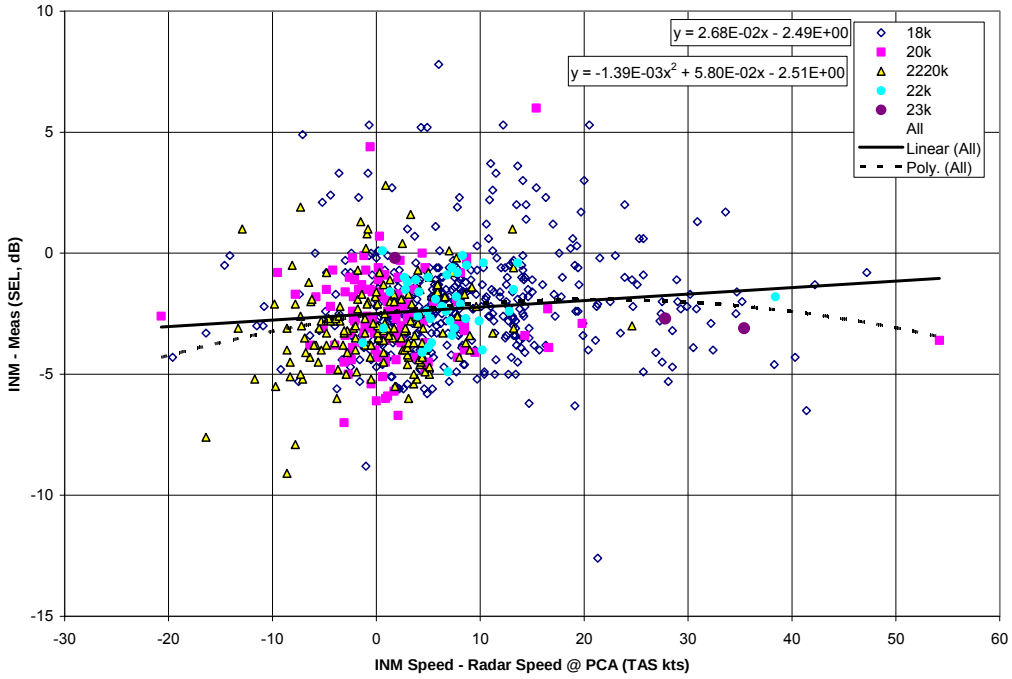


Figure 5-13. Prediction Accuracy – INM Speed – Radar Speed @ PCA (TAS kts)

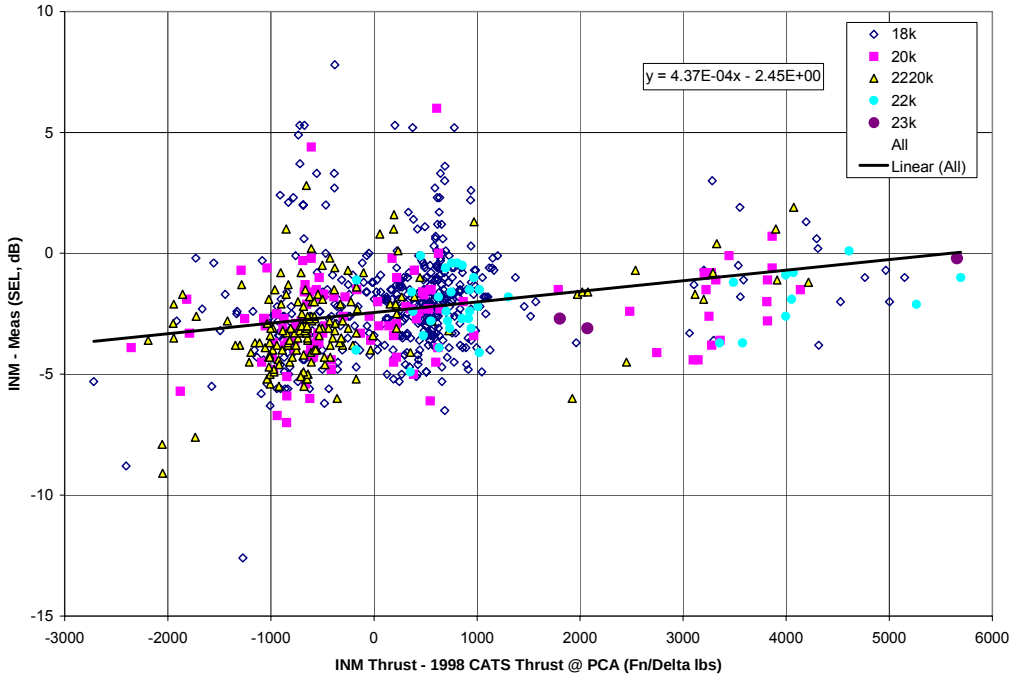


Figure 5-14. Prediction Accuracy – INM Thrust – 1998 CATS Thrust @ PCA (lbs)

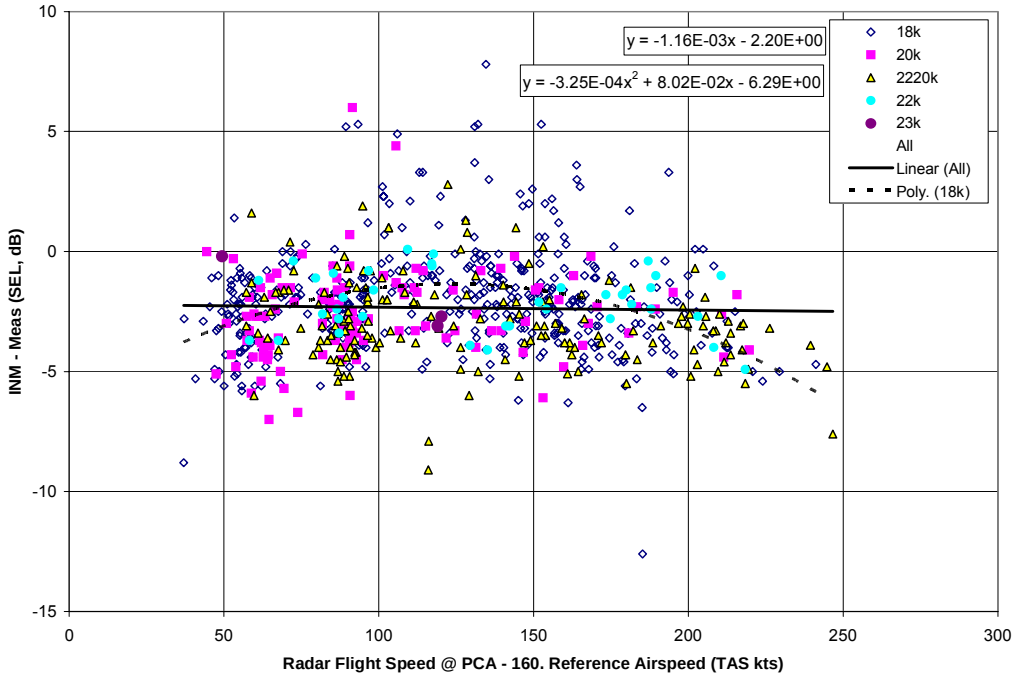


Figure 5-15. Prediction Accuracy – Flight Speed – 160 kt Reference Airspeed

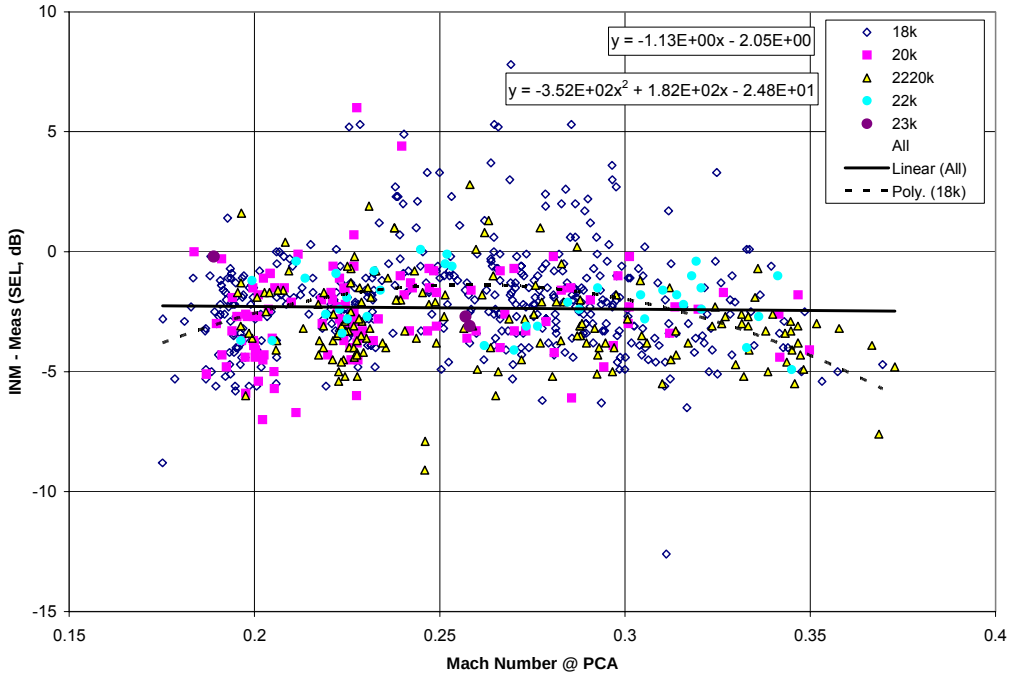


Figure 5-16. Prediction Accuracy – Mach Number at the Point of Closest Approach

6.0 Conclusions and Recommendations

As was shown in Table 5-1, there have been some significant changes in the INM noise predictions since the 1998 Denver Study[1]. For the common set of 742 measurement events, there has been a reduction by 3.49 dB in the mean underprediction between the 1998 (INM 5.2) analyses (-5.83 dB mean) and the best available 2006 (INM 6.2) analysis (-2.34 dB mean). This improvement is due to a combination of incremental changes in:

- aircraft performance and flight profile modeling changes
- improvements to the NPD curves
- changes to the lateral attenuation algorithms in INM
- inclusion of a spectral class absorption/relative humidity capability

In 1998, INM was run using integrated point to point profiles and flight tracks which guaranteed that the aircraft was positioned exactly at the measured radar location. It has been shown in the report that the procedure steps used to model the operations did not result in INM flight trajectories exactly coincident with the measured radar data.

NPD curve changes account for an improvement by 1.09 dB. This is evidenced by comparison using INM 6.2 and changing only the NPD data (-2.34 vs. -3.43 dB).

The effects of absorption modeling were calculated using INM 6.2. The standard SAE-ARP866A absorption is obtained by unselecting the spectral class adjustments, which yielded a mean underprediction of -3.24 dB. Enabling the spectral class adjustments and using the airport recorded humidity, interpolated to the actual departure time, revealed an improvement of 0.90 dB, yielding an underprediction of only -2.34 dB. A sensitivity analysis of INM 6.2 humidity input fidelity showed negligible changes when using humidity by flight (-2.34 dB), by day (-2.35 dB) or by overall average humidity for all flights (-2.35 dB). Switching from the old SAE866A method to the new spectral class method provided the most dramatic improvements.

Improvements in the incremental versions of INM (6.0, 6.1, and 6.2) showed a consistent reduction of the underprediction of the selected 742 noise events modeled. For all three versions of INM the identical procedure steps were input. Due to incremental changes in the flight segment generation module of INM, there were slight differences in the resultant INM flight paths. Using SAE 866A absorption, changing from INM 6.0 to 6.1 yielded a 0.47 dB improvement (-3.71 vs. -3.24 dB) while changing from INM 6.1 to 6.2 yielded no improvement (-3.24 vs. -3.24 dB). However, when the spectral class absorption methodology was enabled the prediction improvements were distributed slightly differently. INM 6.0 to 6.1 yielded a 0.42 dB improvement (-2.81 vs. -2.39 dB) and INM 6.1 to 6.2 provided a slight 0.5 dB improvement (-2.39 vs. -2.34) with spectral class calculations enabled.

As in the prior analysis1, a strong effect of slant range is shown to affect the prediction accuracy (Figure 5-4). There is also a clear sensitivity to elevation angle (Figure 5-7). Improvements have been made to the lateral attenuation algorithms since INM 5.0c. These remaining elevation angle differences could be in part due to aircraft directivity not included in the source model of INM.

The sensitivity of the prediction error (INM - measurement) with the difference between the INM procedure step altitude and the measured radar altitude is shown in Figure 5-12. The polynomial regression,

$$y = (-6.14*10^{-7})x^2 + (9.52*10^{-4})x - 2.40$$

shows three orders of magnitude difference between the linear coefficient ($9.52*10^{-4}$) and the x^2 term coefficient ($6.14*10^{-7}$). The sensitivity of the prediction error with the difference between the INM procedure step speed and the measured radar speed is shown in Figure 5-13. In this case, the polynomial regression,

$$y = (-1.39*10^{-3})x^2 + (5.80*10^{-2})x - 2.51$$

shows about a half order of magnitude difference between the linear coefficient ($5.80*10^{-3}$) and the x^2 term coefficient ($-1.39*10^{-3}$). This stronger relationship for the velocity than the altitude effects suggests that the modeling accuracy is more sensitive to matching the flight speed than the altitude. In regions where the velocity difference between INM and radar exceeds -10 or +30 knots, the most likely cause is a mismatch between the modeled thrust rating and the as-flown thrust. Another possible source of error may be the effects of flight speed and duration adjustments on integrated SEL levels. The duration adjustment for exposure based metrics in INM is given in the technical manual[3] as:

$$DUR_{ADJ} = 10\log_{10}(160/AS_{SEG})$$

where AS_{SEG} is the aircraft speed at the point of closest approach for the segment. The linear regression shown in Figure 5-3 indicates an increase in error with increasing flight speed. Figure 5-15 shows the prediction error with 160 kt reference airspeed subtracted from the radar airspeed at the point of closest approach. A third possible source of error is the absence of INM including any additional noise sources that might appear for high altitude, high speed operations, such as shock cell noise. Figure 5-16 shows the prediction accuracy as a function of Mach number at the radar point of closest approach.

Recommendations for future analyses include the following:

- Measurement of the noise source characteristics from aircraft operating at higher altitudes and flight speeds. The NPD curves are obtained by extrapolating certification data which has been corrected to sea level standard day conditions. Certification data is typically measured within a few thousand feet of the aircraft and the aircraft operating at nominally sea level conditions. Any changes in the noise source characteristics when operating at higher altitudes and flight speeds are not included in INM.
- Assessment of reduced thrust procedure step departures from other aircraft types. This study included only Boeing 737 flights and utilized INM jet coefficients developed specifically for B737 reduced thrust operations. A 1.2 dB effect is evident in the 1998 Study (-4.44 dB versus -5.83 dB) when comparing multiple aircraft types with just 737 aircraft. It is not clear why the 737 modeling was less accurate than the other aircraft types in 1998. Furthermore, it would be useful to understand if that trend holds true of other aircraft if using the INM procedure step modeling approach.
- Improvements to the automated INM procedure step builder process. A significant amount of time was spent developing the software to create profiles using INM procedure steps. In the interest of the scope of the current contract several simplifications were made to the iterative process, primarily because the introduction of more independent variables caused instabilities in the procedure step convergence process.
- Assess the impact of the thrust split on the profile matching process and determine the Lift to Drag for a given climb segment. No attempts were made to 'trick' INM into using a different thrust split. Some of the radar flight profiles contained segments with more aggressive climb segments containing constant or even decelerating flight speeds.

Acknowledgements

The author would like to thank David Forsyth for his excellent technical support and stimulating discussions detailing aircraft flight performance.

References

1. Page, Juliet A., et al."Validation of Aircraft Noise Prediction Models at Low Levels of Exposure", NASA CR-2000-210112, April 2000.
2. "Integrated Noise Model (INM) Version 5.0 User's Guide", FAA-AEE-95 01, August 1995.
3. "Integrated Noise Model (INM) Version 6.0 Technical Manual", FAA-AEE-02-01, January 2002.
4. Forsyth, D.W., Guilding, J., DiPardo, J., "Review of Integrated Noise Model (INM) Equations and Processes", NASA CR-2003-212414, May 2003.
5. "Air Traffic Training Publication N-9, NAS Operational Equipment, ARTS III", Air Traffic Branch, Federal Aviation Administration Academy, March 1973.
6. "ARTS III, Collection and Editing System (ACES) for Noise Monitoring, Technical Reference and User's Manual", Dimensions International, Inc., February 1994.
7. Fleming, G.G., et al., "Integrated Noise Model (INM) Version 5.1 Technical Manual", Report No. FAA-AEE-97-04, December 1997.
8. Page, Juliet A., "Noise Data Acquisition and Display System (NDADS3) User's Guide and Tutorial", AFRL-HE-WP-TR-2004-0068, May 1999.
9. Plotkin, Kenneth J., et al, "Examination of the Lateral Attenuation of Aircraft Noise", NASA/CR-2000-210111, April 2000.
10. "Procedure for the Calculation of Airplane Noise in the Vicinity of Airports", SAE AIR 1845, March 1986.
11. "Boeing Climbout Program (BCOP)", Presentation to the Airlines at the Boeing Performance and Flight Operations Engineering Conference, September 2003.
12. Society of Automotive Engineers, Aerospace Recommended Practice, "Standard Values of Atmospheric Absorption as a Function of Temperature and Humidity," SAE ARP 866A, March 1975.

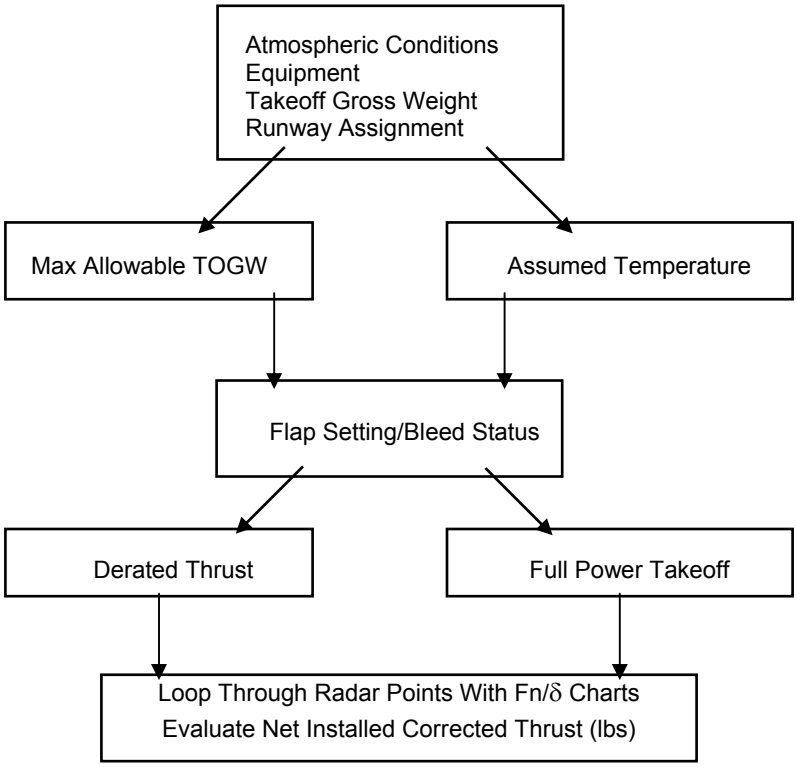
APPENDIX A

Summary of the CATS (Climb and Throttle Scheduler) Code Thrust Calculation Procedure

A.1 Departure Thrust Prediction Based on Operational Procedures

A performance prediction method was used for evaluating the departure throttle settings. This methodology is based heavily on pilot training procedures developed by United Airlines. In order to predict throttle settings, additional data is required for each flight. This data, including exact airframe/engine equipment usage, takeoff gross weight, and atmospheric data, is required. For this project, only commercial flight departure operations FROM United and Delta Airlines were considered. Table A-1 contains a flowchart of the performance prediction process.

Table A-1. Takeoff Thrust Prediction Methodology Flowchart



The prediction of thrust for a given commercial aircraft departure requires knowledge of local airfield atmospheric conditions. The pilot decisions regarding details of the departure procedures is based on local weather reporting station information, updated at least hourly, or as required by changing local conditions. Key information from an aircraft performance perspective is Outside Air Temperature (OAT) and atmospheric pressure. Engine performance is affected significantly by changes in both airfield temperature and pressure. These effects are even more critical for operations from a high-altitude airport such as DIA. Data from the weather services were interpolated linearly to the departure time for the thrust prediction process.

Actual equipment usage, such as the exact airframe and engine models used for the flight, are also required. This data, obtained directly from the airlines, allowed a more exact knowledge of performance capabilities of the particular aircraft. The radar interfacility message stream contains only four character descriptors for the aircraft type. As such, the particular model and engine type are not identified. Also, airlines occasionally make equipment substitutions after the initial automatic flight plan has been logged into the ARTS system. The airline information obtained for this study contains factual historical information from the maintenance records.

Another key parameter required for takeoff thrust prediction is the takeoff gross weight of the aircraft. As with the equipment usage, FAA mandates require all airlines to log such information. This database was also received for the measurement period for United and Delta Airlines departures.

Runway assignment was based on the actual radar track, as variable wind and traffic conditions often dictate last-minute departure changes. Assignments considered the direction and location of the departing flight and the available runways. This information evaluated in the radar processing phase was stored in the output powered flight track and profile RAT file.

Assessment of the Maximum Allowable TOGW was based on the tables provided by the airlines for each airframe/engine combination on all available runways. Detailed performance analyses completed in-house at the airlines considered such variables as headwinds, runway gradients, airframe aerodynamic performance including a range of flap settings, and detailed engine efficiencies over a range of TOGW and atmospheric conditions. The resulting matrix of cases was built into tables such as the one shown in Table A-2, the Max Allowable TOGW for the B737-500 CFM-56-3-B1 for 5-degree flaps and bleeds ON. This chart contains temperatures along the leftmost column, with various runways across the top. The last column reflects the performance-limited case. Contained within each chart element is the max allowable TOGW in thousands of pounds for the particular airframe/engine combination on the given runway at the selected temperature for the specified flap and bleed setting. These data tables were created in the flap sequence as specified in the airframe manufacturer performance manuals and the United Airlines pilot training procedure documentation, and contained within the United Airlines aircraft flight manual. The sequence of flap schedules is airframe/engine and airline specific; however, much commonality occurs among airframes and airlines. These MATOGW charts are screened in the appropriate sequence to determine the flap setting. The chart is entered with the actual OAT for the particular runway, and the MATOGW linearly interpolated. This value is then compared with the Actual TOGW (ATOG) and the flaps increased if necessary. If the ATOG exceeds the MATOGW for all flap settings and bleeds “ON”, then the analysis proceeds through the Bleeds “OFF” data.

Table A-2. Maximum Allowable Takeoff Weight Chart for the B737-500, Flaps 5, Bleeds ON

```
PART 07 OF 16 PARTS

B-737-500 CFM56-3-B1
DENVER, CO   DENVER INTERNATIONAL
DEN/KDEN - ELEV 5431
TAKEOFF - BLEEDS ON
FLAP 5
   RWY    7     8     8E    16    17L   17LF  17R   17RG  PERF
LENGTH 12000 12000 11700 12000 12000 11690 12000 11670 LIMIT
 NOTES    .     .     E     T1    T1    FT1   T1    GT1     .
 DEG F
   -20 119.7 124.6 124.6 124.6 124.6 124.6 124.6 124.6 118.0
   -10 119.4 124.5 124.5 124.5 124.5 124.5 124.5 124.5 117.9
     0 119.2 124.4 124.4 124.4 124.4 124.4 124.4 124.4 117.8
    10 118.9 124.2 124.2 124.2 124.2 124.2 124.2 124.2 117.7
    20 118.7 124.1 124.1 124.1 124.1 124.1 124.1 124.1 117.6
    30 118.5 124.0 124.0 124.0 124.0 124.0 124.0 124.0 117.5
    40 118.2 123.8 123.8 123.8 123.8 123.8 123.8 123.8 117.4
    50 117.9 123.5 123.5 123.5 123.5 123.5 123.5 123.5 117.2
    60 117.5 123.1 123.1 123.1 123.1 123.1 123.1 123.1 117.0
    70 117.2 122.6 122.6 122.6 122.6 122.6 122.6 122.6 116.8
    79 116.9 121.9 121.9 121.9 121.9 121.9 121.9 121.9 116.6
    80 116.7 121.7 121.7 121.7 121.7 121.7 121.7 121.7 116.4
    90 112.0 117.0 117.0 117.0 117.0 117.0 117.0 117.0 111.4
   100 107.0 111.1 111.1 111.1 111.1 111.1 111.1 111.1 106.1
   102 105.7 109.4 109.4 109.4 109.4 109.4 109.4 109.4 104.7
   110 102.2 104.7 104.7 104.7 104.7 104.7 104.7 104.7 100.6
 LB/KT    60     0     0     0     0     0     0     0    0F
  HEAD    60     0     0     0     0     0     0     0  100F
 LB/KT   380     0     0     0     0     0     0     0    0F
  TAIL   380     0     0     0     0     0     0     0  100F
-E-
RWY 8 TKOF FM TWY R9 W/ E 11700FT AVBL  (RWY 8E).

-F-
RWY 17L TKOF FM TWY P9 W/ S 11690FT AVBL  (RWY 17LF).

-G-
RWY 17R TKOF FM TWY M9 W/ S 11670FT AVBL  (RWY 17RG).

-T1-
IN CASE OF ENGINE FAILURE ON TAKEOFF FROM RUNWAYS
16-17L/R, BEGIN LEFT TURN TO 080 DEG MAG AT D4.0 S OF
DEN DME.
END OF PART 07 OF 16 PARTS
_08011559 108362 0803
```

These charts and specified flap sequences are runway specific and contain the various aerodynamic and performance tradeoffs between extra runway length and TOGW. At high altitudes such as DIA, a simple increase in flap setting utilizing the minimum defined field length does not always allow for a gain in TOGW, since the engines are usually operating at their maximum thrust rated limit. Instead the "Improved" flap settings, such as the 1I setting for the B737-200, make use of the extra runway length at DIA for achieving higher V2 speeds. Procedural requirements by the airframe manufacturer and/or airline operator may prohibit the use of derated thrust for these improved flap schedules for higher ATOGs.

During this interpolation process for evaluating the flap setting based on MATOGW and Actual OAT, the ATOG is also considered. If an interpolation at the final flap setting based on ATOG indicates that a higher temperature departure is possible, this higher temperature becomes the basis for derated thrusts. Physically, the difference between this higher "Assumed Temperature" ATEMP and the actual OAT represents excess departure performance. Given high-maintenance cost savings return for reduced-power takeoffs, airlines strongly urge pilots to perform derated thrusts whenever possible. One should note, however, that the interpolation procedure and evaluation of the ATEMP varies from one airline to the next. For example, United allows the ATEMP to be determined as a floating value driven by performance margins. Delta Airlines, on the other hand, prescribes a standard ATEMP threshold for derated thrusts. The actual airline departure procedures must therefore be considered when predicting derated takeoff thrust levels.

The second segment of the departure profile is the Climb segment. The process by which this throttle setting is determined is considerably easier than for takeoff. The Maximum Climb Thrust tables, provided by the airlines, Table A-3, contains Total Air Temperature down the left column and pressure altitude across the top row. A linear interpolation in two dimensions is used to determine the climb N1 or EPR. As before, these charts are a function of the exact airframe/engine combination.

FAA regulations do not permit derated thrust levels which are lower than the climb segment thrust level. After the climb thrust has been calculated, for derated takeoffs, the thrust must be increased to the climb thrust if necessary. This requirement applies only to the actual N1 or EPR setting. The net corrected installed thrust in lbs. may in fact be less for second segment when considering altitude and Mach effects, even though the throttle setting is identical.

Table A-3. Maximum Takeoff Thrust – PMC on 737-300 (B1/C1 20K)

NOTE
The heavy line in the table is used for the Reduced Thrust calculation.

Assumed Temp or OAT (°F)	Pressure Altitude (1000 Feet)									
	-1000	SL	1	2	3	4	5	6	7	8
130	90.0	90.6	91.2	91.9	NA	NA	NA	NA	NA	NA
120	90.7	91.1	91.7	92.3	93.7	94.7	NA	NA	NA	NA
110	91.3	91.7	92.2	92.7	94.0	95.0	95.0	95.0	NA	NA
102	91.8	92.2	92.6	93.0	94.2	95.4	95.4	95.4	95.1	94.7
100	91.9	92.3	92.7	93.1	94.3	95.6	95.6	95.5	95.1	94.6
94	92.0	92.5	93.0	93.4	94.7	96.0	96.0	95.9	95.2	94.4
90	92.1	92.6	93.1	93.5	95.0	96.3	96.2	96.1	95.4	94.6
88	91.9	92.7	93.2	93.6	95.1	96.4	96.3	96.2	95.5	94.8
86	91.8	92.8	93.2	93.6	95.0	96.5	96.4	96.3	95.6	94.9
85	91.7	92.7	93.2	93.6	94.9	96.5	96.5	96.4	95.7	94.9
82	91.4	92.4	93.3	93.7	94.7	96.3	96.4	96.5	95.9	95.2
80	91.3	92.3	93.1	93.7	94.6	96.1	96.4	96.7	96.0	95.3
79	91.2	92.2	93.0	93.7	94.6	96.0	96.4	96.7	96.1	95.4
78	91.1	92.1	92.9	93.6	94.5	95.9	96.4	96.8	96.2	95.5
76	90.9	91.9	92.8	93.5	94.4	95.7	96.2	96.7	96.2	95.6
70	90.4	91.4	92.2	92.9	93.9	95.2	95.7	96.1	96.1	96.0
60	89.6	90.5	91.4	92.1	93.1	94.3	94.8	95.2	95.3	95.4
56	89.3	90.2	91.0	91.7	92.7	93.9	94.4	94.9	95.1	95.2
50	88.7	89.7	90.5	91.2	92.1	93.4	93.8	94.2	94.4	94.5
-40	87.8	88.8	89.6	90.2	91.2	92.5	92.9	93.3	93.5	93.6
30	87.0	87.9	88.7	89.3	90.3	91.6	92.0	92.4	92.6	92.7
20	86.1	87.0	87.7	88.4	89.4	90.6	91.0	91.4	91.6	91.7
10	85.2	86.1	86.8	87.5	88.4	89.6	90.1	90.5	90.6	90.7
0	84.3	85.1	85.9	86.6	87.5	88.7	89.1	89.5	89.7	89.8
-10	83.3	84.2	85.0	85.6	86.5	87.7	88.1	88.5	88.7	88.8
-20	82.4	83.3	84.0	84.7	85.6	86.7	87.1	87.5	87.7	87.8
-40	80.5	81.5	82.1	82.7	83.6	84.7	85.2	85.6	85.7	85.8

Bleed Correction
Engine Bleeds off: + .8% N_1
No correction required for engine anti-ice on.

In the cockpit the pilot sets the throttle level, either N1 or EPR, depending on the engine type. The onboard control system for virtually all modern commercial aircraft holds the engines at the prescribed throttle position until a command control change is input. Other than subtle differences between rolling increasing throttle starts versus max throttle brake release starts which primarily affect noise near the airport grounds and the transition between takeoff and climb thrusts, we can assume the throttle setting to be constant. A further refinement to this assumption might be made in the future via speed and rotation point data analysis; however, these details were not available at DIA for this particular measurement program, due to the radar system resolution limitations. Additional measurements, such as video tape triangulation technologies, would be required for such a study.

Table A-4. Reduced Takeoff Thrust %N_1 Adjustment

Reduced Takeoff Thrust – 737-300 (B1)										
Assumed Temp (°F)	%N_1 Adjustment									
	OAT (°F)									
	-40	0	40	50	60	70	80	90	100	110
120	0	0	-6.7	-5.8	-5.0	-4.0	-3.1	-2.3	-1.6	-.8
110	0	0	-5.9	-5.1	-4.2	-3.3	-2.4	-1.6	-.8	0
100	-12.5	-8.8	-5.1	-4.3	-3.4	-2.6	-1.7	-.8	0	0
90	-11.9	-8.0	-4.4	-3.5	-2.6	-1.7	-.8	0	0	0
80	-11.2	-7.3	-3.5	-2.7	-1.7	-.8	0	0	0	0
70	-10.5	-6.4	-2.6	-1.8	-.8	0	0	0	0	0
60	-9.7	-5.6	-1.8	-.7	0	0	0	0	0	0

Table A-5. United Airlines Maximum Climb Thrust (N_1) 737-300 (B1/C1-20K)

TAT	Pressure Altitude (1000 Feet)								
°C	SL	5	10	15	20	25	30	35	37
50	88.9	89.0	89.2	NA	NA	NA	NA	NA	NA
40	89.8	90.0	90.2	90.7	NA	NA	NA	NA	NA
30	89.9	90.4	91.1	91.6	91.9	92.1	NA	NA	NA
20	88.4	90.5	91.8	92.5	92.8	93.0	93.2	NA	NA
10	86.8	88.9	91.0	92.7	93.5	93.8	94.0	94.0	94.0
0	85.3	87.4	89.4	91.1	93.1	94.4	94.6	94.6	94.6
-10	83.7	85.7	87.7	89.4	91.3	93.1	94.6	95.2	95.2
-20	82.1	84.1	86.0	87.7	89.6	91.3	92.8	95.7	96.0
-30	80.5	82.4	84.3	85.9	87.8	89.5	90.9	93.8	94.5
-40	78.8	80.7	82.6	84.1	86.0	87.6	89.0	91.9	92.5

Bleed Correction (%N_1)

Engine Bleeds off:	+.7	Engine anti-ice on:	-.9
Packs high:	-.5	Wing anti-ice on:	-1.6

With this fixed throttle setting, a prediction of net corrected installed thrust in lbs., as required by the INM, must be performed using the actual installed performance engine performance charts. Thrust in lbs. was calculated as a function of Mach number and altitude and N1 or EPR as appropriate. These Fn/δ charts are considered manufacturer proprietary property and as such are not published in this document.

At this stage of the analysis, each point in the radar track in the initial takeoff segment is analyzed in sequence. Based on the local atmospheric conditions, Mach number, and N1/EPR, the Fn/δ is determined for input into the INM. The atmospheric variations with altitude were based on interpolation of atmospheric weather balloon data to the flight departure time. The local velocity

as reported by the ARTS system was converted to calibrated airspeed and the temperature converted to Total Temperature as required by the particular prediction method and Fn/δ charts.

Standard departure procedures in place at DIA require climb at takeoff thrust to 1,000 feet above ground level (AGL). A scan of the departure profiles and an evaluation of the altitude where the "knee in the curve" occurs, indicated that the majority of departures were adhering to this guideline.

When looping through all the radar points, a switch from the takeoff N1/EPR to the climb N1/EPR is made at radar point closest to or above 1,000 feet AGL. This new N1/EPR value is used when interpolating in the Fn/δ charts to predict the thrust. Future refinements to this methodology may include a pattern recognition method for determining the transition point between takeoff and climb throttle settings, as well as a gradual rather than an instantaneous change between settings. Discussions with United Airlines flight training personnel indicated that the throttle and flap cleanup technique was highly pilot dependent and could not be reliably predicted. Guidelines such as X seconds per flap retraction for acceleration before changing throttles, despite detailed airline studies, were not available. It might be possible to determine the extent of the transition from flaps to clean and acceleration with change to climb segment thrust based on radar data; however, such methods were not employed in this study.

REPORT DOCUMENTATION PAGE

Form Approved
OMB No. 0704-0188

The public reporting burden for this collection of information is estimated to average 1 hour per response, including the time for reviewing instructions, searching existing data sources, gathering and maintaining the data needed, and completing and reviewing the collection of information. Send comments regarding this burden estimate or any other aspect of this collection of information, including suggestions for reducing this burden, to Department of Defense, Washington Headquarters Services, Directorate for Information Operations and Reports (0704-0188), 1215 Jefferson Davis Highway, Suite 1204, Arlington, VA 22202-4302. Respondents should be aware that notwithstanding any other provision of law, no person shall be subject to any penalty for failing to comply with a collection of information if it does not display a currently valid OMB control number.
PLEASE DO NOT RETURN YOUR FORM TO THE ABOVE ADDRESS.

1. REPORT DATE *(DD-MM-YYYY)*	2. REPORT TYPE	3. DATES COVERED *(From - To)*
01- 10 - 2006	Contractor Report	

4. TITLE AND SUBTITLE

Improved Airport Noise Modeling for High Altitudes and Flexible Flight Operations

5a. CONTRACT NUMBER

NAS1-00086

5b. GRANT NUMBER

5c. PROGRAM ELEMENT NUMBER

6. AUTHOR(S)

Forsyth, David W.; and Follet, Jesse I.

5d. PROJECT NUMBER

5e. TASK NUMBER

5f. WORK UNIT NUMBER

23-781-50-21

7. PERFORMING ORGANIZATION NAME(S) AND ADDRESS(ES)

NASA Langley Research Center
Hampton, VA 23681-2199

Boeing Commercial Airplane Company
Seattle, WA 98124

8. PERFORMING ORGANIZATION REPORT NUMBER

9. SPONSORING/MONITORING AGENCY NAME(S) AND ADDRESS(ES)

National Aeronautics and Space Administration
Washington, DC 20546-0001

10. SPONSOR/MONITOR'S ACRONYM(S)

NASA

11. SPONSOR/MONITOR'S REPORT NUMBER(S)

NASA/CR-2006-214511

12. DISTRIBUTION/AVAILABILITY STATEMENT

Unclassified - Unlimited
Subject Category 71
Availability: NASA CASI (301) 621-0390

13. SUPPLEMENTARY NOTES

Langley Technical Monitor: Kevin P. Shepherd
An electronic version can be found at http://ntrs.nasa.gov

14. ABSTRACT

The FAA's Integrated Noise Model (INM) is widely used to estimate noise in the vicinity of airports. This study supports the development of standards by which the fleet data in the INM can be updated. A comparison of weather corrections to noise data using INM Spectral Classes is made with the Boeing integrated method. The INM spectral class method is shown to work well, capturing noise level differences due to weather especially at long distances. Two studies conducted at the Denver International Airport are included in the appendices. The two studies adopted different approaches to modeling flight operations at the airport. When compared to the original, year 2000, results, it is apparent that changes made to the INM in terms of modeling processes and databases have resulted in improved agreement between predicted and measured noise levels.

15. SUBJECT TERMS

Aircraft Noise; Airport Noise; Noise Prediction

16. SECURITY CLASSIFICATION OF:			17. LIMITATION OF ABSTRACT	18. NUMBER OF PAGES	19a. NAME OF RESPONSIBLE PERSON
a. REPORT	b. ABSTRACT	c. THIS PAGE			STI Help Desk (email: help@sti.nasa.gov)
					19b. TELEPHONE NUMBER *(Include area code)*
U	U	U	UU	265	(301) 621-0390